

https://dspace.org/

37 kDa LRP::FLAG enhances telomerase activity and reduces ageing markers in vitro and in vivo

Otgaar, Tyrone C

2020
https://hdl.handle.net/10539/30173

Downloaded from a DSpace repository. https://dspace.org/

School of Molecular and Cell Biology
University of the Witwatersrand
Braamfontein
Johannesburg

37 kDa LRP::FLAG enhances telomerase activity and reduces ageing markers in vitro and in vivo

by

Tyrone C. Otgaar (568652)

THESIS

Submitted in fulfilment of the degree

Philosophiae doctor (PhD.)

in

BIOCHEMISTRY AND CELL BIOLOGY

in the

FACULTY OF SCIENCE

22 May 2020

Supervisor: Prof. Stefan. F.T. Weiss

Co-Supervisor: Dr. E. van der Merwe

Declaration

I, **Tyrone C. Otgaar (568652)**, am a student registered for the degree of Doctor of Philosophy Science by Thesis (PhD) in the academic year 2020.

I hereby declare the following:

- I am aware that plagiarism (the use of someone else's work without their permission and/or without acknowledging the original source) is wrong.
- I confirm that the work submitted for assessment for the above degree is my own unaided work except where explicitly indicated otherwise.
- I have not submitted this work before for any other degree or examination at this or any other University.
- I have followed the required conventions in referencing the thoughts and ideas of others.
- I understand that the University of the Witwatersrand may take disciplinary action against me if there is a belief that this is not my own unaided work or that I have failed to acknowledge the source of the ideas or words in my writing.

Signed: 22nd day of May 2020



Abstract

Ageing is a degenerative process characterised by detrimental changes which accumulate to cause a decline in physiological functioning of the organism. It is characterised by stem cell exhaustion, mitochondrial dysfunction as well as genomic instability. One of the core regulators of cellular ageing are telomeres, repetitive DNA sequences of TTAGGG that cap the ends of chromosomes and are maintained by the ribonucleoprotein DNA polymerase complex, telomerase. Age-dependent progressive loss of telomere functions due to the "end replication" problem and insufficient telomerase activity eventually induces cell cycle exit for the induction of either replicative senescence or apoptosis. To bypass senescence, most epithelial and tumorigenic cells re-activate telomerase allowing for telomere extension thereby, extending their proliferative potential and promoting overall cell viability. It was recently established that knockdown of the 37kDa/ 67kDa laminin receptor (LRP/LR), a proliferative-related protein which maintains cell viability in cancerous and normal cells, reduces telomerase activity. Therefore, it was hypothesized that elevating LRP/LR may increase telomerase activity and hinder the ageing process. The core aims of this research included: To prove *in vitro* that LRP::FLAG overexpression influences telomere dynamics and senescent related proteins in cells. Thereafter, to prove *in vivo* that LRP::FLAG overexpression (i) has an effect on the ageing process, (ii) positively impacts on telomere dynamics and (iii) significantly reduces the levels of tissue senescence in aged C57BL/6J mice. To this end, cell lines were successfully developed that stably overexpressed LRP::FLAG and have further overexpressed LRP::FLAG in aged C57BL/6J mouse models. Western blotting, confocal microscopy and qPCR were used to assess the effects of overexpression of LRP::FLAG on ageing markers as well as telomere dynamics in both cell lines and mice. In addition, various physiological tests (balance beam, puzzle box, nesting, wirehang, social interaction, open field and hair greying tests) and histological analyses were performed to assess overall mouse fitness as well as to discern the treatments ability at reducing tissue degeneration and atrophy. In terms of the *in vitro* research, it was found that the overexpression of LRP::FLAG induced a significant elevation hTERT levels, telomerase activity and telomere length. Concomitantly, it was shown that LRP::FLAG overexpression also reduced the levels of

the senescence/ageing markers β-galactosidase and λH2AX in both HEK293 and MRC 5 cells. Moreover, for the *in vivo* component it was found that mice overexpressing LRP::FLAG displayed improved physiological characteristics and markedly less tissue degeneration and atrophy when compared to control and non-treated mice. Alongside these improvements, certain organs displayed increased telomerase activity with a corresponding elongation in average telomere length, further substantiating that a functional relationship exists between LRP and telomerase. In addition to the improved aspects of telomere biology it was found that the overexpression of LRP::FLAG significantly improved various proliferative and anti-ageing associated proteins (Klotho, MDM2, SIRT1, Akt and c-Myc) while causing a concomitant decrease in senescent associated proteins (p16, NFkB and γH2AX). These findings are indicative of a novel function of LRP/LR impeding the onset of senescence, while also promoting healthier ageing through elevating TERT and telomerase activity. Therefore, LRP::FLAG could act as a novel drug for healthier ageing through the impediment of the cellular ageing process.

Acknowledgments

I would like to firstly thank my supervisor Prof. Stefan Weiss for providing me with all the unique opportunities that he did, as well as all the guidance he has given me since Honours. It is this guidance that has shaped me into the researcher that I am today and has also allowed me to hone a unique set of skills. You also provided a relaxed and friendly environment in addition to a range of unique, humorous and unforgettable experiences and memories.

I would also like to give a special thank you to my co-supervisor Dr Eloise van der Merwe, who was not only a mentor, but a very close and dear friend. It is thanks to you that I survived this PhD and without your aid and support, this research would not even be half of what it currently is. The advice, knowledge, stories and jokes we shared will never be forgotten.

Thank you to Prof Veale, your advice proved invaluable during my PhD research. In addition, I would also like to thank you for your aid with interpreting the histochemical data, without you I would have been more than a little lost.

I would also like to thank Dr Meyer for the enormous amount of advice during the course of my PhD. I now have a much deeper understanding of both advanced statistical analysis as well as gene expression analysis by qPCR. This knowledge will serve will serve me well in the future and for that I am deeply thankful.

A very big thank must also be given to my family for all their love and support. Especially my parents for tolerating me when I was most stressed out, and always being there to offer advice or words of encouragement. Furthermore, I want to thank both of you for allowing me to complete a part of my dreams by studying to finally obtain my PhD, and hope that the works and possible discoveries that may come from this degree will continue to make you proud in the future.

Thank you to my brother, Travis, for not only did you provide support and a lot of laughs over the years, you specifically contributed towards my PhD research by building some of the equipment used during this study.

A special thank you to Liang Gu. Thank you for your patience, especially when having to deal with me, when I was irritable from work or was demotivated. You provided constant motivation and helped, wherever possible during my entire post graduate journey with only the barest of complaints. Thank you for encouraging me to never give up and ensuring that I was also able to work at my best.

Thank you to my best friend and practically second brother, Matthew Wilson. Your constant curiosity and excitement about my research always motivated me to aim for greater achievements. Thanks for being the best friend or "bro" a person could ask for, without you I would not have become the person I am today.

Thank you to my close friend Shaun especially for those late night calls that helped me through some of the all-nighters I pulled. The laughs, talks and debates were a welcome relief after a long week in the lab.

Thank you to both Monique Bignoux and Martin Bernert. You were both super lab colleagues and also exceptionally good friends. You guys were always there and willing to help, a fact I never plan on forgetting. You guys with Eloise made this PhD journey in the lab an unforgettable experience.

Thank you to all my past and present colleagues Prof Weiss' Research Laboratory for your support and for helping me grow scientifically.

I would also like to acknowledge and thank the staff at CAS, especially Patrick Selahle, for all their hard work in caring for the mice during the study.

I would also like to thank Ms. Hasiena Ali, Senior Technician, School of Anatomical Sciences, Faculty of Health Sciences, University of Witwatersrand (Johannesburg,

South Africa). It is thanks to her that all the tissue sectioning and staining was carried out on the tissues.

Finally I would like to offer this thesis in dedication to Dr Letsolo. You were an awe inspiring supervisor and mentor. You touched my life in a profound manner, where I believe you helped bring out some of my best traits. Aside from being a mentor you were also a close friend, where I will sorely miss the four hour long debates over science and life in general. May you rest in peace and receive nothing but blessings in the afterlife.

Financial aid:

Wits Postgraduate Merit Award (2016, 2018-2019)
National Research Foundation (NRF) – Block grant (2016-2017)
National Research Foundation (NRF) – Free Standing (2018-2019)
The South African Medical Research Council (SAMRC)

Research outputs

First Author publications:

Otgaar, T.C., Ferreira, E., Malindisa, S., Bernert, M., Letsolo, B.T., Weiss, S.F.T. (2017). 37 kDa LRP::FLAG enhances telomerase activity and reduces senescent markers *in vitro*. Oncotarget, 8, 86646-56

Co-Author Publications (Not forming part of PhD thesis):

Ferreira, E., Bignoux, M.J., **Otgaar, T.C.,** Tagliatti, N., Jovanovic, K., Letsolo, B.T., and Weiss, S.F. T. (2018). LRP/LR specific antibody IgG1-iS18 impedes neurodegeneration in Alzheimer's disease mice. Oncotarget 9, 27059-73.

Bignoux, M.J., Cuttler, K., **Otgaar, T.C.,** Ferreira, E., Letsolo, B.T. and Weiss, S.F.T. (2019). LRP::FLAG rescues cells from Aβ- mediated cytotoxicity through increased TERT levels and telomerase activity. J. Alzheimer's Disease, 69, 729-741.

Vania, L., Morris, G., **Otgaar, T.C.,** Bignoux, M.J., Bernert, M., Burns, J., Gabathuse, A., Singh, E., Ferreira, E., Weiss, S.F. Patented therapeutic approaches targeting LRP/LR for cancer treatment. Expert Opin Ther Pat. 2019; 29: 987-1009.

Co-authored Patents:

PCT International Application PCT/IB2016/056686, Date of Submission: 7 Nov 2016, is in the name of the University of the Witwatersrand entitled "Compounds for use in the treatment of telomere related diseases and/or telomere related medical conditions". Inventors: Prof. Stefan F T Weiss, Dr. Boitelo Letsolo, Kerrilyn Naidoo and **Tyrone Otgaar**. Priority date is 5 November, 2015. (Espacenet: no citations)

Provisional South Africa patent application NO. 2018/04509 is in the name of the University of the Witwatersrand entitled: "Biopharmaceutical agents for use in reducing lipid content in cells". Inventors: **Tyrone Otgaar**, Martin Bernet, Dr. Eloise van der Merwe, Dr. Gavin Morris, Prof. Stefan F T Weiss. This application has a priority date of 6 July 2018. (Espacenet: no citations) (this patent application has been completed as PCT application PCT/IB2019/055788)

Provisional South Africa patent application NO. 2018/04507 is in the name of the University of the Witwatersrand entitled: "Pharmaceutical composition for the site specific delivery of a biopharmaceutical agent." Inventors: **Tyrone Otgaar**, Martin Bernet, Dr. Eloise van der Merwe, Dr. Gavin Morris, Prof. Stefan F T Weiss. This application has a priority date of 6 July 2018. (Espacenet: no citations) (this patent application has been completed as PCT application PCT/IB2019/055788)

PCT International Application PCT/IB2019/055788, Date of submission 6 July 2019 is in the name of the University of the Witwatersrand entitled: "Biopharmaceutical agents for use in reducing lipid content in cells". Inventors: **Tyrone Otgaar**, Martin Bernet, Dr. Eloise van der Merwe, Dr. Gavin Morris, Prof. Stefan F T Weiss. This application has a priority date of 6 July 2018. (Espacenet: no citations)

Provisional South Africa patent application No. 2019/02879 is in the name of the University of the Witwatersrand entitled: "A method of decreasing concentration of tau (τ) protein and/or phosphorylated tau (τ) protein". Inventors: Katelyn Cuttler, **Tyrone Otgaar**, Monique Bignoux, Dr. Eloise van der Merwe and Prof Stefan F T Weiss. Priority date is 9 May, 2019. (Espacenet: no citations) (this patent application has been completed as PCT application PCT/IB2020/054443)

PCT International Application PCT/IB2020/054443, Date of submission 11 May 2020 is in the name of the University of the Witwatersrand entitled: “A method of decreasing concentration of tau (τ) protein and/or phosphorylated tau (τ) protein”. Inventors: Katelyn Cuttler, **Tyrone Otgaar**, Monique Bignoux, Dr. Eloise van der Merwe and Prof Stefan F T Weiss. This application has a priority date of 11 May 2019. (Espacenet: no citations)

Conferences:

Otgaar, T. C., Ferreira, E., Malindisa, S., Bernert, M., Letsolo, B. T., Weiss, S.F.T. (2018, November 29). 37 kDa LRP::FLAG enhances telomerase activity and reduces ageing markers *in vitro* and *in vivo*. Oral presentation, The Molecular Biosciences Research Thrust (MBRT) Research Day, University of the Witwatersrand, Johannesburg, South Africa.

Otgaar, T. C., Ferreira, E., Malindisa, S., Bernert, M., Letsolo, B. T., Weiss, S.F.T. (2018, July 8-11). 37 kDa LRP::FLAG enhances telomerase activity and reduces ageing markers *in vitro* and *in vivo*. Oral presentation, SASBMB-FASBMB Conference, North West University, Potchefstroom, South Africa.

Otgaar, T. C., Ferreira, E., Malindisa, S., Bernert, M., Letsolo, B. T., Weiss, S.F.T. (2017, November 15). 37 kDa LRP::FLAG enhances telomerase activity and reduces ageing markers *in vitro* and *in vivo*.
Poster presentation, The Molecular Biosciences Research Thrust (MBRT) Research Day, University of the Witwatersrand, Johannesburg, South Africa.

Otgaar, T. C., Ferreira, E., Malindisa, S., Bernert, M., Letsolo, B. T.,
Weiss, S.F.T. (2016, December 6). The role of LRP/LR and telomerase in the ageing process. Poster Presentation, The Molecular Biosciences Research Thrust (MBRT) Research Day, University of the Witwatersrand, Johannesburg, South Africa.

Otgaar, T. C., Ferreira, E., Malindisa, S., Bernert, M., Letsolo, B. T.,
Weiss, S.F.T. (2016, July 11-13). The role of LRP/LR and telomerase in the ageing process. Poster presentation, The South African Society for Biochemistry and Molecular Biology (SASBMB) Congress, East London, South Africa.

Table of contents

Abstract ..... **iii**

Acknowledgments ..... **v**

FINANCIAL AID: ..... **VII**

Research outputs ..... **viii**

FIRST AUTHOR PUBLICATIONS: ..... **VIII**

CO-AUTHOR PUBLICATIONS (NOT FORMING PART OF PHD THESIS): ..... **VIII**

CO-AUTHORED PATENTS: ..... **IX**

CONFERENCES: ..... **XI**

Table of Figures ..... **xix**

List of Tables: ..... **xxiii**

LIST OF ABBREVIATION ..... **XXIV**

1. Literature Review ..... **- 1 -**

1.1 Ageing and cell senescence ..... **- 1 -**

1.1.1 Stem cell model of ageing ..... *- 1 -*

1.1.2 Senescence model of ageing ..... *- 3 -*

1.1.3 The senescence process and the senescence associated secretory phenotype ..... *- 4 -*

1.2 Stress-dependent senescence ..... **- 5 -**

1.2.1 Mitochondrial induced senescence ..... *- 6 -*

1.2.2 Inflamm-ageing ..... *- 7 -*

1.2.3 Oncogene induced senescence ..... *- 7 -*

1.3 Telomere dependent senescence ..... **- 8 -**

1.3.1 Telomere-dependent senescence and Reactive Oxygen Species ..... *- 9 -*

1.3.2 Signalling cascades involved in telomere-dependent senescence ..... *- 10 -*

1.3.3 Impediment of telomere-dependent senescence ..... *- 11 -*

1.4 Telomere biology ..... **- 11 -**

1.4.1 Structure and function of the telomeres ..... *- 11 -*

1.4.2 Telomeres and the shelterin complex ..... - 12 -
1.4.3 Shelterin, telomeres and generation of the telomere loop ..... - 14 -
1.4.4 Shelterin and its role in telomere maintenance ..... - 14 -
1.5 Telomerase and TERT ..... - 15 -
1.5.1 Structure and function of the telomerase complex ..... - 15 -
1.5.2 Regulation of TERT and telomerase ..... - 17 -
1.5.3 Transcriptional and post-translational regulation of TERT ..... - 18 -
1.5.4 TERT and telomerase activity in humans and mice ..... - 20 -
1.6 Extra-telomeric functions of TERT and telomerase ..... - 21 -
1.6.1 The mitochondrial functions of TERT ..... - 22 -
1.6.2 TERT in DNA repair and apoptosis ..... - 23 -
1.6.3 TERT in the regulation of gene expression and signalling cascades ..... - 25 -
1.7 Telomeres, Telomerase and roles in pathological processes ..... - 26 -
1.7.1 Telomerase and telomeres in carcinogenesis ..... - 26 -
1.7.2 The role of TERT and telomerase in CVD and diabetes ..... - 27 -
1.7.3 The influence of telomerase and telomeres in neurodegenerative disorders - 28 -
1.8 The 37kDa/67kDA Laminin Receptor ..... - 29 -
1.8.1 Cellular distribution of LRP/LR and its role as a cell surface receptor ..... - 29 -
1.8.2 LRP/LR and angiogenesis ..... - 30 -
1.8.3 LRP/LR and its interaction with the cytoskeleton ..... - 31 -
1.8.4 The ribosomal functions of LRP/LR ..... - 32 -
1.8.5 Nuclear functions of LRP/LR ..... - 33 -
1.8.6 The role of LRP/LR in differentiation and development ..... - 34 -
1.8.7 The role of LRP/LR in signalling cascades ..... - 35 -
1.9 LRP/LR and its role in pathological processes ..... - 36 -
1.9.1 The Role of LRP/ LR in Bacterial and Viral infections ..... - 37 -
1.9.2 The Role of LRP/ LR in Neurodegenerative disorders ..... - 37 -
LRP/LR and Prion disorders ..... - 37 -
LRP/LR and Alzheimer's disease ..... - 38 -
1.9.3 The role of LRP/ LR in carcinogenesis ..... - 39 -
1.10 Relationship between LRP/LR and telomerase ..... - 39 -
2. Aims and objectives ..... - 41 -

2.1 ***In vitro* Study Aim:** **- 41 -**
2.1.1 *In vitro Study Objectives:* *- 41 -*
2.2 *In vivo* Study Aims**:** **- 41 -**
2.2.1 *In vivo Study Objectives:* *- 41 -*
3. Methodology - 43 -
3.1 Production of the pCIneo-moLRP::FLAG plasmid - 43 -
3.1.1 *Bacterial Transformation and plasmid expression* *- 43 -*
3.1.2 *Plasmid DNA Isolation by the Alkaline Lysis Method* *- 44 -*
3.2 Cell Culture - 44 -
3.3 LRP::FLAG overexpression in HEK293 and MRC 5 cells - 45 -
3.4 Protein extraction from cells and Bicinchoninic acid (BCA) protein assay - 46 -
3.5 Western blotting for *in vitro* analysis of HEK293 and MRC 5 protein levels - 47 -
3.5.1 *Sample preparation* *- 47 -*
3.6 Assessment of co-localisation between TERT and LRP *in vitro* using confocal microscopy - 48 -
3.7 Assessment of cell senescence *in vitro* by use of the β-Galactosidase assay - 48 -
3.8 Assessment of telomerase activity in HEK293 and MRC 5 cells - 49 -
3.9 DNA isolation from HEK293 and MRC 5 cells for telomere length assessment - 50 -
3.9.1 *DNA isolation from cell pellets* *- 50 -*
3.9.2 *Assessment of mean telomere length from cultured cells* *- 51 -*
3.10 Animal trials and treatments - 51 -
3.11 Hair greying analysis - 53 -
3.12 Physiological tests to assess organism fitness - 53 - - 53 -
3.12.1 *Puzzle box test* *- 53 -*
3.12.2 *Nesting Test* *- 54 -*
3.12.3 *Motor function analysis using the balance beam test* *- 55 -*

3.13 Organ harvest ..... - 55 -

3.14 Histological analysis ..... - 56 -

3.15 Assessment of proliferative and senescent gene expression in various mouse organs by qPCR ..... - 57 -

3.15.1 Tissue RNA extraction ..... - 57 -

3.15.2 cDNA synthesis from tissue isolated RNA ..... - 58 -

3.15.3 Mouse gene expression analysis by qPCR ..... - 59 -

3.16 Assessment of proliferative and senescent protein marker levels ..... - 59 -

3.16.1 Protein extraction from tissue ..... - 60 -

3.16.2 Tissue protein profiles assessed by SDS PAGE and western blotting ..... - 60 -

3.17 Assessment of telomerase activity in mice tissue ..... - 61 -

3.18 Telomere length and mitochondrial DNA content determination in mouse tissue by qPCR ..... - 62 -

3.18.1 DNA extraction from mice tissue ..... - 62 -

3.18.2 Relative Telomere length determination in mouse tissue by qPCR ..... - 62 -

3.18.3 Mouse tissue mitochondrial DNA content analysis by qPCR ..... - 63 -

3.19 Data and Statistical analysis ..... - 63 -

4. Results ..... - 66 -

4.1 Overexpression of LRP::FLAG in HEK293 and MRC 5 transfected cells... - 66 -

4.2 hTERT co-localises with LRP/LR and LRP::FLAG *in vitro* ..... - 66 -

4.3 LRP::FLAG overexpression positively influences telomere dynamics to induce a significant increase in hTERT levels telomerase activity, and telomere length *in vitro* - 69 -

4.4 LRP::FLAG overexpression induces a significant reduction in tested senescent markers: β-galactosidase activity and γH2AX levels *in vitro* ..... - 71 -

4.5 LRP::FLAG overexpression induced a significant improvement in various physiological parameters within the aged mice ..... - 73 -

4.5.1 Overexpression of LRP::FLAG impedes the age associated process of hair greying - 73 -

4.5.2 LRP::FLAG overexpression significantly improved cognitive function in aged mice - 75 -

4.5.3 LRP::FLAG overexpression significantly improved nesting abilities in aged mice - 77 -

4.5.4 Overexpression of LRP::FLAG causes a significant improvement in motor function and balance ..... - 79 -

4.6 The overexpression of LRP::FLAG impedes the formation of histopathological markers that constitute tissue ageing ..... - 80 -

4.6.1 Mice overexpressing LRP::FLAG showed less neurodegeneration in the hippocampal regions of the brain ..... - 80 -

4.6.2 Mice overexpressing LRP::FLAG showed less signs of kidney tissue ageing and degeneration - 82 -

4.7 LRP::FLAG overexpression significantly increases total LRP levels in aged mice - 84 -

4.8 LRP::FLAG overexpression positively affects proliferative markers in aged mice - 87 -

4.8.1 LRP::FLAG overexpression increases Akt levels in the brain as well as pAKT levels in liver of aged mice ..... - 87 -

4.8.2 LRP::FLAG overexpression increases c-Myc protein levels in the brain and liver of aged mice ..... - 90 -

4.8.3 Overexpression of LRP::FLAG increases MDM2 levels in the brain while inducing no significant change in pMDM2 levels of the aged mice..... - 93 -

4.9 Overexpression of LRP::FLAG induces a significant elevation in anti-ageing proteins within the aged mice..... - 96 -

4.9.1 LRP::FLAG overexpression significantly increases the levels of the anti-ageing protein SIRT1 in aged mice ..... - 96 -

4.9.2 LRP::FLAG overexpression significantly increased the levels of the anti-ageing protein α-Klotho in aged mice..... - 99 -

4.10 The overexpression of LRP::FLAG significantly elevates the levels of the senescence-associated protein, p53 in aged mice ..... - 101 -

4.11 The overexpression of LRP::FLAG significantly impedes the accumulation of senescent markers, p16 and γH2AX in aged mice ..... - 104 -

4.11.1 LRP::FLAG overexpression decreases p16 levels in aged mice..... - 104 -

4.11.2 LRP::FLAG overexpression prevents the age-dependent accumulation of γH2AX levels within the aged mice ..... - 106 -

4.12 The overexpression of LRP::FLAG lessens the effects of mitochondrial dysfunction by decreasing mitochondrial DNA content in various organs of the aged mice - 107 -

4.13 LRP::FLAG overexpression induces a significant improvement of telomere dynamics within the aged mice .....- 109 -

4.13.1 LRP::FLAG overexpression causes a significant increase in TERT and pTERT levels in aged mice .....- 109 -

4.13.2 LRP::FLAG overexpression causes an increase in relative telomerase activity in the kidney and liver of aged mice.....- 112 -

4.13.3 LRP::FLAG overexpression causes a significant increase in mean telomere length in kidney and liver of aged mice.....- 114 -

5. Discussion .....- 116 -

5.1 LRP and LRP::FLAG co-localise with TERT *in vitro*.....- 117 -

5.2 Overexpression of LRP::FLAG improves telomere dynamics in aged cells *in vitro* - 117 -

5.3 LRP::FLAG overexpression influences the accumulation of senescent markers *in vitro* .....- 118 -

5.4 Overexpression of LRP::FLAG improves physiological functioning in aged mice - 120 -

5.4.1 LRP::FLAG overexpression prevents the accumulation of grey hair.....- 120 -

5.4.2 LRP::FLAG overexpression improves cognitive function in aged mice .....- 120 -

5.4.3 Overexpression of LRP::FLAG improves motor function.....- 121 -

5.5 The overexpression of LRP::FLAG improves tissue pathology in aged mice - 122 -

5.6 Overexpression of LRP::FLAG postivley effects proliferative markers in aged mice - 124 -

5.6.1 LRP::FLAG overexpression increases Akt and pAkt in aged mice.....- 124 -

5.6.2 LRP::FLAG overexpression elevates the transcription factor c-Myc.....- 126 -

5.6.3 LRP::FLAG overexpression positively influences MDM2 and its phosphorylation.....- 126 -

5.7 Overexpression of LRP::FLAG increases anti-ageing proteins in aged mice - 128 -

5.7.1 LRP::FLAG overexpression significantly elevates SIRT1 .....- 128 -

5.7.2 LRP::FLAG overexpression increases both full length and secreted isoforms of klotho - 129 -

5.8 Overexpression of LRP::FLAG increases the senescent-related protein p53 in aged mice - 131 -

5.9 Overexpression of LRP::FLAG reduces the levels of tested senescent markers in aged mice .....- 132 -

5.9.1 LRP::FLAG overexpression decreases senescent marker p16 .....- 132 -

5.9.2 LRP::FLAG overexpression reduces the DNA damage marker γH2AX .....- 133 -

5.10 Overexpression of LRP::FLAG lowers mitochondrial DNA content in aged mice - 134 -

5.11 Overexpression of LRP::FLAG telomere dynamics in aged mice.....- 136 -

6. Conclusion .....- 140 -

6.1 Future Studies .....- 142 -

6.2 Study Limitations.....- 143 -

7. References.....- 145 -

8. Appendices .....- 175 -

Table of Figures

Figure 1.1: The stem cell model of ageing. ..... - 2 -
Figure 1.2: The autocrine and paracrine signalling roles of the senescent associated secretory phenotype in propagating and maintaining the senescence process. . - 5 -
Figure 1.3: The mechanism behind telomere-dependent senescence, and how telomerase reactivation induces replicative immortality by replenishment of the telomeres. ..... - 9 -
Figure 1.4: Schematic diagram featuring the structure and function of the telomeres together with the shelterin complex and TERRA to form the T and D-loop for enhanced genomic protection. ..... - 13 -
Figure 1.5: The ribonucleo reverse transcriptase telomerase performing its primary function of telomeric extension. ..... - 16 -
Figure 1.6: The multitude of regulatory elements dictating TERT expression and telomerase activity. ..... - 19 -
Figure 1.7: TERT and telomerase and its extra-telomeric functions aside from telomere maintenance. ..... - 22 -
Figure 1.8: The extra telomeric functions of TERT in promoting cell proliferation and survival. ..... - 25 -
Figure 1.9: Schematic representation of the 37 kDa Laminin Receptor Precursor/67 kDa High affinity Laminin Receptor and a few of its associated binding partners. ..... - 31 -
Figure 1.10: The various isoforms of LRP/LR also known as LAMR or RPSA and their respective functions. ..... - 34 -
Figure 1.11: The various pathological processes that exploit LRP/LR. ..... - 36 -
Figure 3.1: Flow diagram depicting timing of treatments to be received by each group. ..... - 65 -
Figure 4.1: Overexpression of LRP::FLAG in HEK293 and MRC5 cells. ..... - 66 -
Figure 4.2: LRP and LRP::FLAG co-localizes with hTERT. ..... - 69 -
Figure 4.3: LRP::FLAG overexpression significantly elevates hTERT levels, telomerase activity and telomere length. ..... - 71 -
Figure 4.4: LRP::FLAG overexpression significantly decreases the levels of senescent markers. ..... - 73 -
Figure 4.5: Overexpression of LRP::FLAG reduces the amount of hair greying in mice. ..... - 75 -
Figure 4.6: Overexpression of LRP::FLAG prevents age associated cognitive decline by improving short and long term memory as well as puzzle solving ability. ..... - 77 -
Figure 4.7: Aged mice treated to overexpress LRP::FLAG displayed improved nest building abilities. ..... - 78 -
Figure 4.8: LRP::FLAG overexpression induced a significant improvement in motor function and balance in aged mice. ..... - 80 -
Figure 4.9: Histological analysis revealing that LRP::FLAG overexpression aids in preventing neuro-tissue degeneration in the hippocampus. ..... - 82 -
Figure 4.10: Overexpression of LRP::FLAG prevented the age-dependent tissue

decline of the kidney in aged mice.....- 84 -
Figure 4.11: Overexpression of LRP::FLAG induces an overall increase in LRP/LR gene expression and protein levels. .....- 86 -
Figure 4.12: qPCR and Western blot analysis illustrated that the overexpression of LRP::FLAG positively affected Akt. .....- 90 -
Figure 4.13: LRP::FLAG overexpression significantly elevates c-Myc gene expression and protein levels in aged mice......- 92 -
Figure 4.14: Overexpression of LRP::FLAG increases MDM2 levels in the brain while not affecting the extent of protein phosphorylation in both the brain and liver of aged mice. .....- 96 -
Figure 4.15: Mice overexpressing LRP::FLAG displayed significantly elevated SIRT1 gene expression and protein levels......- 98 -
Figure 4.16: The overexpression of LRP::FLAG increased the levels of both the full length and secreted isoform of α-klotho in aged mice. .....- 100 -
Figure 4.17: Overexpression of LRP::FLAG induced an increase of the tumor suppressor protein, p53 in aged mice. .....- 103 -
Figure 4.18: LRP::FLAG overexpression significantly reduces the senescent marker p16 in aged mice......- 105 -
Figure 4.19: The overexpression of LRP::FLAG induces a significant reduction in the DNA damage marker γH2AX within the aged mice. .....- 107 -
Figure 4.20: The overexpression of LRP::FLAG significantly reduces total mitochondrial DNA content in aged mice. .....- 108 -
Figure 4.21: LRP::FLAG overexpression significantly elevated total TERT and active pTERT levels in aged mice. .....- 112 -
Figure 4.22: The overexpression of LRP::FLAG caused a significant elevation in relative telomerase activity within the kidney and liver of aged mice......- 113 -
Figure 4.23: The overexpression of LRP::FLAG causes a substantial increase in mean telomere length within the kidney and liver of the aged mice......- 115 -
Figure 8.1: The overexpression of LRP::FLAG reduces IL6 in the brain and kidney in aged mice. .....- 175 -
Figure 8.2: The overexpression of LRP::FLAG caused a non-significant reduction in IL8 within the brain and kidney of aged mice......- 176 -
Figure 8.3: The overexpression of LRP::FLAG induces a significant increase in TRF1 and TRF2 within the liver of the aged mice. .....- 177 -
Figure 8.4: Agarose gel electrophoresis displaying the pCIneo-moLRP::FLAG and empty pCIneo- vector......- 178 -
Figure 8.5: Sequencing alignment and BLAST data for the LRP::FLAG gene. - 179 -
Figure 8.6: Agarose gel electrophoresis displaying RNA extracted samples from the brain. .....- 180 -
Figure 8.7: Agarose gel electrophoresis displaying RNA extracted samples from the liver......- 180 -
Figure 8.8: Agarose gel electrophoresis displaying RNA extracted samples from the kidney. .....- 181 -
Figure 8.9: Agarose gel electrophoresis displaying DNA extracted samples from the brain. .....- 181 -
Figure 8.10: Agarose gel electrophoresis displaying DNA extracted samples from

the liver. ..... - 182 -
Figure 8.11: Agarose gel electrophoresis displaying DNA extracted samples from the kidney. ..... - 182 -
Figure 8.12: Amplification curve and Melt peak analysis of the reference gene GAPDH. ..... - 183 -
Figure 8.13: Amplification curve and Melt peak analysis of the reference gene RPLPO. ..... - 184 -
Figure 8.14: Amplification curve and Melt peak analysis of the LRP gene. ..... - 185 -
Figure 8.15: Amplification curve and Melt peak analysis of the Akt gene. ..... - 186 -
Figure 8.16: Amplification curve and Melt peak analysis of the c-Myc gene. ..- 187 -
Figure 8.17: Amplification curve and Melt peak analysis of the MDM2 gene. - 188 -
Figure 8.18: Amplification curve and Melt peak analysis of the SIRT1 gene. .- 189 -
Figure 8.19: Amplification curve and Melt peak analysis of the klotho gene. ..- 190 -
Figure 8.20: Amplification curve and Melt peak analysis of the p53 gene. ..... - 191 -
Figure 8.21: Amplification curve and Melt peak analysis of the p16 gene. ..... - 192 -
Figure 8.22: Amplification curve and Melt peak analysis of the TERT gene. ..- 193 -
Figure 8.23: Amplification curve and Melt peak analysis of the IL6 gene. ..... - 194 -
Figure 8.24: Amplification curve and Melt peak analysis of the IL8 gene. ..... - 195 -
Figure 8.25: Amplification curve and Melt peak analysis of the mtDNA and nuclear specific DNA sequence (hexokinase). ..... - 196 -
Figure 8.26: Amplification curves for telomerase activity in the brain, liver and kidney. ..... - 197 -
Figure 8.27: Amplification curve and Melt peak analysis for telomere length as well as the reference gene 36B4. ..... - 198 -
Figure 8.28: Qualitative analysis of mouse hair greying ..... - 199 -
Figure 8.29: LRP::FLAG overexpression significantly elevates total LRP levels in the brain of aged mice. ..... - 200 -
Figure 8.30: LRP::FLAG overexpression significantly elevates total LRP levels in the liver of aged mice. ..... - 201 -
Figure 8.31: LRP::FLAG overexpression significantly elevates total Akt levels in the brain of aged mice. ..... - 202 -
Figure 8.32: LRP::FLAG overexpression induces no significant change in total Akt levels within the liver of aged mice. ..... - 203 -
Figure 8.33: LRP::FLAG overexpression significantly elevates phospho-Akt levels in the liver of aged mice. ..... - 204 -
Figure 8.34: LRP::FLAG overexpression significantly elevates c-Myc levels in the brain of aged mice. ..... - 205 -
Figure 8.35: LRP::FLAG overexpression significantly elevates c-Myc levels in the liver of aged mice. ..... - 206 -
Figure 8.36: LRP::FLAG overexpression significantly elevates total MDM2 levels in the brain of aged mice. ..... - 207 -
Figure 8.37: LRP::FLAG overexpression induces no significant change in total MDM2 levels in the liver of aged mice. ..... - 208 -
Figure 8.38: LRP::FLAG overexpression induces no significant change in phospho-MDM2 levels in the brain of aged mice. ..... - 209 -
Figure 8.39: LRP::FLAG overexpression induces no significant change in phospho-MDM2 levels in the brain of aged mice. ..... - 210 -

Figure 8.40: LRP::FLAG overexpression significantly increases Sirt1 levels in the brain of aged mice. ..... - 211 -
Figure 8.41: LRP::FLAG overexpression significantly elevates Sirt1 levels in the liver of aged mice. ..... - 212 -
Figure 8.42: LRP::FLAG overexpression significantly elevates full length and secreted klotho levels in the brain of aged mice. ..... - 213 -
Figure 8.43: LRP::FLAG overexpression significantly elevates secreted klotho levels in the liver of aged mice. ..... - 214 -
Figure 8.44: LRP::FLAG overexpression significantly elevates p53 levels in the brain of aged mice. ..... - 215 -
Figure 8.45: LRP::FLAG overexpression significantly elevates p53 levels in the liver of aged mice. ..... - 216 -
Figure 8.46: LRP::FLAG overexpression significantly reduces p16 levels in the brain of aged mice. ..... - 217 -
Figure 8.47: LRP::FLAG overexpression significantly reduces p16 levels in the liver of aged mice. ..... - 218 -
Figure 8.48: LRP::FLAG overexpression significantly reduces γH2AX levels in the brain of aged mice. ..... - 219 -
Figure 8.49: LRP::FLAG overexpression significantly reduces γH2AX levels in the liver of aged mice. ..... - 220 -
Figure 8.50: LRP::FLAG overexpression significantly elevates TERT levels in the brain of aged mice. ..... - 221 -
Figure 8.51: LRP::FLAG overexpression significantly elevates TERT levels in the liver of aged mice. ..... - 222 -
Figure 8.52: LRP::FLAG overexpression significantly elevates phospho-TERT levels in the brain of aged mice. ..... - 223 -
Figure 8.53: LRP::FLAG overexpression significantly elevates phospho-TERT levels in the liver of aged mice. ..... - 224 -

List of Tables:

Table 8.1: Bacterial Nutrient Broth ..... - 225 -
Table 8.2: Bacterial Nutrient Agar ..... - 225 -
Table 8.3: Resuspension Buffer ..... - 226 -
Table 8.4: Bacterial Lysis Buffer ..... - 226 -
Table 8.5: Neutralisation Buffer ..... - 226 -
Table 8.6: Tris-EDTA (TE) Buffer (pH8) ..... - 226 -
Table 8.7: Phosphate Buffered Saline ..... - 227 -
Table 8.8: RIPA Buffer (Radio immunoprecipitation assay lysis buffer) ..... - 227 -
Table 8.9: 10% SDS-PAGE gel recipe ..... - 228 -
Table 8.10: Electrophoresis tank (Running) Buffer (pH 8.3) ..... - 229 -
Table 8.11: 10X Transfer Buffer ..... - 229 -
Table 8.12: 10X Transfer Buffer ..... - 229 -
Table 8.13: Stripping Buffer (pH 2.2) ..... - 230 -
Table 8.14: qPCR master mix ..... - 230 -
Table 8.15: qPCR Trap Master mix ..... - 230 -
Table 8.16: List of primers used for gene expression analysis ..... - 232 -
Table 8.17: Primers used for mtDNA content analysis ..... - 233 -
Table 8.18: Primers used for mean telomere length analysis ..... - 233 -
Table 8.19: Primers used for telomerase activity analysis ..... - 233 -
Table 8.20: Antibodies used for in vitro confocal microscopy and western blotting analysis ..... - 234 -
Table 8.21: Antibodies used for in the vivo study western blotting analysis ..... - 235 -

List of Abbreviation

µg	Microgram
µl	Microlitre
36B4	acidic ribosomal phosphoprotein P0
53B1	p53 binding protein 1
A	Amps
AD	Alzheimer's disease
Akt	Protein kinase B
AMPK	5' adenosine monophosphate-activated protein
APP	Amyloid precursor protein
ARF	ADP ribosylation factor
ATM	Ataxia telangiectasia mutated
ATP	Adenosine triphosphate
ATR	Ataxia telangiectasia and Rad3
Aβ	Amyloid Beta
BBB	Blood brain barrier
BCA	Bicinchoninic acid assay
BSA	Bovine serum albumin
C/EBP-β	CCAAT/enhancer-binding protein beta
CDK4 / 6	Cyclin dependent kinase 4/ 6
cDNA	Complimentary Deoxyribonucleic Acid
CHAPS	(3-((3-cholamidopropyl)dimethylammonio)-1-chromosome 10
CNF1	Cytotoxic necrotizing factor 1
CO_2	Carbon dioxide
Cu	Copper
CVD	Cardiovascular disease
DAPI	4',6-diamidino-2-phenylindole
DDR	DNA damage response
DG	Dentate gyrus
D-loop	Displacement loop

DMEM	Dulbecco’s Modified Eagle’s Medium
DMSO	Dimethyl sulfoxide
DNA	Deoxyribonucleic Acid
dNTP	Deoxynucleotide Triphosphates
DSB	Double stranded breaks
DTT	Dithiothreitol
E. coli	Escherichia coli
ECM	Extracellular matrix
EDTA	Ethylenediaminetetraacetic acid
EGTA	Ethylene glycol bis(2-aminoethyl)tetraacetic acid
EMT	Epithelial–mesenchymal transition
ERK	Extracellular-signal-regulated kinase
FAK	Focal adhesion kinase
FBS	Fetal bovine serum
g	Gram
gDNA	Genomic DNA
H2AX	H2A histone family member X
HEK293	Human Embryonic Kidney Cells
HIP	Hsc70-interacting protein
Hr	Hour
HSC	Heat-shock cognate
HSP70	Heat shock protein 70
HSPG	Heparan sulfate proteoglycan
hTERT	Human Telomerase Reverse Transcription
IL1α	Interleukin 1 alpha
IL6 / 8	Interleukin 6/ 8
JNK	c-Jun N-terminal kinases
Kb	Kilobase
kDa	Kilo Dalton
	kinase
LAMR1	Laminin receptor 1

LRP	Laminin receptor precursor protein
LRP/LR	37 kDa Laminin Receptor Precursor/67 kDa High Affinity Laminin Receptor
MAPK	Mitogen activated protein kinase
MDA MB231	M.D. Anderson Metastatic breast cancer cells 231
MDC1	Mediator Of DNA Damage Checkpoint 1
MDM2	Mouse double minute 2
MFRTA	Mitochondrial free radical theory of aging
MgCl	Magnesium chloride
MHC	Major histocompatibility complex
min	Minutes
MKP1	Mitogen-Activated Protein Kinase Phosphatase 1
ml	Millilitre
mM	Milli-molar
MRC 5	Medical Research Council cell strain 5
mRNA	Messenger RNA
mtDNA	Mitochondrial Deoxyribonucleic Acid
mTERT	Mouse TERT
mV	Milli-volt
MZF2	Myeloid zinc finger protein 2
NaCl	Sodium chloride
NAD^+	Nicotinamide adenine dinucleotide
NBS1	Nibrin
NEDD4	E3 ubiquitin-protein ligase
NFκB	Nuclear factor kappa-light-chain-enhancer of
ng	Nanogram
NMDA	N-methyl-d-aspartate
OIS	Oncogene induced senescence
ONPG	O-Nitrophenyl beta-D-galactopyranoside
PAGE	Polyacrylamide Gel electrophoresis
PBS	Phosphate-buffered saline

PBST	Phosphate-buffered saline tween
PCR	Polymerase Chain Reaction
PEA15	Phosphoprotein enriched in astrocytes 15
PFA	Paraformaldehyde
PinX1	PIN2/TERF1-interacting telomerase inhibitor 1
Pol II	RNA polymerase II
POT1	Protection of telomeres Protein 1
PP1	Protein phosphatase 1
	propanesulfonate)
PrP^{c}	Cellular Prion Protein
PrP^{sc}	Scrapie Prion Protein
PTEN	Phosphatase and tensin homologue deleted on
PVDF	Polyvinylidene fluoride
	pyranoside
qPCR	Quantitative Polymerase Chain Reaction
Rb	Retinoblastoma
RNA	Ribonucleic Acid
RNase	Ribonuclease
RNF8	Ring finger protein 8
ROS	Reactive Oxygen Species
Rpm	Revolutions per minute
RPSA	Ribosomal protein SA
RT	Room temperature
SASP	Senescence Associated Secretory Phenotype
SDS	Sodium Dodecyl Sulphate
shRNA	Small Hairpin RNA
SIPS	Stress induced premature senescence
siRNA	Small Interfering RNA
SIRT1	Sirtuin 1

SP1	Specificity protein 1
STS	Staurosporine
TBE	Tris-Borate-EDTA
TE	Tris-EDTA
TERC	Telomerase RNA Component
TERRA	Telomeric repeat-containing RNA
TERT	Telomerase reverse transcriptase
TF	Transcription factor
TGFβ	Transforming growth factor beta
TIF	Telomere induced foci
TIN2	TERF1-interacting nuclear factor 2
t-loop	Telomere-loop
TNFα	Tumor necrosis factor alpha
TPP1	Tripeptidyl peptidase 1
TRAP	Telomere repeat amplification protocol
TRF1	TTAGGG Repeat Binding Factor 1
TRF2	TTAGGG Repeat Binding Factor 2
Tris-HCl	Tris hydrochloride
V	Volt
v/ v	Volume per volume
v/ w	volume per weight
WT1	Wilms' tumor gene 1
x g	# gravities
X-Gal	5-bromo-4-chloro-3-indolyl-beta-D-galacto-

1. Literature Review

1.1 Ageing and cell senescence

Ageing is a universal process that incorporates the accumulation of adverse changes that ultimately causes a progressive decline of the organism's physiological and biochemical functioning, which are imperative for survival [1]. This functional decline induced by ageing eventually leads to organ failure that in turn gives rise to a host of age-related phenotypic features characteristic of ageing. These features can include benign changes from hair greying and the thinning of the skin to more severe/ pathological features like: loss of lung tissue elasticity, bones becoming brittle, accumulation of fatty deposits and loss of flexibility in blood vessels, as well as a reduced ability for healing/ regeneration of the tissues [2, 3]. In turn, these features culminate in a time dependent loss of tissue and organ function, which effectively elevates the risk of mortality. Although the ageing process exhibits numerous features similar to a pathology, it is still considered a normal cellular process and not a disease [4]. However, the overall functional decline induced by ageing drastically elevate an organism's susceptibility, especially humans, to a number of age-related pathologies. These include: diabetes, cancer, cardiovascular diseases such as atherosclerosis and neurodegenerative disorders like Alzheimer's (AD) or Parkinson's disease [1, 2, 5, 6].

1.1.1 Stem cell model of ageing

The process of ageing is believed to be governed by two generally accepted models namely, the depletion of adult stem cell niches or secondly the gradual accumulation of senescent cells in various tissues of the body [2]. These tissue specific stem cells are essentially uncharacterised cells that retain the ability to differentiate into specialised cells of any cell type of the organ they reside within [6, 7]. In this way, these cells serve as efficient reservoir cells for organs and allow for regeneration, healing and expansion of the tissue [(Figure 1.1) [3]]. These cells however, have been shown to have finite proliferative capacities, owing in part to the accumulation of cellular damage as well as the restrictions imposed by the length of their telomeres, repetitive genetic elements (TTAGGG repeats) that cap the ends of chromosomes [(Figure 1.1) [8-11]]. In turn, when these stem cell reserves are eventually depleted the organs are unable to adequately replace the damaged tissue and cells, which leads to the characteristic phenotypic alterations that generally constitute ageing [(Figure 1.1) [6, 7]].

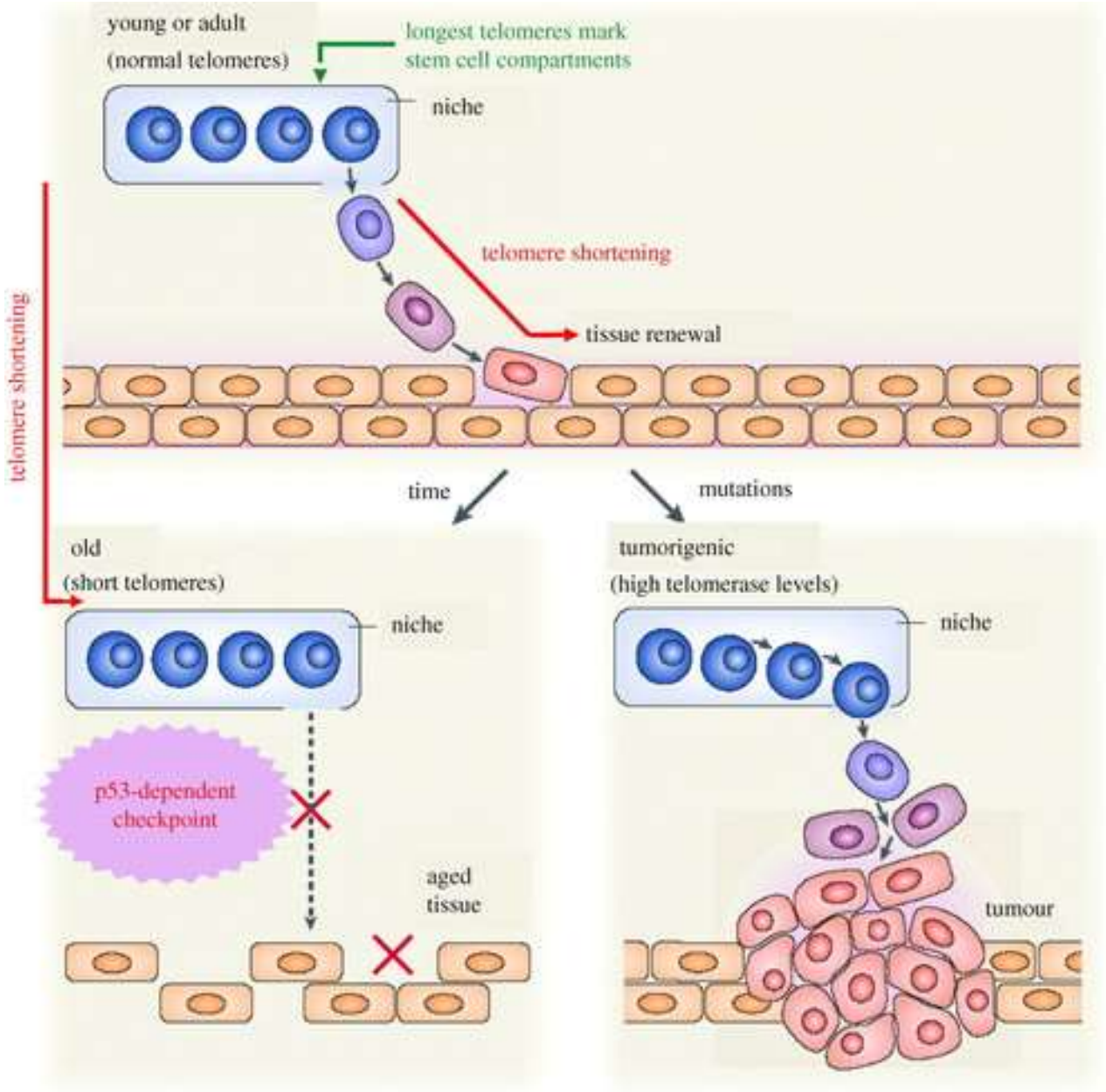


Figure 1.1: The stem cell model of ageing.
The figure illustrates a theoretical model to potentially explain the ageing process, or at the very least, an aspect of it. Adult stem cell niches are known to act almost as a repository for the organs/ tissue they reside in, where the stem cell niches operate to replace damaged or senescent cells with fresh and healthy ones. This occurs throughout the organism's lifespan until the stem cell niches become depleted. This occurs due to an accumulation of damage within the stem cells, as well as extensive replication, which induces senescence by critical shortening of the telomeres. As a result, the organ/ tissue accumulates damaged or senescent cells that can no longer be replaced, which continues until organ failure or mortality occurs. Alternatively, should genomic mutations accumulate within the stem cell population, they can induce the formation of cancer stem cells. These cells are then fed into the tissue in an attempt to carry out tissue renewal, however, the cancer stem cells instead induce tumor formation. Adopted from: Donate and Blasco, 2011 [12].

1.1.2 Senescence model of ageing

The second model of ageing was primarily based off the observation that as an organism ages there is a notable increase in the number of senescent cells throughout the body. Senescence is defined as the complete and irreversible loss of proliferative potential in somatic cells, although they may remain metabolically active and viable [13, 14]. The process was historically discovered *in vitro* where normal human fibroblasts were found to enter a state of permanent cell cycle arrest after extensive sub-culturing, otherwise known as the Hayflick limit [15-17]. The senescence process itself, is a consequence of how a cell responds to both acute and chronic cellular stress [1, 13]. In addition, it is believed that the process of cellular senescence arose as an evolutionary defence mechanism against carcinogenesis [13, 18]. In this regard, senescence would not only prevent the accumulation of mutations, a direct consequence of extensive proliferation and DNA damage, but also effectively prevent the propagation of pre-malignant cells.

In ageing the senescence process is governed by oxidative stress caused by the accumulation of reactive oxygen species (ROS) but can also be influenced by other biological, chemical and physical stresses. These stresses induce genotoxic and proteotoxic damage that is gradually assimilated during each subsequent round of cell division [13, 18, 19]. Other factors that ROS influences to modulate ageing and senescence include: inducing persistent inflammation, mitochondrial dysfunction, forming non-telomeric DNA aberrations, and most importantly, telomeric DNA erosion [1, 19-23]. Once the protein and DNA damage surpasses a critical point the cell undergoes a range of genetic and phenotypic alterations that primarily serve to limit or prevent further proliferation [13, 24-26]. A few of these alterations include: an elevation in key tumor suppressor pathways (p53, pRb and p16INK4A), a silencing of active proto-oncogenic pathways, decline of anti-ageing related proteins like klotho and Sirtuin 1 (SIRT1), altered metabolic pathways as well as sustained activation of inflammatory processes and secretory pathways [13, 25, 26]. In addition, cells adopt an enlarged, flattened and granular morphology with increased amounts of vacuolization [19, 27-30]. These changes are primarily brought about by chromatin remodelling and altered epigenetic profiles, which cause a subsequent change in gene expression patterns [30-32].

1.1.3 The senescence process and the senescence associated secretory phenotype

The altered expression profiles exhibited during cellular ageing allow senescent cells to secrete biomolecules (inflammatory cytokines, chemokines, proteases and extracellular matrix (ECM) remodelling factors) capable of inducing potent paracrine effects [(Figure 1.2) [29, 33, 34]]. These secreted molecules serve to alter the tissue microenvironment in order to propagate the stress or senescent phenotype to neighbouring cells (Figure 1.2). This occurs through a process otherwise known as the senescent associated secretory phenotype (SASP) [33, 35, 36]. Once activated, the senescence process and SASP can take several days, to weeks to become fully established and irreversible. This extended process towards irreversible growth arrest is further enhanced by an intracellular signalling loop where ROS-linked DNA damage responses (DDRs), NFκB (nuclear factor kappa-light-chain-enhancer of activated B cells), transforming growth factor-β (TGF-β) as well as inflammatory cytokines IL1α and IL6 and CCAAT enhancer binding protein-β (C/EBP-β) together form a loop to exacerbate the spread of the senescent state [29, 34, 37-39]. In addition, the process is further reliant on two core inflammatory cytokines, namely; IL6 and IL8, among others, that aid in the recruitment of immune cells [34, 39, 40]. As the number of immune cells accumulates, it eventually induces chronic inflammation, which is commonly associated with a number of age-related pathologies and advanced ageing (inflamm-ageing) [41-43]. Furthermore, these two cytokines have also been implicated in ensuring that senescence associated growth arrest is maintained among the senescent cells and surrounding tissue by operating in both an autocrine and paracrine manner [(Figure 1.2) [34, 35, 39, 40]]. In contrast, under non-ageing conditions the SASP could offer a number of benefits including: promoting the clearance of damaged cells, resolving tissue damage, epithelial to mesenchymal transitions (important for wound healing as well as cancer), and act as a form of protection against infections [30, 44-47]. However, as damaged and aged cells accumulate, the normal functions of the SASP become dysregulated as the damaged tissue can no longer be repaired or replaced with new cells. Instead, the aforementioned senescent-related functions occur, thus indicating the vital role that the SASP plays in maintaining and progressing the senescent phenotype.

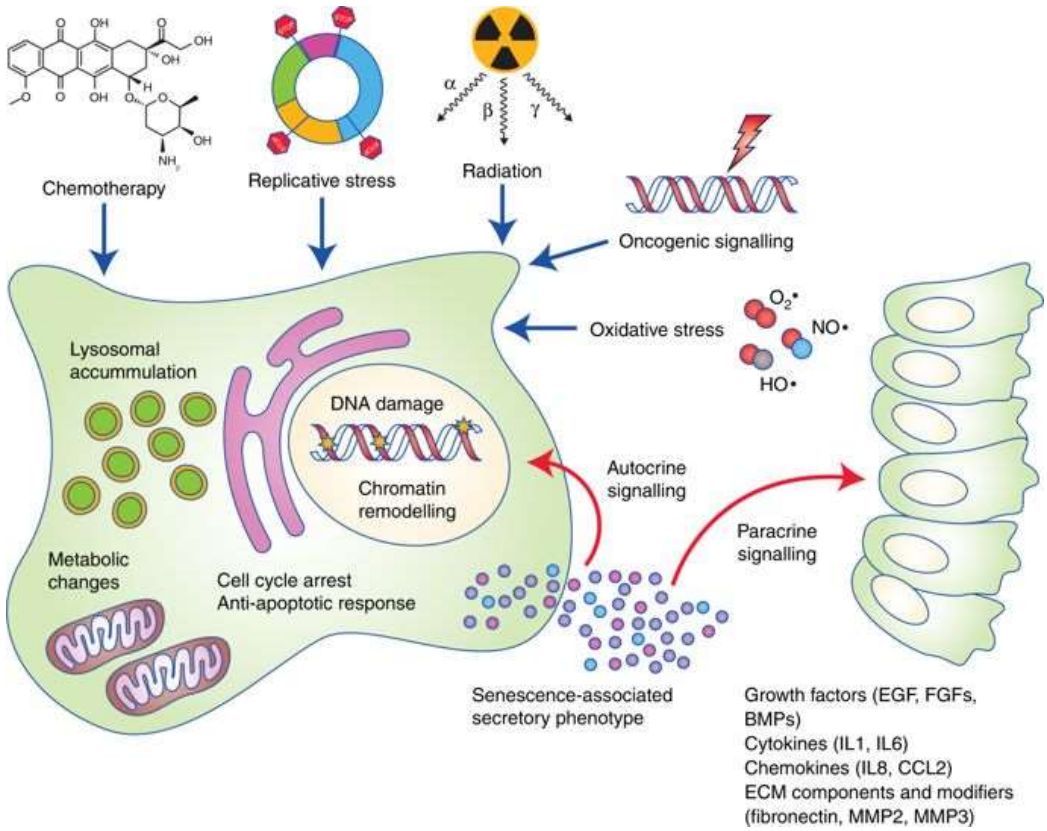


Figure 1.2: The autocrine and paracrine signalling roles of the senescent associated secretory phenotype in propagating and maintaining the senescence process.
The senescent associated secretory phenotype (SASP) is ultimately brought about by the accumulation of senescent cells. This occurs whereby, normal functioning cells accumulate damage induced by various stresses (Chemotherapy, oxidative stress from mitochondrial dysfunction, dysregulated oncogenic signalling, radiation and replicative stress ie: critical telomere erosion). This induces a host of alterations in the cells for permanent cell cycle arrest. In this state the cells produce SASP factors at an exponential rate that are comprised of growth factors, inflammatory cytokines, chemokines as well as factors that operate to modify the ECM. These factors firstly, act in an autocrine manner to ensure the persistence of the senescent state in the afflicted cells. Thereafter, these factors also operate to alter the tissue environment (altered ECM and persistent inflammation) to aid in the maintenance of the senescent phenotype. Finally, these SASP factors can also operate in a paracrine manner to spread the senescent state to the surrounding healthy cells, thereby aiding in the propagation of the senescent phenotype. Thus, illustrating the critical roles that the SASP plays in maintaining and propagating the senescent state using both autocrine and paracrine signalling. Adopted from: Gonzalez-Meljem et al, 2018 [48].

1.2 Stress-dependent senescence

The aforementioned factors have led to the identification of two major types of senescence namely stress-dependent senescence and telomere dependent senescence. It must be highlighted that there is normally a dynamic interplay between the two forms of senescence however, stress-dependent senescence can act independently and normally causes the arousal of a condition known as stress induced premature cellular senescence (SIPs) [49]. Other forms of stress-dependent ageing/ senescence that can operate alongside or independently of telomere dependent senescence include: mitochondrial induced senescence, inflamm-ageing, and oncogene induced senescence.

1.2.1 Mitochondrial induced senescence

The mitochondria are the core organelles responsible for the generation of energy as well as cell metabolism and have been heavily implicated in the ageing process. This influence on ageing is believed to be a consequence of the organelles function to produce ATP through oxidative metabolism, where ROS is generated as a by-product of the process [50, 51]. Consequently, during ageing there is a notable decline in the respiratory function of these organelles as well as an excessive generation of ROS, which leads to elevated levels of oxidative stress and mitochondrial dysfunction [52-55]. Once mitochondrial dysfunction sets in there are an array of compounding effects that contribute to the decline in cellular and tissue fitness including: abrogated ROS generation, mutations and/ or damage within mtDNA, as well as a lack of ATP generation. Furthermore, there is a distinctive increase in mitochondrial mass, altered mitochondrial membrane permeability (elevating the risk of apoptotic induction) with Ca+ dysregulation and inflammation [37, 54, 56-60]. In particular, the abrogated generation of ROS alongside the accumulation of mtDNA mutations encompasses one of the leading theories on ageing namely, the mitochondrial free radical theory of aging (MFRTA) [61]. This theory is housed around several noteworthy observations confirming that both ROS production and mtDNA mutations accumulate with age combined with a concomitant decline in ROS neutralising agents [59, 60, 62-64]. This results in a viscous cycle where each of the aforementioned effects elevates the other to cause a compounding effect. Thereafter, the heighted oxidative stress causes widespread DNA, lipid and protein damage which eventually accumulates to cause cellular decline. However, this theory has recently been thrown into disrepute due to a growing body of conflicting data that rules out ROS as the initial cause of ageing [65-68]. Furthermore, certain studies have found no beneficial effects to longevity when using anti-oxidants to prevent the accumulation of ROS [60, 69-71]. This said, mitochondrial dysfunction and especially mtDNA mutations have still been shown to significantly contribute to the senescent phenotype, where it is believed to contribute to the formation of the SASP and act as an effector pathway for both inflammatory induced and oncogene induced ageing [72-78]. Therefore, mitochondrial fitness may still play a large role in senescence by promoting its continued progression alongside other senescent inducers.

1.2.2 Inflamm-ageing

A core feature that occurs during the ageing process is a persistent activation and increase in chronic inflammation with advancing age, which gained the term inflamm-ageing. Generally, inflammation encompasses a series of responses that an organism's inflammatory cytokine system carries out when exposed to pathogens or tissue injury [79]. These inflammatory responses fade when the pro-inflammatory factors like pathogens are resolved or the injury is healed. In contrast, during inflamm-ageing the inflammation persists and moves onto an unresolved state and eventually causes immuno-senescence [80, 81]. Accompanying this state is an elevation in ROS (induced by mitochondrial dysfunction) to promote cellular damage and metabolic alterations, a progressive increase of pro-inflammatory cytokines and increased fat content to house pro-inflammatory mediators [81-84]. A few of these elevated pro-inflammatory cytokine markers include: IL 1, 6, 8, 15 and 18 as well as TNFα [85-90]. These cytokines in high levels operate through the circulatory system to effectively ensure that an inflammatory environment is maintained for tissues and organs [84, 85]. This generates a cyclic event whereby the elevated ROS generated from the inflammatory response induces additional DNA damage. This results in the expression of additional pro-inflammatory cytokines to further progress the senescent state [88, 91, 92]. Aside from this, the elevated cytokines produced further contribute to the establishment and progression of the SASP allowing the senescent state to be spread to the surrounding tissues [93, 94]. Finally, inflamm-ageing has also been implicated in a range of age-related diseases such as Alzheimer's disease (AD), cancer, cardiovascular disease (CVD), diabetes and sarcopenia (a muscle wasting disease), thus highlighting the intricate role that this form of senescence plays in the ageing process and age-related diseases [5, 95-98].

1.2.3 Oncogene induced senescence

One form of senescence clearly linked to the impediment of tumorigenic development is the cellular programme known as oncogene induced senescence (OIS). This form of premature senescence plays a major role in transforming a developing tumor into a benign state by responding to distinct DNA damage and oncogenic stimuli that the cells produce, to remove the early stage tumorigenic cells from the proliferative pool [99, 100]. This potentially lowers the number of pre-neoplastic cells that can actively contribute towards the growing tumor, thus tumorigenic progression is halted, leaving behind a benign growth with no mitotic potential. Usually this process is brought about by genomic mutations that affect either PTEN, RAS, RAF or BRAF, which induces an explosive elevation in oncogenic factors and hyper replication of the cell's DNA allowing for the accumulation of

heterochromatic foci [100-104]. Eventually a persistent DDR (independent of telomere shortening) is elicited by the accumulation of p16INK4A, p53 and ARF in response to the accumulating cellular dysfunction [99, 100, 103]. Interestingly, this type of senescence also incorporates aspects from other types of senescence to further aid in limiting tumor growth, where cells undergoing OIS have been confirmed to accumulate dysfunctional mitochondria [75, 105]. Moreover, OIS like inflamm-ageing utilises distinct cytokines like IL6 and IL8 to activate inflammatory pathways to provide a means to spread the OIS phenotype to the surrounding premalignant cells [34, 106, 107]. Therefore, the dynamic interplay of other senescent processes involved in inducing OIS highlights its importance as acting as a barrier for tumorigenic development both *in vitro* and *in vivo*.

1.3 Telomere dependent senescence

The second major form of senescence which is regulated by telomeric erosion is intricately linked to normal ageing in humans [19-22, 108]. The process is governed by the gradual loss in mean telomere length during subsequent rounds of cell replication [108-110]. This said, the formation of dysfunctional telomeres can in part be attributed to the imperfect synthesising action of DNA polymerase, otherwise known as the "end replication problem" [111]. This is due to the semi-conservative mechanism of the enzyme emplaced by lagging strand synthesis, where around 50 to 200bp of DNA is lost from the 5' end of the lagging strand during each mitotic event [108, 111, 112]. In this way the telomeres serve a vital protective function by preventing degradation of coding genomic DNA (gDNA), as the telomeric ends are shortened instead [108, 110]. This erosion continues to occur throughout the tissues/organism's lifespan until the "Haylick limit" is reached; a pre-determined critical length of the telomeres that signals for the induction of senescence [(Figure 1.3) [15, 17, 108, 113]]. Aside from telomere attrition, senescence can also arise from the perturbation of the telomere related shelterin complex, a protein complex that binds to the telomeres and prevents exposure of the guanine (G) rich overhang, as well as prevents a loss in overall structural integrity [114, 115]. Therefore, the loss of telomere length, or structural stability acts as an efficient means to track cellular ageing by giving a theoretical indication on the number of times a cell can actively divide [108-110, 112].

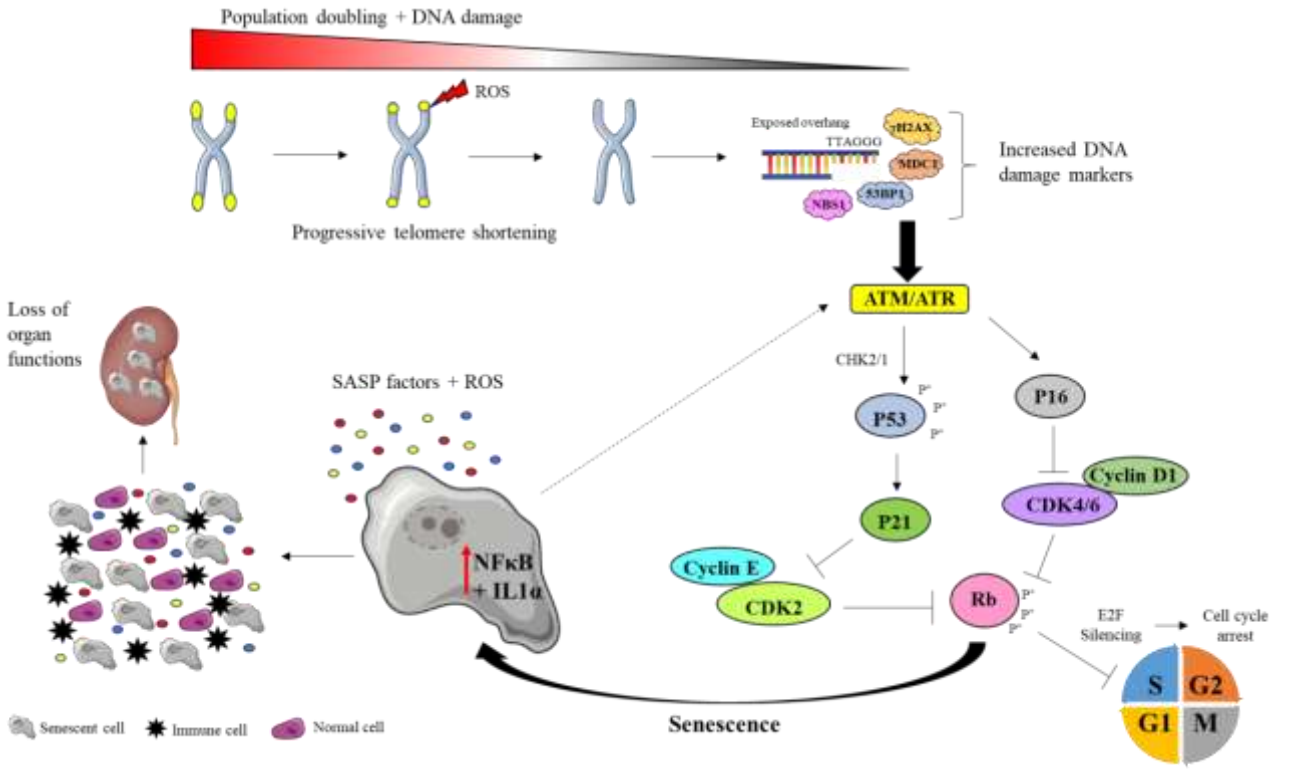


Figure 1.3: The mechanism behind telomere-dependent senescence, and how telomerase reactivation induces replicative immortality by replenishment of the telomeres.
Telomeres continually erode due to replicative stress and ROS related damage until a critical length is reached, causing exposure of the telomeric overhang. Thereafter, DNA damage markers accumulate at the exposed overhangs to eventually elicit a DNA damage response (DDR) that is mediated by p53 or p16 to ensure cell cycle arrest. In this state the cells produce elevated inflammatory markers to ensure the persistence of the DDR, thus ensuring the senescent state is maintained. In addition, these inflammatory markers, also known as senescent associated secretory phenotype (SASP) factors, aid in propagating the senescent state to the surrounding cells and tissue to eventually cause organ failure. Image constructed using: SmartServier.

1.3.1 Telomere-dependent senescence and Reactive Oxygen Species

According to the above mentioned, an additional imperative contributor to telomere dysfunction is the DNA damage caused by ROS. This is due to the rich content of guanine present within the telomeres, which ROS molecules preferentially target, thus illustrating a vital secondary protective function that the telomeres serve [116-118]. This secondary protective function is imperative in post mitotic cells, like neurons, where the major form of DNA damage is derived from sources of oxidative stress like amyloid beta (Aβ) accumulation. This observation was made in several studies, where induced oxidative stress was found to preferentially cause DNA damage at the telomeric regions with higher frequency than within gDNA [117-120]. In conjunction, the oxidative lesions generated at the ends of telomeres are repaired less efficiently than anywhere else in the genome, further contributing to the accumulation of ROS-related DNA damage [121, 122]. This inefficient

repair is a direct consequence of telomere-related binding proteins like, TRF2, that can bind and mask areas of damaged telomeric DNA preventing the recruitment of DNA damage repair proteins [122-124]. In this manner, the telomeres are exceptionally sensitive to this form of damage induced by oxidative stress, where ROS molecules bind to the guanine residues and convert them to 8-oxo-guanine, thereby disrupting the G-quadruplex, a key telomeric structure needed to ensure telomere homeostasis [118, 120, 125, 126]. These 8-oxo-guanines also induce the formation of breaks within the telomeric DNA that expose the overhangs allowing them to be read as a DNA double stranded breaks (DSBs), ultimately signalling for the induction of senescence. [(Figure 1.3) [19, 112, 127]].

1.3.2 Signalling cascades involved in telomere-dependent senescence

This form of senescence occurs as a result of the critically dysfunctional telomeres behaving in a similar manner to DSBs, where it induces a potent DDR effectively halting further cell cycling (Figure 1.3). In turn, a number of DNA damage markers like: γH2A histone family member X (γH2AX), p53 binding protein 1(53BP1), mediator of DNA damage checkpoint (MDC1) and Nibrin (NBS1) localise directly to the exposed ends of dysfunctional telomeres resulting in the formation of telomere- induced foci (TIFs) [26, 128]. It is these TIFs that are recognised as DSBs and elicit the activation of checkpoint PI3 kinases such as ATM (ataxia-telangiectasia mutated) or ATR (ataxia-telangiectasia and Rad3 related) [26, 128, 129]. These kinases go on to phosphorylate a range of downstream factors, leading to the eventual phosphorylation, activation and stabilisation of the tumor suppressor protein, p53 (Figure 1.3). In conjunction, to ensure the continued activity of p53 there is also a corresponding inactivation and degradation of the Mouse double minute 2 (MDM2) protein. Thereafter, p53 stimulates the expression of p21, a cyclin dependent kinase inhibitor, for the inhibition of further cell cycling by activating retinoblastoma protein (Rb) which blocks entry into the S phase of the cell cycle [(Figure 1.3) [129-131]]. Alongside the elevated p21, there is a subsequent activation of the senescent related protein p16, which also induces senescence, albeit at a much lower rate than p53 [(Figure 1.3) [130, 131]]. This takes place by p16 feeding into the process of Rb hyperphosphorylation, thereby causing an inactivation of CDK4 and CDK6 for cell cycle arrest [131, 132]. This said, p16 has been found to be less important than p53 in eliciting a telomere dependent DDR for senescence, but may play an important role in maintaining the senescent state after its establishment [130, 133]. Thereafter, these signalling pathways are persistently activated in order to ensure that a constant DDR is elicited. Alongside a persistent DDR it has been found that the extensive shortening of the telomeres may further contribute to altered epigenetic patterns as well as the development of the SASP through its role in ROS production [(Figure 1.3) [134, 135]]. In turn,

this would allow the telomeric dysfunction as well as the senescent phenotype to spread to the surrounding tissues in order to advance the ageing process.

1.3.3 Impediment of telomere-dependent senescence

This form of senescence can however be prevented or at least obstructed in a controlled manner through the telomere replenishment actions of the enzyme, telomerase. In fact, the maintenance that telomerase affords has essentially been shown to inhibit the activation of a persistent telomere-dependent DDR [110, 136, 137]. Subsequently, this leads to an impediment of cellular ageing as well as an increased proliferative capacity [(Figure 1.1)[136, 138-142]]. This anti-senescence effect has been shown in several studies where, the reactivation of telomerase is an essential requirement for cell immortalization and escape from cell senescence for both normal as well as tumorigenic cells [136, 139-141, 143]. This said, the preservation of the telomeres has been found to aid in conserving normal cell function and also to maintain genomic integrity [136, 143]. In accordance, this telomeric replenishment in a controlled setting does not behave in an oncogenic fashion to stimulate the induction of carcinogenesis [140, 143, 144]. Instead, by maintaining the telomeres it was found to reduce both telomeric and DNA damage, as well as to inhibit the formation of DNA fusion events, which are common phenomena during cancer progression [145-147]. Consequently, this telomeric replenishment further induces a reduction in senescent signalling pathways, with a corresponding elevation in survival/ proliferative pathways, increased expression of anti-ageing proteins like klotho and SIRT1 as well as a marked reduction in the expression of senescent markers like γH2AX and β-galactosidase [136, 140, 143, 144]. Holistically these factors further result in an impediment or reversal of the ageing process on both a tissue and organism level. In relation, cells suffering from certain age-related pathologies like CVD and diabetes, as well as premature ageing syndromes (Werner syndrome), have been found to be positively influenced by telomeric replenishment for an improvement of the disease states [148-150]. Ultimately, this exemplifies the vital role that telomerase plays in impeding ageing and in conserving cell viability.

1.4 Telomere biology

1.4.1 Structure and function of the telomeres

In accordance with the aforementioned, the telomeres which are maintained by telomerase play a vital role in senescence as well as maintaining a juvenile cell state. These tandem genetic elements composed of TTAGGG repeats that end in a vital 3′ single stranded G-rich overhang are located at the termini of eukaryotic chromosomes [(Figure 1.4 A) [151-153]]. This unique composition of the

telomeres in comparison to other genomic DNA has remained evolutionarily conserved, possibly due to a number of factors. A few of which include: constraints imposed by telomerase (specifically the composition of the TERC template), its ability to form a G quartet (four guanines that interact via hydrogen bonding), its unique composition might be imperative for specific association of several telomere-related proteins, which further boost the protective function of telomeres and lastly, its ability to code telomeric RNA known as TERRA [154-158]. These G quartets that the telomeres form have been implicated in telomere protection from damaging agents, suppression of recombination and the inhibition of telomerase activity as they act as poor sites for telomeric extension [154, 159]. Together, the telomeres with its telomere-associated proteins operate synergistically to prevent damage and degradation of coding gDNA [114, 160, 161].

1.4.2 Telomeres and the shelterin complex

The most important of these telomere-related proteins are comprised of a six-protein complex, otherwise known as the shelterin complex that shares a high affinity towards telomeric DNA (Figure 1.4 B). These six proteins namely: POT1, Rap1, TPP1, TIN2 and most importantly TRF1 as well as TRF2, are found with exceedingly high abundance at the telomeric ends during any phase of the cell cycle [(Figure 1.4 B) [115, 161-163]]. In addition, the proteins making up this complex do not accumulate elsewhere, thereby accentuating their telomere-dependent function of "capping" the termini of chromosomes [160]. This exceptional specificity towards the telomeres is owed to the multiple TTAGGG recognition folds that these protein subunits house, specifically within TRF1, TRF2 and POT1, which are all connected through their protein-protein interactions [160, 164, 165]. In this manner, when TRF1 and TRF2 bind to the telomeres, they behave as docking sites and allow the recruitment of POT1, RAP1, TIN2 and TPP1; where TIN2 operates as the linchpin of the complex [160, 162, 163]. This ensures that TPP1 as well as POT1 remain tethered to TRF1/ 2, enabling the stabilisation of TRF2 and in turn, the complex to the telomeres [162, 163]. In this manner, the unique setup of the shelterin complex affords it the ability to perform a number of vital telomere-associated functions.

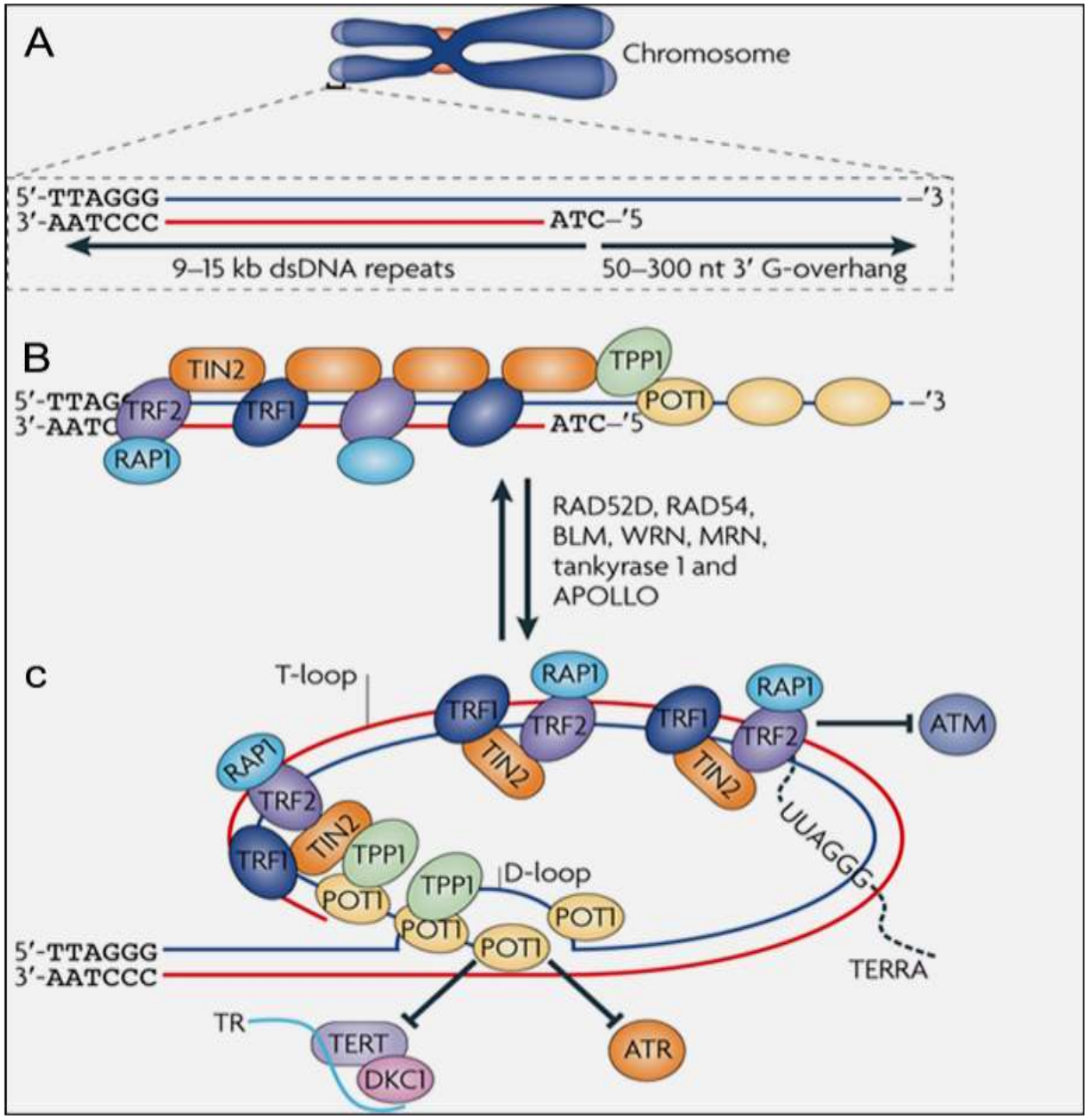


Figure 1.4: Schematic diagram featuring the structure and function of the telomeres together with the shelterin complex and TERRA to form the T and D-loop for enhanced genomic protection.

(A) The figure demonstrates the genetic and structural conformation of the telomeres, where it is made up of tandemly repeated genetic elements of TTAGGG in mammals, that further end in a vital 3′ guanine (G) rich overhang. (B) As these sequences have a highly unique composition, it allows for the recruitment of highly specialised telomere-related proteins, which includes: POT1, RAP1, TIN2, TPP1, TRF1, and TRF2, that bind and interact with each other and the telomeres, to form the shelterin complex, which essentially provides an additional protective function. This said, the binding of the shelterin complex onto the telomeres stimulates the telomeric 3′ G rich overhang to fold over and invade the double stranded telomeric strand and interact with the 5′ cysteine (C) rich strand to form the T-loop. The displaced strand then goes on to form a secondary loop known as the D-loop. The formation of these loop-like structures provides additional protection; especially to the 3′ G rich overhang, as it masks the strand from being read as a double stranded break. Furthermore, the shelterin complex and the T-loop effectively prevent the binding of telomerase to the telomeric ends, thus acting as a negative regulator of telomerase activity. Adopted from O' Sullivan and Karlseder, 2013 [166].

1.4.3 Shelterin, telomeres and generation of the telomere loop

One of the most vital functions pertaining to the shelterin complex, is its ability to aid in the formation and stabilisation of the telomere loop [(T- loop) (Figure 1.4 C)]. The process involves the overhang invading the duplex telomeric repeats and forming bonds with the C- rich strand, inducing the displacement of the G- rich strand, which forms the displacement loop (D- loop) [160, 167]. During the formation of the T- loop both TRF1 and TRF 2 exhibit DNA remodelling capabilities, where TRF2 has specifically been shown to produce the loop-like structures [167]. These structures are essentially formed to cover or shelter the 3′ single stranded overhang from being read as a DSB by DDR-related proteins and also makes the telomeric ends inaccessible to DNA damaging agents [(Figure 1.4 C) [114, 168, 169]]. In fact, in the event that TRF2 is eliminated or inhibited, the chromosomal ends are immediately altered, which causes functional telomeres to behave as though they are dysfunctional eliciting the activation of the ATM/ p53 pathway for senescence or apoptotic induction [114, 169]. Moreover, the abrogation of POT1 can also elicit a persistent DDR albeit in a different mechanism to TRF 2, where the ATR pathway is activated instead [170, 171]. Therefore, this illustrates the vital protective function that both the T- loop and shelterin complex carry out in waylaying DNA damage to the telomeres, as well as preventing the induction of premature senescence.

1.4.4 Shelterin and its role in telomere maintenance

Finally, shelterin carries out a major function in telomere length maintenance. In mammalian organisms, this maintenance has been illustrated to be governed by a negative feedback loop, which inhibits the actions of telomerase, to ensure that the telomeres remain within a set size range [115, 172]. How shelterin governs this process, is by acting as an inhibitor to telomerase (Figure 1.4 C). In this regard, the actions of telomerase are mediated by the number of shelterin present on a given telomere. As the number of these complexes present is more or less proportional to a telomere's length; the enzyme telomerase actively seeks out the telomeres with the fewest number of shelterin present and in this way extends only the shortest telomeres [115, 173]. The inhibitory actions displayed by shelterin is governed by its TRF1, TRF2 and POT1 subunits, where POT1 inhibits telomerase through its ssDNA- binding ability [115, 174, 175]. This is accomplished by POT1 masking the single stranded 3′ terminus, effectively blocking telomerase from gaining access [174, 175]. In contrast, if POT1 acts in partnership with TPP1, it promotes the recruitment of telomerase and allows telomeric extension [176, 177]. This conflicting function occurs as a result of POT1 and TPP1 behaving as a "sliding clamp" where it can slide along the telomeres inducing a constant

folding and unfolding of the telomeres [176]. Thus, when POT1-TPP1 unfolds the telomere ends, it allows for a more relaxed telomeric structure to promote telomerase activity [176]. Therefore, illustrating how POT1 can act as both a positive and negative regulator of telomerase activity.

Alongside shelterin there is an additional structural aspect that aids in telomere maintenance and telomerase activity, namely telomeric repeat containing RNA (TERRA). These long non-coding RNAs are transcribed directly from the telomeres, which is believed to be mediated by TRF1, with its subsequent interaction with Pol II [158]. TERRA has been found to bind telomeres, the shelterin complex, methyl transferases and chromatin remodelling proteins for heterochromatization of the telomeres, as well as regulating telomeric shape, thereby adding a further layer of protection [(Figure 1.4 C) [172, 178, 179]]. Additionally, TERRA can also operate to limit telomerase by either binding the Telomerase RNA component (TERC) subunit directly or by interacting with the catalytic TERT subunit to regulate telomere maintenance [172, 178, 179]. Therefore, the telomeres, in conjunction with the shelterin complex and TERRA provide an effective means to regulate telomerase activity and to shield gDNA from sequence damage or degradation, to conserve cellular and genomic function.

1.5 Telomerase and TERT

1.5.1 Structure and function of the telomerase complex

Telomerase is one of the core regulators involved in the prevention or impediment of telomere-dependent senescence. It is a ribonucleoprotein that operates as an enzyme with a primary function of telomere synthesis for telomere maintenance and elongation [110, 180-182]. This function essentially conserves telomeric structural integrity, which efficiently increases a cell's proliferative capacity; permitting additional cell divisions that exceeds the cell's predetermined limit [136, 142, 180, 183, 184]. Specifically, in humans, the active isoform of this protein is commonly located within immortalised, germline, embryonic, self-renewing stem cell populations and tumorigenic cells [185, 186]. In fact, the presence of telomerase in these cells aids in circumventing senescence, by constantly replenishing the shortest telomeres and in turn, allowing for near limitless DNA replication [136, 142, 185]. The active enzyme is composed of two core sub-units, among others, to form a multi-protein complex which enables telomere replication. These two sub-units are namely: TERC which is read by the catalytic reverse transcriptase component (TERT) for the generation of new TTAGGG repeats [(Figure 1.5) [187, 188]]. Telomerase carries out telomeric extension by recognising the 3′ guanine rich overhang of a telomeric strand where it then introduces the newly

synthesised telomeric repeats in a 3′-5′ direction during the synthesis (S) phase of the cell cycle. The other sub-units (NOP10, GAR, Dyskerin NHP2) that make up the telomerase complex mainly assist in the stabilisation of the complex, and further facilitate the binding of telomerase onto the 3′ G rich overhang of the telomeres [(Figure 1.5) [189-191]]. Once telomerase is attached to the 3′ G rich overhang of the shortest telomere, it carries out telomeric synthesis in a controlled fashion by adding one TTAGGG repeat at a time.

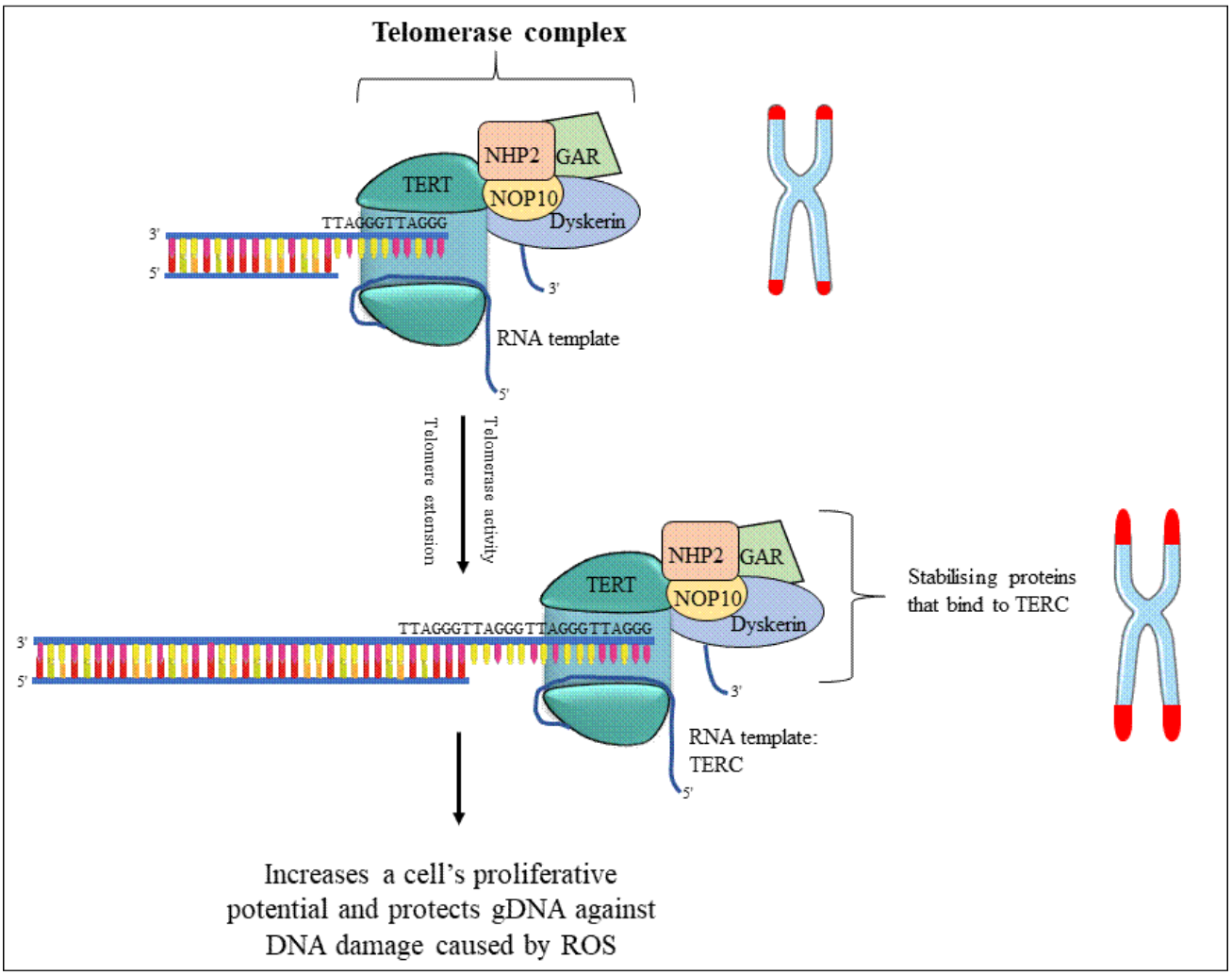


Figure 1.5: The ribonucleo reverse transcriptase telomerase performing its primary function of telomeric extension.
The telomerase complex is composed of two core sub-units among others, namely TERT and TERC that are responsible for performing the catalytic function of telomere synthesis. This function is accomplished by the catalytic component, TERT, reading the RNA template, TERC, to produce the telomeric repeats. The other proteins comprising the complex mainly aid in stabilising the enzyme. These stabilising proteins include: Dyskerin, GAR, NHP2, and NOP10. Together, the subunits of this complex operate to extend the shortest telomeres in a 3′ → 5′ direction [192]. Figure constructed using SmartServier.

1.5.2 Regulation of TERT and telomerase

In humans, telomerase activity is a tightly regulated process where it passes through various phases before telomeric extension can occur. These processes include: regulation of TERT transcription and translation, accumulation of the TERC transcript, the export of the telomerase complex to the nucleus, the activation of telomerase (through phosphorylation) and finally the recruitment of the enzyme to the telomeric ends [(Figure 1.6) [186, 193]]. Although these processes can regulate the extent of telomerase activity that occurs, the greatest limiting factor is the catalytic subunit TERT, where its levels have been confirmed to directly influence the amount of activity that occurs [139, 185, 194]. In fact, it has been proven that TERC expression occurs in most mammalian cells, whereas the expression of the enzymatic isoform of TERT was found to be localised only to cancerous, embryonic and epithelial cells [136, 138, 139]. More surprisingly, it has been shown that the 2 subunits have vastly different half-lives, where TERT remains in the cells for more or less 24 hours [186, 195, 196]. Meanwhile, the TERC transcript can remain for an extraordinary period of five days [186, 195, 196]. Therefore, further emphasising the fact that TERT acts as the limiting factor for regulation of telomerase activity.

Intrinsically, this was found to be a consequence of the strict transcriptional and translational regulation imposed on the human telomerase reverse transcriptase (hTERT) within human somatic cells, therefore causing its low or undetectable levels, as well as the corresponding absence of telomerase activity [136, 138, 139, 186]. On a transcriptional level, there are a multitude of factors that operate to limit expression of the hTERT gene. First and foremost is the unique location that the hTERT gene resides within (chromosome 5p15.33), where its promoter region lies within a highly condensed chromatin domain [197]. This allows for transcriptional repression to be mediated through hypo-acetylation of the core histones, effectively preventing gene activation due to the condensed chromatin [(Figure 1.6 A) [186, 198, 199]]. In conjunction, both histone and CpG methylation, which are responsible for a stable long term repression of particular genes, have been found to influence hTERT regulation [(Figure 1.6 A) [200, 201]]. In turn, this prevents transcription factors (TF) from binding to the TERT promoter region, and further illustrates the tight gene repression regulations imposed on TERT at an epigenetic level.

1.5.3 Transcriptional and post-translational regulation of TERT

Aside from epigenetics, there is also an array of transcriptional silencers that can bind to hTERT or its promoter, to prevent gene expression (Figure 1.6 A). A few such suppressors include: Mad1 (an antagonist to c-Myc), WT1, MZF-2 (a zinc finger transcription factor and a member of the E2F family), E2F1 (believed to counteract c-Myc and TGFβ transcriptional activation of TERT) and p53, among others which is believed to be involved in the negative regulation of TERT (reviewed in: [193]). Aside from direct binding for transcriptional repression other lucrative targets for TERT gene silencing comprise the inactivation or degradation of factors that promote gene expression which include: β-catenin , c-Myc , NFκB, STAT3, STAT5, PAX5 and TGFβ [(Figure 1.6 A) (reviewed in: [193])]. These silencing factors act as efficient insulators and, together with the dramatic alterations to the chromatin environment surrounding TERT, ensure the constant abrogation of its production.

Aside from transcriptional regulation, should the hTERT gene be transcribed, there is a plethora of post-translational regulatory elements that can further limit the enzymes activity. This said, it has been observed that TERT mRNA levels do not correlate with the activity of the enzyme, thereby further supporting the theory of post-translational regulation [202, 203]. It has further been shown that phosphorylation is vital for the formation of the active telomerase enzyme [(Figure 1.6 B) [186, 204-206]]. In fact, hTERT contains a number of putative phosphorylation sites that are exploited by two kinases to regulate the subunit. The two identified kinases responsible for regulating telomerase activity are the proliferative related protein Akt and c-Ab1 [204, 207]. With regards to Akt phosphorylation, it is believed to aid in translocating the hTERT subunit from the cytoplasm to the nucleus for enhanced telomerase activity [(Figure 1.6 B) [204, 205]]. In contrast, the kinase c-Ab1 serves as a negative regulator for telomerase activity in the presence of DNA damage, where c-Ab1 phosphorylates hTERT to induce a decrease in activity [(Figure 1.6) [207]].

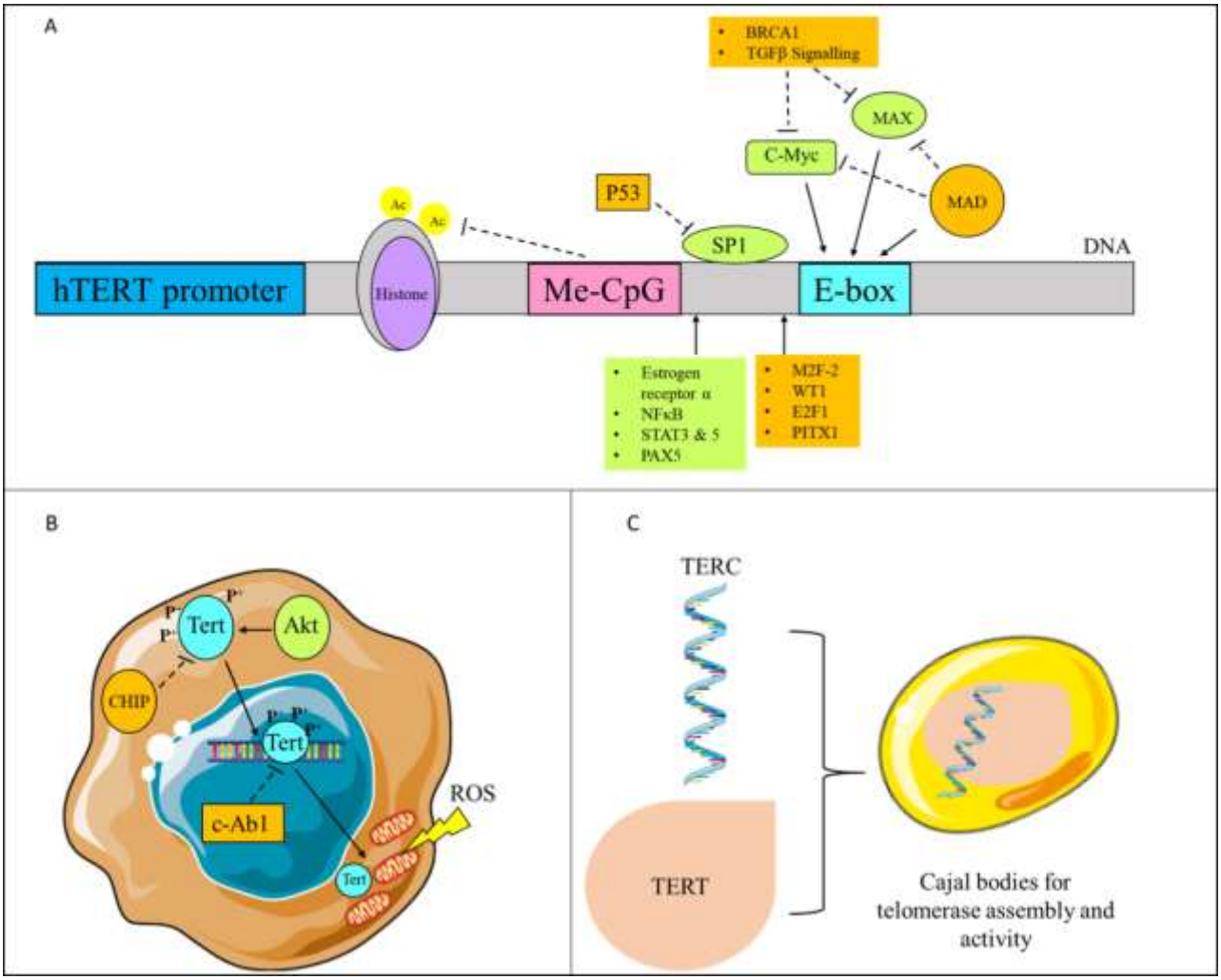


Figure 1.6: The multitude of regulatory elements dictating TERT expression and telomerase activity.
A) Transcription of the hTERT gene is controlled by a host of regulatory elements, including methylated CpG islands and histones for chromatin repression. Other negative regulatory elements include transcriptional repressors like BRCA1, p53, MAD and E2F1 among others (All TF repressors are shown in orange). However, there are a number of transcriptional activators (shown in green) that positively influence TERT, with the most important including: β-catenin, c-Myc NFκB and SP1 [208]. B) On a post-translational level, the hTERT protein requires phosphorylation by Akt for nuclear translocation, however, this can be impeded by CHIP. Moreover, once in the nucleus c-Ab1 can directly inhibit TERT to prevent telomerase activity, especially while under cellular stress. Alternatively, TERT can be signalled to be exported from the nucleus when the mitochondria are exposed to a significant degree of oxidative stress. C) An additional aspect to regulating TERT/ telomerase is the requirement of the TERC component to be processed by Cajal bodies, to allow the assembly of the telomerase complex, as well as to activate the complex in order to carry out telomere synthesis. Figure constructed using SmartServier.

Other factors that can negatively regulate hTERT/ telomerase include polyubiquitination of hTERT by CHIP (C terminus Hsp70 interacting protein) to block entry to the nucleus and for proteolytic degradation [(Figure 1.6 B) [209]]. An additional factor, is the export of the enzyme from the nucleoplasm to the nucleolus following DNA damage [210]. In addition, the TERC subunit needs to

be processed by Cajal bodies before the enzyme can become active [(Figure 1.6 C) [211]] and the protein PinX1 can bind to both the TERT and TERC subunits for inhibition of telomerase activity [186, 212, 213]. Moreover, TERT's presence within the nucleus is limited when cells are exposed to hypoxic or oxidative conditions, as it induces the translocation of TERT to the mitochondria to protect mtDNA, thus preventing telomeric extension [214, 215]. Collectively, these regulatory elements provide strong evidence that TERT behaves as the primary limiting factor for functional telomerase activity.

1.5.4 TERT and telomerase activity in humans and mice

In agreement, it has also been shown that when human or murine cells are exposed to exogenous TERT, it acted as an adequate stimulus for the reactivation of telomerase activity for telomere replenishment, which effectively impeded senescence and ageing [136, 138-140]. Interestingly, TERT expression and telomerase activity in murine species appears to be present throughout most somatic cell types [216]. This in part, explains the large difference in telomere length between mice and humans, where laboratory mice have telomeres ranging from 20-50 kilobases (kb) in length, whereas humans have telomere lengths from 10-15 kb [115, 217, 218]. In fact, it has been theorised that the ageing process of mice is governed by stress induced senescence rather than by telomere shortening [219, 220]. This is due to the fact that even aged mice exhibit longer telomeres than humans, with no critically short telomeres evident, in actively dividing cells as well as post-mitotic cells like neurons [219, 221]. Thus, mice do not age through a telomere-dependent mechanism, but rather accumulate senescent cells through alternative ageing paradigms like Inflamm-ageing or mitochondrial induced senescence. However, it appears that TERT or telomerase based therapies can still exert beneficial effects on aged mice. Studies have confirmed that an overexpression of TERT promotes healthier ageing and longevity, where mice that contain hyper long telomeres from elevated telomerase activity, actually exhibit longer and/ or healthier lifespans without an increased risk of cancer [140, 141, 143, 222-224]. Therefore, although telomere dynamics operate differently between humans and mice, treatments aimed at TERT and telomerase activity upregulation can still provide anti-ageing effects. All together, these findings highlight TERT as the major regulator of telomerase mediated telomere maintenance in both humans and mice, which in turn leads to an influential role in regulating proliferative capacity. In this manner, the maintenance function that telomerase is responsible for allows the continuation of pre-senescent functioning under non-stressed conditions, while also conserving cell viability.

1.6 Extra-telomeric functions of TERT and telomerase

Recently, there has been a growing body of research that strongly indicates that TERT appears to carry out vital functions, independent of its ability to maintain or elongate the telomeric ends. These alternative or extra-telomeric functions all operate to conserve cell viability and improve proliferative capacity. This said, it is often difficult to distinguish between the benefits afforded from telomeric extension and extra-telomeric functions as they generally overlap [(Figure 1.7) [215, 225, 226]]. These extra-telomeric functions are generally centred around the mitochondria, DNA-repair, as well as apoptosis and most importantly the regulation of gene expression. In addition, other non-canonical roles have been attributed to TERT include roles in: cell differentiation and brain development that in turn can regulate the formation of spatial memory. Both these functions are strongly tied to TERT expression rather than TERTs active functional participation [227, 228]. These extra-telomeric functions are especially vital for post-mitotic cells like neurons, where telomere extension plays a negligible role in these cell types.

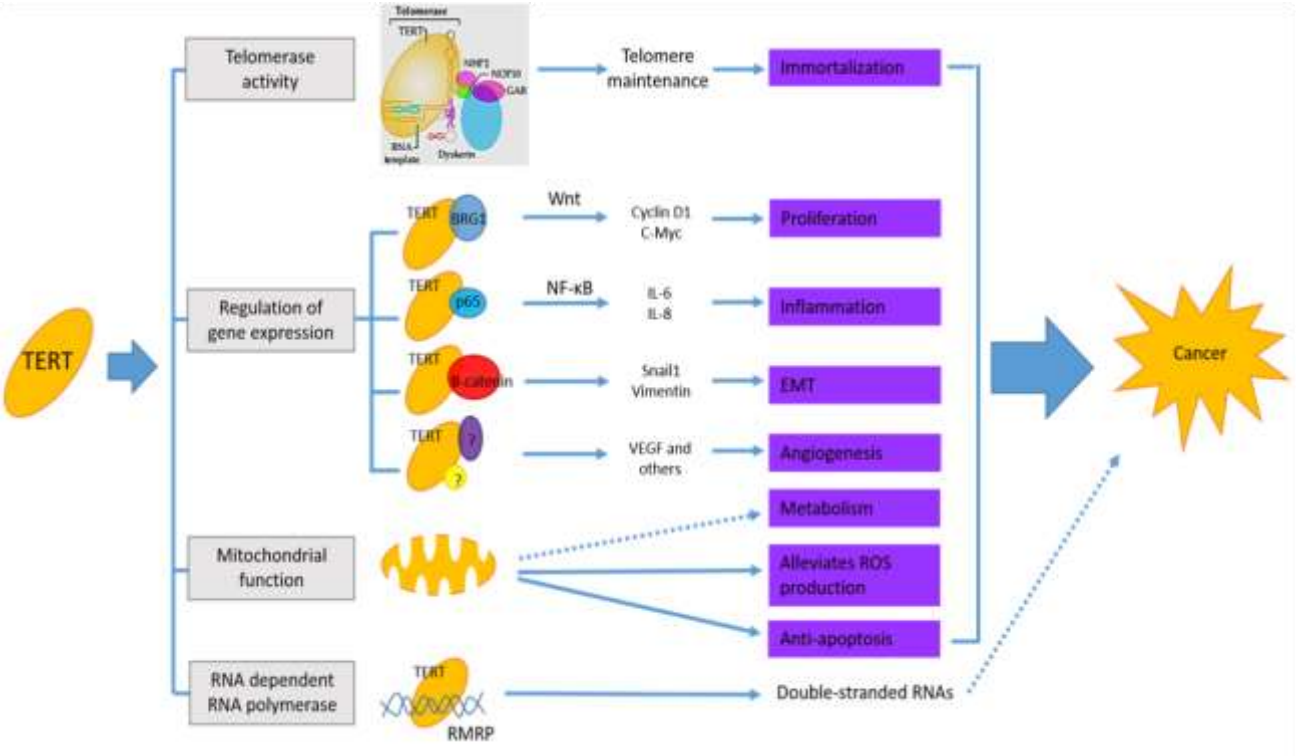


Figure 1.7: TERT and telomerase and its extra-telomeric functions aside from telomere maintenance.
The figure illustrates the numerous extra-telomeric roles that TERT or telomerase have namely, gene expression and pathway regulation, mitochondrial function, as well as its ability to act as an RNA dependent RNA polymerase. TERT's ability to affect gene expression and pathway regulation seems to be focused on the promotion of cell viability, proliferation and survival via the Wnt and Akt pathway. Furthermore, TERT aids in promoting the Epithelial to Mesenchymal transition process (EMT), angiogenesis and inflammatory processes by affecting major pathways, including NFκB and Wnt. In addition, TERT's unique ability to translocate to the mitochondria aids in preventing mitochondrial dysfunction, by affecting mitochondrial metabolism, respiration and the production of ROS . TERT conveys this protective function to ameliorate ROS-related damage done to the mitochondria. However, in the event these aforementioned functions of TERT become dysregulated, it can aid in the stimulation of carcinogenesis. Together, these various functions substantiate TERT's vital presence within both normal and cancerous cells for the promotion of cell viability and survival. Adapted from Ding et al., 2013 [229].

1.6.1 The mitochondrial functions of TERT

These non-canonical functions of TERT at the mitochondria are mainly focused on supporting mitochondrial function, as well as protecting the mitochondria, especially from oxidative stress. In this regard, TERT has been found to readily translocate to the mitochondria, especially when exposed to hypoxic conditions [56, 214, 226, 230]. Intriguingly, it appears that TERT's mitochondrial and telomeric functions co-exist, where around 20- 30 % of total telomerase has been confirmed to be present within the mitochondria under non-hypoxic conditions, in multiple cell types including both mitotic and post mitotic cells [56, 214, 230, 231]. Once TERT gains access to the mitochondria it conveys protection to the mtDNA to prevent further oxidative damage (Figure 1.7). This is especially important in neuronal cells, where brain ageing and age-related neurodenerative

disorders like AD have been closely linked to the inhibition of TERT as well as the accumulation of dysfunctional miochondria. Likewise, telomere-dependent senescent cells have also been confirmed to exhibit increased ROS production, mtDNA damage and mitochondrial mass [56]. How this phenomenon occurs is not exclusively known, however, a few potential mechanisms have been theorised. Most significantly, it has been shown that cells induced to overexpress TERT under stressed conditions resulted in not only a reduction in ROS, but also improved mitochondrial function and decreased the amount of mtDNA damage [(Figure 1.8) [214, 232, 233]]. This might be a consequence of TERT interacting with RNAs implicated in mediating the repair and replication of mtDNA [215, 234]. Conflictingly, it appears that TERT may promote mtDNA damage and apoptosis, however it may act as a selective mechanism to ensure that cells which house mitochondria with extensive damage are removed from the replication pool [215, 235, 236]. Alternatively, TERTs protective function in the mitochondria could be dependent on the type of oxidative stress that the cells are exposed to. These mitochondrial-related functions of TERT clearly demonstrate the importance of this protein in mitochondrial functioning. Furthermore, since both mitochondrial dysfunction and oxidative stress are large culprits, in the ageing process these specific extra-telomeric functions further highlights TERT's importance in telomere independent-senescence.

1.6.2 TERT in DNA repair and apoptosis

Two other noteworthy events that TERT appears to influence in both activley dividing cells and post mitotic cells like neurons are DNA repair and apoptosis. The latter function was known to be influenced through telomerase's ability of telomere maintenance, thereby preventing the accumulation of TIFs and subsequent induction of p53-dependent apoptosis. However, it appears TERTs ability to influence apoptosis extends beyond the telomeres, where it has been noted to associate with the anti-apoptotic protein Bcl-2 [237]. In fact, overexpression of Bcl-2 was found to cause a corresponding elevation in TERT and telomerase activity, with a corresponding decrease in apoptosis [237-239]. Furthermore, TERT has also been observed to act as a repressor for mitochondrial pathway apoptosis in multiple studies. One such study illustrated that when cells were treated with (N-methyl-D-aspartic acid (NMDA) and Staurosporine (STS)), which that induced the translocation of BAX into the mitochondria, for apoptotic activation was impeded by TERT [226, 240]. This may occur either by preventing the accumulation Ca+ ions within the mitochondria, TERT preventing the translocation of BAX or at another pre-mitochondrial step [226, 240]. Conflictingly, TERT may also influence apoptotic induction through its ability to alter mitochondrial

membrane potential and/ or metal homeostasis within the mitochondria, for activation of apoptosis [226, 235]. Nevertheless, this illustrates that TERT carries out an important role in the regulation of apoptosis.

In addition, TERT has also been shown to affect apoptosis within the nucleus, however this is mainly through its ability to affect DNA repair [232, 241]. The telomere replenishment that telomerase carries out at telomeric ends can be considered a form of DNA repair, although it seems this repair is not just limited to the telomeres. Recent evidence suggests that telomerase itself may play a role in the repair of non-telomeric DNA, where intrachromosomal breaks have been infrequently repaired by the insertion of telomeric repeats [226, 242]. Adding further weight behind this possible function, is that TERT has been confirmed to associate with primase, a DNA replication protein known to carry out DNA repair [226, 241]. This interaction coupled with TERT's ability to induce an upregulation in various DNA repair proteins, reaffirms the important role it plays in DNA repair [226, 241, 243].

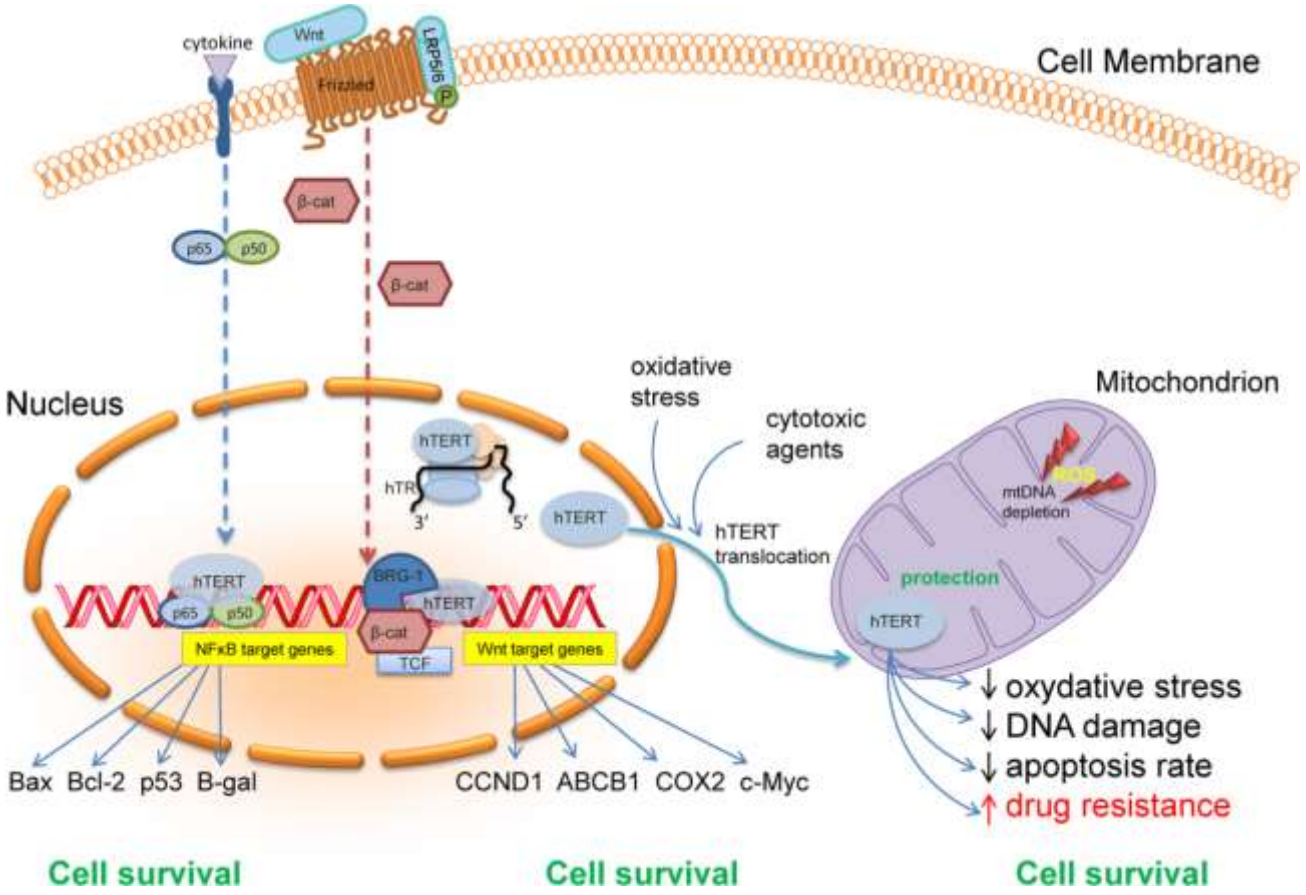


Figure 1.8: The extra telomeric functions of TERT in promoting cell proliferation and survival. The non-canonical roles that TERT is involved in are highlighted in the above figure, which is all centred on promoting cell survival. Importantly, within the nucleus, TERT has been implicated in various signalling cascades to promote gene expression. Specifically, TERT has been found to interact with the p50 and p65 subunits of NFκB, where it binds to target genes (Bax, Bcl-2, p53 and B-gal) that the NFκB pathway transcriptionally activates. Moreover, TERT has also been shown to interact with BRG-1 and β-catenin to induce the transcriptional activation of genes (c-Myc, COX2, ABCB1 and CCND1) targeted by Wnt the pathway. This clearly establishes a role that TERT carries out by promoting inflammatory (NFκB) and proliferative (Wnt) pathways. Aside from pathway regulation, TERT has also been shown to carry out a variety of functions to prevent mitochondrial dysfunction, thereby promoting cell survival. This occurs under hypoxic conditions, whereby TERT readily translocates from the nucleus to the mitochondria, where it provides a protective function to the mitochondria. This effectively reduces mitochondrial related damage to the mtDNA and reduces ROS production to lower oxidative stress. Adopted from: Romaniuk et al.,2019 [244].

1.6.3 TERT in the regulation of gene expression and signalling cascades

One of the major extra-telomeric roles that TERT carries out, is the ability to alter gene expression profiles and subsequently influence various signalling cascades [(Figure 1.7); (Figure 1.8) [245-247]]. This ability of TERT has been confirmed through multiple microarray analyses, where TERT was found to influence proteins that play a role in apoptosis, cell cycle regulation, cell signalling, differentiation, and metabolism. In fact, TERT has been directly implicated in the Wnt pathway, which is commonly known to mediate stem cell maintenance and proliferation as well as aid in

cellular transformation. In this pathway, TERT acts as a transcription factor with β-catenin complexes to promote the expression of several β-catenin target genes such as cyclin D1 and c-Myc, where it is involved in a positive feedback loop with c-Myc to promote its expression [(Figure 1.8) [225, 245, 246]]. In essence, this relationship illustrates that TERT acts as a driving force for the regulation of cell cycle and stem cell maintenance [226, 245, 248]. Other than the Wnt pathway, TERT has been confirmed to influence the NFκB pathway, where it has even been observed that TERT can act as a transcriptional activator of NFκB target genes [(Figure 1.8) [31, 249-251]]. In addition, TERT can also associate with the p65 subunit of NFκB for nuclear translocation [252]. In this manner, TERT aids in the activation of NFκB target genes, essentially implicating TERT in NFκB regulated functions, like inflammation, wound repair and metabolic processes. Holistically, TERT's extra-telomeric function in gene expression and signalling cascades, coupled with its other aforementioned functions, clearly highlight the importance of this protein in normal cell function.

1.7 Telomeres, Telomerase and roles in pathological processes

1.7.1 Telomerase and telomeres in carcinogenesis

The diverse functionality of TERT coupled with its ability to influence gene expression has unfortunately allowed it to be a key target in multiple pathological processes like cancer, CVD, diabetes, as well as neurodegenerative, disorders like AD. Probably one of the most iconic pathological processes that telomere biology plays a role in, is carcinogenesis, where telomerase reactivation has been confirmed in ±90% of all cancers [194]. Cancer is a disease characterised by the loss of normal cellular homeostasis in favour of a dysregulated and hyper-proliferative state. Indeed, the pathological process that governs tumorigenic development is governed by: mutation accumulation, an overrepresentation of oncogenic factors, dysregulation of senescent as well as apoptotic pathways and uncontrolled telomerase reactivation for uncontrolled proliferation [157, 253, 254]. This circumvention of senescence coupled with dysfunctional telomeres, enables the formation of telomeric fusions to induce genomic rearrangements to drive tumorigenic development, especially within premalignant cells [145, 147, 254-257]. In accordance, this elevates the rate and accumulation of mutations characteristic of tumors, however, the risk of cell crisis occuring also increases due to the accruement of potentially detrimental mutations [257, 258]. Therefore, telomerase is reactivated and upregulated to compensate for the telomere loss induced by the fusion events and extensive proliferation occurs, ensuring conservation of the disease state [185, 254, 257, 258]. In conjunction, many of TERT's extra-telomeric roles are further altered to promote various tumorigenic hallmarks and convey chemo-therapeutic resistance. This is especially true with regards to TERT's ability to

influence proliferative pathways through its ability to upregulate c-Myc, a protein upregulated in most cancers [245, 246]. This is vital to not only sustain the tumors enhanced proliferation but to also protect against oncogene induced senescence. In addition, TERT's capacity to impede apoptosis through its association to Bcl-2 and the mitochondria, are further exploited to sustain neoplasm viability [259, 260]. Therefore, together the various aspects of telomere biology exploited during tumorigenic development highlight its vital role in sustaining this particular pathological process.

1.7.2 The role of TERT and telomerase in CVD and diabetes

Two age-related and metabolic disorders that are heavily influenced by telomere dynamics and the accumulation of senescent cells is CVD and diabetes type 2. Both disorders, aside from being influenced by ageing, are also brought about by genetic, environmental and behavioural risk factors [261]. In particular, diabetes is characterised by insulin insensitivity, hyperglycemia and β-cell dysfunction, which, if not treated correctly, can lead to the development of CVD [262-265]. Telomere dysfunction is intricately tied to diabetes disease progression, where several studies have confirmed critically shortened telomeres, especially within the insulin producing pancreatic β-cells [266-269]. Consequently, this telomeric dysfunction results in the induction of premature senescence which leads to β-cell failure and impaired insulin secretion [268-270] . In turn, the accumulation of these senescent cells eventually induces a deterioration of glucose tolerance [268-270]. Moreover, it has been confirmed that telomerase activity and TERT expression in pancreatic islets declines with age, which further contributes to the impaired glucose tolerance [268-270]. Interestingly, it has been reported that the elevation of telomerase activity within diabetic tissues, is capable of counteracting the senescence induced by the hyperglycemic state and has even been confirmed to improve insulin resistance [148, 149, 271]. These factors illustrate the critical importance of reduced telomerase activity, coupled with dysfunctional telomeres, in aiding the development and progression of the diabetic disease state.

As previously mentioned, improper management of diabetes can lead to the onset of CVD, which encompasses a group of progressive diseases that are characterised by atherosclerosis, hypertension (high blood pressure) and myocardial infarctions [272]. Primarily, these symptoms are induced by the complete or partial occlusion of major and minor blood vessels by atherosclerotic plaques, which are formed by the accumulation of leukocytes, macrophages, cholesterol and ROS [272, 273]. In particular, an intricate relationship has been confirmed to exist between cell senescence, oxidative stress, telomere biology and atherosclerosis, where telomere length acts as an efficient marker to

track CVD risk [274-277]. Indeed, multiple cardiac cell types especially vascular endothelial cells and leukocytes, are pre-disposed to high levels of hemodynamic and oxidative stress, which enhances telomeric shortening due to a high cell turn over [278-281]. In addition, this stress and telomeric dysfunction is further exacerbated around atherosclerotic lesions, causing the surrounding tissue to adopt a senescent phenotype with a CVD related protein expression profile. This expression profile, alongside the enhanced oxidative stress, leads to the development of chronic inflammation, which impedes telomerase activity, thereby enabling disease progression [282]. In fact, telomere dysfunction without telomerase activity within cardio myocytes, impedes proliferation and elevates hypertrophy of the tissue, which may eventually lead to heart failure. Unsurprisingly, it has been shown in a number of studies that elevated levels of telomerase activity and telomere maintenance improved the disease state and promoted survival [223, 224, 283]. These findings highlight the interplay between cardiac dysfunction, cell senescence and dysfunctional telomeres in the development of heart disease.

1.7.3 The influence of telomerase and telomeres in neurodegenerative disorders

A growing body of research has implicated TERT/ telomerase in the pathological processes of AD. The disease is characterised by two core pathological hallmarks namely: amyloid beta (Aβ) aggregation and the generation of neurofibrillary tangles caused by the hyper-phosphorylation of tau [284]. These factors accumulate to cause synaptic loss, which eventually leads to the formation of the dementia associated symptoms of the disease. One such manner where telomere biology has been found to influence AD, is that sufferers of the disease have been found to have shorter than normal telomeres in both their neuronal and T cells [285-287]. Additionally, the accumulation of Aβ42 has been confirmed to actively impede telomerase activity, where Aβ binds to the DNA-RNA complex of TERC and the telomeres, preventing telomerase's synthesizing function [288]. Likewise, it has also been illustrated that Aβ localises to the telomeres, where it actively induces telomere shortening and senescence [288]. Moreover, it has been confirmed that the presence of TERT appears to attenuate the pathological effects of both hyperphosphorylated tau [289] and Aβ cytotoxicity [290]. These factors point towards an antagonistic relationship shared between telomerase, Aβ and tau, which drives cellular senescence to promote a loss of neuronal cells resulting in AD-associated neurodegeneration.

1.8 The 37kDa/67kDA Laminin Receptor

The 37 kDa Laminin Receptor Precursor/67 kDa High affinity Laminin Receptor (LRP/LR) was recently found to interact with TERT to influence telomerase activity [291-294]. In a similar manner to TERT, this protein has been found to be intricately linked to preserving cell viability and has even been implicated in similar diseases. LRP/LR, also known as ribosomal protein SA (RPSA), p40 and LAMR1, serves as a cell surface receptor, as well as a vital component of the 40S ribosomal subunit [295-297]. The protein is encoded by the RPSA gene located on the short arm of chromosome 3 in humans with a total of 64 pseudogenes, lending credence to the fact that the gene is ancient [298, 299]. This is further supported by the high level of conservation across various organisms, where the protein is produced in both pro- and eukaryotes [298]. The LRP protein transcribed from the RPSA gene is approximately 295 amino acids long with a molecular weight of 37 kDa, although, how the 67 kDa isoform, arises remains a matter of deep debate. This is owed to the fact that both the 37 kDa and 67 kDa share amino acid sequence homology which suggested the possibility of homodimerization as being a probable cause for the formation of the mature 67 kDa isoform [300, 301]. This however, was later thrown into contention, where it is now believed that the mature isoform may arise from post-translational modifications, such as the addition of heperan sulphates, sumoylation or acylation [298, 300, 302]. Furthermore, it is known that acylation of LRP/LR promotes the interaction with the fatty acid residues of other LRP monomers or acylated protein partners, which could give rise to the mature isoform [298]. Thus, the process and composition of how the mature 67 kDa laminin receptor arises is still subject to extensive debate.

1.8.1 Cellular distribution of LRP/LR and its role as a cell surface receptor

Despite the ambiguity behind the structural aspects of the receptor it is common place in many areas of the cell governing a broad range of vital physiologic functions, which are necessary for cellular/ tissue homeostasis [292, 298]. The protein has been mapped to the cell surface of the plasma membrane residing within the lipid rafts [(Figure 1.9) [303-305]], various cytoplasmic regions [292, 298, 306] as well as within the nuclear compartments [298, 307-309], specifically the perinuclear and perichromosomal regions. Thus, further illustrating the protein's importance by its broad-spanning localisation. It is however, predominately localised to the cell surface, where it carries out major functions as a non-intergrin transmembrane protein by binding to laminin- 1 within the ECM, with high affinity [(Figure 1.9) [292, 296, 297]]. Intriguingly, this vital ability of the ribosomal protein LRP to bind laminin has been confirmed to be an evolutionary gain of function, where it serves to mediate the cells ability for cell adhesion and migration [292, 298, 310-313]. Moreover,

LRP's ability to bind laminin maybe important for neuronal function, where it has been associated with roles in neuronal development, as well as migration axonal development and guidance, although the extent and exact mechanisms are not completely understood [298, 314, 315]. In addition to binding laminin-1, this receptor may in fact be capable of modifying other ECM proteins, to ultimately alter cell adhesive and motility properties in both actively dividing cells and post mitotic cells [298]. Intriguingly, the 67 kDa laminin receptor (LR) could have the ability to be shed from the cell surface, and is theorised to partake in laminin modifications to alter adhesion and further facilitate with cell motility [298, 316].

Aside from laminin-1, LRP has also been found to interact or bind a range of extracellular biomolecules and proteins, including: carbohydrates, elastin, heparin, heparan proteoglycans in most cell types, as well as Aβ and prion proteins (PRP^c) especially within neurons [(Figure 1.9) [292, 317, 318]]. This binding plasticity is owed, in part, to the fact that many of these biomolecule's binding sites overlap namely, the 161- 180 aa region referred to as the peptide G region, which binds both laminin-1 and heparin [(Figure 1.9) [298, 305]]. One of the other binding sites, which spans the 205-229 aa region and is known as the "direct binding region", could potentially bind laminin- 1 as well as PRP^c [(Figure 1.9) [298, 305]]. This ability to interact with such a broad range of extracellular components has afforded LRP/LR the ability to influence a number of physiological parameters outside of migration and adhesion such as: angiogenesis, morphogenesis, aid in neuronal tissue development, and tissue differentiation, in order to preserve cell viability [292, 298].

1.8.2 LRP/LR and angiogenesis

In fact, the cleaved LRP isoform is believed to modify the levels of angiostatin that is produced by plasmin, where it interferes with the required selfhydryl reduction needed to form plasmin [319]. Essentially, this inhibits the anti-angiogenic activity of plasmin as it normally activates collagenases and degrades ECM components. Other aspects of angiogenesis that LRP appears to regulate are the migration and neovascularisation of haemopoietic stem cells (HSCs), which stimulates angiogenesis via the production of new endothelial cells [308, 320]. Moreover, high LRP/LR levels have been detected on the surface of human umbilical vein endothelial (HUVE) cells, which effectively enhances their invasive potential by allowing the secretion of type IV collagenase for degradation of the basal lamina [292, 308, 321]. In effect this may allow the HUVE cells to migrate towards pro-angiogenic stimuli, as well as make space for the development of tubular structures for the generation of new blood vessels. In this manner, LRP/ LR promotes the process of angiogenesis.

However, certain diseases have been shown to exploit this functionality and broad binding capability, where the receptor has been confirmed to interact with numerous pathological elements to promote disease progression. A few of these pathological agents include: bacteria [322, 323], viral species [324-327], as well as pathological proteins like the scrapie Prion protein (PRP^{Sc}) [305, 318, 328] and the cytotoxic amyloid β_{42} (Aβ) [329-333]. Essentially, these pathological agents use LRP/ LR to gain intracellular access to the cell in order to carry out their cytotoxic effects.

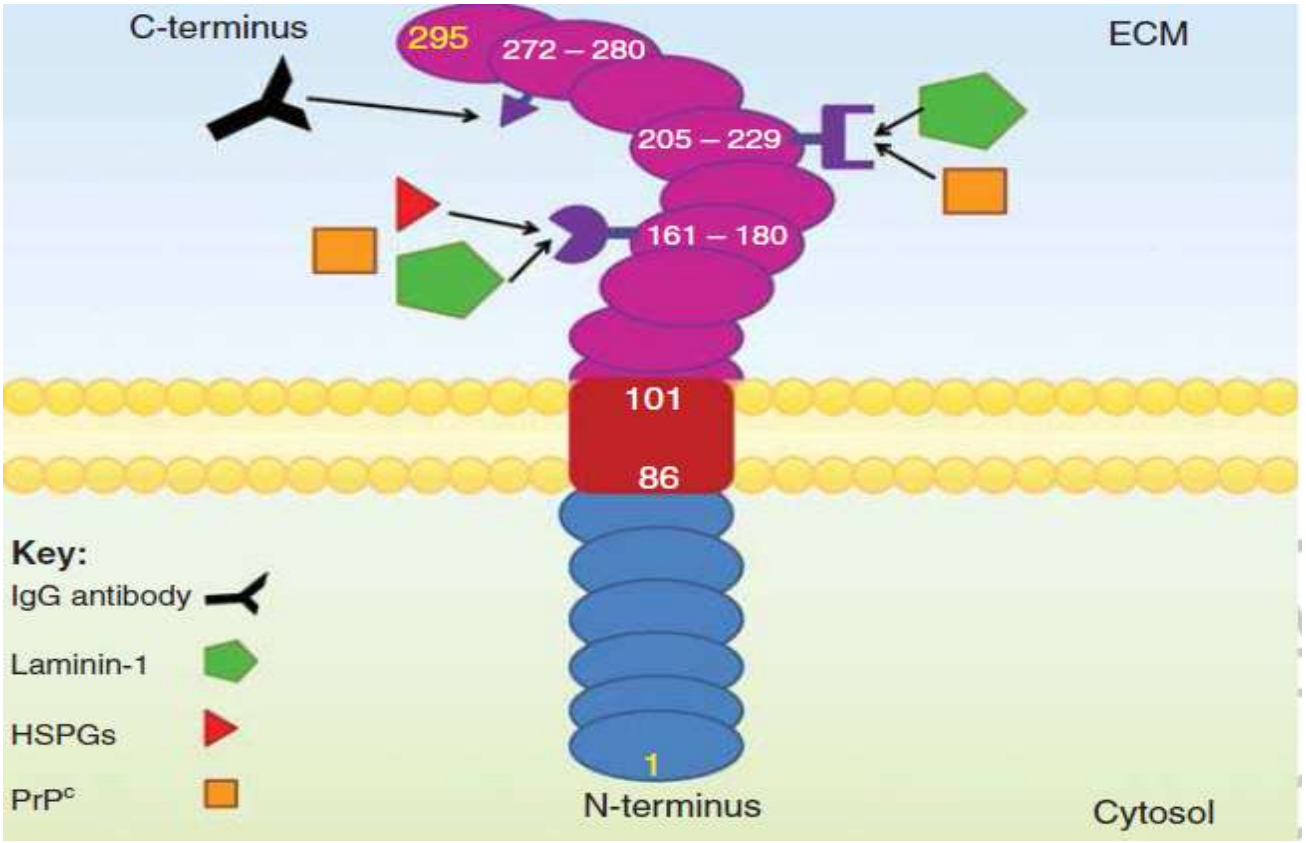


Figure 1.9: Schematic representation of the 37 kDa Laminin Receptor Precursor/67 kDa High affinity Laminin Receptor and a few of its associated binding partners.
The schematic diagram illustrates the structure and role that LRP/LR serves as a transmembrane receptor, with its C-terminus (amino acid 161-295) located extracellularly. Its multiple overlapping binding sites on the C-terminus are capable of interacting with various components of the ECM including: laminin-1, PrP^{c}, and HSPGs, which enables LRP/LR to regulate a variety of functions such as adhesion and motility. Furthermore, the receptor's N-terminus (amino acid 1-85) is located internally, within the cytosol, where it is believed to serve as a conduit between laminin-1 and the cytoskeleton, among other functions. Adopted from: Jovanovic et al., 2015 [292].

1.8.3 LRP/LR and its interaction with the cytoskeleton

According to what was previously mentioned, LRP/ LR's range of functions is not limited to just the cell surface, where its intracellular functions can be categorised into a number of broad sets namely: cytoskeletal, ribosomal, nuclear, cell signalling and development, as well as differentiation functions.

With regards to the cytoskeletal functions, it has been illustrated that cytosolic LRP/LR directly interacts with cytoskeletal stress fibre features and actin, thus suggesting that this protein may serve as a connection or conduit between laminin and the cytoskeleton in most cell types including neurons [(Figure 1.10) [312, 313, 334, 335]]. Additionally, it is known that upon laminin binding by LRP/ LR, this interaction is able to evoke widespread cytoskeletal reorganisation in order to stimulate cell motility [298, 312, 313]. Perhaps LRP/LR's most significant cytoskeletal function, is its tight binding to the cytoskeletal protein, tubulin. In turn, the ribosomal complexes then use LRP/LR as an anchor, for the ribosomes to associate with the cytoskeleton [312]. What makes this association so critical, is that upon reducing or removing LRP/LR, it induces a corresponding loss in ribosomal complexes that localise to the cytoskeleton [306, 312]. Ultimately, this results in major protein synthesis dysfunction, which severely impacts cell fitness.

1.8.4 The ribosomal functions of LRP/LR

Aside from providing structural support there are a number of intricate functions that LRP/LR carries out to ensure the proper functioning of the ribosomes. As mentioned previously, LRP/LR's ribosomal-related functions predates its other functions and has remained evolutionarily conserved across phyla [298, 308, 336]. The first confirmation that LRP/LR was involved in protein synthesis, was the identification of p40 interacting with ribosomal particles in mice [306]. Subsequently, when that protein was isolated and sequenced, it was found to perfectly match the 37 kDa LRP sequence [295]. It is now known that LRP interacts with the 40S subunit of the ribosomes, especially at the commencement of translation [(Figure 1.10) [298, 308, 337-339]]. In fact, the N-terminal portion is responsible for interacting with the ribosome, while the C-terminal domain may be responsible for binding additional proteins of the ribosomal complex or it is involved in the stabilisation and/ or binding of rRNA [307, 338, 339]. This binding of the N-terminal is so imperative, that the knockdown of LRP has been shown to induce subsequent translational defects. Aside from direct ribosomal function, the protein is vital for the processing of the 21S pre- RNA into the mature 18S rRNA allowing for the release of pre-40S particles from the nucleolus [(Figure 1.10) [298, 338, 340, 341]]. Therefore, indicating a role that LRP carries out in regulating the nucleolar export of ribosomal subunits. Collectively, these factors illustrate the crucial role that LRP plays in protein synthesis and ribosome biogenesis.

1.8.5 Nuclear functions of LRP/LR

Although LRP's presence in the nucleus has been confirmed to aid in the export of ribosomal particles, there are additional functions that it appears to be implicated in. One such role is the ability of LRP to interact moderately with chromatin and more tightly with histones, specifically H2A, H2B and H4 [(Figure 1.10) [309]. This ability to interact with DNA could point to a role in maintaining and stabilising nuclear structures, through multiple associations between the chromatin, histones and LRP. Likewise, LRP has also been shown to interact with Midkine, a growth factor that promotes cell viability, which may further assist with LRP binding to the nuclear envelope for chromatin stabilisation [(Figure 1.10) [342]]. Furthermore, the significance of LRP within the nucleus may be greater than what was firstly envisaged, as its DNA binding ability opens the potential for the protein to operate as a potential transcription factor, or as a chromatin modifying agent, however this still needs to be researched.

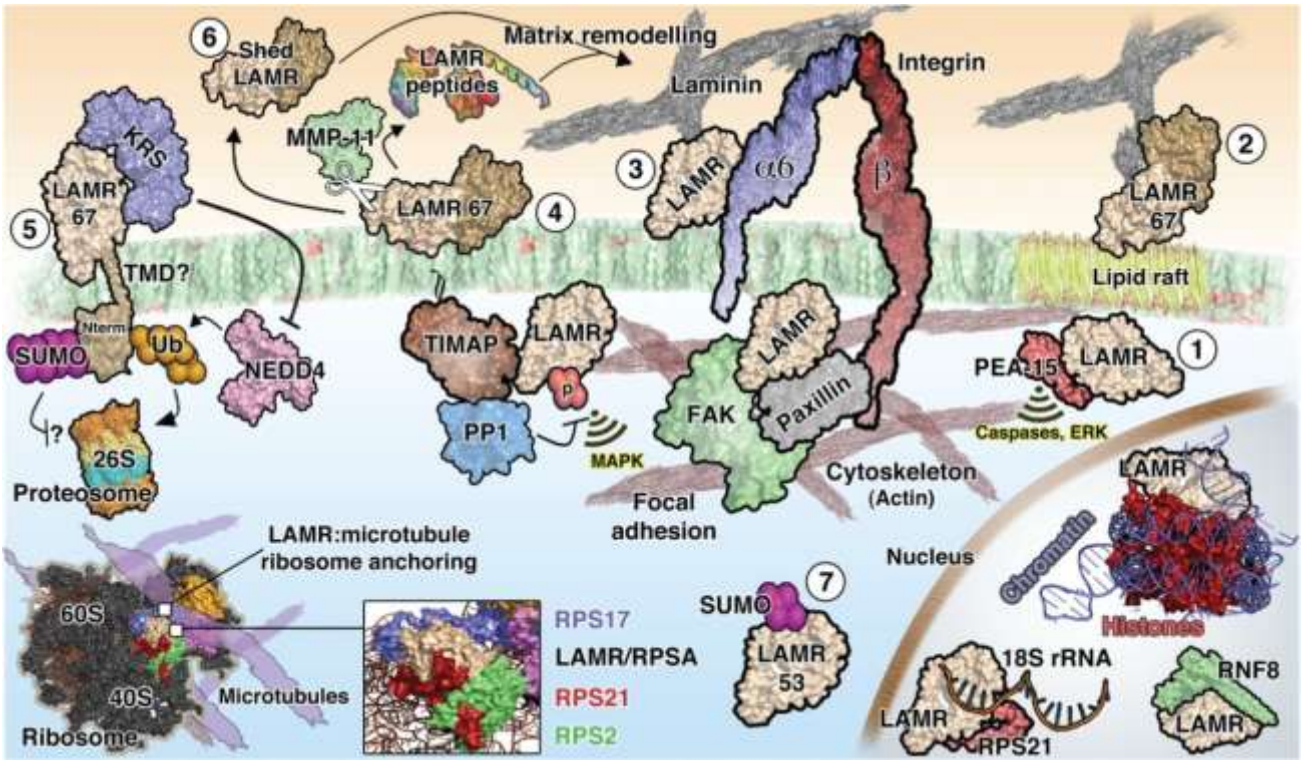


Figure 1.10: The various isoforms of LRP/LR also known as LAMR or RPSA and their respective functions.

The figure clearly depicts that LRP/LR, otherwise known as LAMR1 or RPSA, has several different forms and each is associated with a particular set of functions. (1) Represents intracellular LRP that in the cytosol plays a role in ribosome assembly and anchorage, as well as interacting with the cytoskeleton. In addition, the cytosolic forms of LRP potentially play a role in various signalling cascades including: the mitogen activated protein kinase (MAPK), extracellular regulated kinase (ERK) and focal adhesion kinase (FAK) pathways. Aside from signalling cascades, LRP is also known to share a number of interactions, some of which include: NEDD4 (neural precursor cell expressed developmentally down-regulated protein 4), PEA-15 (phosphoprotein enriched in astrocytes-15) and PP1 (protein phosphatase-1). Aside from the cytosol, this form of LRP/LR can also be found in the nucleus, where it interacts with histones (for nuclear stabilisation), RNF8 (ring finger protein 8) and 18S rRNA (for nuclear export). (2) Illustrates LRP/LR acting as a peripheral membrane protein interacting with laminin-1. (3) Also displays LRP/LR as an extracellular membrane protein but supporting laminin-1 binding through interactions with integrins for establishing a link between the cytoskeleton and the ECM. (4) Displays the maturation of the 67 kDa receptor as a result of either being a hetero or homomer. (5) Shows LRP/LR with its extracellular C-terminus, theoretical transmembrane domain extending through the phospholipid bi-layer and its N-terminus that extends into the cytosol. (6) Shows the shed form of LRP/LR, believed to play a role in chromatin remodelling and angiogenesis, which is generated by matrix metalloproteinase-11 (MMP-11). 7) Displays the SUMOylated 53kDa isoform of LRP/LR. Adopted from: DiGiacomo and Meruelo, 2015 [298].

1.8.6 The role of LRP/LR in differentiation and development

Given LRP/ LR's importance in various aspects of cellular function it is not surprising that the protein has been shown to govern key roles in developmental programmes and differentiation. Admittedly, LRP has been closely tied to limb bud development in chicks [343], cardiomyopathy in mice [344] and spleen development in humans [298, 345]. Interestingly, this protein like TERT, is expressed in high amounts in developing and undifferentiated tissue, with a subsequent decline after

differentiation and more importantly, with increased age [298, 346-349]. How LRP is able to exert such an influence on development and differentiation, is that its levels can be regulated by hormone or cytokine signals such as transforming growth factor (TGF) and tumor necrosis factor (TNF), which bring about chemotaxis, a vital aspect of developmental biology [350, 351].

1.8.7 The role of LRP/LR in signalling cascades

There has been a collection of mounting evidence pointing towards LRP's ability to influence signal transduction pathways, especially those involved in cell growth and apoptotic evasion. This is evident, where LRP/ LR has been shown to interact and phosphorylate focal adhesion kinases (FAK), inducing a subsequent activation of MEK/ERK 1/2 and PI3-kinase/ Akt pro-survival pathways [(Figure 1.10) [352]]. In turn, these pathways effectively inhibit caspase 8 and 9 pathways to prevent the induction of apoptosis in both actively dividing cells as well as in post mitotic cells like neurons. Other pathways that LRP has been shown to interact with and influence include: granulocyte-macrophage colony stimulation factor (GM-CSF) receptor, which leads to STAT5 (One of the TFs responsible for the activation and expression of the TERT gene) phosphorylation for the stimulation of proliferation [353, 354]. Additionally, LRP has been found to influence insulin-like growth factor receptors I and II; both of which regulate proliferation and cell survival [355]. One of the core pathways regulated by LRP, and importantly its binding to laminin-1, is the Mitogen Activated Protein Kinase signal transduction pathway [(MAPK) (Figure 1.10)]. This said, the expression levels of LRP are known to affect the phosphorylation and de-phosphorylation of key proteins within the MAPK signalling cascade including: p38, ERKs and JNK [356, 357]. How this may occur, is that LRP is able to regulate the expression of PAC1 and MKP1, which are MAPK phosphateses responsible for the de-phosphorylation of the aforementioned proteins [358]. In this manner, LRP is able to influence the entry of cells into cell cycling, proliferation and differentiation. Moreover, it has been shown that this laminin-1- LRP- MAPK interaction can increase the phosphorylation and activation of the transcription factor (TF) c- Myc [357]. What makes this so intriguing is that, aside from aiding in proliferation, this TF carries out an additional function of inducing the expression of TERT, as previously mentioned.

Recently, a potentially novel function of LRP has come to light; namely, the interaction or association with TERT to promote telomerase activity for sustained cell viability and prevention of senescence onset [291, 293, 310]. The relationship shared between these two proteins was confirmed, firstly in tumorigenic cells, and later in non-tumorigenic cells, where it appears that LRP

is able to stimulate telomerase activity, which would essentially prevent both senescence and apoptotic induction in cells. Holistically, all the aforementioned functions pertaining to LRP/LR, alongside the tight evolutionary constraints imposed, clearly highlight this protein's far spread importance in maintaining tissue and cellular homeostasis.

1.9 LRP/LR and its role in pathological processes

LRP/LR's functional plasticity coupled with its broad binding range, has made LRP/LR a lucrative target for disease initiation and progression. In fact, it has been broadly implicated in several diseases, especially age-related diseases, where it plays vital roles in promoting and establishing the disease. Furthermore, the diseases that this receptor has been associated with, have been found to comprise of both communicable and non-communicable diseases that include: viral, as well as bacterial infections, prion disorders, AD and most importantly cancer [(Figure 1.11) [292, 298]].

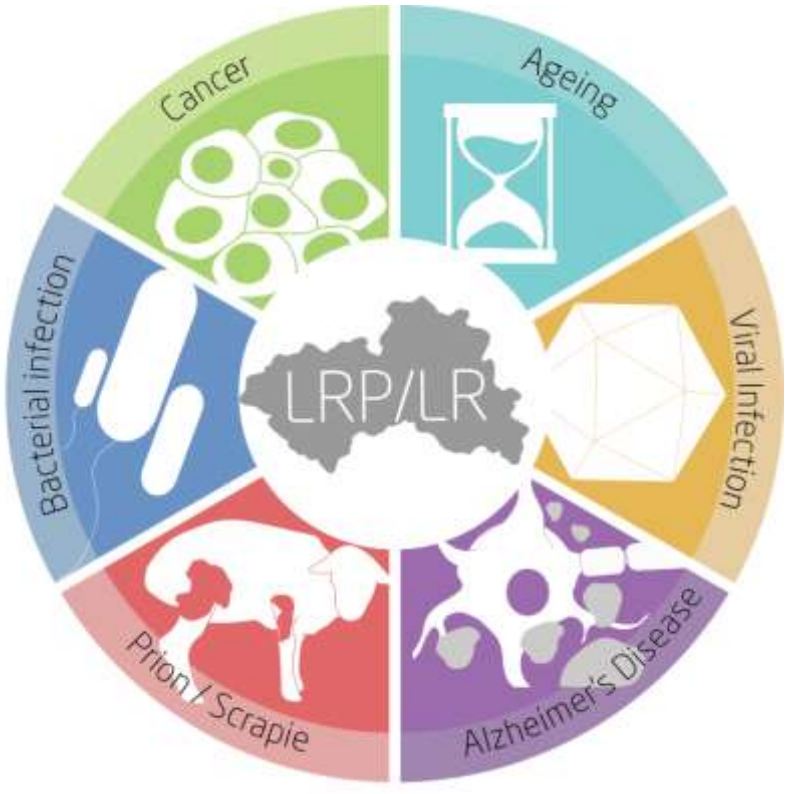


Figure 1.11: The various pathological processes that exploit LRP/LR.
Numerous studies have elucidated that LRP/LR is heavily implicated in a range of pathological processes. Three major reasons for this include: LRP/LR's functional plasticity, its vast cellular distribution patterns and that the receptor contains multiple binding sites. This has allowed LRP/LR to interact with various bacteria, viruses and infectious/ cytotoxic proteins (PRP^{Sc} and Aβ). Furthermore, the protein is commonly overexpressed in tumorigenic cells, where it plays a role in enhanced cell survival, as well as angiogenic and metastatic potential. Adopted from Vania et al., 2019 [308].

1.9.1 The Role of LRP/ LR in Bacterial and Viral infections

Since LRP/ LR's major function is to serve as a cell surface receptor a number of viral and bacterial species exploit it to gain intracellular access to the cell. A few of these viral species include: Adenoviruses, Dengue, Sindbis, Tick-borne encephalitis (TBE), Venezuelan equine encephalitis and West Nile viruses [324-327, 359]. Although these viruses can interact with LRP/LR, it is not the only or primary receptor that is used to infect the cells, however LRP/LR's presence does appear to enhance the aforementioned viruses' primary receptor interactions. In a similar manner, the receptor has been reported to be used by a number of bacterial species. Among them, several bacterial species that induce the cerebral infection meningitis (*Escherichia coli* (*E. coli*), *Haemophilus influenza*, *Neisseria meningitidis* and *Streptococcus pneumoniae*) have been correlated to LRP/ LR binding [322, 323, 360]. These bacteria utilise LRP/LR for surface adhesions; especially for binding to the blood brain barrier (BBB) as well as to gain intracellular access [322, 323, 361]. In particular, the large amounts of LRP/LR present on the surface of human brain microvascular endothelial cells, which make up the BBB, allow the bacteria to bind and adhere tightly [322]. Once bound, these bacteria are then taken up by the cells, thus allowing passage through the BBB, allowing bacterial meningitis to ensue. In addition, to adhesion the K1 strain of E. coli produce the cytotoxic necrotizing factor (CNF1), which is a toxin that LRP/LR binds and internalises [322, 360]. Therefore, LRP/ LR appears to play a central role in establishing microbial infections, specifically those impacting the central nervous system (CNS).

1.9.2 The Role of LRP/ LR in Neurodegenerative disorders

LRP/LR and Prion disorders

Aside from establishing communicable diseases, the receptor has been extensively shown to influence the development of cerebral or neuronal disorders; like prion disorders and AD. For prion disorders, LRP/LR acts as the major receptor which binds and internalises the infectious PrP^{Sc} with high affinity [328, 362-364]. The PRP^{Sc} isoform is generated by the conversion of normal PRP^{c} to the infectious isoform either within endocytotic vesicles or on the cell surface [365, 366]. What makes this particular protein isoform so dangerous, is that it is protease resistant, and thus allows for the accumulation of this pathological agent within neuronal cells [318, 328, 367]. The intracellular accumulation of this infectious protein induces cell death and neurodegeneration to cause the formation of bovine spongiform encephalopathy in cattle and Creutzfeldt-Jakob disease in humans [292, 364]. Since LRP/LR has been implicated in the propagation, internalisation and aggregation of PrP^{Sc}; it highlights the fact that the receptor plays a central role in the establishment and progression

of the disease [362, 368]. This was further evidenced when the receptor was targeted and blocked by antibodies, where it resulted in a subsequent hampering of PrP^{Sc} propagation and its associated cytotoxic effects both *in vitro* and *in vivo* [369, 370]. Therefore, this illustrates the therapeutic potential in targeting LRP/ LR for the treatment of prion disorders.

LRP/LR and Alzheimer's disease

An additional neurodegenerative disorder and age-related disease that has been intricately tied to LRP/ LR is AD. As mentioned previously, two of the most studied neuro-pathological hallmarks include: Aβ aggregation and the generation of neurofibrillary tangles caused by the hyper-phosphorylation of tau [284]. How LRP/ LR is so heavily implicated in AD pathogenesis, is that it promotes the shedding of the etiological agent Aβ from the amyloid precursor protein (APP), where it interacts with both γ- and β- secretase for the cleavage and generation of the neurotoxic $A\beta_{42}$ peptide [331]. Moreover, LRP/LR also acts as the major receptor involved in the shedding, internalisation and intracellular aggregation of Aβ within neuronal cells [292, 329-332, 371]. Aside from just aggregating, this neurotoxic peptide has also been shown to drive other adverse programmes that are detrimental to the cells through its interaction with certain cell surface receptors. A few of these adverse functions include: protein degradation, lipid oxidation and increases in general oxidative stress [333, 372, 373]. These processes are believed to potentially drive disease progression by inducing neuronal damage, cell cytotoxicity and ultimately cell death. In fact, the mechanism by which Aβ induced cytotoxicity occurs, is believed to be a consequence of the interaction between LRP/LR and $A\beta_{42}$-PrP^{c} [371]. The importance of LRP/LR in promoting the pathogenesis of Aβ was further established, when LRP/LR was knocked down with specific shRNAs targeting the mRNA of the receptor, as well as blockade of the receptor using a highly specific anti-LRP/ LR antibody (IgG1-iS18 or W3) [292, 329-332, 363, 374]. Both forms of treatment were found to efficiently inhibit the shedding and internalisation of the cytotoxic Aβ peptide, which in turn significantly reduced Aβ induced cytotoxicity, thus improving overall cell viability *in vitro* [292, 329, 330, 332, 371]. In conjunction, the IgG1-iS18 antibody has also been proven to be effective *in vivo*, where treatment with the antibody was found to significantly reduce $A\beta_{42}$ levels, with a corresponding increase in APP and mTERT levels [374]. Consequently, this resulted in reduced Aβ plaque formation and a striking improvement in memory [374]. Therefore, this convincingly illustrates LRP/LR's potential as a therapeutic target for the treatment of AD.

1.9.3 The role of LRP/ LR in carcinogenesis

In addition to neurodegenerative disorders, LRP/LR has been shown to be crucial for the induction and establishment of carcinogenesis by carrying out a range of tumorigenic functions. Similarly to TERT, LRP/ LR has been found to be overexpressed in most cancer types, where this overexpression aids in the regulation and promotion of key cancer hallmarks. The core hallmarks that LRP/LR has been confirmed to influence include: sustained angiogenesis, apoptotic resistance, increased adhesion, as well as invasion for enhanced metastatic potential and more than likely, aiding in the upregulation of growth signals [308, 321, 375]. These hallmarks act as the core forces that drive tumorigenic progression. Consequently, the majority of these tumorigenic processes that LRP mediates are a consequence of the hyper-upregulation of its normal functions. This is due to the increased amount of LRP present, as well as a lack of functional tumor suppressor signalling cascades [292, 296, 308].

Interestingly, it has recently been uncovered that LRP/LR carries out an additional function through a unique ability to interact with the enzymatic component of the telomerase enzyme, TERT [291, 292, 310]. This interaction within tumorigenic cells points to the possibility that LRP/ LR overexpression and telomerase reactivation may be linked. In addition, as the receptor seems capable of stimulating or elevating telomerase activity, it may then infer that LRP/LR plays a role in another tumorigenic hallmark, namely, limitless replicative potential. In a similar manner to neurodegenerative disorders, the blockade of LRP/LR using the LRP-specific IgG1-iS18 antibody or downregulation by specific siRNA, were found to efficiently impede tumorigenic progression. The antibody treatments were found to significantly hamper adhesive, invasive and angiogenic processes of the tumor cells *in vitro*; to ultimately reduce metastatic potential [321, 369, 375-380]. Alternatively, the specific knockdown of LRP/ LR by siRNA was found to induce apoptosis by both the extrinsic and intrinsic pathways, while causing a further concomitant decrease in telomerase activity [291, 381-385]. The impediment of these hallmarks adversely impacts cell viability and induces cell death in tumorigenic cells, highlighting LRP/LR's potential as a therapeutic target for the treatment of cancer.

1.10 Relationship between LRP/LR and telomerase

The functional relationship shared between LRP/LR and telomerase seems to be centred around cellular survival and viability functions, however what molecular mechanisms are governed to bring about these functions are still not entirely understood. Intriguingly, like TERT, LRP/LR appears to

be expressed less in ageing tissue, while it is overexpressed in the hyper-proliferative disease, cancer. Furthermore, it has been shown in metastatic breast cancer cells (MDA MB-231) and in the normal cell line human embryonic kidney cells (HEK293), that LRP/LR and TERT interact [291]. Moreover, it was found that upon siRNA-mediated down-regulation of LRP/LR it induced a concomitant decrease in telomerase activity [291]. This influence on TERT and telomerase was found to be shared in non-cancerous cells, where an overexpression of LRP::FLAG positively influenced various aspects of telomere biology in aged cells [293]. In relation, a similar effect was also found in cells mimicking an AD pathology (cells treated with cytotoxic levels of Aβ), when LRP::FLAG was overexpressed [294]. In fact, LRP::FLAG overexpression rescued HEK293 and SH-SY5Y cells from Aβ-mediated cytotoxicity and improved overall cell viability [294]. Interestingly, it was also found that this overexpression of LRP::FLAG was even capable of enhancing telomerase activity while in the presence of cytotoxic amounts of Aβ [294]. Collectively, these findings support the theory that a functional relationship exists between these two proteins, to ultimately promote proliferation and viability in both normal and pathological settings. Therefore, understanding the molecular mechanisms shared between these two proteins as well as the extent of this relationship on a whole-organism scale, may afford the opportunity to develop a novel and powerful tool to combat cellular ageing and age-related diseases.

2. Aims and objectives

Hypothesis

Based off the aforementioned previous published findings and that the two proteins share a broad range of similar functions we hypothesised that the elevation of total LRP/LR (by overexpressing LRP::FLAG) may induce a corresponding elevation in telomerase and other potential anti-ageing proteins to elicit an anti-ageing or anti-senescent effect.

2.1 *In vitro* Study Aim:

To investigate the role that LRP/LR has on telomerase activity, hTERT expression, telomere length and levels of the ageing markers β-galactosidase as well as γH2AX as a possible anti-ageing therapy.

2.1.1 In vitro Study Objectives:

1) To transfect MRC-5 (somatic) cells and HEK293 (embryonic) cells with the pCIneo-moLRP::FLAG plasmid to overexpress the full length LRP::FLAG protein.

2) To investigate whether over-expression of LRP::FLAG has a significant effect on telomerase activity, hTERT expression levels and telomere length *in vitro*.

3) To determine the levels of selected senescence markers including: β-galactosidase activity and γH2AX levels in transfected and non-transfected cell lines.

2.2 *In vivo* Study Aims:

To investigate the role that LRP::FLAG exerts in modulating the organism ageing and whether its overexpression positively influences telomere dynamics as well as prevents the accumulation of senescent markers.

2.2.1 In vivo Study Objectives:

1) To overexpress LRP::FLAG within the C57BL/6J mice by intravenous tail vein injections and intramuscular injections with the pCIneo-moLRP::FLAG plasmid.

2) To perform physiological analyses post transfection on the C57BL/6J mice to assess the effects of LRP::FLAG overexpression on memory, social behavior and motor function, among others.

3) To investigate the effect that LRP::FLAG overexpression had on the ageing process within the tissue of the aged C57BL/6J mice. To test the degree of tissue atrophy and degeneration by performing histochemical analysis.

4) Investigating whether LRP::FLAG overexpression elevates hTERT expression, telomerase activity and telomere length in the aged C57BL/6J mice using qPCR and western blotting.

5) To assess the effect that LRP::FLAG overexpression has on major proliferative and senescent proteins in the aged C57BL/6J mice by quantifying mRNA expression levels by qPCR and protein levels by western blotting.

6) To assess the effect that LRP::FLAG overexpression has on the longevity of the C57BL/6J mice.

3. Methodology

All buffers and chemical reagent recipes used during the course of this research can be found in Appendix D. In addition, all chemicals used during the course of this research were obtained from Sigma-Aldrich (Missouri, USA) unless specified otherwise.

3.1 Production of the pCIneo-moLRP::FLAG plasmid

3.1.1 Bacterial Transformation and plasmid expression

The pCIneo-moLRP-FLAG expression vector used during the course of this study was previously generated by Vana and Weiss (2006) [386]. Therefore, the only requirement before commencing with the study was to produce a large enough quantity of plasmid for both *in vitro* and *in vivo* use. Plasmid generation was performed by transforming chemically competent bacterial cells (Invitrogen, Thermo Fisher, USA) with the plasmid followed by cultivation, and thereafter isolation and purification of the plasmid. Firstly, competent cells were thawed on ice and 50 µl of the cell suspension was aliquoted into sterile eppendorf tubes. The pCIneo-moLRP-FLAG plasmid (10 ng) was then added with gentle mixing which was allowed to incubate on ice for 30 min. Thereafter, the bacterial cells were heat shocked at 42°C for 20 sec and were then immediately placed on ice for 2 min in order to facilitate uptake of the plasmid by the cells. Pre-warmed bacterial nutrient broth [(950 µl) (Table 8.1)] was then added to the cells, which was then incubated for 1 hr at 37 °C with gentle agitation (rocking shaker at 225 rpm) to allow for bacterial growth to occur. Following the 1 hr incubation 200 µl of the cell suspension was then spread onto Ampicillin [(100 µg/ ml) (Melford Laboratories, Suffolk, UK)] selective Bacterial Nutrient Agar plates (Table 8.2) which was then incubated at 37 °C overnight. This selective treatment was done to ensure that only bacteria containing the plasmid grew. In this regard, any colonies present on the plate the following day were representative of transformed bacteria. In order to cultivate the transformed bacteria, 1-3 bacterial colonies were selected and using a sterile loop were lifted from the agar and transferred into 1 ml of pre-warmed bacterial nutrient broth. This was then incubated for 1 hr at 37 °C with gentle agitation (rocking shaker at 225 rpm), after which it was transferred into 1 litre of pre-warmed selective bacterial broth (ampicillin at 100 µg/ ml). The broth containing the transformed cells was then incubated overnight to allow for exponential bacterial growth. Thereafter, the broth was kept at 4°C until plasmid isolation was carried out.

3.1.2 Plasmid DNA Isolation by the Alkaline Lysis Method

Following bacterial cultivation, the broth was transferred into new eppendorf tubes and centrifuged at 14 000 xg for 1 min to pellet the transformed bacteria. This was repeated until a sizeable pellet was obtained (the adding of broth and centrifugation were generally repeated 6 times). Once the pellet was a satisfactory size the bacterial cells were resuspended in 150 µl Resuspension buffer (Table 8.3) by vortexing. Subsequently, 200 µl of bacterial lysis solution (Table 8.4) was added and thoroughly mixed by inversion until the solution became viscous. Thereafter, 300 µl of neutralization solution (Table 8.5) was added and mixed by inversion to halt the lysis reaction. The mixture was then centrifuged at 14 000 xg for 5 min and the supernatant was transferred to a new eppendorf tube. A 1: 1 volume of 100 % isopropanol was added to the solution and mixed by inversion, which was then incubated at -20 ˚C overnight in order to precipitate the plasmid DNA. The following day the solution was centrifuged at 14 000 xg for 5 min to pellet the plasmid DNA and the supernatant was discarded. An ethanol wash was then performed using 600 µl of 70 % ethanol to dislodge the pellet and remove any salts, which was followed by centrifugation at 14 000 xg for 5 min. The supernatant was discarded, and the pellet was air-dried for 30 min at room temperature (RT) to ensure evaporation of residual ethanol. Finally, the plasmid pellet was resuspended in 100 µl of nuclease free TE-buffer [(pH 8) (Table 8.6)] and was resolved on a 1 % agarose gel to assess quality and integrity of the plasmid (Table 8.4). In addition, the plasmid samples were also quantified by nanodropping using the NanoDrop® ND-1000 (Thermo Fisher Scientific, Waltham, Massachusetts, USA) and were also sent away for sequencing to ensure that the LRP::FLAG gene was present and not mutated (Table 8.5).

3.2 Cell Culture

Non-tumorigenic, Human Embryonic Kidney cells (HEK293) obtained from ATCC (USA) was used due to their detectable expression of TERT and in turn levels of telomerase activity. This was in order to observe the effect that the overexpression of LRP::FLAG had on telomerase activity in an already immortalised cell line. Non-tumorigenic, Human lung fibroblasts (MRC 5) from Fox Chase Cancer Center (USA) were used as the ageing model due to its undetectable levels of TERT and limited replications before reaching senescence. Additionally, this line readily exhibits increases in various senescent markers after extensive sub-cultivation allowing for efficient monitoring of the senescent phenotype. This line was used to confirm that an overexpression of LRP::FLAG could potentially stimulate the expression of TERT, and subsequently induce an activation of telomerase activity within a somatic cell line.

All cell lines were cultured under the same physiological conditions in 5 % CO_2 at 37 °C in sterile 75 cm^3 cell culture flasks (NeST Technology, Virginia, USA), while being maintained in the same composition of media namely, Dulbecco's modified Eagle's medium (DMEM) with high glucose (4.5 g/l) (Hyclone, GE Life Sciences, Massachusetts, USA) containing 4 mM L-Glutamine, 10 % foetal bovine serum (FBS) (Biowest, Nuaillé, France) and 1 % penicillin/streptomycin (Thermo Fisher Scientific, Massachusetts, USA). All cell lines were sub-cultivated upon reaching a confluency of approximately 80 %. Prior to trypsinization the cells were washed with 5 ml of 1X phosphate buffered saline solution [(PBS) (Table S2.7)]. After discarding the wash, the cells were incubated in 2 ml of trypsin/EDTA (Biowest, Nuaillé, France) at 37 °C for 10 min to allow for the detachment of the cells. Thereafter, 8 ml of fresh media was added to the cells to halt the trypsinization process and cells were then split in a 1:10 ratio for the HEK293 transfected and non-transfected lines, while the MRC 5 transfected and non-transfected lines were split at a 1:4 ratio. The sub-cultivated cells were then replenished with an appropriate amount of fresh media to make up a final volume of 10ml. In the event that cryopreserved cell stocks were made for HEK293 and MRC 5 cells the following procedure was used: Firstly, cells were trypsinised and centrifuged at 500 xg for 5 min. The pelleted cells were then resuspended in 1 ml of a 10 % (v/v) dimethyl sulfoxide (DMSO): 90% (v/v) FBS solution and transferred into cryogenic tubes. The stocks were then frozen at -20 °C for 3 hr and afterwards stored at -80 °C. When cryopreserved stocks were taken out to restart a cell line, the stocks were thawed in a 37 °C water bath and were subsequently aspirated and transferred into a fresh 75 cm^3 culture flask containing 10 ml of supplemented DMEM.

3.3 LRP::FLAG overexpression in HEK293 and MRC 5 cells

The HEK293 and MRC 5 cells were stably transfected to cause an overexpression of the LRP::FLAG protein, essentially elevating total levels of LRP/LR within the cell [386]. The transfection procedure was carried out using Lipofectamine 3000 (Invitrogen, Carlsbad, California, USA), according to the manufacturer's protocol on cells that were at a confluency of around 60 %. Briefly, 5000 ng of the pCIneo-moLRP-FLAG, 56.1 µl P3000 reagent and 56.1 µl of the Lipofectamine reagent were mixed in 250 µl Optimem (Gibco, Life Technologies, California, USA) and incubated at RT for 10- 15 min. This was to allow for the formation of the lipophilic complexes around the plasmid DNA. The cells were then treated with 250 µl of the mixture and incubated for 48 hr to allow uptake of the plasmid complexes by the cells, as well as the expression of both the LRP::FLAG protein and selectable marker. Following the 48 hr incubation, the cells underwent a

selective treatment using geneticin (Gibco, Life Technologies, California, USA) at a concentration of 800 ng/ml for 1 week. This high concentration effectively ensured that all non-transfected cells were removed from the culture line. Thereafter, cells were maintained in a constant low concentration of 300 ng/ml, in order to ensure transfection stability and that the cells actively transcribed the plasmid. Finally, the success of the treatment was confirmed by western blotting using an antibody that specifically targeted the FLAG tag.

3.4 Protein extraction from cells and Bicinchoninic acid (BCA) protein assay

Prior to carrying out any experimental procedures that required protein samples, flasks of confluent cells were harvested. This involved discarding the media and washing the cells in 5 ml of PBS. Thereafter, the cells were trypsinized and pelleted by centrifugation at 2000 xg for 10 min. The trysin was then discarded and the pellets were resuspended in Radioimmunoprecipitation assay (RIPA) buffer (Table 8.8), where they were then placed on ice for 20 min to facilitate cell lysis and protein extraction. This was followed by an additional centrifugation step at 10 000 xg for 20 min in order to pellet the cell debris. The protein extracts were then transferred to a new eppendorf tube and kept frozen at -20°C until required for downstream applications.

BCA assays were performed prior to western blotting to quantify the protein lysate samples for normalisation and ensure equal protein concentrations were used for downstream assays. This assay produces its colorimetric reaction based off the reduction of Cu^{2+} present in the BCA solution to Cu^{+} caused by the peptide bonds present in proteins. Briefly, a series of Bovine serum albumin (BSA) standards of known concentrations were made by serial dilutions (0, 0.2, 0.4, 0.6, 0.8 and 1 mg/ml) and pippetted into individual wells of a 96 well plate. Thereafter, 5 µl of protein sample for each cell extract was pippetted in triplicate into individual wells and diluted 1:5 with RIPA buffer. The BCA mixture (1:50 ratio of Copper sulphate and Bicinchoninic) was added to each well containing either standard or protein sample, and then incubated at 37 °C for 30 min to allow the colorimetric reaction to occur. This colour change was then measured at 562 nm using the Sunrise™ ELISA reader (Tecan, Männedorf, Switzerland). The standard curve was generated, and the cell extract's protein concentration was calculated from the curve.

3.5 Western blotting for *in vitro* analysis of HEK293 and MRC 5 protein levels

3.5.1 Sample preparation

Western blotting was used to confirm that cells were successfully transfected and expressing the LRP::FLAG protein, where endogenous LRP/LR was also assessed. Apart from confirming the presence of LRP::FLAG, western blotting was also used for the relative quantification of hTERT levels and the senescent marker γH2AX. Following the BCA assay the extracted protein samples were incubated with Blue Loading Buffer (New England Biolabs, Massachusetts, USA) with 40 mM of dithiothreitol (DTT) for 5 min at 95 °C. The relative amount of protein sample used for each western blot was approximately: 10 µg/µl for LRP/LR and the LRP::FLAG protein, while due to the low protein expression levels of hTERT and γH2AX 50 µg/µl of protein lysate was used. Alongside these proteins of interest, the reference protein β-actin was assessed to ensure equal concentrations of lysates were used. In addition to the samples a pre-stained molecular weight marker (PageRuler Prestained Protein Ladder, Thermo Fisher Scientific, Massachusetts, USA) was loaded onto each gel in order to determine the relative size of the proteins of interest.

The samples were then resolved by Sodium Dodecyl sulphate polyacrylamide gel electrophoresis (SDS- PAGE) using the Mini Protean gel system (Bio- Rad, California, USA) and loaded into a 10 % Polyacrylamide gel (Table 8.9). The gels were run at 150 V, 0.15 A per a gel with 1 x Electrophoresis Tank buffer (Table 8.10) and were resolved until the dye front reached the bottom of the gel, allowing for protein seperation by size. Thereafter, the resolved proteins were transferred onto a polyvinylidine fluoride (PVDF) membrane (Pall, New York, USA) with 1 × transfer buffer (Table 8.11) using the PerfectBlue™ 'Semi-Dry' Electro Blotter system (Peqlab Biotechnologie GmbH, Erlangen, Germany) at 350 mV for 50 min. These membranes were then blocked in 3 % BSA (Glentham Life Sciences, Corsham, UK) in PBS and 0.1 % Tween 20 (PBST) for 1 hr at RT with gentle agitation. This was done to coat or block all regions of the membrane that did not have protein bound; to ensure that the antibodies used did not bind to the membranes non-specifically. The membranes were then incubated with the appropriate primary antibody overnight at 4 °C with gentle agitation. Thereafter, the membranes were washed in PBST 5 times for a period of 5 min each, to remove any unbound antibody from the membrane. This was then followed by a 1 hr incubation with the relevant secondary antibody at RT. The primary and secondary antibodies as well as their concentrations that were utilized for western blots are detailed in Table 8.20. The membranes were then washed as detailed above and incubated for 5 min in Clarity™ Western ECL Blotting Substrate (Bio- Rad, California, USA) that the HRP present on the secondary antibody reacts with, prior to

detection. The proteins were then visualized with the ChemiDoc™ Imaging System (Bio- Rad, California, USA) and densitometric analysis was performed with Image Lab 5.1 software (Bio- Rad, Hercules, California, USA).

3.6 Assessment of co-localisation between TERT and LRP *in vitro* using confocal microscopy

This experimental procedure was used to determine the extent of co-localization between LRP::FLAG, endogenous LRP/LR and hTERT. These proteins were assessed intracellularly, for transfected and non-transfected HEK293 as well as MRC 5 cells. Firstly, confluent cells were seeded onto coverslips and were cultured until a 70 % cell confluency was reached. Thereafter, the cells were fixed in 4 % paraformaldehyde (PFA) for 20 min, after which the cells were washed thrice in 1X PBS. All successive washing steps were performed a total of three times. In order to allow the antibodies to gain intracellular access to the cells; the cells were permeabilized in 0.1 % Triton X in PBS for 15 min, which was followed by additional washes in 1X PBS. In order to prevent non-specific binding of the antibody a 20 min blocking step in 0.5 % BSA in 1X PBST was carried out. Subsequently, the cells were incubated with the primary antibodies for hTERT (1:100) and LRP/LR or LRP::FLAG [(1:100) (Table 8.20)] overnight. Following the overnight incubation, the cells were washed thrice with 1X PBS and were then incubated with the appropriate fluorescent secondary antibodies, either a FITC-coupled or APC-coupled secondary antibody (see Table 8.20), at a 1:100 dilution in 0.5 % BSA in PBST for 1 hr. This was followed by an additional three washes where afterwards the cells were incubated in 10 µl of Dapi [(10 µg/ml) (Sigma-Aldrich, Missouri, USA)] for 10 min to allow for nuclear staining. A final set of washes were performed and was followed by mounting the coverslips onto glass slides using Gelmount (Sigma-Aldrich, Missouri, USA). The slides were viewed with the Zeiss LSM 780 confocal microscope (Zeiss, Oberkochen, Germany) at 450x and 630x magnification, respectively.

3.7 Assessment of cell senescence *in vitro* by use of the β-Galactosidase assay

In order to determine whether the overexpression of LRP::FLAG subsequently influenced the senescent marker β-galactosidase *in vitro,* an altered form of the β-Galactosidase Enzyme Assay System with Reporter Lysis Buffer (Promega, Wisconsin, USA) by Lee et al., (2006) [387] was used to determine endogenous levels of β-Galactosidase post-transfection. It must also be noted that prior to assessing this marker all the cell lines were allowed to undergo ±20 population doublings before being assessed. Briefly, cells were seeded into 6 well dishes and were allowed to proliferate until a

confluency of about 80% was reached. It must be noted that during the cultivation period daily media changes were performed to prevent a stress related (from nutrient starvation) or metabolic related activation of β-galactosidase. Thereafter, the cells were harvested, washed in 1X PBS and then lysed with 200 µl of Reporter lysis buffer provided in the kit. The lysates were then centrifuged at 10 000 xg to pellet the cell debris and the supernatant was transferred to a new eppendorf tube. The lysates were then quantified by a BCA assay (see section 3.4) and standardized to 1 mg/ ml. This was followed by plating 50 µl of the samples into separate wells of a 96 well plate where the lysates were incubated in 50 µl of 2X Assay buffer composed of: ortho-nitrophenyl-β-D-galactopyranoside (ONPG), MgCl2, and sodium phosphate all of which were utilised by Lee et al., (2006) for their soluble β-galactosidase assay. The mixture was incubated at 37 °C and allowed to react over a sixteen hour period. It must be noted that negative controls comprised of lysis buffer and assay buffer only were included in the experimental procedure. Afterwards 150 µl of sodium carbonate was added to the mixture to halt the reaction, where the plate was then read at 420 nm using the Sunrise™ ELISA reader (Tecan, Männedorf, Switzerland). The procedure was performed in triplicate with three biological repeats for both transfected and non-transfected HEK293 and MRC 5 cells.

3.8 Assessment of telomerase activity in HEK293 and MRC 5 cells

In order to determine whether the overexpression of LRP::FLAG subsequently influenced telomerase activity *in vitro* the TRAPeze RT Telomerase detection Kit (Merck Millipore, USA) was used. The procedure was carried out according to the manufacturer's protocols with a few minor amendments. Firstly, cells were harvested and washed in 1X PBS, after which they were suspended and lysed in 200 µl of CHAPS lysis buffer ((3-((3-cholamidopropyl) dimethylammonio)-1-propanesulfonate)) containing: 1 % CHAPS, EDTA, NaCl, and Tris-HCl that was provided with the kit. This lysis buffer was utilized as it is non-denaturing and capable of extracting active enzymes. The samples were then incubated in the lysis solution for 30 min at 4 °C with constant agitation. After the incubation the samples were centrifuged at 10 000 xg for 30 min at 4 °C to pellet all cell debris. The samples were transferred to new eppendorf tubes and an aliquot of 20 µl was taken for protein quantification using the NanoDrop® ND-1000 (Thermo Fisher Scientific, Massachusetts, USA). Thereafter, the samples were standardised to 500 ng/µl for all: samples, positive controls and heat treated controls. Prior to qPCR analysis, the heat treated controls were incubated at 85 °C for 20 min to inactivate and denature the enzymes within the samples. All samples were then subjected to experimental analysis by qPCR accompanied by: series dilution (1:10) of TSR8 standards (20–0.2 amoles) for generation

of a standard curve, positive control (cell extract confirmed to exhibit telomerase activity) and three negative controls: CHAPs lysis buffer only controls, no template control (water), and the heat treated samples. The qPCR reactions were carried out in the Roche LightCycler LC480 (Roche, Basel, Switzerland) where all experiments were performed in triplicates with the following cycling conditions: 37 °C for 30 min to allow the extracted telomerase enzymes to extend the telomeric substrate, 95 °C for 2 min and 45 cycles of 95 °C for 15 sec, 59 °C for 60 sec and 45 °C for 10 sec (where the fluorescent reads were taken). Thereafter, telomerase activity was calculated from the TSR8 standard curve and the data was analysed using the LightCycler1 Software version 1.5.1.

3.9 DNA isolation from HEK293 and MRC 5 cells for telomere length assessment

3.9.1 DNA isolation from cell pellets

Prior to assessing relative telomere length in the cells, DNA isolation was first carried out on harvested cell pellets using the Gene Jet DNA extraction kit (Thermo Fisher Scientific, Waltham, Massachusetts, USA) following the manufacturer's instructions. Briefly, cells were harvested and washed in 1X PBS and incubated in a mixture of 200 µl TE buffer (Table 8.6), 200 µl lysis solution and 20 µl proteinase K for 10 min at 56 °C with occasional vortexing. Thereafter, the mixture was supplemented with 20 µl of RNase and incubated for an additional 10 min in order to remove all RNA contaminants. Following RNA removal 400 µl of 50 % ethanol was mixed to precipitate the DNA and the mixtures were then transferred to purification columns. The columns were centrifuged at 6000 xg for 1 min to allow the mixture to flow through the column where DNA was selectively bound. Following this, the purification columns went through two rounds of washes, where the first wash was performed by adding 500 µl of wash buffer onto the columns and centrifuging the columns at 8000 xg for 1 min. The second wash was performed in a similar manner except the columns were centrifuged at max speed for 3 min to dry the column and ensure the complete removal of ethanol (present in the wash buffer). DNA samples were then eluted into DNase/ RNase free eppendorf tubes by adding 200 µl of elution buffer to the columns and subsequently centrifuging at 8000 xg for 1 min. The DNA was then resolved on a 1% agarose gel to assess genomic integrity and subsequently quantified using the NanoDrop® ND-1000 (Thermo Scientific, Massachusetts, USA) to a working concentration of 50 ng/ µl. All DNA samples were then frozen and kept at -20 °C until used in downstream applications.

3.9.2 Assessment of mean telomere length from cultured cells

The relative mean telomere length was assessed in order to determine whether the overexpression of LRP::FLAG aided in the stimulation of telomeric extension. To this end the qPCR-based procedure described by Cawthon et al., (2002)[388] was used. All qPCR reactions were performed using the appropriate primers and Sensi-Fast SYBR green master mix [(Bioline, London, UK) (Table 8.14)]. Samples were plated in triplicates and a set of controls were included for every run: a positive control (DNA isolated from HEK293 cells that was previously confirmed to amplify) as well as a no template control (negative control). Firstly, the reference gene acidic ribosomal phosphoprotein [(36B4) (for primers see Supplementary Table 8.18)] was quantified for normalisation purposes in order to account for any sample to sample variance between the isolated DNA samples, thus ensuring the accuracy of the assay. After ensuring that the reference genes exhibited more or less equivalent reads; qPCR was undertaken to assess telomere length by use of the Tel 1 and Tel 2 primers (Supplementary Table 8.18). All plated samples for both 36B4 and telomere length analysis were run in the Roche LightCycler 480 (Roche, Basel, Switzerland) with the following cycling programme: Denaturation at 95 °C for 10 min followed by 45 amplification cycles of: 95 °C for 10 sec, 58 °C for 10 sec and 72 °C for 60 sec. Post amplification the reads generated were analysed where the [2ΔCT (telomeres)/2ΔCT (36B4)] equation was used to calculate the mean telomere length that was then compared between samples.

3.10 Animal trials and treatments

The study included the use of female C57BL/6J mice at approximately 12 months of age that were obtained from Charles River Laboratories, USA. Forty mice were acquired and 36 of these mice were randomized into the 3 treatment groups. These groups included group 1, which received the pCIneo-moLRP::FLAG plasmid and TurboFect^{TM} *in vivo* Transfection Reagent (Thermo Fisher Scientific, Massachusetts, USA) to induce an overexpression of LRP::FLAG. Group 2 received the empty pCIneo plasmid and transfection reagent which served as a vector control. Lastly group 3, which received a 5% glucose solution that served as a vehicle control. The TurboFect^{TM} transfection reagent was used as it has been shown to improve gene delivery to various organs and improve overall transfection efficiency. The mice were housed in separate cages (standard plexiglass, 28x 12x 16cm) with sawdust for bedding and provided with free intake of food and water, 22±2 ℃, humidity 50–60 % and a 12 hr light: dark cycle. Additionally, mice were supplied with paper towel for nest building as well as plastic blocks and balls for entertainment. Before the commencement of the study one mouse had to be terminated due to a persistent rectal prolapse that caused terminal weight loss.

The remaining 3 mice were used to optimise the treatment plan. This included assessing two different treatment plans: 2 tail vein injections spaced 10 days apart as well as a tail vein injection and an intramuscular injection spaced 10 days apart. Thereafter, telomerase activity and general mouse fitness was assessed to select the optimal treatment plan.

The selected treatment plan involved the use of 2 different administration routes namely: a tail vein injection to the lateral tail vein and an intramuscular injection into the right and left quadriceps of the mice with treatments spaced 10 days apart. Thereafter, the treatment was repeated ±5 months after the initial treatment. The treatments were conducted in this manner to ensure a widespread delivery of the plasmid to various tissue sites and ensure an ideal transfection efficiency is maintained. All treatments were performed according to the manufacturer's recommendations. Briefly, the tail vein injection involved diluting 50 µg of purified plasmid DNA in 400 µl of sterile 5 % glucose solution with the addition of 6 µl of the TurboFect™ *in vivo* Transfection Reagent, which followed the manufacturers recommendations. After a 15-20 min incubation at RT to allow the cationic polymers in the transfection reagent to form positively charged complexes with the plasmid DNA, the mice received 400 µl of the plasmid solution via tail vein injection or 400 µl 5 % glucose as vehicle control. The intramuscular injection involved diluting 85 µg of purified plasmid to a volume of 86 µl in sterile 5 % glucose with the addition of 4 µl of the TurboFectTM *in vivo* Transfection Reagent. The amount of plasmid utilised for the intramuscular injections was based off recommended amounts from Tripathy et al., (1996) [389]. Moreover this particular amount was selected to ensure that each quadriceps received 40 µg of plasmid for optimal transfection efficiency. Following, a 15 min incubation at RT, the mice received 100 µl of the plasmid solution or 100 µl of 5 % glucose as vehicle control by intramuscular injection at to the right and left quadriceps (50 µl per injection).

After the treatments were administered the mice were monitored daily for the formation of any adverse side effects or inflammation. Thereafter, physiological tests were carried out 2 months after the first round of treatments to allow for a sufficient span of time to induce a measurable change. The second round of treatment was performed 10 days before euthanization to ensure a biochemical change would be detected. The mice were terminated at approximately 19 months of age, as between 18-24 months the mice are considered "old" according to The Jackson Laboratory (Hagan, C., https://www.jax.org/ news-and-insights/jax-blog/2017/november/when-are-mice-considered-old,Accessed 2019/09/01). Furthermore, it is from 18 months of age that senescent changes in most biomarkers become evident. No mice were set aside for a survival test as 3 mice from the control group died during the course of the second treatment from anaemia, a common condition in senior

mammals. Other mice that had to be terminated prematurely included: 1 mouse from the treated group due to the development of cancer (severely enlarged spleen with evidence of metastases), 1 mouse from the control group due to a persistent anal prolapse, 1 mouse from the control group inflicted extensive self harm by mutilating both ears and experienced terminal weight loss overtime, 1 mouse from the control group as it developed a bacterial or viral infection and 1 mouse from the non-treated group due to a persistent rectal prolapse. All experimental procedures were performed with approval by the University of the Witwatersrand Animal Ethics Screening Committee (clearance certificate number: 2016/08/38/B).

3.11 Hair greying analysis

Hair greying is a common consquence of ageing due to a loss of melanocytes and persistent oxidative stress where normal pigmentation is gradually lost. This accumulation of senescent hair follicles offers a relatively simple approach to track progression of the ageing process. The technique encompassed imaging all the mice prior to termination, in a brightly lit room where they were placed on a neutral green background to minimise light and colour interferance. Thereafter, the mice were coaxed to grab a wooden rod with their forepaws and gently streched out, where they were then imaged using a Canon E05 450D. These images were then analysed using Gandalf the Grey, an in-house developed software by Dr G. Morris. The software measured the amount of grey and white pixels present on a mouse's coat. This data was then presented as a percentage when compared to the total amount of black pixels present on the coat.

3.12 Physiological tests to assess organism fitness

3.12.1 Puzzle box test

This test was carried out to assess the effects that the treatment (overexpression of LRP::FLAG) exhibited on the following cognitive abilities of the mice: short and long term memory as well as puzzle solving ability. The protocol was adapted from Ben Abdallah et al., (2011) [390] and slight modifications were incorporated. The testing arena comprised of a white container separated by a detachable barrier into two compartments: an empty brightly lit start zone (67 cm long, 25.5 cm wide) and a smaller dark and covered goal zone (15 cm long, 25.5 cm wide) filled with sawdust to mimic a nesting area. The mice were placed into the testing arena with no barrier in place and were allowed to habituate the box for 5 min. Thereafter, the mice were removed from the container while the barrier was put into place before re-introducing the mice into the start zone. This allowed them to travel into the goal zone by entering a narrow underpass (±4 cm) set into the barrier. The mice were

then subjected to a total of 9 trials (T1- T9) of increased complexity over a 3 day period, with 3 trials per day. During this period the mice had to solve challenges where the underpass was blocked with various obstructions (with each new succeeding obstruction deemed to be more challenging). On the first day (which was considered training) the mice were tasked with entering the underpass that was un-obstructed. During T1 the top of the underpass was uncovered while in T2 and T3 the top of the underpass was covered, and the mice were timed until they entered the underpass. On the second day (burrowing puzzle), T4 was carried out in the exact same manner as T2 and T3. During T5 and T6, the first puzzle was introduced where the underpass was filled with sawdust and mice had to dig through the sawdust to locate and enter the underpass. On the third day (plug puzzle), T7 was performed as a repetition of T5 and T6. However, during T8 and T9 a more complex puzzle was introduced, where mice were challenged with the plug puzzle. This involved obstructing the underpass with rolled up gauze that was covered in sawdust, which required the mice to firstly burrow and then use their paws and teeth to pull or push the gauze out of the underpass to enter the goal zone. The setup of these trials in this manner allowed for the assessment of problem solving ability (T5 and T8), learning and short term memory (T3, T6 and T9), while the repetition on the next day provided an efficient means of evaluating long term memory (T4 and T7). The mice were assessed based on their performance by measuring the time taken to enter the goal zone with all 4 paws or the trial was ended after a period of 3 min. All tests were video recorded using a Canon E05 450D to aid in obtaining accurate time points.

3.12.2 Nesting Test

Nest building is a common behaviour in mice that has been shown to become impaired during cognitive dysfunction or decline [391]. As ageing causes a decline in motor function, natural behaviour and cognitive function, this test therefore allows a non-stressful and efficient means of assessing behaviour deterioration in aged mice. Morover, this detrioration in nest building ability has been confirmed in the C57BL/6J mouse strain [392]. The test was carried out in the mouse's "home" cage and involved firstly removing all old nesting material from the cages. A single sheet of paper towel was then placed into each cage in more or less the same location and left overnight. The nests the mice constructed were then imaged and graded the following day according to a 6 point scoring system: (1) Paper towel was not noticeably touched or manipulated, (2) Paper towel exhibited slight folding with no tearing or flat paper towel with minimal tearing, (3) Partial folding and minimal tearing of paper towel, (4) Identifiable nest, with partial folding and shredded material, (5) Nest with

well-developed walls, with a distinct amount of folding and/ or shredding, (6) Nest in the shape of a cocoon with partial or complete roof. All nests were imaged with a Canon E05 450D for analysis.

3.12.3 Motor function analysis using the balance beam test

One of the core physiological parameters affected by age-dependent decline is motor function, which includes balance co-ordination due to the degeneration of muscle tissue and a stiffening of the joints. Therefore, tests aimed at assessing these physiological aspects provide an efficient means of evaluating age retardation treatments efficacy. The test that was utilised to assess these parameters was the balance beam test [393], which assessed whether the overexpression of LRP::FLAG was able to prevent a loss of muscle strength and balance in mice as it is commonly associated with aged individuals. The procedure involved using 1 m long beams with a width of 12 mm that was suspended between two poles; approximately 50 cm above the surface. In order to ensure that the mice would not injure themselves in the event of falling, a box containing copious amounts of cushioning material (sawdust and paper towel) was placed underneath the beam. The mice were then placed at one end of the beam while the other end housed a platform and goal box containing nesting material from the home cage as well as food [393]. Thereafter, the mice were allowed to traverse the beam. All tests were video recorded using a Canon E05 450D for data collection purposes where the time it took the mice to traverse the beam as well as the approximate number of foot-slips was analysed [393].

3.13 Organ harvest

After all the physiological tests and the second round of treatments had been completed the mice were euthanized and transcardially perfused with cold 1X PBS in order to remove the blood from the organs. This was to ensure that the blood did not coagulate within the organs and thereby compromise histological and biochemical analysis of the tissues. The mice were approximately 19 months of age at the time of euthanization. The total number of mice terminated at the end of the study included: 10 mice from the treated group, 7 mice from the vector control group and 11 mice from the vechile control group (Non-treated). The following organs were dissected from the mice: brain, colon, heart, kidney, liver, lung, muscle tissue and spleen. Each organ was sectioned into 2 portions; 1 portion for biochemical analysis and the other for histological analysis. The organ portions for biochemical analysis were snap-frozen in liquid nitrogen and stored at –80 °C until used. This was performed to preserve the nucleic acids, proteins and enzymatic activities of the various tissues and minimise sample degradation. The organ portions for histological analysis were placed in

specimen jars and fixed in 4 % PFA. This was done to preserve the tissue structure for efficient identification of structural patterns or differences between the treatment groups during histological analysis. Briefly, the organs were fixed for 24 hr at 4 °C after which they were rinsed with 1X PBS. Thereafter, the organs were placed in a 30 % sucrose solution and incubated for 3 days in order to displace all water from the organs as paraffin (used in downstream processing) is hydrophobic and will not penetrate wet tissue. The samples were then stored in 4 % PFA to prevent contamination until further analysis was performed. It must be noted that organs from 1 mouse in the non-treated group and 1 mouse from the group treated to overexpress LRP::FLAG were harvested, but were not analysed further due to the possible formation of cancer as enlarged spleens similar to the previously mentioned treated mouse were observed.

3.14 Histological analysis

Histological sectioning and staining of the following organs: skin, brain, kidney, liver, and muscle were performed by Ms. Hasiena Ali, Senior Technician, School of Anatomical Sciences, Faculty of Health Sciences, University of Witwatersrand (Johannesburg, South Africa). All organ samples were firstly embedded into paraffin, where the process involved: immersion in 70 % ethanol with two changes of solution (1 hr for each change), thereafter the samples were moved into 80 % ethanol with a single change of the solution after an hour. The organs were then immersed for 1 hr in 95 % ethanol, which was followed by three 1.5 hr changes in 100 % ethanol. The use of an ethanol gradient was done to ensure all water content in the organs had been removed. The samples were then cleared in Xylene with three changes of the solution (1.5 hr each), which essentially bleaches the tissue to ensure that the only form of colour observed on the sections will be a consequence of the respective tissue stain used. Organ samples were finally immersed in molten paraffin wax (58-60 °C) for 2 hr with 2 changes in wax performed to allow complete paraffin penetration of the tissues. These samples were then embedded into paraffin blocks. The blocks were then trimmed and 5 µm thick sections were cut using a microtome. The sectioned tissue (paraffin ribbons) were then placed into a water bath (40- 45 °C) and floated onto glass slides. These slides were then allowed to air dry overnight followed by a deparaffinising step where sections were cleared in 2-3 changes of chloroform (10 min each). Sections were then rehydrated by: 2 changes in absolute ethanol (5 min each), 95 % ethanol for 2 min and 70 % ethanol for 2 min. The rehydrated sections were then briefly washed with distilled water, where afterwards they were stained with Hematoxylin solution (8 min) and washed under warm running water for 10 min. Prior to counterstaining in Eosin (1 min) sections were rinsed in distilled water and dipped in ethanol up to 10 times. Upon staining completion, the

sections were dehydrated in 95 % ethanol (2 changes of 5 min each) and were again cleared in chloroform (2 changes of 5 min each) to remove excess stain. Finally, samples were mounted in a mounting medium where they were then visualised and imaged using the Zeiss Primovert microscope (Zeiss, Oberkochen, Germany). Images were assessed with the aid of Prof R. B. Veale. In this manner the images were assessed for tissue atrophication and degeneration to confirm whether overexpression of LRP::FLAG prevented or impeded the age-dependent decline of various tissue types.

3.15 Assessment of proliferative and senescent gene expression in various mouse organs by qPCR

The mRNA expression levels of various genes involved in key proliferative and senescent pathways were assessed to observe how the overexpression of LRP::FLAG influenced these markers. The procedure involved the extraction of RNA from mouse tissue samples and subsequent cDNA synthesis, prior to qPCR amplification.

3.15.1 Tissue RNA extraction

RNA was extracted from frozen tissue samples of the brain, kidney and liver for the quantification of various proliferative as well as senescent gene expression levels. The RNA was extracted using the Nucleospin® RNA kit (Macherey-Nagel GmbH & Co. KG, Düren, Germany) by following the manufacturer's protocol. Firstly, about 30 mg of frozen tissue was weighed out per organ and placed into sterile RNase free tubes containing 350 µl of lysis buffer RA1 as well as 3.5 µl of β-mercaptoethanol. The samples were then homogenised with a Dounce homogenizer for 30 sec to disrupt the tissue and allow for a more efficient lysis of the cells. Thereafter, the homogenates were passed through a 20 gauge needle around 5-6 times to further facilitate cell lysis and shear the genomic DNA. This aided in DNA digestion and DNA removal during the subsequent steps. The lysates were then loaded onto a NucleoSpin® filter column and were centrifuged at 11 000 xg for 1 min, in order to filter out tissue debris and reduce the viscosity of the solution. Thereafter, the column was discarded and 350 µl of 70 % ethanol was added to the filtrate followed by mixing through gentle pipetting to ensure adequate precipitation of the RNA.

This was followed by loading the lysates onto NucleoSpin® RNA columns which selectively bound the genomic material and were centrifuged at 11 000 xg for 30 sec. After discarding the filtrate, the columns were then desalted using 350 µl of membrane desalting buffer (MDB) that was centrifuged

at 11 000 xg for 1 min. This desalting step aided in making the subsequent DNase treatment more effective. The on column DNase treatment was carried out in order to remove residual DNA thereby preventing off target amplification during qPCR. The DNase treatment was prepared by mixing 10 µl of rDNase with 90 µl of Reaction Buffer, which was loaded onto the columns and incubated at RT for 15 min. The RNA was then washed with 200 µl of Buffer RAW2 to inactivate the DNase, which was then removed by centrifugation at 11 000 xg for 30 sec. The columns were transferred into new collection tubes and a second wash was performed using 600 µl of Buffer RA3, where the flow through was then discarded after centrifugation at 11 000 xg for 30 sec. This was followed by a third wash using 250 µl of Buffer RA3 which was cleared by centrifugation at 11 000 xg for 2 min to completely dry the column. Finally, the RNA was eluted from the column using 70 µl of RNase-free H_2O and centrifuging at 11 000 xg.

As tissues are rich in DNA content, often an on column DNase treatment is not sufficient to remove all the DNA contaminants. Therefore, to ensure that all extracted RNA samples were completely DNA free, an additional in-solution DNase treatment was performed using the Turbo DNA- free™ kit (Thermo Fisher Scientific, Massachusetts, USA). The procedure involved gently mixing 0.1 volumes of 10x Turbo DNase Buffer and 1 µl of Turbo DNase to the RNA samples. The samples were then incubated at RT for 30 min. After DNA digestion was completed, 0.1 volumes of DNase Inactivation Reagent was added to the samples and incubated for 5 min with occasional mixing. The samples were centrifuged at 10 000 xg to pellet the DNase that was coupled to the inactivation reagent. The purified RNA samples were transferred to a new Eppendorf tube where an aliquot was taken to resolve on a 1 % agarose gel (w/ v) to assess RNA integrity (see supplementary Table 8.6-8.8) and also quantify using the Nanodrop One (Thermo Scientific, Massachusetts, USA).

3.15.2 cDNA synthesis from tissue isolated RNA

Total RNA was quantified for each sample using the NanoDrop One (Thermo Fisher Scientific, Massachusetts, USA) and cDNA was synthesised using the SensiFAST™ cDNA Synthesis Kit (Bioline, London, UK) following the manufacturers protocol. Briefly, for each sample 1 µg of pure RNA was mixed with 4 µl 5x TransAmp Buffer, 1 µl of reverse transcriptase and was made up to 20 µl using DNase/ RNase free water. In addition, a no reverse transcriptase (RT) control was made up for each sample by following the above recipe with the exclusion of the reverse transcriptase. Thereafter, the samples were placed in the MultiGene™ OptiMax thermal cycler (Labnet, New Jersey, USA) with the following amplification programme: 25 °C for 10 min (to allow primer

annealing), 42 °C for 15 min (for reverse transcription), 48 °C for 15 min (to compensate for highly structured RNA), and 85 °C for 5 min in order to stop the reaction. Thereafter, the cDNA was stored at -20 °C until required for downstream qPCR.

3.15.3 Mouse gene expression analysis by qPCR

After the successful production of cDNA, qPCR analysis was carried out to determine the gene expression levels of a number of markers tightly linked to the ageing process (Table 8.16). Prior to assessing the genes of interest (Table 8.16), two reference genes (GAPDH and RPLPO) were evaluated in order to normalize the genes of interest to eliminate sample to sample variation. Briefly, a master mix containing Luna® Universal qPCR Mastermix (New England Biolabs, Massachusetts, USA), primers and water (Table 8.14) were plated into individual wells of a 96 well plate. Thereafter, cDNA from each sample was loaded into separate wells and qPCR was conducted with the CFX96™ Touch qPCR System (Bio- Rad, California, USA) using the following cycling parameters: an initial denaturation at 95 °C for 3 min was followed by 40 cycles of denaturation at 95 °C for 10 sec and a combined annealing/ extension step carried out at a primer specific temperature (Table 8.16) for 30 sec. In addition, a melt curve was also generated to ensure amplification specificity, and that only a single product was produced (Appendix B, Figure 8.12-8.24). The threshold cycle (Ct) for each sample was interpreted using the Bio-Rad CFX Maestro analysis software.

3.16 Assessment of proliferative and senescent protein marker levels

SDS PAGE and western blotting was used as the standard experimental procedure for protein quantification of the mouse tissue samples. The tissues selected for protein comparison included: brain and liver. Firstly, LRP::FLAG was assessed in order to confirm its successful overexpression. In addition, total LRP/LR was also assessed in order to provide an indirect confirmation that total LRP levels were elevated in mice treated to overexpress LRP::FLAG (tissues assessed included: brain, kidney and liver). In addition to evaluating LRP::FLAG and LRP/LR, the levels of TERT, pTERT, proliferative related proteins (Akt, pAkt, c-Myc, Klotho, MDM2, and *SIRT1*), senescent related proteins (γH2AX, NFκB, pMDM2, p53, and $p16^{INK4A}$) were quantified in the brain and liver tissue. This allowed for the confirmation of whether the overexpression of LRP::FLAG exerted a comparable effect on the senescence process as was observed in the *in vitro* study.

3.16.1 Protein extraction from tissue

All steps performed were carried out at 4 °C on ice. The frozen organ samples were firstly rinsed in 1X PBS containing protease inhibitors. Thereafter, the organs were transferred to a new 1.5 ml eppendorf tube and homogenized in 400 µl of cold 1X PBS with protease inhibitors using a Dounce homogenizer. This was carried out for 30 sec or until the solid tissue had been dissociated into the solution. The homogenized samples were then fractionated for varying downstream applications, where separate aliquots of 50 µl were taken for DNA extraction and assessment of telomerase activity. These aliquots were immediately snap-frozen on dry ice and stored at -80 °C until further analysis was performed. The remaining 300 µl of homogenate was then supplemented with 300 µl of 2x RIPA buffer and were re-homogenized for 20 sec. The samples were then incubated at 4°C for 30 min with agitation to allow for sample lysis. The samples were then centrifuged at 16 000 xg for 20 min to pellet all cell/ tissue debris, where the supernatant containing the soluble proteins was harvested and stored at -20 °C until further analysis was performed.

In order to normalise and ensure equal protein concentrations between samples were used in downstream applications, a BCA assay was performed as detailed in (section 3.4) with minor amendments. This included using BSA standards made by serial dilution (1:2) from 5 mg/ml to 0 mg/ml (5, 2.5, 1.25, 0.625, 0.313, 0.157 and 0 mg/ml), which was used to construct the standard curve that was utilised to determine the protein concentration of the various mouse organ samples. In addition, the plates were analysed using the Multiskan™ GO Microplate Spectrophotometer (Thermo Fisher Scientific, Massachusetts, USA) for the generation of the absorbance values.

3.16.2 Tissue protein profiles assessed by SDS PAGE and western blotting

All western blotting procedures performed for the *in vivo* study followed the same procedure outlined in section 3.5 with minor amendments. In regard to the transfer step of the procedure an alternative transfer apparatus was used namely, the Trans-Blot® Turbo™ Transfer system (Bio- Rad, California, USA) where transfer was performed at 25 V – 1.0 A for 30 min. In addition, all primary and secondary antibodies that were utilised for the mouse study are detailed in Table 8.21. Following the detection of the proteins of interest, the membranes were stripped of their respective antibodies and re-probed with antibodies targeting β-actin, which served as the reference protein for normalisation purposes. The procedure included washing the viewed blots in PBST twice for 5 min to remove the substrate. Thereafter, membranes were incubated in 10 ml of stripping buffer (Table 8.13) for 10 min with gentle agitation at RT, which was repeated once. The stripped membranes

were then subjected to three 5 min washes in PBST at RT with gentle agitation. The membranes were then blocked in 3 % BSA in PBST for 1 hr at RT with gentle agitation. The subsequent steps followed the general western blotting procedure detailed in (section 3.5). This protocol was followed for each protein analysed. In terms of analysis, the samples were fitted across 4 blots with a minimum of three samples per group. In addition one random technical repeat was performed for each group for blot 2, 3 and 4.

3.17 Assessment of telomerase activity in mice tissue

A modified version of the Telomerase Repeated Amplification Protocol was used to determine the effect of overexpression of LRP::FLAG on telomerase activity in the various aged mice organs (brain, kidney and liver). The fractionated homogenates [(40- 50 mg) (refer to section 3.15.1)] were placed into 200 µl of ice cold CHAPS lysis buffer and re-homogenized for 30 sec. The samples were then incubated for 30 min at 4 °C with constant agitation, to allow the tissue to be broken apart and for a complete lysis to occur. After lysis was complete the samples were centrifuged at 16 000 xg for 20 min at 4 °C to pellet the tissue and cell debris. The supernatant containing the isolated active proteins and RNA was snap frozen on dry ice for downstream analysis. Prior, to snap freezing a 20 µl aliquot was taken and used for protein quantification, which was performed using the NanoDrop One (Thermo Fisher Scientific, Massachusetts, USA). This was done to ensure that a final concentration of 5 µg/ µl was used for all experimental and control samples.

Thereafter, an in house TRAP assay was performed to quantify telomerase activity by qPCR. The samples were run alongside a set of TSR8 standards and the same set of controls as used in section 3.8. Briefly, 5 µg/ µl of protein samples were loaded into individual wells on a 96 well plate and mixed with the TRAP reaction mix (Table S2.14) to make up a total volume of 25 µl. The reaction mix was composed of the following: TS primer (this acted as a substrate for the telomerase enzyme), ACX primer (a modified version of the CX primer that contains a 6 base pair ‘anchor’, which aids in preventing primer self-amplification and reduces the formation of primer dimers) (Table 8.19), EGTA (to inhibit RNases and prevent degradation of the TERC template), 0.1 µg/ µl ultra-pure BSA (this acted as a PCR enhancer), Luna® Universal qPCR Mastermix (New England Biolabs, Massachusetts, USA) and DNase/ RNase free H_2O (Table 8.15). Thereafter, the plated samples were placed in the CFX96™ Touch qPCR System (Bio- Rad, California, USA) and qPCR was performed following the same run parameters as outlined in section 3.8; except the telomerase extension step was increased to 1 hr to allow for detectable extension of the substrate by the tissue derived

telomerase. The data generated was then analysed using the Bio-Rad CFX Maestro software which was used to quantify the relative activity of telomerase.

3.18 Telomere length and mitochondrial DNA content determination in mouse tissue by qPCR

3.18.1 DNA extraction from mice tissue

DNA was extracted from frozen tissue homogenates of the brain, kidney and liver for the quantification of telomere length using the Invisorb® Spin Tissue kit (Invitek Molecular, Berlin, Germany) and followed the manufacturer's protocol. Briefly, 400 µl of Lysis Buffer G and 40 µl of Proteinase S were added to the frozen tissue homogenates and vortexed for ±15 sec. The tube was then incubated at 52 °C with agitation until lysis was complete (when majority of homogenate had gone into solution). Thereafter, the samples were centrifuged at 11 000 xg to spin down tissue debris and the supernatant was transferred to a new eppendorf tube. The samples were supplemented with 40 µl of RNase A (10 mg/ml) and vortexed followed by a 5 min incubation at RT to allow for the degradation of the RNA within the samples. Prior, to loading the samples into the Spin Filter (in a 2 ml receiver tube), 200 µl of Binding Buffer A was added to the samples and vortexed for 10 secs. The samples were then allowed to incubate for 1 min with the Spin Filter to facilitate DNA binding before the samples were centrifuged at 13 500 xg for 3 min. After discarding the filtrate, 550 µl of the Wash Buffer was added to the spin column and centrifuged at 11 000 xg for 1 min, after which the flow through was discarded. The washing step was repeated once and followed by an additional centrifugation step at maximum speed to remove any residual ethanol from the Spin Filter. Finally, the Spin Filter was placed into a new eppendorf tube where 100 µl of pre-warmed elution buffer (52 °C) was added and incubated for 3 min. The samples were then centrifuged at 11 000 xg for 1 min to elute the DNA. Thereafter, sample aliquots were taken to resolve on a 1% agarose to assess intergrity (Figure 8.9-8.11) and were also nanodropped using the NanoDrop One (Thermo Scientific, Massachusetts, USA). The samples were then stored at -20 °C until further analysis was performed.

3.18.2 Relative Telomere length determination in mouse tissue by qPCR

This procedure was utilized to assess any changes in relative telomere length post-transfection in murine tissue; specifically within the brain, liver, kidney and spleen. This qPCR procedure followed the same setup as section 3.9.2 with minor amendments. This included the design of mouse specific primers for the reference gene 36B4 (Supplementary Table 8.18). In addition, both telomere length and 36B4 were quantified on the same plate for each organ assessed, where plates were run in

triplicates for each organ. The qPCR machine used for these procedures was the CFX96™ Touch qPCR System (Bio- Rad, California, USA) and the data generated was analysed using the Bio-Rad CFX Maestro software.

3.18.3 Mouse tissue mitochondrial DNA content analysis by qPCR

This procedure was carried out as mitochondrial DNA content acts as an efficient marker to track the senescence/ ageing process. In fact, aged cells readily produce an elevated amount of mitochondrial mass/ content, however these mitochondria are generally dysfunctional. This is due to the accumulation of mtDNA damage and mutations that induces an increased production of ROS for enhanced oxidative stress. In this regard, we assessed whether the overexpression of LRP::FLAG was able to aid the tissue in retaining a more juvenile state with a lower mitochondrial mass. To this end, primers specifically targeting the mitochondrial DNA as well as another set of primers targeting a reference gDNA region were used [(Table 8.17) [394]]. The procedure involved analysing both mtDNA and reference gDNA qPCRs on the same plate to ensure the greatest possible accuracy. Briefly, the master mix (Table 8.14) containing: Sensi-Fast™ SYBR green master mix (Bioline, London, UK), primers, nuclease free H_2O and each sample was pipetted into separate wells on a 96 well plate. In addition, a set of NTC controls were included for each primer set. Thereafter the CFX96™ Touch qPCR System (Bio- Rad, California, USA) was used with the following cycling parameters: an initial denaturation at 95 °C for 3 min was followed by 40 cycles of denaturation at 95 °C for 10 sec and a combined annealing/ extension step carried out at 60 °C (Table 8.17) for 30 sec. In addition, a melt curve was generated to ensure that only a single product was evident (Appendix B, Figure 8.25). Finally, the Ct for each sample was analysed using the Bio-Rad CFX Maestro analysis software.

3.19 Data and Statistical analysis

All experimental data collected was subjected to statistical analysis using Graphpad Prism, Microsoft Excel 365 ProPlus (Microsoft Corporation) and QuickCalcs Outlier Calculator ©2017 that makes use of the Grubbs test for the identification of outlier data points. All experimental procedures were performed with a minimum of 7 biological repeats with error bars representing standard deviation. This said all physiological tests were performed with Mice overexpressing LRP::FLAG (Treated): n = 10; Empty vector treated mice (Control): n = 11; Non-treated mice: n = 11. For histology, and all biochemical analyses with the exception of mRNA gene expression analysis the following group sample sizes were used: Treated: n = 9; Control: n = 7; Non-treated: n = 10 (except for western

blotting where n = 9 due to protein yield from one of the mice). It must be noted that due to time constraints only the brain and liver samples were assessed at a protein level by western blotting. These sample sizes were a consquence of all the pre-mature mouse deaths and terminations that are outlined in: section 3.10 and 3.13. In terms of the mRNA analysis the the following sample sizes were used for the 3 different organs: Brain: Treated: n = 6, Control: n = 5, Non-treated: n = 7; Liver: Treated: n = 9, Control: n = 7, Non-treated: n = 10 and Kidney: Treated: n = 9, Control: n = 7, Non-treated: n = 10. The brain samples had a reduced sample size due to poor RNA extraction within certain samples as the kit used was not specially tailored for brain extractions. These low extraction numbers for the brain RNA may then account for the lack of significance produced among the different genes tested. Therefore, the kit could not adqueatly process the samples due to the high fat content. In addition, it is unfortunate to note that the majority of the proteins could not be assessed in the kidney due to time contraints. This is also true for H2AX, where this protein could not be analysed due to time constraints, and furthermore a new antbody needed to be ordered in order to assess this marker these tissues. In terms of statistical analysis, the One-way ANOVA and Welch's *t-test* coupled with a *post hoc* Bonferroni correction were performed at a 95% confidence interval; where p values < 0.05 were considered statistically significant ($*p < 0.05$, $**p < 0.01$ and $***p < 0.001$)**.**

Brief overview of the ageing mouse study

The flow diagram below (Figure 3.1) gives a summarised overview of how the in vivo study was carried in a step wise manner, as well as what experimental procedures were carried out at a particular point. All procedures outlined were carried out on each of the three groups (Treated, control and non-treated mice).

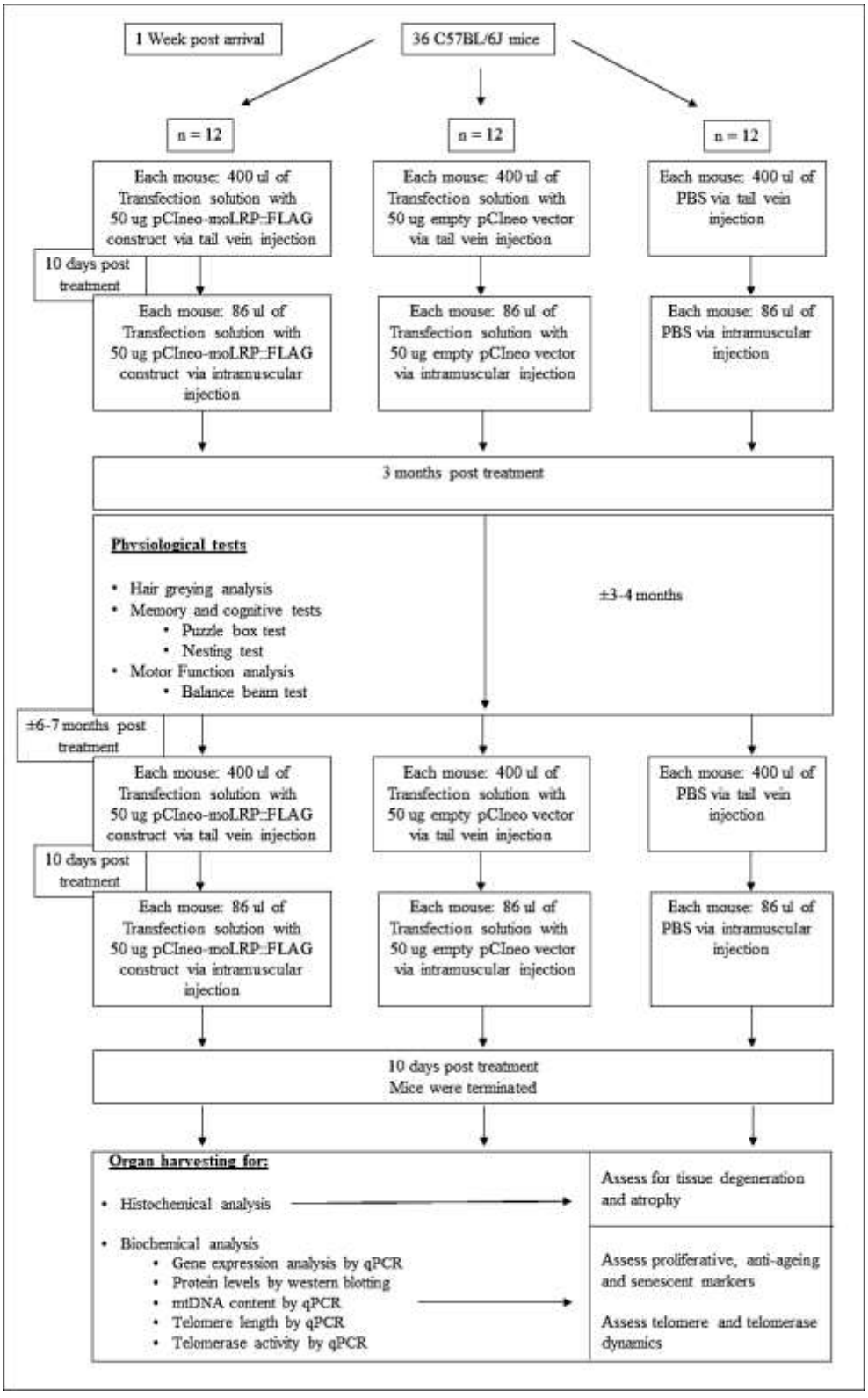


Figure 3.1: Flow diagram depicting timing of treatments to be received by each group.
A brief outline of the workflow that was performed during the ageing *in vivo* study to assess whether the overexpression of LRP::FLAG could impede the senescence process. Treatment procedures and time points are displayed as well as when the various different experimental procedures were carried out on the aged C57BL/6J mice.

4. Results

4.1 Overexpression of LRP::FLAG in HEK293 and MRC 5 transfected cells

In order to validate that LRP/LR does indeed influence the ageing process by affecting various aspects of telomere biology, stably transfected HEK293 and MRC 5 cell lines were generated utilising the pCIneo-moLRP::FLAG mammalian expression vector. This was essentially performed to induce an overexpression of LRP::FLAG, and thereby elevate the total amount of LRP/LR present within the cells. The successful overexpression of LRP::FLAG was confirmed by western blotting, where detection of the FLAG tag was only observed in the transfected HEK293 and MRC 5 cells (Figure 4.1 a,b illustrated in lanes 1-3). In addition, both LRP and the loading control β-actin were also assessed, where it was visually confirmed that the overexpression of LRP::FLAG caused an increase in total LRP levels (Figure 5.1).

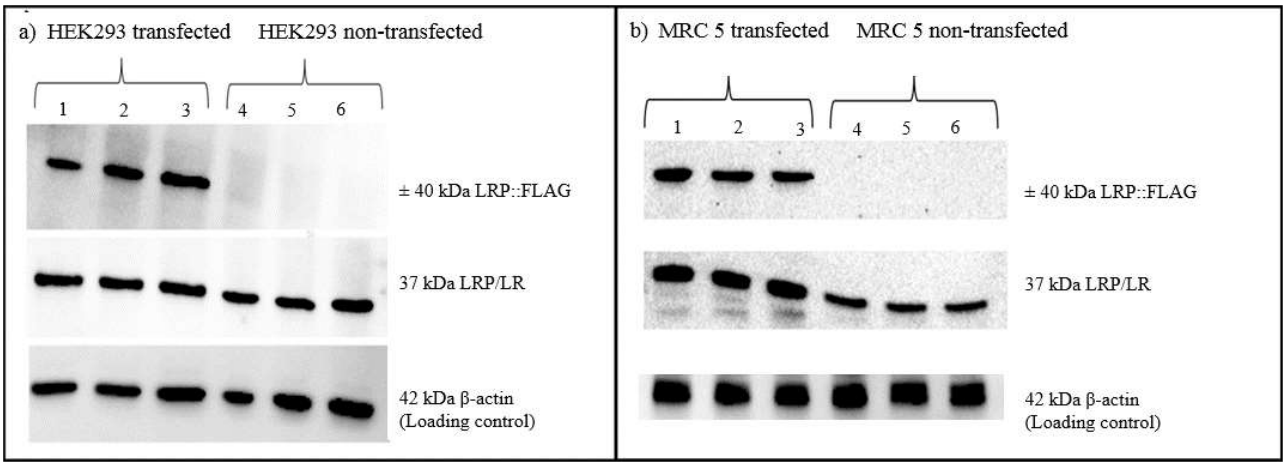
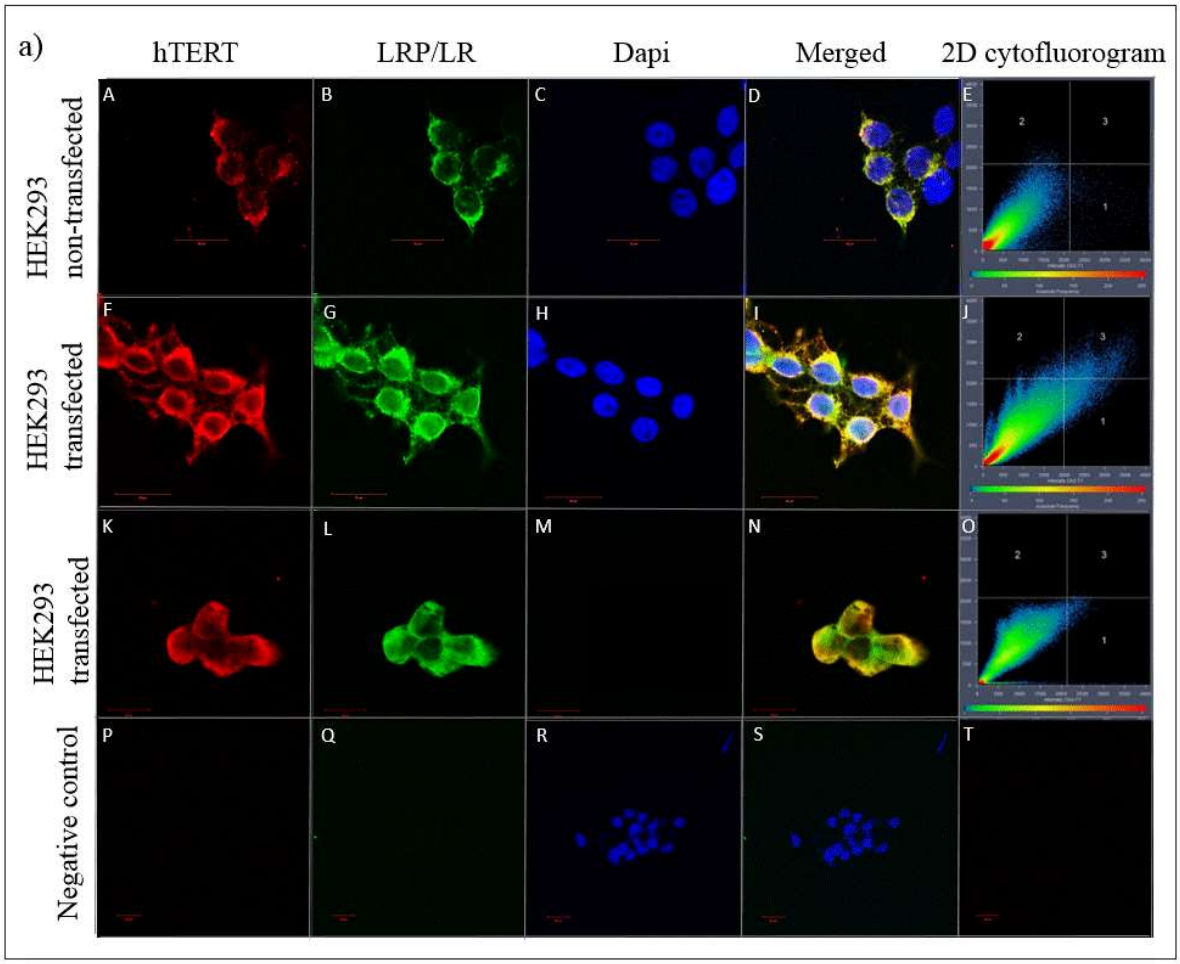


Figure 4.1: Overexpression of LRP::FLAG in HEK293 and MRC5 cells.
The expression of the LRP::FLAG protein was determined for both HEK293 and MRC 5 cells transfected with the pCIneo-moLRP::FLAG construct (lane 1-3) as well as non-transfected HEK293 and MRC 5 cell samples (lane 4-6). Analysis revealed that LRP::FLAG was found to only be expressed in HEK293 and MRC 5 transfected cell samples, with no LRP::FLAG detection in the non-transfected cell samples. Adapted from Otgaar et al., 2017 [293].

4.2 hTERT co-localises with LRP/LR and LRP::FLAG *in vitro*

Upon confirming the successful transfection of both the HEK293 and MRC 5 cells, immunofluorescence microscopy was employed; to firstly confirm the co-localisation in HEK293 cells and assess whether a similar effect was exerted in the somatic MRC 5 cell line. This was undertaken to evaluate whether a similar relationship existed in a somatic cell line with low to

undetectable levels of hTERT following the overexpression of LRP::FLAG. In addition, the technique was further utilised to assess the cellular localisation patterns of TERT and LRP and how the overexpression affects distribution patterns of the two proteins. The merged panels (Figure 4.2 a, b) are a representative of the red fluorescence (hTERT) and green fluorescence (LRP/LR and LRP::FLAG), where points of yellow fluorescence demonstrate a spatial overlap or co-localisation of the two proteins. In turn, this overlap also point towards a potential interaction that could exist between the two proteins. This said, co-localisation was observed between LRP/LR and hTERT in transfected as well as non-transfected HEK293 cells. In fact, this co-localisation was predominantly located intracellularly especially within the cytoplasmic and perinuclear domains of the cell confirming our previous findings [291]. Moreover, when transfected and non-transfected HEK293 cells were compared it was found that the overexpression of LRP::FLAG induced a pronounced increase in fluorescence intensity and co-localisation between LRP/LR and hTERT (Figure 4.2a; Panels: A, B, D, F, G and I). These findings were further validated by the 2D-Cytoflurograms (Figure 4.2a; Panels E and J) which displayed a much greater degree of co-localisation for the transfected HEK293 cell line. Surprisingly, upon analysing the MRC 5 cell lines a striking increase in LRP/LR and hTERT fluorescence was noted in cells overexpressing LRP::FLAG, when compared to the non-transfected cell lines which displayed negligible fluorescence for hTERT (Figure 4.2b; Panels A, B, C, E, F and G). This offered a clear display that LRP/LR was able to influence the expression and production of the TERT protein. In addition, like the HEK293 transfected cell line, the MRC 5 transfected cells displayed a pronounced co-localisation between LRP/LR and hTERT clearly indicating a potential interaction and relationship between the two proteins (Figure 4.2b; Panels C, and G). Finally to ensure that LRP::FLAG behaved in a similar manner to endogenous LRP/LR and also interacted with hTERT, the localisation of the protein was assessed in HEK293 cells only. To this end it was noted that LRP::FLAG shared a similar protein distribution pattern to LRP/LR and further co-localised with hTERT in a similar fashion (Figure 4.2a; Panels K, L, N and O). These findings indicated that the plasmid successfully produced LRP::FLAG and that it appeared to be fully functional and behaved in a similar manner to the endogenous protein.


a)
hTERT
LRP/LR
Dapi
Merged
2D cytofluorogram
HEK293 non-transfected
HEK293 transfected
HEK293 transfected
Negative control
A
B
C
D
E
F
G
H
I
J
K
L
M
N
O
P
Q
R
S
T
1
2
3

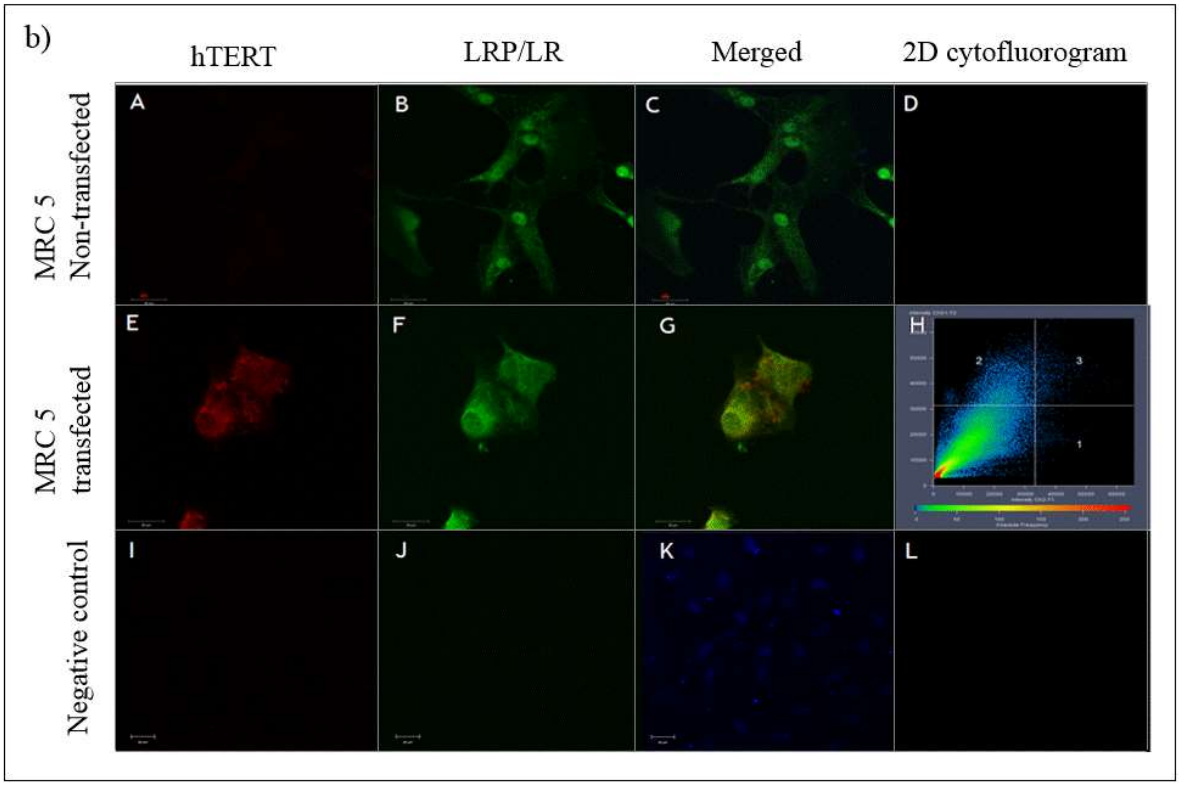

b)
hTERT
LRP/LR
Merged
2D cytofluorogram
MRC 5 Non-transfected
MRC 5 transfected
Negative control
A
B
C
D
E
F
G
H
I
J
K
L
1
2
3

Figure 4.2: LRP and LRP::FLAG co-localizes with hTERT.
a, b. Intracellular localization and co-localization patterns of hTERT and LRP/LR and hTERT and LRP::FLAG in transfected as well as non-transfected HEK293 and MRC 5cells. hTERT was detected with anti-hTERT primary and APC coupled secondary antibodies(a-A, a-F, a-K, b-A, b-E); LRP/LR was detected with anti-LRP/LR IgG1-iS18 primary and FITC coupled secondary antibodies (a-B, a-G, b-B, b-F); LRP::FLAG detected with anti-FLAG and FITC coupled secondary antibodies (a-L); Dapi nuclear staining (a-C, a-H, a-M, a-R); merge between LRP/LR and hTERT (a-D, a-I, b-C, a-G) and LRP::FLAG and hTERT (N) illustrates co-localization caused by the spatial overlap between the proteins. 2D Cytoflurograms confirmed that the overlap observed was co-localization between the proteins (a-E, a-J, a-O, b-H). Secondary antibody controls confirmed no auto-fluorescence or non-specific binding (a-P, a-Q, a-R, a-S, a-T, b-I, b-J, b-K, b-L). Images were taken at 630x and negative controls were obtained at 400x magnification. All scale bars are 20µm. Adapted from Otgaar et al., 2017 [293].

4.3 LRP::FLAG overexpression positively influences telomere dynamics to induce a significant increase in hTERT levels telomerase activity, and telomere length *in vitro*

The increased hTERT observed, especially within the MRC 5 transfected cells from confocal imaging, prompted the assessment of the various aspects of telomere biology. Moreover, the stimulation of telomerase by elevating TERT is sufficient to positively influence the ageing/ senescence process. This said, telomere attrition has been intricately tied to human ageing, due to the limited maintenance afforded by telomerase, thus providing additional motivation into its assessment. Firstly, western blotting was performed to confirm whether the overexpression of LRP::FLAG did indeed influence the TERT protein levels. Subsequent densitometric analysis revealed that the overexpression of LRP::FLAG in both HEK293 and MRC 5 cells induced a significant increase in total TERT levels when compared to their non-transfected counterparts (Figure 4.3 a1- b2). In fact, transfected HEK293 and MRC 5 cells displayed a 76.4% (n= 3, p= 0.0014, *t* test) and 433.11% increase (n= 3, p= 0.0312, *t* test) in hTERT, respectively when compared to their non-transfected counterparts (Figure 4.3 a1- b2). These results convincingly indicate that LRP/LR influences the production of TERT either through transcriptional or translational processes. What lends this observation further credence is that non-transfected MRC 5 cells displayed negligible TERT levels, whereas MRC 5 cells overexpressing LRP::FLAG displayed a distinct increase in TERT protein levels. Therefore, clearly indicating that LRP/LR may play a role in the transcriptional activation of the TERT gene.

In order to confirm whether the increased hTERT caused a subsequent elevation in telomerase activity following the overexpression of LRP::FLAG, real time qPCR with the TRAPeze RT telomerase detection kit (Merck Millipore) was performed. This was prudent to discern as elevated telomerase activity is the core factor that can aid in the impediment of telomere-dependent

senescence through its telomere maintenance ability. Similarly, it was found that the overexpression of LRP::FLAG caused a striking elevation in telomerase activity in both cell lines (Figure 4.3 c and d). Transfected HEK293 displayed a 2.937 fold increase (n=4, p=2.91E-05, *t* test) in activity, when compared to its respective non-transfected counterpart (Figure 4.3 c). Moreover, a similar trend was revealed in the MRC 5 cell lines, where overexpression of LRP::FLAG induced a striking 52.195 fold increase (n=4, p=2.38E-05, *t* test) in telomerase activity when compared to the non-transfected cells which displayed negligible activity of the enzyme (Figure 4.3 d). Thus, indicating that LRP/LR may play a role in the activation of the telomerase enzyme.

In order to elucidate if the elevated telomerase activity observed in both transfected cell lines was capable of providing a maintenance effect to the telomeric ends, qPCR was carried out following Cawthon et al., (2002) [388] and using the $[2^{\Delta CT\ (telomeres)}/2^{\Delta CT\ (36B4)}]$ equation. Prior to assessing telomere length, the reference gene 36B4 was evaluated to ensure an equivalent DNA content was utilized between the transfected and non-transfected cell lines. Thereafter, telomere analysis was carried out where a significant difference in mean telomere length was observed for both transfected HEK293 and MRC 5 cell lines after normalizing against the reference gene (Figure 4.3 e, f). The transfected HEK293 cells were found to exhibit a 2.236 fold increase (n= 4, p= 0.001909, *t* test) in average telomere length, while the MRC transfected cells at population doubling ±40 displayed a similar 2.839 fold increase (n= 4, p= 0.0002, *t* test) in length, when compared to their non-transfected counterparts (Figure 4.3 e, f). Therefore, confirming that the enhanced telomerase activity mediated by LRP::FLAG overexpression is capable of elongating the telomeres.

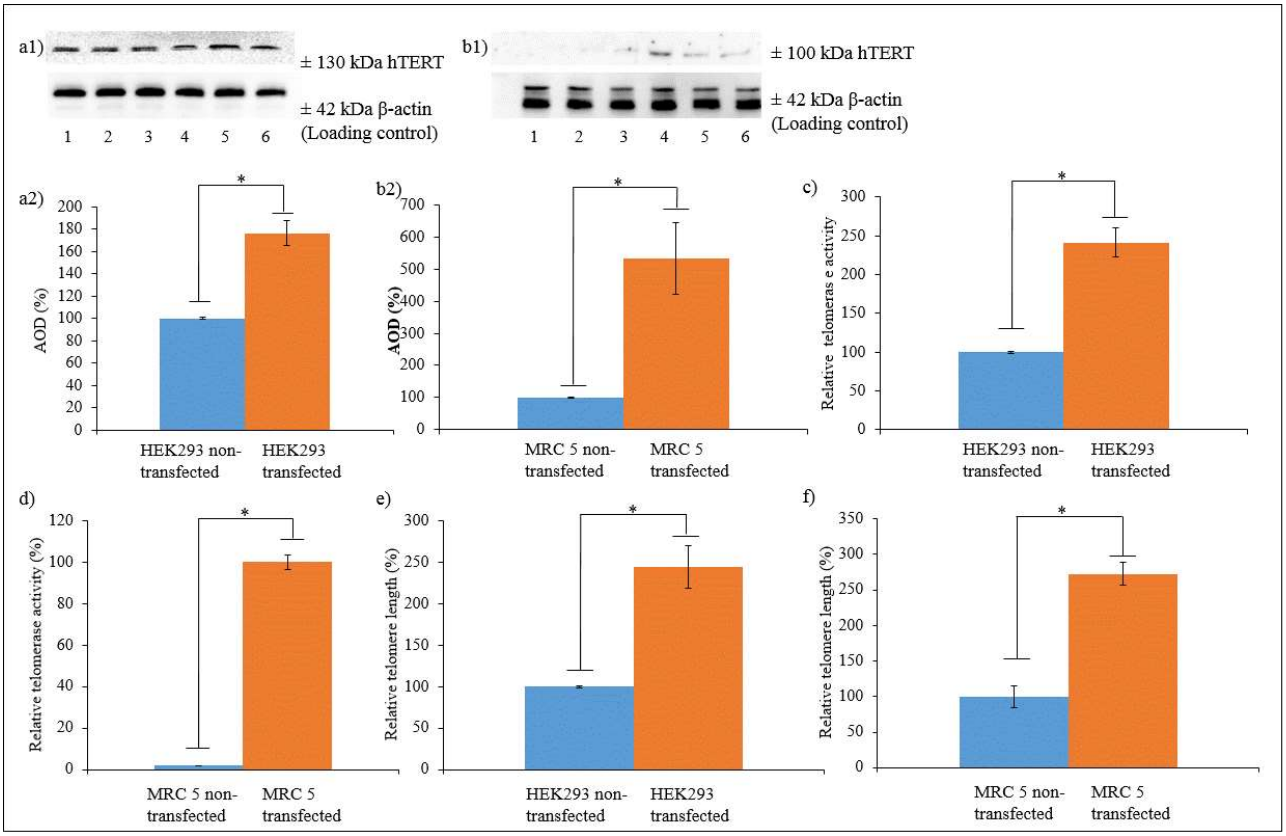


Figure 4.3: LRP::FLAG overexpression significantly elevates hTERT levels, telomerase activity and telomere length.
a-b, Western blot of hTERT levels in non- transfected (lane 1-3), and transfected (lane 4-6) HEK293 cells (a) as well as non-transfected (lane 1-3), and transfected (lane 4-6) MRC 5 cells (b). Densitometric analysis of hTERT expressed as a relative percentage in change respective to the non-transfected samples. c-d, Relative telomerase activity (RU=relative units) in non-transfected and transfected HEK293 (c) as well as MRC 5 (d) cells shown in Log concentration (Log amole). e-f, Relative telomere length in transfected and non-transfected HEK293 (e) as well as MRC 5 (f) lines as a telomere/36B4 (T/S) ratio to illustrate mean telomere length between samples. Sample size n= 3 biological repeats per cell line. Data as a mean ±SD. *p<0.05, **p<0.01, ***p<0.001 by paired *t-test*. Adapted from Otgaar et al., 2017 [293].

4.4 LRP::FLAG overexpression induces a significant reduction in tested senescent markers: β-galactosidase activity and γH2AX levels *in vitro*

As previously stated, the various aspects of telomere biology carry out essential roles in regulating the senescence or ageing process. The positive changes in telomere dynamics induced by LRP::FLAG overexpression provided sufficient motivation to assess whether an impediment of the senescence process had indeed occurred. To this end, the accumulation of two distinct senescent markers was assessed in response to the overexpression of LRP::FLAG. Firstly, β-galactosidase activity was assessed as the enzyme is known to be influenced by telomere shortening/ dysfunction and further accumulates within aged or senescent cells [387, 395]. In addition, this marker has been utilised in a number of studies to track or measure cellular ageing [387, 395]. Prior to assessment, all cell lines were allowed to undergo around 20 population doublings to ensure the accumulation of this

marker. The enzyme's activity was evaluated in all cell lines by incubating cell lysates with an assay buffer that contained ortho-Nitrophenyl-β-galactoside at pH 6 (reporter lysis β-galactosidase assay, Promega), that when reduced allows for the quantification of senescent associated β-galactosidase [387]. Interestingly, even though HEK293 cells displayed basal levels of enzymatic activity, owing to the fact that it is an immortalised embryonic cell line, a significant reduction of 0.111 fold [(10%) (n=3, p= 4,22E-05, *t* test)] in β-galactosidase activity was observed for HEK293 cells overexpressing LRP::FLAG (Figure 4.4 a). Furthermore, a significant decrease of 0.362 fold (±40%) in β-galactosidase activity (n= 3, p= 0.0008, *t* test) was also observed for MRC 5 cells overexpressing LRP::FLAG (Figure 4.4 b). Therefore, the decrease of this senescent marker in both transfected cell lines, especially the MRC 5 cells indicates the occurrence of a potential anti-ageing effect.

To further substantiate the results observed for β-galactosidase and that an impediment of the senescence process had indeed occurred, the levels of an additional senescent marker known as γH2AX foci were also assessed. These foci are histones that are specifically phosphorylated at Serine139 which ultimately act as markers to indicate areas of DNA damage, especially double stranded breaks [143, 396]. These markers are known to accumulate as cells age due to a combination of unresolved genomic damage and the continuous loss of the telomeric ends [143, 396]. Western blotting was performed and revealed that the overexpression of LRP::FLAG in both HEK293 and MRC 5 cells induced a significant decrease in γH2AX levels (Figure 4.4 c and d). In fact, transfected HEK293 cells exhibited a 60.78% (n= 3, p= 0.0017, *t* test) decrease, while transfected MRC 5 cells revealed a 40% (n= 3, p= 0.009, *t* test) reduction in γH2AX levels when compared to their respective non-transfected cell lines. The reduction of this marker alongside the reduced β-galactosidase activity clearly indicates that the overexpression of LRP::FLAG *in vitro* is capable of impeding the senescence process. Although, the HEK293 cell line displayed a significant reduction in both senescent markers, it must be highlighted that the levels of these markers, even in the non-transfected lines, were exceptionally low (basal levels). Therefore, these reductions may in part be due to the extensive sub-culturing or other appropriate stresses that these cells were exposed to. Additionally, basal levels of these markers have been previously reported in exceptionally low amounts [397, 398].

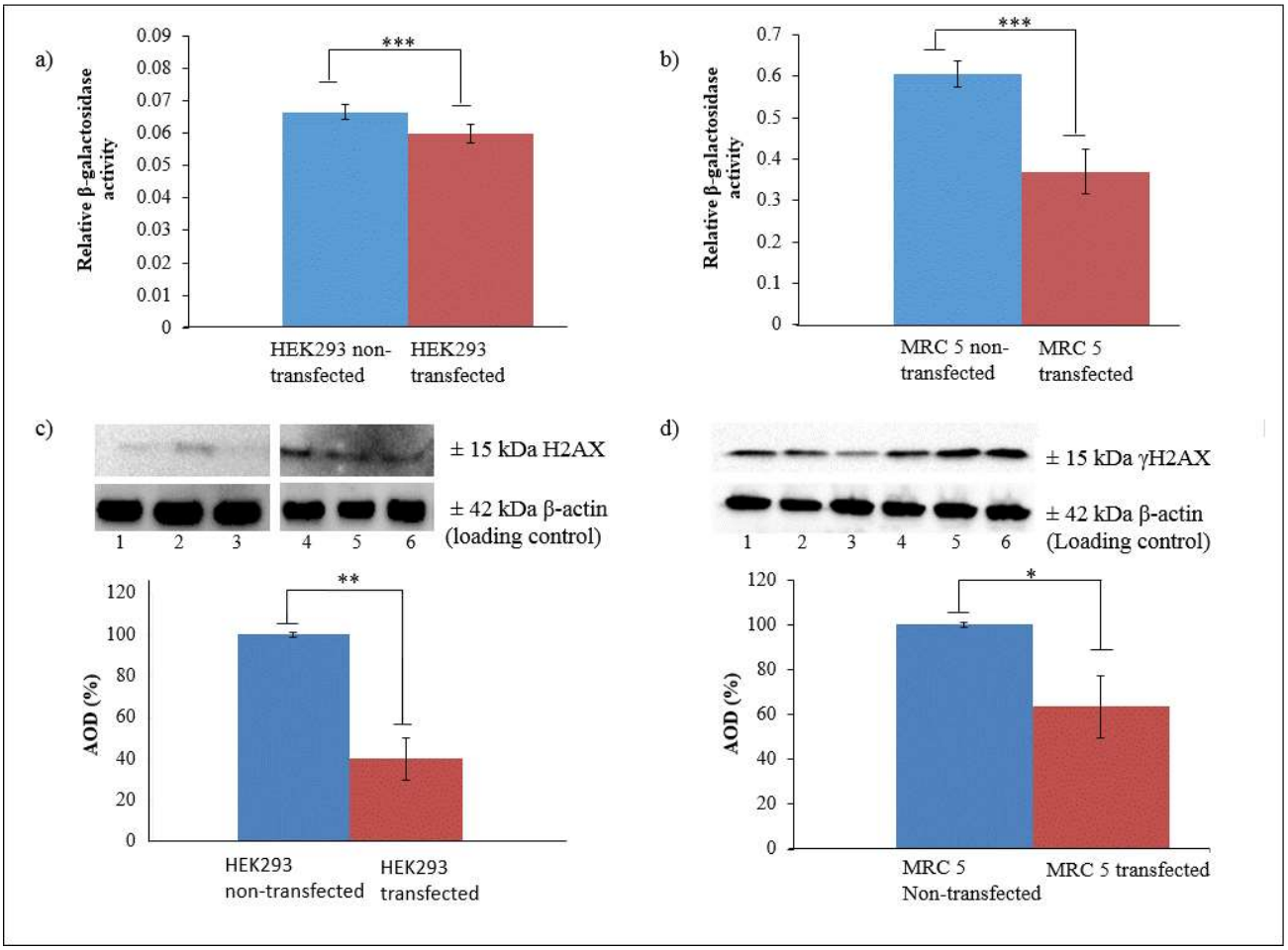


Figure 4.4: LRP::FLAG overexpression significantly decreases the levels of senescent markers. a-b, Change in enzymatic activity of β-galactosidase following LRP::FLAG overexpression in HEK293 (a) and MRC 5 (b) cells when compared to the non-transfected cell lines. c, d Western blotting and densitometric analysis of γH2AX levels expressed as a percentage change with non-transfected (lanes 1-3) compared to transfected lines (lanes 4- 6) for both HEK293 (c) and MRC 5 (d). Sample size n= 3 biological repeats per cell line. Data as a mean ±SD. *p<0.05, **p<0.01, ***p<0.001 by paired *t-test*. Adapted from Otgaar et al., 2017 [293].

4.5 LRP::FLAG overexpression induced a significant improvement in various physiological parameters within the aged mice

4.5.1 Overexpression of LRP::FLAG impedes the age associated process of hair greying

The positive data acquired during the *in vitro* component of this research, which indicated that LRP/LR could be targeted to cause a profound effect on cellular ageing/ senescence, prompted further perusal to observe if the effects found *in vitro* could be validated in an *in vivo* context. Prior to the termination of the mice, it was prudent to assess whether the overexpression of LRP::FLAG was capable of inducing a strong enough effect to waylay the effects of physiologic ageing. To this end an array of procedures were carried out to assess how the overexpression of LRP::FLAG

influenced: cognitive, cosmetic, general well-being and motor function parameters in the aged C57BL/6J mice.

The first marker of physiologic ageing assessed was hair greying, as it is probably one of the most distinguishing phenotypic markers of mammalian ageing. This is especially true for both humans and mice (confirmed in C57BL/6J mouse strain). What governs the process of hair greying is not entirely understood, but it has been linked to a dysregulation or apoptosis of the melanocytes, depletion of melanocyte stem cell niches and a disruption of the processes that govern the development of pigment. Importantly, all these factors can be tied to an age dependent decline in function. Upon analysis using a One-way ANOVA, it was observed that mice treated to overexpress LRP::FLAG (treated mice) displayed a significant difference ($p = 0.004$) in hair greying when compared to the control (empty vector treated mice) and non-treated mice groups (Figure 4.5). Additional statistical analysis using Welch's *t-test* coupled with a *post hoc* Bonferroni correction found that the overexpression of LRP::FLAG caused a significant reduction in hair greying when compared to the control ($p = 0.0086$) and non-treated mice (0.005). It is also noteworthy that although not quantified, it was visually observed that the treated mice appeared to show less signs of hair thinning and balding when compared to the control and non-treated groups (enlarged images for clarity purposes can be observed in Appendix C, Figure8.28). This said, it was observed that the control mice on average exhibited around 44.42% (SD: 10.58%) total hair greying and the non-treated mouse group displayed an average of 46.68% (SD: 12.59%) total hair greying. This was in stark contrast to the treated group which only displayed an average of 25.38% (SD: 14.11%) total hair greying illustrating an approximate 20% reduction when compared to the controls and non-treated groups. This therefore, offers the first potential indication that the overexpression of LRP::FLAG may delay or offset the effects of cellular senescence.

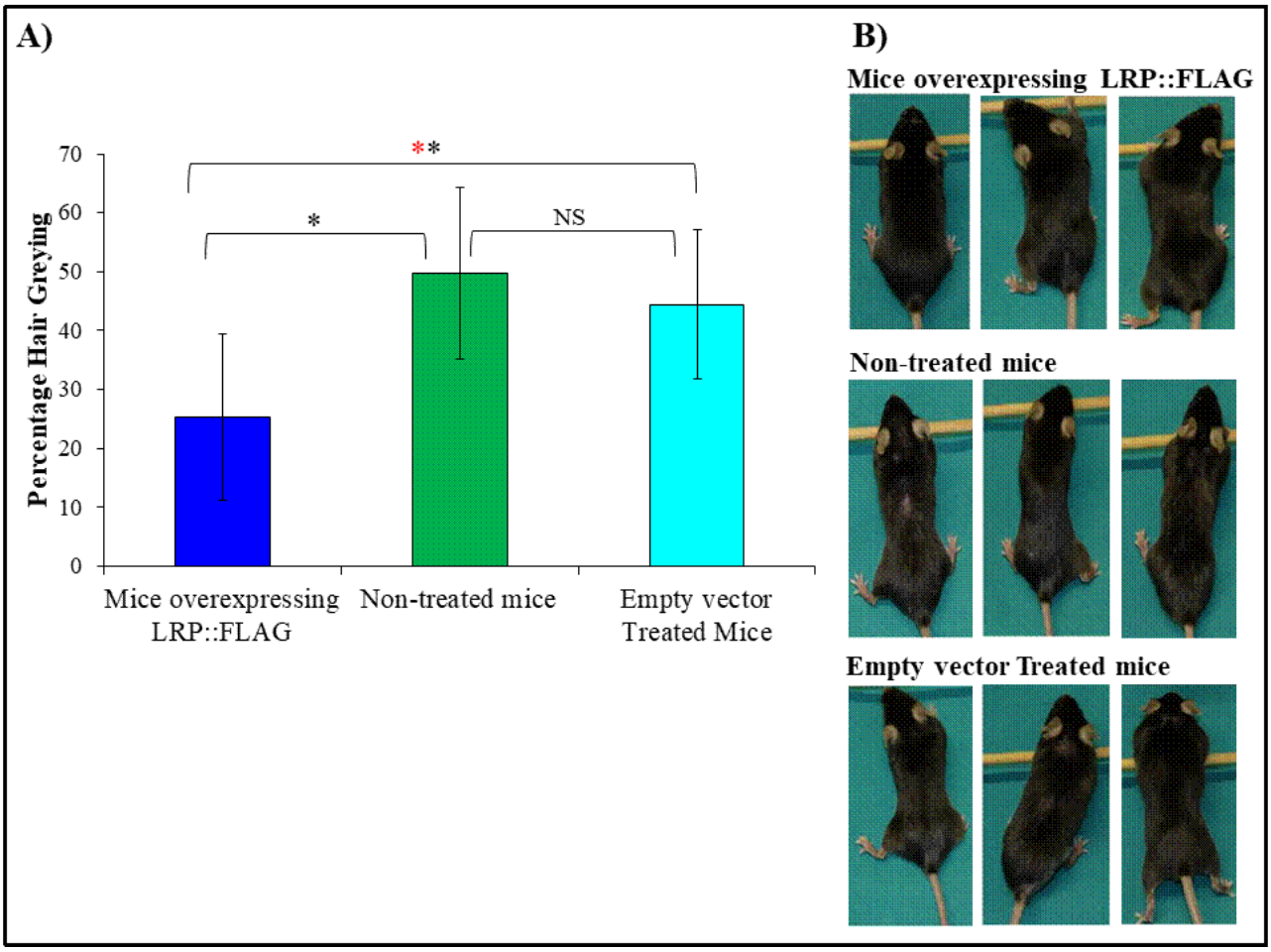
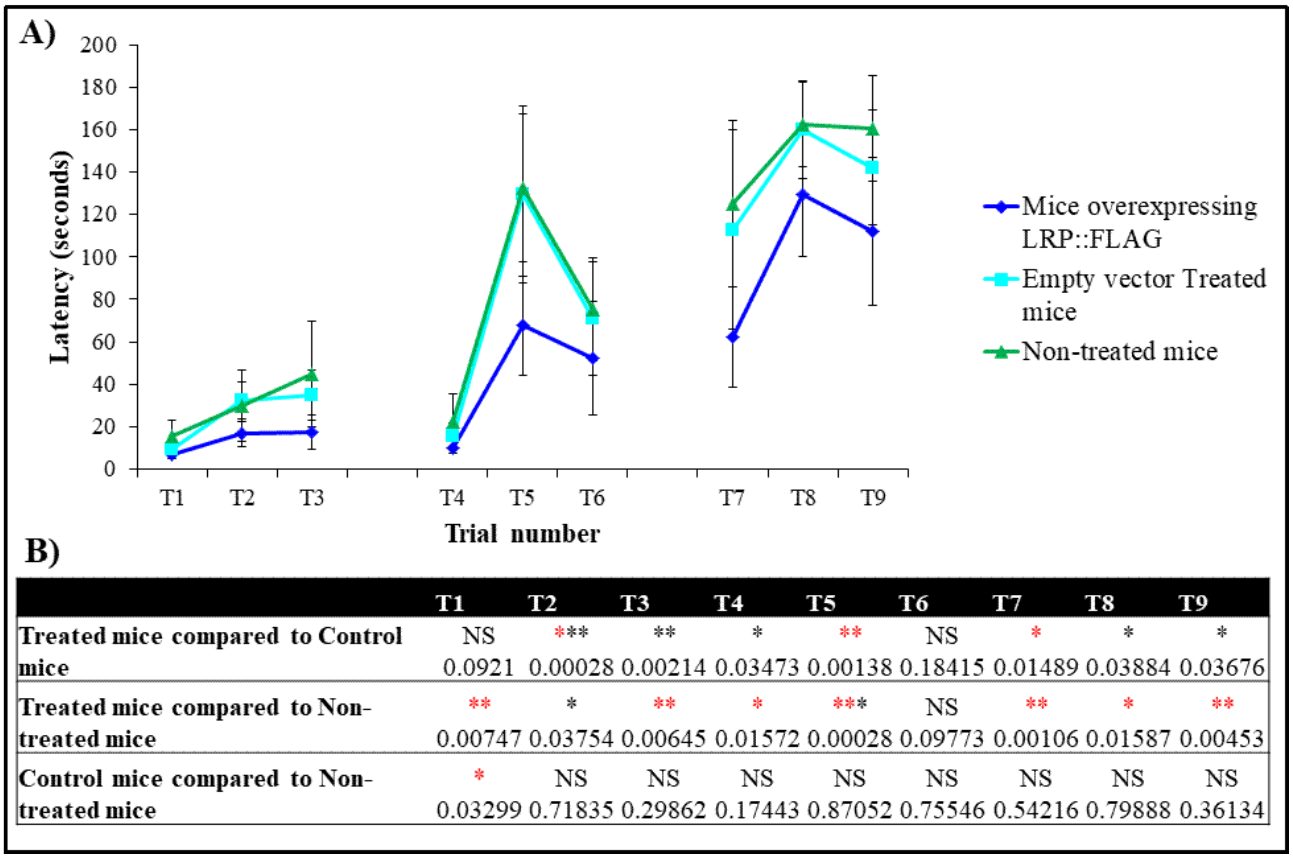


Figure 4.5: Overexpression of LRP::FLAG reduces the amount of hair greying in mice.
Hair greying analysis was performed on 18 month old mice. A) Analysis showed a ±25% reduction in grey hair for the treated mice when compared to the non-treated and control mice. B) Representative images illustrating that the treated mice not only contained less hair greying but also less balding. Sample size: Mice overexpressing LRP::FLAG (Treated): n = 8; Non-treated mice (Non-treated): n = 9 Empty vector treated mice (Control): n = 9. Data as a mean ±SD. *p < 0.05, **p < 0.01, ***p < 0.001, NS: p>0.05, non-significant; One-way ANOVA and Welch's *t-test* coupled with a post hoc Bonferroni correction. The number of '*' irrespective of colour represent the level of significance according to Welch's *t-test*, whereas '*' in red indicate data that is significant following the Bonferroni correction.

4.5.2 LRP::FLAG overexpression significantly improved cognitive function in aged mice

A well-documented phenotypic characteristic that declines with age is cognitive function. This decline of function can be attributed to the accumulation of senescent neuronal tissues that ultimately drive neurodegeneration, and further results in the benign senescent associated forgetfulness that is commonplace among the elderly. In order to discern whether the overexpression of LRP::FLAG could influence cognitive function the puzzle box test was carried out to assess short and long term memory as well as puzzle-solving ability. It must be noted that all data collected was subjected to a One-way ANOVA followed up with a Welch's *t-test*, and a *post hoc* Bonferroni correction to ensure the statistical validity of the data (Figure 4.6 B). Overall, it was found that the overexpression of

LRP::FLAG was able to induce a significant improvement in all three aforementioned cognitive abilities when compared to the non-treated and control mouse groups (Figure 4.6 A, B). More specifically, upon analysis of the trials that represented short term memory (T3, T6 and T9) it was revealed that both the non-treated and control groups had much higher latencies in reaching the goal zone than the treated mice, although T6 was not significantly higher. The same was true for the trials that measured long term memory, where the treated mice exhibited significantly shorter latencies in reaching the goal zone for both T4 and T7. This essentially indicated that the overexpression of LRP::FLAG improved working and long term memory within the aged mice. The final cognitive aspect that the puzzle box test assessed was puzzle solving ability (T5 and T8), where the treated mice displayed significantly enhanced learning capabilities. This said, the treated mice displayed acute remembrance of the opening, burrow puzzle and plug puzzle, which resulted in significantly reduced latencies in reaching the goal zone when compared to the control and non-treated mouse groups. These data essentially reveal that the overexpression of LRP::FLAG positively affects cognitive function to potentially waylay the effects of age-associated cognitive decline.



B)

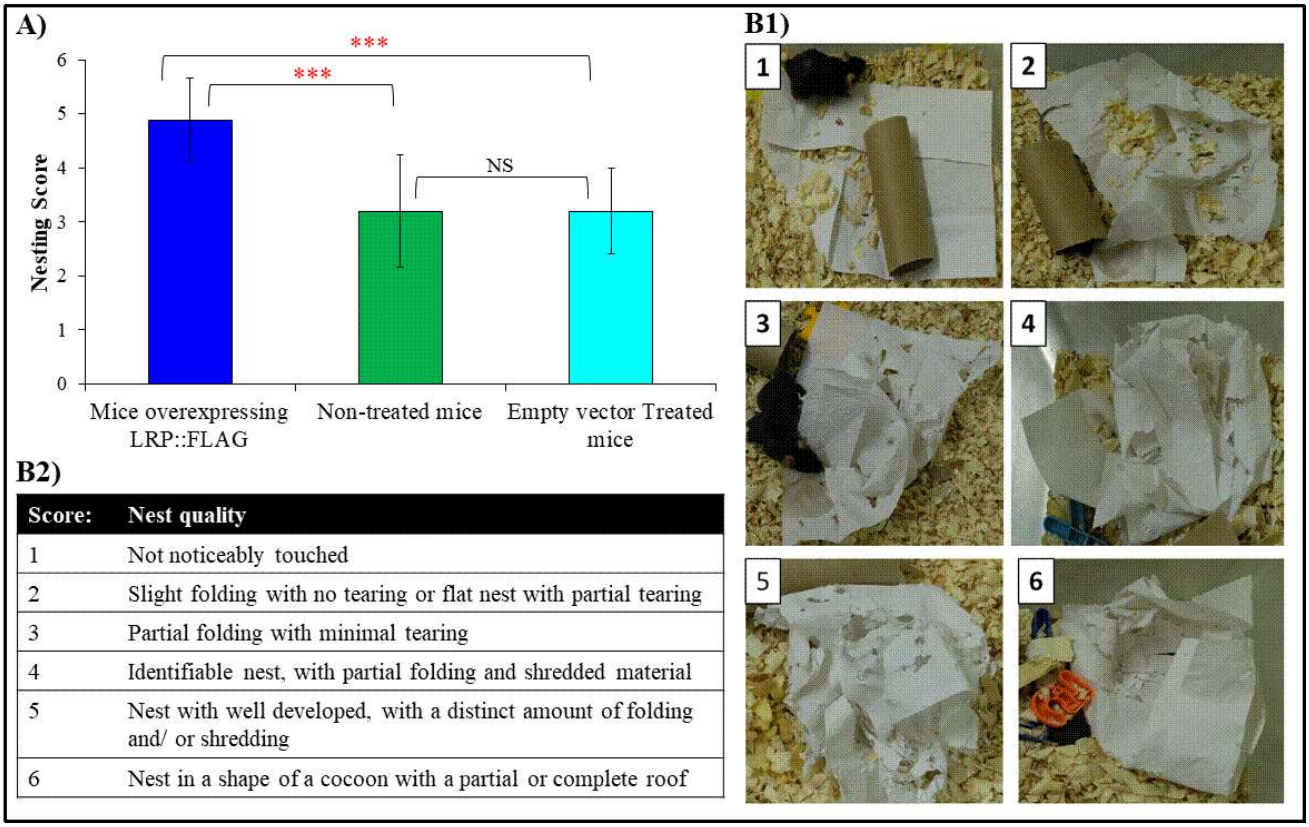
	T1	T2	T3	T4	T5	T6	T7	T8	T9
Treated mice compared to Control mice	NS	***	**	*	**	NS	*	*	*
	0.0921	0.00028	0.00214	0.03473	0.00138	0.18415	0.01489	0.03884	0.03676
Treated mice compared to Non-treated mice	**	*	**	*	***	NS	**	*	**
	0.00747	0.03754	0.00645	0.01572	0.00028	0.09773	0.00106	0.01587	0.00453
Control mice compared to Non-treated mice	*	NS	NS	NS	NS	NS	NS	NS	NS
	0.03299	0.71835	0.29862	0.17443	0.87052	0.75546	0.54216	0.79888	0.36134

Figure 4.6: Overexpression of LRP::FLAG prevents age associated cognitive decline by improving short and long term memory as well as puzzle solving ability.
The puzzle box test measured the latency (time) of the mice to solve cognitive related tasks over a coarse of 9 distinct trials. Tasks that were assessed included: Day 1 (training), T1 - underpass uncovered and un-blocked, thereafter T2 and T3 involved the top being covered and mice having to enter the goal zone by use of the underpass. Day 2 (burrowing puzzle), T4 was a repeat of T2 and T3 to assess long term memory. T5 and T6 (T6 assessed short term memory) – introduced a novel puzzle where the underpass was filled with sawdust. Day 3 (plug puzzle), T7, was a repetition of T5 and T6 to assess long term memory. For T8 and T9 (T9 assessed short term memory) the underpass was obstructed by plugging the cavity with gauze and covering with sawdust. Treated: n = 10; Control: n = 11 and Non-treated: 11. Data as a mean ±SD. *p < 0.05, **p < 0.01, ***p < 0.001, NS: p>0.05, non-significant; One-way ANOVA and Welch's *t-test* coupled with a post hoc Bonferroni correction. The number of '*' irrespective of colour represent the level of significance according to Welch's *t-test*, whereas '*' in red indicate data that is significant following the Bonferroni correction.

4.5.3 LRP::FLAG overexpression significantly improved nesting abilities in aged mice

To further validate the improved cognitive function displayed by mice overexpressing LRP::FLAG the nesting test was also performed. Nesting generally forms part of spontaneous behaviors and thus provided an alternative means to assess cognitive function as well as general well-being of the mice. In addition, this form of spontaneous behavior has been confirmed to decline with age in C57BL/6J mouse models [399]. Upon analysis and scoring of the nests it was found that mice treated to overexpress LRP::FLAG displayed significantly superior nest constructing abilities in comparison to the non-treated and control mouse groups (Figure 4.7). In addition, all data was validated by a One-

way ANOVA (p = 0.0003), Welch's *t-test* and a *post hoc* Bonferroni correction. It was noted that on average the non-treated and control mice displayed limited nesting capabilities, where the paper towel that was provided only showed partial folding with minimal tearing. These groups were issued with an average score of 3.2 for both control (Mean: 3.2, SD: 1.03, p = 0.00096) and non-treated (Mean: 3.2, SD: 0.79, p = 0.00022). Meanwhile, the majority of the treated mice were found to construct nests that ranked a score of around 4-5 (Mean: 4.89, SD: 0.782), thus indicating that the mice were able to construct well developed nests that contained distinct amounts of folding and tearing. Therefore, this suggests that the overexpression of LRP::FLAG could potentially waylay the effects of age-associated behavioral decline.



B2)

Score:	Nest quality
1	Not noticeably touched
2	Slight folding with no tearing or flat nest with partial tearing
3	Partial folding with minimal tearing
4	Identifiable nest, with partial folding and shredded material
5	Nest with well developed, with a distinct amount of folding and/ or shredding
6	Nest in a shape of a cocoon with a partial or complete roof

Figure 4.7: Aged mice treated to overexpress LRP::FLAG displayed improved nest building abilities.

A) Analysis of the nesting scores revealed that mice overexpressing LRP::FLAG were able to build better and more complete nests in comparison to the non-treated and control. B 1,2) Representative table and images of the scoring mechanism used to grade the nests. Sample size: Treated: n = 9; Control: n = 10 and Non-treated: n = 10. Data as a mean ±SD. *p < 0.05, **p < 0.01, ***p < 0.001, NS: p>0.05, non-significant; One-way ANOVA and Welch's *t-test* coupled with a post hoc Bonferroni correction. The number of '*' irrespective of colour represent the level of significance according to Welch's *t-test*, whereas '*' in red indicate data that is significant following the Bonferroni correction.

4.5.4 Overexpression of LRP::FLAG causes a significant improvement in motor function and balance

The next aspect of physiologic ageing assessed was motor function. As previously mentioned, the age-dependent loss in motor function provides an ideal phenotypic marker to track organism ageing. This decline in function is a direct consequence induced by a loss in muscle tissue, which causes a gradual limitation in what physical tasks an aged organism can efficiently perform. The first aspect that was assessed was motor function where mice were scored on their physical ability to traverse the balance beam. A One-way ANOVA revealed that a significant difference ($p = 4.18E-05$) was observed when scoring the different mouse groups on motor function. Overall, it was found that the treated mice displayed a significant improvement in motor function and balance when compared to the non-treated and control mice, where the treated mice (Mean score: 4.25, SD: 0.775) were able to traverse the beam using all four limbs albeit with a large number of slips (Figure 4.8 A). Astonishingly, it was found that both the non-treated and control mice were unable to efficiently use their hindlimbs, and had to resort to traversing majority of the beam by dragging their hindlimbs with some attempted, but failed, use of their hindlimbs. As a consequence the non-treated mice scored 2.625 (SD: 0.72, $p = 9.15E-07$) while the empty vector treated mice scored 2.8125 (SD: 0.403, $p = 2.75E-07$).

The second component of the test focused on assessing the length of time it took the mice to traverse the 1 m long beam. A One-way ANOVA revealed that a significant difference ($p = 0.0001$) was observed when analysing the times the different mouse groups took to traverse the beam. In fact, it was confirmed using Welch's *t-test* with a Bonferroni correction, that the treated mice were able to traverse the beam in a significantly shorter span of time than both the control and non-treated groups (Figure 4.8 B). Analysis revealed that the treated mice took on average 16.375 sec (SD: 4.14 sec) while the non-treated and control took 25 sec (SD: 4.43 sec, $p = 0.0013$) and 26.813 sec (SD: 3.90 sec, $p = 0.0001$), respectively. These data illustrate a remarkable difference in motor function, where it appeared that the control and non-treated mice displayed signs of severe loss in motor function. This was possibly due to the onset of arthritis as the mice appeared unable to use their hindlimbs to its full extent. This essentially highlights the profound effect that the overexpression of LRP::FLAG has on impeding the age dependent decline of motor function.

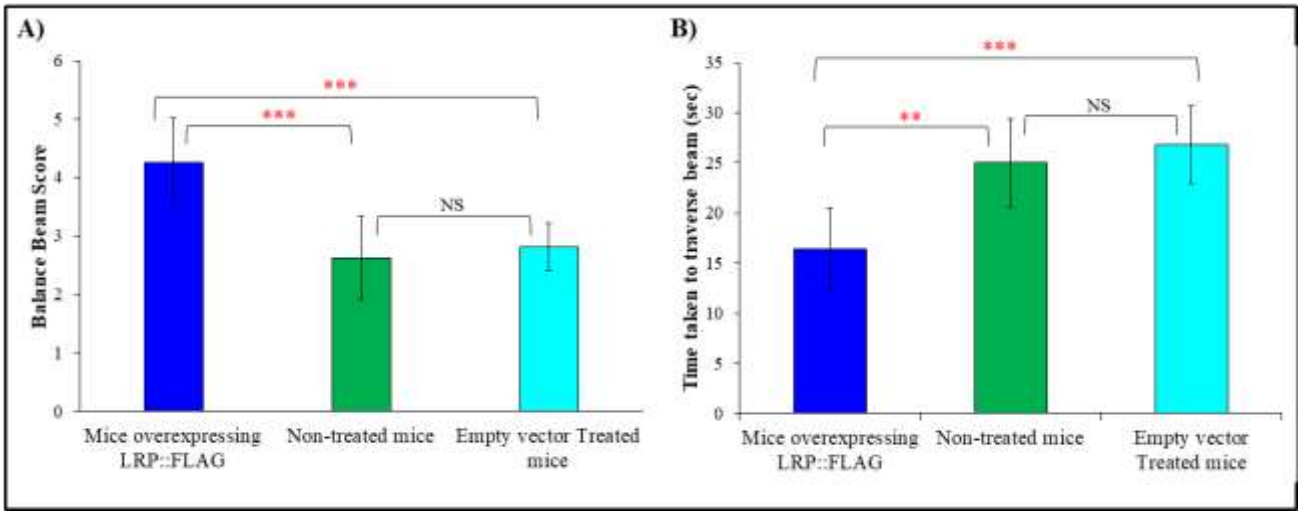


Figure 4.8: LRP::FLAG overexpression induced a significant improvement in motor function and balance in aged mice.
A) Scoring of the mice's ability to traverse the beam indicated that the overexpression of LRP::FLAG improved motor function allowing for a ±2 point score difference. B) Illustrates the difference in time taken to traverse the beam, where mice overexpressing LRP::FLAG on average traversed the beam ±10 sec faster than the control and non-treated mice. Data shown is representative of two averaged technical repeats for each biological replicate. Sample size: Treated: n = 8; Control: n = 8 and Non-treated: n = 8. Data as a mean ±SD. *p < 0.05, **p < 0.01, ***p < 0.001, NS: p>0.05, non-significant; One-way ANOVA and Welch's *t-test* coupled with a post hoc Bonferroni correction. The number of '*' irrespective of colour represent the level of significance according to Welch's *t-test*, whereas '*' in red indicate data that is significant following the Bonferroni correction.

4.6 The overexpression of LRP::FLAG impedes the formation of histopathological markers that constitute tissue ageing

4.6.1 Mice overexpressing LRP::FLAG showed less neurodegeneration in the hippocampal regions of the brain

The stark improvement in cognitive function following the overexpression of LRP::FLAG, warranted the assessment of the brain tissue at a histological level. To this end, histological analysis was performed on the hippocampus region. This neuronal area comprises part of the limbic system where it plays an imperative role in learning and long term memory [400]. In addition, it is the age associated functional decline of this tissue that ultimately causes forgetfulness and learning impairments in the elderly [400]. Histological assessment of this tissue structure involved staining all the sections with H&E, and was subsequently imaged using an inverted microscope at 40x and 200x magnification. Firstly, analysis revealed that all mice did show mild signs of age-dependent tissue decline, however these age-related alterations were present to a higher degree in the non-treated and control mouse groups, when compared to the treated mice (Figure 4.9). This said, the combined overall morphology of the hippocampus for the treated mice appeared better proportioned, which

essentially reflects a hippocampus in good condition (health). More specifically, within the molecular layer it was found that the treated mice on average appeared to showed less vacuolisation and enlarged neurons in comparison to the control and non-treated mice (Figure 4.9 B, F, J). Moreover, when analysing the dentate gyrus (DG) it was evident that the control and non-treated mice displayed a less defined DG on average, as well as a larger distribution of pyramidal cells housing pyknotic nuclei in comparison to the treated mice. Moreover, the non-treated and control mice also displayed a greater incidence of vacuolisation, while the treated mice displayed microglia with more distinct nuclei. These collective morphological features noted in the non-treated and control mice offer a clear indication of a senescing hippocampus, while mice treated to overexpress LRP::FLAG displayed healthier neuronal tissue on average. These data together with the physiological findings clearly demonstrate that LRP::FLAG served a rescuing effect by preventing age-related cognitive decline and neurodegeneration. Therefore, corroborating with previous *in vitro* data (Bignoux et al., 2019) and suggesting that LRP/LR could be utilised as a potential target to waylay the detrimental effects of brain ageing.

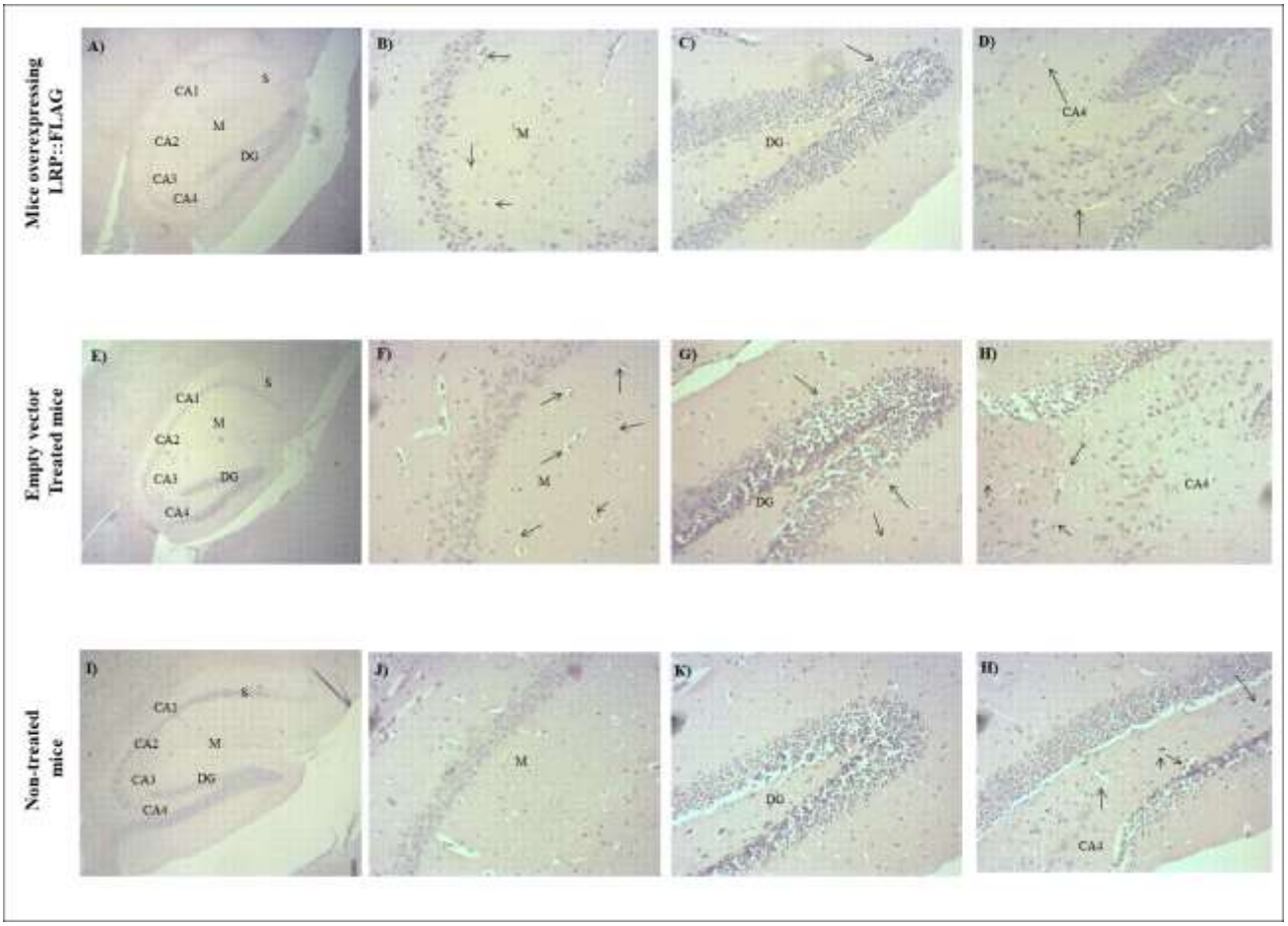


Figure 4.9: Histological analysis revealing that LRP::FLAG overexpression aids in preventing neuro-tissue degeneration in the hippocampus.
Histological analysis of the brain sections targetting the hippocampus was used to assess age-related pathological features following the overexpression of LRP::FLAG. All sections were subjected to H&E staining and images were taken at 40x (A, E, I) and 200x (B-D, F-H, J-L) magnification. The following hippocampus structures were assessed: Cornu Amonis 1-4 (CA1-CA4), Dentate gyrus (DG), Subiculum (S) and the Molecular layer (M). Evaluation of the molecular layer (B, F, J) revealed that the treated mice on average showed less vacuolation (indicated by arrows), and enlarged neurons. Assessment of the dentate gyrus (C, G, K) showed that the treated mice showed less signs of tissue vacuolation (indicated by arrows) when compared to the control and non-treated mice. Analysis of the Cornu Ammonis (D, H, L) indicated that the control and non-treated mice exhibited more necrotic cells and tissue disorganisation in comparison to the control and non-treated mice.

4.6.2 Mice overexpressing LRP::FLAG showed less signs of kidney tissue ageing and degeneration

In order to assess whether the overexpression of LRP::FLAG prevented an age-dependent functional decline within the kidneys of the aged mice, histological analysis was carried out. This decline in organ function is commonly caused by modifications to the tissue structure specifically within the glomerular and tubular structures. The analysis of the tissue sections revealed that for the most part,

all the mice did house a number of glomeruli with increased diameters which occurs as the mice age (Figure 4.10). Interestingly though, the control and non-treated mice on average did appear to show slightly more advanced signs of ageing in comparison to the treated mice. These signs included: an increased infiltration of inflammatory or lymphocytic cells (glial cells) throughout the tissue, some degree of tubular vacuolation and displayed signs of glomerular shrinkage and mild atrophy (Figure 4.10 D-I). In addition, a subset of the control and non-treated mice actually displayed signs of advanced kidney degeneration, where severe glomerular atrophy and sclerosis was evident. Admittedly, in some glomeruli, it even appeared that the various tissues that generally constitute this tissue structure were replaced with fibrous tissue. This said, the treated mice did also display slight shrinkage and increased Bowman's space in some glomeruli, but to a much lower degree than the control and non-treated mice. Therefore, this indicates that the overexpression of LRP::FLAG may be capable of preventing an age associated functional decline within the kidneys.

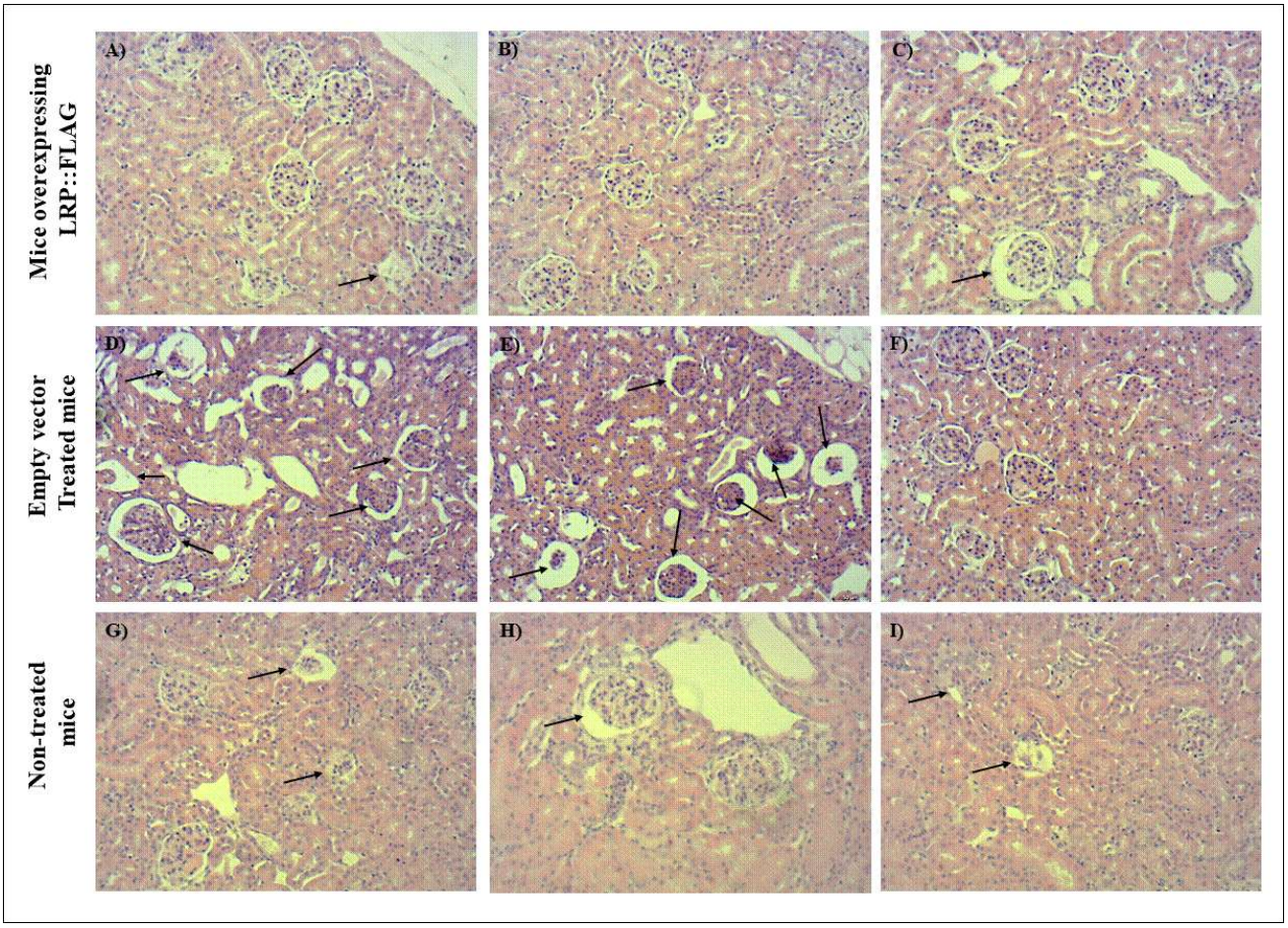


Figure 4.10: Overexpression of LRP::FLAG prevented the age-dependent tissue decline of the kidney in aged mice

Histological analysis of the kidney sections following the overexpression of LRP::FLAG was carried out to assess age-related pathological features. All sections were subjected to H&E staining and images were taken at 200x magnification. (A- C) The treated mice for the most part exhibited fairly normal renal structures with only slight glomerular shrinkage and a finite number of glomeruli with increased diameters. (D-F) The control mice and (G-I) non-treated mice displayed distinct glomerular atrophy and sclerosis (indicated by the arrows) for some biological replicates while overall showing a larger accumulation of age related pathological features including: degree of glomerular shrinkage, vacuolation and increased inflammatory infiltration (glial cells (tiny blue structures dispersed through the tissue section)) than the treated mice.

4.7 LRP::FLAG overexpression significantly increases total LRP levels in aged mice

Considering the vast improvements observed on both a physiological and histological level, it was vital to corroborate this data and ensure that it occurred on a biochemical level so that the potential mechanisms involved could be discerned. It must be noted that enlarged images for all the western blots can be observed in Appendix C from Figure 8.29 to Figure 8.53 that provides higher resolution to more efficiently distinguish differences qualitativley. Firstly, the overexpression of LRP::FLAG had to be confirmed in order to demonstrate that a successful transfection had occurred.

Unfortunately, the tag could not be successfully identified via western blotting due to the non-specificity of the various antibodies used (or that the epitope of the FLAG tag was not sufficiently unique for use in an *in vivo* setting). To this end, three different antibodies that targeted the FLAG tag were tested at various concentrations; however at all conditions tested a non-specific band was detected at the size range for LRP::FLAG. Instead the overexpression of LRP::FLAG was confirmed in an indirect manner, where total LRP mRNA and protein levels were quantified. This said, the FLAG tag does not alter the composition or structure of LRP nor does it convey any other properties other than to allow the discernment between endogenously or exogenously produced protein. Thus, an average/ holistic increase in total LRP within the treated mouse group would suggest a successful overexpression of LRP::FLAG. Analysis by qPCR (Figure 4.11 A-C) and western blotting with densitometry (Figure 4.11 D-F), which were subjected to a One-way ANOVA, revealed that a significant difference was observed for total LRP levels at an mRNA (Brain: $p = 0.6454$; Kidney: $p = 0.0111$ and Liver: $p = 0.0079$) for the kidney and liver as well as at a protein level (Brain: $p = 0.0045$, Kidney: $p = 0.000062$ and Liver: $p = 0.0003$) for all three tested organs.

Furthermore, a Welch's *t-test* and *post hoc* analysis using the Bonferroni correction confirmed that the treated mice (Brain: Mean = 1.27, SD = 0.23; Kidney: Mean = 1.85, SD = 0.59 and Liver: Mean = 1.435, SD = 0.557) displayed a significant elevation in gene expression for LRP when compared to the non-treated (Brain: Mean = 1.10, SD = 0.53, $p = 0.46$; Kidney: Mean = 1.13, SD = 0.59, $p = 0.0297$ Liver: Mean = 0.932, SD = 0.328 $p = 0.012578$) and control mice (Brain: Mean = 1.30, SD = 0.34, $p = 0.88$; Kidney: Mean = 1.00, SD = 0.36, $p = 0.000839$ and Liver: Mean = 0.738, SD = 0.114 $p = 0.005389$) for both the kidney and liver. Similarly, a significant elevation in total LRP protein levels was also noted when the treated mice (Brain: Mean = 121.92%, SD = 14.52%; Kidney: Mean = 128.24%, SD = 25.97% and Liver: Mean = 144.91%, SD = 33.06%) were compared to the non-treated (Brain: Mean = 100%, SD = 15.45%, $p = 0.0021$; Kidney: Mean = 91.51%, SD = 16.31%, $p = 0.000136$ and Liver: Mean = 100%, SD = 22.67% $p = 0.0031$) and control mice (Brain: Mean = 101.12, SD = 18.16, $p = 0.0138$; Kidney: Mean = 82.62%, SD = 16.30%, $p = 0.000722$ and Liver: Mean = 91.35%, SD = 18.42% $p = 0.0008$) in all three tested organs. It must be noted that as LRP mRNA levels in the brain were not significantly elevated it suggests that gene transfer did not occur, possibly due to the BBB. As such all improvements noted within the brain may just be the result of an additive effect caused by a rejuvenation of most of the tissues and not LRP::FLAG. However, the significant increase in both gene expression and protein levels of LRP within the kidney and liver does suggest that the treatment was successful. This therefore, indirectly confirms that treatment

with the pCIneo-moLRP::FLAG vector elevated total LRP/LR levels by allowing for the expression of LRP::FLAG.

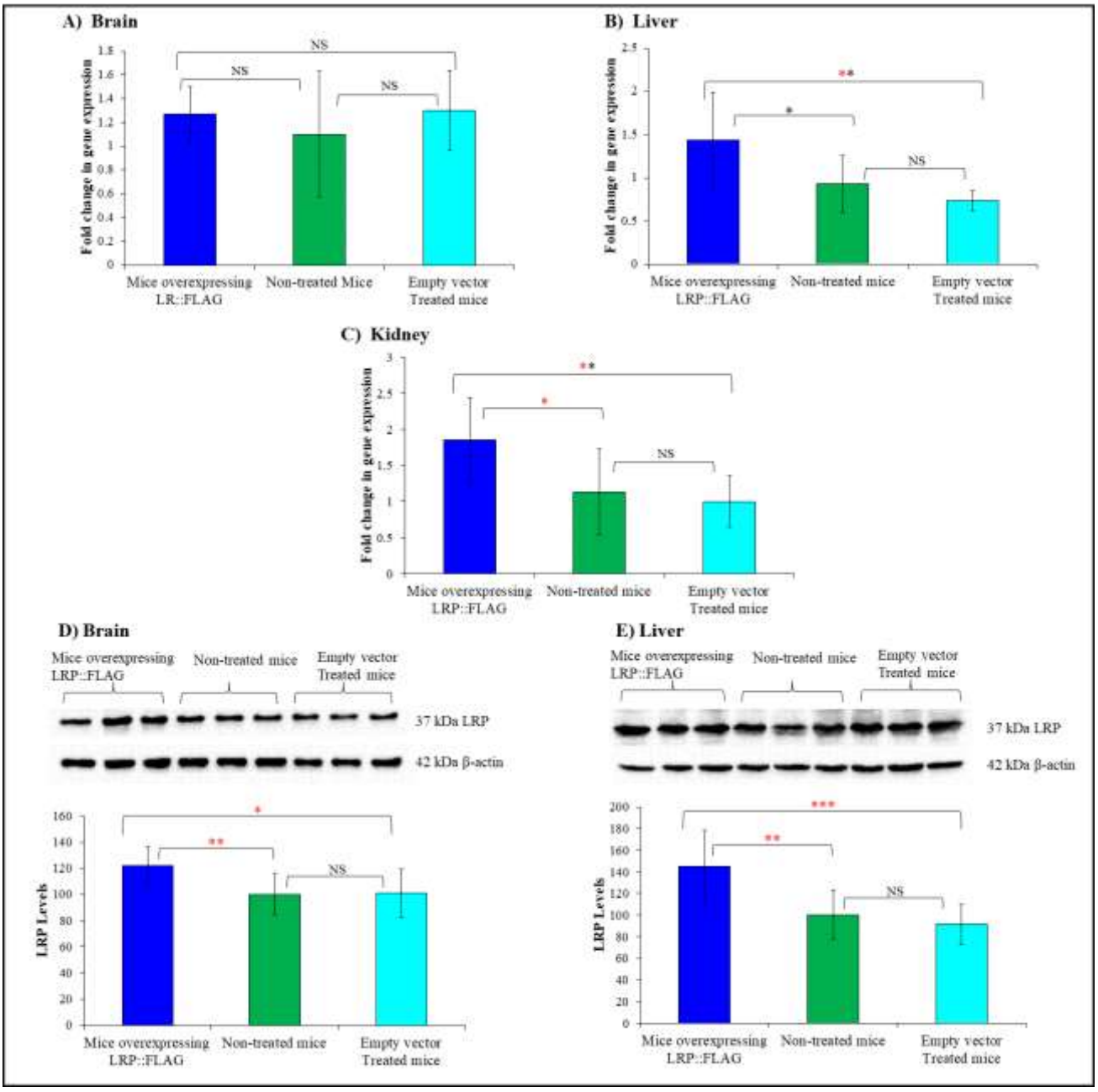


Figure 4.11: Overexpression of LRP::FLAG induces an overall increase in LRP/LR gene expression and protein levels.

LRP/LR gene expression levels in the (A) brain (B) liver and (C) kidney were compared between the different mouse treatment groups. It was found that overexpression of LRP::FLAG induced a significant increase of ±0.5 fold in the liver and ±0.7 fold in the kidney while no difference was observed in the brain. Sample size: Treated: n = 5; Control: n = 5 and Non-treated mice: n = 6; Liver: Treated: n = 9; control: n = 6 and Non-treated: n = 7; Kidney: Treated: n = 8; Control: n = 7 and Non-treated: n = 8. (A, B, C) GAPDH and RPLPO were used as reference genes for sample normalisation. Thereafter, total LRP/LR protein levels were assessed by western blotting in the (D) brain, (E) liver and (F) kidney. It was found that LRP::FLAG overexpression induced a ±20%, ±40% and ±40% increase within the brain, kidney and liver, respectivley. Sample size: Brain: Treated: n = 11; Control: n = 9 and Non-treated: n = 12. Liver: Treated: n = 11; Control: n = 8 and

Non-treated: n = 12. Kidney: Treated: n = 12; Control: n = 8 and Non-treated: n = 10. (D, E) β-actin was used as a reference protein and all illustrated blots are representative where 4 blots were performed to assess all biological replicates. Data as a mean ±SD. *p < 0.05, **p < 0.01, ***p < 0.001, NS: p>0.05, non-significant; One-way ANOVA and Welch's *t-test* coupled with a *post hoc* Bonferroni correction were performed for all experiments. The number of '*' irrespective of colour represent the level of significance according to Welch's *t-test*, whereas '*' in red indicate data that is significant following the Bonferroni correction.

4.8 LRP::FLAG overexpression positively affects proliferative markers in aged mice

4.8.1 LRP::FLAG overexpression increases Akt levels in the brain as well as pAKT levels in liver of aged mice

Following the confirmation that the plasmid induced an increased production in total LRP, an oncogenic protein, it was prudent to assess the downstream effects that this protein would exert on proliferative pathways. This is due to an over representation of proliferative proteins being commonplace to cancer, whilst in ageing a decline is often observed, thus a balance is required to promote a safe/ healthy anti-ageing effect. The first proliferative marker assessed was Akt, an enzyme that plays a pivotal role in processes like proliferation, survival and metabolism through the Akt-PI3K pathway. Moreover, it is this enzyme and its associated signalling cascade that is responsible for the expression and stimulation of TERT. Gene expression analysis by qPCR coupled with a One-way ANOVA revealed that all three tested organs (Brain: p = 0.8845, Kidney: p = 0.4307 and Liver: p = 0.5292) displayed no significant difference when comparing between each group's (treated, control and non-treated) RNA profiles (Figure 4.12 A-C).

Subsequent densitometric analysis alongside a One-way ANOVA illustrated that the overexpression of LRP::FLAG induced no significant alteration in Akt protein levels in the liver (p = 0.8034). In contrast, a significant difference was observed for the brain (p = 0.0077) when analysed under the same conditions leading to further analysis by Welch's *t-test* and Post hoc analysis using the Bonferroni correction (Figure 4.12 D, E). It was found that the mice treated to overexpress LRP::FLAG (Mean = 122.71%, SD = 17.70%) displayed a significant increase in total Akt levels within the brain tissue when compared to the non-treated (Mean = 99.99, SD = 12.94, p = 0.0025) and control mice (Mean = 95.12%, SD = 28.39%, p = 0.0249). The increase in this protein within the brain may imply that the tissue has an increased propensity to carry out metabolic, survival and proliferative related functioning.

In order for Akt to carry out its aforementioned functioning; the enzyme needs to be phosphorylated specifically at S473 in order to be fully activated. Once activated the protein can go on to act as a

transcription factor to initiate gene expression, or can act as a pathway regulator by directly causing the phosphorylation of target proteins. This highlights the requirement to confirm both, total protein levels and the amount of phosphorylated protein in order to draw meaningful conclusions. Unfortunatley, due to time constraints only the liver samples could be assessed for pAkt. Western blotting analysis and One-way ANOVA revealed a significant difference existed within the liver samples when comparing between the different mouse groups (Figure 4.12 F). A more in depth analysis using Welch's *t-test* and Bonferroni correction revealed that mice overexpressing LRP::FLAG contained significantly elevated levels of phospho-Akt (Mean = 147.57%, SD = 36.21%), when compared to the non-treated (Mean = 100%, SD = 16.88%; p = 0.000839) and control mice (Mean = 98.96%, SD = 24.73%; p = 0.001703). Therefore, indicating that LRP/LR may play a role in the phosphorylation of this protein, thereby influencing the Akt-PI3K pathway to aid in cell viability and survival.

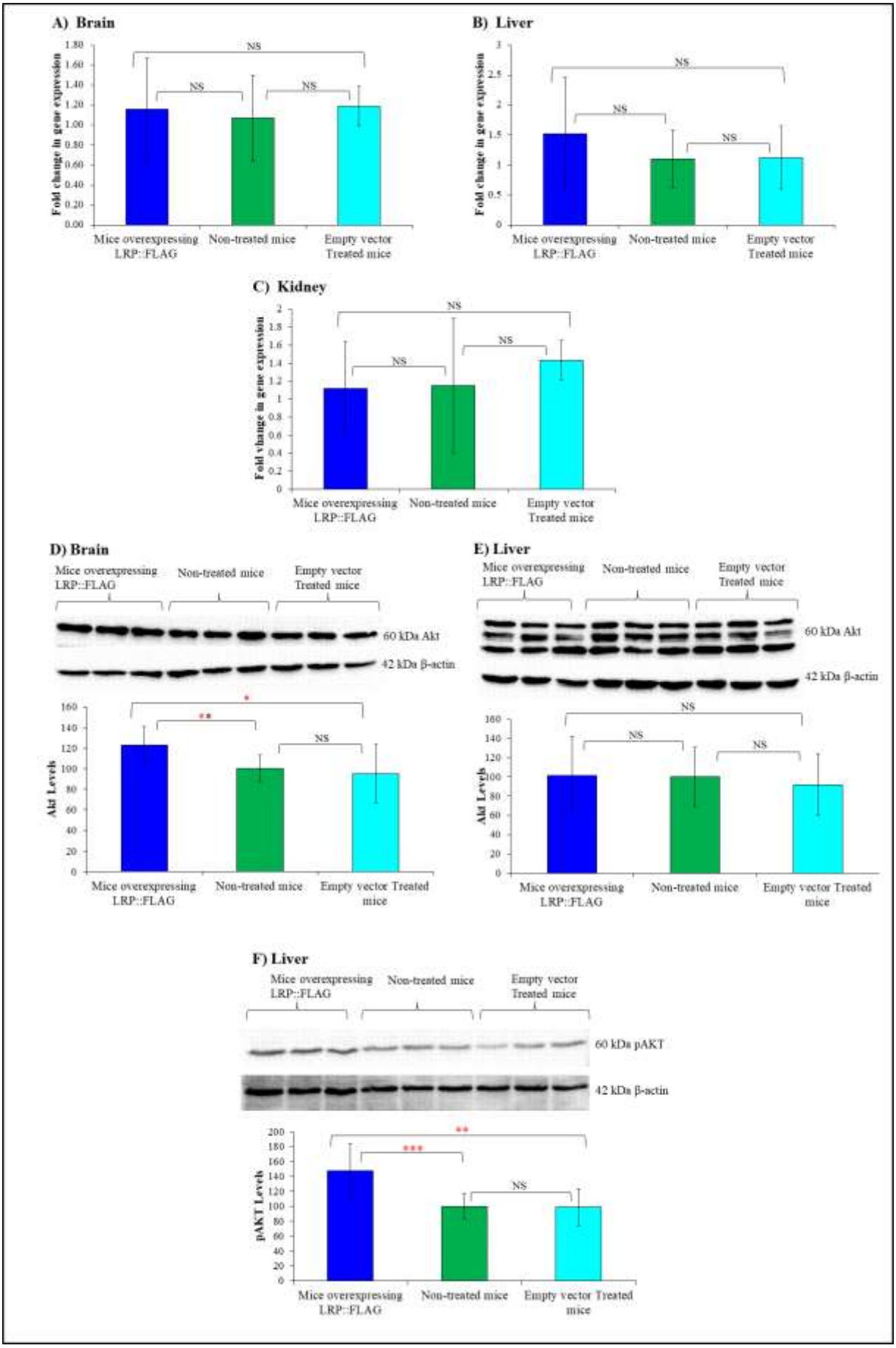

A) Brain
Fold change in gene expression
NS
NS
NS
Mice overexpressing LRP::FLAG
Non-treated mice
Empty vector Treated mice
B) Liver
Fold change in gene expression
NS
NS
NS
Mice overexpressing LRP::FLAG
Non-treated mice
Empty vector Treated mice
C) Kidney
Fold change in gene expression
NS
NS
NS
Mice overexpressing LRP::FLAG
Non-treated mice
Empty vector Treated mice
D) Brain
Mice overexpressing LRP::FLAG
Non-treated mice
Empty vector Treated mice
60 kDa Akt
42 kDa β-actin
Akt Levels
*
**
NS
Mice overexpressing LRP::FLAG
Non-treated mice
Empty vector Treated mice
E) Liver
Mice overexpressing LRP::FLAG
Non-treated mice
Empty vector Treated mice
60 kDa Akt
42 kDa β-actin
Akt Levels
NS
NS
NS
Mice overexpressing LRP::FLAG
Non-treated mice
Empty vector Treated mice
F) Liver
Mice overexpressing LRP::FLAG
Non-treated mice
Empty vector Treated mice
60 kDa pAKT
42 kDa β-actin
pAKT Levels
**
***
NS
Mice overexpressing LRP::FLAG
Non-treated mice
Empty vector Treated mice

Figure 4.12: qPCR and Western blot analysis illustrated that the overexpression of LRP::FLAG positively affected Akt.
Akt gene expression levels in the (A) brain (B) liver and (C) kidney were compared between the different mouse treatment groups. It was found that overexpression of LRP::FLAG induced no difference in Akt expression for any of the tested organs. Sample size: Brain: Treated: n = 6; Control: n = 4 and Non-treated: n = 7. Liver: Treated: n = 9; Control: n = 6 and Non-treated: n = 7. Kidney: Treated: n = 8; Control: n = 7 and Non-treated: n = 7. (A, B, C) GAPDH and RPLPO were used as reference genes for sample normalisation. Thereafter, total Akt protein levels were assessed by western blotting in the (D) brain and (E) liver. Specifically for the liver samples, densitometric analysis was carried out on the bottom protein band (third band). It was found that LRP::FLAG overexpression induced a ±20%, increase within the brain and no significant change for the liver. Sample size: Brain: Treated: n = 11; Control: n = 9 and Non-treated: n = 12. Liver: Treated: n = 11; Control: n = 9 and Non-treated: n = 12. (F) Protein levels of phosphorylated Akt were assessed by western blotting in the liver. It was found that the treated mice contained ±50% more Akt when compared to the non-treated and control groups. Sample size: Liver: Treated: n = 12; Control: n = 9 and Non-treated: n = 12. (D, E, F) β-actin was used as a reference protein and all illustrated blots are representative where 4 blots were performed to assess all biological replicates. Data as a mean ±SD. *$p < 0.05$, **$p < 0.01$, ***$p < 0.001$, NS: $p>0.05$, non-significant; One-way ANOVA and Welch's *t-test* coupled with a *post hoc* Bonferroni correction were performed for all experiments. The number of '*' irrespective of colour represent the level of significance according to Welch's *t-test*, whereas '*' in red indicate data that is significant following the Bonferroni correction.

4.8.2 LRP::FLAG overexpression increases c-Myc protein levels in the brain and liver of aged mice

The changes observed in Akt following the overexpression LRP::FLAG warranted the assessment of other proteins involved TERT regulation. One such protein that was selected was c-Myc a transcription factor responsible for the activation and expression of a number of proliferative related proteins. This TF has been intricately tied to stem cell function (specifically reprogramming into a pluripotent state) and metabolism. Perhaps, c-Myc's most notable function pertaining to this study is that it acts as a major TF for TERT expression and can further enter a positive feedback loop with TERT to drive increased expression of both proteins. Gene expression analysis by qPCR and a One-way ANOVA showed no significant change in c-Myc expression following the overexpression of LRP::FLAG within the brain ($p = 0.9818$). In contrast, a significant difference in gene expression was observed for the kidney (0.0082) and liver ($p = 0.0252$) between the three groups when analysed by One-way ANOVA (Figure 4.13 A-C). This was further validated by use of Welch's *t-test* and Bonferroni correction, where it was found that for the kidney the treated mice (Mean = 1.73, SD = 0.47) had significantly elevated c-Myc expression when compared to the non-treated mice (Mean = 1.01, SD = 0.18, $p = 0.0063$) and a non-significant increase in comparison to the control (Mean = 1.24, SD = 0.35, $p = 0.0573$). In addition, the liver samples showed a similar trend where mice overexpressing LRP::FLAG (Mean = 1.41, SD = 0.372) displayed a significant increase in c-Myc expression in comparison to the control mouse group (Mean = 0.83 SD = 0.186, $p = 0.002851$) and a

non-significant increase when compared to the non-treated mice (Mean = 1.18, SD = 0.505, p = 0.372).

Thereafter, densitometry alongside a One-way ANOVA revealed a significant difference in c-Myc protein levels following LRP::FLAG overexpression [(Brain: p = 0.0009; Liver: p = 0.002) (Figure 4.13 D, E)]. Further analysis by Welch's *t-test* and Bonferroni correction illustrated that the treated mice contained significantly elevated levels of c- Myc in both the brain (Mean = 185.98%, SD = 74.01%) and liver (Mean = 140.15%, SD = 41.12%) when compared to their respective non-treated (Brain: Mean = 98.96, SD = 24.73; p = 0.000839; Liver: Mean = 99.99%, SD = 24.67% p = 0.012578) and control mouse samples (Brain: Mean = 98.96%, SD = 24.73%; p = 0.000839; Liver: Mean = 89.51%, SD = 23.64%, p = 0.003224). The observed upregulation of this TF following overexpression of LRP::FLAG validates that LRP/LR influences signalling cascades and gene expression to promote increased proliferation and survival.

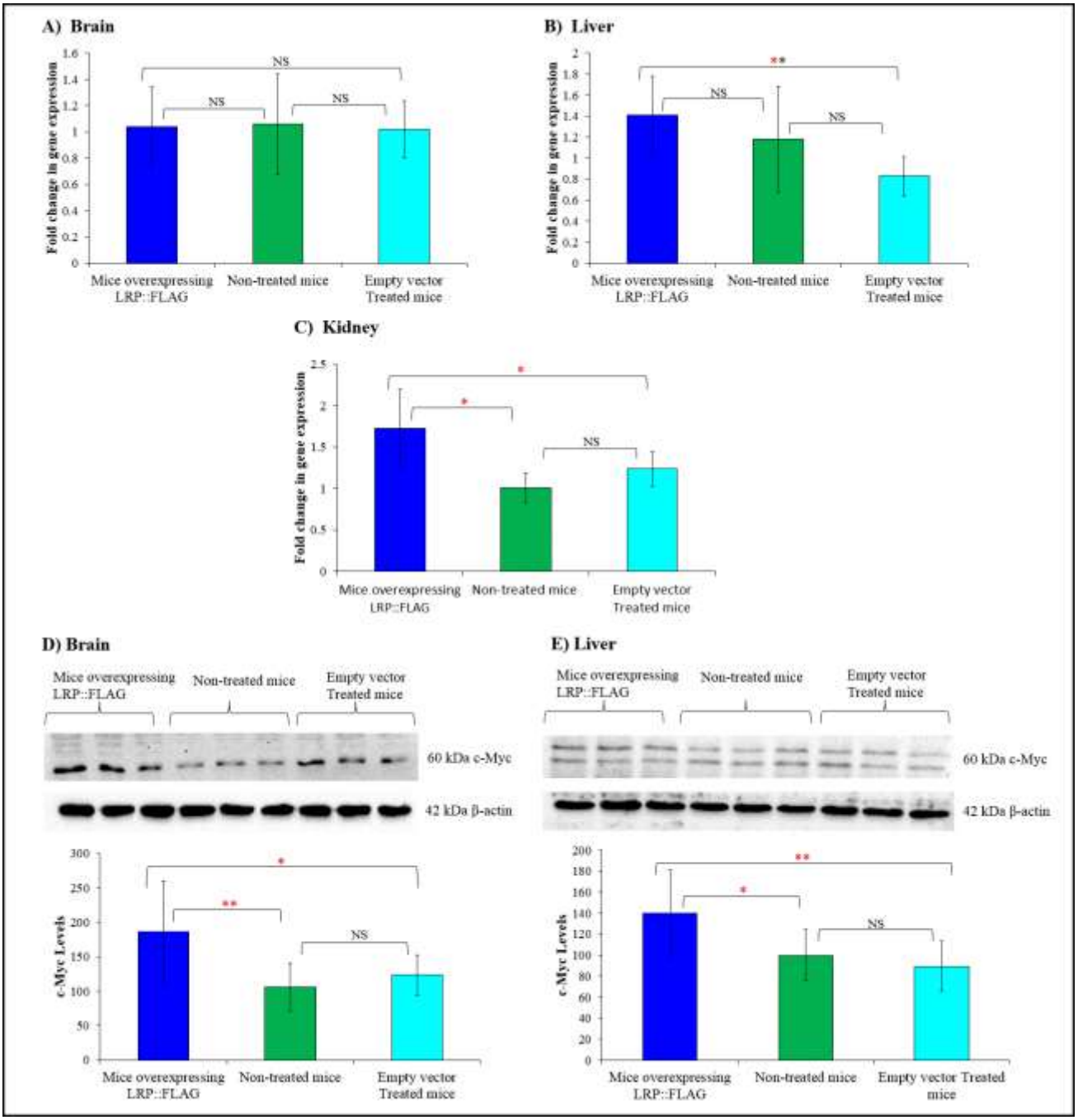


Figure 4.13: LRP::FLAG overexpression significantly elevates c-Myc gene expression and protein levels in aged mice.

c-Myc gene expression levels in the (A) brain (B) liver and (C) kidney were compared between the different mouse treatment groups. It was found that overexpression of LRP::FLAG induced no difference in c-Myc expression for the brain while a significant ±0.4 and 0.6 fold increase was evident in the liver and kidny when compared to the control an non-treatede. Sample size: Brain: Treated: n = 6; Control: n = 5 and Non-treated: n = 7. Liver: Treated: n = 8; Control: n = 7 and Non-treated: n = 6. Kidney: Treated: n = 7; Control: n = 6 and Non-treated: n = 6. (A, B, C) GAPDH and RPLPO were used as reference genes for sample normalisation. Thereafter, c-Myc protein levels were assessed by western blotting in the (D) brain and (E) liver. Densitometry was performed on the the top band for the liver samples. It was found that treated mice had a ±70% and ±40% increase within the brain and liver when compared to the non-treated and control groups. Sample size: Brain: Treated: n = 10; Control: n = 8 and Non-treated: n = 11. Liver: Treated: n = 11; Control: n = 9 and Non-treated: n = 12. (D, E) β-actin was used as a reference protein and all illustrated blots are representative where 4 blots were performed to assess all biological replicates. Data as a mean ±SD. *p <

0.05, **p < 0.01, ***p < 0.001, NS: p>0.05, non-significant; One-way ANOVA and Welch's *t-test* coupled with a *post hoc* Bonferroni correction were performed for all experiments. The number of '*' irrespective of colour represent the level of significance according to Welch's *t-test*, whereas '*' in red indicate data that is significant following the Bonferroni correction.

4.8.3 Overexpression of LRP::FLAG increases MDM2 levels in the brain while inducing no significant change in pMDM2 levels of the aged mice

An additional protein influenced by Akt, and that serves a major role in cell survival by circumvention of apoptosis, is the protein MDM2 [401]. This protein serves as an imperative E3-ubiquitin ligase for the negative regulation of p53 which essentially regulates p53-mediated apoptosis [402, 403]. In this regard, a MDM2/p53 axis has been found to govern processes like tumorigenesis, DNA repair, apoptosis and ageing [404]. Importantly, in ageing this axis is believed to be dysregulated with correspondingly elevated levels of p53, while MDM2 is reduced to drive the senescent phenotype [404]. To this end, gene expression and protein levels of MDM2 were assessed. qPCR analysis subjected to a One-way ANOVA illustrated that the overexpression of LRP::FLAG caused no significant change in *MDM2* gene expression between the different mouse groups for all three tested organs [(Brain: $p = 0.4097$; Kidney: $p = 0.2588$ and Liver: $p = 0.2381$) (Figure 4.14 A-C)].

Following gene expression analysis, the total protein levels of MDM2 were assessed. Densitometric analysis and subsequent One-way ANOVA showed that like Akt a significant difference in protein levels was observed for the brain samples ($p = 0.006$) in the treated mice while no significant difference was noted for the liver samples ($p = 0.073$) when compared to the non-treated and control mice samples (Figure 4.14 D, E). Moreover, a more detailed analysis using the Welch's *t-test* and Bonferroni correction revealed that mice overexpressing LRP::FLAG (Mean = 149.73%, SD = 60.26%) had significantly elevated MDM2 protein levels within their brain tissue when compared to the control (Mean = 96.65%, SD = 30.72%; $p = 0.0175$) and non-treated mice (Mean = 99.99%, SD = 12.98%; $p = 0.0162$). This suggests that the overexpression of LRP::FLAG may influence MDM2 levels to further regulate or inactivate p53 to allow for increased survival, proliferation and an anti-senescence effect. In a similar fashion to Akt, the protein MDM2 requires phosphorylation in order to be fully active. In fact, phosphorylation at S166 has been directly tied to allowing MDM2 to carry out its ubiquinating function for p53 proteosomal degradation. Western blotting analysis of pMDM2 with a One-way ANOVA found that mice treated to overexpress LRP::LAG displayed no significant difference when compared to the control and non-treated mice groups for both tested organs [(Brain: $p = 0.6682$ and Liver: $p = 0.1715$) (Figure 4.14 F, G)]. Essentially these data show that although total

MDM2 does increase in the brains of the treated mice there is no difference in the levels of the active form of this protein in either organ. Furthermore, this potentially indicates that no dysregulated or excessive cell cycling occurred, thus suggesting that functional cell cycle controls were in place to regulate the increased amount of observed oncogenic proteins.

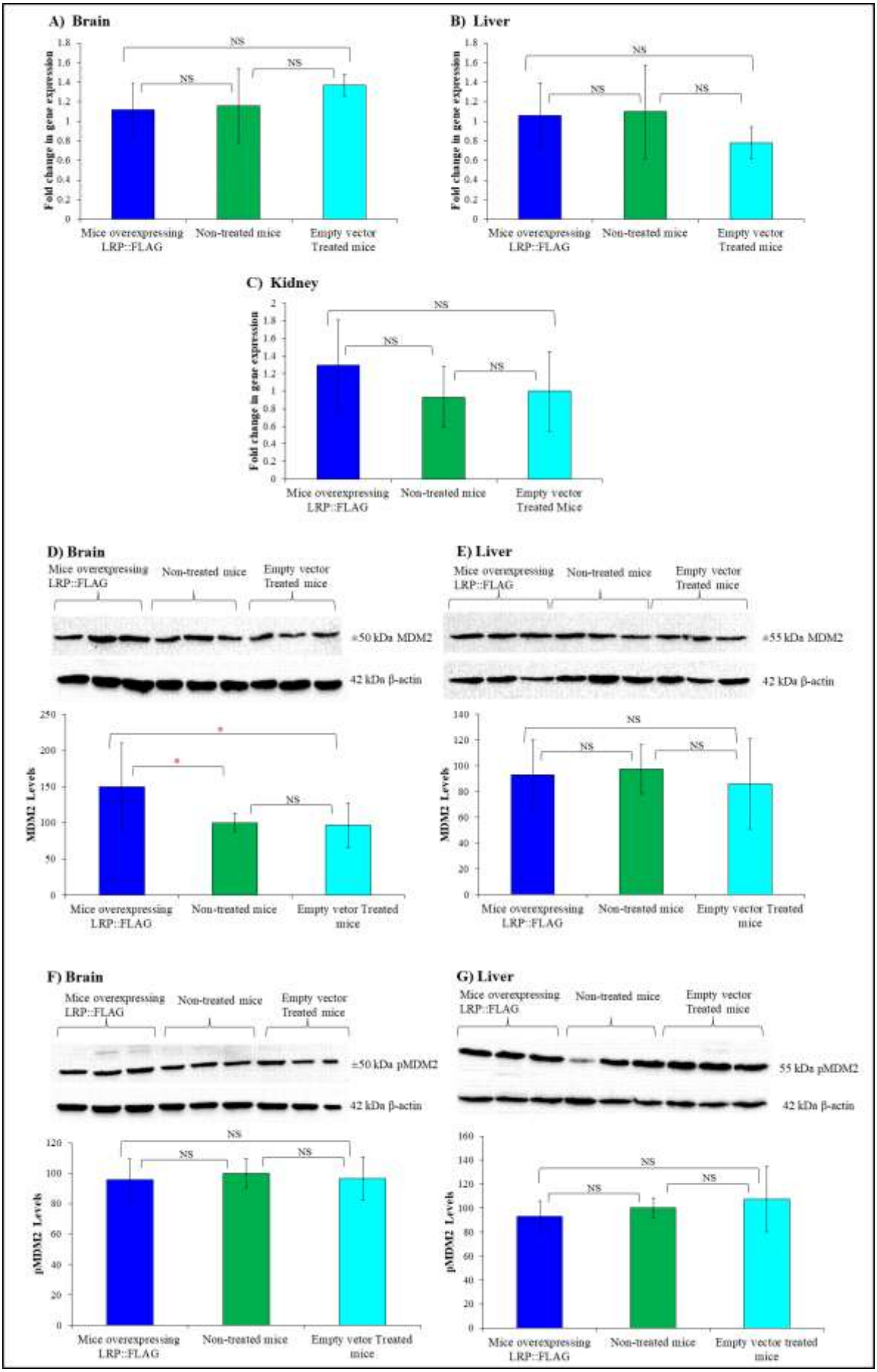

A) Brain
Fold change in gene expression
NS
NS
NS
Mice overexpressing LRP::FLAG
Non-treated mice
Empty vector Treated mice
B) Liver
Fold change in gene expression
NS
NS
NS
Mice overexpressing LRP::FLAG
Non-treated mice
Empty vector Treated mice
C) Kidney
Fold change in gene expression
NS
NS
NS
Mice overexpressing LRP::FLAG
Non-treated mice
Empty vector Treated Mice
D) Brain
Mice overexpressing LRP::FLAG
Non-treated mice
Empty vector Treated mice
±50 kDa MDM2
42 kDa β-actin
MDM2 Levels
*
*
NS
Mice overexpressing LRP::FLAG
Non-treated mice
Empty vetor Treated mice
E) Liver
Mice overexpressing LRP::FLAG
Non-treated mice
Empty vector Treated mice
±55 kDa MDM2
42 kDa β-actin
MDM2 Levels
NS
NS
NS
Mice overexpressing LRP::FLAG
Non-treated mice
Empty vector Treated mice
F) Brain
Mice overexpressing LRP::FLAG
Non-treated mice
Empty vector Treated mice
±50 kDa pMDM2
42 kDa β-actin
pMDM2 Levels
NS
NS
NS
Mice overexpressing LRP::FLAG
Non-treated mice
Empty vetor Treated mice
G) Liver
Mice overexpressing LRP::FLAG
Non-treated mice
Empty vector Treated mice
55 kDa pMDM2
42 kDa β-actin
pMDM2 Levels
NS
NS
NS
Mice overexpressing LRP::FLAG
Non-treated mice
Empty vector treated mice

Figure 4.14: Overexpression of LRP::FLAG increases MDM2 levels in the brain while not affecting the extent of protein phosphorylation in both the brain and liver of aged mice.
MDM2 gene expression levels in the (A) brain (B) liver and (C) kidney were compared between the different mouse treatment groups. It was found that overexpression of LRP::FLAG induced no difference in the brain, liver and kidney when compared to the non-treated and control. Sample size: Brain: Treated: n = 6; Control: n = 4 and Non-treated: n = 6. Liver: Treated: n = 9; Control: n = 6 and Non-treated: n = 8. Kidney: Treated: n = 8; Control: n = 7 and Non-treated: n = 9. (A, B, C) GAPDH and RPLPO were used as reference genes for sample normalisation. Thereafter, MDM2 protein levels were assessed by western blotting in the (D) brain and (E) liver. It was found that LRP::FLAG overexpression induced a ±50% increase within the brain and no difference within the liver. Sample size: Brain: Treated: n = 12; Control: n = 9 and Non-treated: n = 12. Liver: Treated: n = 11; Control: n = 9 and Non-treated: n = 12. Protein levels of phosphorylated MDM2 were assessed by western blotting in the brain (F) and liver (G). No significant difference in pMDM2 protein levels was observed between the three groups. Sample size: Liver: Treated: n = 12; Control: n = 9 and Non-treated mice: n = 12. (D, E, F, G) β-actin was used as a reference protein and all illustrated blots are representative where 4 blots were performed to assess all biological replicates. Data as a mean ±SD. *$p < 0.05$, **$p < 0.01$, ***$p < 0.001$, NS: $p>0.05$, non-significant; One-way ANOVA and Welch's *t-test* coupled with a *post hoc* Bonferroni correction were performed for all experiments. The number of '*' irrespective of colour represent the level of significance according to Welch's *t-test*, whereas '*' in red indicate data that is significant following the Bonferroni correction.

4.9 Overexpression of LRP::FLAG induces a significant elevation in anti-ageing proteins within the aged mice

4.9.1 LRP::FLAG overexpression significantly increases the levels of the anti-ageing protein SIRT1 in aged mice

Upon confirming an improved proliferative response in the aged mice overexpressing LRP::FLAG the next group of proteins assessed were those directly involved in longevity. These anti-ageing proteins have been shown in a number of studies to gradually decline with increased age, and therefore elevations in these proteins are generally associated with an anti-ageing effect. The first anti-ageing marker assessed was the protein SIRT1, a NAD-dependent deacetylase that plays a regulatory function in gene expression and longevity by deacetylating histones (for regulating gene expression), TFs and cytosolic proteins. Specifically, in an ageing context the enzyme is intricately involved in DNA repair, inflammation (regulating antioxidant defences), and has even been tied to the stimulation of TERT as well as p53. Therefore, the stimulation of this enzyme would provide a profound benefit in eliciting an anti-senescence or anti-ageing response.

To this end, *SIRT1* gene expression was assessed by qPCR to discern whether LRP::FLAG could influence this enzyme to affect the senescence process. Subsequent gene expression analysis coupled with a One-way ANOVA revealed a significant difference in SIRT1 expression between the treated, control and non-treated mouse groups within the kidney ($p = 0.0114$) and liver ($p = 0.0038$) samples while a non-significant difference was observed for the brain samples [($p = 0.9074$) (Figure 4.15 A-

C)]. Further analysis by Welch's *t-test* and Bonferroni correction ascertained that the treated mice (Kidney: Mean = 1.761, SD = 0.794 and Liver: Mean = 1.35, SD = 0.139) had significantly increased SIRT1 mRNA expression in both organs (liver and kidney) when compared to both the control (Kidney: Mean = 1.023, SD = 0.225, p = 0.02489 and Liver: Mean = 0.92, SD = 0.186, p = 0.0000343) and non-treated mice (Kidney: Mean = 1.006%, SD = 0.369, p = 0.02479 and Liver: Mean = 1.03, SD = 0.288, p = 0.02264). Furthermore, when the protein levels of this enzyme was assessed a similar trend was observed. Admittedly, upon densitometric analysis with a One-way ANOVA it was found that a significant difference existed within the brain (p = 1.922E-08) and liver (p = 0.0002) of the aged mice (Figure 4.15 D, E). Additional scrutinization using Welch's *t-test* and Bonferroni correction confirmed that the mice treated to overexpress LRP::FLAG (Brain: Mean = 139.64%, SD = 15.95% and Liver: Mean = 260.22%, SD = 119.87%) demonstrated significantly enhanced SIRT1 protein levels within the brain as well as liver samples in comparison to the control (Brain: Mean = 100.47%, SD = 12.96%, p = 6.099E-06 and Liver: Mean = 140.35%, SD = 48.48%, p = 0.0092) and non-treated mice groups (Brain: Mean = 100%, SD = 9.96%, p = 7.584E-07and Liver: Mean = 100.42%, SD = 31.59%, p = 0.0012). This increase in SIRT1 post LRP::FLAG overexpression clearly points towards a longevity promoting function of LRP/LR in potentially waylaying the effects of oxidative stress or inflammation through SIRT1.

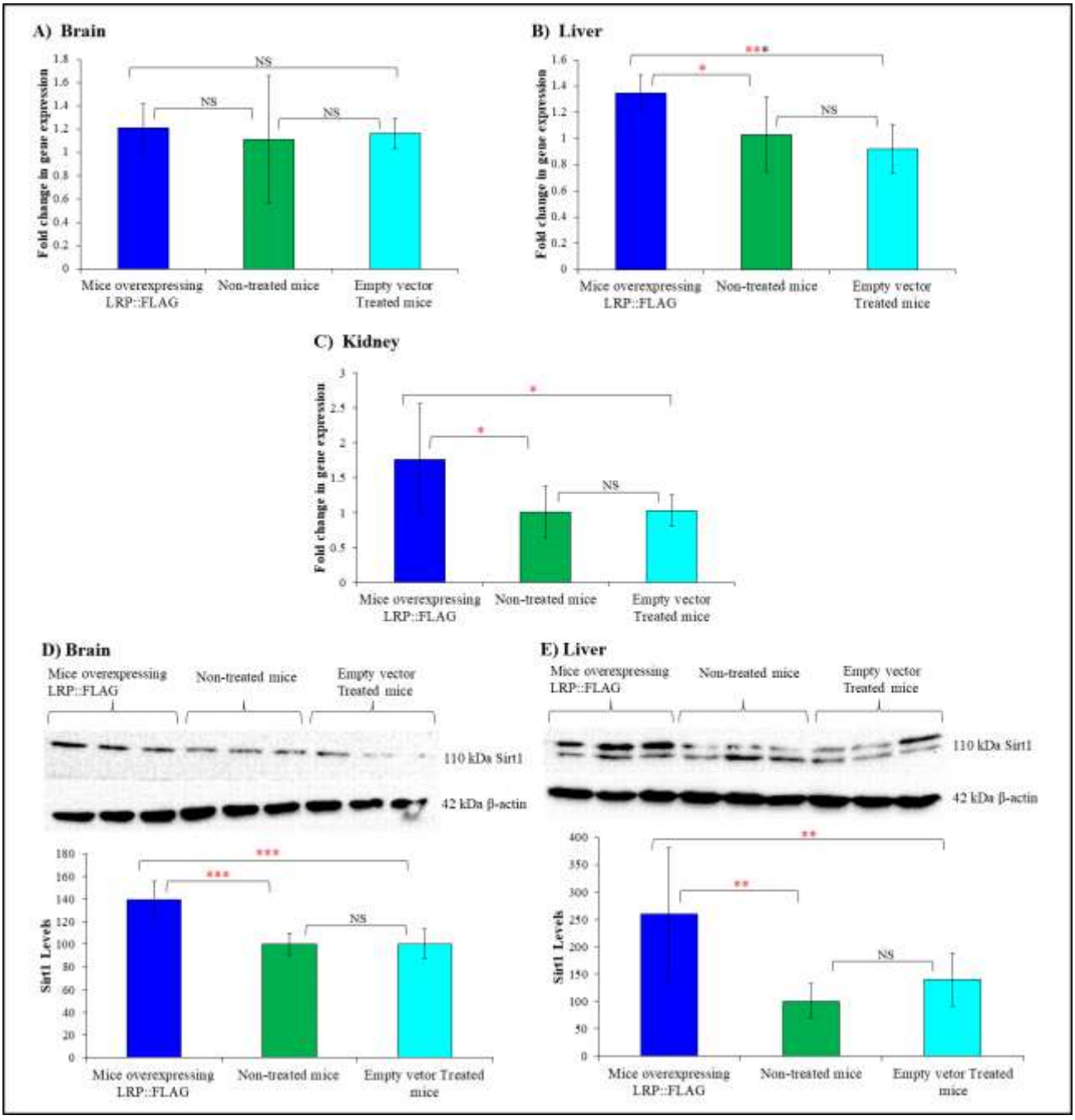


Figure 4.15: Mice overexpressing LRP::FLAG displayed significantly elevated SIRT1 gene expression and protein levels.

SIRT1 gene expression levels in the (A) brain (B) liver and (C) kidney were compared between the different mouse treatment groups. It was found that overexpression of LRP::FLAG induced a significant increase of ±0.3 and ±0.7 fold for the liver and kidney while no difference was observed for the brain. Sample size: Brain: Treated: n = 6; Control: n = 4 and Non-treated: n = 6. Liver: Treated: n = 7; Control: n = 7 and Non-treated: n = 7. Kidney: Treated: n = 9; Control: n = 7 and Non-treated: n = 8. (A, B, C) GAPDH and RPLPO were used as reference genes for sample normalisation. Thereafter, SIRT1 protein levels were assessed by western blotting in the (D) brain and (E) liver. Densitometry was performed on the the top band for the liver samples. It was found that LRP::FLAG overexpression induced a ±40% and ±120% increase within the brain and liver. Sample size: Brain: Treated: n = 12; Control: n = 9 and Non-treated: n = 12. Liver: Treated: n = 11; Control: n = 9 and Non-treated: n = 12. (D, E) β-actin was used as a reference protein and all illustrated blots are representative where 4 blots were performed to assess all biological replicates. Data as a mean ±SD. *p < 0.05, **p < 0.01, ***p < 0.001, NS: p>0.05, non-significant; One-way ANOVA and Welch's *t-test* coupled

with a *post hoc* Bonferroni correction were performed for all experiments. The number of '*' irrespective of colour represent the level of significance according to Welch's *t-test*, whereas '*' in red indicate data that is significant following the Bonferroni correction.

4.9.2 LRP::FLAG overexpression significantly increased the levels of the anti-ageing protein α-Klotho in aged mice

In order to confirm that anti-ageing processes were indeed being favoured post LRP::FLAG overexpression in the aged mice, a second anti-ageing marker was assessed. The marker selected was α-klotho, a transmembrane protein that can also produce a secreted isoform that plays a vital role in regulating insulin signalling and protecting against oxidative stress to elicit an anti-ageing effect. In addition, it also appears that α-klotho may share a functional relationship with other longevity related proteins like SIRT1 and TERT to further carry out this anti-ageing effect. Accordingly, gene expression analysis by qPCR and further assessment by One-way ANOVA illustrated that a significant difference occurred between the different mouse groups (treated, control and non-treated) in the kidneys of the aged mice ($p = 0.0221$) while a non-significant difference was found in the brain [($p = 0.5419$) (Figure 4.16 A, B)]. This was then further validated by the use of a Welch's *t-test* and Bonferroni correction which showed that the treated mice (Mean = 1.86, SD = 0.555) exhibited significantly higher α-klotho mRNA levels within the kidney when compared to the non-treated (Mean = 1.12, SD = 0.518, $p = 0.0153$) and control mice (Mean = 1.24, SD = 0.470, $p = 0.0369$). It must be noted that while not significant the treated mice (Mean = 1.33, SD = 0.415) did exhibit an increased expression of α-klotho in comparison to the non-treated (Mean = 1.07, SD = 0.438, $p = 0.324$) and control mouse groups (Mean = 1.15, SD = 0.239, $p = 0.445$). It must be noted that the gene expression of *α-klotho* is tissue specific and is mainly expressed in the brain and kidney, while it is not expressed in the liver, hence why gene expression analysis was not performed in this organ.

This increase was then further validated by assessing the protein levels by western blotting. Subsequent, densitometric analysis alongside a One-way ANOVA verified that a significant difference in full length α-klotho was observed within the brain between the different groups of mice [($p = 7.594E-06$) (Figure 4.16 C)]. Moreover, a significant difference in secreted α-klotho was also noted in the brain and liver of the various mouse groups [(Brain: $p = 0.0002$ and Liver: $p = 0.0062$) (Figure 4.16 C, D)]. In a similar fashion, Welch's *t-test* alongside a Bonferroni correction ascertained that mice overexpressing LRP::FLAG (Mean = 239.98%, SD = 76.65%) were found to have significantly higher levels of full length α-klotho within the brain, when compared to the control (Mean = 92.23%, SD = 74.95%, $p = 0.00034$) and non-treated mice (Mean = 99.99%, SD = 44.73%, $p = 0.000036$). Furthermore, this trend followed through for the secreted isoform of α-klotho, where

treated mice (Brain: Mean = 121.23%, SD = 18.31% and Liver: Mean = 157.22%, SD = 71.38%) displayed a significant increase of this protein isoform in the brain and liver when compared to the non-treated (Brain: Mean = 97.63%, SD = 12.69%, p = 0.0025 and Liver: Mean = 100%, SD = 21.85%, p = 0.0258) and control groups (Brain: Mean = 83.50%, SD = 21.78%, p = 0.0008 and Liver: Mean = 94.04%, SD = 26.49%, p = 0.0174). These data together with SIRT1 highlight that LRP/LR clearly has longevity functionality either by being directly involved in the ageing process or by acting as a regulatory element for anti-ageing signalling cascades.

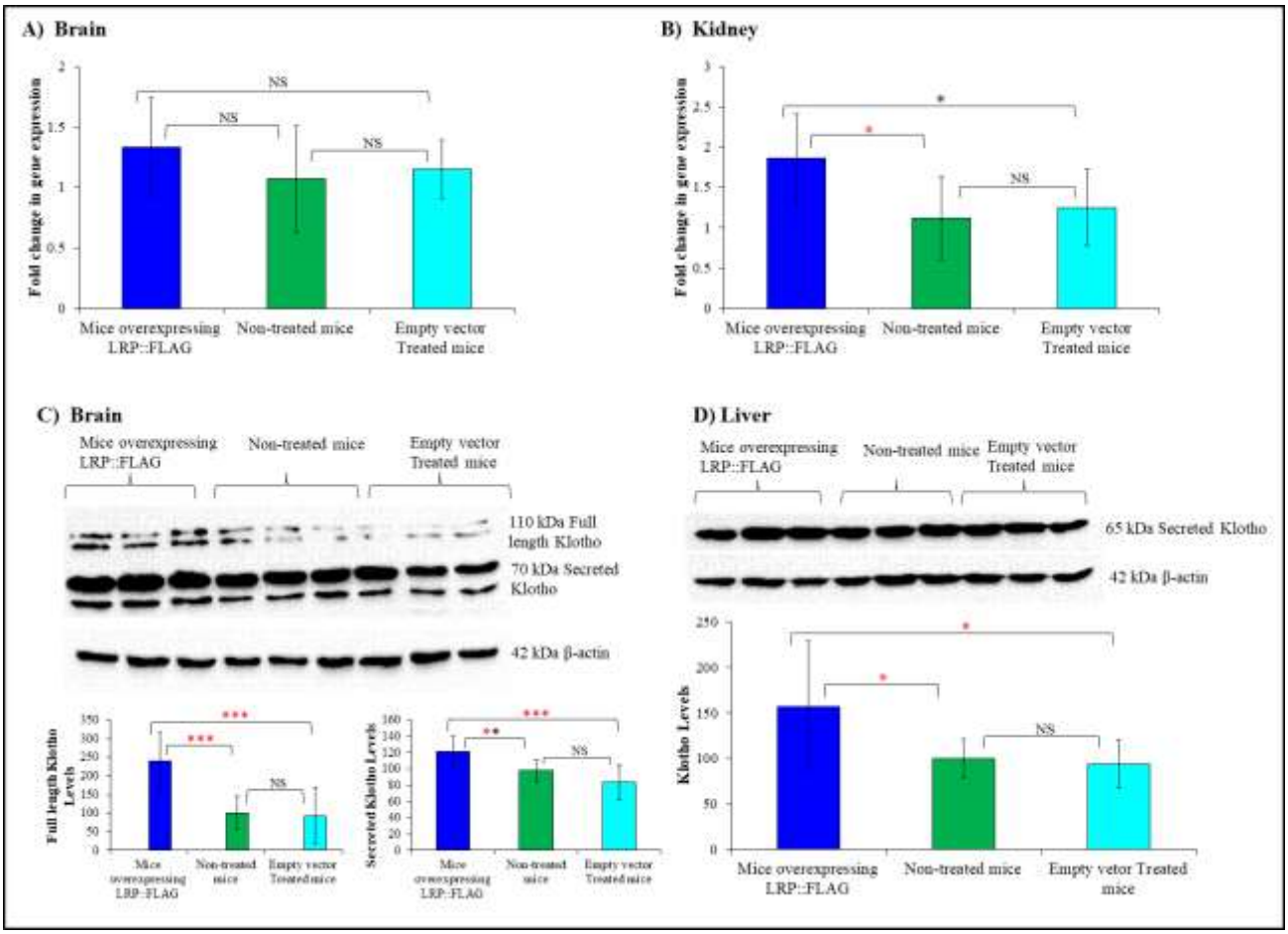


Figure 4.16: The overexpression of LRP::FLAG increased the levels of both the full length and secreted isoform of α-klotho in aged mice.

α-*Klotho* gene expression levels in the (A) brain (B) liver kidney were compared between the different mouse treatment groups. The mice treated to overexpress LRP::FLAG exhibited a significant increase of ±0.6 fold for the kidney while the brain showed a non-significant increase of ±0.2 fold when compared to the control and non-treated. Sample size: Brain: Treated: n = 5; Control: n = 4 and Non-treated: n = 7. Kidney: Treated: n = 8; Control: n = 7 and Non-treated: n = 8. (A, B) GAPDH and RPLPO were used as reference genes for sample normalisation. Thereafter, protein levels for both full length and secreted α-klotho were assessed by western blotting in the (C) brain and (D) liver. In regard to the brain, densitometry was performed on the first set of bands for the full length isoform, while the third band was quantified for the secreted isoform of α-klotho. It was found that LRP::FLAG overexpression induced a ±150% and ±20% increase for full length and secreted α-klotho, respectively within the brain. The liver of the treated mice was observed to contain ±60% more secreted α-klotho in comparison to the control and non-treated. Sample size: Brain: Treated: n = 12 (full

length) and 11 (secreted); Control: n = 9 (for both full length and secreted) and Non-treated: n = 12 (full length) and 11 (secreted). Liver: Treated: n = 11; Control: n = 9 and Non-treated: n = 12. (C, D) β-actin was used as a reference protein and all illustrated blots are representative where 4 blots were performed to assess all biological replicates. Data as a mean ±SD. *p < 0.05, **p < 0.01, ***p < 0.001, NS: p>0.05, non-significant; One-way ANOVA and Welch's *t-test* coupled with a *post hoc* Bonferroni correction were performed for all experiments. The number of '*' irrespective of colour represent the level of significance according to Welch's *t-test*, whereas '*' in red indicate data that is significant following the Bonferroni correction.

4.10 The overexpression of LRP::FLAG significantly elevates the levels of the senescence-associated protein, p53 in aged mice

Considering the positive influence that the overexpression of LRP::FLAG exerted on various proliferative and longevity markers *in vivo*, coupled with the observed reduction in senescent markers *in vitro*, warranted the assessment as to whether the overexpression of LRP::FLAG could effectively prevent the accumulation of senescent markers *in vivo.* The first senescent marker assessed was p53 due to its major aforementioned role in telomere dependent senescence, DNA repair and apoptosis. Moreover, a dysregulated reduction of this protein is commonly associated with carcinogenesis illustrating the importance of assessing this marker in anti-ageing research. Gene expression analysis by qPCR and a One-way ANOVA demonstrated a significant difference in p53 expression was evident within the liver (p = 0.0202) and kidney (p = 0.0363) of the different mouse groups (treated, control and non-treated). In contrast, no significant difference in p53 gene expression was observed between the brain samples [(p = 0.9246) (Figure 4.17 A-C)]. Surprisingly, further analysis using the Welch's *t-test* and Bonferroni correction confirmed that a significant elevation in p53 expression had occurred in kidney of the treated mice (Kidney: Mean = 1.87, SD = 0.609) when compared to the non-treated groups (Kidney: Mean = 1.18, SD = 0.564, p = 0.0302) and a non-significant increase when compared to the control mouse group (Kidney: Mean = 1.29, SD = 0.312, p = 0.0402). A similar pattern was observed in the liver where mice treated to overexpress LRP::FLAG (Mean = 1.38, SD = 0.472) had significantly elevated levels of p53 mRNA when compared to the control (Mean = 0.75, SD = 0.184, p = 0.00648), but only a non-significant increase in comparison to the non-treated (Mean = 0.937, SD = 0.475, p = 0.0853).

Likewise, a similar trend was observed at a protein level where densitometric analysis and One-way ANOVA revealed a significant difference in total p53 levels between the various groups in both the brain (p = 0.0038) and liver [(p = 0.0045) (Figure 4.17 D, E)]. This was further validated by use of a Welch's *t-test* and Bonferroni correction that illustrated that mice treated to overexpress LRP::FLAG (Brain: Mean = 183.70%, SD = 58.70% and Liver: Mean = 135.71%, SD = 30.03%) exhibited

significantly higher levels of p53 in comparison to the non-treated (Brain: Mean = 125.10%, SD = 34.81%, p = 0.0148 and Liver: Mean = 108.55%, SD = 29.71%, p = 0.0447) and control mice (Brain: Mean = 111.89%, SD = 42.88%, p = 0.0072 and Liver: Mean = 95.80%, SD = 23.09%, p = 0.00123) for both brain and liver samples. Although these data demonstrate a marked elevation in p53 that is normally associated with telomere-dependent senescence; certain evidence suggests that p53 induces the elimination of cells exhibiting telomere damage rather than promoting further senescence progression [405]. Therefore the increase in p53 observed post LRP::FLAG overexpression may not be causing an ageing effect, and may in fact require the accumulation of additional senescent markers to promote ageing.

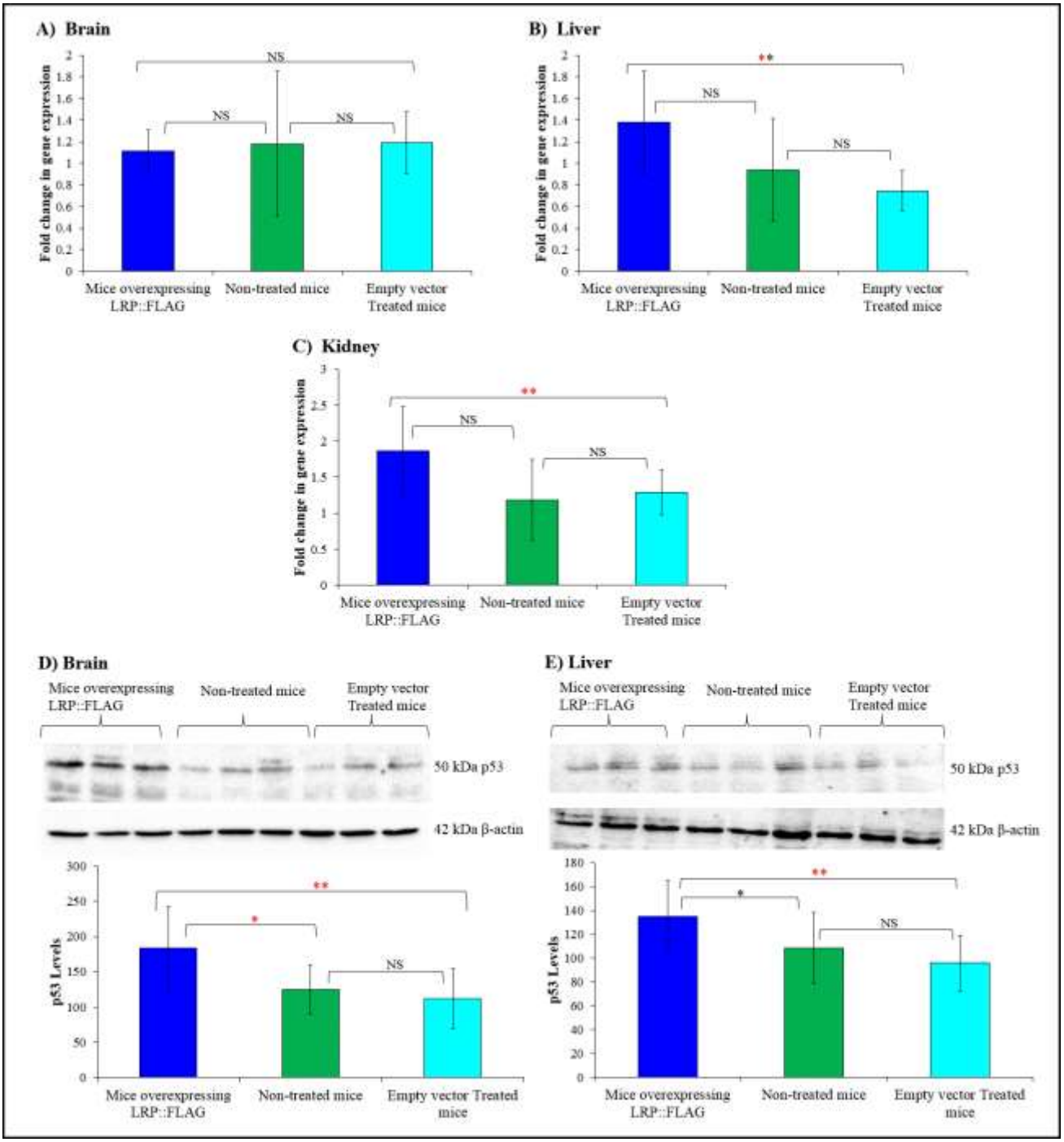


Figure 4.17: Overexpression of LRP::FLAG induced an increase of the tumor suppressor protein, p53 in aged mice.

p53 gene expression levels in the (A) brain (B) liver and (C) kidney were compared between the different mouse treatment groups. Following LRP::FLAG overexpression the treated mice were observed to house a significant elevation of ±0.5 and ±0.6 fold for the liver and kidney, respectively, while no difference was observed for the brain. Sample size: Brain: Treated: n = 6; Control: n = 5 and Non-treated: n = 7. Liver: Treated: n = 8; Control: n = 7 and Non-treated: n = 8. Kidney: Treated: n = 8; Control: n = 6 and Non-treated: n = 9. (A, B, C) GAPDH and RPLPO were used as reference genes for sample normalisation. Subsequently, p53 protein levels were assessed by western blotting in the (D) brain and (E) liver. It was found that LRP::FLAG overexpression induced a ±70% and ±40% increase within the brain and liver. Sample size: Brain: Treated: n = 10; Control: n = 9 and Non-treated: n = 12. Liver: Treated: n = 12; Control: n = 9 and Non-treated: n = 12. (D, E) β-actin was used as a reference protein and all illustrated blots are representative where 4 blots were performed to assess all biological replicates. Data as a mean ±SD. *$p < 0.05$, **$p < 0.01$,

***p < 0.001, NS: p>0.05, non-significant; One-way ANOVA and Welch's *t-test* coupled with a *post hoc* Bonferroni correction were performed for all experiments. The number of '*' irrespective of colour represent the level of significance according to Welch's *t-test*, whereas '*' in red indicate data that is significant following the Bonferroni correction.

4.11 The overexpression of LRP::FLAG significantly impedes the accumulation of senescent markers, p16 and γH2AX in aged mice

4.11.1 LRP::FLAG overexpression decreases p16 levels in aged mice

Following the observed changes to p53 post LRP::FLAG overexpression in the mice it was prudent to confirm the effect that elevating total LRP had on other senescent markers. One of the markers selected was $p16^{INK4A}$, a cyclin dependent kinase inhibitor that serves as a tumor suppressor protein by inhibiting cell cycle progression. Importantly, this protein has been tied to telomere dependent senescence, albeit in a lesser fashion to p53, however it has also been found to play a vital role in telomere-independent senescence processes. Moreover, the accumulation of this protein especially within mice has been tied to the progression of the ageing phenotype. In fact, the reduction or eradication of p16 within senescent cells and tissues has been found to reverse the ageing process and improve longevity [35, 406].

To this end, gene expression analysis coupled with a One-way ANOVA revealed no significant difference in p16 gene expression for all three tested organs when the treated, control and non-treated mouse groups were compared [(Brain: p = 0.3325; Kidney: p = 0.1079 and Liver: p = 0.1031) (Figure 4.18 A-C)]. A more detailed analysis using the Welch's *t-test* and Bonferroni correction found that p16 expression within the kidney of the treated mice (Mean = 0.793, SD = 0.096) was significantly lower than the non-treated (Mean = 1.011, SD = 0.171, p = 0.0268) mice but exhibited a non-significant decrease when compared to the control (Mean = 1.189, SD = 0.489, p = 0.105). In addition, the brain samples also showed a non-significant decrease in p16 expression when the treated mice (Mean = 0.99, SD = 0.286) were compared to the non-treated (Mean = 1.5, SD = 0.782, p = 0.2023) and control mice (Mean = 1.64, SD = 0.872, p = 0.3387). Although p16 expression was non-significantly reduced in the liver when comparing treated to non-treated mice, there was however a suprising increase in p16 expression when comparingh the treated to the control mice. These results were suspected to be a consquence of experiemntal error when plating and therefore will need to be repeated. Thereafter, the protein levels of p16 was assessed by densitometry and One-way ANOVA, where it was revealed that a significant difference in p16 levels existed between the treated, control and non-treated mice within the brain (p = 0.0134) and liver [(p = 0.0141) (Figure 4.18 D, E)]. Upon a deeper scrutinization of the data using Welch's *t-test* and Bonferroni correction

it was validated that the overexpression of LRP::FLAG induced a significant reduction in p16 for the treated mice (Brain: Mean = 65.11%, SD = 20.52%, and Liver: Mean = 38.71%, SD = 30.70%) when compared to the control (Brain: Mean = 89.71%, SD = 35.04%, p = 0.163 and Liver: Mean = 79.81%, SD = 21.85%, p = 0.0045) and non-treated mice (Brain: Mean = 103.79%, SD = 26.23%, p = 0.00057 and Liver: Mean = 99.47%, SD = 62.55%, p = 0.0162). Therefore, suggesting that the overexpression of LRP::FLAG is capable of preventing the accumulation of p16, and thereby effectively delay or impede the progression of the ageing phenotype.

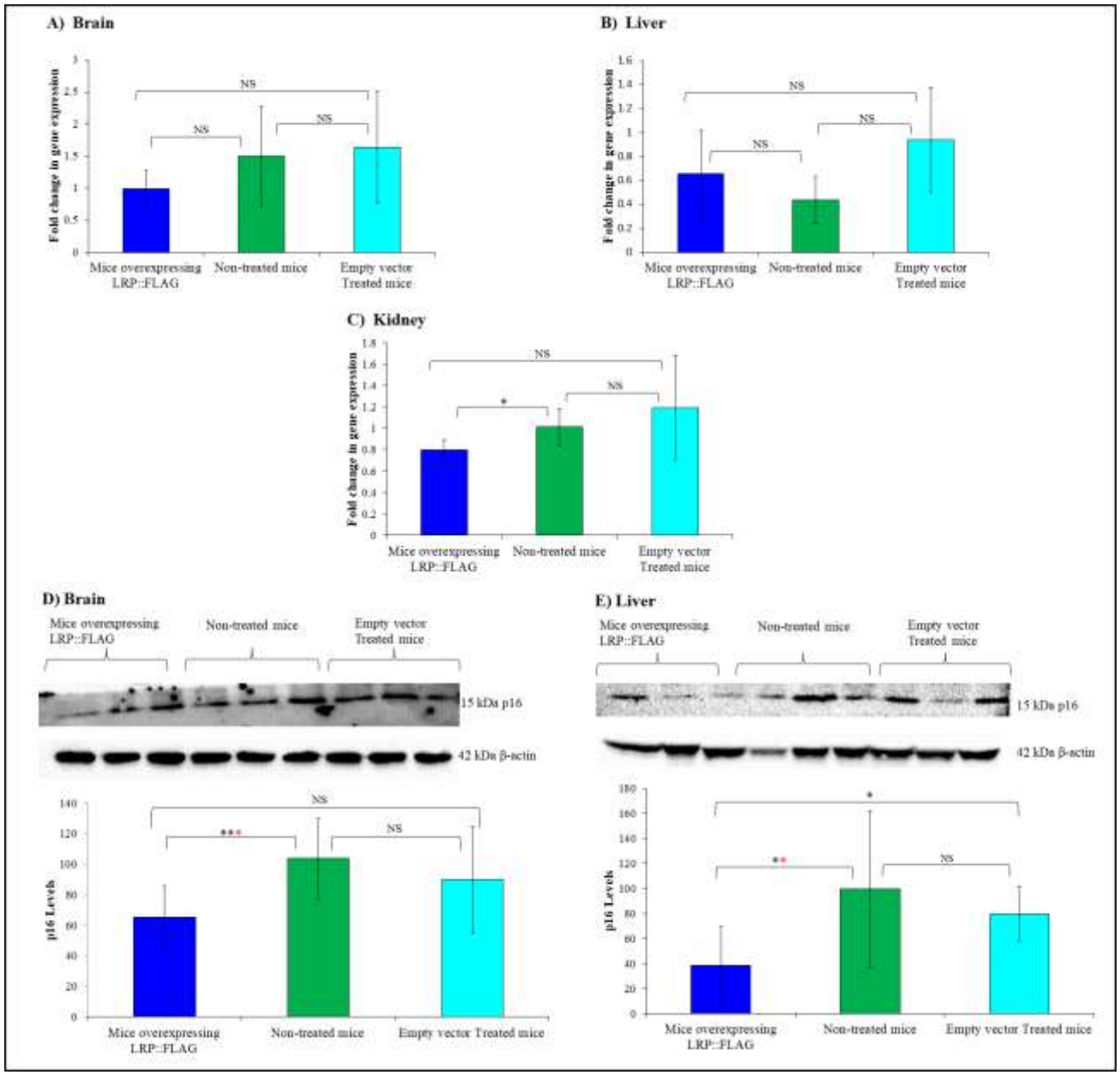


Figure 4.18: LRP::FLAG overexpression significantly reduces the senescent marker p16 in aged mice.

p16 gene expression levels in the (A) brain (B) liver and (C) kidney were compared between the different mouse treatment groups. The treated mice displayed a decrease of ±0.5 and ±0.2 fold for the brain and kidney,

respectively while no difference was observed for the liver. Sample size: Brain: Treated: n = 5; Control: n = 5 and Non-treated: n = 6. Liver: Treated: n = 6; Control: n = 4 and Non-treated: n = 7. Kidney: Treated: n = 6; Control: n = 6 and Non-treated: n = 6. (A, B, C) GAPDH and RPLPO were used as reference genes for sample normalisation. Subsequent assessment of p16 protein levels by western blotting in the (D) brain and (E) liver revealed that LRP::FLAG overexpression induced a ±30% and ±40% reduction within the brain and liver, respectively. Sample size: Brain: Treated: n = 9; Control: n = 7 and Non-treated: n = 11. Liver: Treated: n = 10; Control: n = 8 and Non-treated: n = 10. (D, E) β-actin was used as a reference protein and all illustrated blots are representative where 4 blots were performed to assess all biological replicates. Data as a mean ±SD. *p < 0.05, **p < 0.01, ***p < 0.001, NS: p>0.05, non-significant; One-way ANOVA and Welch's *t-test* coupled with a *post hoc* Bonferroni correction were performed for all experiments. The number of '*' irrespective of colour represent the level of significance according to Welch's *t-test*, whereas '*' in red indicate data that is significant following the Bonferroni correction.

4.11.2 LRP::FLAG overexpression prevents the age-dependent accumulation of γH2AX levels within the aged mice

The confirmed reduction in p16 following the overexpression of LRP::FLAG prompted the assessment of an additional factor that influences ageing, namely the accumulation of DNA damage. To this end, the DNA damage marker γH2AX was assessed. As previously mentioned, γH2AX marks the sites of DNA damage like DSBs and is known to accumulate with age to cause the formation of hetrochromatic foci as well as telomere-induced foci. These foci are then responsible for causing the initial activation for a senescent-dependent DDR thereby making this an ideal marker to track ageing both *in vitro* and *in vivo*. Western blotting and subsequent densitometric analysis with a One-way ANOVA indicated that a significant difference in γH2AX levels was evident between the three mouse groups (treated, control and non-treated) for both brain (p = 0.000016) and liver (p = 0.000012) samples (Figure 4.19 A, B). Additionally, a more in-depth analysis using Welch's *t-test* and Bonferroni correction verified that mice overexpressing LRP::FLAG (Brain: Mean = 55.73%, SD = 17.24%, and Liver: Mean = 52.86%, SD = 14.02%) had a significant reduction in γH2AX levels for both the brain and liver when compared to the non-treated (Brain: Mean = 100%, SD = 13.86%, p = 7.4688E-07 and Liver: Mean = 100.18%, SD = 23.71%, p = 0.0000129) and control (Brain: Mean = 88.88%, SD = 26.59%, p = 0.0161 and Liver: Mean = 95.20%, SD = 26.69%, p = 0.00112) mouse groups. This essentially confirms the *in vitro* data that the overexpression of LRP::FLAG is able to either prevent the accumulation of DNA damage or induce effective DNA repair processes to reduce DNA damage and thereby potentially impede the onset of cell senescence.

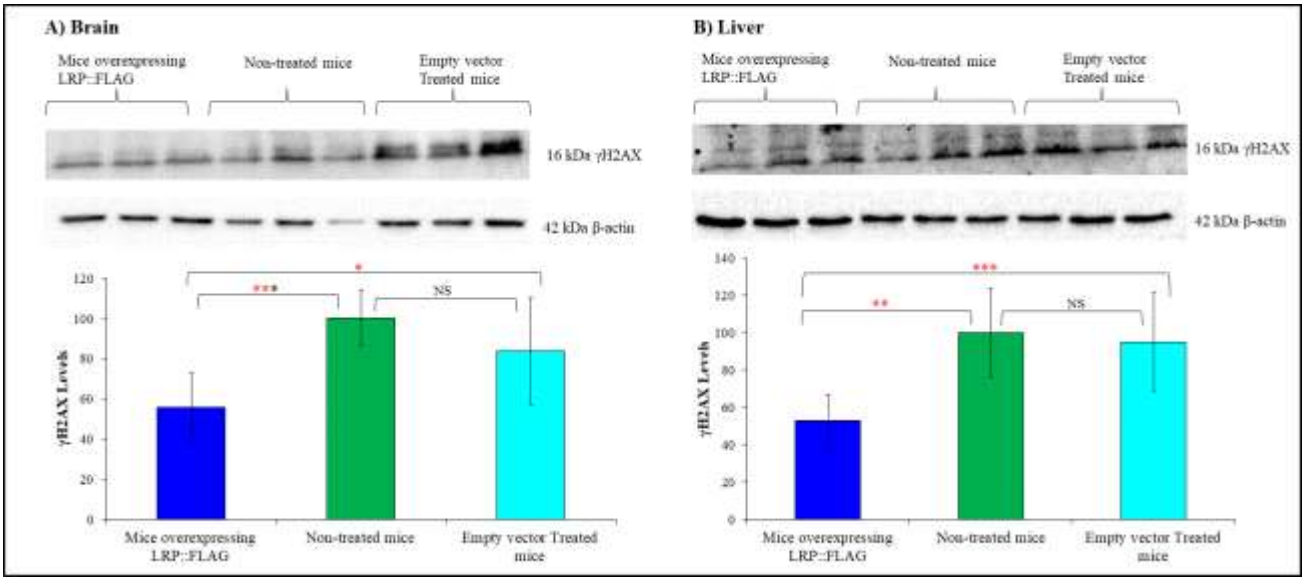


Figure 4.19: The overexpression of LRP::FLAG induces a significant reduction in the DNA damage marker γH2AX within the aged mice.
Protein level assessment of γH2AX levels by western blotting in the (A) brain and (B) liver. Densitomteric analysis was was performed on the bottom bands. Analysis revealed that LRP::FLAG overexpression induced a ±40% and ±50% reduction within the brain and liver, respectively. Sample size: Brain: Treated: n = 12; Control: n = 9 and Non-treated: n = 12. Liver: Treated: n = 12; Control: n = 9 and Non-treated: n = 12. (A, B) β-actin was used as a reference protein and all illustrated blots are representative where 4 blots were performed to assess all biological replicates. Data as a mean ±SD. *p < 0.05, **p < 0.01, ***p < 0.001, NS: p>0.05, non-significant; One-way ANOVA and Welch's *t-test* coupled with a *post hoc* Bonferroni correction were performed for all experiments. The number of '*' irrespective of colour represent the level of significance according to Welch's *t-test*, whereas '*' in red indicate data that is significant following the Bonferroni correction.

4.12 The overexpression of LRP::FLAG lessens the effects of mitochondrial dysfunction by decreasing mitochondrial DNA content in various organs of the aged mice

As previously mentioned, mitochondrial dysfunction forms a major part of the ageing process, where most age-related diseases to some extent are affected by compromised mitochondria. This dysfunction ultimately induces lowered ATP generation and severely heightens ROS production, which in turn allows mtDNA damage as well as mutations to accumulate. In an attempt to ameliorate these effects the cells produce additional mitochondria (increase in mitochondrial mass), however this just results in a cyclic event to further drive mitochondrial dysfunction. Thereafter, the increased oxidative stress targets genomic and telomeric DNA to exacerbate the senescence process. In this regard, assessing the relative mitochondrial DNA content serves to track not only mitochondrial dysfunction but ageing as well. qPCR analysis followed by a One-way ANOVA illustrated that the overexpression of LRP::FLAG significantly affected total mitochondrial DNA content [(Brain: p = 0.0129; Kidney: p = 0.0009 and Liver: p = 0.0132) (Figure 4.20 A-C)]. Additional analysis by

Welch's *t-test* and Bonferroni correction demonstrated that the treated mice (Brain: Mean = 0.721, SD = 0.170; Kidney: Mean = 0.776, SD = 0.220 and Liver: Mean = 0.65, SD = 0.12) contained significantly less mitochondrial DNA in all three tested organs (brain, kidney and liver) in comparison to the non-treated (Brain: Mean = 1.035, SD = 0.187, p = 0.00153; Kidney: Mean = 1.057, SD = 0.301, p = 0.0322 and Liver: Mean = 1.06, SD = 0.363, p = 0.0069) and control mice (Brain: Mean = 1.117, SD = 0.398, p = 0.0407; Kidney: Mean = 1.386, SD = 0.369, p = 0.0036 and Liver: Mean = 1.16, SD = 0.408, p =0.0274). These data essentially illustrate that the overexpression of LRP::FLAG may prevent senescence-associated mitochondrial dysfunction. Therefore, the reduced mitochondrial DNA content together with the effects on the other senescent markers suggests that LRP/LR may indeed play an imperative role in influencing the process of cellular ageing.

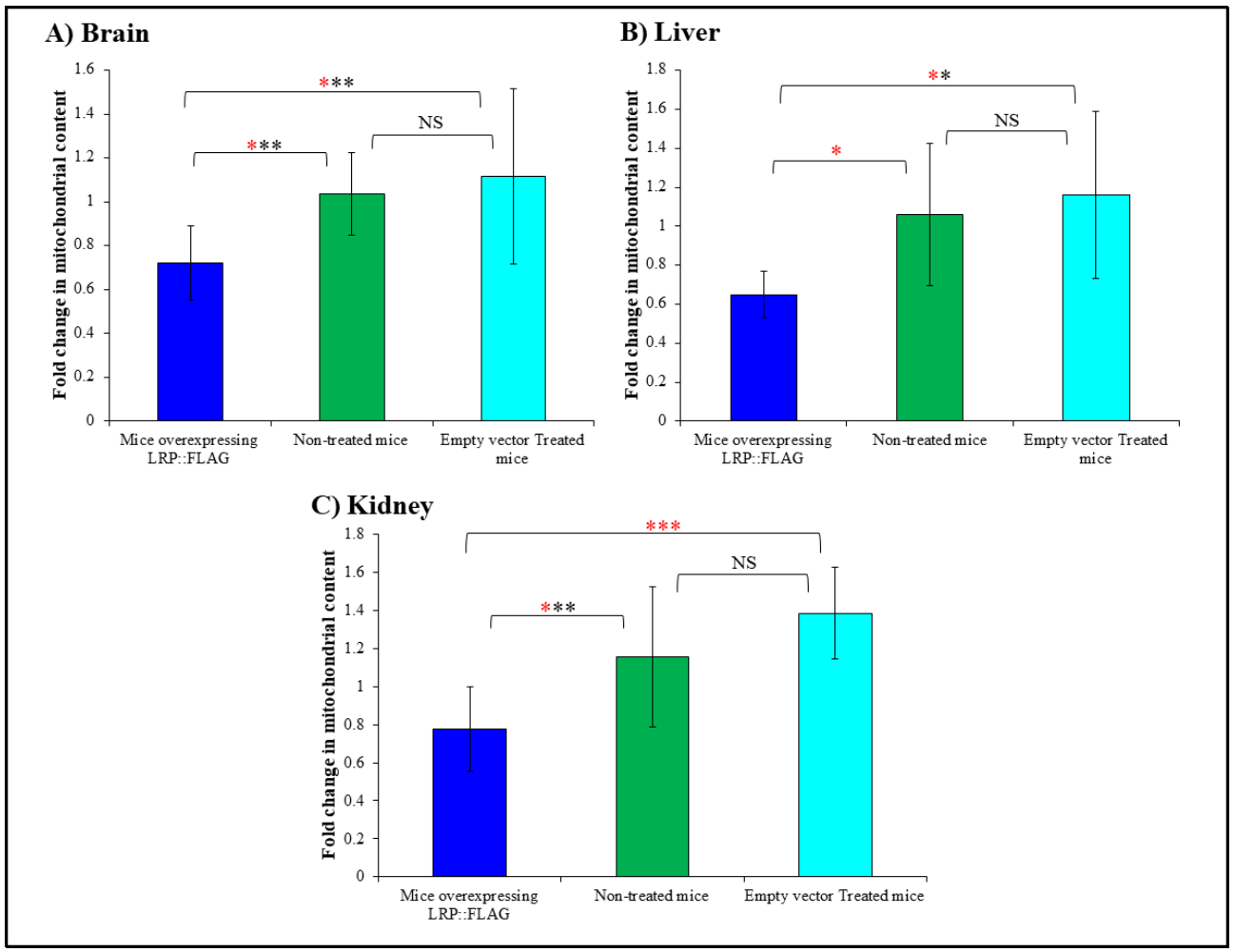


Figure 4.20: The overexpression of LRP::FLAG significantly reduces total mitochondrial DNA content in aged mice.

Mitochondrial DNA content assessment by qPCR revealed that LRP::FLAG overexpression induced a ±0.3, ±0.4 and ±0.4 fold reduction within the (A) brain, (B) liver and kidney (C). Sample size: Brain: Treated: n = 8; Control: n = 7 and Non-treated: n = 11. Liver: Treated: n = 8; Control: n = 6 and Non-treated: n = 10 and

Kidney: Treated: n = 9; Control: n = 7 and Non-treated: n = 10. Nuclear specific primers for hexokinase 2 gene, intron 9 were used as reference genes for sample normalisation. Data shown for all three organs is representative of three averaged technical repeats for each biological replicate. Data as a mean ±SD. *p < 0.05, **p < 0.01, ***p < 0.001, NS: p>0.05, non-significant; One-way ANOVA and Welch's *t-test* coupled with a *post hoc* Bonferroni correction were performed for all experiments. The number of '*' irrespective of colour represent the level of significance according to Welch's *t-test*, whereas '*' in red indicate data that is significant following the Bonferroni correction.

4.13 LRP::FLAG overexpression induces a significant improvement of telomere dynamics within the aged mice

4.13.1 LRP::FLAG overexpression causes a significant increase in TERT and pTERT levels in aged mice

As the overexpression of LRP::FLAG was found to improve various aspects of telomere dynamics *in vitro* coupled with the positive effects on proliferative, anti-ageing and senescent markers *in vivo* made it prudent to discern, whether a similar effect could be induced on telomere dynamics *in vivo*. To this end both TERT and its active form pTERT were assessed. As previously mentioned, TERT acts as the limiting factor to telomerase activity and thus is one of the major reasons for telomere erosion due to a lack of maintenance. In addition, the functions of this protein are imperative for carrying out an anti-ageing effect not only in an *in vitro* setting but within an *in vivo* setting as well. Firstly, gene expression analysis by qPCR was undertaken with a One-way ANOVA, where a significant difference in TERT mRNA levels was found in the kidney [(p = 0.0351) (Figure 21 A)]. Meanwhile, the brain (p = 0.392) and liver (p = 0.1031) displayed a non-significant difference when comparing the treated, control and non-treated mouse groups (Figure 21 B, C). Further analysis by Welch's *t-test* and Bonferroni correction illustrated that the treated mice displayed a significant increase in mTERT gene expression for the kidney (Mean = 2.16, SD = 0.95) and a non-significant increase for the brain (Mean = 1.4, SD = 0.224) and liver (Mean = 1.64, SD = 0.89) when compared to the non-treated (Brain: Mean = 1.01, SD = 0.566, p = 0.298; Kidney: Mean = 1.14, SD = 0.572, p = 0.0483 and Liver: Mean = 1.079, SD = 0.433, p = 0.121) and control mice (Brain: Mean = 1.12, SD = 0.502, p = 0.167; Kidney: Mean = 1.23, SD = 0.573, p = 0.0725 and Liver: Mean = 1.021, SD = 0.352, p = 0.082).

Following gene expression analysis, the total protein levels of mTERT were assessed. Subsequent densitometric analysis and One-way ANOVA confirmed that there was a significant difference between the treated, non-treated groups [(Brain: p = 0.0046 and Liver: p = 0.0071) (Figure 21 D, E)]. Upon further analysis using the Welch's *t-test* and Bonferroni correction it was validated that the overexpression of LRP::FLAG within the treated mice (Brain: Mean = 153.36%, SD = 62.44% and

Liver: Mean = 144.70%, SD = 45.55%) induced a significant increase in total mTERT protein levels for both the brain and liver when compared to the control (Brain: Mean = 82.14%, SD = 39.93%, p = 0.0118 and Liver: Mean = 94.87%, SD = 22.91%, p =0.0094) and non-treated mice (Brain: Mean = 100%, SD = 27.77%, p = 0.0138 and Liver: Mean = 100%, SD = 28.11, p =0.0185). This confirms the *in vitro* findings that the overexpression of LRP::FLAG is capable of influencing TERT levels. Following these findings it was imperative to assess, whether the increased TERT observed was being phosphorylated to induce the proteins activation to allow for an increase in its activity for telomeric extension. Similarly, densitometry and One-way ANOVA of pTERT blots confirmed that there was a significant difference between the three groups (treated, control and non-treated) for both the brain (p = 0.0003) and liver [(p = 0.002) (Figure 21 F, G)]. In addition, a more detailed analysis using the Welch's *t-test* and Bonferroni correction found that mice treated to overexpress LRP::FLAG (Brain: Mean = 148.53%, SD = 35.58% and Liver: Mean = 135.15%, SD = 42.60%) displayed a greater degree of "active" pTERT in both the brain and liver when compared to the non-treated (Brain: Mean = 100%, SD = 18.35%, p = 0.00064 and Liver: Mean = 95.96%, SD = 24.50%, p = 0.0138) and control (Brain: Mean = 117.20%, SD = 22.80%, p = 0.0122 and Liver: Mean = 86.33%, SD = 12.96%, p =0.0023) samples. These data indicate that not only does LRP/LR appear capable of influencing TERT levels; it may also play a role in the activation of this protein so that it can form the active telomerase complex to carry out telomere maintenance effects.

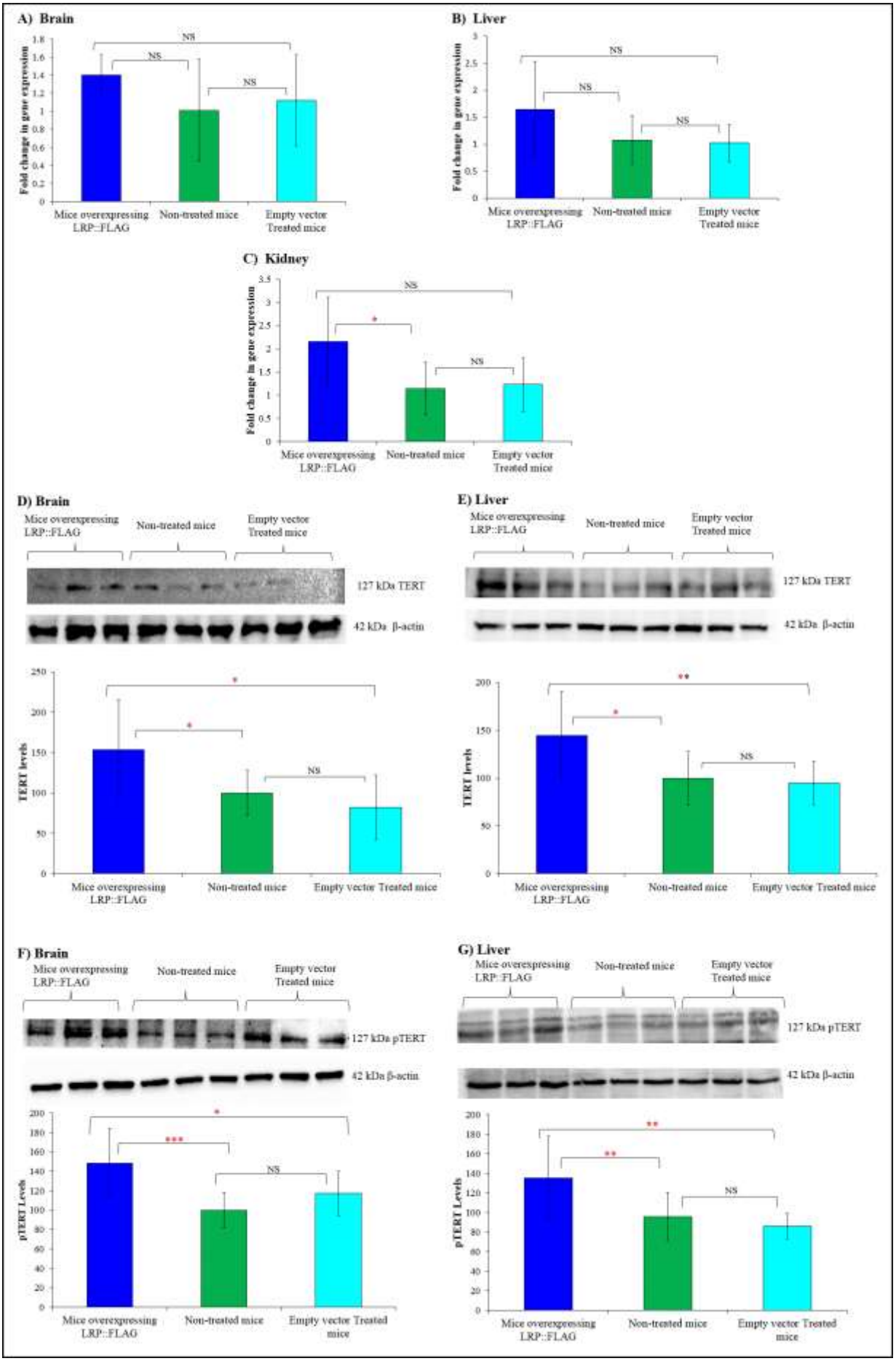

A) Brain
Fold change in gene expression
NS
NS
NS
Mice overexpressing LRP::FLAG
Non-treated mice
Empty vector Treated mice
B) Liver
Fold change in gene expression
NS
NS
NS
Mice overexpressing LRP::FLAG
Non-treated mice
Empty vector Treated mice
C) Kidney
Fold change in gene expression
NS
*
NS
Mice overexpressing LRP::FLAG
Non-treated mice
Empty vector Treated mice
D) Brain
Mice overexpressing LRP::FLAG
Non-treated mice
Empty vector Treated mice
127 kDa TERT
42 kDa β-actin
TERT levels
*
*
NS
Mice overexpressing LRP::FLAG
Non-treated mice
Empty vector Treated mice
E) Liver
Mice overexpressing LRP::FLAG
Non-treated mice
Empty vector Treated mice
127 kDa TERT
42 kDa β-actin
TERT levels
**
*
NS
Mice overexpressing LRP::FLAG
Non-treated mice
Empty vector Treated mice
F) Brain
Mice overexpressing LRP::FLAG
Non-treated mice
Empty vector Treated mice
127 kDa pTERT
42 kDa β-actin
pTERT Levels
*
***
NS
Mice overexpressing LRP::FLAG
Non-treated mice
Empty vector Treated mice
G) Liver
Mice overexpressing LRP::FLAG
Non-treated mice
Empty vector Treated mice
127 kDa pTERT
42 kDa β-actin
pTERT Levels
**
**
NS
Mice overexpressing LRP::FLAG
Non-treated mice
Empty vector Treated mice

Figure 4.21: LRP::FLAG overexpression significantly elevated total TERT and active pTERT levels in aged mice.
TERT gene expression analysis by qPCR was performed in the (A) brain (B) liver and (C) kidney to compare expression differences between the different mouse treatment groups. It was observed that overexpression of LRP::FLAG induced a significant ±0.8 fold increase for the kidney, while a non-significant increase of ±0.4 and ±0.6 fold was evident in the brain and liver, when compared to the non-treated and control. Sample size: Brain: Treated: n = 5; Control: n = 5 and Non-treated: n = 6. Liver: Treated: n = 8; Control: n = 7 and Non-treated: n = 7. Kidney: Treated: n = 6; Control: n = 6 and Non-treated: n = 8. (A, B, C) GAPDH and RPLPO were used as reference genes for sample normalisation. Thereafter, total TERT protein levels were assessed by western blotting in the (D) brain and (E) liver. It was found that LRP::FLAG overexpression induced a ±50% and ±40% increase within the brain and liver. Sample size: Brain: Treated: n = 11; Control: n = 8 and Non-treated: n = 12. Liver: Treated: n = 10; Control: n = 8 and Non-treated: n = 10. In addition, protein levels of phosphorylated TERT (pTERT) were assessed by western blotting in the brain (F) and liver (G). It was noted that the treated mice displayed a significant increase of ±30% and 40% was noted when compared to the non-treated and control. Sample size: Brain: Treated: n = 12; Control: n = 8 and Non-treated mice: n = 12 and Liver: Treated: n = 12; Control: n = 9 and Non-treated mice: n = 11. (D, E, F, G) β-actin was used as a reference protein and all illustrated blots are representative where 4 blots were performed to assess all biological replicates. Data as a mean ±SD. *p < 0.05, **p < 0.01, ***p < 0.001, NS: p>0.05, non-significant; One-way ANOVA and Welch's *t-test* coupled with a *post hoc* Bonferroni correction were performed for all experiments. The number of '*' irrespective of colour represent the level of significance according to Welch's *t-test*, whereas '*' in red indicate data that is significant following the Bonferroni correction.

4.13.2 LRP::FLAG overexpression causes an increase in relative telomerase activity in the kidney and liver of aged mice

In order to confirm that the increased TERT and pTERT observed was causing a subsequent increase in telomerase activity post LRP::FLAG overexpression, an in house TRAP assay using qPCR was performed. Initial qPCR analysis coupled with a One-way ANOVA illustrated that the overexpression of LRP::FLAG did induce a significant change in telomerase activity within the kidney and liver samples, when compared to the non-treated and control mouse groups [(Kidney: p = 0.0037 and Liver: p = 0.0177) (Figure 4.22 B, C)]. In addition, it was also found that no significant difference was observed in the brain when comparing between the different mouse groups [(p = 0.1765) (Figure 4.22 A)]. This lack of change in telomerase activity within the brain may be explained by the fact that even in juvenile mice there is only a basal level of telomerase activity, as majority of the TERT expressed within the brain appears to play extra-telomeric functions. Moreover, a deeper analysis using Welch's *t-test* and Bonferroni correction revealed that the treated mice (Kidney: Mean = 0.0025 amole, SD = 0.00075 amole and Liver: Mean = 0.0047 amole, SD = 0.0019 amole) exhibited a significantly greater elevation in telomerase activity within the kidney and liver when compared to the non-treated (Kidney: Mean = 0.0013 amole, SD = 0.00028 amole, p = 0.0072 and Liver: Mean = 0.0024 amole, SD = 0.00096 amole, p = 0.0319) and control mice (Kidney: Mean = 0.0016 amole, SD = 0.00033 amole, p = 0.0254 and Liver: Mean = 0.0026 amole, SD = 0.00068 amole, p = 0.0399). These data in conjuction with the *in vitro* results clearly suggests

that LRP/LR may play an influential role in mediating telomerase activity, and therefore alterations in LRP/LR levels may play a pivotal role in regulating telomere dependent senescence.

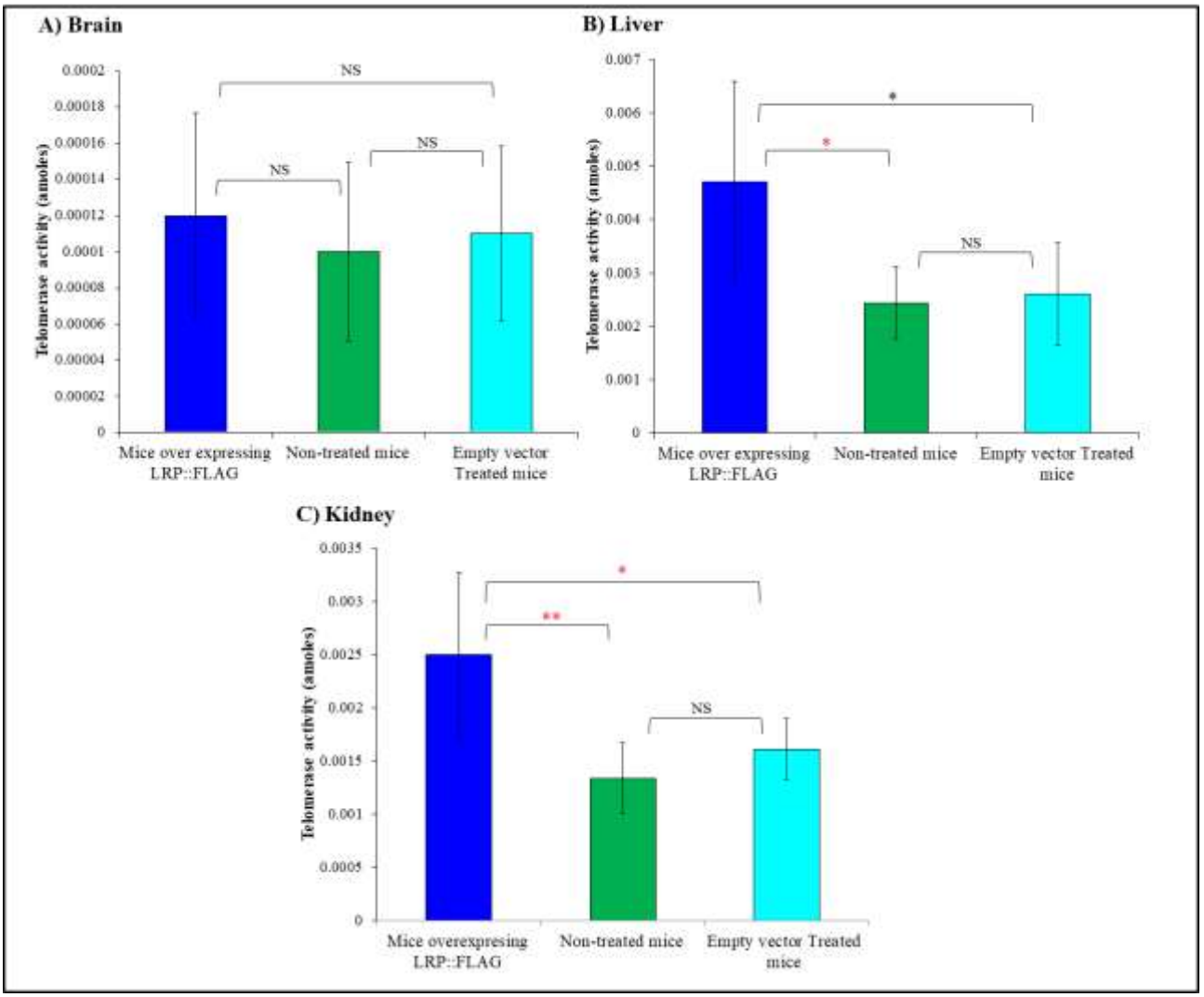


Figure 4.22: The overexpression of LRP::FLAG caused a significant elevation in relative telomerase activity within the kidney and liver of aged mice.

Relative telomerase activity was quantified by qTRAP and real time PCR. (A) Analysis for the brain displayed no significant difference in telomerase activity between the three groups. (B, C) Quantification of telomerase activity within the liver and kidney revealed a significant 0.002 and 0.001(log amole) elevation in activity for the treated mice, when compared to the non-treated and control mice. Data shown for all three organs is representative of sample data subtracted from the heat treated control. Sample size: Brain: n = 7 biological replicates for all three groups. Liver: n = 6 biological replicates for the treated and non-treated groups while n = 5 biological replicates for the control group. Kidney: n = 6 biological replicates for all three mouse groups. Data as a mean ±SD. *p < 0.05, **p < 0.01, ***p < 0.001, NS: p>0.05, non-significant; One-way ANOVA and Welch's *t-test* coupled with a post hoc Bonferroni correction. The number of '*' irrespective of colour represent the level of significance according to Welch's *t-test*, whereas '*' in red indicate data that is significant following the Bonferroni correction.

4.13.3 LRP::FLAG overexpression causes a significant increase in mean telomere length in kidney and liver of aged mice

The final aspect assessed for the *in vivo* study was whether LRP/LR could influence the mean telomere length within tissue to attenuate the senescence process on an organism scale. To this end telomere length was assessed using the protocol outlined by Cawthon, et al., (2002)[388]. Subsequent analysis by qPCR and One-way ANOVA illustrated that when the three groups (treated, control and non-treated) a significant difference was noted in the kidney and liver while no significant difference was observed for the brain [(Brain: $p = 0.9332$; Kidney: $p = 0.0065$ and Liver: $p = 0.0072$) (Figure 4.23 A-C)]. In fact, further analysis utilising Welch's *t-test* and Bonferroni correction verified that the treated mice's (Kidney: Mean = 1.56, SD = 0.167 and Liver: Mean = 1.59, SD = 0.514) average telomere length was significantly greater in comparison to both the control (Kidney: Mean = 1.02, SD = 0.319, $p = 0.0191$ and Liver: Mean = 0.93, SD = 0.392, $p = 0.0269$) and non-treated (Kidney: Mean = 1.01, SD = 0.470, $p = 0.0337$ and Liver: Mean = 0.98, SD = 0.376, $p = 0.0266$) mice within the liver and kidney samples. In regards to the brain, the fact that there was no significant change in mean telomere length may be a consequence of the lack of change in telomerase actvity observed. Moreover, it can be directly attributed to the tissue being poorly proliferative, and would therefore not display signs of extensive telomere erosion like the other organs. These data further corroborate what was observed *in vitro* that the overexpression of LRP::FLAG is capable of stimulating telomerase for an enhanced telomere maintenance effect. Therefore, this indicates that LRP/LR could be utilised or targeted to specifically impede telomere-dependent senescence to improve organism fitness and allow for a healthier form of ageing.

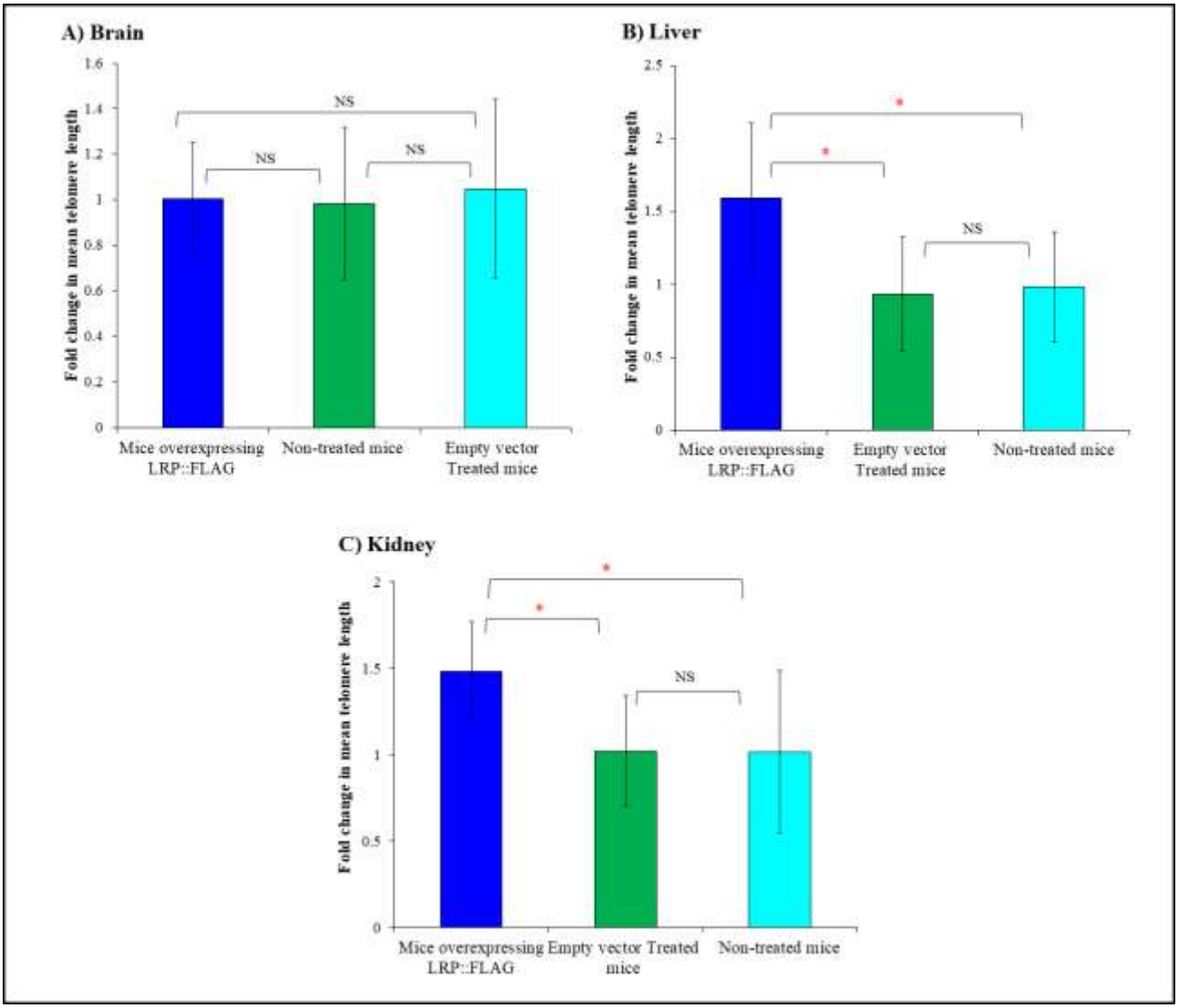


Figure 4.23: The overexpression of LRP::FLAG causes a substantial increase in mean telomere length within the kidney and liver of the aged mice.

Mean telomere length was measured by qPCR and normalised to the reference gene 36B4 to generate a telomere/ 36B4 (T/S) ratio. (A) Brain samples showed no significant difference in relative telomere length across all three mouse groups. (B) A significant ±0.6 fold increase in telomere length was evident in the treated mice when compared to the non-treated and control mouse groups for the liver. (C) Analysis revealed a significant increase of ±0.5 fold in relative telomere in the treated mice when compared to the non-treated and control mouse groups. Error bars are indicative of standard deviation. Data shown for all three organs is representative of three averaged technical repeats for each biological replicate. Brain: n = 7 biological replicates for all three groups. Liver: n = 7 biological replicates for the treated and non-treated groups while n = 6 biological replicates for the control group. Kidney: n = 9 biological replicates for the treated and non-treated groups while n = 7 biological replicates. Data as a mean ±SD. *p < 0.05, **p < 0.01, ***p < 0.001, NS: p>0.05, non-significant; One-way ANOVA and Welch's *t-test* coupled with a post hoc Bonferroni correction. The number of '*' irrespective of colour represent the level of significance according to Welch's *t-test*, whereas '*' in red indicate data that is significant following the Bonferroni correction.

5. Discussion

The research areas pertaining to healthy ageing and longevity extensions have been a prime target of scientific investigation for decades. These areas have garnered intense interest due to the enticing prospect of increasing the average human lifespan. However, an additional factor that has stimulated increased research motivation into this field, is that an ever-increasing number of diseases have been shown to be tied to ageing. In fact, anti-ageing or anti-senescent strategies have shown lucrative results in treating or managing these diseases. This said, the ageing process has been found to be attenuated by a variety of different strategies including: diet; specifically caloric restriction (which influences insulin signalling and oxidative stress to retard ageing), reducing DNA damage by use of NAD+ (stimulates DNA damage repair), senolytics (selective elimination of senescent cells) as well as using or targeting anti-ageing proteins like SIRT1, klotho and TERT [140, 407-409]. In regard to TERT and telomerase activity, it is more than likely one of the most well studied proteins in both the fields of ageing as well as cancer. It is well known that a lack of telomerase activity, induced by the absence of TERT allows the accumulation of short/damaged telomeres to elicit a permanent DDR. Subsequently, causing a loss/ decline in regenerative capacity for systemic organismal ageing in both humans and mice [143, 221, 410].

Indeed, the reactivation of telomerase, through genetic manipulation and/ or targeting the TERT gene with specific proteins like c-Myc or using biomolecules like TA-65 as an activator, has proven to impede cell senescence and allow for tissue rejuvenation in both an *in vitro* and *in vivo* research aspect [141, 411, 412]. The current study serves to demonstrate for the first time that the proliferative protein LRP/ LR could induce a similar effect for the stimulation of telomerase. Moreover, this particular protein may house other anti-ageing properties aside from influencing TERT, due to its apparent broad spanning effect on other senescent markers and anti-ageing proteins. Prior to discussing LRPs potential anti-ageing properties it is important to note that it shares a number of similar characteristics with TERT. This includes similar localisations, functions, diseases (like cancer and AD) and most interestingly both proteins are found in high abundance during embryonic development (specifically in undifferentiated cells). Subsequently, during differentiation and increasing age there is a gradual decline in the levels of both proteins. This link between TERT and LRP was further solidified when the two proteins were confirmed to interact *in vitro* within tumorigenic cells. Furthermore, it was shown that knock down of LRP/LR induced a subsequent

decrease in telomerase activity, thereby justifying the link between these two proteins in a cancer context.

5.1 LRP and LRP::FLAG co-localise with TERT *in vitro*

The functional relationship and shared localisation between LRP/LR and TERT was further confirmed in the current study, where post LRP::FLAG overexpression (Figure 4.1 a, b) a distinct amount of co-localisation occurred in both HEK293 and MRC 5 cell lines (Figure 4.2 a, b). Interestingly, the only way such a co-localisation would have been possible within the MRC 5's is that the increased LRP levels stimulated the production of TERT; as most somatic lines like MRC 5 produce negligible levels of TERT *in vitro*. Consequently, it was further established that both the transfected lines appeared to not only have increased TERT levels, but also an increased amount of co-localisation between the two proteins within the peri-nuclear and cytosolic regions (Figure 4.2 a, b). Although this distribution is uncommon for TERT in non-tumorigenic cells, a number of studies have established that the shuttling of TERT between the cytoplasm and the nucleus occurs in both tumorigenic as well as non-tumorigenic lines [215, 230, 233]. This shuttling of TERT is vital for cell immortalisation as it allows TERT to carry out extra-telomeric functions aside from telomerase activity, like aiding in mitochondrial protection and function [215, 230, 233]. Alternatively, the widespread distribution of TERT could be a result of other factors. Firstly, it is known that the TERT gene has the ability to produce multiple splice variants (the epitope that the antibody recognises could be conserved across multiple variants of TERT), where these different isoforms normally carry out functions independent of telomerase activity [225, 413]. Secondly, it is known that a portion of the TERT gene encodes for a component of the major histocompatibility complex (MHC), which would further explain the fluorescence noted on the surface of the cells [414].

5.2 Overexpression of LRP::FLAG improves telomere dynamics in aged cells *in vitro*

The seemingly increased levels of TERT observed within the cells during confocal microscopy following LRP::FLAG overexpression was further validated by western blotting. In fact, the striking increases observed for the 120 kDa fully functional TERT in both cell lines, especially within the fibroblast MRC 5 line (which normally contains negligible levels of TERT), suggests that LRP may stimulate the production of TERT for telomerase activity [(Figure 4.3 a1-b2) [291, 292]]. Consequently, this increased production in TERT appeared to follow the central dogma in telomere biology, as a corresponding elevation in telomerase activity was evident in both cell lines. This

dogma states that the ectopic expression of TERT or the stimulation of its production at any stage within the cell cycle is sufficient to elevate telomerase activity for enhanced telomeric maintenance and cell immortalisation *in vitro* [136, 139, 184, 415]. The increased telomerase activity observed post LRP::FLAG overexpression (Figure 4.3 c, d) could indicate, that aside from elevating TERT, LRP could potentially play a role in forming the active telomerase complex. Either through the recruitment of telomerase associated proteins, promoting the association of TERT and TERC or even in aiding in the shuttling of telomerase components within the cell. These observations were made based off the previously seen co-localisation and that LRP appears to influence telomerase activity in both normal and tumorigenic cells.

Moreover, these results clearly resemble other telomerase modulating strategies like TA-65 or gene based therapies [136, 140, 141]. This clearly illustrates that the elevation of both TERT and telomerase activity by LRP::FLAG overexpression is sufficient to potentially stimulate telomere maintenance for an enhanced proliferative lifespan [136, 140, 141, 293]. This was further supported by the large difference in mean telomere length noted between both transfected and non-transfected cell lines indicating that a telomere maintenance effect had indeed occurred (Figure 4.3 e, f). However, the average telomere length does not provide a detailed insight as to whether the maintenance effect observed was targeting the shortest telomeres to prevent the critical loss and exposure of the overhangs. Prior studies do offer imperative insight, where telomerase has been shown to preferentially extend the shortest telomeres, which it identifies according to the number of shelterin present on each telomere. Therefore this suggests that the telomeric extension provided by the increased telomerase activity post LRP::FLAG overexpression provided sufficient maintenance to prevent the accumulation of critically shortened telomeres [293]. In turn, this would prevent the induction of telomere-dependent senescence thereby impeding cellular ageing, at least *in vitro* [136, 184, 415, 416].

5.3 LRP::FLAG overexpression influences the accumulation of senescent markers *in vitro*

The increased telomere length and potential impediment of senescence was further confirmed by the reduction in both tested senescent markers; β-galactosidase and γH2AX (Figure 4.4 a-d). More specifically β-galactosidase is an enzyme housed within the lysosomes that serves as a hydrolase, especially in senescent cells, by cleaving the β-linked terminal galactosyl residues of substrates [395]. This said, as cells age and enter senescence, there is a gradual increased production in

lysosomal mass and β-galactosidase. This increase has been theorised to be a result of an accumulation of non-degradable macromolecules and organelles housed in autophagic vacuoles [2, 395]. Secondly, the increased lysosomal content is further brought about by age-related changes to epigenetic patterns allowing senescent pathways to be favoured [2]. Ultimately, these epigenetic alterations can be linked to telomere dysfunction and thereby illustrates that increased β-galactosidase activity can be used to track cellular ageing [395, 417]. Therefore, the observed reduction in β-galactosidase activity in both cell lines clearly points towards an anti-senescence effect (Figure 4.4 a, b).

A similar effect was also noted when assessing the second senescent marker γH2AX, where stark reductions in this DNA damage marker was noted in both transfected cell lines (Figure 4.4 c, d). This implies that LRP may play a role in DNA damage response either by aiding in the prevention of damage or playing an active part in ameliorating the damage and thus preventing an age-dependent accumulation. Moreover, this reduction alongside the increased telomere length signifies that not only is DNA damage being reduced it may also aid in preventing the generation of telomere induced foci. These positive effects exerted on the DNA damage response following LRP::FLAG overexpression could be a consequence of two proposed mechanisms. Firstly, the increased TERT induced by LRP::FLAG could be performing extra-telomeric functions aside from telomere maintenance. As previously stated, TERT has been proven to exhibit DNA repair functionality that can act on both heterochromatic foci and TIFs [129, 225, 232]. This occurs by telomerase acting as a substitute repair enzyme (fills in DNA breaks with telomeric repeats) or TERT can aid in the recruitment of DNA repair proteins [129, 225, 232]. Alternatively, LRP itself could aid in the recruitment of DNA repair proteins due to the supporting role it plays in the nucleus [292, 298, 418]. In fact, the increased LRP present within the transfected cells could provide additional nuclear structural support to prevent further damage. Instead LRP may also have chromatin modification abilities, through its histone association, and may therefore allow chromatin repression so that DNA repair proteins could access the sites of DNA damage with ease. Therefore, the reduction in both senescent markers within the transfected cells strongly indicates that LRP may have anti-senescent functionality [293].

Finally, at the culmination of the *in vitro* study it was noted that the non-transfected MRC 5 cells entered senescence at around passage doubling 49-50, while its transfected counterpart underwent an additional 20 population doublings before concluding the study. Collectively, these findings strongly indicate that the overexpression of LRP::FLAG was sufficient to influence telomere dynamics to

allow for the state and processing of juvenile cells to be retained, by impeding the ageing process *in vitro* [136, 140, 143, 184, 293].

5.4 Overexpression of LRP::FLAG improves physiological functioning in aged mice

5.4.1 LRP::FLAG overexpression prevents the accumulation of grey hair

Based off the highly promising data collected from the *in vitro* study it was prudent to confirm if the potential anti-ageing functionality that LRP illustrated *in vitro* could be replicated on an organism scale *in vivo*. Accordingly, aged mice were treated to overexpress LRP::FLAG after which various physiological and histological parameters were performed. The first parameter that provided an indication that the overexpression of LRP::FLAG was indeed providing an anti-senescence effect was the marked decrease in hair greying of the treated mice (Figure 4.5). Although, the C57BL/6J mouse strain does exhibit a fairly homogenous dark coat throughout their lifespan, a gradual accumulation in the amount of grey hairs was evident. Interestingly, it must be pointed out that no hair thinning/ balding was evident within any of the treated mice, while 2-3 mice from the control and non-treated group each displayed signs of thinning and balding. This reduction in hair greying could be attributed to a replenishment of melanocyte stem cells or the conservation of the pigment production machinery within the treated mice [419]. Moreover, the absence of hair thinning and balding in the treated mice clearly indicates that the hair follicles are not being lost through senescence onset. In part, the improved telomere length observed both at an *in vitro* (Figure 4.3 e, f) and *in vivo* (Figure 4.23) level coupled with the reduced mitochondrial DNA content (Figure 4.20), IL 6 and 8 levels (Supplementary Figure 8.1 and 8.2), which indirectly indicates a reduction in oxidative stress, could provide a maintenance effect to prevent melanocyte stem cell depletion [419-422]. This therefore, indicates that the overexpression of LRP::FLAG potentially stimulated these factors positively to induce the observed reduction in hair greying.

5.4.2 LRP::FLAG overexpression improves cognitive function in aged mice

Normally with ageing there is a corresponding reduction in cognitive function. This is mainly manifested through a gradual decline in higher order function centering around short and long term memory as well as working ability, planning and puzzle solving ability. This age-dependent decline is brought about in part by a loss in neuronal tissue, especially within the hippocampus and negative alterations (like disruptions in mTOR signalling) to neuro-based signalling pathways [423]. Two distinct cognitive tests were performed (puzzle box and nesting test) to confirm whether LRP::FLAG

had the ability to prevent age-related cognitive decline. From the results obtained, it was evident that the overexpression of LRP::FLAG had a profound effect on cognitive function. Firstly, the puzzle box test clearly illustrated that the treated mice had superior short and long term memory, as well as puzzle solving ability when compared to their non-treated and control counterparts (Figure 4.6). This was illustrated, where all treated mice exhibited largely reduced latencies in solving the puzzles and reaching the goal zone. In turn, this implied that the treated mice showed greater spatial recognition and reference memory suggesting that neural plasticity within the hippocampus was maintained, explaining the observed memory enhancement [400].

These data were further corroborated by the nesting test results, where mice treated to overexpress LRP::FLAG exhibited improved nesting ability (Figure 4.7). In this regard, the ability to successfully build a complete nest relies heavily on hippocampal integrity (for spatial memory) and a fully functioning medial prefrontal cortex [392]. This said, the significant improvement in nest building ability, alongside the improved short and long term memory as well as puzzle solving ability, indicate that the overexpression of LRP::FLAG likely impeded the age-dependent neurodegeneration of the hippocampus for enhanced cognitive function. This was further confirmed by histopathological analysis where less tissue degeneration was noted in the treated mice. In addition, these improvements could be a result of multiple consequences that have been previously confirmed to positively influence brain ageing. A few of these factors include; conservation of neuronal signalling, reduced age-related inflammation (decreased expression of IL6 and 8 within neuronal tissue (Supplementary Figure 8.1 and 8.2), reduced oxidative stress from the increased levels of TERT (both *in vitro* (Figure 4.3 a1-b2) and *in vivo* (Figure 4.21)), mitochondrial content (Figure 4.20) and klotho's anti-oxidant capabilities (Figure 4.16) [285, 399, 424-426]. In fact, elevated levels of secreted klotho especially in the hippocampal region of the brain has been shown to not only improve memory related functions, but nesting abilities as well [399]. All of these factors observed post LRP::FLAG overexpression would act in a synergistic manner to prevent or reduce the effects of neurological ageing. Therefore, this infers that the use of LRP::FLAG or stimulation of LRP/LR could act as a potent cognitive enhancer for aged mice.

5.4.3 Overexpression of LRP::FLAG improves motor function

The final physiological aspect that displayed a significant improvement post LRP::FLAG overexpression in the aged mice was motor function and balance co-ordination (Figure 4.8). These two physiological parameters have been well documented to decline with increased age, where

C57BL/6J mouse models have been confirmed to exhibit stark motor skill deficits with increased age [427-429]. This motor function decline is potentially brought about by the loss in muscle fibres from muscular atrophy, low grade persistent inflammation (increased oxidative stress) with a corresponding low bioavailability of Nitric Oxide (NO) (required for muscle contractions) as well as reduced energy production due to mitochondrial dysfunction [430, 431]. This said, the stark improvements in motor function and balance that the treated mice displayed offers unequivocal proof that senescence/ age retardation had occurred following the overexpression of LRP::FLAG. Moreover, the control and non-treated mice aside from displaying deficits in motor function and balance, generally hooked their hindlimbs around the beam for additional support. This observation has been previously confirmed to indicate a gross inability to maintain balance and further substantiates that LRP::FLAG was able to prevent the age-dependent induction of motor function decline [427]. This result may have been a consequence of the reduced mitochondrial dysfunction (Figure 4.20), which would have allowed for reduced oxidative stress as well as more efficient energy production [431, 432]. Alternatively, the increased production of TERT (Figure 4.21) and other proliferative markers observed (Figure 4.12- 4.14), may have allowed the muscle tissue to replenish its lost mass by filling the tissue with non-senescent and functional muscle cells [240, 407, 433]. Therefore, the widespread improvement noted for most tested physiological parameters suggests that LRP/LR could effectively waylay the effects of physiologic ageing for increased gross motor co-ordination as well as organism fitness.

5.5 The overexpression of LRP::FLAG improves tissue pathology in aged mice

The stark improvements in physiologic functioning observed post overexpression of LRP::FLAG, was further corroborated by widespread improvements to tissue structure and form, noted during histochemical analysis. In this respect, the brain tissue of the mice overexpressing LRP::FLAG, specifically the hippocampus, were found on average to be more defined with fewer tissue abnormalities. More, specifically the treated mice were shown to contain less vacuolation and pyknotic nuclei (indicative of apoptosis) in comparison to the control and non-treated mice, clearly demonstrating an anti-senescence effect. This effect may have been brought about by the treatment inducing neurogenesis [434], to allow for neuronal tissue replenishment, however this would need to be confirmed. This said, the improvement in the hippocampus convincingly explains the large improvements in short and long term memory as well as puzzle solving and nesting ability. This is due to the fact that the hippocampus forms part of the limbic system, where it plays an imperative role in learning and long term memory [400].

It must be noted these tissue changes while not extensive, it does coincide with parts of the biochemical data and suggests that only a moderate anti-ageing/ senescence was induced in the brain, possibly due to a lack of LRP::FLAG present in the brain. In fact, as the plasmid may not have been able to traverse the BBB, the positive effects seen in the brain of the treated mice may just be a consequence of an additive effect caused by the systemic improvement of the rest of the tissues and organs. Alternatively, as LRP protein levels were shown to be slightly elevated in the brain it may be induced, firstly by an accumulation of the shed isoform of LRP, possibly brought to the brain by the circulatory system. Secondly, as LRP is known to decrease with age, the increased levels of LRP within the neuronal tissues may just be a consequence of the aforementioned additive effect of impeding the ageing process [298]. Nevertheless, the improvements noted in the brain clearly display the potential ant-ageing effects that can be induced by elevating total LRP.

The second tissue type assessed via histochemical analysis was the kidney as it commonly develops various age-related tissue pathologies even within the C57BL/6J mouse strain [435, 436]. Assessment of the sections revealed that the non-treated and control mice on average displayed a greater accumulation of pathological markers such as glomerular shrinkage, as well as atrophic and sclerotic glomeruli in comparison to the mice treated to overexpress LRP::FLAG (Figure 4.10). These findings for the non-treated and control mice fit in line with previous findings, where aged post-menopausal female mice show heightened development of glomerulosclerosis [435, 437]. Moreover, a subset of the control and non-treated mice also displayed severe atrophy and replacement of the glomeruli tissue with fibrous tissue hinting at the development of an age-related kidney disease. In stark contrast, the treated mice, for the most part, displayed healthier kidney tissue with normal glomeruli structure and shape with only a portion of glomeruli displaying increased diameters (Figure 4.10 A-C). This clearly indicates that the gene based treatment to overexpress LRP::FLAG is providing a restorative effect to the tissues, where renal ageing was impeded.

One such possibility that could explain these findings is that Wnt signalling, which is generally upregulated during ageing to cause reduced progenitor cell proliferation and increased fibrosis, was reduced in the treated mice [438, 439]. This proposed reduction in Wnt signalling could be induced by the increase in klotho expression observed in both brain and kidney (Figure 4.16 B)[399, 439, 440]. This anti-ageing protein is highly expressed in the kidney and is responsible for maintaining renal functions like renal mineral metabolism as well as renal ageing [441]. Moreover, this protein is also produced in the brain and is imperative for preserving cognitive function. In fact, depletion of

this protein has even been associated with AD development in brain tissue [399, 442]. Although the Wnt pathway can be up-regulated through TERT's extra-telomeric functionality [247, 443], we propose that the increased TERT observed in the kidney (Figure 4.21) is primarily carrying out a telomere maintenance effect, which may prevent senescence mediated kidney dysfunction [140, 444]. Whereas, within the brain tissue the elevated TERT may be favouring its mitochondrial related functions to prevent mitochondrial dysfunction and extensive ROS generation [225, 288]. Otherwise, the increased TERT present in the brain may aid in preventing the accumulation of Aβ, a peptide known to cause age-related neurodegeneration [288, 294]. Alternativley, as the treated mice appeared to still have functional pathway controls in place, a compensatory mechanism could have been activated to regulate Wnt signalling such as the increased p53 (Figure 4.17) that was observed [440, 445]. A final possibility that could account for the observed restorative effects within the brain and kidney is that there was a potential reduction in tissue damage caused from oxidative stress. The proposed reduction in oxidative stress may have been a result of firstly the reduced mitochondrial DNA content (Figure 4.20), suggesting that less ROS would be produced. Secondly, oxidative stress could be ameliorated by the increased SIRT1 levels observed (Figure 4.15), which would subsquently reduce PGC-1α signalling lowering adenosine monophosphate activated protein kinase (AMPK) for reduced oxidative stress [446, 447]. Collectivley, this illustrates that LRP could be utilised or targeted to reduce the effects of renal ageing.

5.6 Overexpression of LRP::FLAG postivley effects proliferative markers in aged mice

5.6.1 LRP::FLAG overexpression increases Akt and pAkt in aged mice

The improved physiological and histological parameters confirmed post LRP::FLAG overexpression was identified to be a consequence of stark improvements on multiple biochemical aspects including proliferative markers, anti-ageing proteins, senescent markers as well as telomere dynamics [13, 25, 26]. This said, advanced ageing is often correlated with an overall lack in proliferation that culminates in a loss of tissue replenishment, whereas the restoration of controlled and active proliferative signalling has been associated with tissue restoration [13, 25, 26]. The current study falls in line with this sentiment, where Akt was positively affected in both tested organs. This protein is the major constituent of the Akt/PI3K pathway, which has been shown to play controversial roles in ageing. This pathway is generally attributed to regulating apoptosis, cell survival, glucose metabolism and protein synthesis among others [448]. Interestingly, this pathway is also known to share a role with the current study's two major proteins of interest; TERT and LRP/LR [204, 352].

The protein has three distinct isoforms that are expressed, to various degrees, in different organs to carry out its aforementioned functioning. The expression of Akt1 has been found to be fairly uniform for the different tissues [449], while expression of Akt 2 occurs in organs that mainly respond to insulin signalling, like the liver, for mediating glucose metabolism [450], whereas Akt 3 is more commonly expressed in the brain and kidney [448, 451].

In regard to ageing and development, it has been noted that knockout of Akt 1 leads to a shortened lifespan [449], while a loss of Akt 2; can induce the development of the age-related disease, diabetes [452] and loss of Akt3 results in reduced brain size [451]. Furthermore, reductions in Akt or a reduction in its phosphorylation at Ser473 during ageing has been correlated to the following: muscle atrophy and reduced insulin sensitivity [453], a loss of osteogenic capacity in the skeletal system [448, 454] and a suppression of telomerase activity in memory T cells as well as the vascular system [448, 455, 456]. In stark contrast, the over-activation of Akt has been tied to some pathological aspects of ageing such as increased oxidative stress [457, 458] and has been shown to play a potential role in senescence activation [459]. Moreover, increased amounts of phosphorylated Akt have been tied to a number of aged organs including the brain, muscle and heart [460-462]. The controversial roles that this protein plays in ageing could be attributed to its signalling targets mTOR, which carries out both autophagy and protein synthesis based roles, and TERT, which is known to play a role in immortalisation and anti-ageing [204, 456, 463].

Regarding the current study, a significant increase in Akt protein was observed within the brain samples of treated mice (Figure 4.12 D). While no change was observed in in the liver (Figure 4.12 E). However, a significant elevation in pAkt was observed in the liver (Figure 4.12 F). We propose that the aforementioned increases served a beneficial effect within the mice overexpressing LRP::FLAG. This is in accordance with the increased pTERT (Figure 4.21 F, G) and telomerase activity (Figure 4.22), which corresponds with a previous study that illustrated that resveratrol treatment increased telomerase activity through the PI3K-Akt signalling cascade [464]. This is due to Akt's function in phosphorylating TERT, which allows its translocation from the cytoplasm to the nucleus for enhanced telomerase activity [204, 205]. Moreover, this is further evidenced by the increased TRF1 exhibited in the liver (Supplementary Figure 8.3) following LRP::FLAG overexpression. In fact, the stability and telomere binding function of TRF1 is highly dependent on its phosphorylation by Akt [465]. This effectively establishes that in the current study it appears that the increased active Akt may be favouring its longevity related functions by causing various improvements telomere dynamics and telomere associated proteins [465]. Finally, we propose that

the increased LRP (Figure 4.11) present activates FAK to stimulate Akt and its signalling cascade to carry out these beneficial functions [352]. More specifically, it offers a potential mechanism as to how LRP may upregulate TERT.

5.6.2 LRP::FLAG overexpression elevates the transcription factor c-Myc

Alongside the observed improvements in the proliferative signalling marker, Akt, there was also a corresponding improvement in c-Myc, for mice overexpressing LRP::FLAG. Notably, c-Myc is a protein whose expression and stabilisation is also influenced by Akt and plays a major role in proliferation, apoptosis, EMT (plays a role in stem cell like functions), TERT regulation and the process of tumorigenesis through its ability as a TF [412, 466-468]. More specifically, in tumorigenesis, this TF is hyper upregulated to drive uncontrolled proliferation and telomerase activity. In contrast, c-Myc has been noted to play controversial roles in ageing. Increased expression and activity of c-Myc has been associated with senescence and more specifically in driving oncogene induced senescence provided that p16 and p53 are functional, in order to limit neoplasm development [469, 470]. However, a large body of evidence has found that inhibition or reduced c-Myc alongside active p16 and p19 has been implicated in senescence as well [466, 471, 472]. In fact, overexpression of c-Myc in normal cells has been found to circumvent Rb/$p16^{INK4a}$ based senescence for immortalisation [473, 474]. One other manner c-Myc promotes circumvention of senescence is through its ability to upregulate TERT expression for enhanced telomerase activity [198, 412]. This said, the increased gene expression and protein levels of c-Myc observed (Figure 4.13) following LRP::FLAG overexpression, was found to provide a beneficial effect in all tested organs. Several interconnected findings validated this observation, where firstly the decreased p16 (Figure 4.18) alongside the elevated c-Myc would aid in obstructing senescence. Moreover, the increase in TERT further substantiated that an anti-senescent effect had occurred and thus offered an additional mechanism as to how LRP is able to induce an increased production of TERT [193]. Hence, in the context of this study, the increase in c-Myc following the overexpression of LRP::FLAG improves proliferative functioning while impeding senescence to ultimately improve organism fitness.

5.6.3 LRP::FLAG overexpression positively influences MDM2 and its phosphorylation

Alongside the significant increases in c-Myc post LRP::FLAG overexpression, *in vivo*, it was also noted that MDM2 and its phosphorylation was positively affected. Interestingly, like c-Myc, the activation and stabilisation of the MDM2 protein is dependent on Akt phosphorylation [401]. This oncogenic protein acts as a ubiquitin ligase for p53 allowing it to carry out an imperative role in the

stability and regulation of p53 [402, 403]. This ubiquitinating action affords MDM2 anti-apoptotic functionality via the repression and degradation of p53 [402, 403]. This relationship between these two proteins is further evidenced by the auto-regulatory feedback loop present, where p53 positively influences MDM2 gene expression while MDM2 negatively regulates p53 [402]. This feedback loop allows for the establishment of a p53-MDM2 axis for cell cycle regulation and is often a target for dysregulation in both tumorigenic and ageing processes. In regard to cancer, this axis is often dysregulated by favouring the increased expression of MDM2 to promote apoptotic evasion and uncontrolled proliferation. Meanwhile in ageing, this axis is often modified to favour an elevation in p53 that can induce either early or delayed ageing onset depending on the presence of other ageing/ senescent markers (like telomere shortening) [404]. This said, a number of studies have found that ablation of this p53-MDM2 axis does contribute to the ageing phenotype both *in vitro* where it induces p53 dependent growth arrest as well as *in vivo* [475-477].

The current study revealed that post LRP::FLAG overexpression there was no difference in MDM2 gene expression (Figure 4.14 A-C). Likewise, no significant change was noted in the protein levels of MDM2 within the liver samples when comparing the three mouse groups (Figure 4.14 E). This finding could potentially be attributed to the fact that the liver is a highly regenerative organ and would thus already display higher levels of MDM2. Therefore, any additional alterations to raising this protein could prove deregulatory and may provide ideal conditions for carcinogenic development. In contrast, the brain did display elevated levels of MDM2 within the treated mice (Figure 4.14 D), possibly to allow for increased proliferative potential and tissue replenishment of neuronal cells that can propagate. Alternatively, the increased MDM2 observed could be a consequence of the increased p53 observed in order to maintain the p53-MDM2 axis for proper functioning and ensure that the ATM/ATR pathways were not inappropriately favoured for senescent onset [404]. In accordance with maintaining proper cell signalling, it was also noted that the overexpression of LRP::FLAG caused no significant increase in pMDM2 (Figure 4.14 F, G), the active form of this protein, for either organ. This potentially indicates that proper cell functioning and cell cycle controls are still in place that would prevent exhaustive proliferation and conserve chromosomal stability to act as a preventative towards tumorigenic development [404, 478].

5.7 Overexpression of LRP::FLAG increases anti-ageing proteins in aged mice

5.7.1 LRP::FLAG overexpression significantly elevates SIRT1

A further indicator behind LRP/LR's suggested anti-senescent functionality, is that it was able to positivley influence proteins directly involved in anti-ageing and longevity responses. As mentioned previously these anti-ageing proteins; SIRT1 and klotho, have been confirmed to decline during the senenescence process [479, 480]. Whereas, a subsquent increase of these markers have been shown to retard ageing [479, 481-483]. In this regard, the increase in both gene expression and protein levels of SIRT1 following LRP::FLAG overexpression (Figure 4.15), clearly indicates an impediment of senescence. This protein is a NAD-dependent deacetylase that is known to deacetylate not only histones but also TFs and other other cytsolic proteins. This function allows SIRT1 to play a regulatory role in gene expression and in subsequent signalling cascades for NFκB, p53, E2F1, forkhead transcriptional factors, AMPK (5' adenosine monophosphate-activated protein kinase) and importantly TERT [484, 485]. Additionally, the regulation of these various pathways allow SIRT1 to influence DNA repair, metabolism and longevity [484, 485]. Aside from these functions, SIRT1 has also been implicated in reducing the effects of oxidative stress, as well as inflammation while enhancing DNA stabilisation, and most importantly it has been found to act as a potent tumor supperssor (by consquence of its other aformentioned functions) [482, 486, 487]. These functions collectivley are responsible for both impeding the ageing process as well as promoting healthier ageing.

The benefits to cell longevity that SIRT1 provides was clearly evidenced in the mice treated to overexpress LRP::FLAG. In fact, the increased SIRT1 (Figure 4.15) observed may have potentially played a role in the reduction of γH2AX through enhancing DNA repair [488]. In turn, these data together offer an additional mechanism as to how LRP::FLAG was able to reduce DNA damage and accumulation of the senescent marker; γH2AX both *in vitro* (Figure 4.4 c, d) an *in vivo* (Figure 4.19). Alongside the reduction in γH2AX, it was further suggested that the increased SIRT1 aided in reducing oxidative stress to induce the observed reduction in the senescent marker p16 [(Figure 4.18) [489, 490]]. An additional snescent marker that SIRT1 may have influenced in line with this study is p53, where SIRT1 is known to regulate its function by acetylation [491]. In this manner, SIRT1 could regulate p53 activity to ensure it carries out its function in DDR in a controlled manner that would not induce senescence [491, 492]. Aside from ameliorating DNA damage, it can be further suggested that the elevated SIRT1 aided in maintaining telomere length either by influencing telomerase activity or affecting the telomeres or shelterin directly [(Figure 4.21- 4.23) [493]]. In

addition, the increased SIRT1 may also have aided in reducing or preventing the accumulation of senescent-related inflammatory markers IL6 and 8 (Figure 8.1 and 8.2) by deacetylating and inactivating NFκB [494, 495]. The interconnections and positive effects that these data present ultimately indicate that elevated LRP increases the anti-ageing protein SIRT1 through translational processes or by influencing signalling cascades to bring about an anti-senescent effect for healthier ageing.

5.7.2 LRP::FLAG overexpression increases both full length and secreted isoforms of klotho

The second anti-ageing protein that LRP::FLAG was found to influence was α-klotho; a single pass transmembrane protein that can occur in three distinct isoforms (full length, shed and secreted α-klotho) [496]. This protein is predominantly expressed in the kidney and brain but is also expressed to a lesser extent in the ovary, testis and placenta [497]. Although this protein is only expressed in a subset of organs, its dysregulation can induce widespread and systemic effects to aggravate either the natural ageing processes or the development of age-related diseases [479, 498]. The full length isoform of this protein is known to act as an obligate co-receptor for FGF23 and further associates with fibroblast growth factor receptors (FGFR) to play a critical role in endocrine based metabolism of calcium, phosphate and vitamin D [496]. In fact, defects in the α-klotho-FGF23 endocrine axis leads to a retention of the aforementioned minerals to induce a premature ageing phenotype. This retention, especially in phosphate, has been known to cause increased insulin sensitivity and ROS production/ oxidative stress, caused by the mitochondrial uptake of cytoplasmic phosphate for oxidative phosphorylation, thereby inducing a state of accelerated ageing [496, 499, 500].

In addition, the secreted form of α-klotho, whose levels decline with increased age, also plays a major role in promoting longevity [498]. This isoform is able to interact with various ion channels and growth factor receptors to further regulate ageing [479]. Importantly, secreted klotho has also been found to influence Wnt signalling by binding to Wnt-related proteins to prevent exhaustive proliferation and thus depletion of stem cell niches [440]. Moreover, secreted α-klotho present within the blood and cerebrospinal fluid, has also been associated with ameliorating oxidative stress through a negative regulation of insulin/IGF-1 signalling [483]. This negative regulation induces the expression of manganese superoxide dismutase, which is responsible for the removal of ROS [483]. Hence, why the age dependent decline in secreted α-klotho accelerates ageing due to the increased insulin signalling and oxidative stress evident within aged cells.

In line with these published findings (reviewed in: [479]), the present study found that in mice overexpressing LRP::FLAG a significant increase in α-*klotho* gene expression (Figure 4.16 A, B) was noted for the kidney, while a non-significant increase was noted in the brain. This was further substantiated by an increase in both full length and secreted klotho in the brain (Figure 4.16 C), while a subsequent increase in secreted α-klotho was noted in the liver (Figure 4.16 D). In regard to the liver findings, it is known that β-klotho rather than α-klotho is expressed [501]. However, due to secreted klotho's presence within the blood system, coupled with its hormone related functions, may enable it to operate within organs that do not transcribe it. In fact, studies have revealed that reduced secreted klotho levels have impacted the liver by attenuating expression of multiple growth hormones responsive genes [409] and may be further responsible for attenuating TGFβ- signalling in multiple different organs [479]. This said, the increased klotho observed within the treated mice essentially coincides with the increased SIRT1 (Figure 4.15) to suggest that an anti- ageing or anti-senescence had indeed occurred. Additional substantiation is that it has been previously confirmed that klotho appears to exert some form of regulation over SIRT1 activity for longevity functionality [502]. Further contributing to this anti-senescent effect, is that klotho has been confirmed to influence TERT and telomerase activity [503]. Thus, the increased klotho may have aided in stimulating the observed increase in TERT (Figure 4.21) expression following LRP::FLAG overexpression thereby potentially aiding LRP with enhancing telomerase activity (Figure 4.22). Aside from all these aforementioned functions of klotho, the final manner in which it could be carrying out an anti-ageing effect is its ability to reduce the expression of inflammatory related markers (such as IL6 and 8 (Figure 8.1 and 8.2)) [504]. This occurs by klotho reducing the effects of oxidative stress as well as diminishing NFκB's activity via preventing its translocation to the nucleus [504]. In contrast to the increased klotho observed, there was also an increase in Akt and its phosphorylation at Ser473, which klotho normally down regulates to protect against oxidative stress and hypoxia [505, 506]. However, other studies have shown conflicting results where enhancing klotho expression in the brain was shown to cause a subsequent increase in pAkt to improve synaptic plasticity [399]. In accordance other studies have found that klotho can increase Akt expression [507] and that pAkt, through rapamycin, allows for klotho expression [508], thus suggesting that the relationship between Akt and klotho is treatment and environment dependent. This said, we propose that klotho and Akt in the current study positively regulates one another to allow for increased anti-ageing functionality. Therefore, to summarise, the data suggests that LRP::FLAG overexpression is able to induce an increase in klotho production to prevent the accumulation of inflammatory markers and oxidative stress, while positively influencing SIRT1 and telomerase for an anti-senescent effect.

5.8 Overexpression of LRP::FLAG increases the senescent-related protein p53 in aged mice

An exceptionally surprising finding observed during the course of this study was the apparent elevation in gene expression and protein levels of p53 following LRP::FLAG overexpression. This particular tumor suppressor, which famously doubles up as a senescent marker, has broad spanning roles in cancer, apoptosis, DNA repair, and senescence (reviewed in: [509]). These roles allow p53 to act as a guard to conserve normal cell functioning and prevent tumorigensis. In fact, p53 is well characterised as the central mediator in telomere dependent senescence, where the activation of ATM/ATR signalling cascades from critical telomeric erosion activates this protein to ensure a state of permanent cell arrest [129-131]. This has been further confirmed in mice engineered to express a mutant p53 or overexpression of p53 with other pathways that are also dysregulated [510, 511]. Although these mice are extremely cancer resistant, they did unfortunately display signs of acclerated ageing [510, 511]. In contrast, accumulating evidence has shown that p53's roles in ageing is not as clear cut as originally thought. Interestingly, p53 has been tied to longevity functioning, where it has been shown to be capable of stimulating the activation of genes, like sistrin, which are involved in reducing oxidative stress; provided the stress is not of a high intensity [512-514]. Should a high intensity stress affect the cells then p53 switches roles in favour of apoptosis where it interacts with the mitochondria for additional ROS generation and to intiate mitochondria-dependent apoptosis [512, 515]. Futhermore, other mouse studies focused on overexpressing wildtype p53 showed signs that the ageing process was impeded [512]. In further support, p53 has also been shown to play an inhibitory role towards insulin and Akt signalling, both of which have been tied to pro-ageing functionality [516, 517]. Alongside the previously mentioned p53-MDM2 axis, it is abundantly clear that the role p53 plays in a given moment is highly dependent on the environment (like stress) and presence of other manipulating factors, like the accumulation of senescent markers [475-477].

This said, we propose the increased p53 noted in the current study can be ascribed to promoting longevity. This is due to prior published findings that mice engineered with extra copies of the wild-type p53 showed ordinary ageing patterns, even in the face of increased p53 [518, 519]. Moreover, it was found in another study that increased p53, alongside $p19^{ARF}$ in mice, induced a heightened resistance to tumor development as well as a significant increase in longevity [512]. One possibility that could account for the increased p53 present in the mice overexpressing LRP::FLAG is that the alteration of LRP, like MDM2, has been shown to stimulate p53 expression [520]. Thus, the

increased p53 observed may have been a compensatory mechanism carried out by the tissue. This would have ensured that the proliferative and potential anti-ageing functions of LRP were tightly regulated to protect against any potential tumorigenic onset. Alternativley, the increase in p53 observed, specifically in the brain, may have been a consquence of the increased MDM2 in order to maintain the p53-MDM2 axis to ensure normal and controlled functioning. Further supporting this proposed longevity functioning of p53 is the increase in both anti-ageing proteins and mean telomere length (Figure 4.15, 4.16, 4.23) with the concomittant decrease in DNA damage marker, γH2AX (Figure 4.19). This co-incides with previous findings that increased p53 activity does not necessarily accelerate or impede telomere driven senescence but rather promotes the removal of telomere damaged cells [405]. In this context, the removal of the damaged cells would further promote the establishment of a healthier phenotype in the treated mice in conjunction to waylaying senescence.

5.9 Overexpression of LRP::FLAG reduces the levels of tested senescent markers in aged mice

5.9.1 LRP::FLAG overexpression decreases senescent marker p16

The conclusions made following the observed increases in p53 and other longevity markers was further substantiated by the stark decrease in p16 protein levels. This tumor suppressor protein acts as a cyclin-dependent kinase inhibitor that induces cell cycle arrest at the G1 checkpoint or activates Rb to elicit growth arrest by suppressing cdk 4 and 6 [131, 132]. This protein is commonly expressed or activated when the cells are exposed to extensive stress (exhaustive replication, oxidative stress and or metabolic stress) implicating the involvement of this protein in the process of senescence [131, 132]. In fact, p16 may even act as the master regulator of senescence, especially in mice. This is due to the fact that mice age along a stress-dependent senescence process as they exhibit a lack of critically shortened telomeres during their lifespan [219, 220]. Moreover, this protein has been confirmed to accumulate in various human and mouse tissues with increased age and also plays a role in maintaining the senescent phenotype [24, 521]. This said, it must still be noted that p16 can influence telomere-dependent senescence, but to a lower degree in comparsion to p53. Further ascertaining p16's role in the ageing process, is that the eradication of p16 within senescent cells or the targeted removal of these cells has been found to reverse the ageing phenotype [35, 406].

The current study falls in line with this sentiment, where the decreased gene expression and lowered protein levels of p16 appeared to positively affect tissue and organism fitness. In support, majority of the other tested senescent markers (Figure: 4.19; γH2AX, Figure: 8.1 and 8.2; IL6 and IL8) were also

diminished and thereby provides strong evidence that the senescence process was impeded [522, 523]. Conflictingly though, elevated PI3K/ Akt/ mTOR signalling alongside increased p16 has been implicated in senescence [459]. Although, an increase in Akt and pAkt was noted in the current study, (Figure 4.12), we propose that it was not contributing to the senescent phenotype through mTOR signalling [459], but was rather being utilised for longevity related functions like TERT activation [204, 205]. This inhibition of senescence was further validated by the elevation in c-Myc previously noted within the treated mice (Figure 4.13). This is due to prior findings that have shown that an elevation in both p19 and p16 is capable of inducing an inhibition of c-Myc during DDR-independent senescence [524]. Thus, an elevation of c-Myc with reduced p16 expression would indicate an impediment of senescence. Moreover, elevated levels in klotho (Figure 4.16) and SIRT1 (Figure 4.15) have been shown separately, to reduce p16 in aged organisms to promote longevity [482, 490, 525]. Therefore, the reduction in p16, alongside the improvements noted on a biochemical, histological and physiological clearly show that LRP plays an imperative role in ageing and senescence.

5.9.2 LRP::FLAG overexpression reduces the DNA damage marker γH2AX

The stark reduction in p16 alongside the increased p53 induced by LRP::FLAG overexpression prompted the assessment of DNA damage accumulation; one of the lead driving forces in ageing. DSBs have been closely linked to senescence by inducing permanent cell cycle arrest at stalled replication forks [526]. In response to the presence of DSBs caused by ROS, metabolic stress or UV, the cells firstly phosphorlate the histone H2AX (a variant of H2A) at Ser139, by ATM and ATR, to elicit a DDR [527, 528]. Thereafter, the presence of phospho-H2AX (γH2AX) ensures the persistance of the DDR until the damage is resolved. Moreover, γH2AX increases DNA accessibility and also aids in the recruitment of DDR proteins. This marker then persists throughout the repair process and is only de-phosphorylated in normal cells after the damage has been ameliorated. In turn, the persistant presence of this marker during DDR allows it to modulate cell cycle checkpoints to ensure growth arrest is maintained (21-24). In an ageing context, senescent cells accumulate γH2AX that eventually form foci, which represent a portion of lesions that are resistant to repair [529]. These lesions accumulate especially at the telomeric ends, due to crtical telomere erosion, and eventually induce a state of permanent cell cycle arrest typical of senescence [529]. This phenomenon has been extensivley confirmed both *in vitro* and *in vivo*, where it plays a key role in determing the rate of ageing [20, 26, 128]. Thus, a reduction in this marker in aged organisms following a particular treatment can be attributed to an anti-ageing or senescent effect.

Accordingly, the significant reduction in γH2AX following LRP::FLAG overexpression both *in vitro* (Figure 4.4 c, d) and *in vivo* (Figure 4.19) clearly points towards an anti-senescent effect. This finding was further substantiated by the reductions in p16 (Figure 4.18) levels as well as IL6 and 8 expression (Figure 8.1 and 8.2) that was observed. In fact, previous studies have shown that marked reductions in γH2AX not only suppressed DDR-dependent senescence but also reduced IL6 secretion thereby corroborating the current findings [530, 531]. Moreover, the reduction in γH2AX alongside the increase in mean telomere length (Figure 4.23) suggests global genomic integrity was maintained in the treated mice (telomere dysfunction was averted) [529]. This said, there are a number of possibilities that could have accounted for this phenomenon including that the increased LRP may have played a role in resolving the DNA damage through its ability to maintain nuclear structure and integrity [292, 418]. In addition, LRP could aid in the recruitment of DNA repair proteins possibly through its ability to interact with histones [309]. Alternativley, Akt is also known to regulate phosphorylation of H2AX to regulate apoptosis, where it has been known to aid cancer progression by diminishing γH2AX during DNA repair [532, 533]. However, the current study suggests that Akt's functioning is not pro-tumorigenic due to the high presence of proteins that play a role in tumor suppression (p53, SIRT1 and klotho). Moreover, the increased SIRT (Figure 4.15) may also aid in reducing γH2AX as it is known to localise to DNA damage sites to promote repair [534, 535]. Another potential mechanism that could account for this reduction both *in vitro* and *in vivo* is that the increased TERT (Figure 4.21) present may have been carrying out extra-telomeric functioning. This extra-telomeric functioning of TERT refers to its ability to prevent DNA damage accumulation and also to mediate in the DNA repair process to effectivley reduce the number of foci present [225, 232]. Holistically, the reduction of γH2AX alongside all the other positive aspects that overexpression of LRP::FLAG wrought clearly indicate an improvement of tissue fitness.

5.10 Overexpression of LRP::FLAG lowers mitochondrial DNA content in aged mice

In order to further substantiate that LRP::FLAG had indeed aided in the impediment of senescence, mitochondrial fitness was assessed. One of the most common occurrences during ageing and age-related diseases is the development of mitochondrial dysfunction. This process is characterised by a deterioration in respiratory function of the mitochondria that leads to enhanced oxidative stress causing extensive DNA, lipid and protein damage to accelerate the senescence process [536]. As mentioned previously this dysfunction generally comes about as a result of excessive generation of

ROS during ATP synthesis with impaired anti-oxidant defences that eventually induces extensive mtDNA damage accumulation [537, 538]. An additional factor contributing to mitochondrial decline is defective mitochondrial biogenesis through altered rates of fission and fusion, thereby causing disruptions in the lifecycle of the mitochondria [539]. This said, even though extensive research has been performed in elucidating the exact mechanisms behind mitochondrial dysfunction, there is much controversy with no clearly agreed upon explanation consolidating changes to mtDNA content (reviewed in: [536, 540]). What is agreed upon though, is that during ageing (aside from the accumulation of mtDNA mutations) there is a stark increase in mtDNA deletions, which negatively impacts the electron transport chain leading to the aforementioned increase in free radicals (reviewed in: [536, 540]). However, with regards to mtDNA copy number glaring, discrepancies are apparent, where increases, decreases and no apparent changes in copy number during ageing have been reported for both humans and rodents (reviewed in: [536, 540]). In relation, these discrepancies cannot be attributed to be being tissue-specific as conflicting data has been generated in the same tissue. However, one possibility that could at least in part account for this is the selection of mitochondrial and nuclear amplicons, where overlaps between mtDNA and genomic DNA or cases where the amplicon can be mapped to multiple sites can lead to confounding and even misleading results [536]. Alternatively, mitochondrial numbers may be regulated by a series of different signalling cascades and protein axes, and therefore alterations in its numbers maybe dependent on the patterns of signalling cascades that are favoured.

Nevertheless, both increases and decreases in mtDNA copy number can be reasonably consolidated in the ageing process. In regard to a decreased copy number during ageing, this may be the result of extensive mitophagy where damaged mitochondria are degraded without a compensatory replenishment by biogenesis [541]. Moreover, this decline in mtDNA copy number could also be a consequence of aged mtDNA being a poor template for replication [542]. In addition, any aberrations to mitochondrial-based signalling cascades and anti-oxidant defences could abolish mitochondrial replication, thus lowering the mtDNA copy number. Alternatively, the increase in mtDNA copy number observed in prior ageing-based studies may also be a result of dysregulated fission and biogenesis. In this regard, impairments in mitophagy may prevent the degradation of damaged mitochondria and thereby allow their accumulation. Likewise, the increase in mtDNA could be a result of an attempted compensatory mechanism to counteract the accumulation of damaged mitochondria [543-545]. Moreover, elevated oxidative stress, a common feature in ageing, has been shown to stimulate mitochondrial biogenesis [546, 547]. Based on the aforementioned possibilities, it appears that changes in the copy number of mtDNA with age, cannot be consolidated, and therefore

data pertaining to mtDNA must be interpreted alongside other biochemical changes to draw reasonable conclusions.

The data generated from the current study proposes that the overexpression of LRP::FLAG in aged mice reduces mtDNA content to elicit an anti-ageing effect (Figure 4.20). In fact our data coincides with Correia et al. (2016) [548], who found that reductions in mtDNA copy number prevented tissue senescence within the liver *in vivo*. Moreover, Masuyama et al. (2005) [544] further showed that as mice age there is a corresponding increase in brain and kidney mtDNA content, which indicates that the observed reductions in these tissues post LRP::FLAG overexpression could potentially be attributed to an anti-senescent effect. Further corroborating these findings, is the stark reductions in γH2AX (Figure 4.19), IL6 and IL8 (Figure 8.1 and 8.2) as well as increased telomere length (Figure 4.23) that were noted. These findings collectively suggest an impediment of excessive ROS production and inflammation, which in turn would reduce the senescence-promoting effects of the SASP [548, 549]. In turn, this would not just improve mitochondrial function but whole cell functioning as well for improved tissue fitness. From these data, it can be construed that mitochondrial dysfunction was impeded by the preservation of mitochondrial fission and fusion processes, thereby allowing the selective degradation of damaged mitochondria. Alternatively, oxidative stress could have been reduced to prevent excessive mitochondrial biogenesis. Although, Akt through the mTORC pathway has been shown to adversely affect mitochondrial function during ageing, to promote ROS production, we propose that the increased Akt (Figure 4.12) is not favouring mTORC signalling, but is rather focused on pathways promoting longevity [548]. Alternatively, a compensatory mechanism, like elevated TERT or klotho, may be in place to stem excessive mitochondrial biogenesis, regulate Akt signalling and also protect against ROS [225, 483]. In fact, TERT is known to play a dual extra-telomeric role in the mitochondria, where it aids in protecting mtDNA from oxidative damage [215, 235, 236]. However, if the damage is too extensive TERT can aid in the initiation of mitophagy for its removal [215, 235, 236]. Therefore, the potential improvement in mitochondrial function alongside the improvements noted in physiologic function and tissue state further substantiate LRP as an ideal candidate to influence organism health and fitness.

5.11 Overexpression of LRP::FLAG telomere dynamics in aged mice

The final and perhaps most important aspect for LRP::FLAG overexpression that was assessed within the mice was validating the *in vitro* findings that LRP::FLAG overexpression positively

influenced telomere biology through telomerase. Although, the dynamics that govern telomere biology in ageing are fundamentally different between humans and mice, there are still common features that can be assessed to gain possible insights as to what may happen in humans. This said, mice do exhibit significantly longer telomeres than humans with no critically short telomeres evident, even at advanced ages, in either actively dividing cells or post-mitotic cells like neurons [219, 221]. Thus, mice do not age via a telomere-driven replicative senescence mechanism, but rather through the accumulation of stresses like oxidative stress commonly observed in inflamm-ageing or mitochondrial induced senescence. However, treatments that modulate telomerase and the telomeres can still produce comparable anti-ageing effects, especially for healthier ageing, in both humans and mice. In addition, studies have also shown that mice like humans may also suffer from critical telomere erosion or dysfunction at old age [405, 550]. Similarly to the *in vitro* study, it was validated that the overexpression of LRP::FLAG not only caused a significant increase in mTERT protein, but also stimulated its expression at a gene level (Figure 4.21). This would suggest that LRP may have the potential to stimulate TERT expression through the stimulation of appropriate signalling cascades like MAPK or Wnt [292]. Moreover, the TERT gene is known to reside in an area of highly condensed chromatin domain that is subjected to histone hypoacetylation. Thus, LRP's ability to interact with histones may aid in chromatin relaxation to allow for transcription. Alternatively, due to LRP's nuclear related functioning and suspected potential TF capabilities it may play a more direct role in TERT expression [298, 418].

In regard to the increased TERT protein levels, the elevated LRP could have had a potential hand in this as well, where it's ribosomal functioning may allow for additional translational processing, effectively elevating TERT [298, 551]. This elevation in TERT, aside from allowing it to perform additional telomeric extension, may also allow for enhanced extra-telomeric functioning. Further supporting this theory, was the improved mtDNA content (Figure 4.20) and elevated c-Myc (Figure 4.13). This indicated that the elevated TERT may have aided in preserving mitochondrial function and protected the mitochondria against oxidative mediated damage [225]. Moreover, the increased c-Myc could suggest that TERT was aiding in Wnt pathway signalling, specifically through its positive feedback loop with c-Myc [225, 245, 246]. Alongside the increased TERT, there was also a corresponding increase in the phosphorylated form of this protein. This suggests that that the increased Akt may have allowed a corresponding elevation in TERT activation for subsequent translocation to the nucleus for construction of the active telomerase complex [204, 205].

In line with the increased phospho-TERT there was a corresponding elevation in telomerase activity within the kidney and liver following LRP::FLAG overexpression in the treated mice (Figure 4.22). This corroborates the *in vitro* findings that LRP can be utilised to influence telomerase and telomere dynamics [293]. In accordance, this data was further validated by the fact that like telomerase activity the average telomere length was longer in the liver and kidney of the treated mice (Figure 4.23) and thus confirmed that the elevated telomerase activity was having a replenishing effect. More specifically, this increase in telomere length was further confirmed by the elevated levels of TRF1 and TRF2 observed in the liver (Figure 8.3), where comparatively higher TRF1 and 2 has been previously confirmed to illustrate the presence of longer telomeres. One last assurance that telomerase activity and telomere length had indeed improved was the elevated SIRT1 (Figure 4.15) that was also noted. How SIRT1 positively influences telomere biology is that it stabilises the telomeres and promotes their extension [493, 552]. Moreover, the improved mtDNA content (Figure 4.20), telomere length and elevated telomerase activity coupled with the significant decreases in multiple senescent markers (γH2AX (Figure 4.19), p16 (Figure 4.18), IL6 and IL8 (Figure 8.1 and 8.2) further establishes that an impediment of the senescent process had indeed occurred [136, 140, 144, 553]. In turn, this telomeric extension would allow for a re-population of the treated mice tissues with non-senescent cells, further backing up the improved tissue observed during histopathological analysis [140, 554].

Lastly, it must be pointed out that a slightly larger number of treated mice contracted cancer in comparison to the control or non-treated mice. Now while this is not a significantly large (8%) increase to cancer susceptibility, it does mimic other gene altering longevity based studies, further corroborating our findings that altering LRP can be used to modulate telomerase activity [555-557]. This said, the marginal increase could just indicate that LRP can be modulated to impede senescence onset, provided all cell cycle controls are functional and the organism is not predisposed to tumorigenic development (does not have genomic mutations that could alter tumor suppressor protein function). Moreover, the increased functional p53 could further operate as a cancer deterrent. Therefore, treatments that target LRP in a non-genetic altering manner, may provide a potentially powerful therapeutic to impede the senescence process and possibly even treat age-related diseases influenced by telomerase. Holistically, all the aforementioned improvements to mouse physiologic, histologic and biochemical function clearly point towards a healthier form of ageing. It is unfortunate to note that an increase in longevity could not be confirmed post LRP::FLAG overexpression. This was due to a significant loss of control mice prior to the planned terminations for subsequent histological and biochemical analysis. These premature deaths, mainly from age-related conditions,

do offer some testament that the ageing process may have been impeded; however this should be further confirmed by a longevity-based study in the future. Moreover, these premature age-related deaths alongside the apparent increase in cellular proliferative capacity suggest that elevation of LRP could be used to potentially treat age-related diseases like AD, CVD, diabetes, age-related macular degeneration and possibly accelerated ageing disorders [136, 558, 559]. This is especially true for diseases or ageing syndromes that are affected by cell senescence, dysfunctional telomeres as well as telomerase. A fact confirmed by Bignoux et al., (2019)[294] that showed that LRP::FLAG could rescue cells, mimicking AD, from Aβ-induced cytotoxicity *in vitro*. Therefore, based off both the *in vitro* and *in vivo* ageing studies, strategies aimed at elevating LRP/LR could be used to improve not only telomere dynamics, but also allow the elevation of anti-ageing proteins while impeding the accumulation of senescent markers to revert or impede cellular senescence.

6. Conclusion

This study provided an in-depth analysis into the effects of overexpressing LRP::FLAG *in vitro* and thereafter, *in vivo* demonstrated, from an ageing perspective, the potential of using LRP as a target for modulating the ageing process. This should come as little surprise due to the extensive roles it plays in cancer. In fact, it was in tumorigenic cells that a relationship between LRP and TERT was first established. The current study confirmed that this relationship between LRP and TERT extended into normal cells, where a co-localization between both proteins was observed predominantly within the perinuclear and cytosolic domains of the cells. Thereafter, the overexpression of LRP::FLAG was confirmed to induce a significant reduction in both γH2AX and β-galactosidase in aged embryonic (HEK293) and somatic (MRC 5) cells. This reduction in both tested senescent markers, suggested an impediment of the senescent process *in vitro.* This was validated by the subsequent elevation in hTERT, telomerase activity and telomere length in both cell lines transfected to stably overexpress LRP::FLAG. This indicates that LRP is able to hinder telomere-dependent senescence to impede cellular ageing.

Further corroborating these findings, it was found that the overexpression of LRP::FLAG in aged mice exhibited drastically improved health and well-being. In this regard, the treated mice, on average, displayed less hair greying as well as fewer signs of hair thinning and balding. This was followed up with stark improvements in cognitive and motor function, where the treated mice solved puzzles of increasing complexity within a shorter period than the control mice and non-treated mice. Therefore, illustrating distinct improvements in short- and long-term memory, as well as puzzle solving ability. This improvement of cognitive function was further supported by the improved nesting ability displayed by the treated mice. Moreover, significant improvements in motor functions and balance were noted, where the treated mice traversed the beam, on average, 10 sec faster. Overall, these physiological improvements were proposed to be due to holistic improvements observed at a tissue level. Histological analysis showed that, on average, mice overexpressing LRP::FLAG displayed fewer signs of tissue atrophy, degeneration, disorganization and shrinkage, in both the brain and liver tissue. Thus, further highlighting the restorative effects conveyed by LRP::FLAG.

The compelling benefits noted at both a physiologic and histologic level in the treated mice were further substantiated upon biochemical analysis. In this respect, the confirmed elevation in total LRP was found to significantly improve distinct proliferative pathways, including the PI3-Akt (via Akt) and Wnt (via c-Myc) pathway. In fact, the significant elevation in both total and active Akt, also indicates, that additional TERT protein may have been phosphorylated for nuclear translocation. Moreover, the increase in the TF c-Myc not only indicated an increase in Wnt proliferative and survival signaling, but also suggested an increase in TERT expression. This improvement in proliferative potential was further confirmed, in part, by the elevated MDM2 within the brain. Alternatively, this may have simply acted as a compensatory mechanism against the observed increase of p53. Although this increase in MDM2 was noted in the brain, there was no change in total MDM2 in the liver, as well as no observable difference in active pMDM2 in these organs. Accordingly, this indicates a preservation of cell cycle controls and that no dysregulated or extensive proliferation had occurred.

Coinciding with the improvement in proliferative signalling, it was subsequently noted that LRP::FLAG overexpression significantly enhanced the levels of the anti-ageing proteins, SIRT1 and klotho. Both of these proteins are positively implicated in telomere and telomerase regulation, and have been confirmed to induce a healthier ageing and longevity effect. Surprisingly, in conjunction with these improvements, there was a significant increase in p53 levels in the treated mice. These elevated levels more than likely acted as a compensatory mechanism against the enhanced proliferative markers (especially LRP and MDM2), to ensure functional cell cycle controls were in place, and this would have made the mice (that displayed these increases) more resistant to tumorigenic development. Interestingly, although p53 was increased in the treated mice, a significant reduction was noted in all other tested senescent markers (γH2AX, p16, IL6 and IL8), thereby confirming that LRP::FLAG impeded the senescence process *in vivo*. More specifically, it also indicates a reduction in both DNA damage and inflammatory responses, which are normally central to progressing the ageing phenotype. Collectively, the elevation in multiple proliferative and anti-ageing proteins coupled with the observed decrease of the various senescent markers clearly demonstrate that elevation of LRP/LR exerted an anti-ageing effect within the mice. Finally, this potential impediment of the senescence process was further confirmed by the substantial improvements observed in the telomere biology of the treated mice. In a similar manner to the *in vitro* study, it was found that LRP::FLAG overexpression within the aged mice induced a significant elevation in mTERT expression, total mTERT protein levels, phospho-TERT and telomerase activity, as well as telomere length, which would have aided in promoting healthier ageing.

In conclusion, these data from both the *in vitro* and *in vivo* studies clearly implicate LRP in a novel role within the process of cellular ageing. This role appears to be centred around modulating telomere biology and anti-ageing proteins, as well as aiding in preventing the accumulation of senescent markers. The considerable data generated during the course of this study offers valuable insight into the process of cellular ageing and further presents the potential for alternative therapeutic design. Therefore, strategies aimed at targeting or elevating LRP may well provide an alternative therapeutic strategy for impeding the effects of ageing and potentially treat age-related diseases.

6.1 Future Studies

Since the process of ageing is a dynamic and multi-faceted process, any future studies surrounding the modulation of LRP for impeding the senescence process should aim at delving into this function with greater detail. In particular, greater attention should be given to determining LRP's role in metabolic and mitochondrial function based off the mtDNA content data generated during the current study. In substantiation, numerous age-related and metabolic disorders like AD, diabetes, CVD and muscular dystrophy, to name a few, are significantly affected by mitochondrial dysfunction. Thus, should LRP be found to have functionality that improves mitochondrial and/ or metabolic function, it could be exploited for therapeutic design. Another avenue of research that could be explored, is performing a proteomic and transcriptomic study to fully elucidate the gene expression patterns, as well as signaling patterns altered by LRP::FLAG overexpression. This would provide valuable insight into the extent to which LRP influences normal cellular functions. Moreover, as LRP is an oncogenic protein, a full risk assessment study should be carried out to evaluate and minimize chances of tumorigenic development during potential drug development.

Perhaps, the most important avenue that this research will take in future studies, will be in drug design. One potential drug design area we aim to pursue, is the use of the LRP protein as a protein-based drug. This area of drug design is particularly attractive as the use of a protein, especially one that is normally produced endogenously, usually produces minimal to negligible side effects. One factor accounting for this, is that it is normally non-gene altering, safe and that several protein-based drugs have been met with large success. Interestingly, protein-based therapeutics have substantial commercial and therapeutic value, comprising approximately 10% of the current pharmaceutical market. A few well-documented cases where protein-based drugs have been used with large success, are epoetin for anemia, rituximab for non-Hodgkin's lymphoma and insulin for diabetes, thereby

highlighting the huge potential this field of drug design has. One large draw-back to protein-based drugs, is their relatively short half-life and their poor ability to pass through physiologic barriers.

To circumvent this issue, we will attempt encapsulating the LRP protein within nanocapsules, specifically using Poly(lactic-co-glycolic acid) (PLGA) nanoparticles, which is already FDA approved. These nanoparticles offer a range of advantages over alternative delivery systems, including low toxicity, high biocompatibility, and a controlled release of the drug due to its biodegradability. Therefore, encapsulating LRP in PLGA nanocapsules will protect the drug from degradation and allow it to pass physiological barriers, in addition to having a longer half-life for enhanced therapeutic properties. Once synthesized, this drug's therapeutic potential would firstly need to be assessed *in vitro* on cultured cells and thereafter *in vivo* on various animal models, where toxicity profiling would also need to be done. Should positive data be generated on all these fronts pre-clinical and clinical studies could then be possibly initiated. On an interesting side note, once the LRP protein-based drug is developed we can perform studies that assess its effectiveness against other anti-ageing drugs like TA-65, senolytics, klotho, resveratrol and NAD^+. These studies would offer valuable knowledge to discern how the different drugs measure up comparably to one another, especially with regards to our LRP-based drug. Ultimately, the targeting or use of LRP/LR to impede the senescence process may provide an invaluable opportunity for therapeutic design; for the potential treatment of age-related disorders, as well as allow for healthier ageing and extended longevity.

6.2 Study Limitations

There were a number of additional parameters and alterations that could have been made to improve the current study. Firstly, a larger sample size for the mouse study could have been used to definitively confirm all of the aforementioned effects that LRP::FLAG induced, in a larger cohort. Moreover, the use of a larger sample size would have allowed for a more accurate statistical representation. An additional shortcoming, is that an additional mouse group should have been used during the study. This group would have included younger C57BL/6J mice to distinguish the extent to which overexpression of LRP::FLAG induces an anti-ageing effect. In addition, an alternative vector system could have been used for the overexpression of LRP. If overexpression of LRP had been performed by a viral system (lenti-viral) or by CRISPR/CAS9, this would have presented a much larger and further reaching overexpression which may have allowed for efficient deection of the FLAG tag. In turn, this may have induced a much greater effect on all the different markers that

were assessed. As mentioned previously, a large discrepency exists around mtDNA content, therefore a better alternative, such as assessing mtDNA mutations, may have provided a more definitive finding. Finally, with regards to the assessment of telomere length and telomerase activity, alternative techniques could have been performed together with the qPCR to act as further validation.

7. References

1. López-Otín C, Blasco MA, Partridge L, Serrano M, Kroemer G. The hallmarks of aging. Cell. 2013; 153: 1194-217. doi:
2. Lowe D, Horvath S, Raj K. Epigenetic clock analyses of cellular senescence and ageing. Oncotarget. 2016; 7: 8524. doi:
3. Ho AD, Wagner W, Mahlknecht U. Stem cells and ageing. EMBO Rep. 2005; 6: S35-S8. doi:
4. Bulterijs S, Hull RS, Björk VC, Roy AG. It is time to classify biological aging as a disease. Frontiers in genetics. 2015; 6: 205. doi:
5. Singh T, Newman AB. Inflammatory markers in population studies of aging. Ageing research reviews. 2011; 10: 319-29. doi:
6. Pekovic V, Hutchison CJ. Adult stem cell maintenance and tissue regeneration in the ageing context: the role for A-type lamins as intrinsic modulators of ageing in adult stem cells and their niches. Journal of anatomy. 2008; 213: 5-25. doi:
7. Jones DL, Rando TA. Emerging models and paradigms for stem cell ageing. Nature cell biology. 2011; 13: 506-12. doi:
8. Vaziri H, Schächter F, Uchida I, Wei L, Zhu X, Effros R, Cohen D, Harley CB. Loss of telomeric DNA during aging of normal and trisomy 21 human lymphocytes. American journal of human genetics. 1993; 52: 661. doi:
9. Torella D, Rota M, Nurzynska D, Musso E, Monsen A, Shiraishi I, Zias E, Walsh K, Rosenzweig A, Sussman MA. Cardiac stem cell and myocyte aging, heart failure, and insulin-like growth factor-1 overexpression. Circulation research. 2004; 94: 514-24. doi:
10. Yudoh K, Matsuno H, Nakazawa F, Katayama R, Kimura T. Reconstituting telomerase activity using the telomerase catalytic subunit prevents the telomere shorting and replicative senescence in human osteoblasts. Journal of Bone and Mineral Research. 2001; 16: 1453-64. doi:
11. Flach J, Bakker ST, Mohrin M, Conroy PC, Pietras EM, Reynaud D, Alvarez S, Diolaiti ME, Ugarte F, Forsberg EC. Replication stress is a potent driver of functional decline in ageing haematopoietic stem cells. Nature. 2014; 512: 198. doi:
12. Donate LE, Blasco MA. Telomeres in cancer and ageing. Philosophical Transactions of the Royal Society B: Biological Sciences. 2011; 366: 76-84. doi:
13. Campisi J, d'Adda di Fagagna F. Cellular senescence: when bad things happen to good cells. Nat Rev Mol Cell Biol. 2007; 8: 729-40. doi: 10.1038/nrm2233.
14. Stein GH, Drullinger LF, Robetorye RS, Pereira-Smith OM, Smith JR. Senescent cells fail to express cdc2, cycA, and cycB in response to mitogen stimulation. Proceedings of the National Academy of Sciences. 1991; 88: 11012-6. doi:
15. Hayflick L. The limited in vitro lifetime of human diploid cell strains. Exp Cell Res. 1965; 37: 614-36. doi:
16. Hayflick L, Moorhead PS. The serial cultivation of human diploid cell strains. Exp Cell Res. 1961; 25: 585-621. doi:
17. Shay JW, Wright WE. Hayflick, his limit, and cellular ageing. Nature reviews Molecular cell biology. 2000; 1: 72. doi:
18. Lowe SW, Cepero E, Evan G. Intrinsic tumour suppression. Nature. 2004; 432: 307. doi:
19. Shay J, Wright W. Hallmarks of telomeres in ageing research. J Pathol. 2007; 211: 114-23. doi:
20. Blasco MA. Telomeres and human disease: ageing, cancer and beyond. Nature Reviews Genetics. 2005; 6: 611-22. doi:
21. Granger MP, Wright, W.E. and Shay, J.W. Telomerase in cancer and aging. Critical reviews in oncology/hematology. 2002; 41: 29-40. doi:
22. Harley CB, Vaziri H, Counter CM, Allsopp RC. The telomere hypothesis of cellular aging. Exp Gerontol. 1992; 27: 375-82. doi:

23. Aubert G, Lansdorp PM. Telomeres and aging. Physiological reviews. 2008; 88: 557-79. doi:
24. Krishnamurthy J, Ramsey MR, Ligon KL, Torrice C, Koh A, Bonner-Weir S, Sharpless NE. p16INK4a induces an age-dependent decline in islet regenerative potential. Nature. 2006; 443: 453. doi:
25. Prieur A, Peeper DS. Cellular senescence in vivo: a barrier to tumorigenesis. Curr Opin Cell Biol. 2008; 20: 150-5. doi: 10.1016/j.ceb.2008.01.007.
26. di Fagagna FdA, Reaper PM, Clay6-Farrace L, Flegler H. A DNA damage checkpoint response in telomere-initiated senescence. Nature. 2003; 426: 194. doi:
27. Dimri GP, Lee X, Basile G, Acosta M, Scott G, Roskelley C, Medrano EE, Linskens M, Rubelj I, Pereira-Smith O. A biomarker that identifies senescent human cells in culture and in aging skin in vivo. Proceedings of the National Academy of Sciences. 1995; 92: 9363-7. doi:
28. De Cecco M, Jeyapalan J, Zhao X, Tamamori-Adachi M, Sedivy JM. Nuclear protein accumulation in cellular senescence and organismal aging revealed with a novel single-cell resolution fluorescence microscopy assay. Aging (Albany NY). 2011; 3: 955. doi:
29. Freund A, Orjalo AV, Desprez P-Y, Campisi J. Inflammatory networks during cellular senescence: causes and consequences. Trends in molecular medicine. 2010; 16: 238-46. doi:
30. Tchkonia T, Zhu Y, Van Deursen J, Campisi J, Kirkland JL. Cellular senescence and the senescent secretory phenotype: therapeutic opportunities. J Clin Invest. 2013; 123: 966-72. doi:
31. Zhang J, Rane G, Dai X, Shanmugam MK, Arfuso F, Samy RP, Lai MKP, Kappei D, Kumar AP, Sethi G. Ageing and the telomere connection: An intimate relationship with inflammation. Ageing research reviews. 2016; 25: 55-69. doi:
32. De Cecco M, Criscione SW, Peckham EJ, Hillenmeyer S, Hamm EA, Manivannan J, Peterson AL, Kreiling JA, Neretti N, Sedivy JM. Genomes of replicatively senescent cells undergo global epigenetic changes leading to gene silencing and activation of transposable elements. Aging cell. 2013; 12: 247-56. doi:
33. Acosta JC, Banito A, Wuestefeld T, Georgilis A, Janich P, Morton JP, Athineos D, Kang T-W, Lasitschka F, Andrulis M. A complex secretory program orchestrated by the inflammasome controls paracrine senescence. Nature cell biology. 2013; 15: 978. doi:
34. Kuilman T, Michaloglou C, Vredeveld LC, Douma S, van Doorn R, Desmet CJ, Aarden LA, Mooi WJ, Peeper DS. Oncogene-induced senescence relayed by an interleukin-dependent inflammatory network. Cell. 2008; 133: 1019-31. doi:
35. Baker DJ, Wijshake T, Tchkonia T, LeBrasseur NK, Childs BG, Van De Sluis B, Kirkland JL, van Deursen JM. Clearance of p16 Ink4a-positive senescent cells delays ageing-associated disorders. Nature. 2011; 479: 232. doi:
36. Parrinello S, Coppe J-P, Krtolica A, Campisi J. Stromal-epithelial interactions in aging and cancer: senescent fibroblasts alter epithelial cell differentiation. J Cell Sci. 2005; 118: 485-96. doi:
37. Passos JF, Nelson G, Wang C, Richter T, Simillion C, Proctor CJ, Miwa S, Olijslagers S, Hallinan J, Wipat A. Feedback between p21 and reactive oxygen production is necessary for cell senescence. Molecular systems biology. 2010; 6. doi:
38. Kuilman T, Michaloglou C, Mooi WJ, Peeper DS. The essence of senescence. Genes Dev. 2010; 24: 2463-79. doi: 10.1101/gad.1971610.
39. Acosta JC, O'Loghlen A, Banito A, Guijarro MV, Augert A, Raguz S, Fumagalli M, Da Costa M, Brown C, Popov N. Chemokine signaling via the CXCR2 receptor reinforces senescence. Cell. 2008; 133: 1006-18. doi:
40. Kortlever RM, Higgins PJ, Bernards R. Plasminogen activator inhibitor-1 is a critical downstream target of p53 in the induction of replicative senescence. Nature cell biology. 2006; 8: 877. doi:
41. Walston JD, Matteini AM, Nievergelt C, Lange LA, Fallin DM, Barzilai N, Ziv E, Pawlikowska L, Kwok P, Cummings SR. Inflammation and stress-related candidate genes, plasma interleukin-6 levels, and longevity in older adults. Exp Gerontol. 2009; 44: 350-5. doi:

42. Ershler WB, Keller ET. Age-associated increased interleukin-6 gene expression, late-life diseases, and frailty. Annual review of medicine. 2000; 51: 245-70. doi:
43. Franceschi C, Campisi J. Chronic inflammation (inflammaging) and its potential contribution to age-associated diseases. Journals of Gerontology Series A: Biomedical Sciences and Medical Sciences. 2014; 69: S4-S9. doi:
44. Krizhanovsky V, Yon M, Dickins RA, Hearn S, Simon J, Miething C, Yee H, Zender L, Lowe SW. Senescence of activated stellate cells limits liver fibrosis. Cell. 2008; 134: 657-67. doi:
45. Ritschka B, Storer M, Mas A, Heinzmann F, Ortells MC, Morton JP, Sansom OJ, Zender L, Keyes WM. The senescence-associated secretory phenotype induces cellular plasticity and tissue regeneration. Genes Dev. 2017; 31: 172-83. doi:
46. Demaria M, Ohtani N, Youssef SA, Rodier F, Toussaint W, Mitchell JR, Laberge R-M, Vijg J, Van Steeg H, Dollé ME. An essential role for senescent cells in optimal wound healing through secretion of PDGF-AA. Developmental cell. 2014; 31: 722-33. doi:
47. Sparmann A, Bar-Sagi D. Ras-induced interleukin-8 expression plays a critical role in tumor growth and angiogenesis. Cancer cell. 2004; 6: 447-58. doi:
48. Gonzalez-Meljem JM, Apps JR, Fraser HC, Martinez-Barbera JP. Paracrine roles of cellular senescence in promoting tumourigenesis. Br J Cancer. 2018; 118: 1283. doi:
49. Toussaint O, Royer V, Salmon M, Remacle J. Stress-induced premature senescence and tissue ageing. Biochemical pharmacology. 2002; 64: 1007-9. doi:
50. Brand MD. Mitochondrial generation of superoxide and hydrogen peroxide as the source of mitochondrial redox signaling. Free Radical Biology and Medicine. 2016; 100: 14-31. doi:
51. Chance B, Sies H, Boveris A. Hydroperoxide metabolism in mammalian organs. Physiological reviews. 1979; 59: 527-605. doi:
52. Jurk D, Wang C, Miwa S, Maddick M, Korolchuk V, Tsolou A, Gonos ES, Thrasivoulou C, Jill Saffrey M, Cameron K. Postmitotic neurons develop a p21-dependent senescence-like phenotype driven by a DNA damage response. Aging cell. 2012; 11: 996-1004. doi:
53. Wang C, Jurk D, Maddick M, Nelson G, Martin-Ruiz C, Von Zglinicki T. DNA damage response and cellular senescence in tissues of aging mice. Aging cell. 2009; 8: 311-23. doi:
54. Trounce I, Byrne E, Marzuki S. Decline in skeletal muscle mitochondrial respiratory chain function: possible factor in ageing. The lancet. 1989; 333: 637-9. doi:
55. Bowling AC, Mutisya EM, Walker LC, Price DL, Cork LC, Beal MH. Age-dependent impairment of mitochondrial function in primate brain. Journal of neurochemistry. 1993; 60: 1964-7. doi:
56. Passos JF, Saretzki G, Ahmed S, Nelson G, Richter T, Peters H, Wappler I, Birket MJ, Harold G, Schaeuble K. Mitochondrial dysfunction accounts for the stochastic heterogeneity in telomere-dependent senescence. PLoS biology. 2007; 5: e110. doi:
57. Zwerschke W, Mazurek S, Stöckl P, HüTTER E, Eigenbrodt E, Jansen-Dürr P. Metabolic analysis of senescent human fibroblasts reveals a role for AMP in cellular senescence. Biochemical Journal. 2003; 376: 403-11. doi:
58. Hutter E, Renner K, Pfister G, Stöckl P, Jansen-Duerr P, Gnaiger E. Senescence-associated changes in respiration and oxidative phosphorylation in primary human fibroblasts. Biochemical Journal. 2004; 380: 919-28. doi:
59. Kadenbach B, Münscher C, Frank V, Müller-Höcker J, Napiwotzki J. Human aging is associated with stochastic somatic mutations of mitochondrial DNA. Mutation Research/DNAging. 1995; 338: 161-72. doi:
60. Correia-Melo C, Passos JF. Mitochondria: are they causal players in cellular senescence? Biochimica et Biophysica Acta (BBA)-Bioenergetics. 2015; 1847: 1373-9. doi:
61. Harman D. The biologic clock: the mitochondria? Journal of the American Geriatrics Society. 1972; 20: 145-7. doi:

62. Trifunovic A, Wredenberg A, Falkenberg M, Spelbrink JN, Rovio AT, Bruder CE, Bohlooly-Y M, Gidlöf S, Oldfors A, Wibom R. Premature ageing in mice expressing defective mitochondrial DNA polymerase. Nature. 2004; 429: 417. doi:
63. Schon E, Rizzuto R, Moraes C. Accumulation of deletions in mtDNA during tissue ageing: analysis by long PCR. Science. 1989; 244: 346. doi:
64. Ozawa T. Mechanism of somatic mitochondrial DNA mutations associated with age and diseases. Biochimica et Biophysica Acta (BBA)-Molecular Basis of Disease. 1995; 1271: 177-89. doi:
65. Doonan R, McElwee JJ, Matthijssens F, Walker GA, Houthoofd K, Back P, Matscheski A, Vanfleteren JR, Gems D. Against the oxidative damage theory of aging: superoxide dismutases protect against oxidative stress but have little or no effect on life span in Caenorhabditis elegans. Genes Dev. 2008; 22: 3236-41. doi:
66. Mockett RJ, Bayne A-CV, Kwong LK, Orr WC, Sohal RS. Ectopic expression of catalase in Drosophila mitochondria increases stress resistance but not longevity. Free Radical Biology and Medicine. 2003; 34: 207-17. doi:
67. Mockett RJ, Sohal BH, Sohal RS. Expression of multiple copies of mitochondrially targeted catalase or genomic Mn superoxide dismutase transgenes does not extend the life span of Drosophila melanogaster. Free Radical Biology and Medicine. 2010; 49: 2028-31. doi:
68. Bratic A, Larsson N-G. The role of mitochondria in aging. J Clin Invest. 2013; 123: 951-7. doi:
69. Hajhashemi V, Vaseghi G, Pourfarzam M, Abdollahi A. Are antioxidants helpful for disease prevention? Research in pharmaceutical sciences. 2010; 5: 1. doi:
70. Bjelakovic G, Nikolova D, Gluud LL, Simonetti RG, Gluud C. Antioxidant supplements for prevention of mortality in healthy participants and patients with various diseases. Cochrane database of systematic reviews. 2012. doi:
71. Walker C. Antioxidant supplements do not improve mortality and may cause harm. American family physician. 2008; 78: 1079-80. doi:
72. Wan M, Hua X, Su J, Thiagarajan D, Frostegård AG, Haeggström JZ, Frostegård J. Oxidized but not native cardiolipin has pro-inflammatory effects, which are inhibited by Annexin A5. Atherosclerosis. 2014; 235: 592-8. doi:
73. Arivazhagan P, Mizutani E, Fujii M, Ayusawa D. Cardiolipin induces premature senescence in normal human fibroblasts. Biochem Biophys Res Commun. 2004; 323: 739-42. doi:
74. Chapman J, Fielder E, Passos JF. Mitochondrial dysfunction and cell senescence: deciphering a complex relationship. FEBS Lett. 2019. doi:
75. Moiseeva O, Bourdeau V, Roux A, Deschênes-Simard X, Ferbeyre G. Mitochondrial dysfunction contributes to oncogene-induced senescence. Mol Cell Biol. 2009; 29: 4495-507. doi:
76. Nakahira K, Haspel JA, Rathinam VA, Lee S-J, Dolinay T, Lam HC, Englert JA, Rabinovitch M, Cernadas M, Kim HP. Autophagy proteins regulate innate immune responses by inhibiting the release of mitochondrial DNA mediated by the NALP3 inflammasome. Nature immunology. 2011; 12: 222. doi:
77. Salminen A, Kaarniranta K, Kauppinen A. Inflammaging: disturbed interplay between autophagy and inflammasomes. Aging (Albany NY). 2012; 4: 166. doi:
78. Wiley CD, Velarde MC, Lecot P, Liu S, Sarnoski EA, Freund A, Shirakawa K, Lim HW, Davis SS, Ramanathan A. Mitochondrial dysfunction induces senescence with a distinct secretory phenotype. Cell metabolism. 2016; 23: 303-14. doi:
79. Portou M, Baker D, Abraham D, Tsui J. The innate immune system, toll-like receptors and dermal wound healing: a review. Vascular pharmacology. 2015; 71: 31-6. doi:
80. Franceschi C, Bonafè M, Valensin S, Olivieri F, De Luca M, Ottaviani E, De Benedictis G. Inflamm-aging: an evolutionary perspective on immunosenescence. Annals of the New York Academy of Sciences. 2000; 908: 244-54. doi:

81. Salvioli S, Capri M, Valensin S, Tieri P, Monti D, Ottaviani E, Franceschi C. Inflamm-aging, cytokines and aging: state of the art, new hypotheses on the role of mitochondria and new perspectives from systems biology. Current pharmaceutical design. 2006; 12: 3161-71. doi:
82. Bruunsgaard H, Pedersen M, Pedersen BK. Aging and proinflammatory cytokines. Current opinion in hematology. 2001; 8: 131-6. doi:
83. Lumeng CN, Bodzin JL, Saltiel AR. Obesity induces a phenotypic switch in adipose tissue macrophage polarization. J Clin Invest. 2007; 117: 175-84. doi:
84. Cannizzo ES, Clement CC, Sahu R, Follo C, Santambrogio L. Oxidative stress, inflamm-aging and immunosenescence. Journal of proteomics. 2011; 74: 2313-23. doi:
85. Lio D, Scola L, Crivello A, Colonna-Romano G, Candore G, Bonafe M, Cavallone L, Marchegiani F, Olivieri F, Franceschi C. Inflammation, genetics, and longevity: further studies on the protective effects in men of IL-10− 1082 promoter SNP and its interaction with TNF-α− 308 promoter SNP. Journal of medical genetics. 2003; 40: 296-9. doi:
86. Fagiolo U, Cossarizza A, Scala E, Fanales-Belasio E, Ortolani C, Cozzi E, Monti D, Franceschi C, Paganelli R. Increased cytokine production in mononuclear cells of healthy elderly people. European journal of immunology. 1993; 23: 2375-8. doi:
87. Franceschi C, Monti D, Sansoni P, Cossarizza A. The immunology of exceptional individuals: the lesson of centenarians. Immunology today. 1995; 16: 12-6. doi:
88. Bartek J, Hodny Z, Lukas J. Cytokine loops driving senescence. Nature cell biology. 2008; 10: 887. doi:
89. Hernanz A, Guayerbas N, Alvarez P, Alvarado C. Changes with age in peritoneal macrophage functions. Implication of leukocytes in the oxidative stress of senescence. Cellular and molecular biology (Noisy-le-Grand, France). 2004; 50: OL683-90. doi:
90. Fujimoto H, Kobayashi H, Ohno M. Age-induced reduction in mitochondrial manganese superoxide dismutase activity and tolerance of macrophages against apoptosis induced by oxidized low density lipoprotein. Circulation Journal. 2010: 0912100547-. doi:
91. Olivieri F, Albertini MC, Orciani M, Ceka A, Cricca M, Procopio AD, Bonafè M. DNA damage response (DDR) and senescence: shuttled inflamma-miRNAs on the stage of inflamm-aging. Oncotarget. 2015; 6: 35509. doi:
92. Sasaki M, Ikeda H, Sato Y, Nakanuma Y. Proinflammatory cytokine-induced cellular senescence of biliary epithelial cells is mediated via oxidative stress and activation of ATM pathway: a culture study. Free radical research. 2008; 42: 625-32. doi:
93. Prattichizzo F, Bonafè M, Ceka A, Giuliani A, Rita Rippo M, Re M, Antonicelli R, Domenico Procopio A, Olivieri F. Endothelial cell senescence and inflammaging: microRNAs as biomarkers and innovative therapeutic tools. Current Drug Targets. 2016; 17: 388-97. doi:
94. Fulop T, Larbi A, Dupuis G, Le Page A, Frost EH, Cohen AA, Witkowski JM, Franceschi C. Immunosenescence and inflamm-aging as two sides of the same coin: friends or foes? Frontiers in immunology. 2018; 8: 1960. doi:
95. Bruunsgaard H. Effects of tumor necrosis factor-alpha and interleukin-6 in elderly populations. European cytokine network. 2002; 13: 389-91. doi:
96. Bruunsgaard H, Andersen-Ranberg K, Jeune B, Pedersen AN, Skinhøj P, Pedersen BK. A high plasma concentration of TNF-α is associated with dementia in centenarians. Journals of Gerontology Series A: Biomedical Sciences and Medical Sciences. 1999; 54: M357-M64. doi:
97. Ershler WB. Interleukin-6: A Cytokine for Gerontolgists. Journal of the American Geriatrics Society. 1993; 41: 176-81. doi:
98. Strandberg TE, Tilvis RS. C-reactive protein, cardiovascular risk factors, and mortality in a prospective study in the elderly. Arteriosclerosis, thrombosis, and vascular biology. 2000; 20: 1057-60. doi:

99. Serrano M, Lin AW, McCurrach ME, Beach D, Lowe SW. Oncogenic ras provokes premature cell senescence associated with accumulation of p53 and p16INK4a. Cell. 1997; 88: 593-602. doi:
100. Bartkova J, Rezaei N, Liontos M, Karakaidos P, Kletsas D, Issaeva N, Vassiliou L-VF, Kolettas E, Niforou K, Zoumpourlis VC. Oncogene-induced senescence is part of the tumorigenesis barrier imposed by DNA damage checkpoints. Nature. 2006; 444: 633. doi:
101. Chen Z, Trotman LC, Shaffer D, Lin H-K, Dotan ZA, Niki M, Koutcher JA, Scher HI, Ludwig T, Gerald W. Crucial role of p53-dependent cellular senescence in suppression of Pten-deficient tumorigenesis. Nature. 2005; 436: 725. doi:
102. Michaloglou C, Vredeveld LC, Soengas MS, Denoyelle C, Kuilman T, Van Der Horst CM, Majoor DM, Shay JW, Mooi WJ, Peeper DS. BRAF E600-associated senescence-like cell cycle arrest of human naevi. Nature. 2005; 436: 720. doi:
103. Courtois-Cox S, Williams SMG, Reczek EE, Johnson BW, McGillicuddy LT, Johannessen CM, Hollstein PE, MacCollin M, Cichowski K. A negative feedback signaling network underlies oncogene-induced senescence. Cancer cell. 2006; 10: 459-72. doi:
104. Di Micco R, Fumagalli M, Cicalese A, Piccinin S, Gasparini P, Luise C, Schurra C, Nuciforo PG, Bensimon A, Maestro R. Oncogene-induced senescence is a DNA damage response triggered by DNA hyper-replication. Nature. 2006; 444: 638. doi:
105. Nakamura M, Ohsawa S, Igaki T. Mitochondrial defects trigger proliferation of neighbouring cells via a senescence-associated secretory phenotype in Drosophila. Nature communications. 2014; 5: 5264. doi:
106. Mason DX, Jackson TJ, Lin AW. Molecular signature of oncogenic ras-induced senescence. Oncogene. 2004; 23: 9238. doi:
107. Narita M, Young AR, Narita M. Autophagy facilitates oncogene-induced senescence. Autophagy. 2009; 5: 1046-7. doi:
108. Harley CB, Futcher, A.B. and Greider, C.W. Telomeres shorten during ageing of human fibroblasts. Nature. 1990; 345: 458-60. doi: 10.1038/345458a0.
109. Harley CB. Telomere loss mitotic clock or genetic time bomb. Mutation Research/DNAging. 1991; 256: 271-82. doi:
110. Blackburn EH. Telomeres and telomerase: their mechanisms of action and the effects of altering their functions. FEBS Lett. 2005; 579: 859-62. doi: 10.1016/j.febslet.2004.11.036.
111. Olovnikov AM. A theory of marginotomy: the incomplete copying of template margin in enzymic synthesis of polynucleotides and biological significance of the phenomenon. Journal of theoretical biology. 1973; 41: 181-90. doi:
112. Allsopp RC, Harley CB. Evidence for a critical telomere length in senescent human fibroblasts. Exp Cell Res. 1995; 219: 130-6. doi:
113. Lindsey J, McGill NI, Lindsey LA, Green DK, Cooke HJ. In vivo loss of telomeric repeats with age in humans. Mutation Research/DNAging. 1991; 256: 45-8. doi:
114. Sfeir A, De Lange T. Removal of shelterin reveals the telomere end-protection problem. Science. 2012; 336: 593-7. doi:
115. Palm W, de Lange T. How shelterin protects mammalian telomeres. Annual review of genetics. 2008; 42: 301-34. doi:
116. Von Zglinicki T. Oxidative stress shortens telomeres. Trends in biochemical sciences. 2002; 27: 339-44. doi:
117. von Zglinicki T, Saretzki G, Döcke W, Lotze C. Mild hyperoxia shortens telomeres and inhibits proliferation of fibroblasts: a model for senescence? Exp Cell Res. 1995; 220: 186-93. doi:
118. Kawanishi S, Oikawa S. Mechanism of telomere shortening by oxidative stress. Annals of the New York Academy of Sciences. 2004; 1019: 278-84. doi:
119. Richter T, von Zglinicki T. A continuous correlation between oxidative stress and telomere shortening in fibroblasts. Exp Gerontol. 2007; 42: 1039-42. doi:

120. Oikawa S, Tada-Oikawa S, Kawanishi S. Site-specific DNA damage at the GGG sequence by UVA involves acceleration of telomere shortening. Biochemistry. 2001; 40: 4763-8. doi:
121. Petersen S, Saretzki G, von Zglinicki T. Preferential accumulation of single-stranded regions in telomeres of human fibroblasts. Exp Cell Res. 1998; 239: 152-60. doi:
122. Houben JM, Moonen HJ, van Schooten FJ, Hageman GJ. Telomere length assessment: biomarker of chronic oxidative stress? Free Radical Biology and Medicine. 2008; 44: 235-46. doi:
123. Ohki R, Ishikawa F. Telomere-bound TRF1 and TRF2 stall the replication fork at telomeric repeats. Nucleic Acids Res. 2004; 32: 1627-37. doi:
124. Richter T, Saretzki G, Nelson G, Melcher M, Olijslagers S, von Zglinicki T. TRF2 overexpression diminishes repair of telomeric single-strand breaks and accelerates telomere shortening in human fibroblasts. Mech Ageing Dev. 2007; 128: 340-5. doi:
125. Lee H-T, Bose A, Lee C-Y, Opresko PL, Myong S. Molecular mechanisms by which oxidative DNA damage promotes telomerase activity. Nucleic Acids Res. 2017; 45: 11752-65. doi:
126. Fouquerel E, Lormand J, Bose A, Lee H-T, Kim GS, Li J, Sobol RW, Freudenthal BD, Myong S, Opresko PL. Oxidative guanine base damage regulates human telomerase activity. Nature structural & molecular biology. 2016; 23: 1092. doi:
127. Fouquerel E, Barnes RP, Uttam S, Watkins SC, Bruchez MP, Opresko PL. Targeted and persistent 8-oxoguanine base damage at telomeres promotes telomere loss and crisis. Molecular cell. 2019; 75: 117-30. e6. doi:
128. Takai H, Smogorzewska A, de Lange T. DNA damage foci at dysfunctional telomeres. Current Biology. 2003; 13: 1549-56. doi:
129. Herbig U, Jobling WA, Chen BP, Chen DJ, Sedivy JM. Telomere shortening triggers senescence of human cells through a pathway involving ATM, p53, and p21 CIP1, but not p16 INK4a. Molecular cell. 2004; 14: 501-13. doi:
130. Stein GH, Drullinger LF, Soulard A, Dulić V. Differential roles for cyclin-dependent kinase inhibitors p21 and p16 in the mechanisms of senescence and differentiation in human fibroblasts. Mol Cell Biol. 1999; 19: 2109-17. doi:
131. Ben-Porath I, Weinberg RA. The signals and pathways activating cellular senescence. The international journal of biochemistry & cell biology. 2005; 37: 961-76. doi:
132. Jacobs JJ, de Lange T. Significant role for p16INK4a in p53-independent telomere-directed senescence. Current Biology. 2004; 14: 2302-8. doi:
133. Wei W, Herbig U, Wei S, Dutriaux A, Sedivy JM. Loss of retinoblastoma but not p16 function allows bypass of replicative senescence in human fibroblasts. EMBO Rep. 2003; 4: 1061-5. doi:
134. Correia-Melo C, Hewitt G, Passos JF. Telomeres, oxidative stress and inflammatory factors: partners in cellular senescence? Longevity & healthspan. 2014; 3: 1. doi:
135. Benetti R, García-Cao M, Blasco MA. Telomere length regulates the epigenetic status of mammalian telomeres and subtelomeres. Nat Genet. 2007; 39: 243-50. doi:
136. Bodnar AG, Ouellette, M., Frolkis, M., Holt, S.E., Chiu, C.P., Morin, G.B., Harley, C.B., Shay, J.W., Lichtsteiner, S. and Wright, W.E. Extension of life-span by introduction of telomerase into normal human cells. Science. 1998; 279: 349-52. doi: 10.1126/science.279.5349.349
137. Masutomi K, Possemato R, Wong JM, Currier JL, Tothova Z, Manola JB, Ganesan S, Lansdorp PM, Collins K, Hahn WC. The telomerase reverse transcriptase regulates chromatin state and DNA damage responses. Proceedings of the National Academy of Sciences. 2005; 102: 8222-7. doi:
138. Counter CM, Avilion, A.A., LeFeuvre, C.E., Stewart, N.G., Greider, C.W., Harley, C.B. and Bacchetti, S. The roles of telomeres and telomerase in cell life span. Mutation Research/Reviews in Genetic Toxicology. 1996; 366: 45-63. doi:

139. Counter CM, Meyerson, M., Eaton, E.N., Ellisen, L.W., Caddle, S.D., Haber, D.A. and Weinberg, R.A. Telomerase activity is restored in human cells by ectopic expression of hTERT (hEST2), the catalytic subunit of telomerase. Oncogene. 1998; 16: 1217-22. doi:
140. de Jesus BB, Vera E, Schneeberger K, Tejera AM, Ayuso E, Bosch F, Blasco MA. Telomerase gene therapy in adult and old mice delays aging and increases longevity without increasing cancer. EMBO molecular medicine. 2012; 4: 691-704. doi:
141. de Jesus BB, Schneeberger K, Vera E, Tejera A, Harley CB, Blasco MA. The telomerase activator TA-65 elongates short telomeres and increases health span of adult/old mice without increasing cancer incidence. Aging cell. 2011; 10: 604-21. doi:
142. Masutomi K, Evan YY, Khurts S, Ben-Porath I, Currier JL, Metz GB, Brooks MW, Kaneko S, Murakami S, DeCaprio JA. Telomerase maintains telomere structure in normal human cells. Cell. 2003; 114: 241-53. doi:
143. Tomas-Loba A, Flores I, Fernandez-Marcos PJ, Cayuela ML, Maraver A, Tejera A, Borras C, Matheu A, Klatt P, Flores JM, Vina J, Serrano M, Blasco MA. Telomerase reverse transcriptase delays aging in cancer-resistant mice. Cell. 2008; 135: 609-22. doi: 10.1016/j.cell.2008.09.034.
144. Counter CM, Avilion, A.A., LeFeuvre, C.E., Stewart, N.G., Greider, C.W., Harley, C.B. and Bacchetti, S. Telomere shortening associated with chromosome instability is arrested in immortal cells which express telomerase activity. . The EMBO journal. 1992; 11: 1921. doi:
145. Capper R, Britt-Compton B, Tankimanova M, Rowson J, Letsolo B, Man S, Haughton M, Baird DM. The nature of telomere fusion and a definition of the critical telomere length in human cells. Genes Dev. 2007; 21: 2495-508. doi: 10.1101/gad.439107.
146. Chan SW-L, Blackburn EH. Telomerase and ATM/Tel1p protect telomeres from nonhomologous end joining. Molecular cell. 2003; 11: 1379-87. doi:
147. Lin TT, Letsolo BT, Jones RE, Rowson J, Pratt G, Hewamana S, Fegan C, Pepper C, Baird DM. Telomere dysfunction and fusion during the progression of chronic lymphocytic leukemia: evidence for a telomere crisis. Blood. 2010; 116: 1899-907. doi: 10.1182/blood-2010-02-272104.
148. Blazer S, Khankin E, Segev Y, Ofir R, Yalon-Hacohen M, Kra-Oz Z, Gottfried Y, Larisch S, Skorecki KL. High glucose-induced replicative senescence: point of no return and effect of telomerase. Biochem Biophys Res Commun. 2002; 296: 93-101. doi:
149. Liew C, Holman A, Kulkarni R. The roles of telomeres and telomerase in β-cell regeneration. Diabetes, Obesity and Metabolism. 2009; 11: 21-9. doi:
150. Wyllie FS, Jones CJ, Skinner JW, Haughton MF, Wallis C, Wynford-Thomas D, Faragher RG, Kipling D. Telomerase prevents the accelerated cell ageing of Werner syndrome fibroblasts. Nat Genet. 2000; 24: 16-7. doi:
151. Henderson ER, Blackburn EH. An overhanging 3'terminus is a conserved feature of telomeres. Mol Cell Biol. 1989; 9: 345-8. doi:
152. Moyzis RK, Buckingham JM, Cram LS, Dani M, Deaven LL, Jones MD, Meyne J, Ratliff RL, Wu J-R. A highly conserved repetitive DNA sequence,(TTAGGG) n, present at the telomeres of human chromosomes. Proceedings of the National Academy of Sciences. 1988; 85: 6622-6. doi:
153. Meyne J, Ratliff RL, MoYzIs RK. Conservation of the human telomere sequence (TTAGGG) n among vertebrates. Proceedings of the National Academy of Sciences. 1989; 86: 7049-53. doi:
154. Zahler AM, Williamson JR, Cech TR, Prescott DM. Inhibition of telomerase by G-quartet DMA structures. Nature. 1991; 350: 718-20. doi:
155. McEachern MJ, Krauskopf A, Blackburn EH. Telomeres and their control. Annual review of genetics. 2000; 34: 331-58. doi:
156. Gilley D, Lee MS, Blackburn EH. Altering specific telomerase RNA template residues affects active site function. Genes Dev. 1995; 9: 2214-26. doi:
157. Harley CB, Villeponteau B. Telomeres and telomerase in aging and cancer. Current opinion in genetics & development. 1995; 5: 249-55. doi:

158. Schoeftner S, Blasco MA. Developmentally regulated transcription of mammalian telomeres by DNA-dependent RNA polymerase II. Nature cell biology. 2008; 10: 228. doi:
159. Oganesian L, Bryan TM. Physiological relevance of telomeric G-quadruplex formation: a potential drug target. Bioessays. 2007; 29: 155-65. doi:
160. De Lange T. Shelterin: the protein complex that shapes and safeguards human telomeres. Genes Dev. 2005; 19: 2100-10. doi:
161. Smogorzewska A, de Lange T. Regulation of telomerase by telomeric proteins. Annu Rev Biochem. 2004; 73: 177-208. doi: 10.1146/annurev.biochem.73.071403.160049.
162. Liu D, O'Connor MS, Qin J, Songyang Z. Telosome, a mammalian telomere-associated complex formed by multiple telomeric proteins. Journal of Biological Chemistry. 2004; 279: 51338-42. doi:
163. Ye JZ-S, Donigian JR, Van Overbeek M, Loayza D, Luo Y, Krutchinsky AN, Chait BT, De Lange T. TIN2 binds TRF1 and TRF2 simultaneously and stabilizes the TRF2 complex on telomeres. Journal of Biological Chemistry. 2004; 279: 47264-71. doi:
164. Chapman L, Fairall L, Rhodes D. How the human telomeric proteins TRF1 and TRF2 recognize telomeric DNA: a view from high-resolution crystal structures. EMBO Rep. 2005; 6: 39-45. doi:
165. Loayza D, Parsons H, Donigian J, Hoke K, de Lange T. DNA Binding Features of Human POT1 A NONAMER 5′-TAGGGTTAG-3′ MINIMAL BINDING SITE, SEQUENCE SPECIFICITY, AND INTERNAL BINDING TO MULTIMERIC SITES. Journal of Biological Chemistry. 2004; 279: 13241-8. doi:
166. O'Sullivan RJ, Karlseder J. Telomeres: protecting chromosomes against genome instability. Nat Rev Mol Cell Biol. 2010; 11: 171. doi:
167. Griffith JD, Comeau L, Rosenfield S, Stansel RM, Bianchi A, Moss H, De Lange T. Mammalian telomeres end in a large duplex loop. Cell. 1999; 97: 503-14. doi:
168. Verdun RE, Karlseder J. Replication and protection of telomeres. Nature. 2007; 447: 924. doi:
169. Karlseder J, Broccoli D, Dai Y, Hardy S, de Lange T. p53-and ATM-dependent apoptosis induced by telomeres lacking TRF2. Science. 1999; 283: 1321-5. doi:
170. Denchi EL, de Lange T. Protection of telomeres through independent control of ATM and ATR by TRF2 and POT1. Nature. 2007; 448: 1068-71. doi:
171. Guo X, Deng Y, Lin Y, Cosme-Blanco W, Chan S, He H, Yuan G, Brown EJ, Chang S. Dysfunctional telomeres activate an ATM-ATR-dependent DNA damage response to suppress tumorigenesis. The EMBO journal. 2007; 26: 4709-19. doi:
172. Mattern KA, Swiggers SJ, Nigg AL, Lowenberg B, Houtsmuller AB, Zijlmans JM. Dynamics of protein binding to telomeres in living cells: implications for telomere structure and function. Mol Cell Biol. 2004; 24: 5587-94. doi: 10.1128/MCB.24.12.5587-5594.2004.
173. Loayza D, De Lange T. POT1 as a terminal transducer of TRF1 telomere length control. Nature. 2003; 423: 1013-8. doi:
174. Kelleher C, Kurth I, Lingner J. Human protection of telomeres 1 (POT1) is a negative regulator of telomerase activity in vitro. Mol Cell Biol. 2005; 25: 808-18. doi:
175. Lei M, Zaug AJ, Podell ER, Cech TR. Switching human telomerase on and off with hPOT1 protein in vitro. Journal of Biological Chemistry. 2005; 280: 20449-56. doi:
176. Hwang H, Buncher N, Opresko PL, Myong S. POT1-TPP1 regulates telomeric overhang structural dynamics. Structure. 2012; 20: 1872-80. doi:
177. Wang F, Podell ER, Zaug AJ, Yang Y, Baciu P, Cech TR, Lei M. The POT1–TPP1 telomere complex is a telomerase processivity factor. Nature. 2007; 445: 506-10. doi:
178. Deng Z, Norseen J, Wiedmer A, Riethman H, Lieberman PM. TERRA RNA binding to TRF2 facilitates heterochromatin formation and ORC recruitment at telomeres. Molecular cell. 2009; 35: 403-13. doi:

179. Redon S, Reichenbach P, Lingner J. The non-coding RNA TERRA is a natural ligand and direct inhibitor of human telomerase. Nucleic Acids Res. 2010; 38: 5797-806. doi:
180. Greider CWaB, E.H. A telomeric sequence in the RNA of Tetrahymena telomerase required for telomere repeat synthesis. Nature. 1989; 337: 331-7. doi:
181. Greider CW, Blackburn EH. Identification of a specific telomere terminal transferase activity in Tetrahymena extracts. Cell. 1985; 43: 405-13. doi:
182. Morin GB. The human telomere terminal transferase enzyme is a ribonucleoprotein that synthesizes TTAGGG repeats. Cell. 1989; 59: 521-9. doi:
183. Weinrich SL, Pruzan R, Ma L, Ouellette M, Tesmer VM, Holt SE, Bodnar AG, Lichtsteiner S, Kim NW, Trager JB. Reconstitution of human telomerase with the template RNA component hTR and the catalytic protein subunit hTRT. Nat Genet. 1997; 17: 498. doi:
184. Morales CP, Holt SE, Ouellette M, Kaur KJ, Yan Y, Wilson KS, White MA, Wright WE, Shay JW. Absence of cancer–associated changes in human fibroblasts immortalized with telomerase. Nat Genet. 1999; 21: 115-8. doi:
185. Kim NW, Piatyszek MA, Prowse KR, Harley CB. Specific association of human telomerase activity with immortal cells and cancer. Science. 1994; 266: 2011. doi:
186. Cifuentes-Rojas C, Shippen DE. Telomerase regulation. Mutation Research/Fundamental and Molecular Mechanisms of Mutagenesis. 2012; 730: 20-7. doi:
187. Nakamura TM, Morin, G.B., Chapman, K.B., Weinrich, S.L., Andrews, W.H., Lingner, J., Harley, C.B. and Cech, T.R. Telomerase catalytic subunit homologs from fission yeast and human. Science. 1997; 277: 955-9. doi:
188. Nakamura TM, Cech TR. Reversing time: origin of telomerase. Cell. 1998; 92: 587-90. doi:
189. Pogacic V, Dragon F, Filipowicz W. Human H/ACA small nucleolar RNPs and telomerase share evolutionarily conserved proteins NHP2 and NOP10. Mol Cell Biol. 2000; 20: 9028-40. doi:
190. Podlevsky JD, Chen JJ-L. It all comes together at the ends: telomerase structure, function, and biogenesis. Mutation Research/Fundamental and Molecular Mechanisms of Mutagenesis. 2012; 730: 3-11. doi:
191. Cohen SB, Graham ME, Lovrecz GO, Bache N, Robinson PJ, Reddel RR. Protein composition of catalytically active human telomerase from immortal cells. Science. 2007; 315: 1850-3. doi:
192. Townsley DM, Dumitriu B, Young NS. Bone marrow failure and the telomeropathies. Blood. 2014; 124: 2775-83. doi:
193. Ramlee M, Wang J, Toh W, Li S. Transcription regulation of the human telomerase reverse transcriptase (hTERT) gene. Genes. 2016; 7: 50. doi:
194. Shay J, Bacchetti S. A survey of telomerase activity in human cancer. European journal of cancer. 1997; 33: 787-91. doi:
195. Holt SE, Aisner DL, Shay JW, Wright WE. Lack of cell cycle regulation of telomerase activity in human cells. Proceedings of the National Academy of Sciences. 1997; 94: 10687-92. doi:
196. Yi X, Tesmer VM, Savre-Train I, Shay JW, Wright WE. Both transcriptional and posttranscriptional mechanisms regulate human telomerase template RNA levels. Mol Cell Biol. 1999; 19: 3989-97. doi:
197. Wang S, Zhu J. Evidence for a relief of repression mechanism for activation of the human telomerase reverse transcriptase promoter. Journal of Biological Chemistry. 2003; 278: 18842-50. doi:
198. Xu D, Popov N, Hou M, Wang Q, Björkholm M, Gruber A, Menkel AR, Henriksson M. Switch from Myc/Max to Mad1/Max binding and decrease in histone acetylation at the telomerase reverse transcriptase promoter during differentiation of HL60 cells. Proceedings of the National Academy of Sciences. 2001; 98: 3826-31. doi:

199. Wang S, Hu C, Zhu J. Transcriptional silencing of a novel hTERT reporter locus during in vitro differentiation of mouse embryonic stem cells. Molecular biology of the cell. 2007; 18: 669-77. doi:
200. Atkinson SP, Hoare SF, Glasspool RM, Keith WN. Lack of telomerase gene expression in alternative lengthening of telomere cells is associated with chromatin remodeling of the hTR and hTERT gene promoters. Cancer Res. 2005; 65: 7585-90. doi:
201. Wick M, Zubov D, Hagen G. Genomic organization and promoter characterization of the gene encoding the human telomerase reverse transcriptase (hTERT). Gene. 1999; 232: 97-106. doi:
202. Oguchi K, Tamura K, Takahashi H. Characterization of Oryza sativa telomerase reverse transcriptase and possible role of its phosphorylation in the control of telomerase activity. Gene. 2004; 342: 57-66. doi:
203. Rohde V, Sattler H-P, Bund T, Bonkhoff H, Fixemer T, Bachmann C, Lensch R, Unteregger G, Stoeckle M, Wullich B. Expression of the human telomerase reverse transcriptase is not related to telomerase activity in normal and malignant renal tissue. Clinical Cancer Research. 2000; 6: 4803-9. doi:
204. Kang SS, Kwon T, Do SI. Akt protein kinase enhances human telomerase activity through phosphorylation of telomerase reverse transcriptase subunit. Journal of Biological Chemistry. 1999; 274: 13085-90. doi:
205. Minamino T, Mitsialis S, Kourembanas S. Hypoxia extends the life span of vascular smooth muscle cells through telomerase activation. Mol Cell Biol. 2001; 21: 3336-42. doi:
206. Aisner DL, Wright WE, Shay JW. Telomerase regulation: not just flipping the switch. Current opinion in genetics & development. 2002; 12: 80-5. doi:
207. Kharbanda S, Kumar V, Dhar S, Pandey P, Chen C, Majumder P, Yuan Z, Whang Y, Strauss W, Pandita TK. Regulation of the hTERT telomerase catalytic subunit by the c-Abl tyrosine kinase. Current Biology. 2000; 10: 568-75. doi:
208. Horikawa I, Barrett JC. Transcriptional regulation of the telomerase hTERT gene as a target for cellular and viral oncogenic mechanisms. Carcinogenesis. 2003; 24: 1167-76. doi:
209. Lee JH, Khadka P, Baek SH, Chung IK. CHIP promotes human telomerase reverse transcriptase degradation and negatively regulates telomerase activity. Journal of Biological Chemistry. 2010; 285: 42033-45. doi:
210. Wong JM, Kusdra L, Collins K. Subnuclear shuttling of human telomerase induced by transformation and DNA damage. Nature cell biology. 2002; 4: 731. doi:
211. Venteicher AS, Abreu EB, Meng Z, McCann KE, Terns RM, Veenstra TD, Terns MP, Artandi SE. A human telomerase holoenzyme protein required for Cajal body localization and telomere synthesis. Science. 2009; 323: 644-8. doi:
212. Banik SS, Counter CM. Characterization of interactions between PinX1 and human telomerase subunits hTERT and hTR. Journal of Biological Chemistry. 2004; 279: 51745-8. doi:
213. Zhou XZ, Lu KP. The Pin2/TRF1-interacting protein PinX1 is a potent telomerase inhibitor. Cell. 2001; 107: 347-59. doi:
214. Ahmed S, Passos JF, Birket MJ, Beckmann T, Brings S, Peters H, Birch-Machin MA, von Zglinicki T, Saretzki G. Telomerase does not counteract telomere shortening but protects mitochondrial function under oxidative stress. J Cell Sci. 2008; 121: 1046-53. doi: 10.1242/jcs.019372.
215. Saretzki G. Telomerase, mitochondria and oxidative stress. Exp Gerontol. 2009; 44: 485-92. doi: 10.1016/j.exger.2009.05.004.
216. Prowse KR, Greider CW. Developmental and tissue-specific regulation of mouse telomerase and telomere length. Proceedings of the National Academy of Sciences. 1995; 92: 4818-22. doi:
217. Kipling D, Cooke HJ. Hypervariable ultra-long telomeres in mice. Nature. 1990; 347: 400. doi:

218. De Lange T, Shiue L, Myers R, Cox D, Naylor S, Killery A, Varmus H. Structure and variability of human chromosome ends. Mol Cell Biol. 1990; 10: 518-27. doi:
219. Wright WE, Shay JW. Telomere dynamics in cancer progression and prevention: fundamental differences in human and mouse telomere biology. Nat Med. 2000; 6: 849. doi:
220. Parrinello S, Samper E, Krtolica A, Goldstein J, Melov S, Campisi J. Oxygen sensitivity severely limits the replicative lifespan of murine fibroblasts. Nature cell biology. 2003; 5: 741. doi:
221. Blasco MA, Lee, H.W., Hande, M.P., Samper, E., Lansdorp, P.M., DePinho, R.A. and Greider, C.W. Telomere Shortening and Tumor Formation by Mouse Cells Lacking Telomerase RNA. Cell. 1997; 91: 25-34. doi:
222. Muñoz-Lorente MA, Cano-Martin AC, Blasco MA. Mice with hyper-long telomeres show less metabolic aging and longer lifespans. Nature communications. 2019; 10: 1-14. doi:
223. Jaskelioff M, Muller FL, Paik J-H, Thomas E, Jiang S, Adams AC, Sahin E, Kost-Alimova M, Protopopov A, Cadinanos J. Telomerase reactivation reverses tissue degeneration in aged telomerase-deficient mice. Nature. 2011; 469: 102. doi:
224. Bär C, De Jesus BB, Serrano R, Tejera A, Ayuso E, Jimenez V, Formentini I, Bobadilla M, Mizrahi J, De Martino A. Telomerase expression confers cardioprotection in the adult mouse heart after acute myocardial infarction. Nature communications. 2014; 5: 5863. doi:
225. Saretzki G. Extra-telomeric functions of human telomerase: cancer, mitochondria and oxidative stress. Current pharmaceutical design. 2014; 20: 6386-403. doi:
226. Cong Y, Shay JW. Actions of human telomerase beyond telomeres. Cell research. 2008; 18: 725. doi:
227. Klapper W, Shin T, Mattson MP. Differential regulation of telomerase activity and TERT expression during brain development in mice. Journal of neuroscience research. 2001; 64: 252-60. doi:
228. Zhou Q-G, Liu M-Y, Lee H-W, Ishikawa F, Devkota S, Shen X-R, Jin X, Wu H-Y, Liu Z, Liu X. Hippocampal TERT regulates spatial memory formation through modulation of neural development. Stem cell reports. 2017; 9: 543-56. doi:
229. Ding D, Zhou J, Wang M, Cong YS. Implications of telomere-independent activities of telomerase reverse transcriptase in human cancer. The FEBS journal. 2013; 280: 3205-11. doi:
230. Haendeler J, Dröse S, Büchner N, Jakob S, Altschmied J, Goy C, Spyridopoulos I, Zeiher AM, Brandt U, Dimmeler S. Mitochondrial telomerase reverse transcriptase binds to and protects mitochondrial DNA and function from damage. Arteriosclerosis, thrombosis, and vascular biology. 2009; 29: 929-35. doi:
231. Sahin E, Colla S, Liesa M, Moslehi J, Müller FL, Guo M, Cooper M, Kotton D, Fabian AJ, Walkey C. Telomere dysfunction induces metabolic and mitochondrial compromise. Nature. 2011; 470: 359. doi:
232. Sharma GG, Gupta A, Wang H, Scherthan H, Dhar S, Gandhi V, Iliakis G, Shay JW, Young CS, Pandita TK. hTERT associates with human telomeres and enhances genomic stability and DNA repair. Oncogene. 2003; 22: 131-46. doi: 10.1038/sj.onc.1206063.
233. Kovalenko OA, Caron MJ, Ulema P, Medrano C, Thomas AP, Kimura M, Bonini MG, Herbig U, Santos JH. A mutant telomerase defective in nuclear-cytoplasmic shuttling fails to immortalize cells and is associated with mitochondrial dysfunction. Aging cell. 2010; 9: 203-19. doi:
234. Sharma NK, Reyes A, Green P, Caron MJ, Bonini MG, Gordon DM, Holt IJ, Santos JH. Human telomerase acts as a hTR-independent reverse transcriptase in mitochondria. Nucleic Acids Res. 2011; 40: 712-25. doi:
235. Santos JH, Meyer JN, Skorvaga M, Annab LA, Van Houten B. Mitochondrial hTERT exacerbates free-radical-mediated mtDNA damage. Aging cell. 2004; 3: 399-411. doi:
236. Santos JH, Meyer JN, Van Houten B. Mitochondrial localization of telomerase as a determinant for hydrogen peroxide-induced mitochondrial DNA damage and apoptosis. Human molecular genetics. 2006; 15: 1757-68. doi:

237. Mattson MP, Klapper W. Emerging roles for telomerase in neuronal development and apoptosis. Journal of neuroscience research. 2001; 63: 1-9. doi:
238. Mandal M, Kumar R. Bcl-2 modulates telomerase activity. Journal of Biological Chemistry. 1997; 272: 14183-7. doi:
239. Fu W, Begley JG, Killen MW, Mattson MP. Anti-apoptotic role of telomerase in pheochromocytoma cells. Journal of Biological Chemistry. 1999; 274: 7264-71. doi:
240. Lee J, Sung Y, Cheong C, Choi Y, Jeon H, Sun W, Hahn W, Ishikawa F, Lee HW. TERT promotes cellular and organismal survival independently of telomerase activity. Oncogene. 2008; 27: 3754. doi:
241. Ray S, Karamysheva Z, Wang L, Shippen DE, Price CM. Interactions between telomerase and primase physically link the telomere and chromosome replication machinery. Mol Cell Biol. 2002; 22: 5859-68. doi:
242. Stellwagen AE, Haimberger ZW, Veatch JR, Gottschling DE. Ku interacts with telomerase RNA to promote telomere addition at native and broken chromosome ends. Genes Dev. 2003; 17: 2384-95. doi:
243. Sharma GG, Hwang K-k, Pandita RK, Gupta A, Dhar S, Parenteau J, Agarwal M, Worman HJ, Wellinger RJ, Pandita TK. Human heterochromatin protein 1 isoforms HP1Hsα and HP1Hsβ interfere with hTERT-telomere interactions and correlate with changes in cell growth and response to ionizing radiation. Mol Cell Biol. 2003; 23: 8363-76. doi:
244. Romaniuk A, Paszel-Jaworska A, Totoń E, Lisiak N, Hołysz H, Królak A, Grodecka-Gazdecka S, Rubiś B. The non-canonical functions of telomerase: to turn off or not to turn off. Molecular biology reports. 2019; 46: 1401-11. doi:
245. Park J-I, Venteicher AS, Hong JY, Choi J, Jun S, Shkreli M, Chang W, Meng Z, Cheung P, Ji H. Telomerase modulates Wnt signalling by association with target gene chromatin. Nature. 2009; 460: 66-72. doi:
246. Choi J, Southworth LK, Sarin KY, Venteicher AS, Ma W, Chang W, Cheung P, Jun S, Artandi MK, Shah N. TERT promotes epithelial proliferation through transcriptional control of a Myc-and Wnt-related developmental program. PLoS genetics. 2008; 4: e10. doi:
247. Chiodi I, Mondello C. Telomere-independent functions of telomerase in nuclei, cytoplasm, and mitochondria. Front Oncol. 2012; 2: 133. doi: 10.3389/fonc.2012.00133.
248. Wege H, Heim D, Lütgehetmann M, Dierlamm J, Lohse AW, Brümmendorf TH. Forced activation of β-catenin signaling supports the transformation of hTERT-immortalized human fetal hepatocytes. Molecular cancer research. 2011; 9: 1222-31. doi:
249. Ghosh A, Saginc G, Leow SC, Khattar E, Shin EM, Yan TD, Wong M, Zhang Z, Li G, Sung W-K. Telomerase directly regulates NF-κB-dependent transcription. Nature cell biology. 2012; 14: 1270. doi:
250. Ding D, Xi P, Zhou J, Wang M, Cong Y-S. Human telomerase reverse transcriptase regulates MMP expression independently of telomerase activity via NF-κB-dependent transcription. The FASEB Journal. 2013; 27: 4375-83. doi:
251. Wu Y, Bian C, Zhen C, Liu L, Lin Z, Nisar MF, Wang M, Bartsch JW, Huang E, Ji P. Telomerase reverse transcriptase mediates EMT through NF-κB signaling in tongue squamous cell carcinoma. Oncotarget. 2017; 8: 85492. doi:
252. Mattiussi M, Tilman G, Lenglez S, Decottignies A. Human telomerase represses ROS-dependent cellular responses to Tumor Necrosis Factor-α without affecting NF-κB activation. Cellular signalling. 2012; 24: 708-17. doi:
253. Shay JW, Pereira-Smith OM, Wright WE. A role for both RB and p53 in the regulation of human cellular senescence. Exp Cell Res. 1991; 196: 33-9. doi:
254. Artandi SE, DePinho RA. Telomeres and telomerase in cancer. Carcinogenesis. 2009; 31: 9-18. doi:

255. Letsolo BT, Rowson J, Baird DM. Fusion of short telomeres in human cells is characterized by extensive deletion and microhomology, and can result in complex rearrangements. Nucleic Acids Res. 2010; 38: 1841-52. doi: 10.1093/nar/gkp1183.
256. Martínez P, Thanasoula M, Muñoz P, Liao C, Tejera A, McNees C, Flores JM, Fernández-Capetillo O, Tarsounas M, Blasco MA. Increased telomere fragility and fusions resulting from TRF1 deficiency lead to degenerative pathologies and increased cancer in mice. Genes Dev. 2009; 23: 2060-75. doi:
257. Londoño-Vallejo JA. Telomere instability and cancer. Biochimie. 2008; 90: 73-82. doi:
258. Hiyama E, Gollahon L, Kataoka T, Kuroi K, Yokoyama T, Gazdar AF, Hiyama K, Piatyszek MA, Shay JW. Telomerase activity in human breast tumors. Journal of the National Cancer Institute. 1996; 88: 116-22. doi:
259. Singhapol C, Pal D, Czapiewski R, Porika M, Nelson G, Saretzki GC. Mitochondrial telomerase protects cancer cells from nuclear DNA damage and apoptosis. PLoS One. 2013; 8: e52989. doi:
260. Del Bufalo D, Rizzo A, Trisciuoglio D, Cardinali G, Torrisi MR, Zangemeister-Wittke U, Zupi G, Biroccio A. Involvement of hTERT in apoptosis induced by interference with Bcl-2 expression and function. Cell death and differentiation. 2005; 12: 1429. doi:
261. Murea M, Ma L, Freedman BI. Genetic and environmental factors associated with type 2 diabetes and diabetic vascular complications. The review of diabetic studies: RDS. 2012; 9: 6. doi:
262. Reaven GM. Role of insulin resistance in human disease. Diabetes. 1988; 37: 1595-607. doi:
263. Mehta JL, Rasouli N, Sinha AK, Molavi B. Oxidative stress in diabetes: a mechanistic overview of its effects on atherogenesis and myocardial dysfunction. The international journal of biochemistry & cell biology. 2006; 38: 794-803. doi:
264. Melmed S, Polonsky K, Larsen P, Kronenberg H. Williams textbook of endocrinology. 12th. Philadelphia, PA: Saunders Elsevier. 2011. doi:
265. Ripsin CM, Kang H, Urban RJ. Management of blood glucose in type 2 diabetes mellitus. Am Fam Physician. 2009; 79: 29-36. doi:
266. Sampson MJ, Winterbone MS, Hughes JC, Dozio N, Hughes DA. Monocyte telomere shortening and oxidative DNA damage in type 2 diabetes. Diabetes care. 2006; 29: 283-9. doi:
267. Zee RY, Castonguay AJ, Barton NS, Germer S, Martin M. Mean leukocyte telomere length shortening and type 2 diabetes mellitus: a case-control study. Translational research. 2010; 155: 166-9. doi:
268. Halvorsen T, Beattie G, Lopez A, Hayek A, Levine F. Accelerated telomere shortening and senescence in human pancreatic islet cells stimulated to divide in vitro. Journal of Endocrinology. 2000; 166: 103-9. doi:
269. Guo N, Parry EM, Li L-S, Kembou F, Lauder N, Hussain MA, Berggren P-O, Armanios M. Short telomeres compromise β-cell signaling and survival. PLoS One. 2011; 6: e17858. doi:
270. Kuhlow D, Florian S, von Figura G, Weimer S, Schulz N, Petzke KJ, Zarse K, Pfeiffer AF, Rudolph KL, Ristow M. Telomerase deficiency impairs glucose metabolism and insulin secretion. Aging (Albany NY). 2010; 2: 650. doi:
271. Zhang Y, Chen Z, Wang T, Yang J, Li R, Wang S, Liu J, Ye Z. Treatment of diabetes mellitus-induced erectile dysfunction using endothelial progenitor cells genetically modified with human telomerase reverse transcriptase. Oncotarget. 2016; 7: 39302. doi:
272. Libby P. Inflammation and cardiovascular disease mechanisms. The American journal of clinical nutrition. 2006; 83: 456S-60S. doi:
273. Van Gaal LF, Mertens IL, Christophe E. Mechanisms linking obesity with cardiovascular disease. Nature. 2006; 444: 875. doi:
274. Brouilette S, Singh RK, Thompson JR, Goodall AH, Samani NJ. White cell telomere length and risk of premature myocardial infarction. Arteriosclerosis, thrombosis, and vascular biology. 2003; 23: 842-6. doi:

275. Bekaert S, De Meyer T, Rietzschel ER, De Buyzere ML, De Bacquer D, Langlois M, Segers P, Cooman L, Van Damme P, Cassiman P. Telomere length and cardiovascular risk factors in a middle-aged population free of overt cardiovascular disease. Aging cell. 2007; 6: 639-47. doi:
276. Oh H, Wang SC, Prahash A, Sano M, Moravec CS, Taffet GE, Michael LH, Youker KA, Entman ML, Schneider MD. Telomere attrition and Chk2 activation in human heart failure. Proceedings of the National Academy of Sciences. 2003; 100: 5378-83. doi:
277. Chimenti C, Kajstura J, Torella D, Urbanek K, Heleniak H, Colussi C, Di Meglio F, Nadal-Ginard B, Frustaci A, Leri A. Senescence and death of primitive cells and myocytes lead to premature cardiac aging and heart failure. Circulation research. 2003; 93: 604-13. doi:
278. Serrano AL, Andrés V. Telomeres and cardiovascular disease: does size matter? Circulation research. 2004; 94: 575-84. doi:
279. Samani NJ, Boultby R, Butler R, Thompson JR, Goodall AH. Telomere shortening in atherosclerosis. The lancet. 2001; 358: 472-3. doi:
280. Salpea KD, Humphries SE. Telomere length in atherosclerosis and diabetes. Atherosclerosis. 2010; 209: 35-8. doi:
281. . !!! INVALID CITATION !!! doi:
282. Fuster JJ, Andrés V. Telomere biology and cardiovascular disease. Circulation research. 2006; 99: 1167-80. doi:
283. Oh H, Taffet GE, Youker KA, Entman ML, Overbeek PA, Michael LH, Schneider MD. Telomerase reverse transcriptase promotes cardiac muscle cell proliferation, hypertrophy, and survival. Proceedings of the National Academy of Sciences. 2001; 98: 10308-13. doi:
284. Serrano-Pozo A, Frosch MP, Masliah E, Hyman BT. Neuropathological alterations in Alzheimer disease. Cold Spring Harb Perspect Med. 2011; 1: a006189. doi: 10.1101/cshperspect.a006189.
285. Franco S, Blasco MA, Siedlak SL, Harris PL, Moreira PI, Perry G, Smith MA. Telomeres and telomerase in Alzheimer's disease: epiphenomena or a new focus for therapeutic strategy? Alzheimer's & Dementia. 2006; 2: 164-8. doi:
286. Panossian L, Porter V, Valenzuela H, Zhu X, Reback E, Masterman D, Cummings J, Effros R. Telomere shortening in T cells correlates with Alzheimer's disease status. Neurobiology of aging. 2003; 24: 77-84. doi:
287. Liu M, Huo YR, Wang J, Wang C, Liu S, Liu S, Wang J, Ji Y. Telomere shortening in Alzheimer's disease patients. Annals of Clinical & Laboratory Science. 2016; 46: 260-5. doi:
288. Wang J, Zhao C, Zhao A, Li M, Ren J, Qu X. New insights in amyloid beta interactions with human telomerase. Journal of the American Chemical Society. 2015; 137: 1213-9. doi:
289. Spilsbury A, Miwa S, Attems J, Saretzki G. The role of telomerase protein TERT in Alzheimer's disease and in tau-related pathology in vitro. Journal of Neuroscience. 2015; 35: 1659-74. doi:
290. Zhu H, Fu W, Mattson MP. The catalytic subunit of telomerase protects neurons against amyloid β-peptide-induced apoptosis. Journal of neurochemistry. 2000; 75: 117-24. doi:
291. Naidoo K, Malindisa ST, Otgaar TC, Bernert M, Dias BDC, Ferreira E, Reusch U, Knackmuss S, Little M, Weiss SF. Knock-Down of the 37kDa/67kDa Laminin Receptor LRP/LR Impedes Telomerase Activity. PLoS One. 2015; 10: e0141618. doi:
292. Jovanovic K, Chetty CJ, Khumalo T, Da Costa Dias B, Ferreira E, Malindisa ST, Caveney R, Letsolo BT, Weiss SF. Novel patented therapeutic approaches targeting the 37/67 kDa laminin receptor for treatment of cancer and Alzheimer's disease. Expert Opin Ther Pat. 2015; 25: 567-82. doi: 10.1517/13543776.2015.1014802.
293. Otgaar TC, Ferreira E, Malindisa S, Bernert M, Letsolo BT, Weiss SFT. 37 kDa LRP::FLAG enhances telomerase activity and reduces senescent markers in vitro. Oncotarget. 2017; 8: 86646-56. doi: 10.18632.

294. Bignoux MJ, Cuttler K, Otgaar TC, Ferreira E, Letsolo BT, Weiss SF. LRP:: FLAG Rescues Cells from Amyloid-β-Mediated Cytotoxicity Through Increased TERT Levels and Telomerase Activity. Journal of Alzheimer's Disease. 2019: 1-13. doi:
295. Tohgo A, Takasawa S, Munakata H, Yonekura H, Hayashi N, Okamoto H. Structural determination and characterization of a 40 kDa protein isolated from rat 40 S ribosomal subunit. FEBS Lett. 1994; 340: 133-8. doi:
296. Rao N, Barsky S, Terranova V, Liotta L. Isolation of a tumor cell laminin receptor. Biochem Biophys Res Commun. 1983; 111: 804-8. doi:
297. Malinoff HL, Wicha MS. Isolation of a cell surface receptor protein for laminin from murine fibrosarcoma cells. The Journal of Cell Biology. 1983; 96: 1475-9. doi:
298. DiGiacomo V, Meruelo D. Looking into laminin receptor: critical discussion regarding the non-integrin 37/67-kDa laminin receptor/RPSA protein. Biological Reviews. 2016; 91: 288-310. doi:
299. Jackers P, Minoletti F, Belotti D, Clausse N, Sozzi G, Sobel ME, Castronovo V. Isolation from a multigene family of the active human gene of the metastasis-associated multifunctional protein 37LRP/p40 at chromosome 3p21. 3. Oncogene. 1996; 13: 495-503. doi:
300. Butò S, Tagliabue E, Ardini E, Magnifico A, Ghirelli C, van den Brûle F, Castronovo V, Colnaghi MI, Sobel ME, Ménard S. Formation of the 67-kDa laminin receptor by acylation of the precursor. Journal of cellular biochemistry. 1998; 69: 244-51. doi:
301. Landowski T, Dratz E, Starkey J. Studies of the structure of the metastasis-associated 67 kDa laminin binding protein: fatty acid acylation and evidence supporting dimerization of the 32 kDa gene product to form the mature protein. Biochemistry. 1995; 34: 11276-87. doi:
302. Hundt C, Peyrin JM, Haïk S, Gauczynski S, Leucht C, Rieger R, Riley ML, Deslys JP, Dormont D, Lasmézas CI. Identification of interaction domains of the prion protein with its 37-kDa/67-kDa laminin receptor. The EMBO journal. 2001; 20: 5876-86. doi:
303. Fujimura Y, Yamada K, Tachibana H. A lipid raft-associated 67 kDa laminin receptor mediates suppressive effect of epigallocatechin-3-O-gallate on FcεRI expression. Biochem Biophys Res Commun. 2005; 336: 674-81. doi:
304. Liotta L, Hand PH, Rao C, Bryant G, Barsky S, Schlom J. Monoclonal antibodies to the human laminin receptor recognize structurally distinct sites. Exp Cell Res. 1985; 156: 117-26. doi:
305. Gauczynski S, Nikles, D., El-Gogo, S., Papy-Garcia, D., Rey, C., Alban, S., Barritault, D., Lasmézas, C.I. and Weiss, S. The 37-kDa/67-kDa laminin receptor acts as a receptor for infectious prions and is inhibited by polysulfated glycanes. Journal of Infectious Diseases. 2006; 194: 702-9. doi:
306. Auth D, Brawerman G. A 33-kDa polypeptide with homology to the laminin receptor: component of translation machinery. Proceedings of the National Academy of Sciences. 1992; 89: 4368-72. doi:
307. Scheiman J, Jamieson K, Ziello J, Tseng J, Meruelo D. Extraribosomal functions associated with the C terminus of the 37/67 kDa laminin receptor are required for maintaining cell viability. Cell Death Dis. 2010; 1: e42. doi:
308. Vania L, Morris G, Otgaar TC, Bignoux MJ, Bernert M, Burns J, Gabathuse A, Singh E, Ferreira E, Weiss SF. Patented therapeutic approaches targeting LRP/LR for cancer treatment. Expert Opin Ther Pat. 2019; 29: 987-1009. doi:
309. Kinoshita K, Kaneda Y, Sato M, Saeki Y, Wataya-Kaneda M, Hoffmann A, Kaneda Y. LBP-p40 binds DNA tightly through associations with histones H2A, H2B, and H4. Biochem Biophys Res Commun. 1998; 253: 277-82. doi:
310. Weiss SF. Bad Boy with a Twist: Targeting the 37 kDa/67 kDa Laminin Receptor for Treatment of Cancer and Neurodegenerative Diseases and for Changing Telomere Dynamics. Cell Cell Life Sci J. 2017; 2: 000114. doi:
311. Mercurio AM. Laminin receptors: achieving specificity through cooperation. Trends in cell biology. 1995; 5: 419-23. doi:

312. Venticinque L, Jamieson KV, Meruelo D. Interactions between laminin receptor and the cytoskeleton during translation and cell motility. PLoS One. 2011; 6: e15895. doi:
313. Yannariello-Brown J, Wewer U, Liotta L, Madri J. Distribution of a 69-kD laminin-binding protein in aortic and microvascular endothelial cells: modulation during cell attachment, spreading, and migration. The Journal of Cell Biology. 1988; 106: 1773-86. doi:
314. Masuda T, Sakuma C, Kobayashi K, Kikuchi K, Soda E, Shiga T, Kobayashi K, Yaginuma H. Laminin peptide YIGSR and its receptor regulate sensory axonal response to the chemoattractive guidance cue in the chick embryo. Journal of neuroscience research. 2009; 87: 353-9. doi:
315. Gundimeda U, McNeill TH, Barseghian BA, Tzeng WS, Rayudu DV, Cadenas E, Gopalakrishna R. Polyphenols from green tea prevent antineuritogenic action of Nogo-A via 67-kD a laminin receptor and hydrogen peroxide. Journal of neurochemistry. 2015; 132: 70-84. doi:
316. Karpatová M, Tagliabue E, Castronovo V, Magnifico A, Ardini E, Morelli D, Belotti D, Colnaghi MI, Ménard S. Shedding of the 67-kD laminin receptor by human cancer cells. Journal of cellular biochemistry. 1996; 60: 226-34. doi:
317. Gauczynski S, Hundt, C., Leucht, C. and Weiss, S. Interaction of prion proteins with cell surface receptors, molecular chaperones, and other molecules. Advances in protein chemistry. 2001; 57: 229-72. doi:
318. Rieger R, Edenhofer F, Lasmézas CI, Weiss S. The human 37-kDa laminin receptor precursor interacts with the prion protein in eukaryotic cells. Nat Med. 1997; 3: 1383-8. doi:
319. Moss BL, Taubner L, Sample YK, Kazmin DA, Copié V, Starkey JR. Tumor shedding of laminin binding protein modulates angiostatin production in vitro and interferes with plasmin-derived inhibition of angiogenesis in aortic ring cultures. International journal of cancer. 2006; 118: 2421-32. doi:
320. Selleri C, Ragno P, Ricci P, Visconte V, Scarpato N, Carriero MV, Rotoli B, Rossi G, Montuori N. The metastasis-associated 67-kDa laminin receptor is involved in G-CSF–induced hematopoietic stem cell mobilization. Blood. 2006; 108: 2476-84. doi:
321. Khusal R, Dias, B.D.C., Moodley, K., Penny, C., Reusch, U., Knackmuss, S., Little, M. and Weiss, S.F. In vitro inhibition of angiogenesis by antibodies directed against the 37kDa/67kDa laminin receptor. PLoS One. 2013; 8: p.e58888. doi: 10.1371/journal.pone.0058888.g001.
322. Kim KJ, Chung JW, Kim KS. 67-kDa laminin receptor promotes internalization of cytotoxic necrotizing factor 1-expressing Escherichia coli K1 into human brain microvascular endothelial cells. Journal of Biological Chemistry. 2005; 280: 1360-8. doi:
323. Orihuela CJ, Mahdavi J, Thornton J, Mann B, Wooldridge KG, Abouseada N, Oldfield NJ, Self T, Ala'Aldeen DA, Tuomanen EI. Laminin receptor initiates bacterial contact with the blood brain barrier in experimental meningitis models. J Clin Invest. 2009; 119: 1638-46. doi:
324. Akache B, Grimm D, Pandey K, Yant SR, Xu H, Kay MA. The 37/67-kilodalton laminin receptor is a receptor for adeno-associated virus serotypes 8, 2, 3, and 9. J Virol. 2006; 80: 9831-6. doi:
325. Tio PH, Jong WW, Cardosa MJ. Two dimensional VOPBA reveals laminin receptor (LAMR1) interaction with dengue virus serotypes 1, 2 and 3. Virology journal. 2005; 2: 25. doi:
326. Ludwig GV, Kondig JP, Smith JF. A putative receptor for Venezuelan equine encephalitis virus from mosquito cells. J Virol. 1996; 70: 5592-9. doi:
327. Bogachek MV, Protopopova EV, Loktev VB, Zaitsev BN, Favre M, Sekatskii SK, Dietler G. Immunochemical and single molecule force spectroscopy studies of specific interaction between the laminin binding protein and the West Nile virus surface glycoprotein E domain II. Journal of Molecular Recognition: An Interdisciplinary Journal. 2008; 21: 55-62. doi:
328. Gauczynski S, Peyrin, J.M., Haïk, S., Leucht, C., Hundt, C., Rieger, R., Krasemann, S., Deslys, J.P., Dormont, D., Lasmézas, C.I. and Weiss, S. The 37-kDa/67-kDa laminin receptor acts as the cell-surface receptor for the cellular prion protein. The EMBO journal. 2001; 20: 5863-75. doi:

329. Da Costa Dias B, Jovanovic K, Gonsalves D, Moodley K, Reusch U, Knackmuss S, Weinberg MS, Little M, Weiss SF. The 37kDa/67kDa laminin receptor acts as a receptor for Abeta42 internalization. Sci Rep. 2014; 4: 5556. doi: 10.1038/srep05556.
330. Da Costa Dias B, Jovanovic K, Gonsalves D, Moodley K, Reusch U, Knackmuss S, Penny C, Weinberg MS, Little M, Weiss SF. Anti-LRP/LR specific antibody IgG1-iS18 and knock-down of LRP/LR by shRNAs rescue cells from Abeta42 induced cytotoxicity. Sci Rep. 2013; 3: 2702. doi: 10.1038/srep02702.
331. Jovanovic K, Loos B, Da Costa Dias B, Penny C, Weiss SF. High resolution imaging study of interactions between the 37 kDa/67 kDa laminin receptor and APP, beta-secretase and gamma-secretase in Alzheimer's disease. PLoS One. 2014; 9: e100373. doi: 10.1371/journal.pone.0100373.
332. Jovanovic K, Gonsalves D, Da Costa Dias B, Moodley K, Reusch U, Knackmuss S, Penny C, Weinberg MS, Little M, Weiss SF. Anti-LRP/LR specific antibodies and shRNAs impede amyloid beta shedding in Alzheimer's disease. Sci Rep. 2013; 3: 2699. doi: 10.1038/srep02699.
333. Da Costa Dias B, Jovanovic K, Gonsalves D, Weiss SF. Structural and mechanistic commonalities of amyloid-β and the prion protein. Prion. 2011; 5: 126-37. doi:
334. Brown SS, Malinoff HL, Wicha MS. Connectin: cell surface protein that binds both laminin and actin. Proceedings of the National Academy of Sciences. 1983; 80: 5927-30. doi:
335. Keppel E, Schaller H. A 33 kDa protein with sequence homology to the ‘laminin binding protein’is associated with the cytoskeleton in hydra and in mammalian cells. J Cell Sci. 1991; 100: 789-97. doi:
336. Balasubramanian S, Zheng D, Liu Y-J, Fang G, Frankish A, Carriero N, Robilotto R, Cayting P, Gerstein M. Comparative analysis of processed ribosomal protein pseudogenes in four mammalian genomes. Genome biology. 2009; 10: R2. doi:
337. Ben-Shem A, de Loubresse NG, Melnikov S, Jenner L, Yusupova G, Yusupov M. The structure of the eukaryotic ribosome at 3.0 Å resolution. Science. 2011; 334: 1524-9. doi:
338. O’Donohue M-F, Choesmel V, Faubladier M, Fichant G, Gleizes P-E. Functional dichotomy of ribosomal proteins during the synthesis of mammalian 40S ribosomal subunits. The Journal of Cell Biology. 2010; 190: 853-66. doi:
339. Malygin AA, Babaylova ES, Loktev VB, Karpova GG. A region in the C-terminal domain of ribosomal protein SA required for binding of SA to the human 40S ribosomal subunit. Biochimie. 2011; 93: 612-7. doi:
340. Sato M, Saeki Y, Tanaka K, Kaneda Y. Ribosome-associated protein LBP/p40 binds to S21 protein of 40S ribosome: analysis using a yeast two-hybrid system. Biochem Biophys Res Commun. 1999; 256: 385-90. doi:
341. Sato M, Kong CJ, Yoshida H, Nakamura T, Wada A, Shimoda C, Kaneda Y. Ribosomal proteins S0 and S21 are involved in the stability of 18S rRNA in fission yeast, Schizosaccharomyces pombe. Biochem Biophys Res Commun. 2003; 311: 942-7. doi:
342. Salama RH, Muramatsu H, Zou K, Inui T, Kimura T, Muramatsu T. Midkine binds to 37-kDa laminin binding protein precursor, leading to nuclear transport of the complex. Exp Cell Res. 2001; 270: 13-20. doi:
343. Hara K, Satoh K, Ide H. Apical ectodermal ridge-dependent expression of the chick 67 kDa laminin binding protein gene (cLbp) in developing limb bud. Zoological science. 1997; 14: 969-79. doi:
344. Asano Y, Takashima S, Asakura M, Shintani Y, Liao Y, Minamino T, Asanuma H, Sanada S, Kim J, Ogai A. Lamr1 functional retroposon causes right ventricular dysplasia in mice. Nat Genet. 2004; 36: 123. doi:
345. Bolze A, Mahlaoui N, Byun M, Turner B, Trede N, Ellis SR, Abhyankar A, Itan Y, Patin E, Brebner S. Ribosomal protein SA haploinsufficiency in humans with isolated congenital asplenia. Science. 2013; 340: 976-8. doi:

346. Rao M, Manishen WJ, Maheshwari Y, Sykes DE, Siyanova EY, Tyner AL, Weiser MM. Laminin receptor expression in rat intestine and liver during development and differentiation. Gastroenterology. 1994; 107: 764-72. doi:
347. Weeks BS, Kopp JB, Horikoshi S, Cannon FB, Garrett M, Kleinman HK, Klotman PE. Adult and fetal human mesangial cells interact with specific laminin domains. American Journal of Physiology-Renal Physiology. 1991; 261: F688-F95. doi:
348. Laurie G, Horikoshi S, Killen P, Segui-Real B, Yamada Y. In situ hybridization reveals temporal and spatial changes in cellular expression of mRNA for a laminin receptor, laminin, and basement membrane (type IV) collagen in the developing kidney. The Journal of Cell Biology. 1989; 109: 1351-62. doi:
349. Laurie GW, Stone CM, Yamada Y. Elevated 32-kDa LBP and low laminin mRNA expression in developing mouse cerebrum. Differentiation. 1991; 46: 173-9. doi:
350. Wenzel S, Henning K, Habbig A, Forst S, Schreckenberg R, Heger J, Maxeiner H, Schlüter K-D. TGF-β1 improves cardiac performance via up-regulation of laminin receptor 37/67 in adult ventricular cardiomyocytes. Basic research in cardiology. 2010; 105: 621-9. doi:
351. Clausse N, van den Brûle F, Delvenne P, Jacobs N, Franzen-Detrooz E, Jackers P, Castronovo V. TNF-α and IFN-γ down-regulate the expression of the metastasis-associated bi-functional 37LRP/p40 gene and protein in transformed keratinocytes. Biochem Biophys Res Commun. 1998; 251: 564-9. doi:
352. Sun L, Liu L, Liu X, Wang Y, Li M, Yao L, Yang J, Ji G, Guo C, Pan Y. MGr1-Ag/37LRP induces cell adhesion-mediated drug resistance through FAK/PI3K and MAPK pathway in gastric cancer. Cancer science. 2014; 105: 651-9. doi:
353. Chen J, Cárcamo JM, Bórquez-Ojeda O, Erdjument-Bromage H, Tempst P, Golde DW. The laminin receptor modulates granulocyte–macrophage colony-stimulating factor receptor complex formation and modulates its signaling. Proceedings of the National Academy of Sciences. 2003; 100: 14000-5. doi:
354. Ando K, Miyazaki Y, Sawayama Y, Tominaga S, Matsuo E, Yamasaki R, Inoue Y, Iwanaga M, Imanishi D, Tsushima H. High expression of 67-kDa laminin receptor relates to the proliferation of leukemia cells and increases expression of GM-CSF receptor. Experimental hematology. 2011; 39: 179-86. e4. doi:
355. Ku HC, Liu HS, Hung PF, Chen CL, Liu HC, Chang HH, Tsuei YW, Shih LJ, Lin CL, Lin CM. Green tea (–)-epigallocatechin gallate inhibits IGF-I and IGF-II stimulation of 3T3-L 1 preadipocyte mitogenesis via the 67-k D a laminin receptor, but not AMP-activated protein kinase pathway. Molecular nutrition & food research. 2012; 56: 580-92. doi:
356. Givant-Horwitz V, Davidson B, Reich R. Laminin-induced signaling in tumor cells: the role of the Mr 67,000 laminin receptor. Cancer Res. 2004; 64: 3572-9. doi:
357. Duan S-G, Cheng L, Li D-J, Zhu J, Xiong Y, Li X-W, Wang S-G. The role of MAPK-ERK pathway in 67-kDa laminin receptor-induced FasL expression in human cholangiocarcinoma cells. Digestive diseases and sciences. 2010; 55: 2844-52. doi:
358. Givant-Horwitz V, Davidson B, Reich R. Laminin-induced signaling in tumor cells. Cancer letters. 2005; 223: 1-10. doi:
359. Wang K-S, Kuhn RJ, Strauss EG, Ou S, Strauss JH. High-affinity laminin receptor is a receptor for Sindbis virus in mammalian cells. J Virol. 1992; 66: 4992-5001. doi:
360. Chung JW, Hong SJ, Kim KJ, Goti D, Stins MF, Shin S, Dawson VL, Dawson TM, Kim KS. 37-kDa laminin receptor precursor modulates cytotoxic necrotizing factor 1–mediated RhoA activation and bacterial uptake. Journal of Biological Chemistry. 2003; 278: 16857-62. doi:
361. Huang S-H, Jong A. Evolving role of laminin receptors in microbial pathogenesis and therapeutics of CNS infection. Future microbiology. 2009; 4: 959-62. doi:

362. Morel E, Andrieu T, Casagrande F, Gauczynski S, Weiss S, Grassi J, Rousset M, Dormont D, Chambaz J. Bovine prion is endocytosed by human enterocytes via the 37 kDa/67 kDa laminin receptor. The American journal of pathology. 2005; 167: 1033-42. doi:
363. Leucht C, Simoneau S, Rey C, Vana K, Rieger R, Lasmezas CI, Weiss S. The 37 kDa/67 kDa laminin receptor is required for PrP(Sc) propagation in scrapie-infected neuronal cells. EMBO Rep. 2003; 4: 290-5. doi: 10.1038/sj.embor.embor768.
364. Rieger R, Lasmezas C, Weiss S. Role of the 37 kDa laminin receptor precursor in the life cycle of prions. Transfusion clinique et biologique. 1999; 6: 7-16. doi:
365. Campana V, Sarnataro D, Zurzolo C. The highways and byways of prion protein trafficking. Trends in cell biology. 2005; 15: 102-11. doi:
366. Zuber C, Mitteregger G, Pace C, Zerr I, Kretzschmar HA, Weiss S. Anti-LRP/LR antibody W3 hampers peripheral PrPSc propagation in scrapie infected mice. Prion. 2007; 1: 207-12. doi:
367. Simoneau S, Haïk S, Leucht C, Dormont D, Deslys J-P, Weiss S, Lasmézas C. Different isoforms of the non-integrin laminin receptor are present in mouse brain and bind PrP. Biological chemistry. 2003; 384: 243-6. doi:
368. Kolodziejczak D, Dias BDC, Zuber C, Jovanovic K, Omar A, Beck J, Vana K, Mbazima V, Richt J, Brenig B. Prion interaction with the 37-kDa/67-kDa laminin receptor on enterocytes as a cellular model for intestinal uptake of prions. J Mol Biol. 2010; 402: 293-300. doi:
369. Zuber C, Knackmuss S, Zemora G, Reusch U, Vlasova E, Diehl D, Mick V, Hoffmann K, Nikles D, Frohlich T, Arnold GJ, Brenig B, Wolf E, et al. Invasion of tumorigenic HT1080 cells is impeded by blocking or downregulating the 37-kDa/67-kDa laminin receptor. J Mol Biol. 2008; 378: 530-9. doi: 10.1016/j.jmb.2008.02.004.
370. Zuber C, Ludewigs H, Weiss S. Therapeutic approaches targeting the prion receptor LRP/LR. Vet Microbiol. 2007; 123: 387-93. doi: 10.1016/j.vetmic.2007.04.005.
371. Pinnock EC, Jovanovic K, Pinto MG, Ferreira E, Dias BDC, Penny C, Knackmuss S, Reusch U, Little M, Schatzl HM. LRP/LR Antibody Mediated Rescuing of Amyloid-β-Induced Cytotoxicity is Dependent on PrPc in Alzheimer's Disease. Journal of Alzheimer's Disease. 2016; 49: 645-57. doi:
372. Bartzokis G. Alzheimer's disease as homeostatic responses to age-related myelin breakdown. Neurobiology of aging. 2011; 32: 1341-71. doi:
373. Marchesi VT. Alzheimer's dementia begins as a disease of small blood vessels, damaged by oxidative-induced inflammation and dysregulated amyloid metabolism: implications for early detection and therapy. The FASEB Journal. 2011; 25: 5-13. doi:
374. Ferreira E, Bignoux MJ, Otgaar TC, Tagliatti N, Jovanovic K, Letsolo BT, Weiss SF. LRP/LR specific antibody IgG1-iS18 impedes neurodegeneration in Alzheimer's disease mice. Oncotarget. 2018; 9: 27059. doi:
375. Chetty C, Khumalo T, Da Costa Dias B, Reusch U, Knackmuss S, Little M, Weiss SF. Anti-LRP/LR specific antibody IgG1-iS18 impedes adhesion and invasion of liver cancer cells. PLoS One. 2014; 9: e96268. doi: 10.1371/journal.pone.0096268.
376. Vania L, Chetty CJ, Ferreira E, Weiss SF. anti-LRP/LR–Specific antibody igG1-iS18 Significantly impedes adhesion and invasion in Early-and Late-Stage Colorectal Carcinoma Cells. Molecular Medicine. 2016; 22: 664. doi:
377. Rebelo TM, Chetty CJ, Ferreira E, Weiss SF. Anti-LRP/LR-specific antibody IgG1-iS18 impedes adhesion and invasion of pancreatic cancer and neuroblastoma cells. BMC cancer. 2016; 16: 917. doi:
378. Khumalo T, Reusch, U., Knackmuss, S., Little, M., Veale, R.B. and Weiss, S.F. Adhesion and invasion of breast and oesophageal cancer cells are impeded by anti-LRP/LR-specific antibody IgG1-iS18. PLoS One. 2013; 8: p.e66297. doi: 10.1371/journal.pone.0066297.g001.
379. Munien C, Rebelo TM, Ferreira E, Weiss SF. IgG1-iS18 impedes the adhesive and invasive potential of early and late stage malignant melanoma cells. Exp Cell Res. 2017; 351: 135-41. doi:

380. Omar A, Reusch U, Knackmuss S, Little M, Weiss SF. Anti-LRP/LR-specific antibody IgG1-iS18 significantly reduces adhesion and invasion of metastatic lung, cervix, colon and prostate cancer cells. J Mol Biol. 2012; 419: 102-9. doi: 10.1016/j.jmb.2012.02.035.
381. Rebelo TM, Vania L, Ferreira E, Weiss SF. siRNA-mediated LRP/LR knock-down reduces cellular viability of malignant melanoma cells through the activation of apoptotic caspases. Exp Cell Res. 2018; 368: 1-12. doi:
382. Vania L, Rebelo TM, Ferreira E, Weiss SF. Knockdown of LRP/LR induces apoptosis in early and late stage colorectal carcinoma cells through caspase activation. In preparation. 2017. doi:
383. Khumalo T, Ferreira E, Jovanovic K, Veale RB, Weiss SF. Knockdown of LRP/LR induces apoptosis in breast and oesophageal cancer cells. PLoS One. 2015; 10: e0139584. doi:
384. Chetty CJ, Ferreira E, Jovanovic K, Weiss SF. Knockdown of LRP/LR induces apoptosis in pancreatic cancer and neuroblastoma cells through activation of caspases. Exp Cell Res. 2017. doi:
385. Moodley K, Weiss SF. Downregulation of the non-integrin laminin receptor reduces cellular viability by inducing apoptosis in lung and cervical cancer cells. PLoS One. 2013; 8: e57409. doi:
386. Vana K, Weiss S. A trans-dominant negative 37kDa/67kDa laminin receptor mutant impairs PrP(Sc) propagation in scrapie-infected neuronal cells. J Mol Biol. 2006; 358: 57-66. doi: 10.1016/j.jmb.2006.02.011.
387. Lee BY, Han JA, Im JS, Morrone A, Johung K, Goodwin EC, Kleijer WJ, DiMaio D, Hwang ES. Senescence-associated β-galactosidase is lysosomal β-galactosidase. Aging cell. 2006; 5: 187-95. doi:
388. Cawthon RM. Telomere measurement by quantitative PCR. Nucleic Acids Res. 2002; 30: e47-e. doi:
389. Tripathy SK, Svensson EC, Black HB, Goldwasser E, Margalith M, Hobart PM, Leiden JM. Long-term expression of erythropoietin in the systemic circulation of mice after intramuscular injection of a plasmid DNA vector. Proceedings of the National Academy of Sciences. 1996; 93: 10876-80. doi:
390. Nada M-B, Fuss J, Trusel M, Galsworthy MJ, Bobsin K, Colacicco G, Deacon RM, Riva MA, Kellendonk C, Sprengel R. The puzzle box as a simple and efficient behavioral test for exploring impairments of general cognition and executive functions in mouse models of schizophrenia. Experimental neurology. 2011; 227: 42-52. doi:
391. Min Z, Wang S, Wu J, Zhang S. Impairment of nesting behavior in APPswe/PS1dE9 mice. Life Sci J. 2013; 10. doi:
392. Xiong X-D, Xiong W-D, Xiong S-S, Chen G-H. Age-and Gender-Based Differences in Nest-Building Behavior and Learning and Memory Performance Measured Using a Radial Six-Armed Water Maze in C57BL/6 Mice. Behavioural neurology. 2018; 2018. doi:
393. Luong TN, Carlisle HJ, Southwell A, Patterson PH. Assessment of motor balance and coordination in mice using the balance beam. Journal of visualized experiments: JoVE. 2011. doi:
394. Lagouge M, Argmann C, Gerhart-Hines Z, Meziane H, Lerin C, Daussin F, Messadeq N, Milne J, Lambert P, Elliott P. Resveratrol improves mitochondrial function and protects against metabolic disease by activating SIRT1 and PGC-1α. Cell. 2006; 127: 1109-22. doi:
395. Kurz DJ, Decary S, Hong Y, Erusalimsky JD. Senescence-associated (beta)-galactosidase reflects an increase in lysosomal mass during replicative ageing of human endothelial cells. J Cell Sci. 2000; 113: 3613-22. doi:
396. Pospelova TV, Demidenko ZN, Bukreeva EI, Pospelov VA, Gudkov AV, Blagosklonny MV. Pseudo-DNA damage response in senescent cells. Cell cycle. 2009; 8: 4112-8. doi:
397. Bahmani B, Amiri F, Roushandeh AM, Bahadori M, Harati MD, Roudkenar MH. The Lcn2-engineered HEK-293 cells show senescence under stressful condition. Iranian journal of basic medical sciences. 2015; 18: 459. doi:

398. Ryu S, Kawamura R, Naka R, Silberberg YR, Nakamura N, Nakamura C. Nanoneedle insertion into the cell nucleus does not induce double-strand breaks in chromosomal DNA. Journal of bioscience and bioengineering. 2013; 116: 391-6. doi:
399. Behnisch T, Li D, Jing D, Liu Z, Chen Y, Huang F. Enhanced expression of secreted α-Klotho in the hippocampus alters nesting behaviour and memory formation in mice. Frontiers in cellular neuroscience. 2019; 13: 133. doi:
400. Frick KM, Fernandez SM. Enrichment enhances spatial memory and increases synaptophysin levels in aged female mice. Neurobiology of aging. 2003; 24: 615-26. doi:
401. Ogawara Y, Kishishita S, Obata T, Isazawa Y, Suzuki T, Tanaka K, Masuyama N, Gotoh Y. Akt enhances Mdm2-mediated ubiquitination and degradation of p53. Journal of Biological Chemistry. 2002; 277: 21843-50. doi:
402. Wu X, Bayle JH, Olson D, Levine AJ. The p53-mdm-2 autoregulatory feedback loop. Genes Dev. 1993; 7: 1126-32. doi:
403. Haupt Y, Maya R, Kazaz A, Oren M. Mdm2 promotes the rapid degradation of p53. Nature. 1997; 387: 296-9. doi:
404. Wu D, Prives C. Relevance of the p53–MDM2 axis to aging. Cell Death & Differentiation. 2018; 25: 169-79. doi:
405. García-Cao I, García-Cao M, Tomás-Loba A, Martin-Caballero J, Flores JM, Klatt P, Blasco MA, Serrano M. Increased p53 activity does not accelerate telomere-driven ageing. EMBO Rep. 2006; 7: 546-52. doi:
406. Baker DJ, Childs BG, Durik M, Wijers ME, Sieben CJ, Zhong J, Saltness RA, Jeganathan KB, Verzosa GC, Pezeshki A. Naturally occurring p16 Ink4a-positive cells shorten healthy lifespan. Nature. 2016; 530: 184-9. doi:
407. Koltai E, Szabo Z, Atalay M, Boldogh I, Naito H, Goto S, Nyakas C, Radak Z. Exercise alters SIRT1, SIRT6, NAD and NAMPT levels in skeletal muscle of aged rats. Mech Ageing Dev. 2010; 131: 21-8. doi:
408. Zhu Y, Tchkonia T, Pirtskhalava T, Gower AC, Ding H, Giorgadze N, Palmer AK, Ikeno Y, Hubbard GB, Lenburg M. The Achilles' heel of senescent cells: from transcriptome to senolytic drugs. Aging cell. 2015; 14: 644-58. doi:
409. Chen T-H, Kuro-o M, Chen C-H, Sue Y-M, Chen Y-C, Wu H-H, Cheng C-Y. The secreted Klotho protein restores phosphate retention and suppresses accelerated aging in Klotho mutant mice. European journal of pharmacology. 2013; 698: 67-73. doi:
410. Herrera E, Samper E, Martín-Caballero J, Flores JM, Lee HW, Blasco MA. Disease states associated with telomerase deficiency appear earlier in mice with short telomeres. The EMBO journal. 1999; 18: 2950-60. doi:
411. Harley CB, Liu W, Blasco M, Vera E, Andrews WH, Briggs LA, Raffaele JM. A natural product telomerase activator as part of a health maintenance program. Rejuvenation research. 2011; 14: 45-56. doi:
412. Wang J, Xie LY, Allan S, Beach D, Hannon GJ. Myc activates telomerase. Genes Dev. 1998; 12: 1769-74. doi:
413. Teichroeb JH, Kim J, Betts DH. The role of telomeres and telomerase reverse transcriptase isoforms in pluripotency induction and maintenance. RNA biology. 2016; 13: 707-19. doi:
414. Langlade-Demoyen P, Pons FG, Adotevi O, Cardinaud S, Neuveut C, Kosmatopoulos K, Graff-Dubois S, Menez-Jamet J. (2011). Polynucleotides encoding MHC class I-restricted htert epitopes, analogues thereof or polyepitopes. Google Patents).
415. McSharry B, Jones C, Skinner J, Kipling D, Wilkinson G. Human telomerase reverse transcriptase-immortalized MRC-5 and HCA2 human fibroblasts are fully permissive for human cytomegalovirus. Journal of General Virology. 2001; 82: 855-63. doi:

416. Counter CM, Meyerson M, Eaton EN, Ellisen LW, Caddle SD, Haber DA, Weinberg RA. Telomerase activity is restored in human cells by ectopic expression of hTERT (hEST2), the catalytic subunit of telomerase. Oncogene. 1998; 16: 1217-22. doi:
417. Sikora E. Rejuvenation of senescent cells—The road to postponing human aging and age-related disease? Exp Gerontol. 2013; 48: 661-6. doi:
418. Sato M, Kinoshita K, Kaneda Y, Saeki Y, Iwamatsu A, Tanaka K, Kaneda Y. Analysis of nuclear localization of laminin binding protein precursor p40 (LBP/p40). Biochem Biophys Res Commun. 1996; 229: 896-901. doi:
419. Seiberg M. Age-induced hair greying–the multiple effects of oxidative stress. International journal of cosmetic science. 2013; 35: 532-8. doi:
420. Wong K-K, Maser RS, Bachoo RM, Menon J, Carrasco DR, Gu Y, Alt FW, DePinho RA. Telomere dysfunction and Atm deficiency compromises organ homeostasis and accelerates ageing. Nature. 2003; 421: 643-8. doi:
421. Jurk D, Wilson C, Passos JF, Oakley F, Correia-Melo C, Greaves L, Saretzki G, Fox C, Lawless C, Anderson R. Chronic inflammation induces telomere dysfunction and accelerates ageing in mice. Nature communications. 2014; 5: 4172. doi:
422. Endou M, Aoki H, Kobayashi T, Kunisada T. Prevention of hair graying by factors that promote the growth and differentiation of melanocytes. The Journal of dermatology. 2014; 41: 716-23. doi:
423. Yang L, Zhang J, Zheng K, Shen H, Chen X. Long-term ginsenoside Rg1 supplementation improves age-related cognitive decline by promoting synaptic plasticity associated protein expression in C57BL/6J mice. Journals of Gerontology Series A: Biomedical Sciences and Medical Sciences. 2014; 69: 282-94. doi:
424. Tams GE, Tejiri AS, Owolagba G, Ujah W. Evaluation of the neurobehavioural and Histo-architecture changes of the hippocampus and pancreas of the streptozotocin-induced diabetic male wistar rats responding to Z. Officinale extract. doi:
425. Miwa S, Czapiewski R, Wan T, Bell A, Hill KN, von Zglinicki T, Saretzki G. Decreased mTOR signalling reduces mitochondrial ROS in brain via accumulation of the telomerase protein TERT within mitochondria. Aging (Albany NY). 2016; 8: 2551. doi:
426. Dinel A-L, Andre C, Aubert A, Ferreira G, Laye S, Castanon N. Cognitive and emotional alterations are related to hippocampal inflammation in a mouse model of metabolic syndrome. PLoS One. 2011; 6. doi:
427. Tung VW, Burton TJ, Quail SL, Mathews MA, Camp AJ. Motor performance is impaired following vestibular stimulation in ageing mice. Frontiers in aging neuroscience. 2016; 8: 12. doi:
428. Rosenthal MJ, Morley JE, Flood JF, Scarpace PJ. Relationship between behavioral and motor responses of mature and old mice and cerebellar beta-adrenergic receptor density. Mech Ageing Dev. 1988; 45: 231-7. doi:
429. Justice JN, Carter CS, Beck HJ, Gioscia-Ryan RA, McQueen M, Enoka RM, Seals DR. Battery of behavioral tests in mice that models age-associated changes in human motor function. Age. 2014; 36: 583-95. doi:
430. Justice JN, Gioscia-Ryan RA, Johnson LC, Battson ML, de Picciotto NE, Beck HJ, Jiang H, Sindler AL, Bryan NS, Enoka RM. Sodium nitrite supplementation improves motor function and skeletal muscle inflammatory profile in old male mice. Journal of applied physiology. 2015; 118: 163-9. doi:
431. Fulle S, Protasi F, Di Tano G, Pietrangelo T, Beltramin A, Boncompagni S, Vecchiet L, Fanò G. The contribution of reactive oxygen species to sarcopenia and muscle ageing. Exp Gerontol. 2004; 39: 17-24. doi:
432. Rygiel KA, Picard M, Turnbull DM. The ageing neuromuscular system and sarcopenia: a mitochondrial perspective. The Journal of physiology. 2016; 594: 4499-512. doi:

433. Wagatsuma A, Shiozuka M, Takayama Y, Hoshino T, Mabuchi K, Matsuda R. Effects of ageing on expression of the muscle-specific E3 ubiquitin ligases and Akt-dependent regulation of Foxo transcription factors in skeletal muscle. Molecular and cellular biochemistry. 2016; 412: 59-72. doi:
434. Marlatt MW, Potter MC, Lucassen PJ, van Praag H. Running throughout middle-age improves memory function, hippocampal neurogenesis, and BDNF levels in female C57BL/6J mice. Developmental neurobiology. 2012; 72: 943-52. doi:
435. Zheng F, Plati AR, Potier M, Schulman Y, Berho M, Banerjee A, Leclercq B, Zisman A, Striker LJ, Striker GE. Resistance to glomerulosclerosis in B6 mice disappears after menopause. The American journal of pathology. 2003; 162: 1339-48. doi:
436. Lichtig C, Levy J, Gershon D, Reznick AZ. Effect of aging and exercise on the kidney. Gerontology. 1987; 33: 40-8. doi:
437. Yumura W, Sugino N, Nagasawa R, Kubo S, Hirokawa K, Maruyama N. Age-associated changes in renal glomeruli of mice. Exp Gerontol. 1989; 24: 237-49. doi:
438. Brack AS, Conboy MJ, Roy S, Lee M, Kuo CJ, Keller C, Rando TA. Increased Wnt signaling during aging alters muscle stem cell fate and increases fibrosis. Science. 2007; 317: 807-10. doi:
439. Yang H-C, Fogo AB. Fibrosis and renal aging. Kidney international supplements. 2014; 4: 75-8. doi:
440. Liu H, Fergusson MM, Castilho RM, Liu J, Cao L, Chen J, Malide D, Rovira II, Schimel D, Kuo CJ. Augmented Wnt signaling in a mammalian model of accelerated aging. Science. 2007; 317: 803-6. doi:
441. Torres P-U, Prie D, Molina-Bletry V, Beck L, Silve C, Friedlander G. Klotho: an antiaging protein involved in mineral and vitamin D metabolism. Kidney international. 2007; 71: 730-7. doi:
442. German DC, Khobahy I, Pastor J, Kuro-o M, Liu X. Nuclear localization of Klotho in brain: an anti-aging protein. Neurobiology of aging. 2012; 33: 1483. e25-. e30. doi:
443. Shkreli M, Sarin KY, Pech MF, Papeta N, Chang W, Brockman SA, Cheung P, Lee E, Kuhnert F, Olson JL. Reversible cell-cycle entry in adult kidney podocytes through regulated control of telomerase and Wnt signaling. Nat Med. 2012; 18: 111. doi:
444. Nalapareddy K, Jiang H, Gutierrez LMG, Rudolph KL. Determining the influence of telomere dysfunction and DNA damage on stem and progenitor cell aging–what markers can we use? Exp Gerontol. 2008; 43: 998-1004. doi:
445. Kim NH, Kim HS, Kim N-G, Lee I, Choi H-S, Li X-Y, Kang SE, Cha SY, Ryu JK, Na JM. p53 and microRNA-34 are suppressors of canonical Wnt signaling. Science signaling. 2011; 4: ra71-ra. doi:
446. Ruderman NB, Julia Xu X, Nelson L, Cacicedo JM, Saha AK, Lan F, Ido Y. AMPK and SIRT1: a long-standing partnership? American Journal of Physiology-Endocrinology and Metabolism. 2010; 298: E751-E60. doi:
447. Lim JH, Kim EN, Kim MY, Chung S, Shin SJ, Kim HW, Yang CW, Kim Y-S, Chang YS, Park CW. Age-associated molecular changes in the kidney in aged mice. Oxidative medicine and cellular longevity. 2012; 2012. doi:
448. Wu M, Wang B, Fei J, Santanam N, Blough ER. Important roles of Akt/PKB signaling in the aging process. Front Biosci (Schol Ed). 2010; 2: 1169-88. doi:
449. Chen WS, Xu P-Z, Gottlob K, Chen M-L, Sokol K, Shiyanova T, Roninson I, Weng W, Suzuki R, Tobe K. Growth retardation and increased apoptosis in mice with homozygous disruption of the Akt1 gene. Genes Dev. 2001; 15: 2203-8. doi:
450. Altomare DA, Guo K, Cheng JQ, Sonoda G, Walsh K, Testa JR. Cloning, chromosomal localization and expression analysis of the mouse Akt2 oncogene. Oncogene. 1995; 11: 1055-60. doi:
451. Easton RM, Cho H, Roovers K, Shineman DW, Mizrahi M, Forman MS, Lee VM-Y, Szabolcs M, de Jong R, Oltersdorf T. Role for Akt3/protein kinase Bγ in attainment of normal brain size. Mol Cell Biol. 2005; 25: 1869-78. doi:

452. Cho H, Mu J, Kim JK, Thorvaldsen JL, Chu Q, Crenshaw EB, Kaestner KH, Bartolomei MS, Shulman GI, Birnbaum MJ. Insulin resistance and a diabetes mellitus-like syndrome in mice lacking the protein kinase Akt2 (PKBβ). Science. 2001; 292: 1728-31. doi:
453. Stitt TN, Drujan D, Clarke BA, Panaro F, Timofeyva Y, Kline WO, Gonzalez M, Yancopoulos GD, Glass DJ. The IGF-1/PI3K/Akt pathway prevents expression of muscle atrophy-induced ubiquitin ligases by inhibiting FOXO transcription factors. Molecular cell. 2004; 14: 395-403. doi:
454. Cao JJ, Kurimoto P, Boudignon B, Rosen C, Lima F, Halloran BP. Aging impairs IGF-I receptor activation and induces skeletal resistance to IGF-I. Journal of Bone and Mineral Research. 2007; 22: 1271-9. doi:
455. Pérez-Rivero G, Ruiz-Torres MP, Rivas-Elena JV, Jerkic M, Díez-Marques ML, Lopez-Novoa JM, Blasco MA, Rodríguez-Puyol D. CLINICAL PERSPECTIVE. Circulation. 2006; 114: 309-17. doi:
456. Plunkett FJ, Franzese O, Finney HM, Fletcher JM, Belaramani LL, Salmon M, Dokal I, Webster D, Lawson AD, Akbar AN. The loss of telomerase activity in highly differentiated CD8+ CD28− CD27− T cells is associated with decreased Akt (Ser473) phosphorylation. The Journal of Immunology. 2007; 178: 7710-9. doi:
457. Sedding DG. FoxO transcription factors in oxidative stress response and ageing–a new fork on the way to longevity? Biological chemistry. 2008; 389: 279-83. doi:
458. Kim DH, Kim JY, Yu BP, Chung HY. The activation of NF-κB through Akt-induced FOXO1 phosphorylation during aging and its modulation by calorie restriction. Biogerontology. 2008; 9: 33-47. doi:
459. Tan P, Wang Y-J, Li S, Wang Y, He J-Y, Chen Y-Y, Deng H-Q, Huang W, Zhan J-K, Liu Y-S. The PI3K/Akt/mTOR pathway regulates the replicative senescence of human VSMCs. Molecular and cellular biochemistry. 2016; 422: 1-10. doi:
460. Wu M, Katta A, Gadde MK, Liu H, Kakarla SK, Fannin J, Paturi S, Arvapalli RK, Rice KM, Wang Y. Aging-associated dysfunction of Akt/protein kinase B: S-nitrosylation and acetaminophen intervention. PLoS One. 2009; 4. doi:
461. Hua Y, Zhang Y, Ceylan-Isik AF, Wold LE, Nunn JM, Ren J. Chronic Akt activation accentuates aging-induced cardiac hypertrophy and myocardial contractile dysfunction: role of autophagy. Basic research in cardiology. 2011; 106: 1173-91. doi:
462. Jackson TC, Rani A, Kumar A, Foster TC. Regional hippocampal differences in AKT survival signaling across the lifespan: implications for CA1 vulnerability with aging. Cell Death & Differentiation. 2009; 16: 439-48. doi:
463. Hands SL, Proud CG, Wyttenbach A. mTOR's role in ageing: protein synthesis or autophagy? Aging. 2009; 1: 586. doi:
464. Xia L, Wang X, Hu X, Guo X, Shang Y, Chen H, Zeng C, Zhang F, Chen J. Resveratrol reduces endothelial progenitor cells senescence through augmentation of telomerase activity by Akt-dependent mechanisms. British journal of pharmacology. 2008; 155: 387-94. doi:
465. Méndez-Pertuz M, Martínez P, Blanco-Aparicio C, Gómez-Casero E, García AB, Martínez-Torrecuadrada J, Palafox M, Cortés J, Serra V, Pastor J. Modulation of telomere protection by the PI3K/AKT pathway. Nature communications. 2017; 8: 1-17. doi:
466. Wu C-H, Van Riggelen J, Yetil A, Fan AC, Bachireddy P, Felsher DW. Cellular senescence is an important mechanism of tumor regression upon c-Myc inactivation. Proceedings of the National Academy of Sciences. 2007; 104: 13028-33. doi:
467. Li P, Guo X, Lei P, Shi S, Luo S, Cheng X. PI3K/Akt/uncoupling protein 2 signaling pathway may be involved in cell senescence and apoptosis induced by angiotensin II in human vascular endothelial cells. Molecular biology reports. 2014; 41: 6931-7. doi:

468. Domínguez-Cáceres MA, García-Martínez JM, Calcabrini A, Gonzalez L, Porque PG, Leon J, Martín-Pérez J. Prolactin induces c-Myc expression and cell survival through activation of Src/Akt pathway in lymphoid cells. Oncogene. 2004; 23: 7378-90. doi:
469. Pelengaris S, Khan M, Evan G. c-MYC: more than just a matter of life and death. Nature Reviews Cancer. 2002; 2: 764-76. doi:
470. Zhuang D, Mannava S, Grachtchouk V, Tang W, Patil S, Wawrzyniak J, Berman A, Giordano T, Prochownik E, Soengas M. C-MYC overexpression is required for continuous suppression of oncogene-induced senescence in melanoma cells. Oncogene. 2008; 27: 6623-34. doi:
471. Guney I, Sedivy JM. Cellular senescence, epigenetic switches and c-Myc. Cell cycle. 2006; 5: 2319-23. doi:
472. Guney I, Wu S, Sedivy JM. Reduced c-Myc signaling triggers telomere-independent senescence by regulating Bmi-1 and p16INK4a. Proceedings of the National Academy of Sciences. 2006; 103: 3645-50. doi:
473. Kim H-S, Shin J-Y, Yun J-Y, Ahn D-K, Lee J-Y. Immortalization of human embryonic fibroblasts by overexpression of c-myc and simian virus 40 large T antigen. Experimental & molecular medicine. 2001; 33: 293-8. doi:
474. Gil J, Kerai P, Lleonart M, Bernard D, Cigudosa JC, Peters G, Carnero A, Beach D. Immortalization of primary human prostate epithelial cells by c-Myc. Cancer Res. 2005; 65: 2179-85. doi:
475. Lessel D, Wu D, Trujillo C, Ramezani T, Lessel I, Alwasiyah MK, Saha B, Hisama FM, Rading K, Goebel I. Dysfunction of the MDM2/p53 axis is linked to premature aging. J Clin Invest. 2017; 127: 3598-608. doi:
476. Blaydes JP, Wynford-Thomas D. The proliferation of normal human fibroblasts is dependent upon negative regulation of p53 function by mdm2. Oncogene. 1998; 16: 3317-22. doi:
477. Gannon HS, Donehower LA, Lyle S, Jones SN. Mdm2–p53 signaling regulates epidermal stem cell senescence and premature aging phenotypes in mouse skin. Developmental biology. 2011; 353: 1-9. doi:
478. Lushnikova T, Bouska A, Odvody J, Dupont WD, Eischen CM. Aging mice have increased chromosome instability that is exacerbated by elevated Mdm2 expression. Oncogene. 2011; 30: 4622-31. doi:
479. Kuro-o M. Klotho and the aging process. The Korean journal of internal medicine. 2011; 26: 113. doi:
480. Matsuzaki T, Matsushita T, Takayama K, Matsumoto T, Nishida K, Kuroda R, Kurosaka M. Disruption of Sirt1 in chondrocytes causes accelerated progression of osteoarthritis under mechanical stress and during ageing in mice. Annals of the rheumatic diseases. 2014; 73: 1397-404. doi:
481. Herranz D, Serrano M. SIRT1: recent lessons from mouse models. Nature Reviews Cancer. 2010; 10: 819-23. doi:
482. Herranz D, Muñoz-Martin M, Cañamero M, Mulero F, Martinez-Pastor B, Fernandez-Capetillo O, Serrano M. Sirt1 improves healthy ageing and protects from metabolic syndrome-associated cancer. Nature communications. 2010; 1: 1-8. doi:
483. Yamamoto M, Clark JD, Pastor JV, Gurnani P, Nandi A, Kurosu H, Miyoshi M, Ogawa Y, Castrillon DH, Rosenblatt KP. Regulation of oxidative stress by the anti-aging hormone klotho. Journal of Biological Chemistry. 2005; 280: 38029-34. doi:
484. Chen H, Liu X, Zhu W, Chen H, Hu X, Jiang Z, Xu Y, Wang L, Zhou Y, Chen P. SIRT1 ameliorates age-related senescence of mesenchymal stem cells via modulating telomere shelterin. Frontiers in aging neuroscience. 2014; 6: 103. doi:
485. Elibol B, Kilic U. High levels of SIRT1 expression as a protective mechanism against disease-related conditions. Frontiers in endocrinology. 2018; 9: 614. doi:
486. Grabowska W, Sikora E, Bielak-Zmijewska A. Sirtuins, a promising target in slowing down the ageing process. Biogerontology. 2017; 18: 447-76. doi:

487. Deng C-X. SIRT1, is it a tumor promoter or tumor suppressor? International journal of biological sciences. 2009; 5: 147. doi:
488. Jeong J, Juhn K, Lee H, Kim S-H, Min B-H, Lee K-M, Cho M-H, Park G-H, Lee K-H. SIRT1 promotes DNA repair activity and deacetylation of Ku70. Experimental & molecular medicine. 2007; 39: 8-13. doi:
489. Li Y, Tollefsbol TO. p16INK4a suppression by glucose restriction contributes to human cellular lifespan extension through SIRT1-mediated epigenetic and genetic mechanisms. PLoS One. 2011; 6. doi:
490. Huang J, Gan Q, Han L, Li J, Zhang H, Sun Y, Zhang Z, Tong T. SIRT1 overexpression antagonizes cellular senescence with activated ERK/S6k1 signaling in human diploid fibroblasts. PLoS One. 2008; 3. doi:
491. Langley E, Pearson M, Faretta M, Bauer UM, Frye RA, Minucci S, Pelicci PG, Kouzarides T. Human SIR2 deacetylates p53 and antagonizes PML/p53-induced cellular senescence. The EMBO journal. 2002; 21: 2383-96. doi:
492. De Bonis ML, Ortega S, Blasco MA. SIRT1 is necessary for proficient telomere elongation and genomic stability of induced pluripotent stem cells. Stem cell reports. 2014; 2: 690-706. doi:
493. Palacios JA, Herranz D, De Bonis ML, Velasco S, Serrano M, Blasco MA. SIRT1 contributes to telomere maintenance and augments global homologous recombination. Journal of Cell Biology. 2010; 191: 1299-313. doi:
494. Hwang J-w, Yao H, Caito S, Sundar IK, Rahman I. Redox regulation of SIRT1 in inflammation and cellular senescence. Free Radical Biology and Medicine. 2013; 61: 95-110. doi:
495. Chung S, Yao H, Caito S, Hwang J-w, Arunachalam G, Rahman I. Regulation of SIRT1 in cellular functions: role of polyphenols. Archives of biochemistry and biophysics. 2010; 501: 79-90. doi:
496. Kuro-o M. Klotho. Pflügers Archiv-European Journal of Physiology. 2010; 459: 333-43. doi:
497. Kuro-o M, Matsumura Y, Aizawa H, Kawaguchi H, Suga T, Utsugi T, Ohyama Y, Kurabayashi M, Kaname T, Kume E. Mutation of the mouse klotho gene leads to a syndrome resembling ageing. Nature. 1997; 390: 45-51. doi:
498. Kurosu H, Yamamoto M, Clark JD, Pastor JV, Nandi A, Gurnani P, McGuinness OP, Chikuda H, Yamaguchi M, Kawaguchi H. Suppression of aging in mice by the hormone Klotho. Science. 2005; 309: 1829-33. doi:
499. Papa S, Skulachev V. (1997). Reactive oxygen species, mitochondria, apoptosis and aging. Detection of mitochondrial diseases: Springer), pp. 305-19.
500. Nagai T, Yamada K, Kim H-C, Kim Y-S, Noda Y, Imura A, Nabeshima Y-i, Nabeshima T. Cognition impairment in the genetic model of aging klotho gene mutant mice: a role of oxidative stress. The FASEB Journal. 2003; 17: 50-2. doi:
501. Lin BC, Wang M, Blackmore C, Desnoyers LR. Liver-specific activities of FGF19 require Klotho beta. Journal of Biological Chemistry. 2007; 282: 27277-84. doi:
502. Gao D, Zuo Z, Tian J, Ali Q, Lin Y, Lei H, Sun Z. Activation of SIRT1 Attenuates Klotho Deficiency–Induced Arterial Stiffness and Hypertension by Enhancing AMP-Activated Protein Kinase Activity. Hypertension. 2016; 68: 1191-9. doi:
503. Ullah M, Sun Z. Klotho deficiency accelerates stem cells aging by impairing telomerase activity. The Journals of Gerontology: Series A. 2019; 74: 1396-407. doi:
504. Buendía P, Carracedo J, Soriano S, Madueño JA, Ortiz A, Martín-Malo A, Aljama P, Ramírez R. Klotho prevents NFκB translocation and protects endothelial cell from senescence induced by uremia. Journals of Gerontology Series A: Biomedical Sciences and Medical Sciences. 2015; 70: 1198-209. doi:
505. Ai F, Chen M, Li W, Yang Y, Xu G, Gui F, Liu Z, Bai X, Chen Z. Protective role of Klotho on cardiomyocytes upon hypoxia/reoxygenation via downregulation of Akt and FOXO1

phosphorylation Retraction in/10.3892/mmr. 2015.3177. Molecular medicine reports. 2015; 11: 2013-9. doi:
506. Dalton GD, Xie J, An S-W, Huang C-L. New insights into the mechanism of action of soluble klotho. Frontiers in endocrinology. 2017; 8: 323. doi:
507. Yao Y, Wang Y, Zhang Y, Liu C. Klotho ameliorates oxidized low density lipoprotein (ox-LDL)-induced oxidative stress via regulating LOX-1 and PI3K/Akt/eNOS pathways. Lipids in health and disease. 2017; 16: 77. doi:
508. Tataranni T, Biondi G, Cariello M, Mangino M, Colucci G, Rutigliano M, Ditonno P, Schena F, Gesualdo L, Grandaliano G. Rapamycin-Induced Hypophosphatemia and Insulin Resistance Are Associated With mTORC2 Activation and Klotho Expression. American Journal of Transplantation. 2011; 11: 1656-64. doi:
509. Papazoglu C, Mills A. p53: at the crossroad between cancer and ageing. The Journal of Pathology: A Journal of the Pathological Society of Great Britain and Ireland. 2007; 211: 124-33. doi:
510. Maier B, Gluba W, Bernier B, Turner T, Mohammad K, Guise T, Sutherland A, Thorner M, Scrable H. Modulation of mammalian life span by the short isoform of p53. Genes Dev. 2004; 18: 306-19. doi:
511. Tyner SD, Venkatachalam S, Choi J, Jones S, Ghebranious N, Igelmann H, Lu X, Soron G, Cooper B, Brayton C. p53 mutant mice that display early ageing-associated phenotypes. Nature. 2002; 415: 45-53. doi:
512. Borrás C, Gómez-Cabrera MC, Viña J. The dual role of p53: DNA protection and antioxidant. Free radical research. 2011; 45: 643-52. doi:
513. Budanov AV, Karin M. p53 target genes sestrin1 and sestrin2 connect genotoxic stress and mTOR signaling. Cell. 2008; 134: 451-60. doi:
514. Sablina AA, Budanov AV, Ilyinskaya GV, Agapova LS, Kravchenko JE, Chumakov PM. The antioxidant function of the p53 tumor suppressor. Nat Med. 2005; 11: 1306-13. doi:
515. Johnson TM, Yu Z-X, Ferrans VJ, Lowenstein RA, Finkel T. Reactive oxygen species are downstream mediators of p53-dependent apoptosis. Proceedings of the National Academy of Sciences. 1996; 93: 11848-52. doi:
516. Mayo LD, Donner DB. The PTEN, Mdm2, p53 tumor suppressor–oncoprotein network. Trends in biochemical sciences. 2002; 27: 462-7. doi:
517. Salminen A, Kaarniranta K. Insulin/IGF-1 paradox of aging: regulation via AKT/IKK/NF-κB signaling. Cellular signalling. 2010; 22: 573-7. doi:
518. García-Cao I, García-Cao M, Martín-Caballero J, Criado LM, Klatt P, Flores JM, Weill JC, Blasco MA, Serrano M. 'Super p53'mice exhibit enhanced DNA damage response, are tumor resistant and age normally. The EMBO journal. 2002; 21: 6225-35. doi:
519. Matheu A, Maraver A, Klatt P, Flores I, Garcia-Cao I, Borras C, Flores JM, Viña J, Blasco MA, Serrano M. Delayed ageing through damage protection by the Arf/p53 pathway. Nature. 2007; 448: 375-9. doi:
520. Modugno M, Tagliabue E, Ardini E, Berno V, Galmozzi E, De Bortoli M, Castronovo V, Menard S. p53-dependent downregulation of metastasis-associated laminin receptor. Oncogene. 2002; 21: 7478-87. doi:
521. Kim WY, Sharpless NE. The regulation of INK4/ARF in cancer and aging. Cell. 2006; 127: 265-75. doi:
522. Watanabe S, Kawamoto S, Ohtani N, Hara E. Impact of senescence-associated secretory phenotype and its potential as a therapeutic target for senescence-associated diseases. Cancer science. 2017; 108: 563-9. doi:
523. Fumagalli M, di Fagagna FdA. SASPense and DDRama in cancer and ageing. Nature cell biology. 2009; 11: 921-3. doi:
524. Van Deursen JM. The role of senescent cells in ageing. Nature. 2014; 509: 439-46. doi:

525. Sato S, Kawamata Y, Takahashi A, Imai Y, Hanyu A, Okuma A, Takasugi M, Yamakoshi K, Sorimachi H, Kanda H. Ablation of the p16 INK4a tumour suppressor reverses ageing phenotypes of klotho mice. Nature communications. 2015; 6: 1-10. doi:
526. Li H, Mitchell JR, Hasty P. DNA double-strand breaks: a potential causative factor for mammalian aging? Mech Ageing Dev. 2008; 129: 416-24. doi:
527. Falck J, Coates J, Jackson SP. Conserved modes of recruitment of ATM, ATR and DNA-PKcs to sites of DNA damage. Nature. 2005; 434: 605-11. doi:
528. Mah L-J, El-Osta A, Karagiannis TC. γH2AX as a molecular marker of aging and disease. Epigenetics. 2010; 5: 129-36. doi:
529. Sedelnikova OA, Horikawa I, Zimonjic DB, Popescu NC, Bonner WM, Barrett JC. Senescing human cells and ageing mice accumulate DNA lesions with unrepairable double-strand breaks. Nature cell biology. 2004; 6: 168-70. doi:
530. Pazolli E, Alspach E, Milczarek A, Prior J, Piwnica-Worms D, Stewart SA. Chromatin remodeling underlies the senescence-associated secretory phenotype of tumor stromal fibroblasts that supports cancer progression. Cancer Res. 2012; 72: 2251-61. doi:
531. Turinetto V, Giachino C. Multiple facets of histone variant H2AX: a DNA double-strand-break marker with several biological functions. Nucleic Acids Res. 2015; 43: 2489-98. doi:
532. Park JH, Kim CK, Lee SB, Lee K-H, Cho S-W, Ahn J-Y. Akt attenuates apoptotic death through phosphorylation of H2A under hydrogen peroxide-induced oxidative stress in PC12 cells and hippocampal neurons. Sci Rep. 2016; 6: 1-11. doi:
533. Deng R, Tang J, Ma J, Chen S, Xia L, Zhou W, Li D, Feng G, Zeng Y-X, Zhu X-F. PKB/Akt promotes DSB repair in cancer cells through upregulating Mre11 expression following ionizing radiation. Oncogene. 2011; 30: 944-55. doi:
534. Oberdoerffer P, Michan S, McVay M, Mostoslavsky R, Vann J, Park S-K, Hartlerode A, Stegmuller J, Hafner A, Loerch P. SIRT1 redistribution on chromatin promotes genomic stability but alters gene expression during aging. Cell. 2008; 135: 907-18. doi:
535. Song S-H, Lee M-O, Lee J-S, Oh J-S, Cho S-U, Cha H-J. Sirt1 promotes DNA damage repair and cellular survival. Biomolecules & Therapeutics. 2011; 19: 282-7. doi:
536. Malik AN, Czajka A. Is mitochondrial DNA content a potential biomarker of mitochondrial dysfunction? Mitochondrion. 2013; 13: 481-92. doi:
537. Cannon B, Shabalina IG, Kramarova TV, Petrovic N, Nedergaard J. Uncoupling proteins: a role in protection against reactive oxygen species—or not? Biochimica et Biophysica Acta (BBA)-Bioenergetics. 2006; 1757: 449-58. doi:
538. Trifunovic A, Larsson NG. Mitochondrial dysfunction as a cause of ageing. Journal of internal medicine. 2008; 263: 167-78. doi:
539. Palikaras K, Lionaki E, Tavernarakis N. Coordination of mitophagy and mitochondrial biogenesis during ageing in C. elegans. Nature. 2015; 521: 525-8. doi:
540. Kazachkova N, Ramos A, Santos C, Lima M. Mitochondrial DNA damage patterns and aging: revising the evidences for humans and mice. Aging and disease. 2013; 4: 337. doi:
541. Cree L, Patel S, Pyle A, Lynn S, Turnbull D, Chinnery P, Walker M. Age-related decline in mitochondrial DNA copy number in isolated human pancreatic islets. Diabetologia. 2008; 51: 1440-3. doi:
542. Welle S, Bhatt K, Shah B, Needler N, Delehanty JM, Thornton CA. Reduced amount of mitochondrial DNA in aged human muscle. Journal of applied physiology. 2003; 94: 1479-84. doi:
543. Pesce V, Cormio A, Fracasso F, Vecchiet J, Felzani G, Lezza AM, Cantatore P, Gadaleta MN. Age-related mitochondrial genotypic and phenotypic alterations in human skeletal muscle. Free Radical Biology and Medicine. 2001; 30: 1223-33. doi:
544. Masuyama M, Iida R, Takatsuka H, Yasuda T, Matsuki T. Quantitative change in mitochondrial DNA content in various mouse tissues during aging. Biochimica et Biophysica Acta (BBA)-General Subjects. 2005; 1723: 302-8. doi:

545. Santoro A, Salvioli S, Raule N, Capri M, Sevini F, Valensin S, Monti D, Bellizzi D, Passarino G, Rose G. Mitochondrial DNA involvement in human longevity. Biochimica et Biophysica Acta (BBA)-Bioenergetics. 2006; 1757: 1388-99. doi:
546. Kim S-J, Mehta HH, Wan J, Kuehnemann C, Chen J, Hu J-F, Hoffman AR, Cohen P. Mitochondrial peptides modulate mitochondrial function during cellular senescence. Aging (Albany NY). 2018; 10: 1239. doi:
547. LEE H-C, YIN P-H, LU C-Y, CHI C-W, WEI Y-H. Increase of mitochondria and mitochondrial DNA in response to oxidative stress in human cells. Biochemical Journal. 2000; 348: 425-32. doi:
548. Correia-Melo C, Marques FD, Anderson R, Hewitt G, Hewitt R, Cole J, Carroll BM, Miwa S, Birch J, Merz A. Mitochondria are required for pro-ageing features of the senescent phenotype. The EMBO journal. 2016; 35: 724-42. doi:
549. Birch J, Passos JF. Targeting the SASP to combat ageing: Mitochondria as possible intracellular allies? Bioessays. 2017; 39: 1600235. doi:
550. Flores I, Canela A, Vera E, Tejera A, Cotsarelis G, Blasco MA. The longest telomeres: a general signature of adult stem cell compartments. Genes Dev. 2008; 22: 654-67. doi:
551. Scheiman J, Jamieson KV, Ziello J, Tseng JC, Meruelo D. Extraribosomal functions associated with the C terminus of the 37/67 kDa laminin receptor are required for maintaining cell viability. Cell Death Dis. 2010; 1: e42. doi: 10.1038/cddis.2010.19.
552. Yamashita S, Ogawa K, Ikei T, Udono M, Fujiki T, Katakura Y. SIRT1 prevents replicative senescence of normal human umbilical cord fibroblast through potentiating the transcription of human telomerase reverse transcriptase gene. Biochem Biophys Res Commun. 2012; 417: 630-4. doi:
553. Chen R, Zhang K, Chen H, Zhao X, Wang J, Li L, Cong Y, Ju Z, Xu D, Williams BR. Telomerase deficiency causes alveolar stem cell senescence-associated low-grade inflammation in lungs. Journal of Biological Chemistry. 2015; 290: 30813-29. doi:
554. Hao L-Y, Armanios M, Strong MA, Karim B, Feldser DM, Huso D, Greider CW. Short telomeres, even in the presence of telomerase, limit tissue renewal capacity. Cell. 2005; 123: 1121-31. doi:
555. Artandi SE, Alson S, Tietze MK, Sharpless NE, Ye S, Greenberg RA, Castrillon DH, Horner JW, Weiler SR, Carrasco RD. Constitutive telomerase expression promotes mammary carcinomas in aging mice. Proceedings of the National Academy of Sciences. 2002; 99: 8191-6. doi:
556. Rafnar T, Sulem P, Stacey SN, Geller F, Gudmundsson J, Sigurdsson A, Jakobsdottir M, Helgadottir H, Thorlacius S, Aben KK. Sequence variants at the TERT-CLPTM1L locus associate with many cancer types. Nat Genet. 2009; 41: 221. doi:
557. González-Suárez E, Samper E, Ramírez A, Flores JM, Martín-Caballero J, Jorcano JL, Blasco MA. Increased epidermal tumors and increased skin wound healing in transgenic mice overexpressing the catalytic subunit of telomerase, mTERT, in basal keratinocytes. The EMBO journal. 2001; 20: 2619-30. doi:
558. Armanios M. Telomeres and age-related disease: how telomere biology informs clinical paradigms. J Clin Invest. 2013; 123: 996-1002. doi:
559. Li Y, Zhou G, Bruno IG, Cooke JP. Telomerase mRNA reverses senescence in progeria cells. Journal of the American College of Cardiology. 2017; 70: 804-5. doi:

8. Appendices

Appendix A

Additional Data

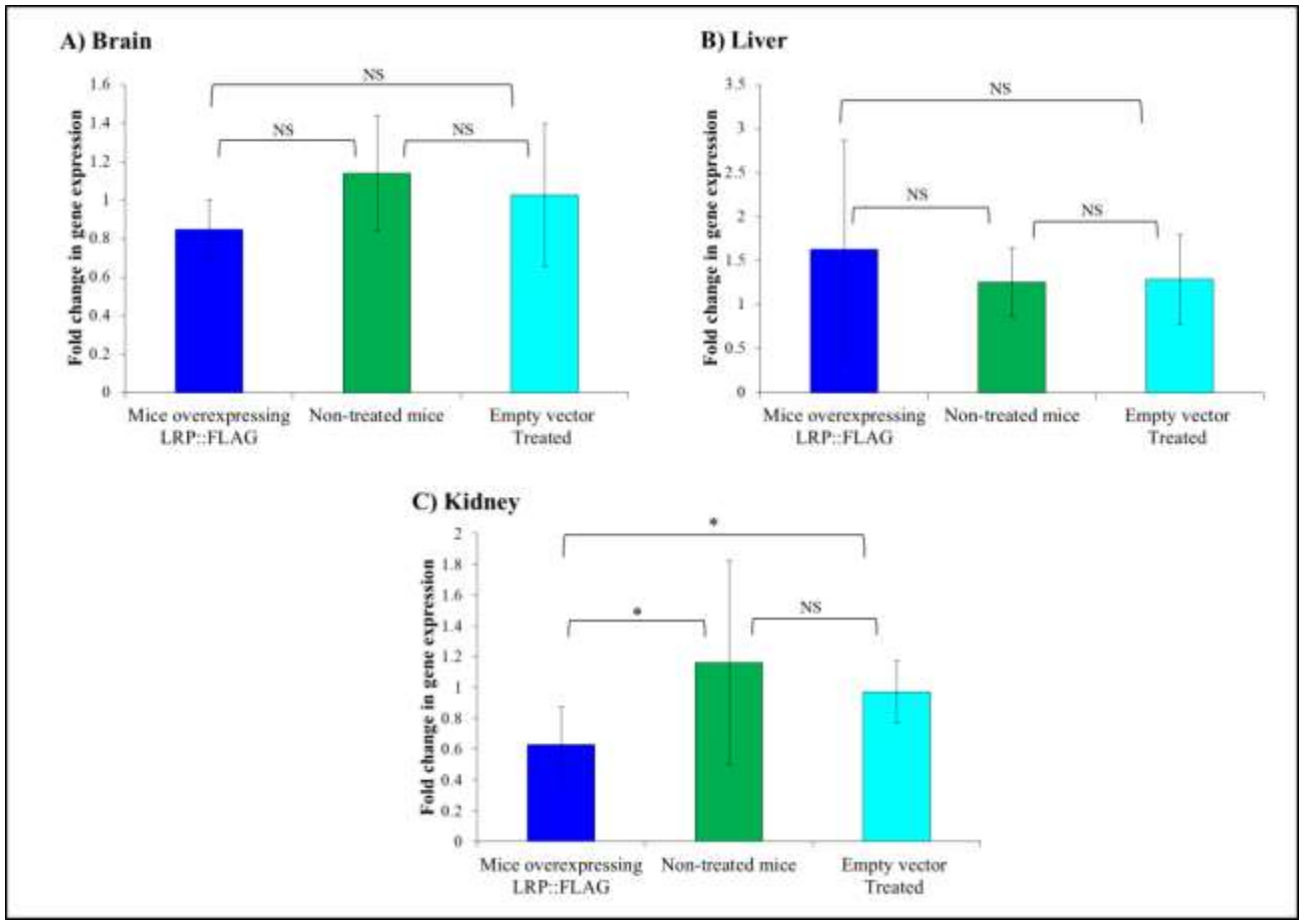


Figure 8.1: The overexpression of LRP::FLAG reduces IL6 in the brain and kidney in aged mice.

IL6 gene expression assessment by qPCR revealed that LRP::FLAG overexpression induced a ±0.2 and ±0.4 fold reduction within the (A) brain and kidney (C), while no difference was observed in the (B) liver. Sample size: Brain: Treated: n = 6; Control: n = 5 and Non-treated: n = 6. Liver: Treated: n = 6; Control: n = 6 and Non-treated: n = 7 and Kidney: Treated: n = 9; Control: n = 5 and Non-treated: n = 10. RPLPO and GAPDH were used as reference genes for normalisation purposes. Data as a mean ±SD. *p < 0.05, **p < 0.01, ***p < 0.001, NS: p>0.05, non-significant; One-way ANOVA and Welch's *t-test* coupled with a post hoc Bonferroni correction were performed for all experiments. The number of '*' irrespective of colour represents the level of significance according to Welch's *t-test*, whereas '*' in red indicate data that is significant following the Bonferroni correction.

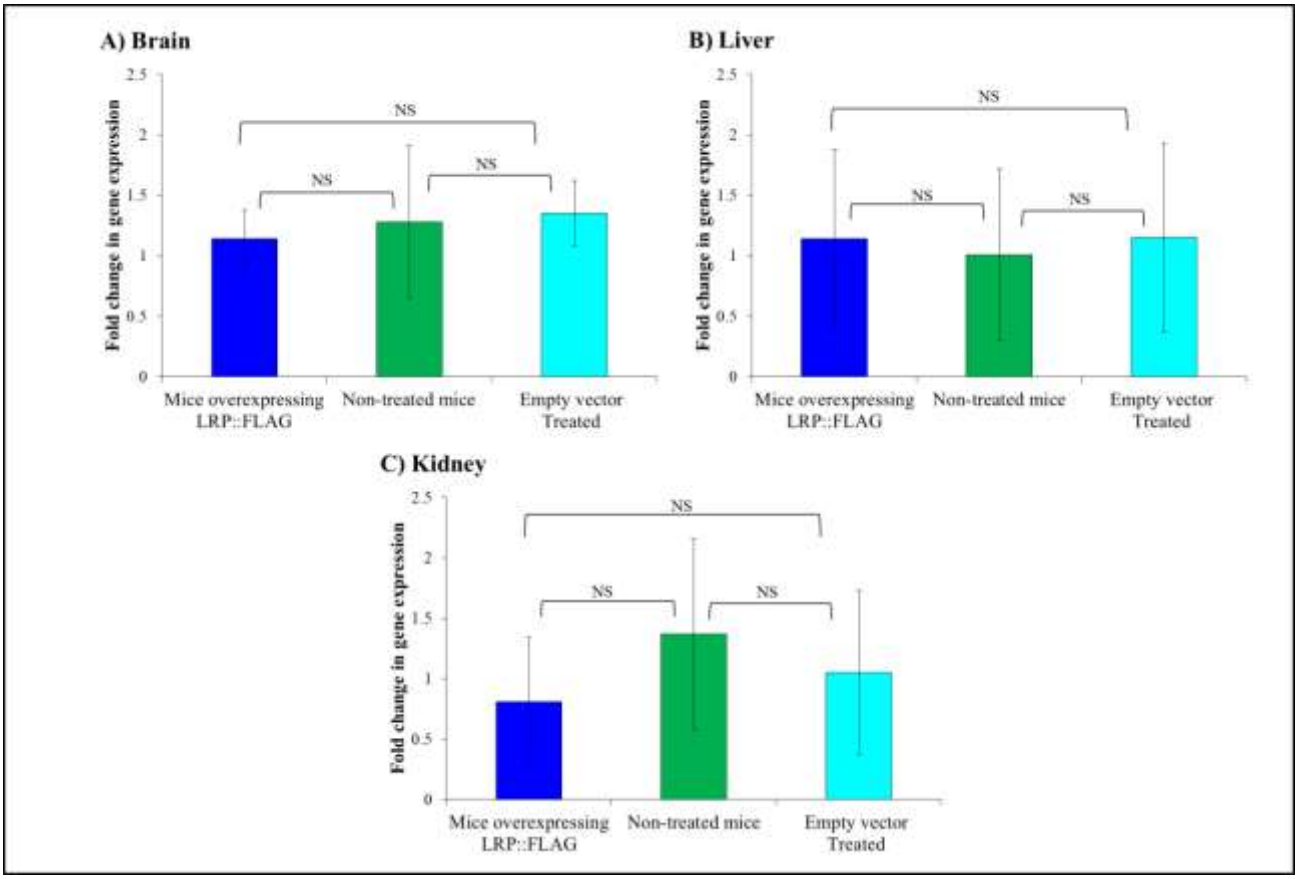


Figure 8.2: The overexpression of LRP::FLAG caused a non-significant reduction in IL8 within the brain and kidney of aged mice.

IL8 gene expression assessment by qPCR revealed that LRP::FLAG overexpression induced a ±0.3, ±0.4 and ±0.4 fold reduction within the (A) brain, (B) liver and kidney (C). Sample size: Brain: Treated: n = 5; Control: n = 5 and Non-treated: n = 6. Liver: Treated: n = 7; Control: n = 7 and Non-treated: n = 8 and Kidney: Treated: n = 6; Control: n = 6 and Non-treated: n = 8. RPLPO and GAPDH were used as reference genes for normalisation purposes. Data as a mean ±SD. *p < 0.05, **p < 0.01, ***p < 0.001, NS: p>0.05, non-significant; One-way ANOVA and Welch's *t-test* coupled with a post hoc Bonferroni correction were performed for all experiments. The number of '*' irrespective of colour represents the level of significance according to Welch's *t-test*, whereas '*' in red indicate data that is significant following the Bonferroni correction.

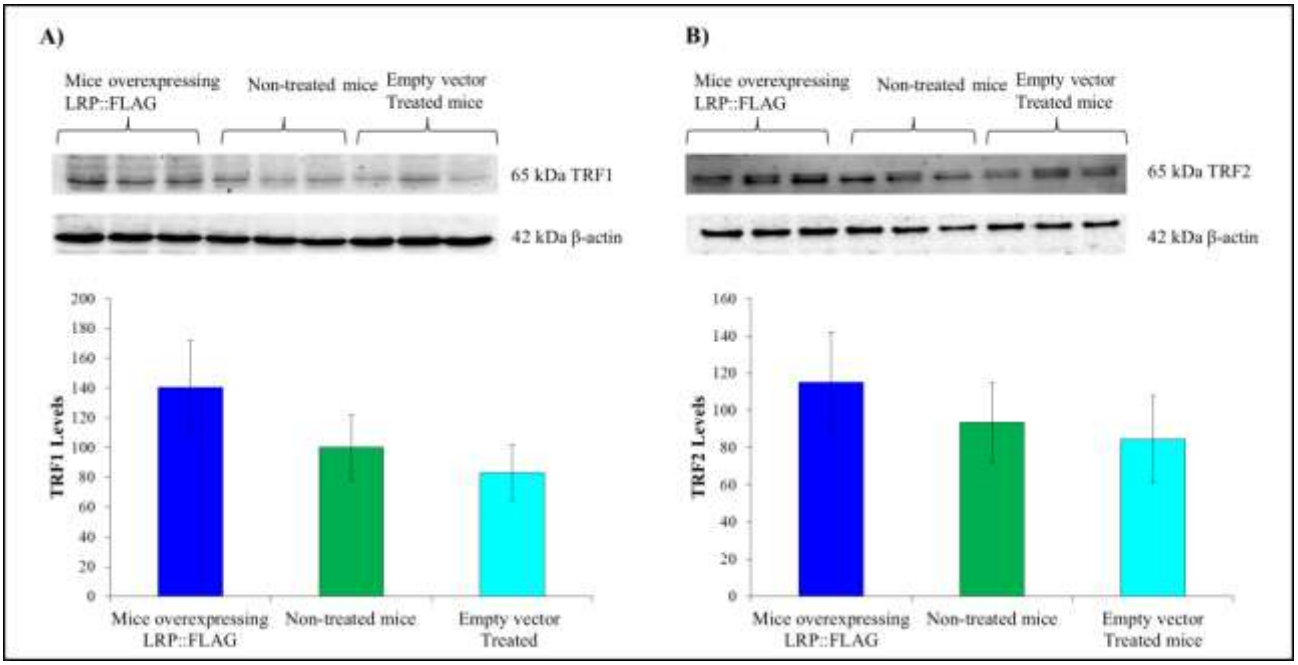


Figure 8.3: The overexpression of LRP::FLAG induces a significant increase in TRF1 and TRF2 within the liver of the aged mice.

Protein level assessment of (A) TRF1 and (B) TRF2 protein levels by western blotting in the liver revealed that LRP::FLAG overexpression induced a ±40% and ±20% elevation for both proteins. Liver TRF1: Treated: n = 12; Control: n = 9 and Non-treated: n = 12. Liver TRF2: Treated: n = 11; Control: n = 9 and Non-treated: n = 10. (A, B) β-actin was used as a reference protein and all illustrated blots are representative where 4 blots were performed to assess all biological replicates. Data as a mean ±SD. *p < 0.05, **p < 0.01, ***p < 0.001, NS: p>0.05, non-significant; One-way ANOVA and Welch's *t-test* coupled with a post hoc Bonferroni correction were performed for all experiments. The number of '*' irrespective of colour represents the level of significance according to Welch's *t-test*, whereas '*' in red indicate data that is significant following the Bonferroni correction.

Appendix B

Supporting Data

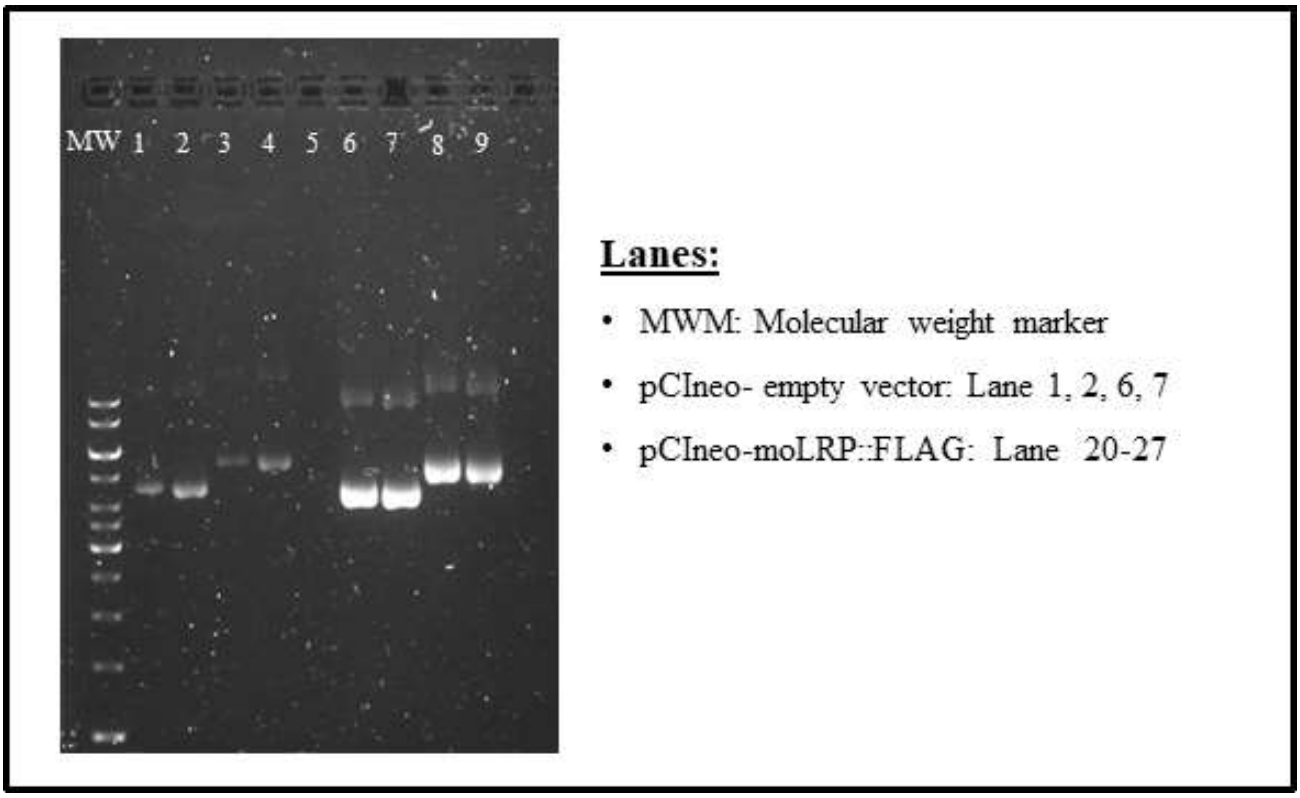


Figure 8.4: Agarose gel electrophoresis displaying the pCIneo-moLRP::FLAG and empty pCIneo- vector.

A 1% agarose gel was utilised to assess plasmid purity and integrity following plasmid expression and isolation. Two distinct bands can be noted in all loaded lanes (lane 1-4 and lane 6-9). The uppermost band (fainter band in each lane) displays nicked plasmid while the second band (brightest and largest band in each lane) illustrates intact supercoiled plasmid. Lanes containing the empty pCIneo-vector include: 1, 2, 6 and 7, while lanes containing the pCIneo-moLRP::FLAG include: 3, 4, 8, 9. Interestingly, the pCIneo-moLRP::FLAG plasmid appeared higher on the gel indicating an extra weight of ±1000 bp, where the LRP::FLAG insert is about ±909 bp thereby rudimentarily confirming that an insert was present.

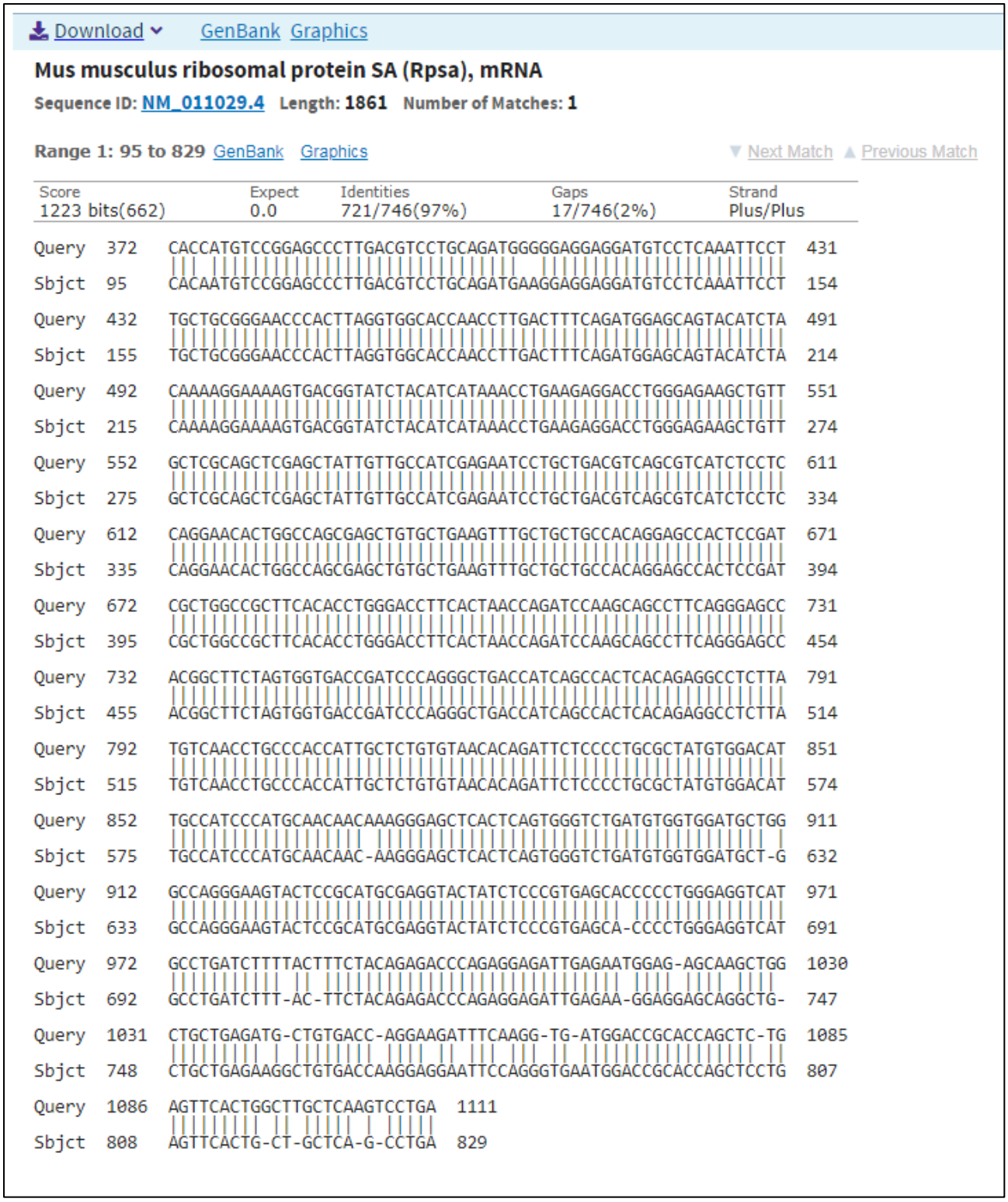


Figure 8.5: Sequencing alignment and BLAST data for the LRP::FLAG gene

The isolated and purified pCIneo-moLRP::FLAG mammalian expression vector was sequenced by Inqaba Biotech™ (South Africa). The sequence data generated was then aligned to the mus musculus LRP (RPSA) gene using Bio-edit. Thereafter, the aligned sequences were BLASTed on NCBI where it was noted that the insert present in the pCIneo-moLRP::FLAG plasmid shared a 97% sequence homology. This confirms that the plasmid used during the *in vitro* and *in vivo* study definitely allowed the overexpression of LRP::FLAG.

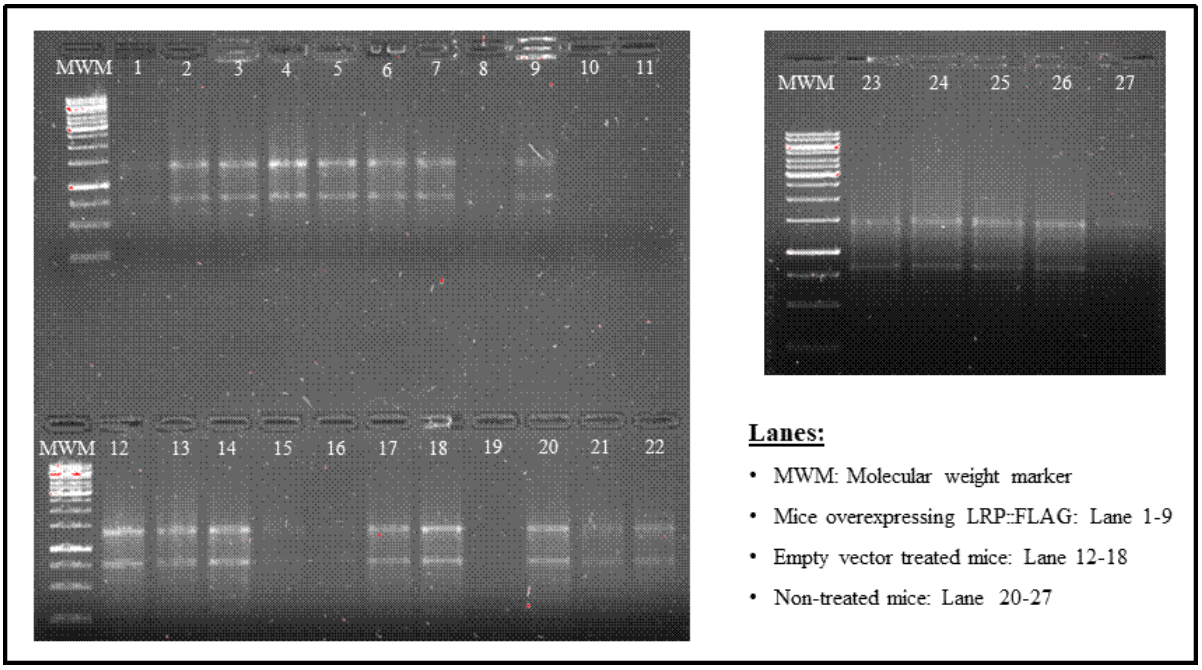


Figure 8.6: Agarose gel electrophoresis displaying RNA extracted samples from the brain.
A 1% agarose gel was utilised to assess RNA purity and integrity following RNA isolation. Two distinct bands representing the ribosomal 28S rRNA and 18S rRNA can be seen for most samples in each gel. In addition, it was observed that no bands were present at the top of the gel confirming that there is no DNA to negligible DNA contamination. Lanes 1-9 represent brain RNA samples from the treated group. Lanes 12-18 represent brain from the RNA samples from the control mouse group, and Lanes 20-27 represent brain RNA samples from the non-treated mouse group. Approximately 200 ng of RNA was loaded for each sample.

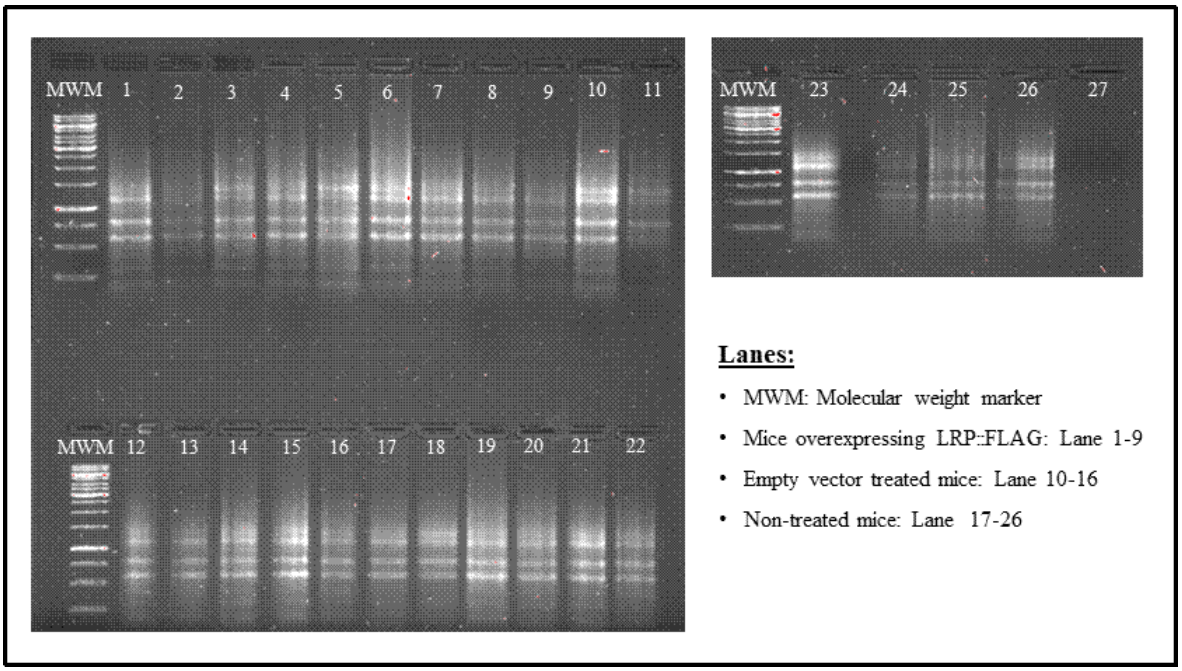


Figure 8.7: Agarose gel electrophoresis displaying RNA extracted samples from the liver.
A 1% agarose gel was utilised to assess RNA purity and integrity following RNA isolation. Two distinct bands representing the ribosomal 28S rRNA and 18S rRNA can be seen for most samples in each gel. In addition, it was observed that no bands were present at the top of the gel confirming that there is no DNA to negligible DNA contamination. Lanes 1-9 represent liver RNA samples from the treated mouse group. Lanes 10-16 represent liver from the RNA samples from the control mouse group, and Lanes 17-26 represent liver RNA samples from the non-treated mouse group. Approximately 200 ng of RNA was loaded for each sample.

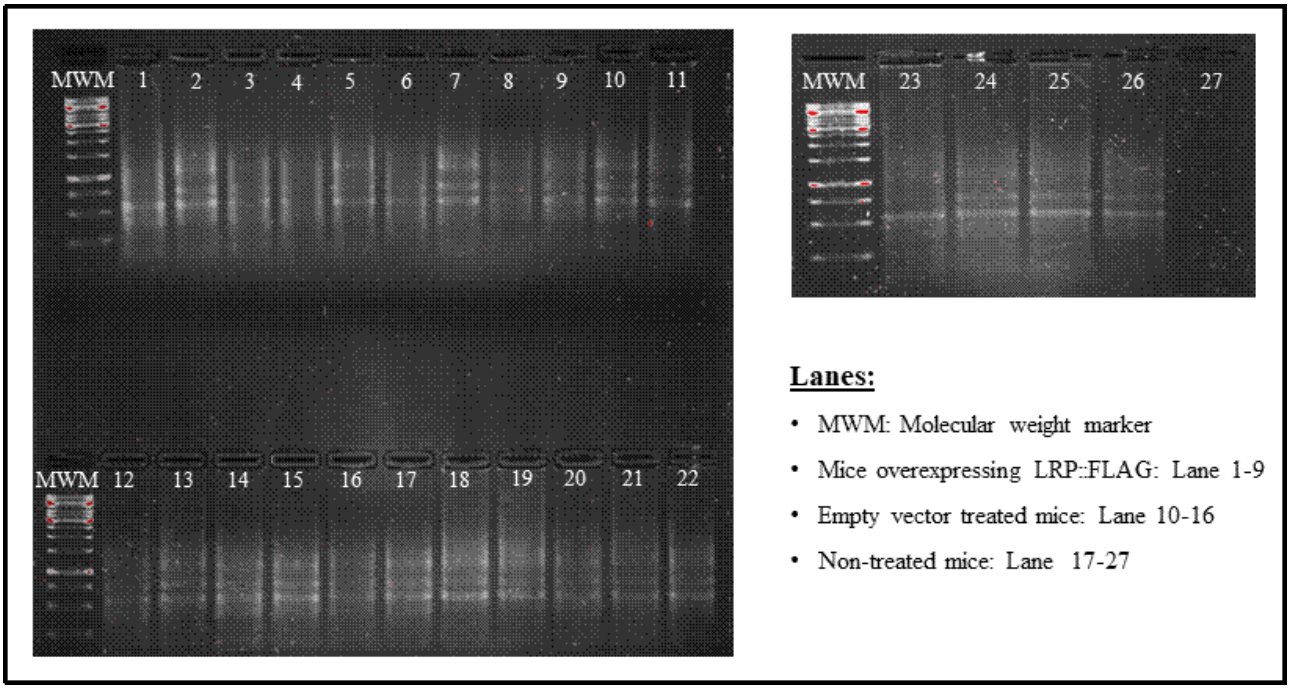


Figure 8.8: Agarose gel electrophoresis displaying RNA extracted samples from the kidney.
A 1% agarose gel was utilised to assess RNA purity and integrity following RNA isolation. Two distinct bands representing the ribosomal 28S rRNA and 18S rRNA can be seen for most samples in each gel. In addition, it was observed that no bands were present at the top of the gel confirming that there is no DNA to negligible DNA contamination. Lanes 1-9 represent kidney RNA samples from the treated mouse group. Lanes 10-16 represent kidney from the RNA samples from the control mouse group, and Lanes 17-26 represent kidney RNA samples from the non-treated mouse group. Approximately 200 ng of RNA was loaded for each sample.

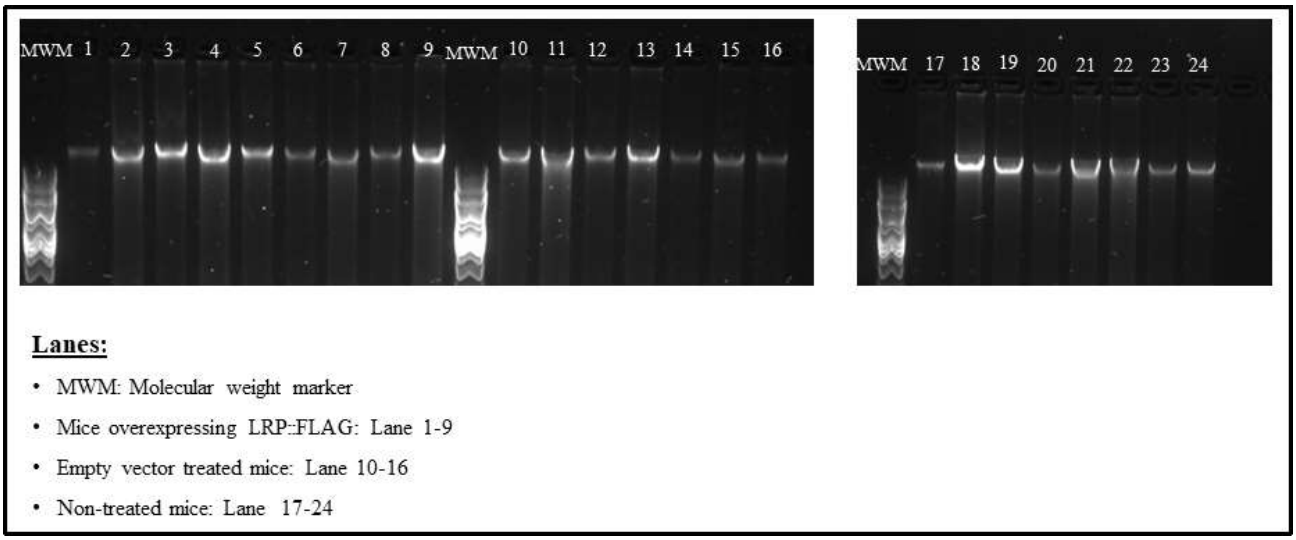


Figure 8.9: Agarose gel electrophoresis displaying DNA extracted samples from the brain.
A 1% agarose gel was utilised to assess DNA integrity following DNA isolation. One distinct band was present at the top of each lane confirming the presence of intact DNA. Lanes 1-9 represent brain DNA samples from the treated mouse group. Lanes 10-16 represent brain from the DNA samples from the control mouse group, and Lanes 17-24 represent brain DNA samples from the non-treated mouse group. Approximately 100 ng of DNA was loaded for each sample.

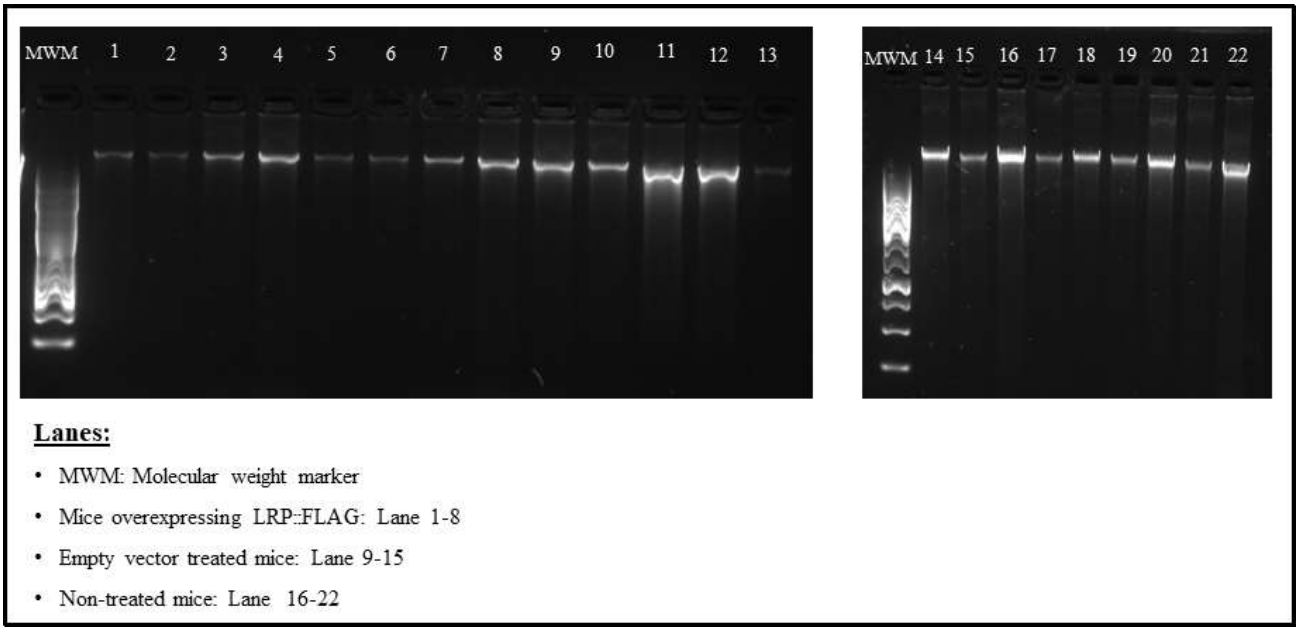


Figure 8.10: Agarose gel electrophoresis displaying DNA extracted samples from the liver.
A 1% agarose gel was utilised to assess DNA integrity following DNA isolation. One distinct band was present at the top of each lane confirming the presence of intact DNA. Lanes 1-8 represent liver DNA samples from the treated mouse group. Lanes 9-15 represent liver from the DNA samples from the control mouse group, and Lanes 16-22 represent liver DNA samples from the non-treated mouse group. Approximately 100 ng of DNA was loaded for each sample.

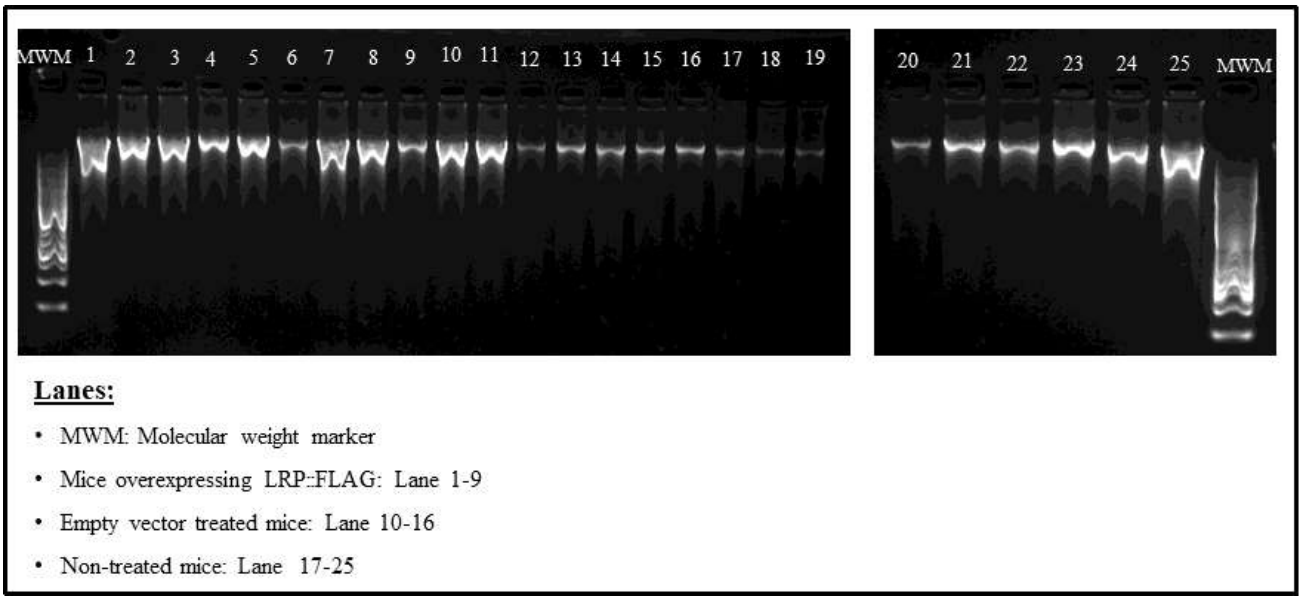


Figure 8.11: Agarose gel electrophoresis displaying DNA extracted samples from the kidney.
A 1% agarose gel was utilised to assess DNA integrity following DNA isolation. One distinct band was present at the top of each lane confirming the presence of intact DNA. Lanes 1-9 represent kidney DNA samples from the treated mouse group. Lanes 10-16 represent kidney from the DNA samples from the control mouse group, and Lanes 17-25 represent kidney DNA samples from the non-treated mouse group. Approximately 100 ng of DNA was loaded for each sample.

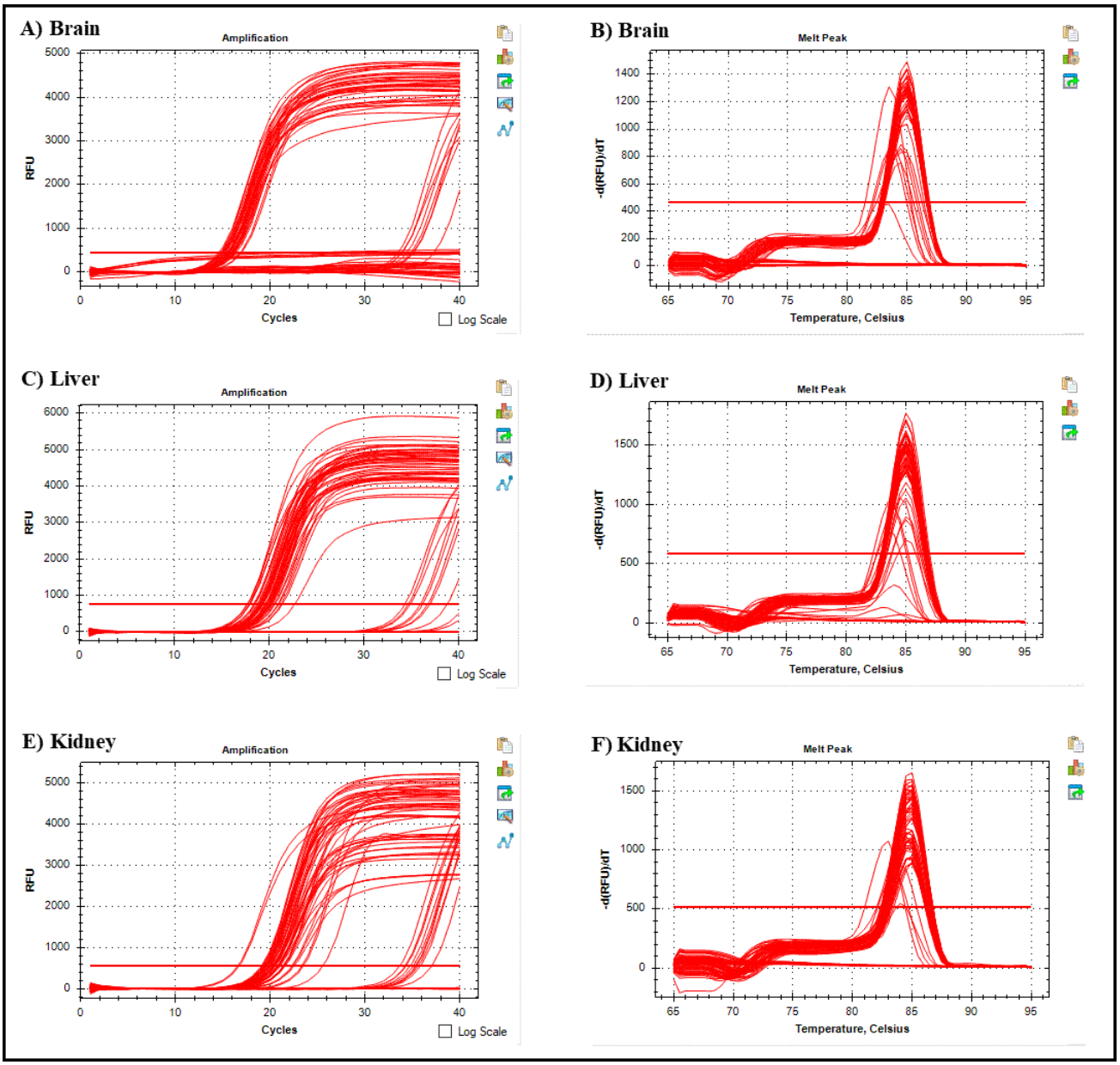


Figure 8.12: Amplification curve and Melt peak analysis of the reference gene GAPDH.
(A, C, E) Amplification curves following qPCR amplification of the reference gene GAPDH in the three different mouse groups, namely: Mice overexpressing LRP::FLAG, Empty vector Treated mice and Non-treated mice. This was done for all three tested organs that included the brain (A), liver (C) and kidney (E). (B, D, F) Representative qPCR melt peak analysis of the reference gene GAPDH in the three different organs of the various mouse groups confirmed that only a single gene product was amplified. No amplification was observed in the no template controls (NTC's) and the no reverse transcriptase controls (no RT's).

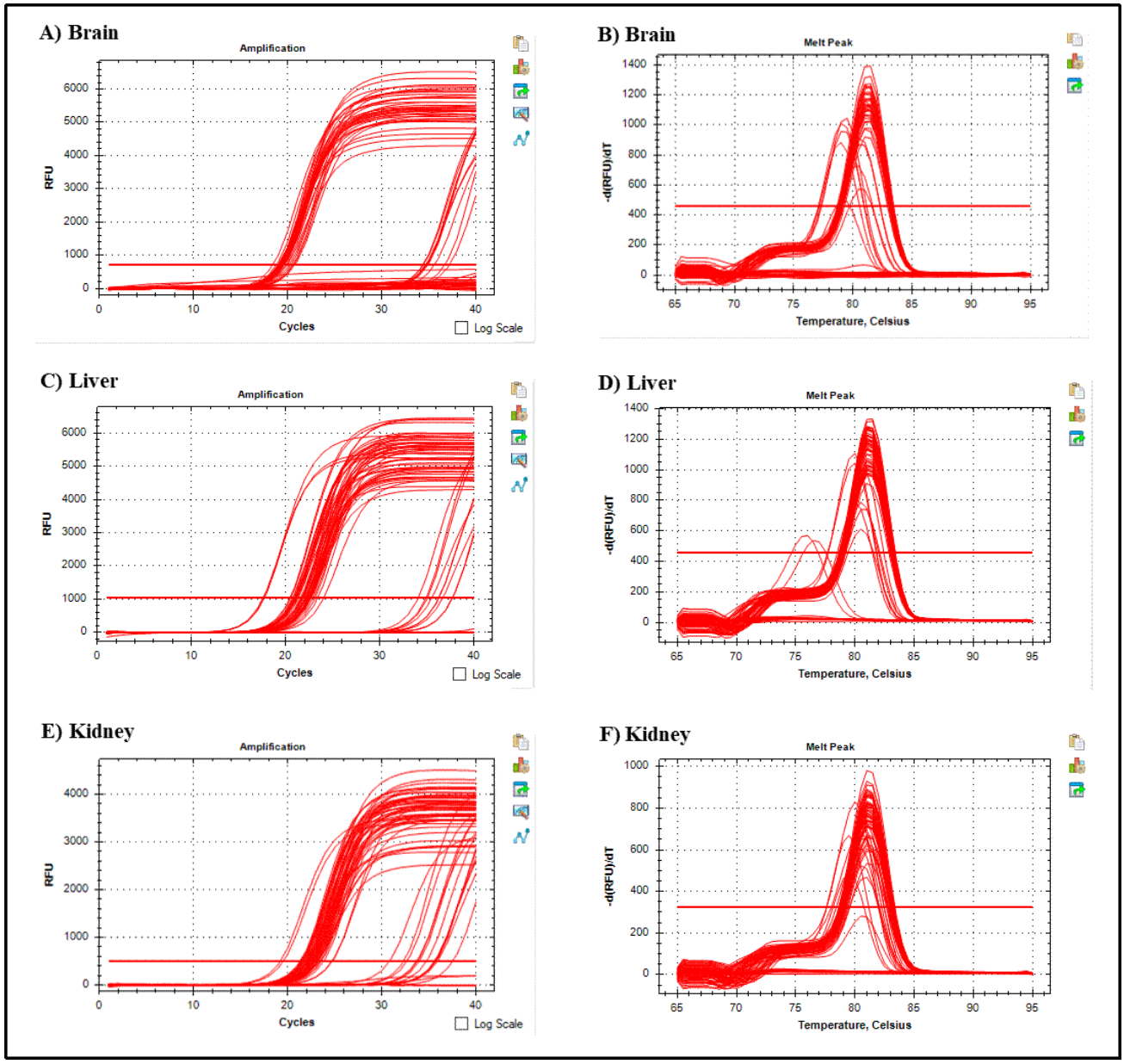


Figure 8.13: Amplification curve and Melt peak analysis of the reference gene RPLPO.
(A, C, E) Amplification curves following qPCR amplification of the reference gene RPLPO in the three different mouse groups, namely: Mice overexpressing LRP::FLAG, Empty vector Treated mice and Non-treated mice. This was done for all three tested organs that included the brain (A), liver (C) and kidney (E). (B, D, F) Representative qPCR melt peak analysis of the reference gene RPLPO in the three different organs of the various mouse groups confirmed that only a single gene product was amplified. No amplification was observed in the NTC's and for majority of the no RT's except for two of the no RT samples in the liver (D).

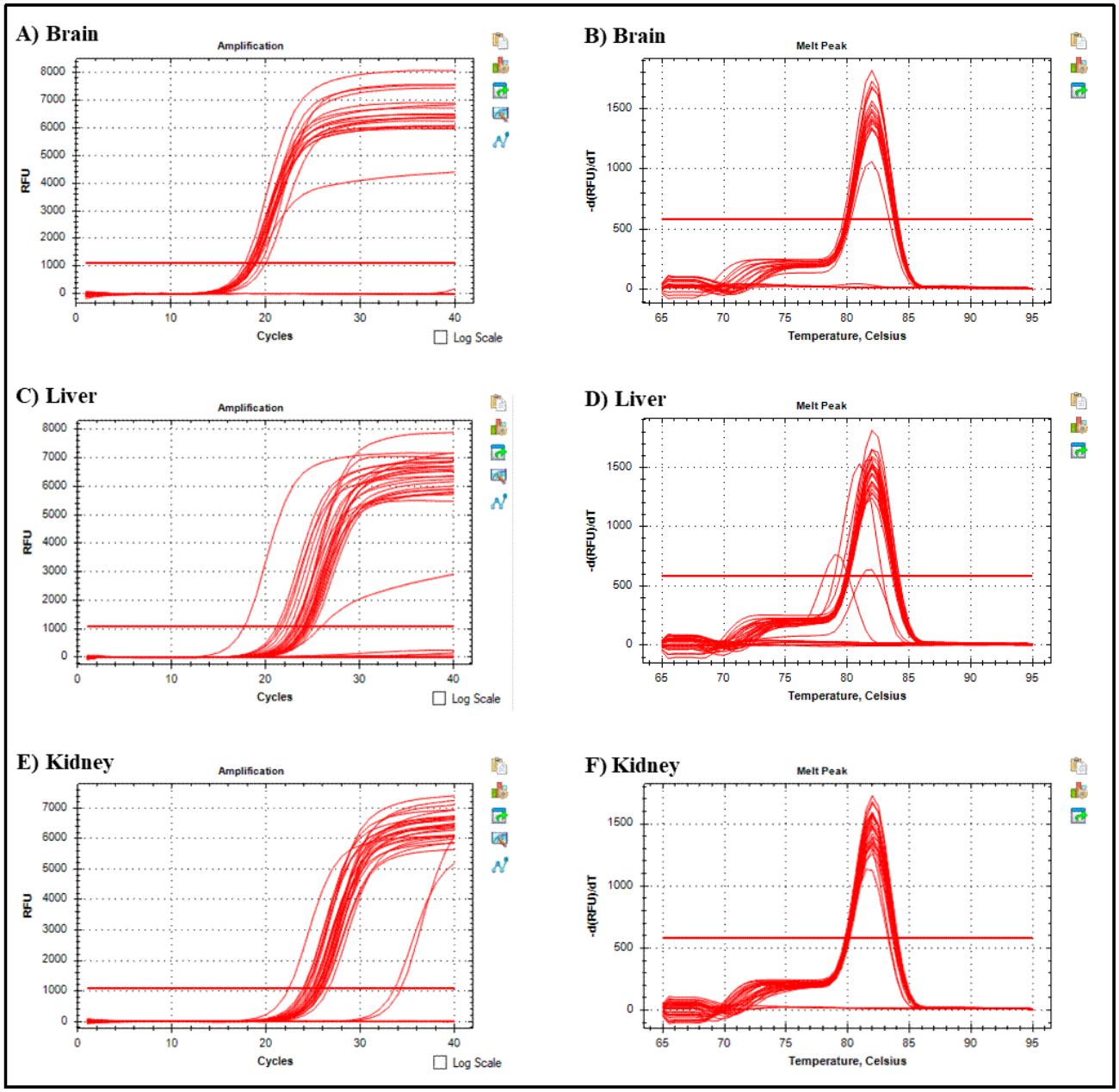


Figure 8.14: Amplification curve and Melt peak analysis of the LRP gene.
(A, C, E) Amplification curves following qPCR amplification of the LRP gene in the three different mouse groups, namely: Mice overexpressing LRP::FLAG, Empty vector Treated mice and Non-treated mice. This was done for all three tested organs that included the brain (A), liver (C) and kidney (E). (B, D, F) Representative qPCR melt peak analysis of the LRP gene in the three different organs of the various mouse groups confirmed that only a single gene product was amplified. No amplification was observed in the NTC's and no RT's.

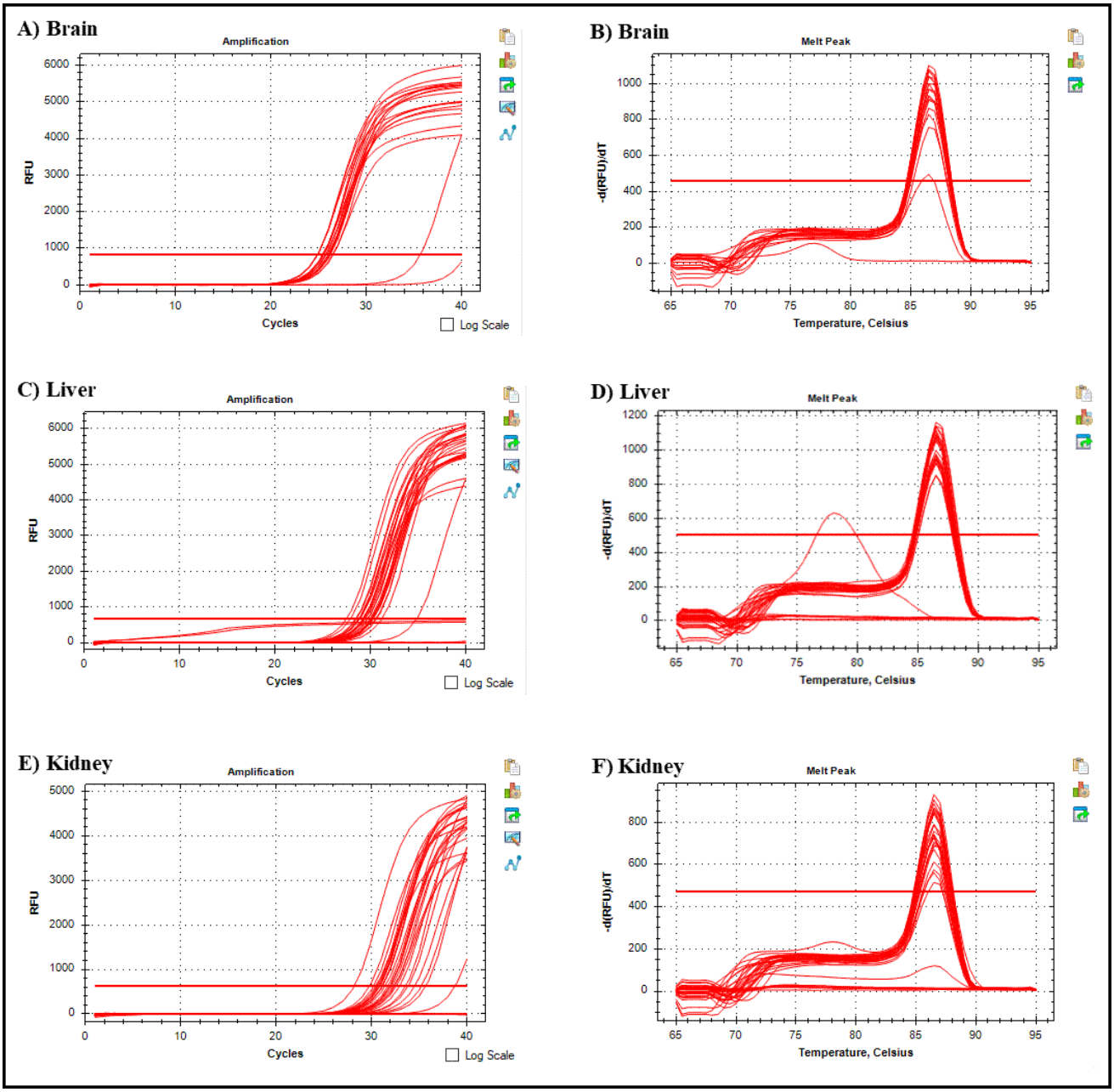


Figure 8.15: Amplification curve and Melt peak analysis of the Akt gene.
(A, C, E) Amplification curves following qPCR amplification of the Akt gene in the three different mouse groups, namely: Mice overexpressing LRP::FLAG, Empty vector Treated mice and Non-treated mice. This was done for all three tested organs that included the brain (A), liver (C) and kidney (E). (B, D, F) Representative qPCR melt peak analysis of the Akt gene in the three different organs of the various mouse groups confirmed that only a single gene product was amplified. There was however one sample that amplified poorly in the (D) liver. No amplification was observed in the NTC's and no RT's.

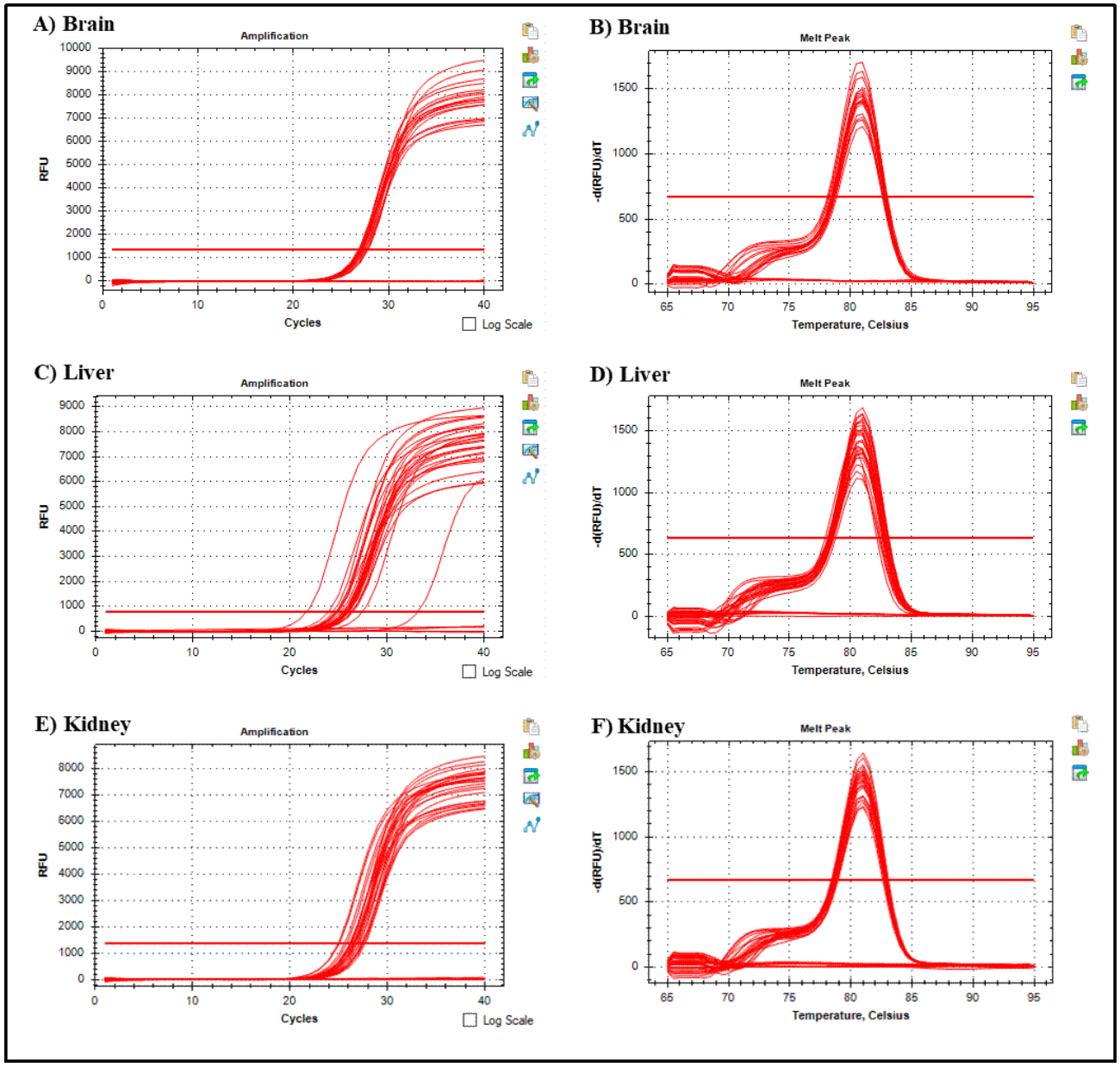


Figure 8.16: Amplification curve and Melt peak analysis of the c-Myc gene.

(A, C, E) Amplification curves following qPCR amplification of the c-Myc gene in the three different mouse groups, namely: Mice overexpressing LRP::FLAG, Empty vector Treated mice and Non-treated mice. This was done for all three tested organs that included the brain (A), liver (C) and kidney (E). (B, D, F) Representative qPCR melt peak analysis of the c-Myc gene in the three different organs of the various mouse groups confirmed that only a single gene product was amplified. No amplification was observed in the NTC's and no RT's.

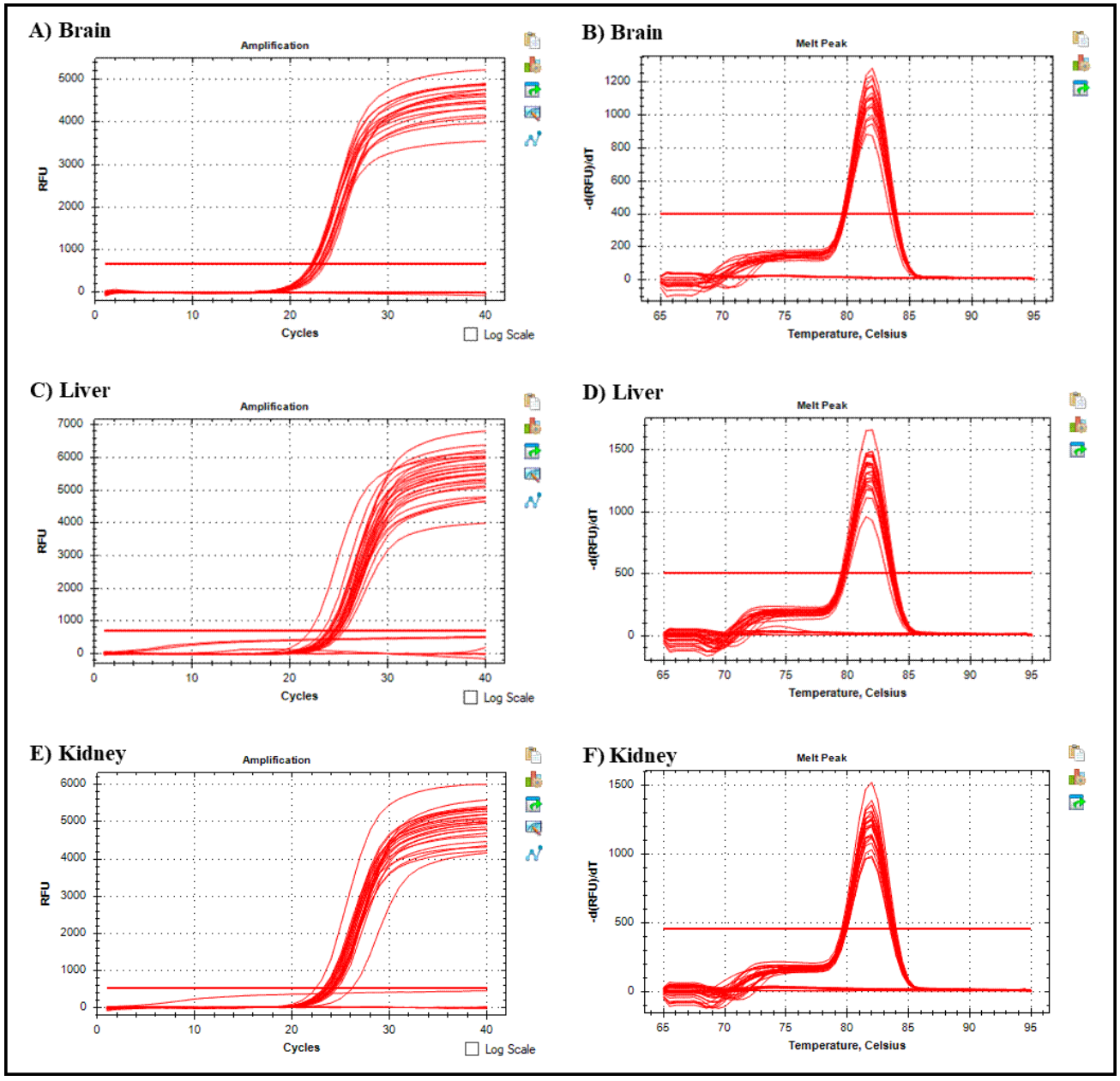


Figure 8.17: Amplification curve and Melt peak analysis of the MDM2 gene.

(A, C, E) Amplification curves following qPCR amplification of the MDM2 gene in the three different mouse groups, namely: Mice overexpressing LRP::FLAG, Empty vector Treated mice and Non-treated mice. This was done for all three tested organs that included the brain (A), liver (C) and kidney (E). (B, D, F) Representative qPCR melt peak analysis of the MDM2 gene in the three different organs of the various mouse groups confirmed that only a single gene product was amplified. No amplification was observed in the NTC's and no RT's.

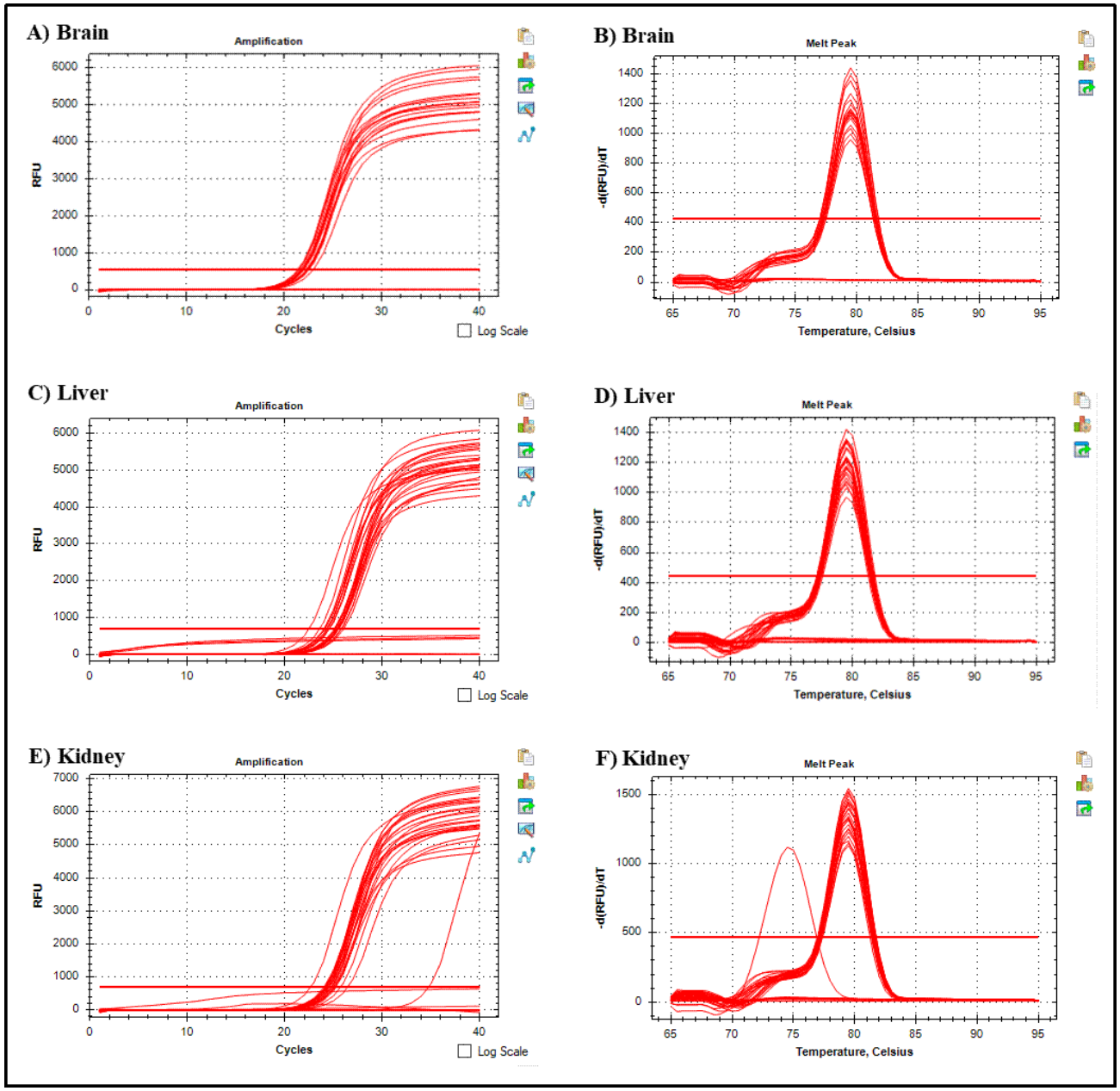


Figure 8.18: Amplification curve and Melt peak analysis of the SIRT1 gene.
(A, C, E) Amplification curves following qPCR amplification of the SIRT1 gene in the three different mouse groups, namely: Mice overexpressing LRP::FLAG, Empty vector Treated mice and Non-treated mice. This was done for all three tested organs that included the brain (A), liver (C) and kidney (E). (B, D, F) Representative qPCR melt peak analysis of the SIRT1 gene in the three different organs of the various mouse groups confirmed that only a single gene product was amplified. However, one sample for the kidney (F) was confirmed to amplify poorly. No amplification was observed in the NTC's and no RT's.

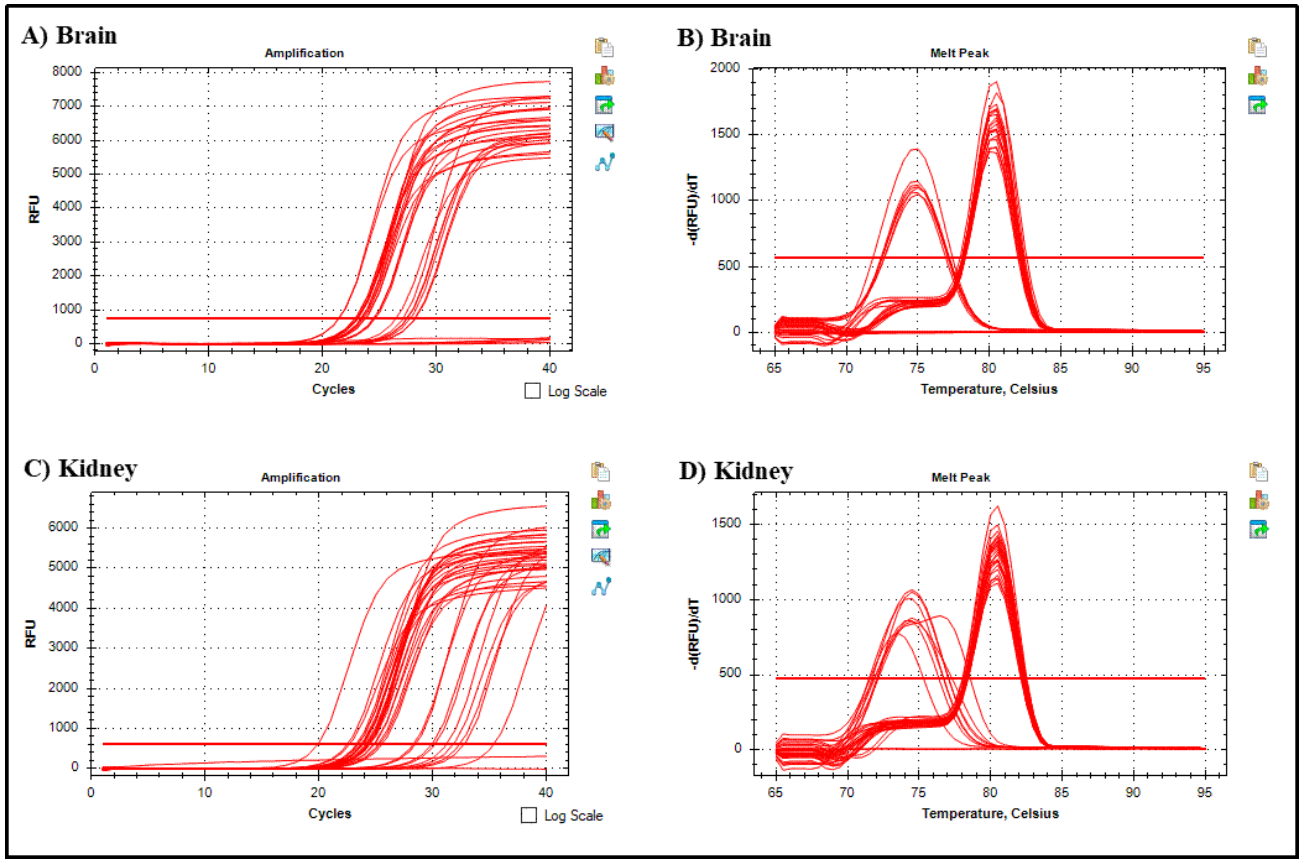


Figure 8.19: Amplification curve and Melt peak analysis of the klotho gene.
(A, C) Amplification curves following qPCR amplification of the klotho gene in the three different mouse groups, namely: Mice overexpressing LRP::FLAG, Empty vector Treated mice and Non-treated mice. This was done for all three tested organs that included the brain (A) and kidney (C). (B, D) Representative qPCR melt peak analysis of the klotho gene in the three different organs of the various mouse groups confirmed that only a single gene product was amplified, however all the no RT's and NTC's displayed low amplification suggesting that primer dimers had occurred.

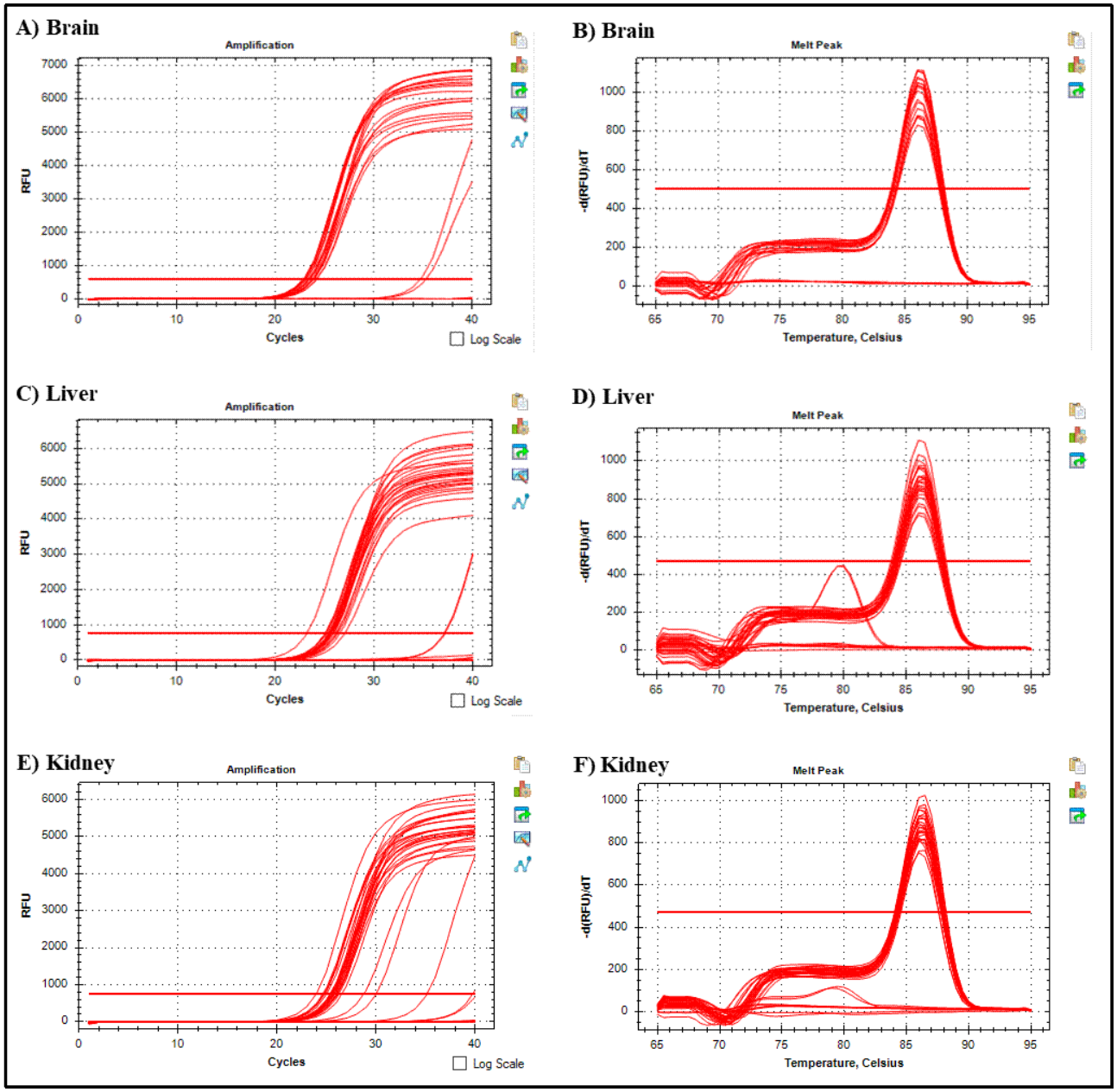


Figure 8.20: Amplification curve and Melt peak analysis of the p53 gene.

(A, C, E) Amplification curves following qPCR amplification of the p53 gene in the three different mouse groups, namely: Mice overexpressing LRP::FLAG, Empty vector Treated mice and Non-treated mice. This was done for all three tested organs that included the brain (A), liver (C) and kidney (E). (B, D, F) Representative qPCR melt peak analysis of the p53 gene in the three different organs of the various mouse groups confirmed that only a single gene product was amplified. No amplification was observed in the NTC's and no RT's.

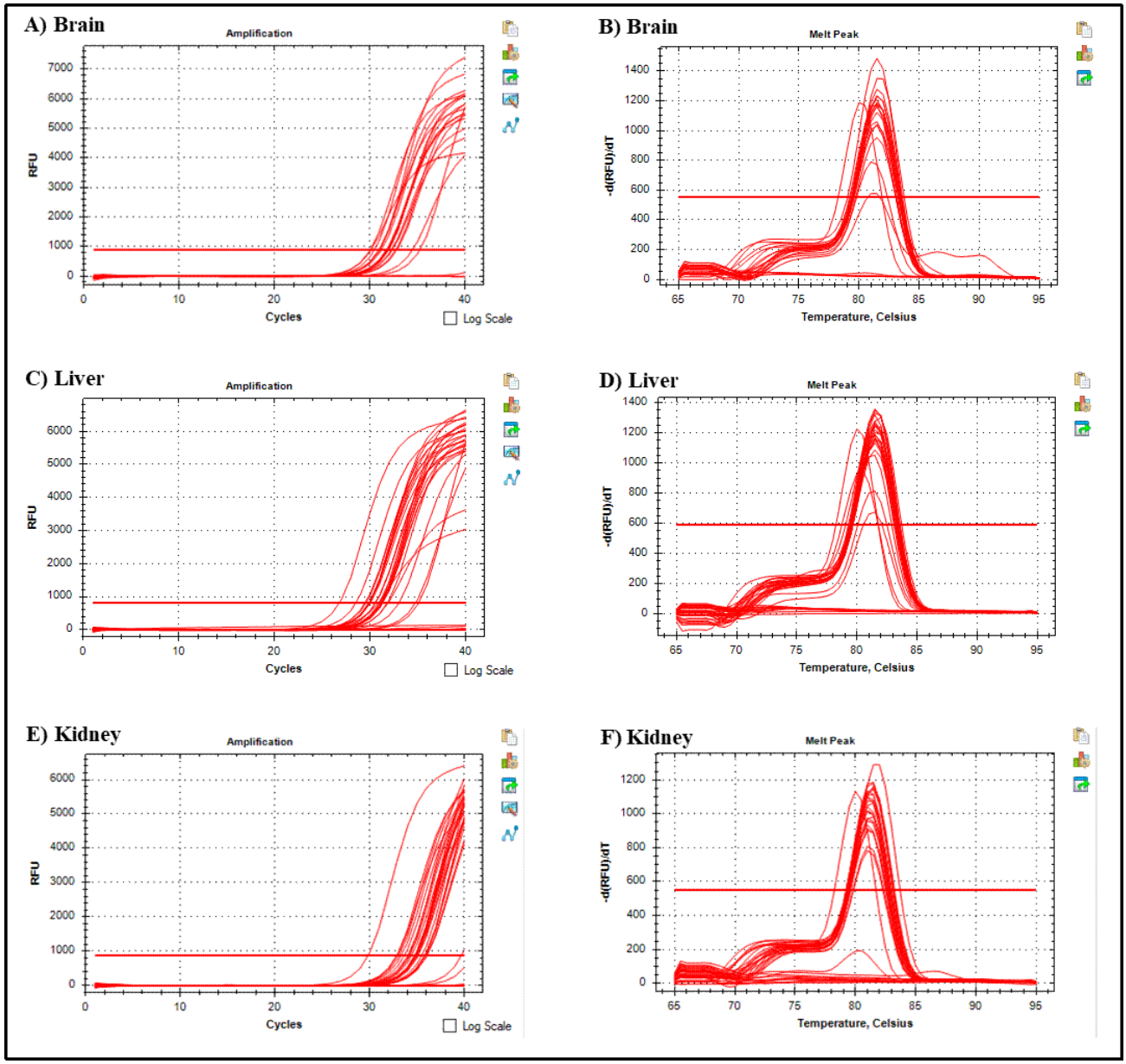


Figure 8.21: Amplification curve and Melt peak analysis of the p16 gene.
(A, C, E) Amplification curves following qPCR amplification of the p16 gene in the three different mouse groups, namely: Mice overexpressing LRP::FLAG, Empty vector Treated mice and Non-treated mice. This was done for all three tested organs that included the brain (A), liver (C) and kidney (E). (B, D, F) Representative qPCR melt peak analysis of the p16 gene in the three different organs of the various mouse groups confirmed that only a single gene product was amplified. No amplification was observed in the NTC's and no RT's.

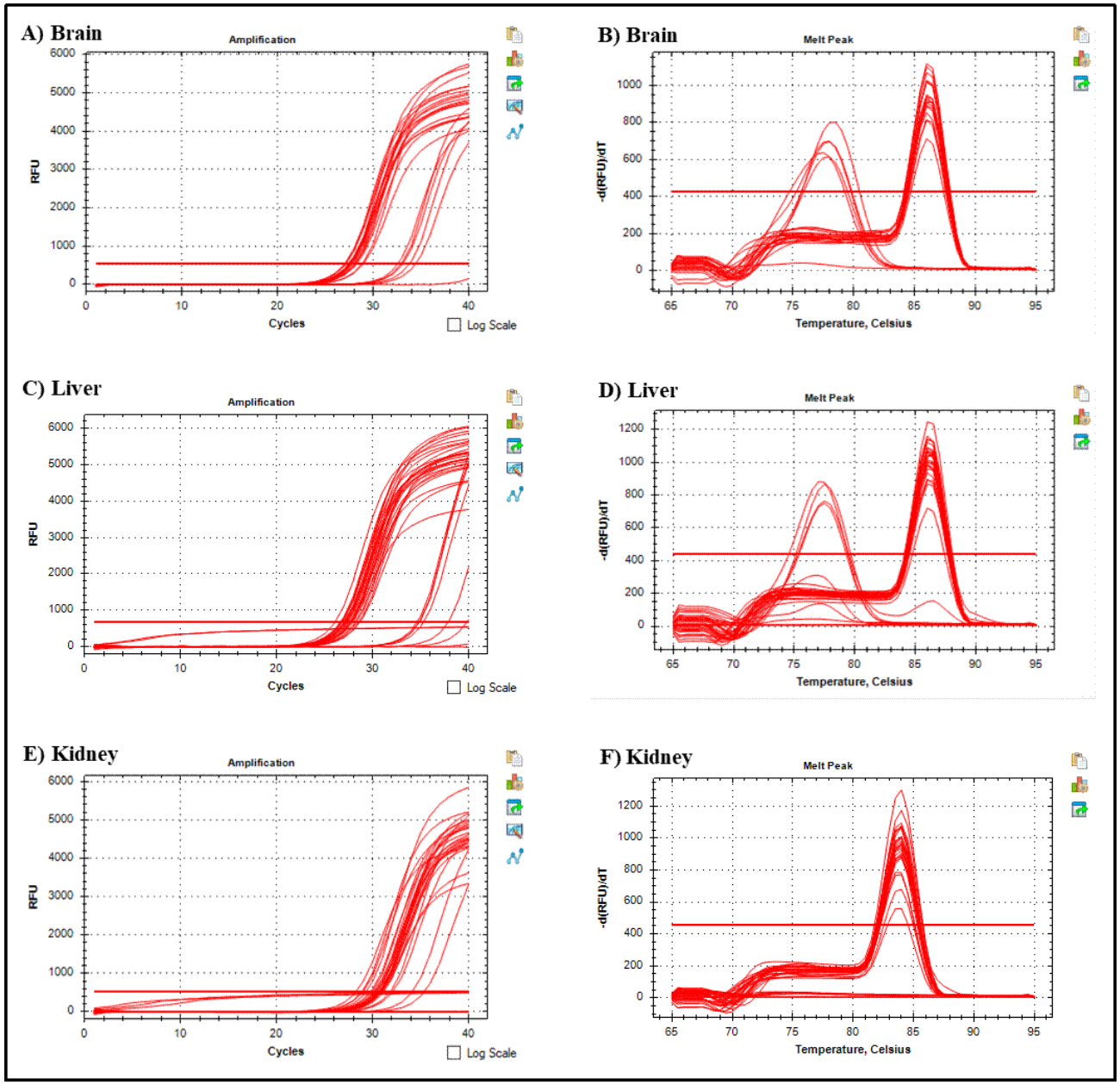


Figure 8.22: Amplification curve and Melt peak analysis of the TERT gene.
(A, C, E) Amplification curves following qPCR amplification of the TERT gene in the three different mouse groups, namely: Mice overexpressing LRP::FLAG, Empty vector Treated mice and Non-treated mice. This was done for all three tested organs that included the brain (A), liver (C) and kidney (E). (B, D, F) Representative qPCR melt peak analysis of the TERT gene in the three different organs of the various mouse groups confirmed that only a single gene product was amplified. There was low amplification for the no RT's and NTC's for the brain (B) and liver (D) suggesting the formation of primer dimers. No amplification was observed in the NTC's and no RT's for the kidney (F).

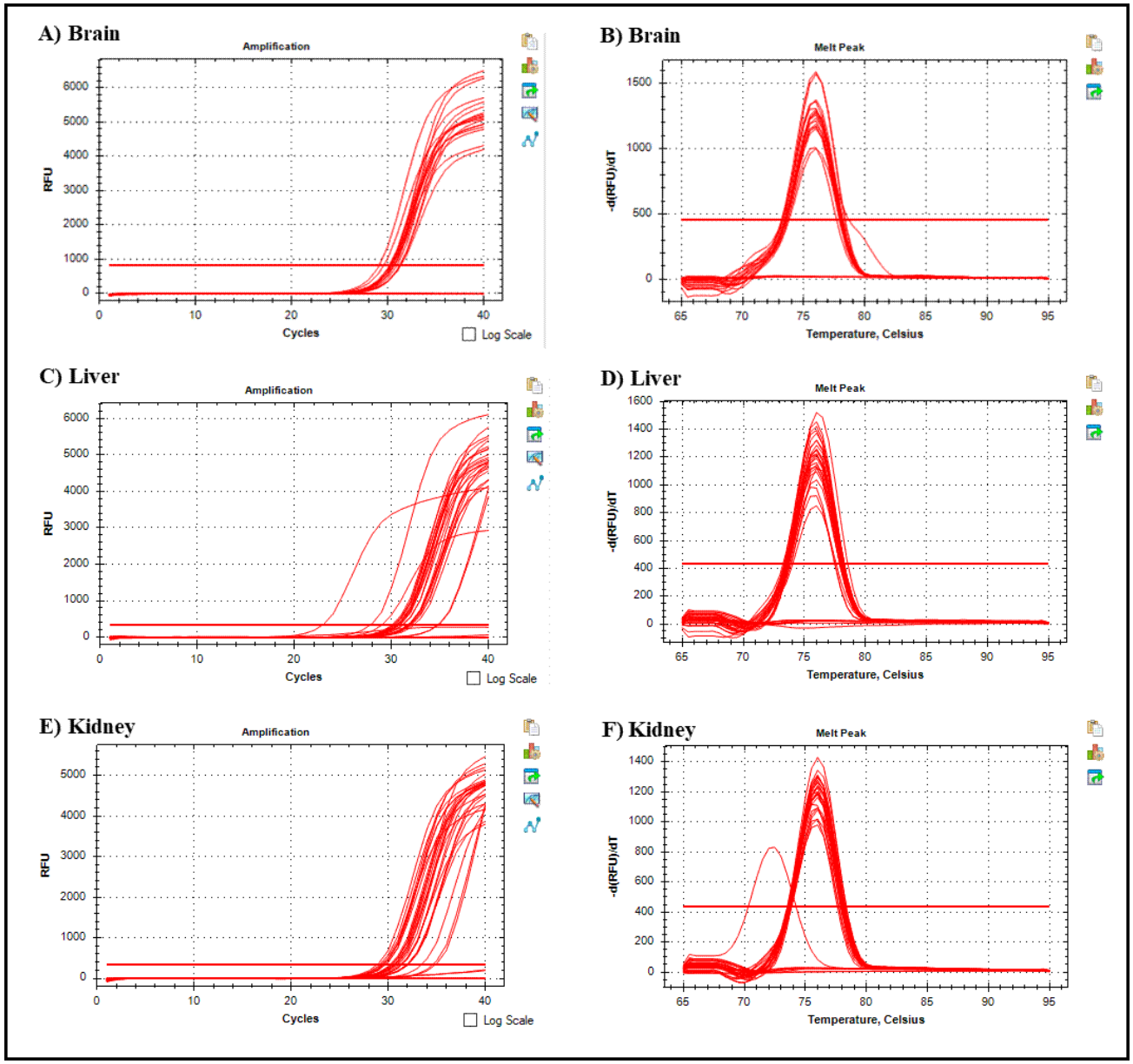


Figure 8.23: Amplification curve and Melt peak analysis of the IL6 gene.
(A, C, E) Amplification curves following qPCR amplification of the IL6 gene in the three different mouse groups, namely: Mice overexpressing LRP::FLAG, Empty vector Treated mice and Non-treated mice. This was done for all three tested organs that included the brain (A), liver (C) and kidney (E). (B, D, F) Representative qPCR melt peak analysis of the IL6 gene in the three different organs of the various mouse groups confirmed that only a single gene product was amplified. However, one sample for the kidney (F) was found to amplify poorly. No amplification was observed in the NTC's and no RT's.

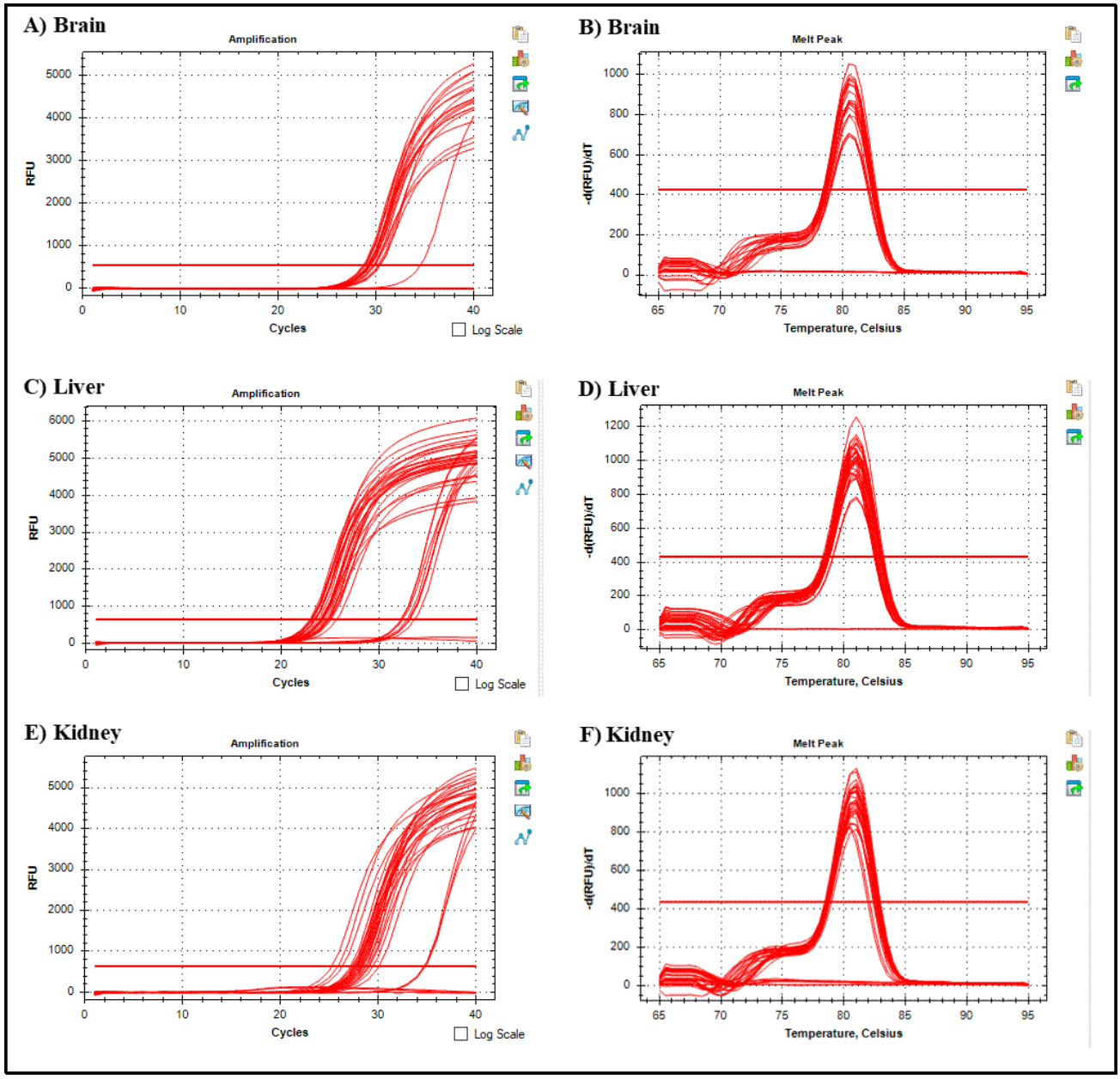


Figure 8.24: Amplification curve and Melt peak analysis of the IL8 gene.
(A, C, E) Amplification curves following qPCR amplification of the IL8 gene in the three different mouse groups, namely: Mice overexpressing LRP::FLAG, Empty vector Treated mice and Non-treated mice. This was done for all three tested organs that included the brain (A), liver (C) and kidney (E). (B, D, F) Representative qPCR melt peak analysis of the IL8 gene in the three different organs of the various mouse groups confirmed that only a single gene product was amplified. No amplification was observed in the NTC's and no RT's.

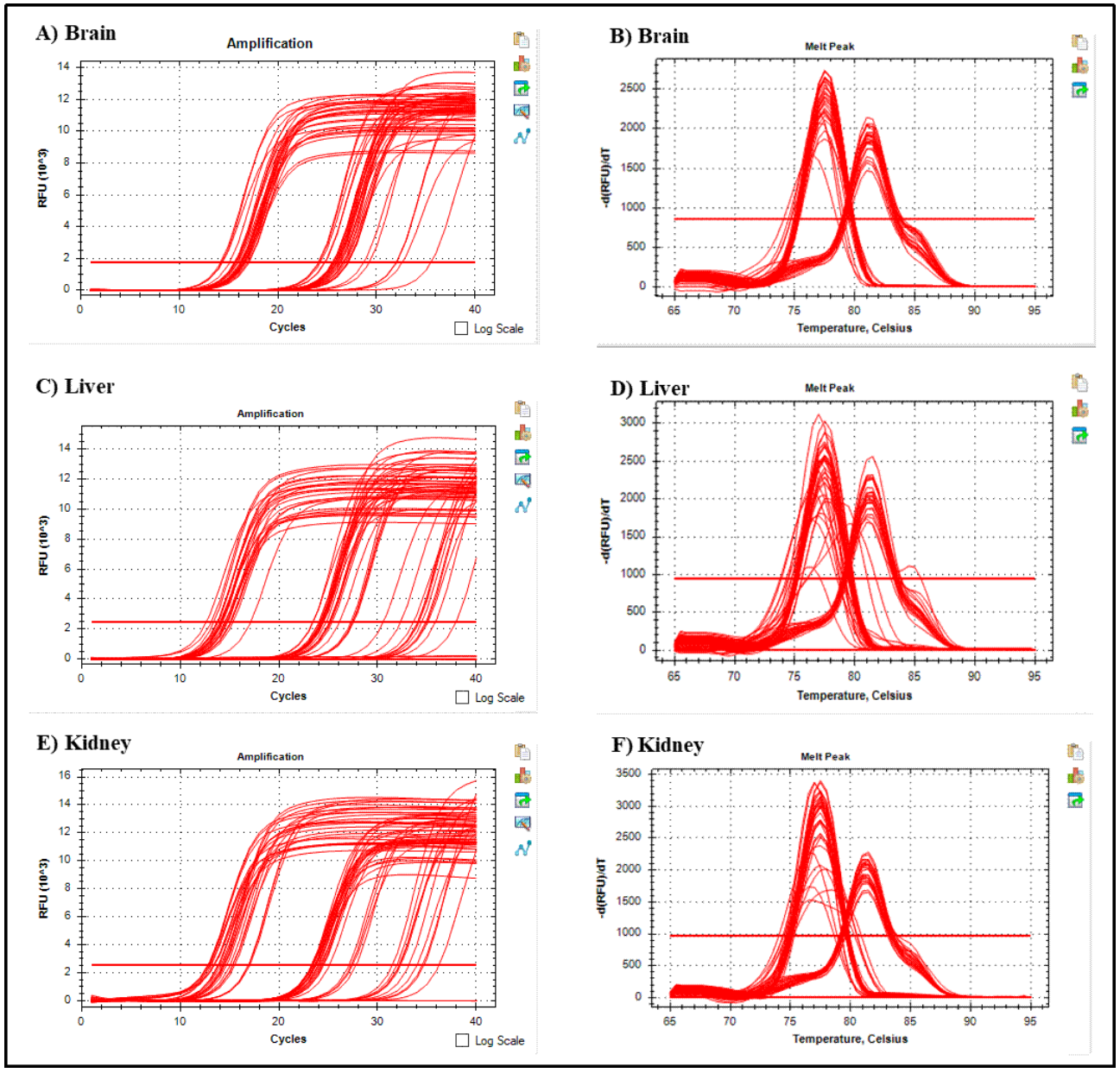


Figure 8.25: Amplification curve and Melt peak analysis of the mtDNA and nuclear specific DNA sequence (hexokinase).

(A, C, E) Amplification curves following qPCR amplification of mtDNA as well as a nuclear specific sequence in the three different mouse groups, namely: Mice overexpressing LRP::FLAG, Empty vector Treated mice and Non-treated mice. The curves show that two distinct genomic products were amplified; one for the mtDNA and the other for the nuclear specific sequence. This was done for all three tested organs that included the brain (A), liver (C) and kidney (E). (B, D, F) Representative qPCR melt peak analysis of the LRP gene in the three different organs of the various mouse groups confirmed that only a single gene product was amplified per primer set evidenced by the two separate peaks. No amplification was observed in the NTC's and no RT's.

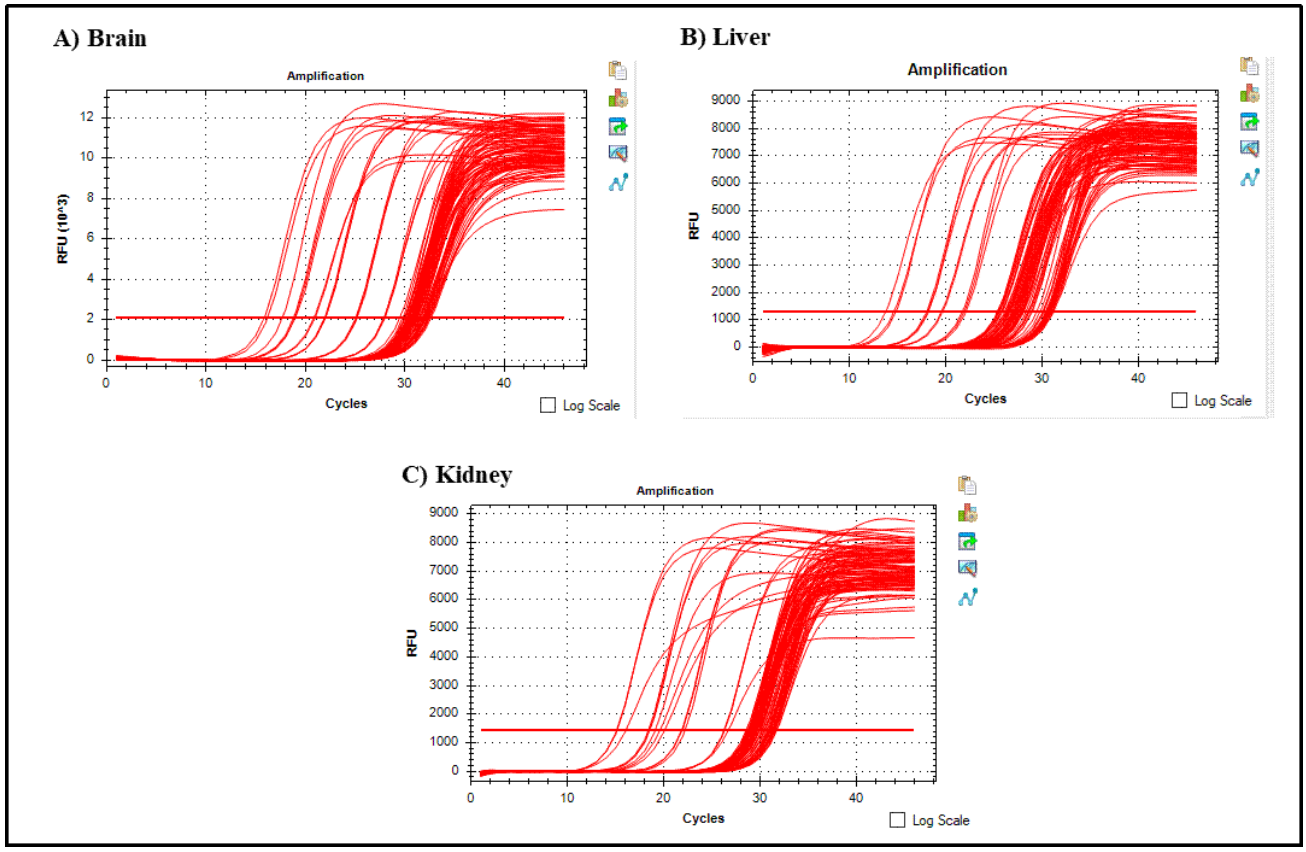


Figure 8.26: Amplification curves for telomerase activity in the brain, liver and kidney.
(A, B, C) Amplification curves following telomerase extension and subsequent qPCR amplification of a telomeric substrate to quantify telomerase activity in the three different mouse groups, namely: Mice overexpressing LRP::FLAG, Empty vector Treated mice and Non-treated mice. This was done for all three tested organs that included the brain (A), liver (C) and kidney (E). Minimal amplification was observed in the NTC's and Heat treated (HT) controls.

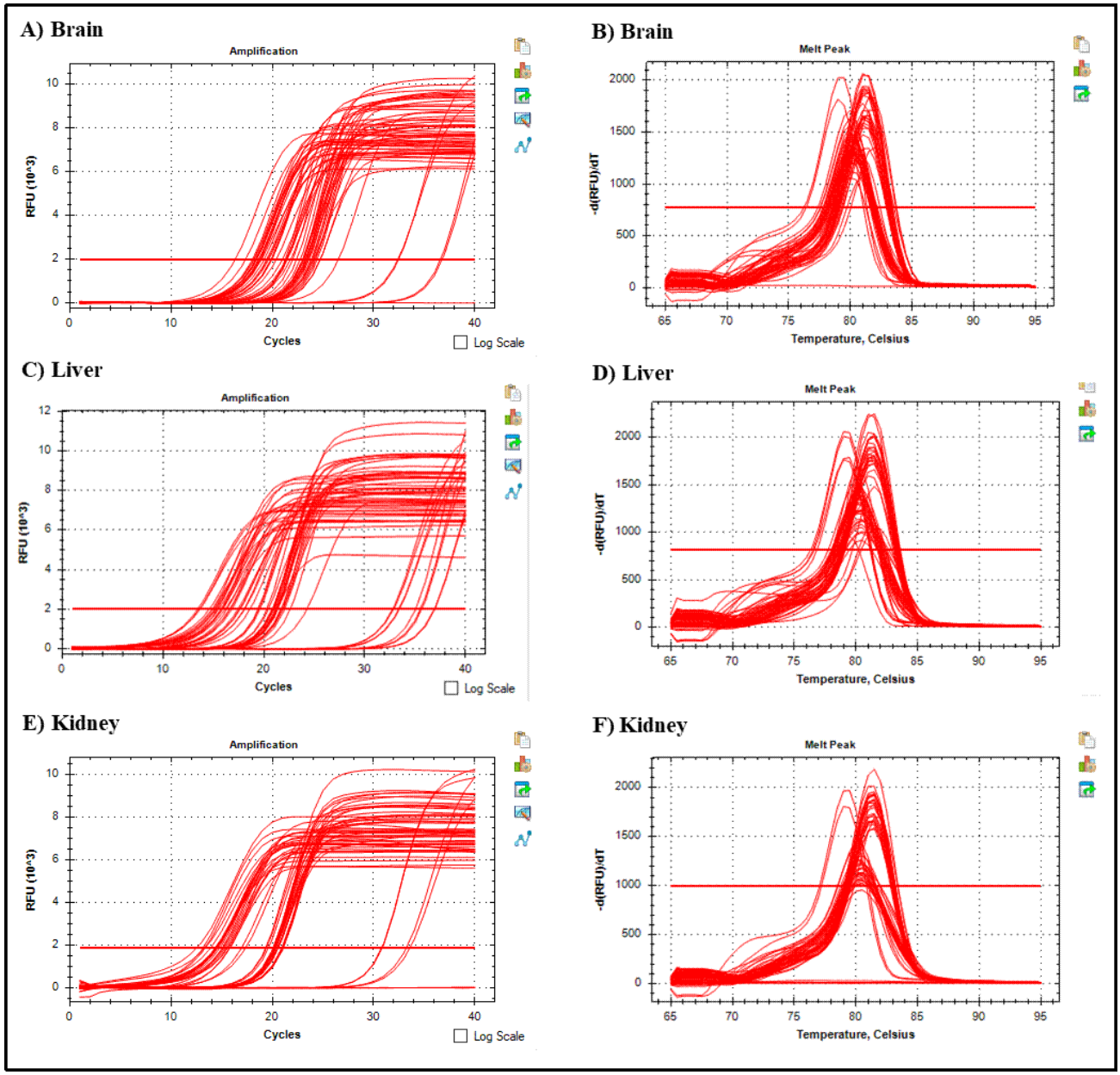


Figure 8.27: Amplification curve and Melt peak analysis for telomere length as well as the reference gene 36B4.

(A, C, E) Amplification curves following qPCR amplification of the 36B4 reference gene as well as the telomeres in the three different mouse groups, namely: Mice overexpressing LRP::FLAG, Empty vector Treated mice and Non-treated mice. The curves show that two distinct genomic products were amplified; one for the amplified telomeres and the other for the reference gene 36B4. This was done for all three tested organs that included the brain (A), liver (C) and kidney (E). (B, D, F) Representative qPCR melt peak analysis of the LRP gene in the three different organs of the various mouse groups confirmed that only a single gene product was amplified per primer set evidenced by the two separate peaks. No amplification was observed in the NTC's and no RT's.

Appendix C

Enlarged Figures

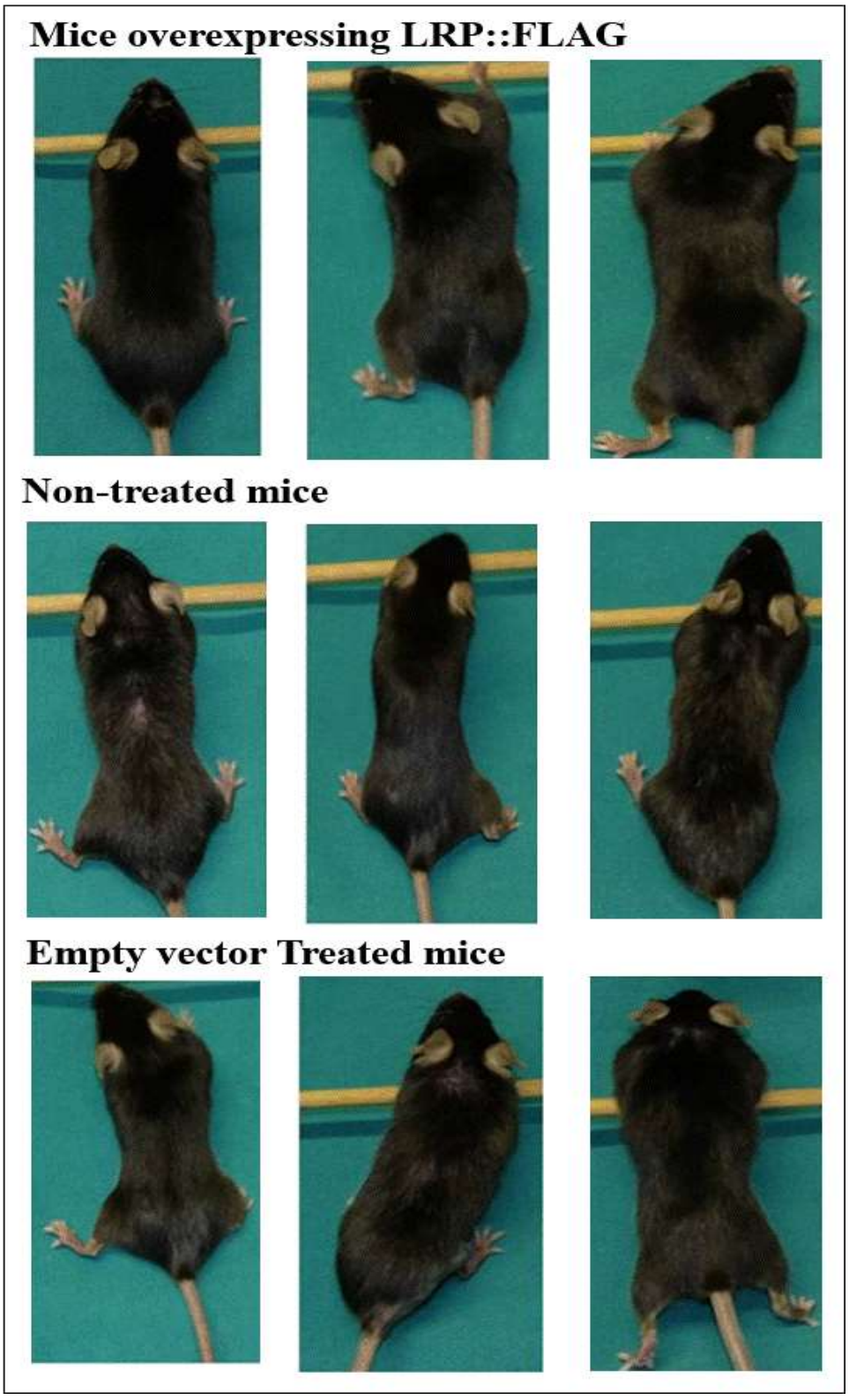


Figure 8.28: Qualitative analysis of mouse hair greying

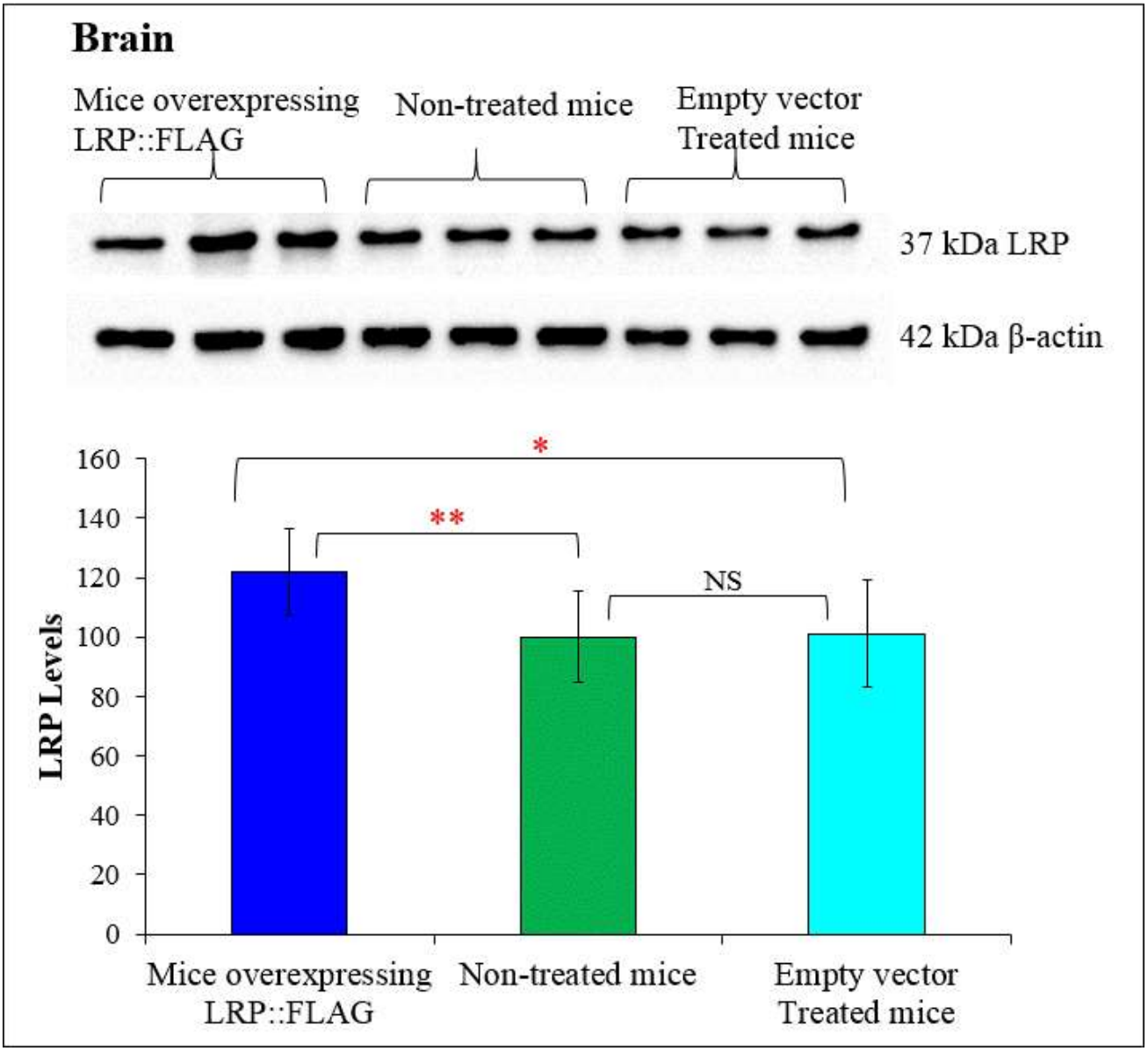


Figure 8.29: LRP::FLAG overexpression significantly elevates total LRP levels in the brain of aged mice.

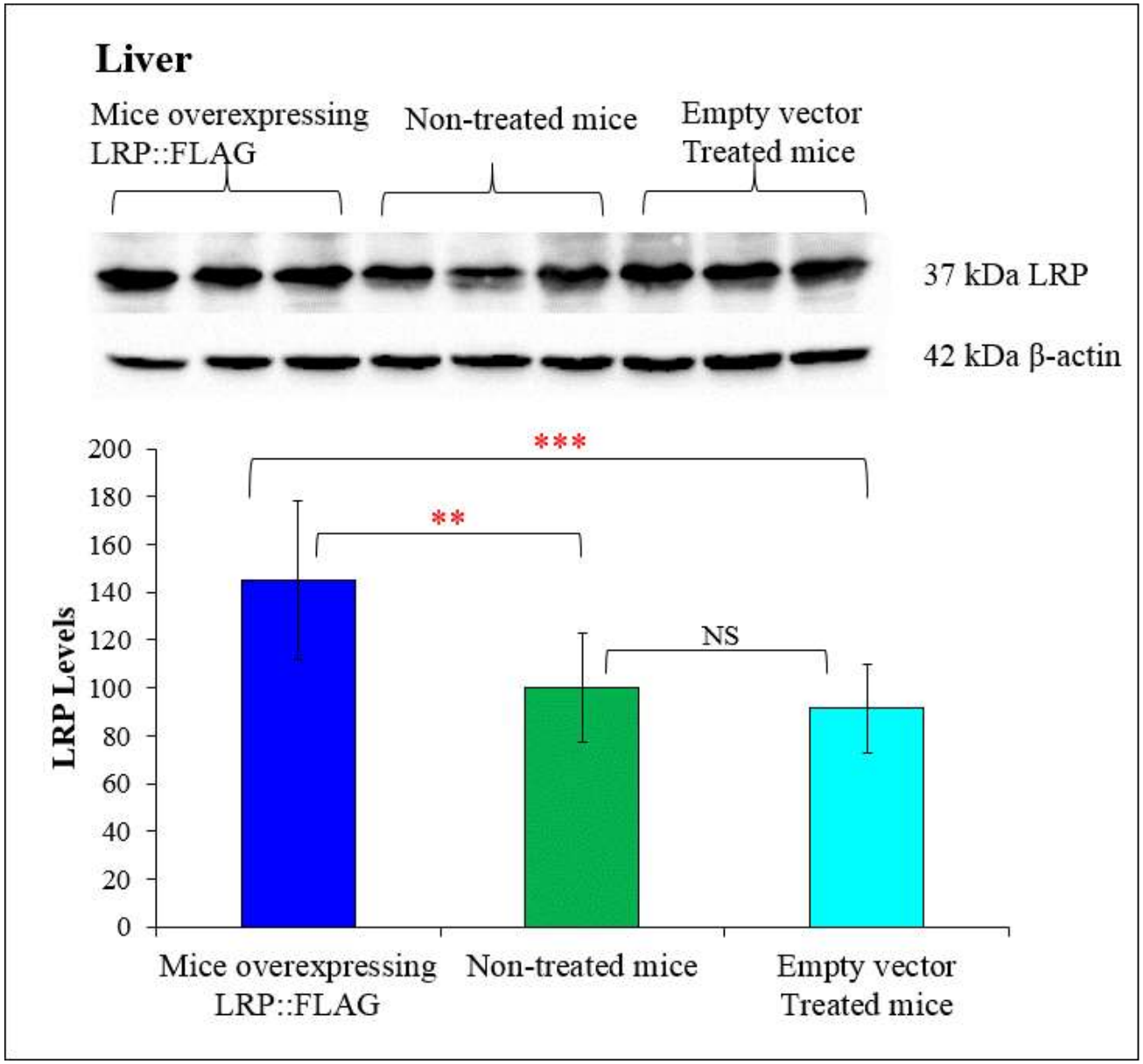


Figure 8.30: LRP::FLAG overexpression significantly elevates total LRP levels in the liver of aged mice.

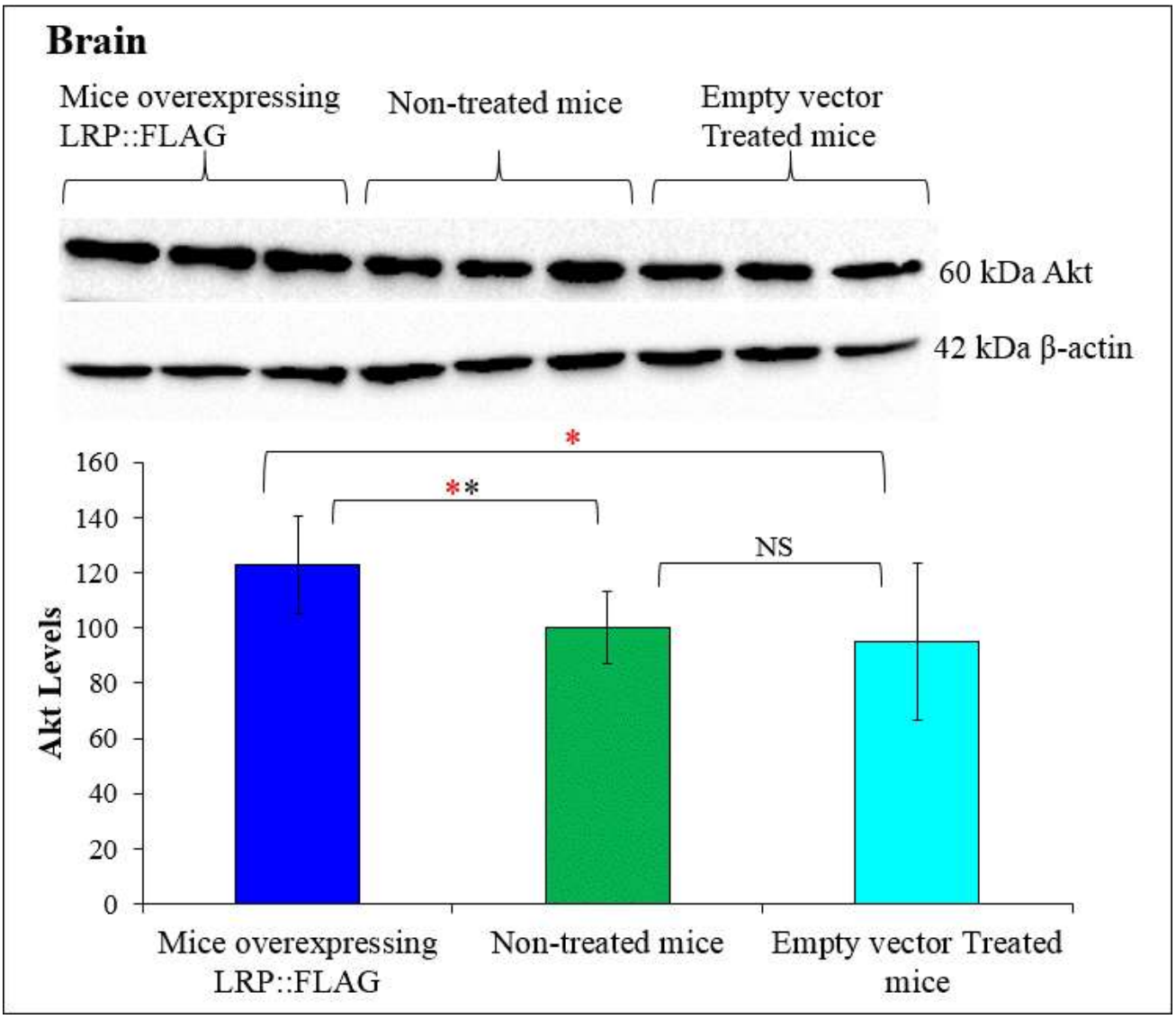


Figure 8.31: LRP::FLAG overexpression significantly elevates total Akt levels in the brain of aged mice.

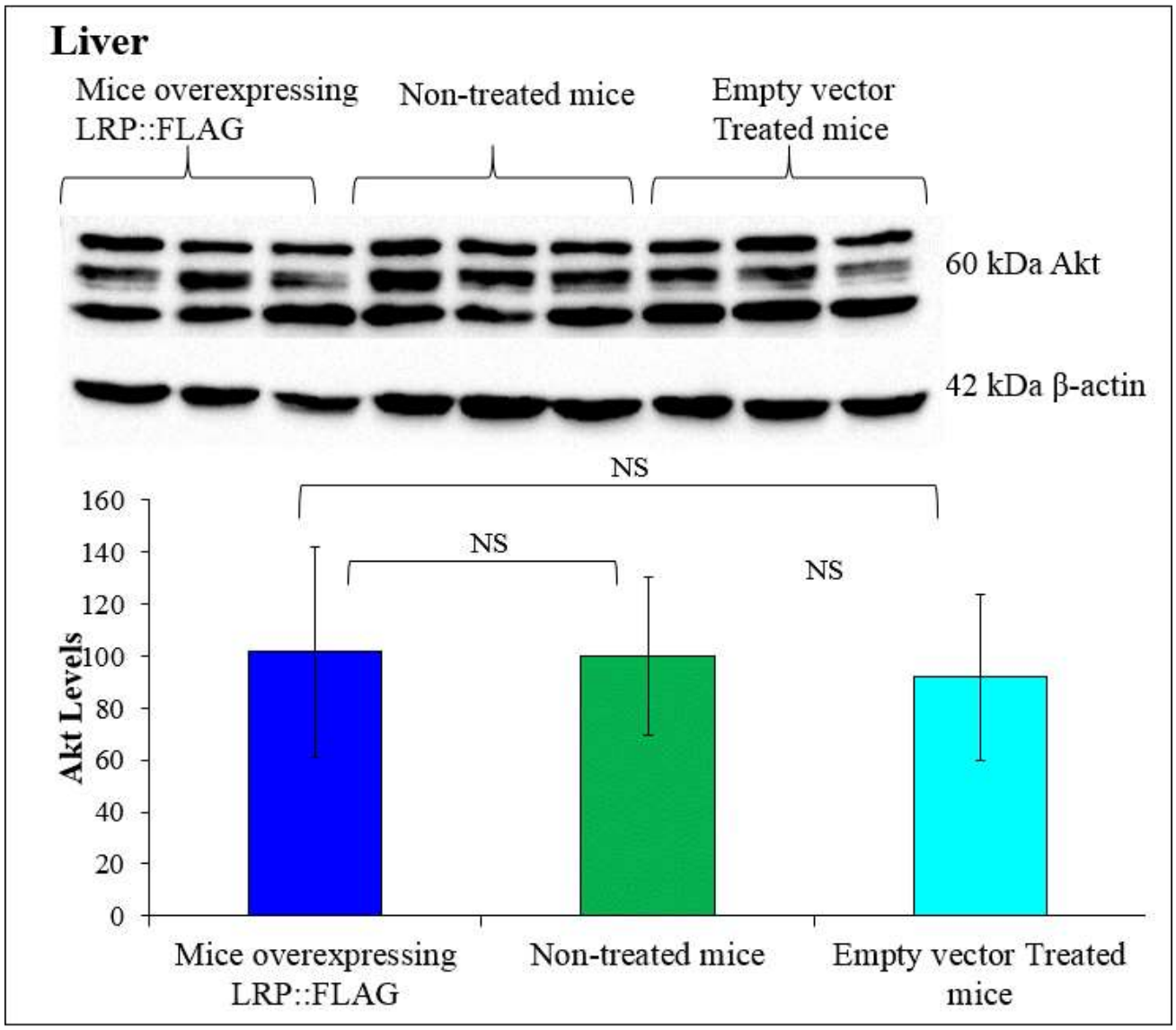


Figure 8.32: LRP::FLAG overexpression induces no significant change in total Akt levels within the liver of aged mice.

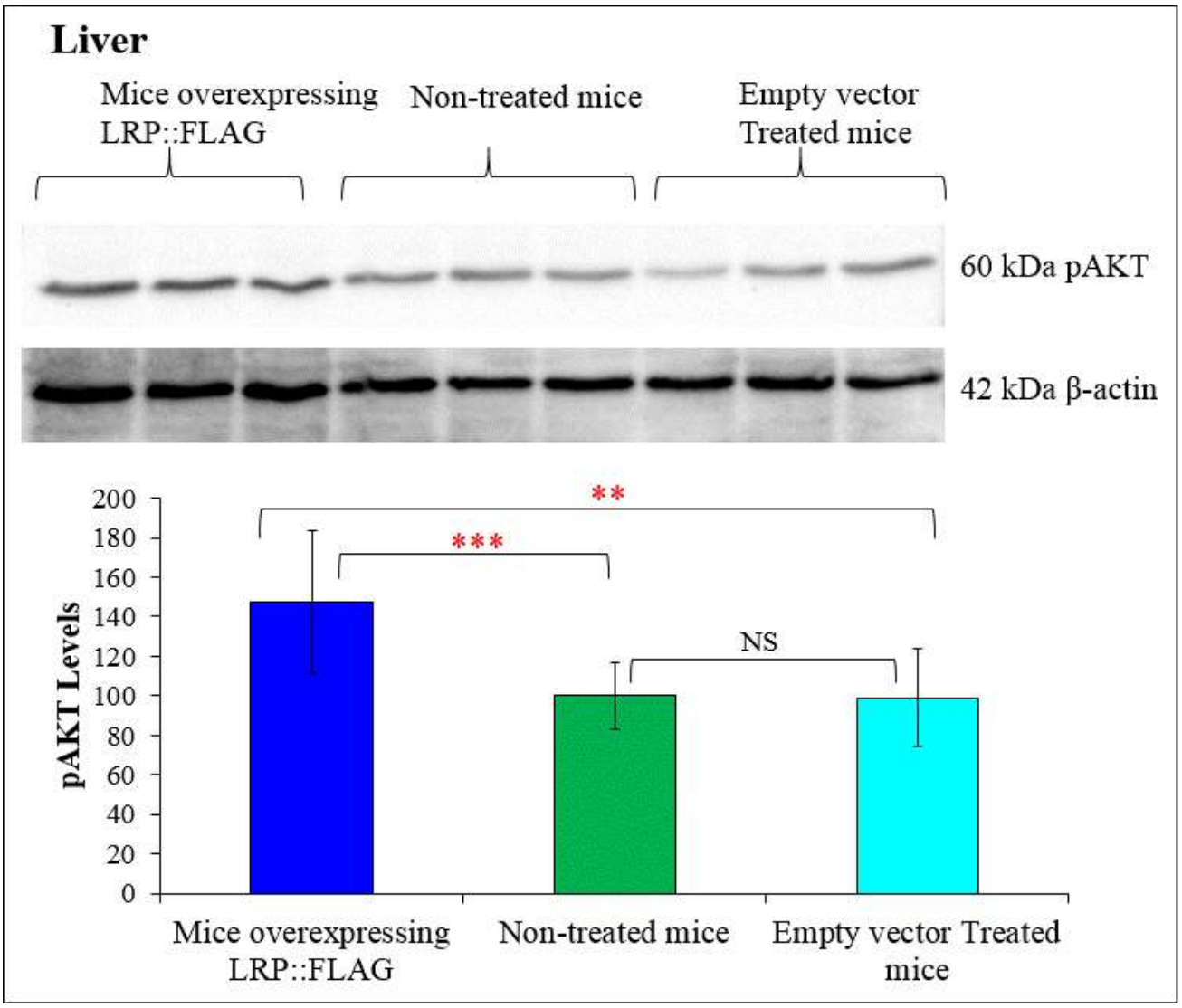


Figure 8.33: LRP::FLAG overexpression significantly elevates phospho-Akt levels in the liver of aged mice.

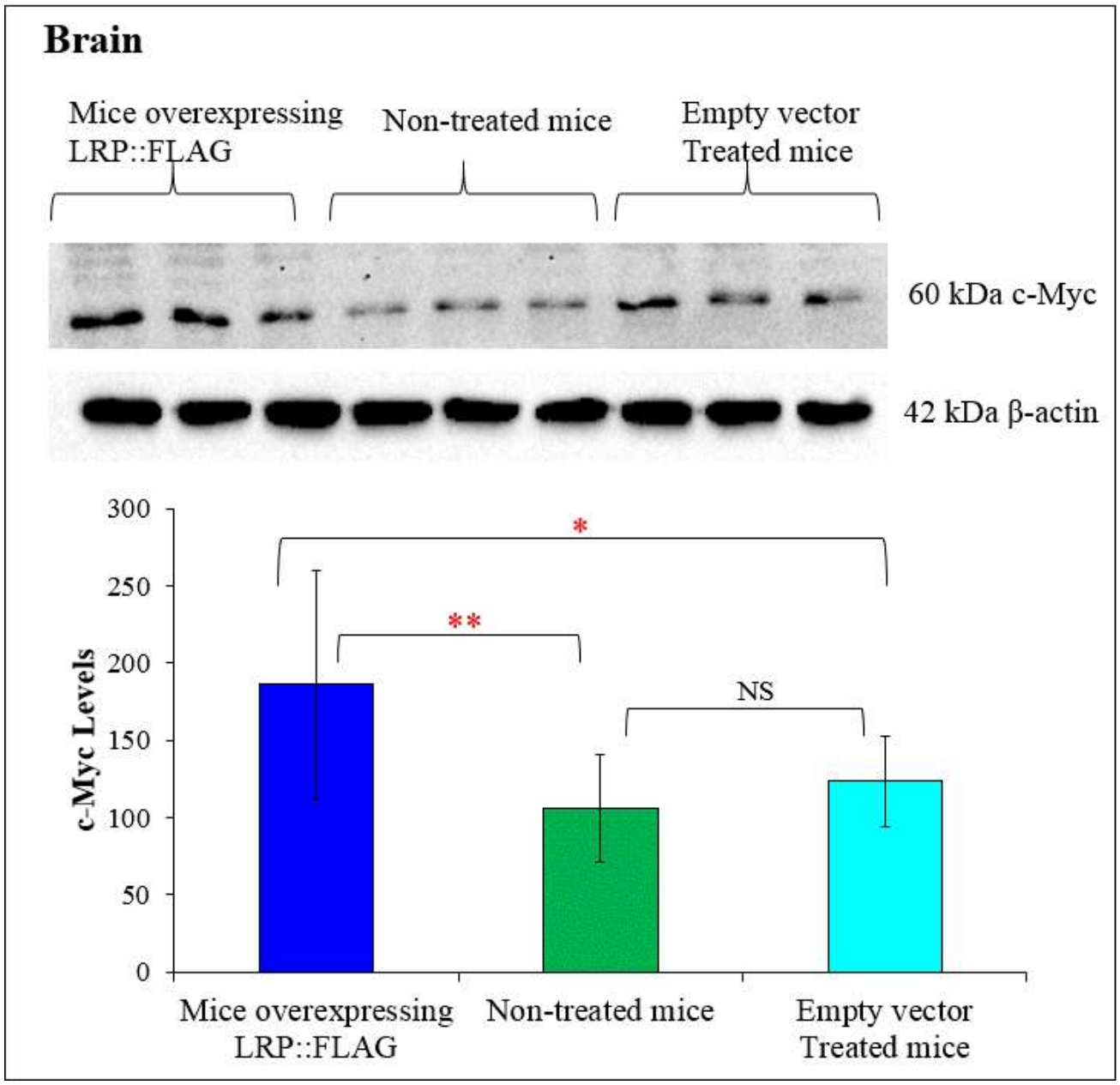


Figure 8.34: LRP::FLAG overexpression significantly elevates c-Myc levels in the brain of aged mice.

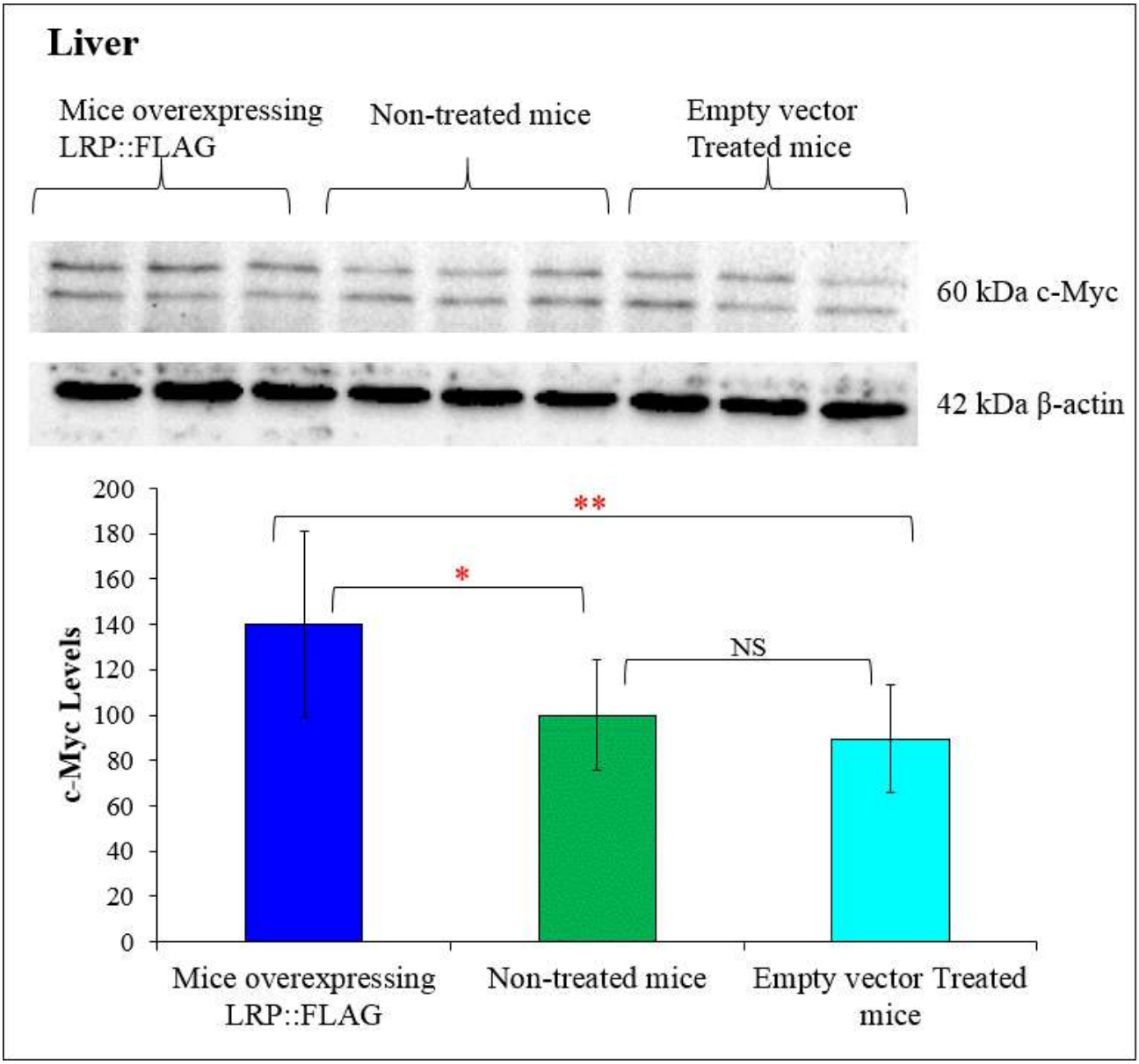


Figure 8.35: LRP::FLAG overexpression significantly elevates c-Myc levels in the liver of aged mice.

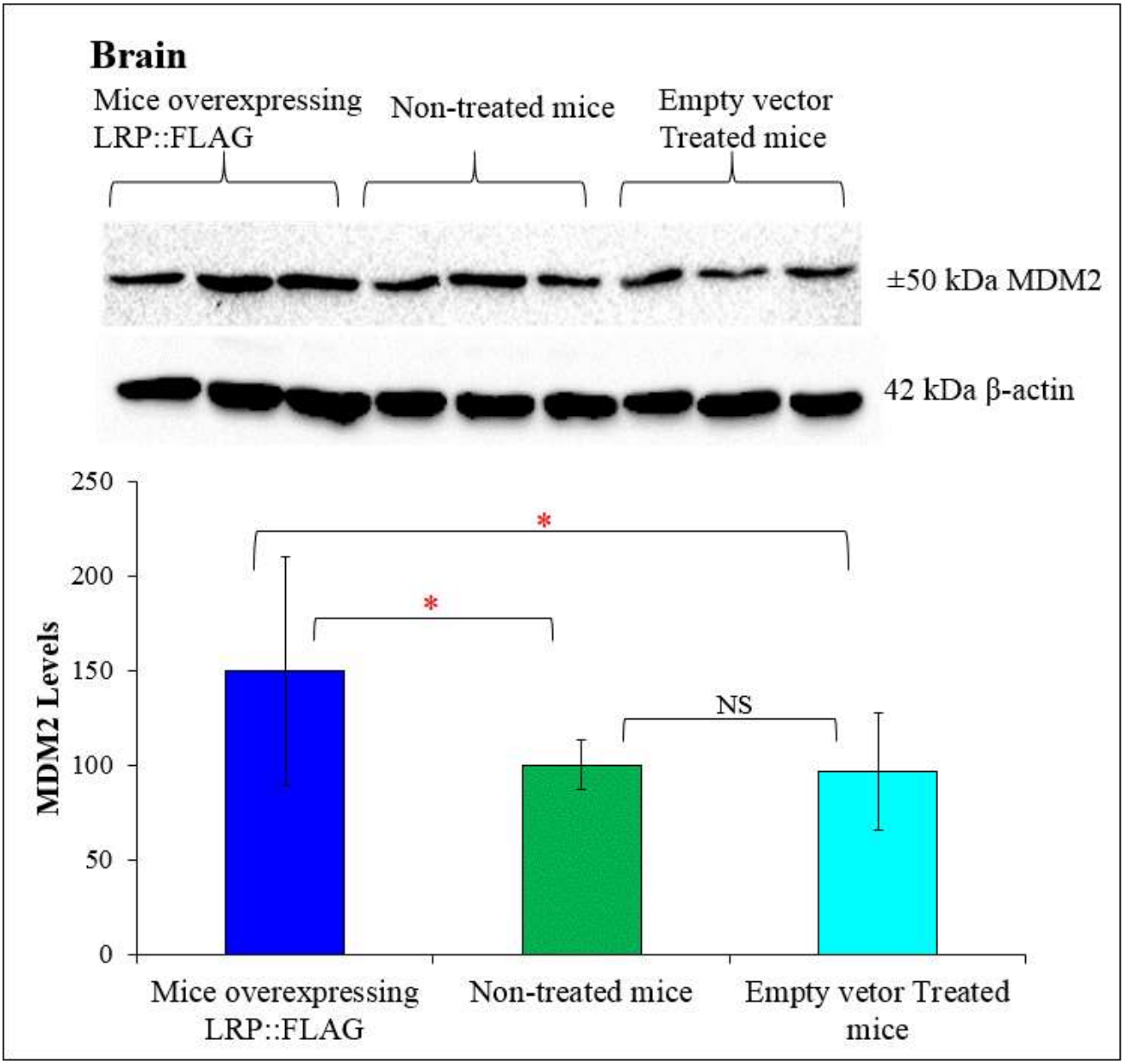


Figure 8.36: LRP::FLAG overexpression significantly elevates total MDM2 levels in the brain of aged mice.

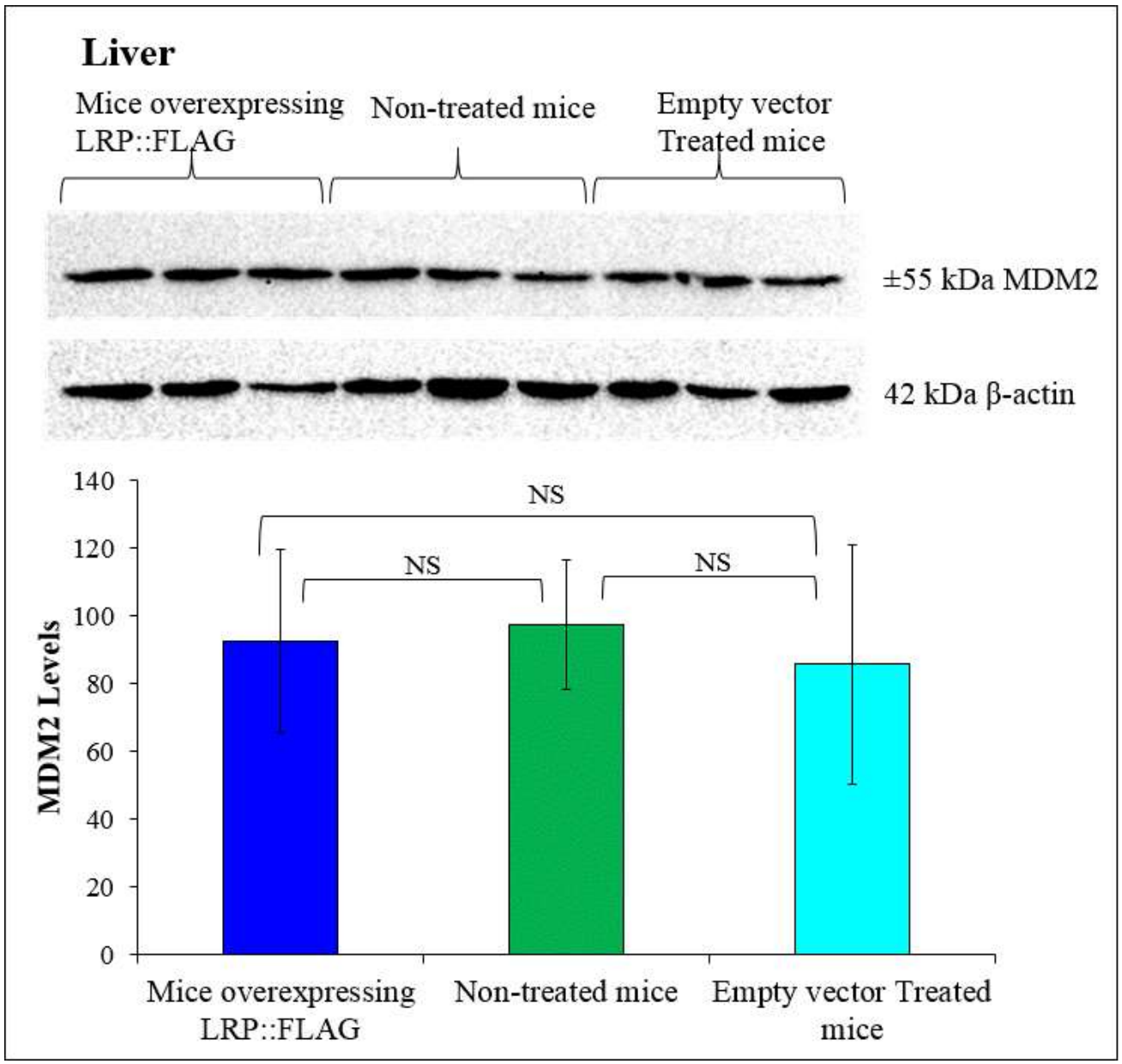


Figure 8.37: LRP::FLAG overexpression induces no significant change in total MDM2 levels in the liver of aged mice.

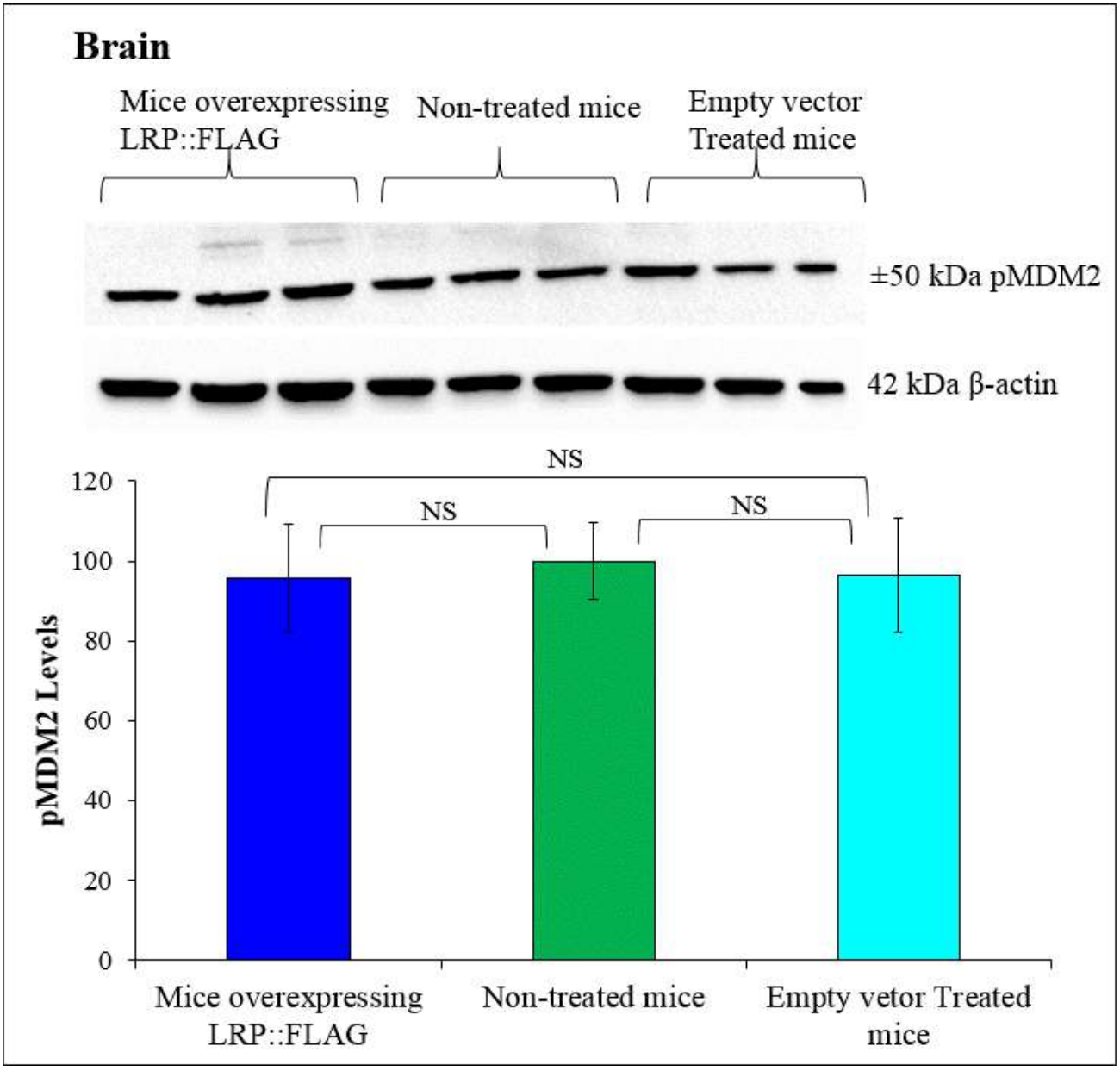


Figure 8.38: LRP::FLAG overexpression induces no significant change in phospho-MDM2 levels in the brain of aged mice.

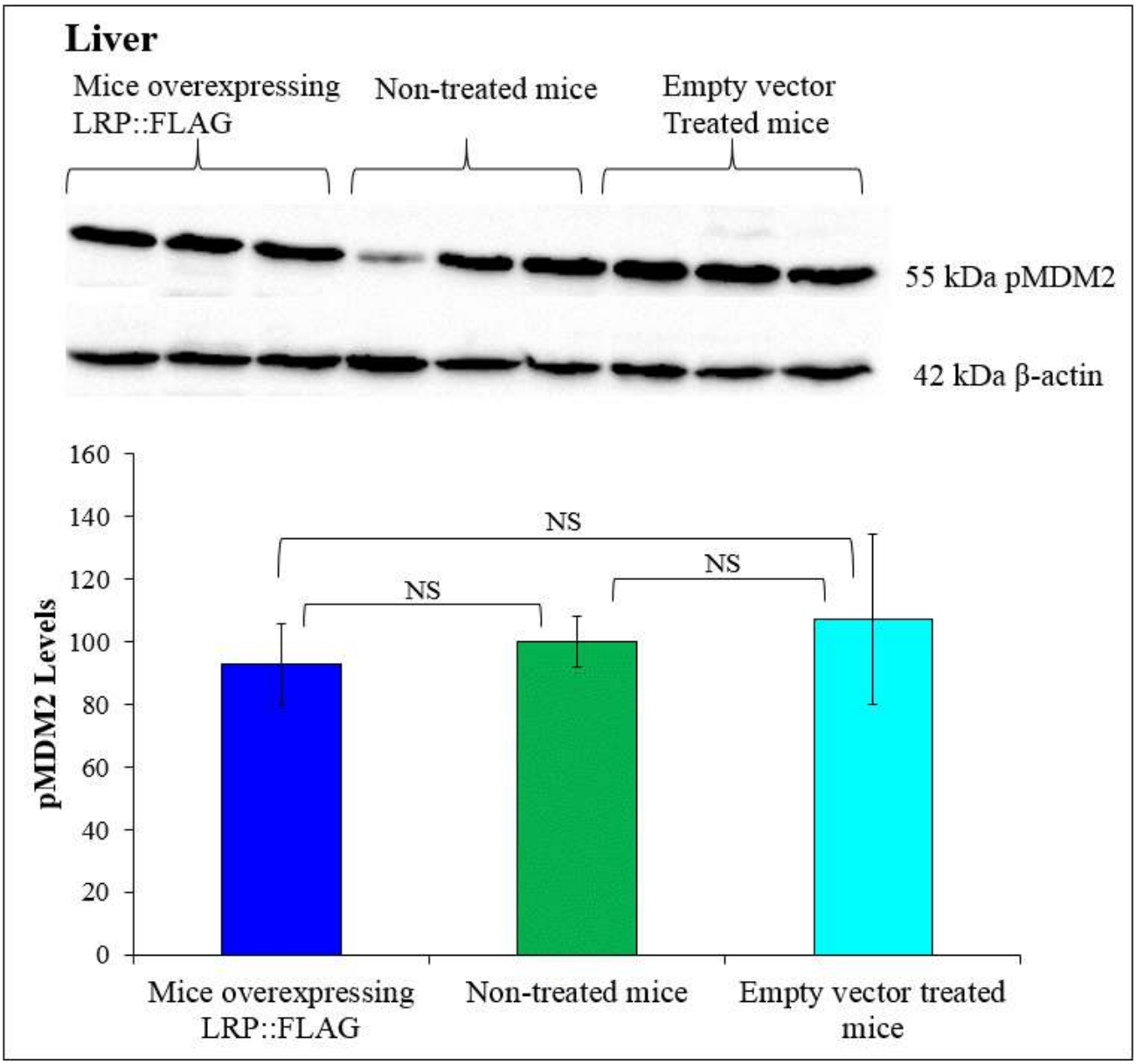


Figure 8.39: LRP::FLAG overexpression induces no significant change in phospho-MDM2 levels in the brain of aged mice.

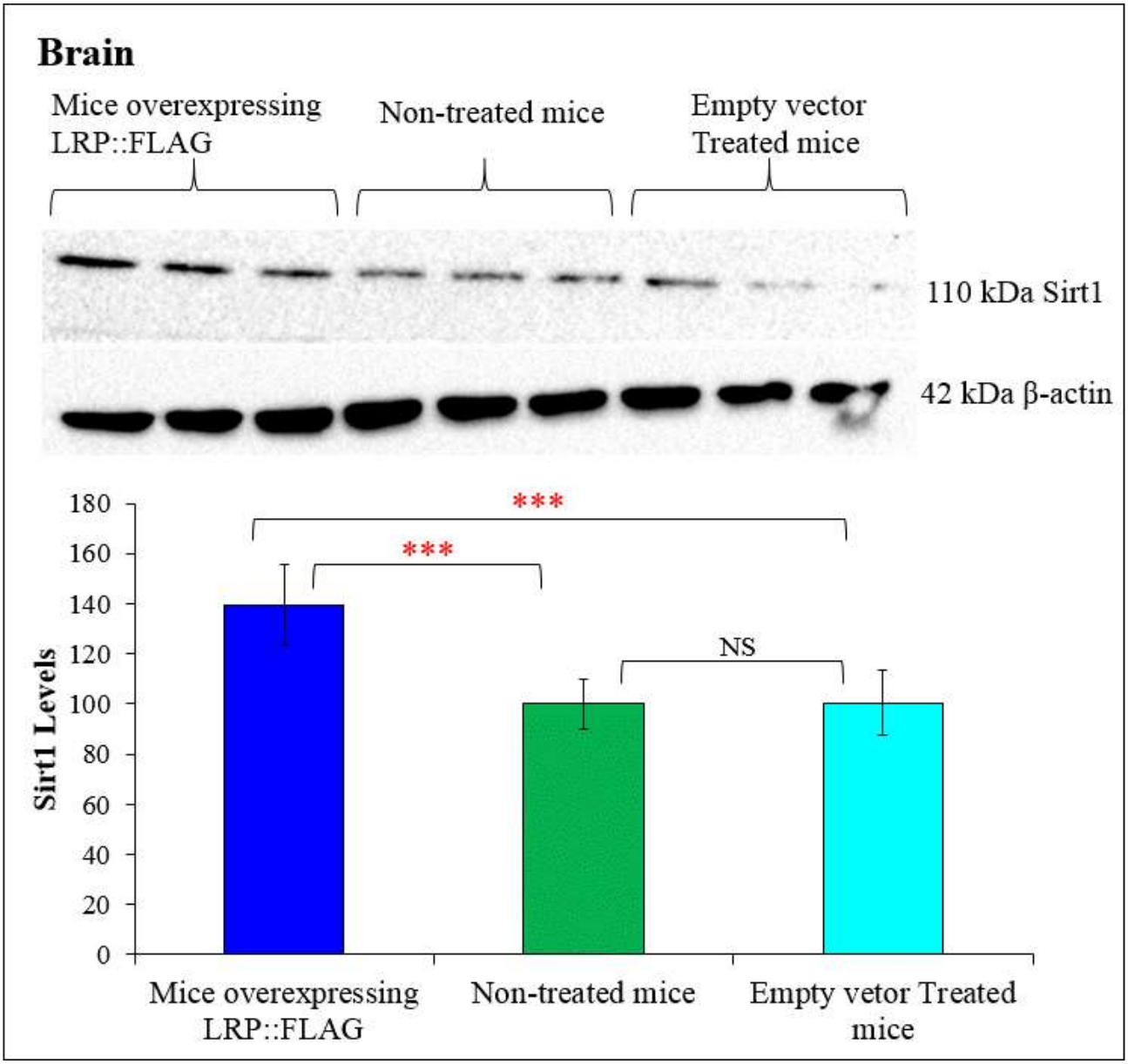


Figure 8.40: LRP::FLAG overexpression significantly increases Sirt1 levels in the brain of aged mice.

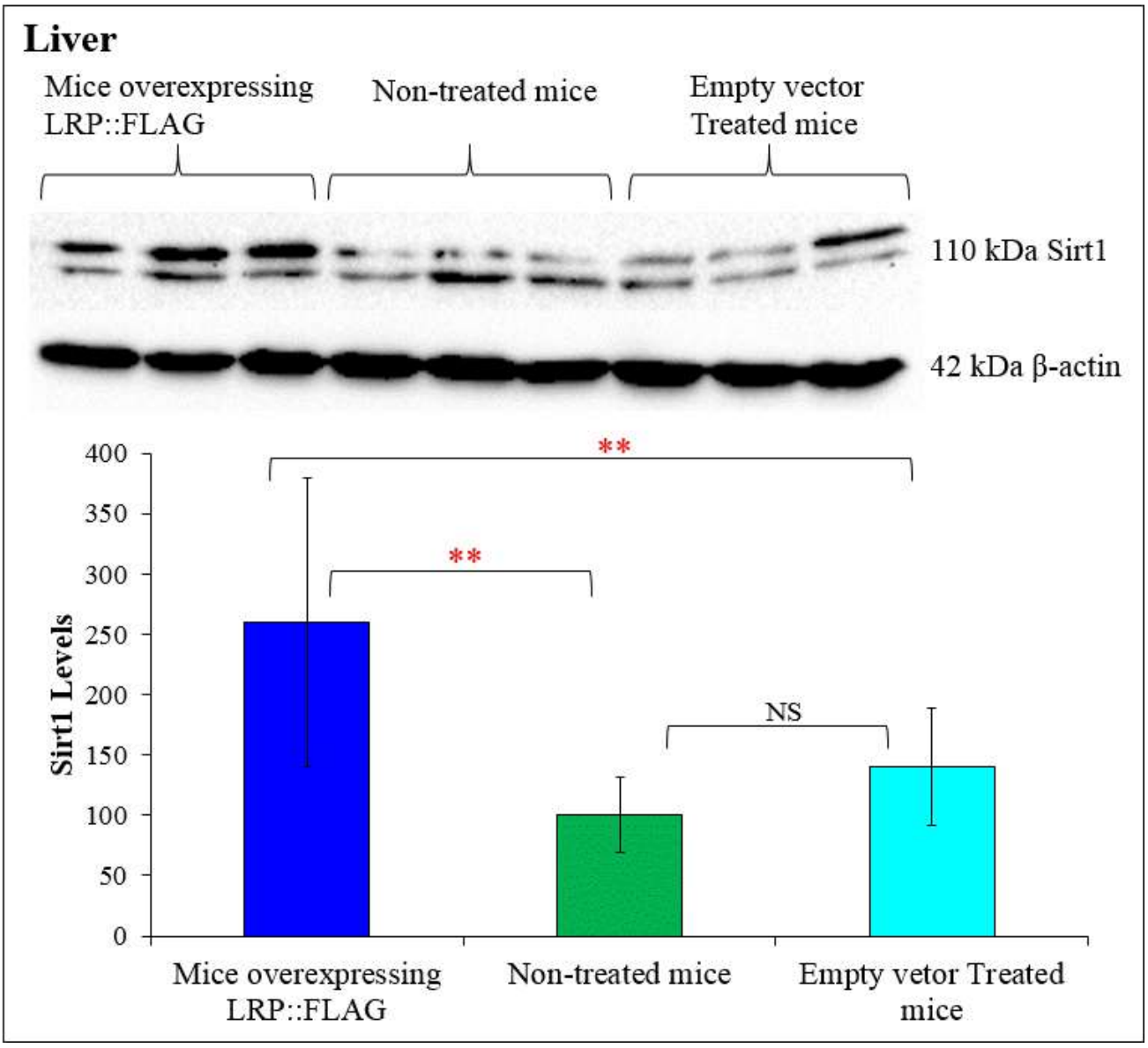


Figure 8.41: LRP::FLAG overexpression significantly elevates Sirt1 levels in the liver of aged mice.

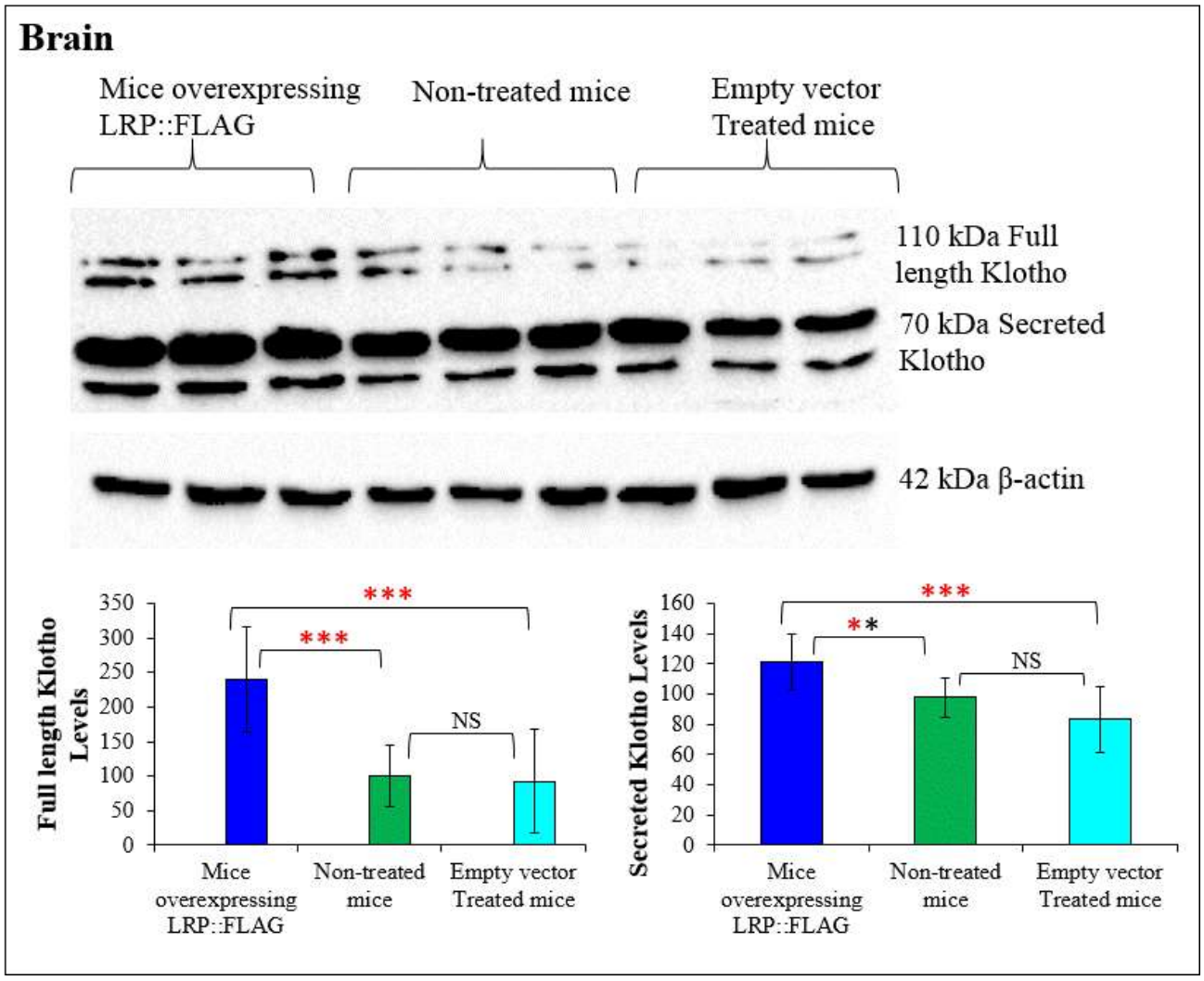


Figure 8.42: LRP::FLAG overexpression significantly elevates full length and secreted klotho levels in the brain of aged mice.

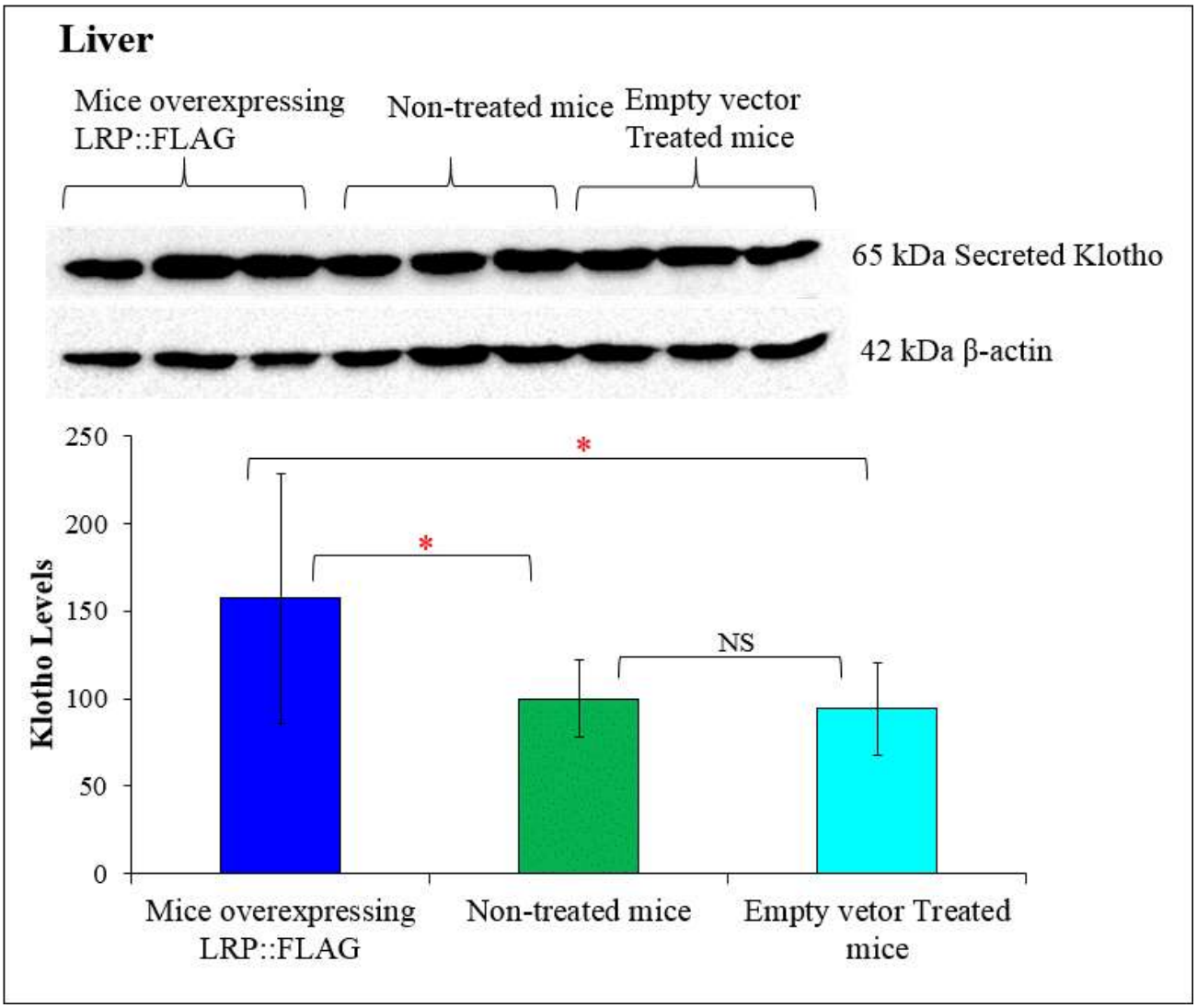


Figure 8.43: LRP::FLAG overexpression significantly elevates secreted klotho levels in the liver of aged mice.

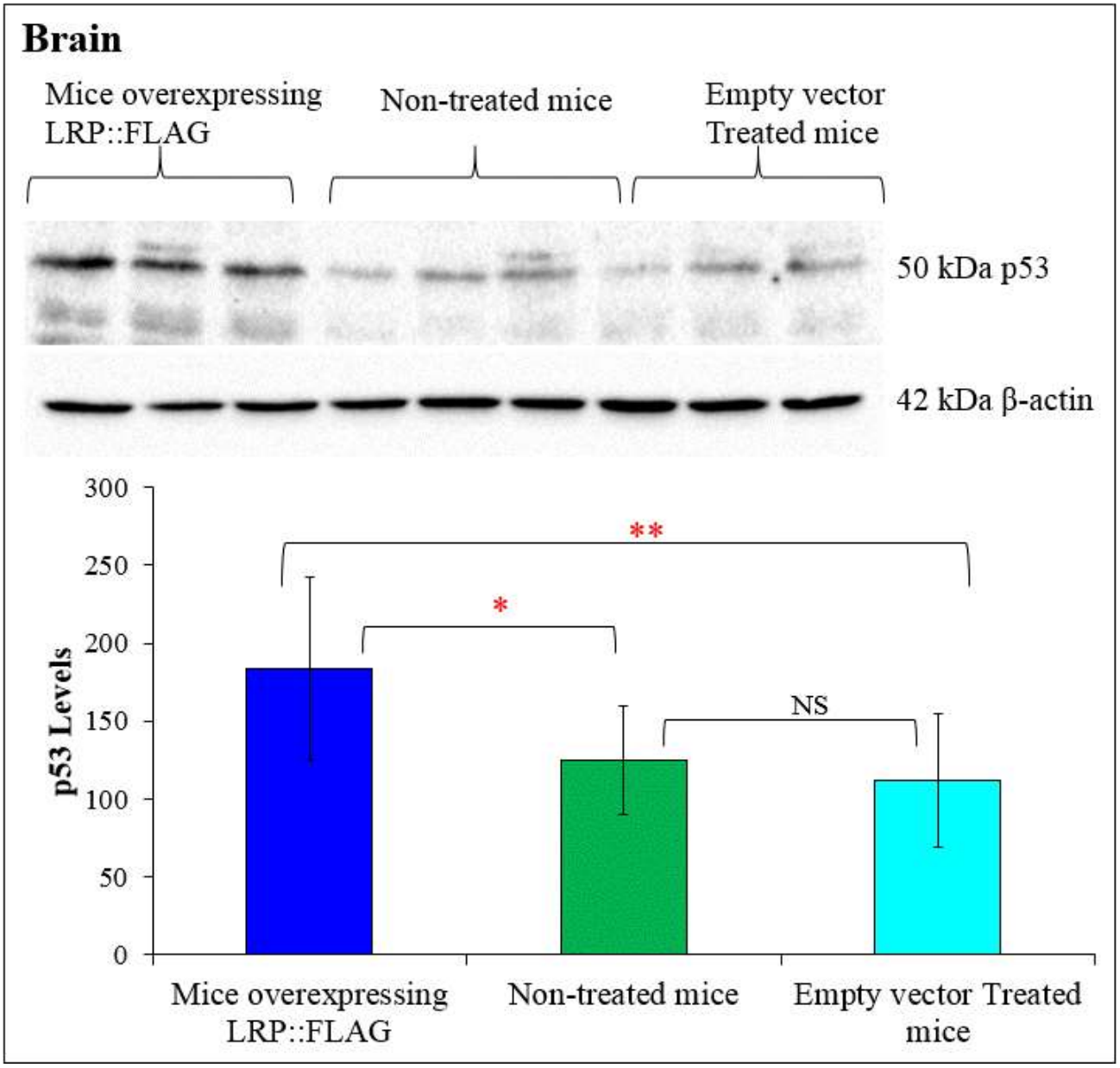


Figure 8.44: LRP::FLAG overexpression significantly elevates p53 levels in the brain of aged mice.

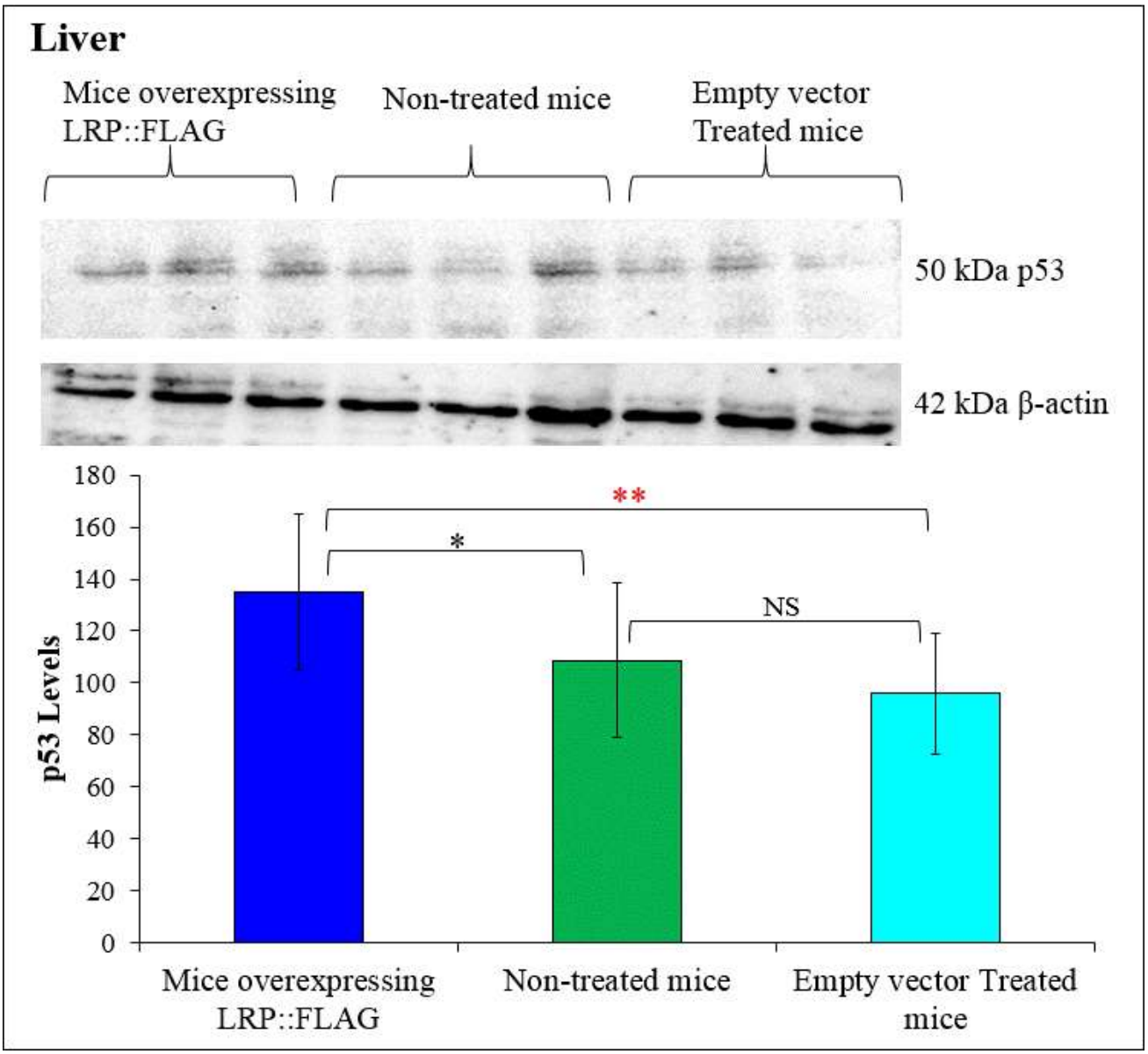


Figure 8.45: LRP::FLAG overexpression significantly elevates p53 levels in the liver of aged mice.

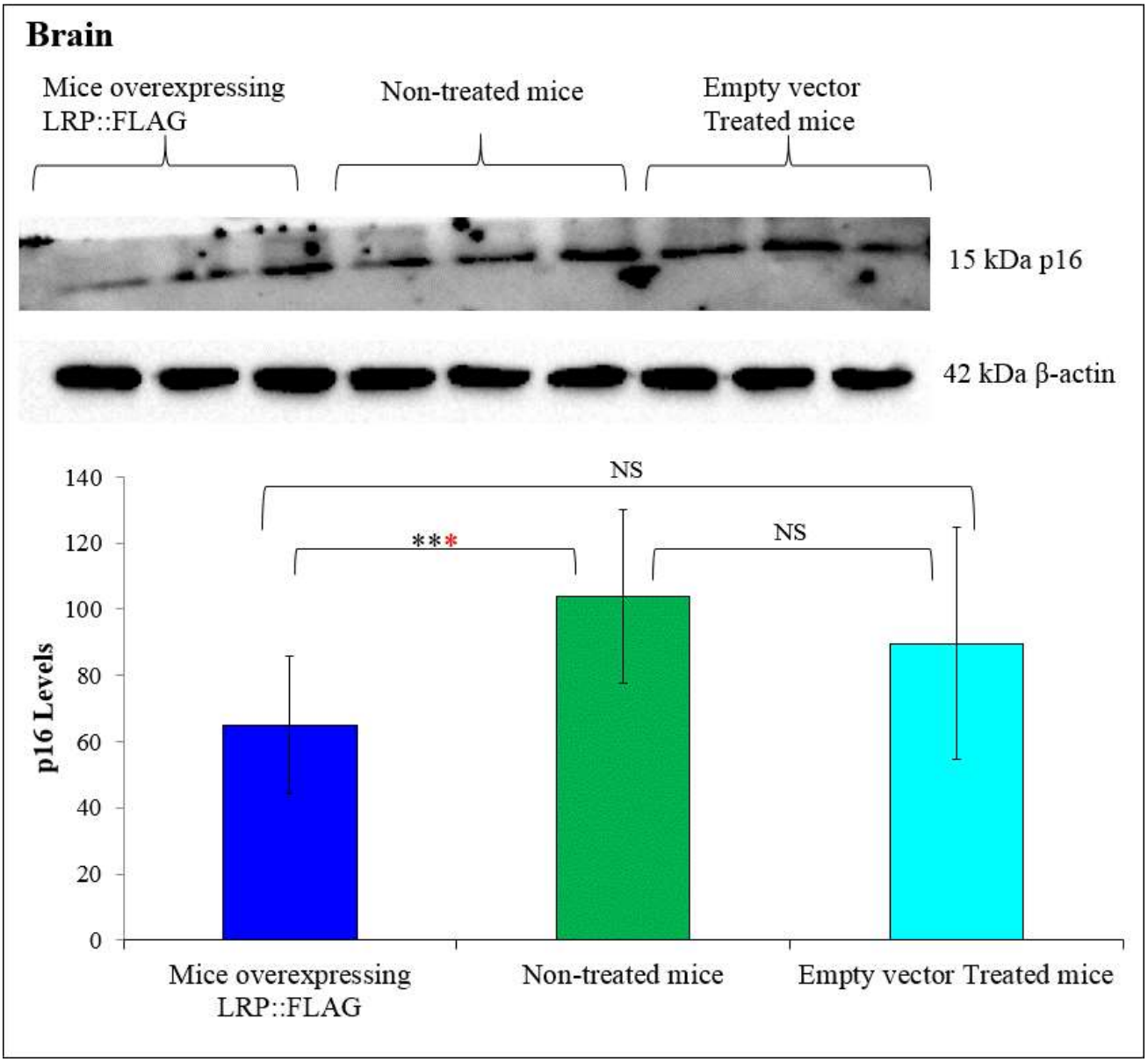


Figure 8.46: LRP::FLAG overexpression significantly reduces p16 levels in the brain of aged mice.

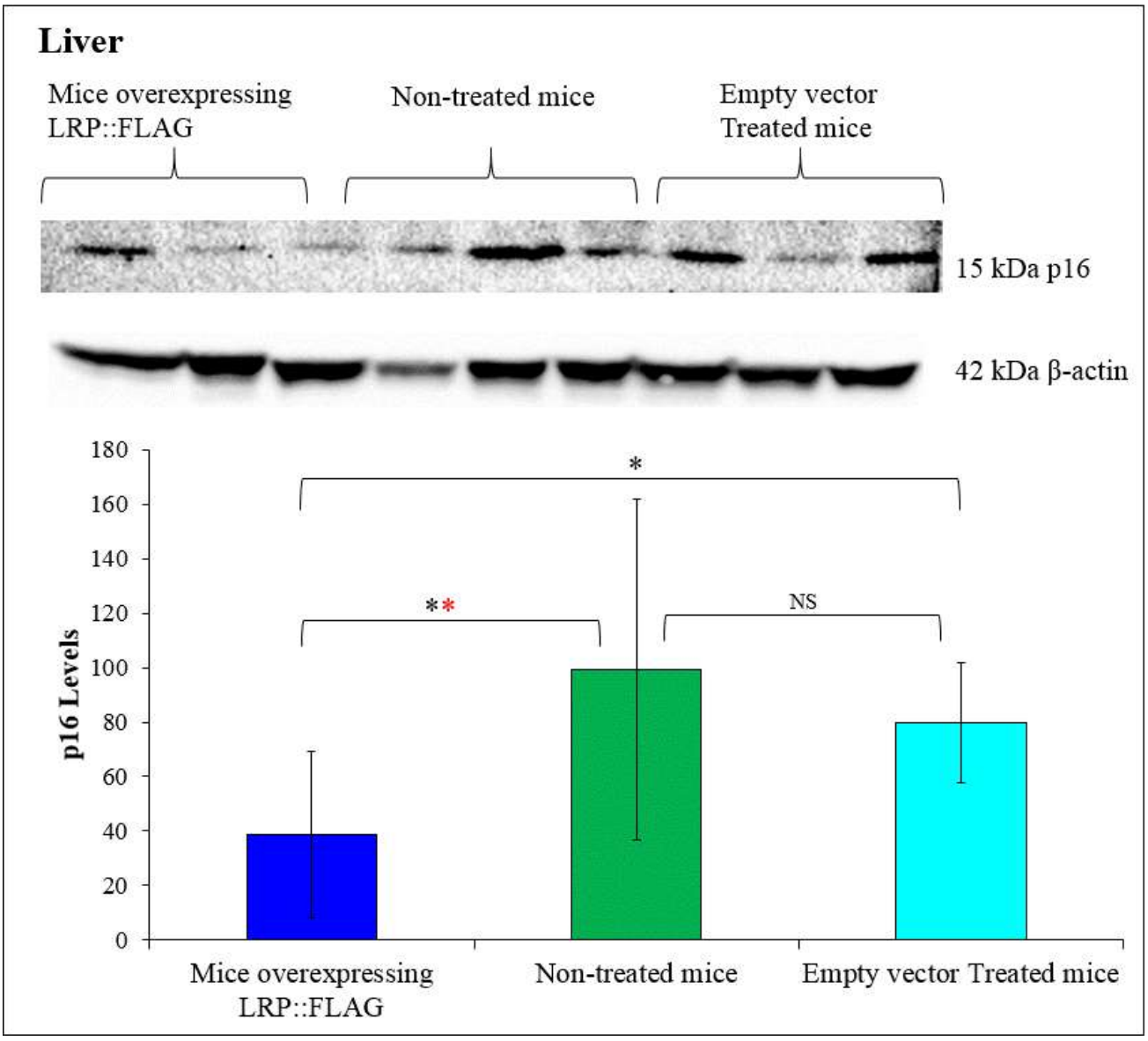


Figure 8.47: LRP::FLAG overexpression significantly reduces p16 levels in the liver of aged mice.

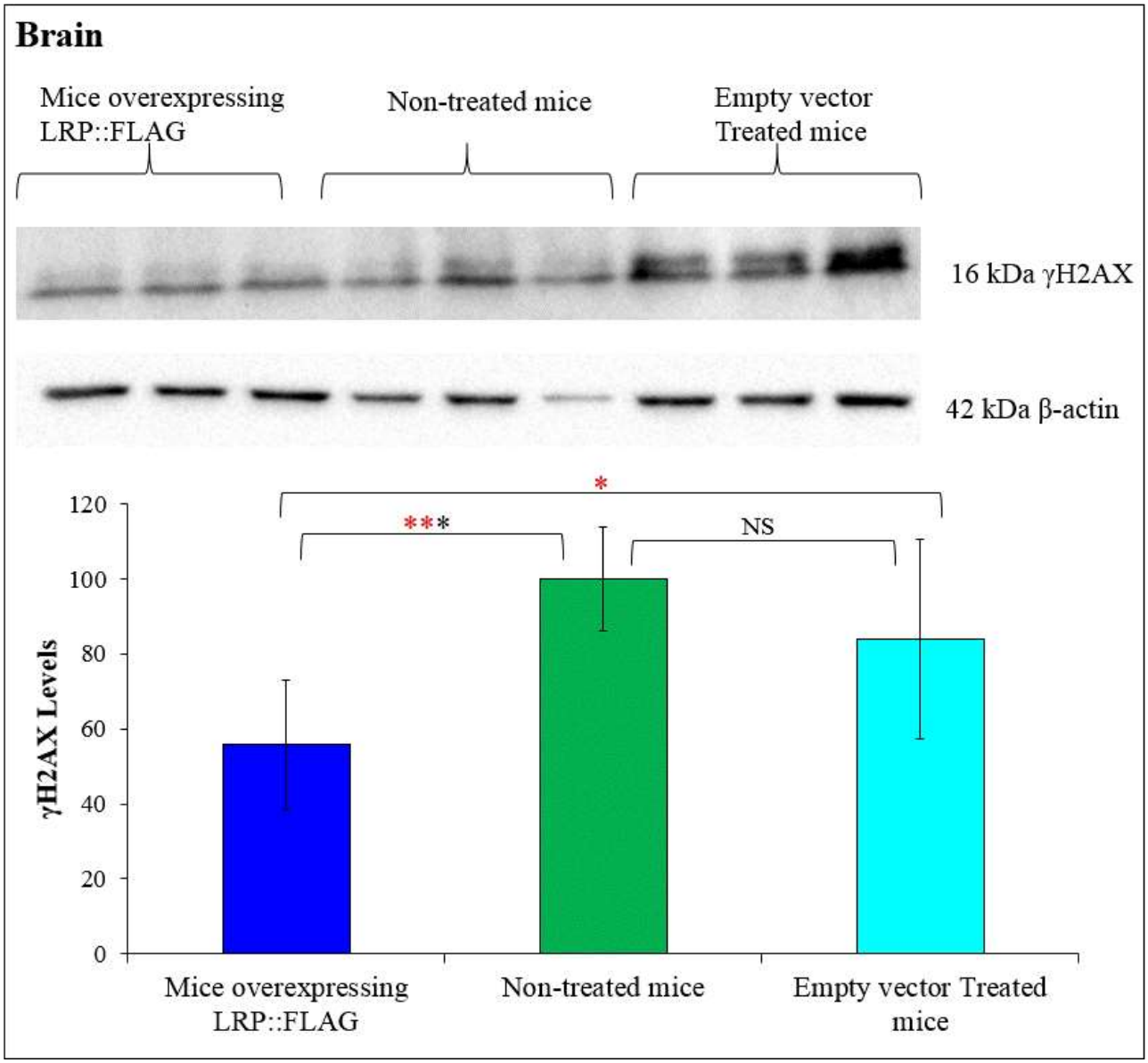


Figure 8.48: LRP::FLAG overexpression significantly reduces γH2AX levels in the brain of aged mice.

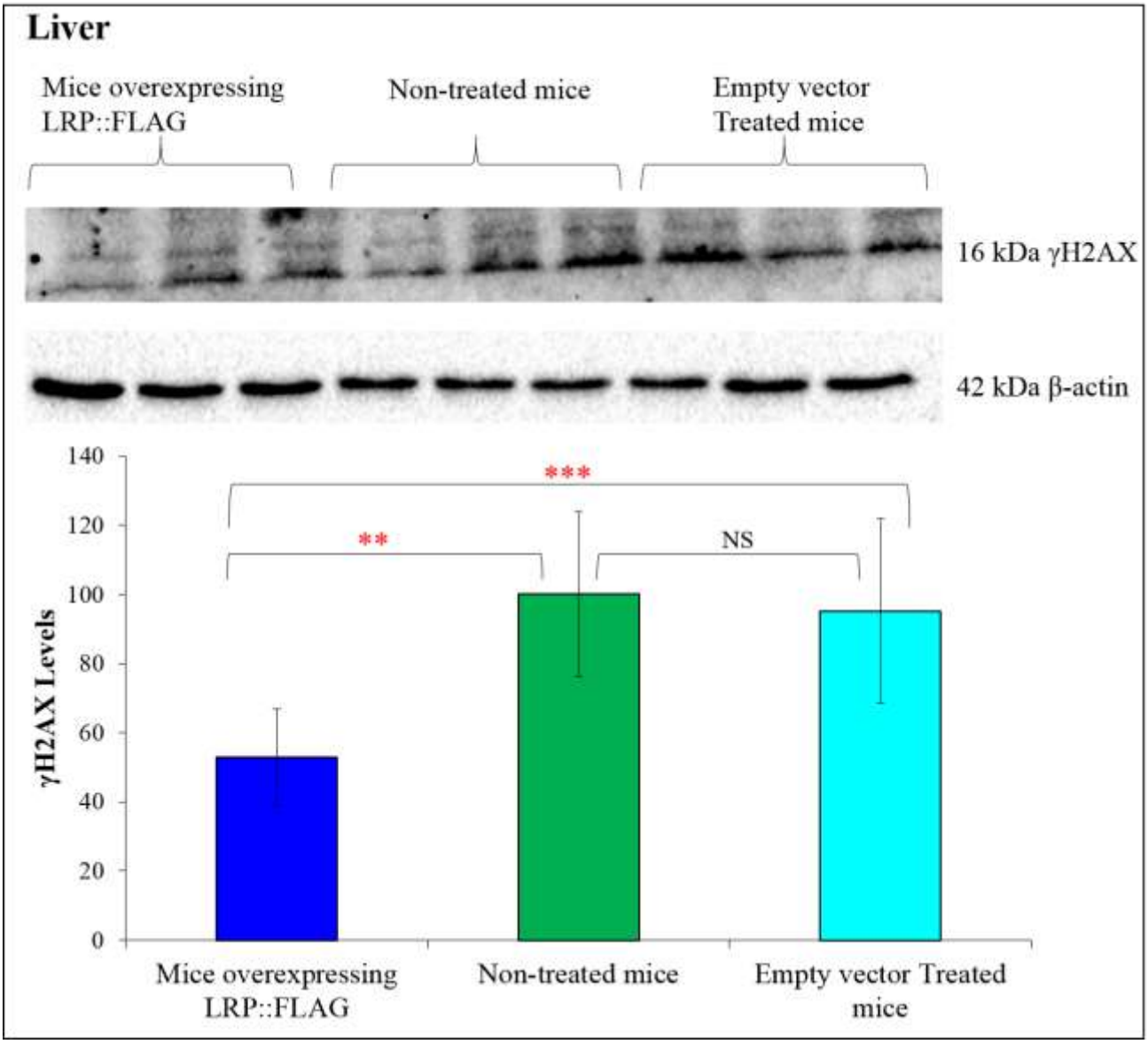


Figure 8.49: LRP::FLAG overexpression significantly reduces γH2AX levels in the liver of aged mice.

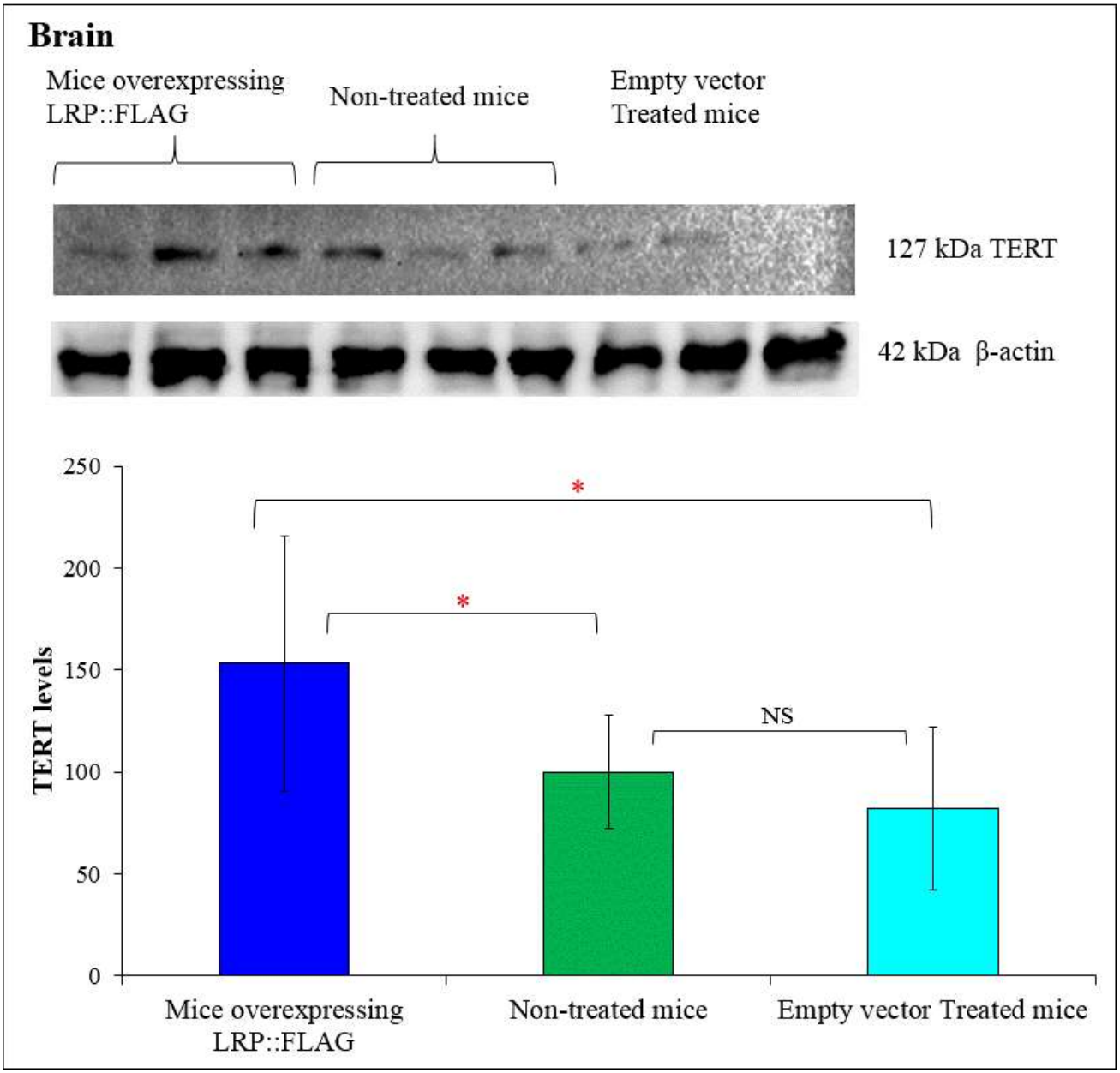


Figure 8.50: LRP::FLAG overexpression significantly elevates TERT levels in the brain of aged mice.

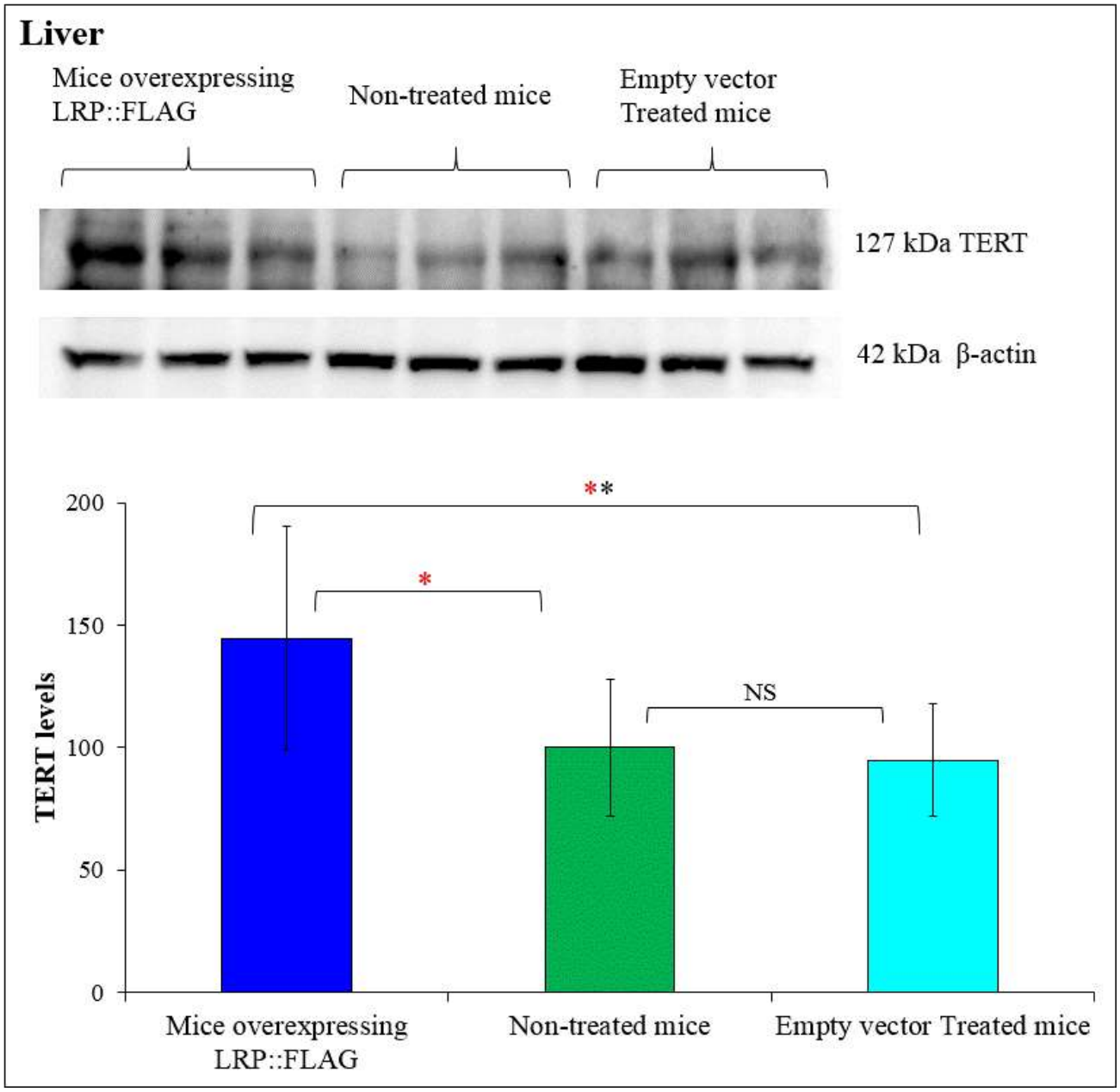


Figure 8.51: LRP::FLAG overexpression significantly elevates TERT levels in the liver of aged mice.

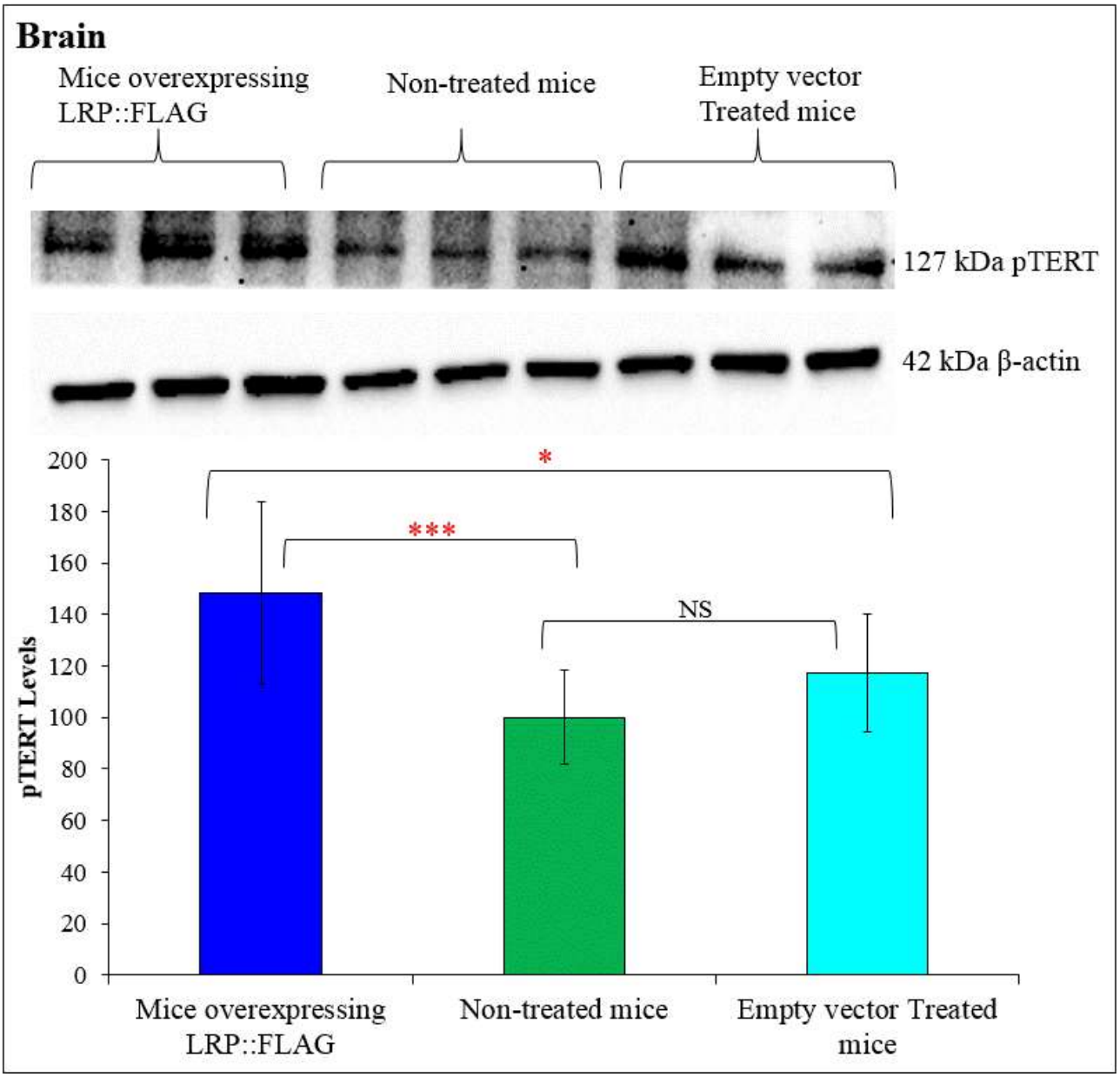


Figure 8.52: LRP::FLAG overexpression significantly elevates phospho-TERT levels in the brain of aged mice.

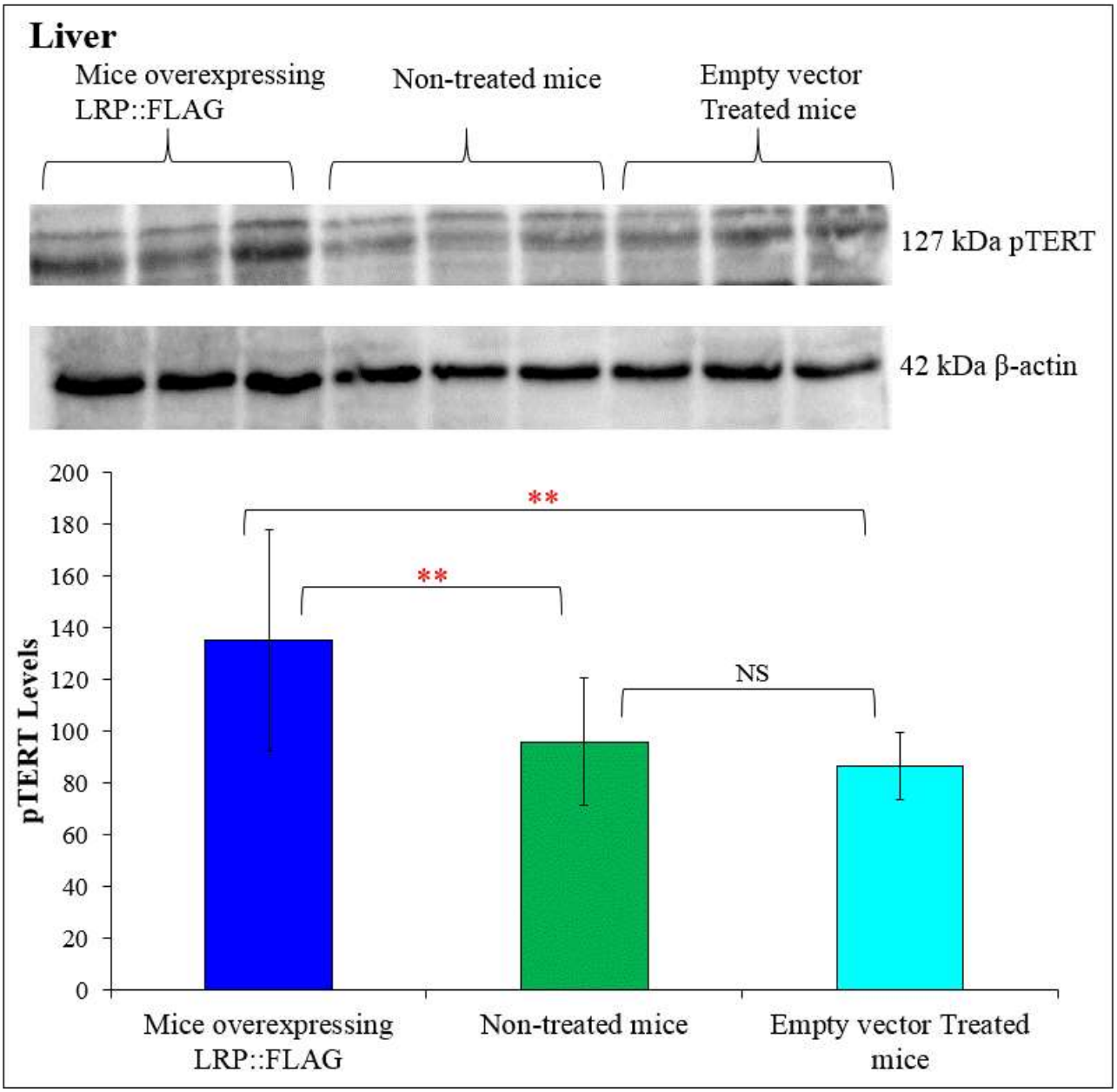


Figure 8.53: LRP::FLAG overexpression significantly elevates phospho-TERT levels in the liver of aged mice.

Appendix D

Table 8.1: Bacterial Nutrient Broth

Reagents	Amount (g)
Tryptone	10
Yeast Extract	5
NaCl	10

- Add ddH20 to 1l
- pH to 7.5
- Autoclave
- (if resistance gene is being used, add 1ml of 100mg/ml Ampicillin after it has cooled)

Table 8.2: Bacterial Nutrient Agar

Reagents	Amount (g)
Tryptone	10
Yeast Extract	5
NaCl	10
Agar	15

- Add dd$H_2$0 to 1l
- pH to 7.5
- Autoclave
- (if resistance gene is being used, add 1ml of 100mg/ml Ampicillin after it has cooled)
    - Creates selective environment

Plasmid DNA Isolation Buffers:

Table 8.3: Resuspension Buffer

Reagents	Volume (ml)
1M Glucose	5
1M Tris- HCl	2.5
1M EDTA	1
ddH_2O	90.5
Total:	100

Table 8.4: Bacterial Lysis Buffer

Reagents	Volume
0.2 M NaOH	0.4
1% (w/ v) SDS	2
ddH_2O	17.6
Total:	20

Table 8.5: Neutralisation Buffer

Reagents	Volume (ml)
5M Potassium acetate	60
Glacial Acetic Acid	11.5
Total:	100

Table 8.6: Tris-EDTA (TE) Buffer (pH8)

Component	Volume (ml)
1M Tris- HCl	1
0.5M EDTA	0.2
ddH_2O	98.8
Total:	100

1M Tris-HCl (50ml):

1. Dissolve 6.057g of Tris-base in 50ml ddH_20
2. Adjust pH with HCl and NaOH
3. Filter sterilize
4. Store at room temperature

500mM / 0.5M EDTA (pH 8.0) (100ml):

- 18.2 g Na_2EDTA
- 80 ml dH_2O
- pH to 8.0 with HCl and NaOH
- Make up to 100ml
- Stored at 4 ºC

Table 8.7: Phosphate Buffered Saline

	Amount		
Reagent	1X	10X	20X
NaCl	8 g	80 g	160 g
KCl	0.2 g	2 g	4 g
Sodium dihydrogen phosphate dodecahydrate (NA2HPO4.12H20)	1.44 g	14.4 g	28.8 g
Monopotassium phosphate	0.24 g	2.4 g	4.8 g

- pH using HCl and NaOH
- Dissolve in 1L with dH_20
- Stored at Room Temperature

Table 8.8: RIPA Buffer (Radio immunoprecipitation assay lysis buffer)

	Amount	
Reagent	1X	2X
NaCl	150 mM	300 mM
Trition X- 100	1 % (v/ v)	2 % (v/ v)
Sodium deoxycholate	0.5 % (w/ v)	1 % (w/ v)
SDS	0.1 % (w/ v)	0.2 % (w/ v)
Tris- HCl (pH 8.0)	50 mM	100 mM
EDTA (pH 8.0)	5 mM	10 mM

- A protease inhibitor cocktail was added to the RIPA buffer used for protein extraction from tissue.
- Made up to 100 ml with dH_2O and stored at 4 ºC.

Table 8.9: 10% SDS-PAGE gel recipe

Reagents/ No. of gels	10 % Separating Gel				5 % Stacking Gel			
No. of gels	1	2	3	4	1	2	3	4
dH_2O (ml)	0.825	1.65	2.475	3.3	1.36	2.73	4.1	5.45
40 % Acrylamide	1.675	3.35	5.025	6.7	0.3	0.6	0.9	1.2
2X Resolving Gel Buffer	2.5	5	7.5	10	-	-	-	-
4X Stacking Gel Buffer	-	-	-	-	0.56	1.125	1.69	2.25
10 % SDS								
10 % Ammonium Persulphate (APS)	37.25	74.5	111.75	149	22.5	45	67.5	90
TEMED (µl)				25	2.25	4.5	6.75	9
Total gel volume								

40 % Acrylamide/ bis-acrylamide:

- Add 380g acrylamide
- Add 20g bis-acrylamide
- Dissolve in up to 1L of water
- Store at 4 ºC

4X Stacking gel buffer (pH 6.8):

500 mM Tris – HCl

- 30.25 g Tris in 400 ml dH_2O, make up to 500 ml
- pH to 6.8 using HCl and NaOH
- Stored at 4 ºC

Resolving/ Separation gel buffer (pH 8.8):

1.5 M Tris – HCl

- 90.85 g Tris in 400 ml dH_2O, make up to 500 ml with water
- pH to 8.8 using HCl and NaOH
- Stored at 4 ºC

Table 8.10: Electrophoresis tank (Running) Buffer (pH 8.3)

	Amount (g)	
Reagent	1X	10X
Tris	3	30
Glycine	14.4	144
SDS	1	10

- Made up to 1L with dH_20
- pH using HCl and NaOH
- Stored at 4 ºC

Table 8.11: 10X Transfer Buffer

	Amount (g)
Reagents	10X
Tris	30
Glycine	144

- Made up to 1L with dH_20
- Stored at 4 ºC

Table 8.12: 10X Transfer Buffer

	Amount (ml)
Reagents	1X
10X Transfer Buffer	100
Methanol	200
dH_2O	700

- Stored at 4 ºC

Table 8.13: Stripping Buffer (pH 2.2)

	Amount		
Reagent	500 ml	250 ml	100 ml
Glycine	7.5 g	3.75 g	1.5 g
SDS	0.5 g	0.25 g	0.1 g
Tween20	5 ml	2.5 ml	1 ml

- Make up to 70% of the total volume with dH_2O
- To pH 2.2 using HCl and NaOH (this may take some time)
- Then make up to the final volume with dH_2O
- Stored at 4 ºC for up to 3 days

Table 8.14: qPCR master mix

Reagent	Amount per well (µl)
SYBR green (Luna or Sensi-Fast)	5
Forward Primer (10 µM)	0.5
Reverse Primer (10 µM)	0.5
DNase/ RNase free dH_2O	3
Sample	1

Table 8.15: qPCR Trap Master mix

Reagent	Amount per well (µl)
SYBR green	12.5
Forward Primer	1
Reverse Primer	1
EGTA	1
BSA (0.1 mg/ ml)	2.5
DNase/ RNase free dH_2O	5
Sample	2

Appendix E

Reagents and Materials

- **Associate chemical enterprise (ACE), Southdale, *RSA***: Methanol; Paraformaldehyde; Acetic acid; Hydrochloric acid; Sodium hydroxide (NaOH)
- **Bioline, London, UK**: Sensi-Fast™ SYBR green master mix
- **Biorad Hercules, CA**: Clarity™ Western ECL Substrate; Laemmli sample buffer; Cell counting slides; Triton X-100
- **Biowest/Gibco, Nuaillé - France**: Penicillin/streptomycin; PBS; Opti-MEM
- **Capricorn Scientific, Hessen, Germany**: FCS
- **Cleaver Scientific Ltd, Warwickshire, UK**: Agarose
- **Corning Inc. Corning, NY, USA**:15 ml and 50 ml centrifuge tube; 1.8 ml cryogenic tube, 24-well, 6-well plates as well as 25 cm^3 and 75 cm^3 cell culture flasks
- **Eppendorf AG, Hamburg, Germany**: 2 ml microfuge tubes
- **Fermentas Life Sciences, Glen Burnie, Burlington, Canada**: Loading buffer
- **GE Life sciences /Hyclone, Massachusetts, USA**: Media (DMEM)
- **Invitrogen, California, USA**: Lipofectamine 3000
- **Labocare, Secunderabad, India**: Microscopy slides and coverslips
- **Lonza Walkersville, MD**: Trypsin/EDTA; Pen/Strep; Gentamycin
- **Macherey-Nagel, Düren, Germany**: RNase A
- **Merck Millipore, Massachusetts, USA**: Tween 20; DMSO; CHAPs lysis buffer; Ethylenediaminetetraacetic acid (EDTA); Glycine; Isopropanol; KCl; Potassium dihydrogen phosphate (KH2PO4); Sodium chloride (NaCl); Sodium dodecyl sulfate *(*SDS); Tris(hydroxymethyl) aminomethane (Tris)
- **New England Biolabs Inc. Massachusetts, USA**: Molecular weight marker; OneTaq® HotStart Taq Polymerase; Luna® Universal qPCR Mastermix
- **Pall corporation, NY, USA**: PVDF membrane
- **Sigma-Aldrich, Missouri, USA**: Non-essential amino acids; BCA reagents; APS; acrylamide; TEMED; fluoromount mounting fluid; SDS; Triton-X; Agarose gel stain; Acrylamide; β-mercaptoethanol; Bisacrylamide; Ammonium persulphate; Formaldehyde; Dapi

- **Thermo Fisher Scientific, Massachusetts, USA**: TurboFect™ *in vivo* Transfection Reagent; GeneRuler 1 kb DNA ladder; PageRuler™ Plus prestained protein ladder; Lipofectamine 3000
- **VWR Life sciences, Pennsylvania, USA**: BSA; Ethanol

Antibodies and primer Tables

Table 8.16: List of primers used for gene expression analysis

Name	Mouse Primers (5'-3')		Annealing Temp (°C)	Reference
α-klotho	Forward	GATGGCAGAGAAATCAACACAGT	60	Sato et al., 2015 (1)
	Reverse	ACTACGTTCAAGTGGACACTACT		
Akt	Forward	GCCAAAGTCCAGCAAGAAGG	58	Hoshino and Sato, 2008 (2)
	Reverse	CTGAACCGCATGGGACACAG		
cMyc	Forward	TGAGGAGACACCGCCCAC	55	Magri et al., 2014 (3)
	Reverse	CAACATCGATTTCTTCCTCATCTTC		
GAPDH	Forward	CAACTACATGGTCTACATGTTC	55	Sato et al., 2015 (1)
	Reverse	CGCCAGTAGACTCCACGAC		
IL-6	Forward	CCAGAGATACAAAGAAATGATGG	58	Li et al., 2010 (4)
	Reverse	ACTCCAGAAGACCAGAGGAAAT		
IL8	Forward	TGTCCCCAAGTAACGGAGAAA	56	Thangavel et al., 2014 (5)
	Reverse	TGTCAGAAGCCAGCGTTCAC		
LRP	Forward	GGT TGG GAT TGC CAG ATG GA	60	-
	Reverse	AAG TGC TAT TCA CAG GCC CC		
Mdm2	Forward	ATTGCCTGGATCAGGATTCAGTT	58	Alder et al., 2015 (6)
	Reverse	ACCTCATCATCCTCATCTGAGA		
p16	Forward	CGGTCGTACCCCGATTCAG	60	Diekman et al., 2018. (7)
	Reverse	GCACCGTAGTTGAGCAGAAGAG		
p53	Forward	CTGTGCAGTTGTGGGTCAGC	60	Kim et al., 2012 (8)
	Reverse	ACCTCCGTCATGTGCTGTGA		
RPLPO	Forward	GGACCCGAGAAGACCTCCTT	60	Lin et al., 2013. (9)
	Reverse	GCACATCACTCAGAATTTCAATGG		
Sirt 1	Forward	TGTGAAGTT ACTGCAGGAGTGTAAA	56	Bai et al., 2011. (10)
	Reverse	GCATAGATACCGTCTCTTGATCTGAA		
TERT	Forward	TGC TAC TGT TGA GCC GAG TG	56	-
	Reverse	GCC TGT AAC TAG CGG ACA CA		

Table 8.17: Primers used for mtDNA content analysis

Name	Mouse Primers (5'-3')		Annealing Temp (°C)	Reference
mtDNA specific (murine)	Forward	CCGCAAGGGAAAGATGAAAGA C	60	Bai et al., 2011 [10]
	Reverse	TCGTTTGGTTTCGGGGTTTC		
nuclear specific (murine)	Forward	GCCAGCCTCTCCTGATTT TAGTGT	60	Bai et al., 2011 [10]
	Reverse	GGGAACACAAAAGACCTC TTCTGG		

Table 8.18: Primers used for mean telomere length analysis

Name	Mouse Primers (5'-3')		Annealing Temp (°C)	Reference
Tel 1	Forward	TCC CGA CTA TCC CTA TCC CTA TCC CTA TCC CTA TCC CTA	60 (mouse) and 58 (human)	Cawthon, 2002. [11]
Tel 2	Reverse	GGT TTT TTG AGG GTG AGG GTG AGG GGT GAG GGT GAG GGT		
36B4 (human)	Forward	CAGCAAGTGGGAAGGTGTAATCC	58	Cawthon, 2002 [11]
	Reverse	CCCATTCTATCATCAACGGGTACAA		
36B4 (mouse)	Forward	ACT GGT CTA GGA CCC GAG AAG	60	O'Callaghan, and Fenech, 2011 [12]
	Reverse	TCA ATG GTG CCT CTG GAG ATT		

Table 8.19: Primers used for telomerase activity analysis

Name	Mouse Primers (5'-3')		Annealing Temp (°C)	Citation
TS	Forward	AATCCGTCGAGCAGAGTT	58	Kim et al., 1997 [13]
ACX	Reverse	GCGCGGCTTACCCTTACCCTTACCCTA		Kim et al. 1997 [13]

Table 8.20: Antibodies used for *in vitro* confocal microscopy and western blotting analysis

Target Protein	**Primary (1°) antibody**	**Secondary (2°) antibody**	**Experiment and dilution factor**
LRP/LR	Human anti-LRP/LR IgG-iS18 (Affimed)	anti-human IgG-HRP (Abcam 6858)	Western blotting **1°:** 1:6500 **2°:** 1:6500
LRP/LR	Human anti-LRP/LR IgG-iS18 (Affimed)	anti-human IgG-FITC (Abcam 6854)	Confocal Microscopy **1°:** 1:100 **2°:** 1:100
LRP::FLAG	Murine anti-FLAG (Sigma F-3165)	anti-murine IgG-HRP (Sigma A4416)	Western blotting **1°:** 1:4000 **2°:** 1: 2500
LRP::FLAG	Murine anti-FLAG (Sigma F-3165)	anti-murine IgG-FITC (Abcam 6785)	Confocal Microscopy **1°:** 1:100 **2°:** 1:100
hTERT	Rabbit anti-hTERT (abcam 183105)	anti-rabbit IgG-HRP (Cell signalling 7074S)	Western blotting **1°:** 1:1000 **2°:** 1: 2500
hTERT	Rabbit anti-hTERT (Abcam 183105)	anti-rabbit IgG-APC (Abcam 72567)	Confocal Microscopy **1°:** 1:100 **2°:** 1:100
β-actin	Murine anti-β-actin-peroxidase. (Sigma A3854)	-	Western blotting **1°:** 1:10 000
Progerin	Murine anti-progerin (Abcam 13A)	anti-murine IgG-HRP (Sigma A4416)	Western blotting **1°:** 1:1000 **2°:** 1: 2500

Table 8.21: Antibodies used for in the *vivo* study western blotting analysis

Target Protein	Primary antibody	Dilution factor for primary antibodies	Secondary antibody	Dilution factor for secondary antibodies
β-actin	Anti-β-actin-peroxidase (Murine) (Sigma A3854)	1:10 000	-	-
γH2AX	Anti-PHOSPHO-H2AFX (Rabbit) (Sigma-Aldrich: SAB4300213)	1: 1000	Anti-rabbit IgG-HRP (Cell signalling Technologies: 7074S)	1: 2500
Akt	Anti-pan-AKT (Rabbit) (Sigma-Aldrich: SAB4301170)	1: 1000	Anti-rabbit IgG-HRP (Cell signalling Technologies: 7074S)	1: 2500
pAkt	Anti-P-Akt (pSer473) (Rabbit) (Cell Signalling Technologies: 9271S)	1: 1000	Anti-rabbit IgG-HRP (Cell signalling Technologies: 7074S)	1: 2500
c-Myc	Anti-MYC (AB-58) (Rabbit) (Sigma-Aldrich: SAB4300318)	1: 1000	Anti-rabbit IgG-HRP (Cell signalling Technologies: 7074S	1: 2500
Klotho	Anti-KL (Rabbit) (Sigma-Aldrich: SAB2101270-50UG)	1: 1000	Anti-rabbit IgG-HRP (Cell signalling Technologies: 7074S)	1: 2500
LRP	Anti-LRP/LR IgG-iS18 (Human) (Affimed Therapeutics)	1: 6500	Anti-human IgG-HRP (Abcam 6858)	1: 6500
MDM2	Anti-MDM2 (Rabbit) (Sigma-Aldrich: SAB4501849)	1: 1000	Anti-rabbit IgG-HRP (Cell signalling Technologies: 7074S)	1: 2500
pMDM2	Anti-phospho-MDM2 (pSer166) (Rabbit) (Sigma-Aldrich: SAB4503937)	1: 1000	Anti-rabbit IgG-HRP (Cell signalling Technologies: 7074S)	1: 2500

p16	Anti-p16 INK, N-Terminal (Rabbit) (Sigma-Aldrich: SAB4500072)	1: 500	Anti-rabbit IgG-HRP (Cell signalling Technologies: 7074S)	1: 2500
p53	Anti-p53, C-Terminal (Rabbit) (Sigma-Aldrich: SAB4503015)	1: 500	Anti-rabbit IgG-HRP (Cell signalling Technologies: 7074S)	1: 2500
SIRT1	Anti-SIRT1 (Rabbit) (Sigma-Aldrich: AV32386-100UL)	1: 1000	Anti-rabbit IgG-HRP (Cell signalling Technologies: 7074S)	1: 2500
TERT	Anti-TERT/ Telomerase (Rabbit) (Lifespan Biosciences: LS-C312849-100	1: 1000	Anti-rabbit IgG-HRP (Cell signalling Technologies: 7074S)	1: 2500
pTERT	Anti-phospho-Telomerase (pSer824) (Rabbit) (Sigma-Aldrich: SAB4504295)	1: 1000	Anti-rabbit IgG-HRP (Cell signalling Technologies: 7074S)	1: 2500
TRF1	Anti-TRF1 (Rabbit) (Sigma-Aldrich: ABE210)	1: 1000	Anti-rabbit IgG-HRP (Cell signalling Technologies: 7074S)	1: 2500
TRF2	Anti-TRF2 (D1Y5D) (Rabbit) (Cell signalling Technologies: 13136S)	1: 1000	Anti-rabbit IgG-HRP (Cell signalling Technologies: 7074S)	1: 2500

References for primers

1. Sato, S., Kawamata, Y., Takahashi, A., Imai, Y., Hanyu, A., Okuma, A., Takasugi, M., Yamakoshi, K., Sorimachi, H., Kanda, H. and Ishikawa, Y., 2015. Ablation of the p16 INK4a tumour suppressor reverses ageing phenotypes of klotho mice. Nature communications, 6(1), pp.1-10.
2. Hoshino, Y. and Sato, E., 2008. Protein kinase B (PKB/Akt) is required for the completion of meiosis in mouse oocytes. Developmental biology, 314(1), pp.215-223.
3. Magri, L., Gacias, M., Wu, M., Swiss, V.A., Janssen, W.G. and Casaccia, P., 2014. c-Myc-dependent transcriptional regulation of cell cycle and nucleosomal histones during oligodendrocyte differentiation. Neuroscience, 276, pp.72-86.
4. Li, P., Lu, M., Nguyen, M.A., Bae, E.J., Chapman, J., Feng, D., Hawkins, M., Pessin, J.E., Sears, D.D., Nguyen, A.K. and Amidi, A., 2010. Functional heterogeneity of CD11c-positive adipose tissue macrophages in diet-induced obese mice. Journal of Biological Chemistry, 285(20), pp.15333-15345.
5. Thangavel, J., Malik, A.B., Elias, H.K., Rajasingh, S., Simpson, A.D., Sundivakkam, P.K., Vogel, S.M., Xuan, Y.T., Dawn, B. and Rajasingh, J., 2014. Combinatorial therapy with acetylation and methylation modifiers attenuates lung vascular hyperpermeability in endotoxemia-induced mouse inflammatory lung injury. The American journal of pathology, 184(8), pp.2237-2249.
6. Alder, J.K., Barkauskas, C.E., Limjunyawong, N., Stanley, S.E., Kembou, F., Tuder, R.M., Hogan, B.L., Mitzner, W. and Armanios, M., 2015. Telomere dysfunction causes alveolar stem cell failure. Proceedings of the National Academy of Sciences, 112(16), pp.5099-5104.
7. Diekman, B.O., Sessions, G.A., Collins, J.A., Knecht, A.K., Strum, S.L., Mitin, N.K., Carlson, C.S., Loeser, R.F. and Sharpless, N.E., 2018. Expression of p16 INK 4a is a biomarker of chondrocyte aging but does not cause osteoarthritis. Aging Cell, 17(4), p.e12771.
8. Kim, J., Roh, M., Doubinskaia, I., Algarroba, G.N., Eltoum, I.A. and Abdulkadir, S.A., 2012. A mouse model of heterogeneous, c-MYC-initiated prostate cancer with loss of Pten and p53. Oncogene, 31(3), pp.322-332.
9. Lin, P., Lan, X., Chen, F., Yang, Y., Jin, Y. and Wang, A., 2013. Reference gene selection for real-time quantitative PCR analysis of the mouse uterus in the peri-implantation period. PloS one, 8(4).
10. Bai, P., Canto, C., Brunyánszki, A., Huber, A., Szántó, M., Cen, Y., Yamamoto, H., Houten, S.M., Kiss, B., Oudart, H. and Gergely, P., 2011. PARP-2 regulates SIRT1 expression and whole-body energy expenditure. Cell metabolism, 13(4), pp.450-460.
11. Cawthon, R.M., 2002. Telomere measurement by quantitative PCR. Nucleic acids research, 30(10), pp.e47-e47.
12. O'Callaghan, N.J. and Fenech, M., 2011. A quantitative PCR method for measuring absolute telomere length. Biological procedures online, 13(1), p.3.
13. Kim, N.W. and Wu, F., 1997. Advances in quantification and characterization of telomerase activity by the telomeric repeat amplification protocol (TRAP). *Nucleic acids research*, *25*(13), pp.2595-2597.

Kits

- Gene Jet DNA extraction kit (Thermo Fisher Scientific, Waltham, Massachusetts, USA)
- Gene Jet DNA extraction kit (Thermo Scientific)
- Invisorb® Spin Tissue kit (Invitek Molecular, Berlin, Germany)
- KAPA Taq PCR kit – Kapa Biosystems
- Nucleospin® RNA kit (Macherey-Nagel GmbH & Co. KG, Düren, Germany)
- SensiFAST™ cDNA Synthesis Kit (Bioline, London, UK)
- TRAPeze RT Telomerase detection Kit (Merck Millipore, USA)
- Turbo DNA-free™ kit Life Technologies
- β -Galactosidase Enzyme Assay System with Reporter Lysis Buffer (Promega, Wisconsin, USA)

Equipment list

- Bright field microscope – Floid cell imaging station
- Canon EOS 4501
- Centrifuge – Eppendorf 5417C
- CFX Maestro™ thermo cycler
- Confocal microscope – Zeiss LSM 710 3-channel
- ELISA reader – Tecan (using Magellan software)
- Gel casting and running apparatus, Chemidoc imaging machine (Roche
- Laminar flow – Labotec
- Multiskan™ GO Microplate Spectrophotometer (Thermo Fisher Scientific, Massachusetts, USA)
- NanoDrop One (Thermo Fisher Scientific, Massachusetts, USA)
- Nanodrop® ND-1000
- pH meter – Eutech instruments
- Pipettes and micropipettes – Eppendorf research
- Roche LightCycler 480 (Germany)
- Trans-Blot® Turbo™ Transfer System – Biorad

Software

- Biorad CFX Maestro™ (version 1.0)
- Gandalf the Grey, grey scale measurement software (Weiss lab)
- GraphPad prism (version 5.03)
- Image Lab (version 5.1)
- Magellan software (For ELISA plate reader)
- Microsoft Excel 365 ProPlus (Microsoft Corporation)
- Panlab Smart video tracking software, Smart 3.0 video tracking software
- Roche LightCycler software version 1.5.1
- Zen v2.6 (Blue edition)
- Zen 2011 software (For the Zeiss confocal microscope)

Appendix F

Original Publications

www.impactjournals.com/oncotarget/ Oncotarget, 2017, Vol. 8, (No. 49), pp: 86646-86656

Research Paper

37 kDa LRP::FLAG enhances telomerase activity and reduces senescent markers *in vitro*

Tyrone C. Otgaar[1], Eloise Ferreira[1], Sibusiso Malindisa[1,2], Martin Bernert[1], Boitelo T. Letsolo[1] and Stefan F.T. Weiss[1]

[1]School of Molecular and Cell Biology, University of the Witwatersrand, Wits 2050, Republic of South Africa

[2]Present Address: Department of Life and Consumer Sciences, University of South Africa, Florida 1710, Republic of South Africa

Correspondence to: Stefan F.T. Weiss, email: stefan.weiss@wits.ac.za

Keywords: aging, LRP/LR, LRP::FLAG, telomerase, telomeres

Received: June 30, 2017 Accepted: August 15, 2017 Published: September 27, 2017

Copyright: Otgaar et al. This is an open-access article distributed under the terms of the Creative Commons Attribution License 3.0 (CC BY 3.0), which permits unrestricted use, distribution, and reproduction in any medium, provided the original author and source are credited.

ABSTRACT

One of the core regulators of cellular aging are telomeres, repetitive DNA sequences at the ends of chromosomes that are maintained by the ribonucleoprotein DNA polymerase complex, telomerase. Recently, we demonstrated that knockdown of the 37kDa/ 67kDa laminin receptor (LRP/LR), a protein that promotes cell viability in tumorigenic and normal cells, reduces telomerase activity. We therefore hypothesized that upregulating LRP/LR might increase telomerase activity and impede aging. Here we show that overexpression of LRP::FLAG resulted in significantly elevated hTERT levels, telomerase activity and telomere length, respectively, with concomitantly reduced levels of senescence markers. These data suggest a novel function of LRP/LR hampering the onset of senescence through elevating hTERT levels and telomerase activity, respectively. LRP::FLAG might therefore act as a potential novel anti-aging drug through the impediment of the cellular aging process.

INTRODUCTION

Aging is a degenerative process characterized by the accumulation of detrimental changes that cause deterioration of the physiological functioning of the organism [1]. The process is characterized in cells by telomere erosion, genomic instability, mitochondrial dysfunction and stem cell exhaustion [1]. These stresses drive cellular senescence by limiting the replicative and regenerative potential of cells, this ultimately drives functional decline and disrupts tissue homeostasis to accelerate the aging process [2, 3]. One of the core regulators of human cellular aging are telomeres, repeated elements of TTAGGG that "cap" chromosome ends [4, 5]. Age-dependent loss of telomere functions, due to the "end replication" problem of DNA polymerases, telomere fusions and insufficient telomerase activity, eventually causes cell cycle arrest to induce a senescent state [4-8]. To circumvent aging, most epithelial and tumorigenic cells re-activate the enzyme telomerase, which can lead to telomere extension [9, 10]. This telomeric extension provided by telomerase maintains and elongates telomere length to effectively increase a cell's replicative capacity [9-11]. Interestingly, there have been a number of findings illustrating that in addition to its role in telomere extension, telomerase and its enzymatic subunit, telomerase reverse transcriptase (TERT), have other functions. These additional functions, otherwise known as extra-telomeric functions, all coincide to preserve cell viability [12]. A few of these include: DNA repair, cell proliferation, mtDNA protection as well as influencing a number of cellular pathways offering pro-proliferative functions [12, 13]. TERT's numerous roles can be attributed to its ability to interact directly or indirectly with various cellular proteins. One such protein, that we have proven to interact with TERT/telomerase, is the 37kDa/ 67kDa laminin receptor (LRP/LR) [14]. LRP/LR is a non-integrin transmembrane protein located predominantly on the cell surface, and to a lesser extent intracellularly in the cytosol, peri-nuclear as well as nuclear domains [14, 15]. The wide-

spread localization of LRP/LR as well as its numerous interactions shared with extracellular matrix proteins allows its key role in multiple processes such as: cell growth, adhesion, differentiation, migration, translational processes and maintenance of nuclear structures required for survival regimens [14-21]. The multi-functionality of LRP/LR includes vital roles in diseases such as cancer [14, 16-21], prion diseases [22, 23] and Alzheimer's disease [24]. Recently, we demonstrated that knockdown of LRP/LR, reduces telomerase activity in tumorigenic and normal cells [14, 15]. This suggests that LRP/LR, which promotes cell viability, plays a pivotal role in cancer processes via influencing telomerase activity [14]. Considering that telomerase and telomeres play antagonistic roles in cancer and aging [25], we postulated that an upregulation of LRP/LR may increase telomerase activity and possibly impede the aging process.

RESULTS

In order to validate that upregulation of LRP/LR does in fact increase telomerase activity, non-tumorigenic MRC 5 cells, at population doubling 23, and HEK293 cells were stably transfected with a pCIneo-moLRP-FLAG plasmid effectively elevating LRP::FLAG levels within the cells (Figure 1A, 1B). Western blotting was performed to confirm the presence of the LRP::FLAG protein and therefore stable transfection of the cells and to further assess LRP levels (Figure 1A, 1B). Upon confirming LRP::FLAG overexpression we proceeded to evaluate the change in expression patterns of LRP and hTERT following transfection. We previously observed co-localization between LRP and hTERT within MDA-MB231 and HEK293 cells [14], however, expression patterns and co-localization between these two proteins have not been confirmed in somatic cells with low/ undetectable levels of TERT. Immunofluorescence microscopy was employed to confirm the co-localization between the proteins in both MRC 5 and HEK293 transfected as well as non-transfected cell lines. The merged panels in Figure 2A, 2B, represent a merge of the red (hTERT) and green (LRP/LR and LRP::FLAG), where areas of yellow fluorescence indicated spatial overlap and possible interaction of the two proteins. The intracellular co-localization of LRP/LR and hTERT was pronounced for both non-transfected and transfected HEK293 cells (Figure 2A). Interestingly, the transfected MRC 5 cells displayed a striking increase in TERT fluorescence and co-localization (between LRP/LR and hTERT) when compared to the non-transfected MRC 5 cells which displayed negligible fluorescence for hTERT and no detectable co-localization (Figure 2B). Since co-localization between hTERT and LRP/LR was observed, we wanted to evaluate whether this pattern was also shared between hTERT and LRP::FLAG. To this end only HEK293 cells were utilized, where we found that LRP::FLAG behaved in a similar fashion to endogenous LRP/LR in localization and also co-localized with hTERT (Figure 2A panels K-N). This further suggested that the plasmid derived protein was correctly post-translationally processed, and was able to perform similar processes and interactions as its endogenous counterpart. The merged images and 2D-Cytofluorograms further revealed that a greater degree of co-localization occurred in cells overexpressing LRP::FLAG (Figure 2A, 2B). The increased hTERT levels post pCIneo-moLRP-FLAG transfection therefore encouraged us to further investigate telomere and telomerase dynamics. Telomere biology is one of the core regulatory mechanisms for the aging process in humans [4, 9] and is therefore a key aspect to assess in senescence and aging. A main factor involved in regulating telomere attrition is insufficient maintenance by telomerase, which in turn is limited by the expression of its catalytic subunit, hTERT [9, 26]. We thus investigated whether overexpression of LRP::FLAG influences hTERT-levels. Interestingly, western blot and subsequent densitometric analysis revealed a significant increase in hTERT levels in pCIneo-moLRP-FLAG transfected versus non-transfected HEK293 and MRC 5 cells (Figure 3A, 3B). HEK293 cells overexpressing LRP::FLAG revealed a 176,4% (n= 3, p= 0.0014, *t* test) increase in hTERT levels, while MRC 5 cells overexpressing LRP::FLAG revealed a 533.11% increase (n= 3, p= 0.0312, *t* test) in hTERT levels. The elevation of hTERT levels via LRP::FLAG overexpression in MRC 5 cells with little or no endogenous hTERT expression [27], indicates that LRP::FLAG enhances hTERT levels. These findings led us to determine whether LRP::FLAG mediated elevated levels of hTERT may subsequently affect the activity of telomerase, a ribonucleo-protein, acting as a key component to counteract telomere-dependent senescence by maintaining telomere length [7, 9]. Telomerase activity was determined with the TRAPeze RT telomerase detection kit (Merck Millipore) via real time qPCR. HEK293 cells overexpressing LRP::FLAG revealed a 2.937 fold increase (n=4, p=2.91*10^{-4}, *t* test) in telomerase activity compared to the non-transfected cells (Figure 3C, 3D). LRP::FLAG overexpression in MRC 5 cells revealed a 52.195 fold increase (n=4, p=2.38*10^{-6}, *t* test) in telomerase activity compared to non-transfected cells with minimal telomerase activity (Figure 3C, 3D). In order to investigate whether the LRP::FLAG mediated increased telomerase activity results in an elongation and maintenance effect of the telomere ends, qPCR was utilized and the data analyzed according to Cawthon et al., (2002) using $(2^{-\Delta CT(telomere)}/2^{-\Delta CT(36B4)})$ [28]. Prior to telomere length analysis, the reference gene, acidic ribosomal phosphoprotein (36B4), was analyzed to ensure equal DNA content between transfected and normal cell lines (Supplementary Figure 1A, 1B) [28]. A significant difference in telomere length was detected for both HEK293 and MRC 5 cells overexpressing LRP::FLAG (Figure 4E, 4F). Transfected HEK293 cells displayed a 2.236 fold increase (n= 4, p= 0.001909, *t* test) and transfected MRC 5 cells at population doubling 40

displayed a 2.839 fold increase (n= 4, p= 0.0002, *t* test) in mean telomere length, compared to their respective non-transfected cell lines. Since telomerase plays a role in cellular senescence and aging, these results regarding telomere dynamics (hTERT level, telomere length and telomerase activity) encouraged us to investigate whether LRP::FLAG may play a role in the senescence process. We therefore assessed the production and accumulation of specific senescence markers in response to LRP::FLAG expression. We selected β-galactosidase activity as our primary senescence marker as this enzyme is influenced by telomere dysfunction and accumulates as cells age or reach senescence [29, 30]. Furthermore, the use of this enzyme in conjunction with an additional marker is broadly utilized to track cellular aging [29, 30]. Transfected and non-transfected cell lines were allowed to undergo a minimum of 20 population doublings before this marker was assessed. To evaluate the enzyme's activity in both transfected and non-transfected cells; cell lysates were incubated with an assay buffer containing ortho-Nitrophenyl-β-galactoside at pH 6 (reporter lysis β-galactosidase assay, Promega), which when reduced allows for a quantitative measurement of β-galactosidase [29]. In fact, Lee et al., (2006) illustrated that senescence associated or lysosomal β-galactosidase can be detected if incubated for an extended period of 12 hours. HEK293 cells overexpressing LRP::FLAG showed a significant 1.111 fold (10%) reduction (n=3, p=4,22E-05, *t* test) in β-galactosidase activity, when compared to non-transfected cells (Figure 4A), whereas MRC 5 fibroblasts revealed a significant 1.638 fold (40%) reduction in β-galactosidase activity (n= 3, p= 0.0008, *t* test) after LRP::FLAG overexpression (Figure 4B). To further substantiate this impediment of the aging process we assessed the levels of an additional senescent marker, γH2AX foci. These foci are histones that are specifically phosphorylated at pSer139 and serve to mark sites of DNA damage as well as double stranded breaks which accumulate with increased cellular age due to the loss of telomeric ends [31, 32]. Overexpression of LRP::FLAG caused a significant decrease in the levels of γH2AX in both cell lines (Figure 4C, 4D). HEK293 cells overexpressing LRP::FLAG exhibited a 60.78% (n= 3, p= 0.0017, *t* test) reduction in γH2AX levels, while MRC 5 cells overexpressing LRP::FLAG displayed a significant 40% (n= 3, p= 0.009, *t* test) decrease in total γH2AX levels. Although, a reduction in both senescence markers was observed in the HEK293 cells it must be noted that these levels were exceptionally low (basal levels) and may in fact be due to extensive sub-culturing or other relevant stresses. In addition, basal levels of these markers have been previously observed in exceptionally low amounts [33, 34].

DISCUSSION

Previous studies have shown LRP/LR and telomerase to play critical roles in carcinogenesis [14, 15, 35, 36]. In addition, it has been found in most cancer types that LRP/LR, hTERT and telomerase are overexpressed to promote cell viability as well as to retain an immortalized state [14, 15, 35, 36]. Moreover, telomerase up-regulation is a necessary requirement for cells to bypass apoptotic and senescence pathways during critical telomere shortening in order to become immortalized or possibly tumorigenic [37, 38]. Recently, we have shown that LRP/LR not only co-localized, but in fact, interacted with hTERT; the catalytic subunit of telomerase via a co-immunoprecipitation assay [14]. In addition, knockdown of LRP/LR reduced telomerase activity in tumorigenic and non-tumorigenic cells [14]. Our hypothesis was further based on the evidence that whilst non-tumorigenic somatic cells senesce due to telomere attrition, introduction of hTERT at any stage of the cell cycle is sufficient to immortalize cells without additional risk of tumorigenic onset [9, 26, 39]. We have shown that aside from tumorigenic and other highly proliferative cell lines that naturally transcribe TERT; a functional relationship between LRP/LR and hTERT exists in somatic cells such as fibroblasts, which are only capable of displaying such an interaction provided TERT production is stimulated. Interestingly, this interaction appears to be localized to the nucleus, peri-nuclear compartments and cytosol. This distribution of TERT, while uncommon, has been shown in studies where shuttling between the nucleus and cytoplasm is imperative for cell immortalization in both tumorigenic and non-tumorigenic cell lines [40-42]. In support of this, a growing amount of data on extra-telomeric functions of TERT has illustrated its cytoplasmic distribution especially for mitochondrial function and protection [40-42]. Using confocal microscopy we have identified that LRP/LR interacts with TERT, where this relationship is further enhanced by the elevation of LRP/LR levels, such as overexpression of the LRP::FLAG protein. In fact, it was found that upon overexpression of LRP::FLAG that the levels of TERT and co-localization between TERT and LRP/LR increased. Our results suggest that LRP/LR shares an interaction/association with hTERT, which was previously reported in HEK293 and metastatic breast cancer cells (MDA-MB231) [14]. The confirmation of such an interaction between LRP/LR and hTERT indicates that targeting LRP/LR could be utilized to alter the functioning of hTERT or telomerase to influence either cancer or aging [14, 15]. LRP::FLAG may also play a direct or indirect role in promoting endogenous hTERT levels [14, 15]. These findings suggest that LRP/LR, aside from interacting with TERT, may play a role in the endogenous production of TERT through translational or transcriptional processes. Additionally, the presence of LRP::FLAG may contribute to these functions and processes performed by endogenous LRP. One such function is its interaction with the ribosomal complex where it facilitates translational processing [43]. Alternatively, LRP could carry out this unique function of

elevating TERT levels by interaction with the nuclear envelope to allow chromatin remodeling to subsequently expose the TERT gene leading to increased transcription [44]. The association of these two proteins as well as the elevation in TERT post LRP::FLAG overexpression appears to positively impact on telomerase dynamics and telomere homeostasis. This can be noted due to the significant elevation in telomerase activity accompanying the increased TERT levels. This correlates with the previous finding that telomerase activator (TA65) elevates TERT levels with a corresponding increase in mean telomere length [45]. Our findings confirm the dogma in telomere biology: the introduction of hTERT or the externally mediated elevation of hTERT levels increases telomerase activity in a non-oncogenic fashion; a common phenomenon in many immortalized cell lines [9, 10, 26,

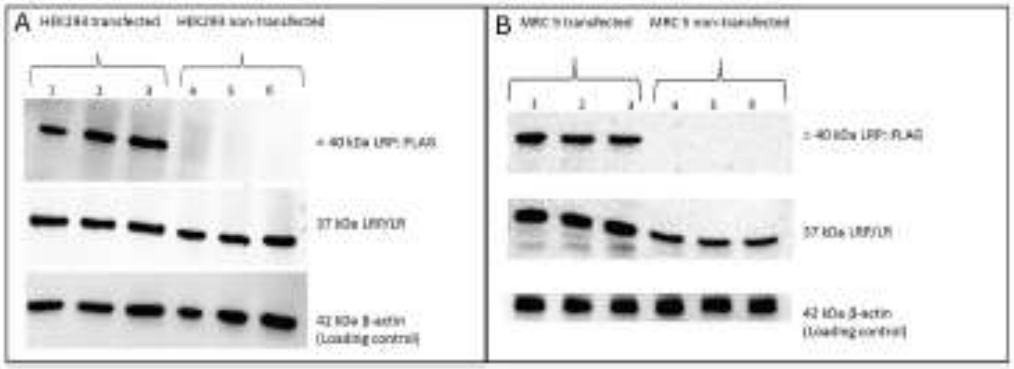


Figure 1: Overexpression of LRP::FLAG in HEK293 and MRC5 cells. (A, B) The expression of the LRP:FLAG protein was determined for both HEK293 and MRC 5 cells transfected with the pCIneo-LRP-FLAG construct (lane 1-3) as well as non-transfected HEK293 and MRC 5 cell samples (lane 4-6). Analysis revealed that LRP::FLAG was found to only be expressed in HEK293 and MRC 5 transfected cell samples, with no LRP::FLAG detection in the non-transfected cell samples.

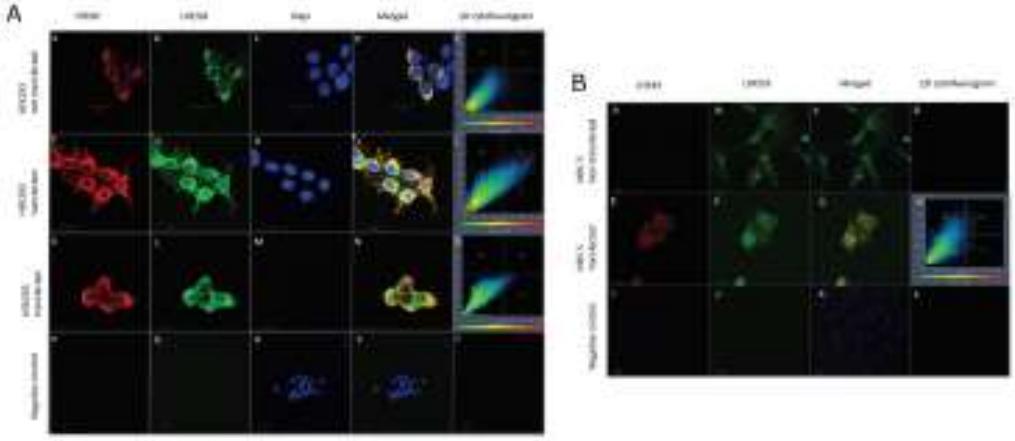


Figure 2: LRP and LRP::FLAG co-localizes with hTERT. (A, B) Intracellular localization and co-localization patterns of hTERT and LRP/LR and hTERT and LRP::FLAG in transfected as well as non-transfected HEK293 and MRC 5 cells. hTERT was detected with anti-hTERT primary and APC coupled secondary antibodies (A-A, A-F, A-K, B-A, B-E); LRP/LR was detected with anti-LRP/LR IgG1-i318 primary and FITC coupled secondary antibodies (A-B, A-G, B-B, B-F); LRP::FLAG detected with anti-FLAG and FITC coupled secondary antibodies (A-L); Dapi nuclear staining (A-C, A-H, A-M, A-R); merge between LRP/LR and hTERT (A-D, A-I, B-C, B-G) and LRP::FLAG and hTERT (A-N) illustrates co-localization caused by the spatial overlap between the proteins. 2D Cytofluorograms confirmed that the overlap observed was co-localization between the proteins (A-E, A-J, A-O, B-H). Secondary antibody controls confirmed no auto-fluorescence or non-specific binding (A-P, A-Q, A-R, A-S, A-T, B-I, B-J, B-K, B-L). Images were taken at 630x and negative controls were obtained at 400x magnification. All scale bars are 20μm.

27, 39, 45]. It must be noted that post transfection with the pCIneo-moLRP-FLAG plasmid there was no apparent phenotypic or morphological alterations indicative of transformed cells (such as loss of contact inhibition or growth in low serum) that may have accounted for elevation in telomerase activity [9]. The telomerase activity described here refers to its core elongating function of attaching telomeric repeats to the terminal ends of chromosomes, and thus enhancing the cell's proliferative potential [10, 35, 46] and preventing cellular senescence [9, 32]. Therefore it appears that LRP::FLAG overexpression aids in increasing telomerase activity sufficiently to increase proliferative potential and inhibit the activation of senescence associated pathways. Aside from increasing hTERT levels, we suggest that LRP/LR and/or LRP::FLAG may play a role in promoting the association of the hTERC and hTERT subunits to form the active telomerase based on the fact that telomerase activity appears to be regulated by LRP levels in both cancer and normal cells where both proteins have been shown to co-localize and interact [14]. In addition, the large difference in telomere length between transfected and non-transfected lines is a clear indicator that telomere length was indeed maintained. This suggests that the increased telomerase activity following the production of LRP::FLAG is sufficient to maintain telomere length and prevent the accumulation of short telomeres, a characteristic of telomere-dependent senescence [9, 10, 46]. This elongation allows cells to reverse and impede the aging process, and essentially immortalize themselves. Alternatively, the difference in telomere length post transfection may indicate a re-population by cells with longer telomeres [10, 47]. The reduction of both molecular aging markers further substantiates that the telomere replenishment occurring is in fact impeding senescence. More specifically the reduction of β-galactosidase, aside from suggesting an impediment to the senescence process also suggests that telomere dysfunction is not occurring [30, 48]. The accumulation of short/damaged telomeres with increased replicative stress and age is believed to be one of the major causatives of DNA damage associated with aging [10, 49]. This damage further accelerates the loss of regenerative

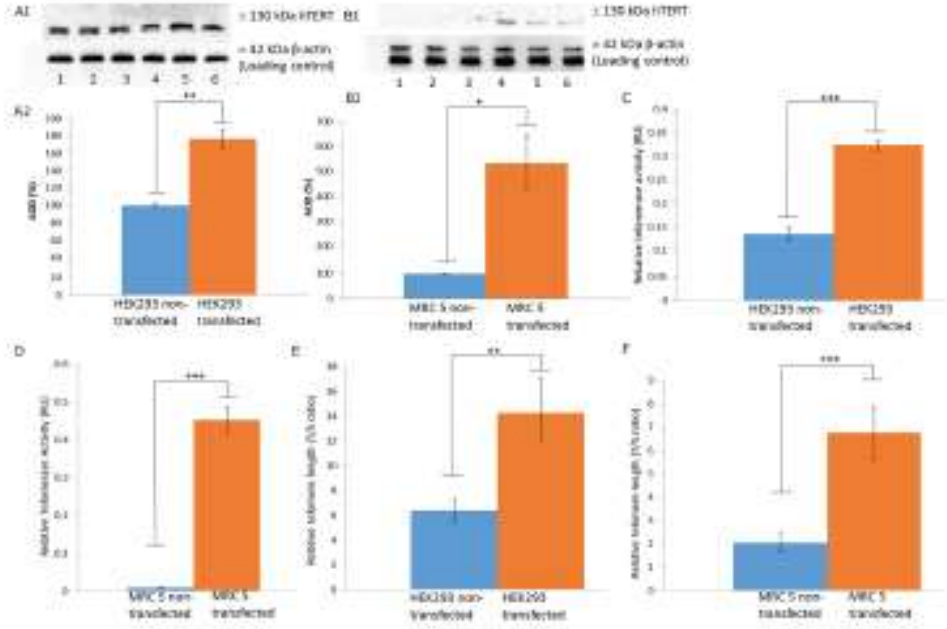


Figure 3: LRP::FLAG overexpression significantly elevates hTERT levels, telomerase activity and telomere length. (A-B), Western blot of hTERT levels in non-transfected (lane 1-3), and transfected (lane 4-6) HEK293 cells (A) as well as non-transfected (lane 1-3), and transfected (lane 4-6) MRC 5 cells (B). Densitometric analysis of hTERT expressed as a relative percentage in change respective to the non-transfected samples. (C-D) Relative telomerase activity (RU=relative units) in non-transfected and transfected HEK293 (C) as well as MRC 5 (D) cells shown in Log concentration (Log amole). (E-F), Relative telomere length in transfected and non-transfected HEK293 (E) as well as MRC 5 (F) lines as a telomere/36B4 (T/S) ratio to illustrate mean telomere length between samples. Sample size n= 3 biological repeats per cell line. Data as a mean ±sd. *p<0.05, **p<0.01, ***p<0.001 by paired *t*-test.

capacity in organisms [10, 49]. The significant decrease in γH2AX concomitantly with the increase in telomere length therefore indicates that the overexpression of LRP::FLAG provides an efficient means of reducing the effects of replicative stress by eliminating or preventing the accumulation of DNA damage [32, 46, 49]. TERT has previously been found to prevent the accumulation of DNA damage or mediate in the repair process to decrease the amount of foci present [12, 49, 50] further suggesting that the increased TERT present may be performing extra-telomeric functions in addition to telomere maintenance [12, 50]. Alternatively, LRP may have a role in DNA protection or in the repair process itself, however the exact nature and function still needs to be assessed. One possible mechanism that may explain this is that LRP/LR is known to play a role in supporting nuclear structure and overexpression of LRP::FLAG may thus provide an additional function of increasing nuclear integrity [15, 44]. This would essentially maintain nuclear shape which could alleviate and prevent additional DNA damage. Collectively, these findings strongly suggest that overexpression of LRP::FLAG in non-tumorigenic cell lines is sufficient to induce a physiological change. This change appears to allow the state and processing of young cells to be retained, by either slowing down or impeding the aging process [10, 32, 39]. In this regard, towards the end of our study the non-transfected MRC 5 cells underwent senescence at around passage doubling 49-50, while the transfected MRC 5 cells underwent an additional 20 passage doublings before the end of the study. Retention of pre-senescent functioning in normal cells holds important implications in the medical and pharmaceutical industries, especially in the form of treating age-related disorders. Cellular senescence and loss of proliferative capacity along with critically shortened telomeres and dysfunctional telomerase activity has also been linked to multiple age-related diseases and aging syndromes including: idiopathic pulmonary fibrosis, bone marrow failure and age-related

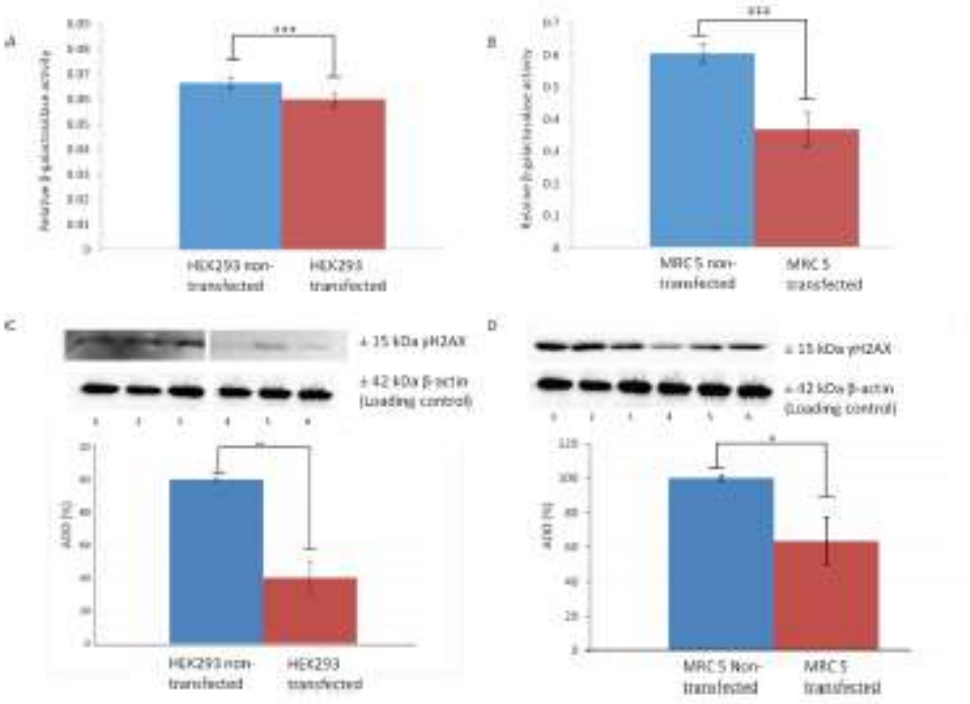


Figure 4: LRP::FLAG overexpression significantly decreases the levels of senescent markers. (A-B) Change in enzymatic activity of β-galactosidase following LRP::FLAG overexpression in HEK293 (A) and MRC 5 (B) cells when compared to the non-transfected cell lines. (C, D) Densitometric analysis of γH2AX levels expressed as a percentage change with non-transfected (lanes 1-3) compared to transfected lines (lanes 4- 6) for both HEK293 (C) and MRC 5 (D). Sample size n= 3 biological repeats per cell line. Data as a mean ±sd. *p<0.05, **p<0.01, ***p<0.001 by paired *t*-test.

macular degeneration [9, 51]. These diseases could be treated or their effects lessened by extending telomeres and elevating proliferative capacity providing an additional potential use for LRP/LR. In conclusion, these findings illustrate a novel function of LRP/LR and telomerase in the process of cellular aging. Furthermore we show that with LRP::FLAG overexpression, it is possible to delay the accumulation of DNA damage or possibly repair it. Therefore, strategies aimed at elevating LRP/LR levels may prove a potential therapeutic treatment in reverting/impeding cellular senescence and, in turn organism aging.

MATERIALS AND METHODS

Cell lines

Non-tumorigenic, Human Embryonic Kidney cells (HEK293) obtained from ATCC were used due to their detectable levels of telomerase activity. Human lung fibroblasts (MRC 5) (Fox Chase Cancer Center) were used as the aging model due to low/undetectable levels of TERT and limited replications before reaching senescence. All cell lines were cultured in 5% CO_2 at 37°C and were maintained in Dulbecco's modified Eagle's medium (DMEM) with high glucose (4.5g/l) (Hyclone) containing 4mM L-Glutamine, 10% foetal bovine serum (FBS) (Biowest) and 1% penicillin/streptomycin (Hyclone) (Thermo scientific).

LRP::FLAG overexpression in HEK293 and MRC 5 cells

Cells were stably transfected to induce an overexpression of the LRP::FLAG protein, to elevate total levels of LRP within the cell [23]. Cells were transfected at a 60% confluency using Lipofectamine 3000 (Invitrogen), according to the manufacturer's protocol. Briefly, 250µl Optimem, 5000ng of the pCIneo-moLRP-FLAG, 56.1µl P3000 and 56.1µl of the Lipofectamine reagent were mixed and incubated at room temperature for 10-15 minutes. Cells were treated with 250µl of the mix and incubated for 48 hours. Two days post treatment cells were exposed to the selective treatment, geneticin at 800ng/ml for 1 week. Thereafter, cells were maintained in 300ng/ml of geneticin to ensure transfection stability. In order to confirm success of the transfection, western blotting was carried out targeting the FLAG tag.

Western blotting

Western blotting was used to determine the protein levels of LRP::FLAG, LRP/LR, hTERT and γH2AX post-transfection with pCIneo-moLRP-FLAG when compared to untreated controls. β-actin used as the loading control. Briefly, cells were lysed, protein levels quantified and 10µg of cell lysate was loaded for LRP/LR, and LRP::FLAG while 50µg was used for TERT and γH2AX. To ensure equal concentrations of lysate were used, β-actin was used as a loading control. These cell lysates were resolved on a SDS polyacrylamide gel and subsequently transferred to a polyvinylidene fluoride (PVDF) membrane using a semi-dry transferring apparatus at 350 mV for 50 minutes. Membranes were then blocked in 3% BSA in 1x PBS Tween (0.1%). Thereafter the appropriate primary antibody was added (see Supplementary Table 1 online) and incubated at 4°C overnight, with gentle agitation. Membranes were then washed in PBS-Tween, and further incubated in a suitably diluted solution of secondary antibody coupled to a HRP enzyme in 3% BSA in PBS-Tween for 1 hour at room temperature (see Supplementary Table 1 online). The membrane was washed as before and incubated with Biorad Clarity™ Western ECL substrate prior to being analyzed with the Biorad Gel Doc XR Imager.

Confocal microscopy

Firstly, cells were seeded onto coverslips and cultured until 70% cell confluency was reached. The cells were fixed in a solution of 4% paraformaldehyde for 20 minutes, followed by three washes in 1X PBS. Cells were further permeabilized in a solution of 0.1% Triton X in PBS for 15 minutes. Thereafter, coverslips were washed thrice and blocked in 0.5% BSA for 20 minutes. The cells were subsequently incubated overnight with the primary antibodies for LRP/LR (1:100) and hTERT [(1:100) (see Supplementary Table 1 online)] and washed thrice with PBS. The cells were then incubated with the secondary antibodies [(1:100 dilution in 0.5% BSA) (see Supplementary Table 1 online)] for 1 hour where after the coverslips were washed and incubated for 10 minutes with 10µl of Dapi (10µg/ml) for nuclear staining. This was followed by additional washes. The cover slips were mounted and viewed at 400x and 630x magnification using the Zeiss LSM 780 confocal microscope.

β-Galactosidase assays

An altered form Lee et al., 2006 [29] of the β-Galactosidase Enzyme Assay System with Reporter Lysis Buffer (Promega) was used to determine endogenous levels of β-Galactosidase within the cells. Briefly, cells were seeded into 6 well dishes and allowed to proliferate until confluent with daily media changes performed to prevent metabolic or stress related activation of β-galactosidase. The cells were harvested, washed in PBS and lysed with a lysis buffer provided in the kit. Lysates were quantified and standardized and thereafter, incubated in 96 well plates with Assay buffer composed of: sodium phosphate, $MgCl_2$, and ortho-nitrophenyl-β-D-galactopyranoside (ONPG) all of which Lee et al., (2006)

used for their soluble β-galactosidase assay. This mixture was then incubated at 37°C and allowed to react for sixteen hours. Negative controls consisting of lysis buffer and assay buffer only were also included. Afterwards sodium carbonate was added to stop the reaction and the plate was read at 420nm in a Sunrise™ ELISA reader (Tecan). The procedure was performed in triplicate with three biological repeats for both transfected and non-transfected HEK293 and MRC 5 cells.

Detection of telomerase activity

Relative telomerase activity was quantified by the TRAPeze RT Telomerase detection Kit (Merck Millipore) following the manufacturers protocols with minor alterations. Briefly, cells were harvested and washed in PBS, after which they were lysed using CHAPS lysis buffer ((3-((3-cholamidopropyl) dimethylammonio)-1-propanesulfonate)). Protein and RNA extractions were collected in the supernatant where protein concentrations were standardized to 500 ng/µl for all experimental and control reactions. All samples were then subjected to experimental analysis by qPCR accompanied by a positive control (cell extract with confirmed telomerase activity) and three negative controls: no template control (water), CHAPs lysis buffer and samples heat treated at 85°C for 10 minutes. All reactions were performed in triplicate. The qPCR reactions were carried out in the LightCycler LC480 (Roche) using the following cycling parameters: 37°C for 30 minutes, 95°C for 2 minutes and 45 cycles of 95°C for 15 seconds, 59°C for 60 seconds and 45°C for 10 seconds. Telomerase activity was estimated by extrapolation from the standard curve generated by 1:10 serial dilutions (20–0.2 amoles) of TSR8 control as per Merck Millipore instructions. The data was analyzed with LightCycler1 Software version 1.5.1.

Assessment of telomere length

The relative telomere length was assessed by use of Tel 1 and Tel 2 primers with qPCR as described by Cawthon *et al*. (2002). DNA was extracted using the Gene Jet DNA extraction kit (Thermo Scientific) following the manufacturer's instructions. In order to normalize the data obtained for telomere length and to ensure accuracy in the quantification of the data obtained, 36B4 was used as a reference gene (List of primers used can be found as online Supplementary Table 2.) [28]. A standard curve was constructed using DNA of a known concentration (35ng/µl to 0.035ng/µl). The reaction was run with a set of positive (DNA samples previously confirmed to amplify) and negative controls (no template control). All experimental and control sample reactions were performed in the Roche LightCycler 480 (Germany) with the following cycling parameters: initial denaturation at 95°C for 10 minutes followed by 45 amplification cycles of: 95°C for 10 seconds, 58°C for 10 seconds and 72°C for 60 seconds. The amplification readings for the experimental samples were then normalized to the standard curve and analyzed.

Statistical evaluations

All statistical evaluations of the data were carried out using Microsoft Excel 2014 (Microsoft Corporation) and Graph Prism Version 5 (Graphpad Software, Inc). All experiments were performed in at least triplicate so that standard deviation could be calculated. The two-tailed Student's *t*-test was performed at a 95% confidence interval; where values *p<0.05 were considered significant, while values **p<0,01 and values ***p<0,001 were considered highly significant.

Abbreviations

36B4: acidic ribosomal phosphoprotein
CHAPS: 3-((3-cholamidopropyl) dimethylammonio)-1-propanesulfonate
DAPI: 4',6-diamidino-2-phenylindole
DDR: DNA Damage Response
DMEM: Dulbecco's Modified Eagle's Medium
DMSO: Dimethyl Sulfoxide
DNA: Deoxyribonucleic Acid
HEK293: Human Embryonic Kidney Cells
hTERT: Human Telomerase Reverse Transcriptase
kDa: Kilo Dalton
LRP/LR: 37 kDa Laminin Receptor Precursor/67 kDa High Affinity Laminin Receptor
MDA-MB231: Metastatic breast cancer cells
MRC-5: Human Lung Fibroblast cells
ONPG: Ortho-nitrophenyl-β-D-galactopyranoside
PAGE: Polyacrylamide Gel electrophoresis
PCR: Polymerase Chain Reaction
RNA: Ribonucleic Acid
TERC: Telomerase RNA Component
TERT: Telomerase Reverse Transcriptase

Author contributions

T. C. O. performed the experiments, T. C. O., E. F., S. M., M. B. analyzed the data. T. C. O. and E. F. wrote the manuscript S. F. T. W. and B. T. L. conceptualized the study and edited the manuscript.

ACKNOWLEDGMENTS

We thank Affimed Therapeutics GmbH, Heidelberg, Germany for providing antibody IgG1-iS18. It is with great sadness to report that Dr. Boitelo T. Letsolo, passed away during the preparation of this manuscript.

CONFLICTS OF INTEREST

There are no conflicts of interest.

FUNDING

This work is based upon research supported by the National Research Foundation (NRF), the Republic of South Africa (RSA). Any opinions, findings and conclusions or recommendations expressed in this material are those of the author(s), and therefore, the National Research Foundation does not accept any liability in this regard thereto. Financial support was further received from the South African Medical Research Council (MRC) under the Wits Common Epithelial Cancer Research Centre (CECRC) grant. Any opinions, findings and conclusions or recommendations expressed in this material are those of the author(s), and therefore, the MRC does not accept any liability in this regard thereto.

REFERENCES

1. Prieur A, Peeper DS. Cellular senescence *in vivo*: a barrier to tumorigenesis. Curr Opin Cell Biol. 2008; 20: 150-155.
2. Allsopp RC, Harley CB. Evidence for a critical telomere length in senescent human fibroblasts. Exp Cell Res. 1995; 219: 130-136.
3. Molofsky AV, Slutsky SG, Joseph NM, He S, Pardal R, Krishnamurthy J, Sharpless NE, Morrison SJ. Increasing p16INK4a expression decreases forebrain progenitors and neurogenesis during ageing. Nature. 2006; 443: 448-452.
4. Harley CB, Futcher AB, Greider CW. Telomeres shorten during ageing of human fibroblasts. Nature. 1990; 345: 458-460.
5. Harley CB, Villeponteau B. Telomeres and telomerase in aging and cancer. Curr Opin Genet Dev. 1995; 5: 249-255.
6. Capper R, Britt-Compton B, Tankimanova M, Rowson J, Letsolo B, Man S, Haughton M, Baird DM. The nature of telomere fusion and a definition of the critical telomere length in human cells. Genes Dev. 2007; 21: 2495-2508.
7. Blackburn EH. Telomeres and telomerase: their mechanisms of action and the effects of altering their functions. FEBS Lett. 2005; 579: 859-862.
8. Letsolo BT, Rowson J, Baird DM. Fusion of short telomeres in human cells is characterized by extensive deletion and microhomology, and can result in complex rearrangements. Nucleic Acids Res. 2010; 38: 1841-1852.
9. Bodnar AG, Ouellette M, Frolkis M, Holt SE, Chiu CP, Morin GB, Harley CB, Shay JW, Lichtsteiner S, Wright WE. Extension of life-span by introduction of telomerase into normal human cells. Science. 1998; 279: 349-352.
10. de Jesus BB, Vera E, Schneeberger K, Tejera AM, Ayuso E, Bosch F, Blasco MA. Telomerase gene therapy in adult and old mice delays aging and increases longevity without increasing cancer. EMBO Mol Med. 2012; 4: 691-704.
11. Greider CW, Blackburn EH. A telomeric sequence in the RNA of Tetrahymena telomerase required for telomere repeat synthesis. Nature. 1989; 337: 331-337.
12. Saretzki G. Extra-telomeric functions of human telomerase: cancer, mitochondria and oxidative stress. Curr Pharm Des. 2014; 20: 6386-6403.
13. Park JI, Venteicher AS, Hong JY, Choi J, Jun S, Shkreli M, Chang W, Meng Z, Cheung P, Ji H. Telomerase modulates Wnt signalling by association with target gene chromatin. Nature. 2009; 460: 66-72.
14. Naidoo K, Malindisa ST, Ogunr TC, Bernert M, Dias BD, Ferreira E, Reusch U, Knackmuss S, Little M, Weiss SF. Knock-Down of the 37kDa/67kDa Laminin Receptor LRP/LR Impedes Telomerase Activity. PLoS One. 2015; 10: e0141618.
15. Jovanovic K, Chetty CJ, Khumalo T, Da Costa Dias B, Ferreira E, Malindisa ST, Caveney R, Letsolo BT, Weiss SF. Novel patented therapeutic approaches targeting the 37/67 kDa laminin receptor for treatment of cancer and Alzheimer's disease. Expert Opin Ther Pat. 2015; 25: 567-582.
16. Omar A, Reusch U, Knackmuss S, Little M, Weiss SF. Anti-LRP/LR-specific antibody IgG1-iS18 significantly reduces adhesion and invasion of metastatic lung, cervix, colon and prostate cancer cells. J Mol Biol. 2012; 419: 102-109.
17. Khumalo T, Reusch U, Knackmuss S, Little M, Veale RB, Weiss SF. Adhesion and invasion of breast and oesophageal cancer cells are impeded by anti-LRP/LR-specific antibody IgG1-iS18. PLoS One. 2013; 8: p.e56297.
18. Moodley K, Weiss SF. Downregulation of the non-integrin laminin receptor reduces cellular viability by inducing apoptosis in lung and cervical cancer cells. PLoS One. 2013; 8: e57409.
19. Rebelo TM, Chetty CJ, Ferreira E, Weiss SF. Anti-LRP/LR-specific antibody IgG1-iS18 impedes adhesion and invasion of pancreatic cancer and neuroblastoma cells. BMC Cancer. 2016; 16: 917.
20. Munien C, Rebelo TM, Ferreira E, Weiss SF. IgG1-iS18 impedes the adhesive and invasive potential of early and late stage malignant melanoma cells. Exp Cell Res. 2017; 351: 135-141.
21. Vania L, Chetty CJ, Ferreira E, Weiss SF. Anti-LRP/LR–Specific antibody igG1-iS18 significantly impedes adhesion and invasion in early-and late-stage colorectal carcinoma cells. Mol Med. 2016; 22: 664-673.
22. Gauczynski S, Nikles D, El-Gogo S, Papy-Garcia D, Rey C, Alban S, Barritault D, Lasmezas CI, Weiss, S. The 37-kDa/67-kDa laminin receptor acts as a receptor for infectious prions and is inhibited by polysulfated glycans. J Infect Dis. 2006; 194: 702-709.
23. Vana K, Weiss S. A trans-dominant negative 37kDa/67kDa laminin receptor mutant impairs PrP(Sc) propagation in

scrapie-infected neuronal cells. J Mol Biol. 2006; 358: 57-66.

24. Jovanovic K, Gonsalves D, Da Costa Dias B, Moodley K, Reusch U, Knackmuss S, Penny C, Weinberg MS, Little M, Weiss SF. Anti-LRP/LR specific antibodies and shRNAs impede amyloid beta shedding in Alzheimer's disease. Sci Rep. 2013; 3: 2699.
25. Blasco MA. Telomeres and human disease: aging, cancer and beyond. Nature Reviews Genetics. 2005; 6: 611-622.
26. Counter CM, Meyerson M, Eaton EN, Ellisen LW, Caddle SD, Haber DA, Weinberg RA. Telomerase activity is restored in human cells by ectopic expression of hTERT (hEST2), the catalytic subunit of telomerase. Oncogene. 1998; 16: 1217-1222.
27. McSharry B, Jones C, Skinner J, Kipling D, Wilkinson G. Human telomerase reverse transcriptase-immortalized MRC-5 and HCA2 human fibroblasts are fully permissive for human cytomegalovirus. J Gen Virol. 2001; 82: 855-863.
28. Cawthon RM. Telomere measurement by quantitative PCR. Nucleic Acids Res. 2002; 30: e47.
29. Lee BY, Han JA, Im JS, Morrone A, Johung K, Goodwin EC, Kleijer WJ, DiMaio D, Hwang ES. Senescence-associated β-galactosidase is lysosomal β-galactosidase. Aging Cell. 2006; 5: 187-195.
30. Kurz DJ, Decary S, Hong Y, Erusalimsky JD. Senescence-associated (beta)-galactosidase reflects an increase in lysosomal mass during replicative aging of human endothelial cells. J Cell Sci. 2000; 113: 3613-3622.
31. Pospelova TV, Demidenko ZN, Bukreeva EI, Pospelov VA, Gudkov AV, Blagosklonny MV. Pseudo-DNA damage response in senescent cells. Cell Cycle. 2009; 8: 4112-4118.
32. Tomas-Loba A, Flores I, Fernandez-Marcos PJ, Cayuela ML, Maraver A, Tejera A, Borras C, Matheu A, Klatt P, Flores JM, Vina J, Serrano M, Blasco MA. Telomerase reverse transcriptase delays aging in cancer-resistant mice. Cell. 2008; 135: 609-622.
33. Bahmani B, Amiri F, Rouhandeh AM, Bahadori M, Harati MD, Roudkenar MH. The Lcn2-engineered HEK-293 cells show senescence under stressful condition. Iran J Basic Med Sci. 2015; 18: 459-464.
34. Ryu S, Kawamura R, Naka R, Silberberg YR, Nakamura N, Nakamura C. Nanoneedle insertion into the cell nucleus does not induce double-strand breaks in chromosomal DNA. J Biosci Bioeng. 2013; 116: 391-396.
35. Kim NW, Piatyszek MA, Prowse KR, Harley CB, West MC, Ho PL, Coviello GM, Wright WE, Weinrich SL, Shay JW. Specific association of human telomerase activity with immortal cells and cancer. Science. 1994; 266: 2011-2015.
36. Shay JW, Zou Y, Hiyama E, Wright WE. Telomerase and cancer. Hum Mol Genet. 2001; 10: 677-685.
37. Wege H, Le HT, Chui MS, Liu L, Wu J, Giri R, Malhi H, Sappal BS, Kumaran V, Gupta S. Telomerase reconstitution immortalizes human fetal hepatocytes without disrupting their differentiation potential. Gastroenterology. 2003; 124: 432-444.
38. Hiyama E, Gollahon L, Kataoka T, Kuroi K, Yokoyama T, Gazdar AF, Hiyama K, Piatyszek MA, Shay JW. Telomerase activity in human breast tumors. J Natl Cancer Inst. 1996; 88: 116-122.
39. Morales CP, Holt SE, Ouellette M, Kaur KJ, Yan Y, Wilson KS, White MA, Wright WE, Shay JW. Absence of cancer-associated changes in human fibroblasts immortalized with telomerase. Nat Genet. 1999; 21: 115-118.
40. Haendeler J, Dröse S, Büchner N, Jakob S, Altschmied J, Goy C, Spyridopoulos I, Zeiher AM, Brandt U, Dimmeler S. Mitochondrial telomerase reverse transcriptase binds to and protects mitochondrial DNA and function from damage. Arterioscler Thromb Vasc Biol. 2009; 29: 929-935.
41. Kovalenko OA, Caron MJ, Ulema P, Medrano C, Thomas AP, Kimura M, Bonini MG, Herbig U, Santos JH. A mutant telomerase defective in nuclear-cytoplasmic shuttling fails to immortalize cells and is associated with mitochondrial dysfunction. Aging Cell. 2010; 9: 203-219.
42. Saretzki G. Telomerase, mitochondria and oxidative stress. Exp Gerontol. 2009; 44: 485-492.
43. Scheiman J, Jamieson K, Ziello J, Tseng J, Meruelo D. Extraribosomal functions associated with the C terminus of the 37/67 kDa laminin receptor are required for maintaining cell viability. Cell Death Dis. 2010; 1: e42.
44. Sato M, Kinoshita K, Kaneda Y, Saeki Y, Iwamatsu A, Tanaka K, Kaneda Y. Analysis of nuclear localization of laminin binding protein precursor p40 (LBP/p40). Biochem Biophys Res Commun. 1996; 229: 896-901.
45. de Jesus BB, Schneeberger K, Vera E, Tejera A, Harley CB, Blasco MA. The telomerase activator TA-65 elongates short telomeres and increases health span of adult/old mice without increasing cancer incidence. Aging Cell. 2011; 10: 604-621.
46. Samper E, Flores JM, Blasco MA. Restoration of telomerase activity rescues chromosomal instability and premature aging in Terc−/− mice with short telomeres. EMBO Rep. 2001; 2: 800-807.
47. Hao LY, Armanios M, Strong MA, Karim B, Feldser DM, Huso D, Greider CW. Short telomeres, even in the presence of telomerase, limit tissue renewal capacity. Cell. 2005; 123: 1121-1131.
48. Matsunaga H, Handa JT, Aotaki-Keen A, Sherwood SW, West MD, Hjelmeland LM. Beta-galactosidase histochemistry and telomere loss in senescent retinal pigment epithelial cells. Invest Ophthalmol Vis Sci. 1999; 40: 197-202.
49. Herbig U, Jobling WA, Chen BP, Chen DJ, Sedivy JM. Telomere shortening triggers senescence of human cells through a pathway involving ATM, p53, and p21 CIP1, but not p16 INK4a. Mol Cell. 2004; 14: 501-513.

50. Sharma GG, Gupta A, Wang H, Scherthan H, Dhar S, Gandhi V, Iliakis G, Shay JW, Young CS, Pandita TK. hTERT associates with human telomeres and enhances genomic stability and DNA repair. Oncogene. 2003; 22: 131-146.

51. Armanios M. Telomeres and age-related disease: how telomere biology informs clinical paradigms. J Clin Invest. 2013; 123: 996-1002.

Appendix G

Co-authored publications (not pertaining to current study)

PLOS | ONE

RESEARCH ARTICLE

Knock-Down of the 37kDa/67kDa Laminin Receptor LRP/LR Impedes Telomerase Activity

Kerrilyn Naidoo[1*], Sibusiso T. Malindisa[1*], Tyrone C. Otgaar[1], Martin Bernert[1], Bianca Da Costa Dias[1*], Eloise Ferreira[1], Uwe Reusch[2], Stefan Knackmuss[2], Melvyn Little[2], Stefan F. T. Weiss[1‡*], Bolleb T. Letsolo[1‡*]

1 School of Molecular and Cell Biology, University of the Witwatersrand, Private Bag 3, Wits, 2050, Johannesburg, Republic of South Africa, 2 Affimed GmbH, Technologiepark, Im Neuenheimer Feld 582, 69120, Heidelberg, Germany

☯ These authors contributed equally to this work.
‡ These authors also contributed equally to this work.
* Stefan.weiss@wits.ac.za (SFTW); Bolleb.Letsolo@wits.ac.za (BTL)

OPEN ACCESS

Citation: Naidoo K, Malindisa ST, Otgaar TC, Bernert M, Da Costa Dias B, Ferreira E, et al. (2015) Knock-Down of the 37kDa/67kDa Laminin Receptor LRP/LR Impedes Telomerase Activity. PLoS ONE 10(11): e0141618. doi:10.1371/journal.pone.0141618

Editor: Ming Tan, University of South Alabama, UNITED STATES

Received: July 22, 2015

Accepted: October 9, 2015

Published: November 6, 2015

Copyright: © 2015 Naidoo et al. This is an open access article distributed under the terms of the Creative Commons Attribution License, which permits unrestricted use, distribution, and reproduction in any medium, provided the original author and source are credited.

Data Availability Statement: All relevant data are within the paper.

Funding: This work was supported by the National Research Foundation, the Republic of South Africa. Any opinions, findings and conclusions or recommendations expressed in this material are those of the authors, and therefore, the National Research Foundation does not accept any liability in this regard thereto. The funders had no role in study design, data collection and analysis, decision to publish or preparation of the manuscript. The research from which this publication emanated was co-funded by the South African Medical Research

Abstract

Cancer has become a major problem worldwide due to its increasing incidence and mortality rates. Both the 37kDa/67kDa laminin receptor (LRP/LR) and telomerase are overexpressed in cancer cells. LRP/LR enhances the invasiveness of cancer cells thereby promoting metastasis, supporting angiogenesis and hampering apoptosis. An essential component of telomerase, hTERT is overexpressed in 85–90% of most cancers. hTERT expression and increased telomerase activity are associated with tumor progression. As LRP/LR and hTERT both play a role in cancer progression, we investigated a possible correlation between LRP/LR and telomerase. LRP/LR and hTERT co-localized in the perinuclear compartment of tumorigenic breast cancer (MDA_MB231) cells and non-tumorigenic human embryonic kidney (HEK293) cells. FLAG® Co-immunoprecipitation assays confirmed an interaction between LRP/LR and hTERT. In addition, flow cytometry revealed that both cell lines displayed high cell surface and intracellular LRP/LR and hTERT levels. Knock-down of LRP/LR by RNAi technology significantly reduced telomerase activity. These results suggest for the first time a novel function of LRP/LR in contributing to telomerase activity. siRNAs targeting LRP/LR may act as a potential alternative therapeutic tool for cancer treatment by (i) blocking metastasis (ii) promoting angiogenesis (iii) inducing apoptosis and (iv) impeding telomerase activity.

Introduction

Cancer has become a major problem worldwide due to its increasing incidence and mortality rates. According to the World Health Organisation (WHO), cancer accounted for 8.2 million deaths in 2012 alone (http://www.who.int/cancer/en/).

Council (SAMRC). The specific roles of these authors are articulated in the 'author contributions' section.

Competing Interests: S.F.T.W. is currently a PLOS ONE Editorial Board Member. The patent, EP 1670826, co-owned by the University of the Witwatersrand and Affinod Therapeutics AG covers LRP/LR specific antibodies used in this study as tools for diagnosis and therapy of cancer. This granted European patent was validated in the United Kingdom, France, Germany, Switzerland and Austria. Further, a South African Provisional Patent Application 2014/08990, owned by the University of the Witwatersrand covers the inhibition of the development of cancer cells by the modification of the levels of LRP/LR. This does not alter the authors' adherence to all the PLOS ONE policies on sharing data and materials. U.R., S.K. and M.L. are affiliated with or employed by Affinod Therapeutics AG, a commercial company which produces therapeutic antibodies for the treatment of cancer and inflammatory diseases. This does not alter our adherence to PLOS ONE policies on sharing data and materials.

The 37kDa/67kDa laminin receptor precursor/ high affinity laminin receptor (LRP/LR) is a high affinity cell surface receptor for laminin-1, an extracellular matrix glycoprotein involved in cell growth, movement, attachment and differentiation (for review: [1, 2]). The relationship between the 67kDa high affinity receptor (LR) and the 37kDa laminin receptor precursor (LRP) remains unknown. LRP/LR is localized on the cell surface as well as in the cytoplasm, perinuclear compartment and the nucleus. The overexpression of LRP/LR is evident in multiple cancer types, and directly correlates with the invasiveness of cancer cells which thereby enhances the risk of cancer metastasis [3–7].

LRP/LR further plays fundamental roles in neurodegenerative disorders such as prion diseases [8–12] and Alzheimer's Disease [13–17].

Telomeres are especialised DNA-protein structures found at the ends of linear eukaryotic chromosomes. The ends of telomeres have the ability to form a telomere-loop (t-loop) structure [18]. The t-loop is stabilised by the "Shelterin" complex [19]. In this conformation, chromosome ends are protected from degradation and illegitimate processing which could results in premature senescence, recombination and end-to-end fusions and ultimately genome instability; a hallmark of cancer [20–22]. During semi-conservative DNA replication, DNA polymerase fails to replicate the chromosomal ends during the lagging strand synthesis, resulting in the loss of terminal sequences, a phenomenon known as "end replication problem" [23–25]. Cells that are unable to compensate for this mechanism experience progressive telomere shortening, which in turn triggers growth arrest called replicative senescence [26–28]. Replicative senescence is a tumor protective mechanism which cells have to bypass to acquire immortality [29].

Telomeres are maintained and replenished by telomerase. Telomerase is a holoenzyme and a cellular ribonucleoprotein that is involved in the addition of TTAGGG repeats to the 3'end of chromosomes. It is composed of two essential components, the enzymatic reverse transcriptase catalytic subunit, hTERT and the integral RNA component, hTR or hTERC [30, 31]. hTERT overexpression and telomerase activity are detected in highly proliferative cells such as embryonic cells, germline cells, adult stem cells and most cancer types [32, 33]. Telomerase stimulates tumor progression by stabilizing the telomeres to prevent the induction of replicative senescence and/or apoptosis. Therefore elevated telomerase activity could prevent a pro-cancer activity and still function as an anti-aging factor by elongating existing telomeres and preventing an accumulation of short telomeres [34, 35].

As LRP/LR and hTERT both play a role in cancer progression and share sub-cellular localizations, we sought to investigate a possible correlation between LRP/LR and telomerase activity.

Materials and Methods

Cell culture

Human embryonic kidney cells (HEK293) were cultured in Dulbecco's Modified Eagle Medium (DMEM) high glucose (Hyclone). MDA_MB231 breast cancer cells were cultured in DMEM/Ham's-F12 (1:1). All media was supplemented with 10% fetal calf serum (FCS) and 1% penicillin/streptomycin. The cells were cultured at 37°C and 5% CO_2. Non-tumorigenic HEK 293 cells were used as the positive control as they exhibit high telomerase activity whereas the tumorigenic MDA_MB231 cells were used as the experimental model as they are tumorigenic and metastatic.

Reagents and antibodies

IgG1-I5 18 was recombinantly produced in a mammalian expression system as described by Zuber et al., (2008) [36].

Flow cytometric analysis of cell surface and intracellular levels

Quantification of cell surface and intracellular levels of LRP/LR and hTERT was conducted using flow cytometry. Trypsin/EDTA was used to facilitate detachment of adherent cells which was followed by centrifugation at 1200 rpm for 10 minutes. Cells were subsequently fixed by re-suspending them for 10 minutes at 4°C in 4% paraformaldehyde. Cells were then permeabilised by resuspension in methanol for 30 minutes to detect intracellular levels. Cells were again centrifuged in FACS buffer which allowed for the preparation of two cell suspensions, one to which anti-LRP/LR specific antibody IgGI -1518 was added to detect LRP/LR and anti-telomerase reverse transcriptase was added to detect hTERT in another. The cell suspension containing only PBS but no antibody was used as the negative control. All suspensions were incubated at room temperature for 1 hour. Following three washing steps with 1X PBS, anti-human-FITC coupled secondary (Sigma Aldrich) was added to each cell suspension to detect LRP/LR and APC-coupled to detect hTERT, followed by another 1 hour incubation period. Furthermore, three post-incubation washes were performed and cell suspensions were analysed using the BD Accuri C6 flow cytometer. The experiments were performed in triplicate and repeated at least three times.

Confocal microscopy

In order to visualize the co-localization of LRP/LR and hTERT on the cell surface and intracellularly, confocal microscopy was employed. Cells were first seeded on coverslips and allowed to reach 70% confluency. Cells were fixed in 4% formaldehyde in PBS for approximately 15 minutes followed by several washes with PBS. Cells were permeabilised for intracellular visualization with Triton-X BSA solution for 15 minutes followed by several washes. Cells were blocked in 0.5% BSA in PBS for 5–10 minutes. After washing with 1 x PBS, excess PBS was blotted off. The coverslips containing cells were placed on a glass slide (with cells facing upwards) and this was followed by addition of primary antibody IgGI -1518 (1:100) diluted in 0.5% BSA and anti-Telomerase reverse transcriptase (1:100) diluted in 0.5% BSA and incubated at 4°C overnight. At the end of incubation period, the coverslips were rinsed thrice in PBS/BSA and incubated with FITC-coupled and APC-coupled secondary antibodies (diluted in 0.5% BSA) for 1 hour in the dark. After which, the cells were again rinsed thrice as before. Thereafter, Hoechst 33342 diluted in PBS was administered for 5–10 minutes. Cells were finally washed once in PBS alone and mounted on to a clean slide using GelMount (Sigma-Aldrich). A period of 45 minutes was allocated to allow for setting to take place. Images were acquired at room temperature with 60X magnification using the Olympus IX71 Immunofluorescence Microscope and Olympus XM10 greyscale camera analysis. Research Image Processing Software was used to capture the images.

FLAG® Co-immunoprecipitation assay (Pull down Assay)

To assess whether there is an interaction between LRP/LR and hTERT, HEK293 cells were transfected with pCIneo-moLRP:FLAG [37] using Lipofectamine 3000 and cultured to stably express the LRP:FLAG as per the manufacturer's instructions (Invitrogen). The cell lysate was produced from both non-transfected HEK293 cells (lacking the LRP:-FLAG) as well as HEK293 cells transfected with pCIneo-moLRP:-FLAG. A modified procedure using FLAG® Immunoprecipitation Kit (Sigma-Aldrich) was then used to selectively bind the FLAG peptide. This involved incubating cell lysates with the Anti-FLAG M2 beads in Eppendorf tubes at 4°C overnight. Thereafter, three washes were performed with 1x wash buffer provided in the kit. The washes were then collected as they contained unbound protein. Proteins were then collected and analysed by western blotting. The murine anti-FLAG (Sigma F-3165)

(1:4000) and rabbit anti-hTERT (Abcam ab 183105) (1:1000) primary antibodies were used to detect LRP::FLAG and hTERT, respectively. These were then detected using anti-rabbit IgG (Cell signalling 7074S) and anti-murine IgG (Sigma A4416) secondary antibodies coupled with an HRP enzyme.

Western blotting and SDS-PAGE

Western blotting was used to determine the protein levels of LRP post-transfection with siRNA-LAMR1 when compared to untreated controls, with β-actin used as the loading control. Briefly, cells were lysed, protein levels quantified and 5μg of cell lysate was resolved on a polyacrylamide gel. The proteins were subsequently transferred to a polyvinylidene fluoride (PVDF) membrane for 45 minutes at 350 mV and a semi-dry transferring apparatus. The membrane was blocked in a 1:10 000 solution of the LRP-specific primary antibody IgG1-I518 in 3% BSA in PBS-Tween at 4°C overnight, with shaking. The membrane was subsequently washed in PBS-Tween, and further incubated in a 1:10 000 solution of anti-human HRP secondary antibody in 3% BSA in PBS-Tween for 1 hour at room temperature with shaking, and washed as before prior to being analysed.

siRNA-mediated down-regulation of LRP

HEK293 and MDA_MB231 cells were transfected for LRP knockdown with siRNA purchased from Dharmacon, Cat # J-013303-08, according to manufacturer's instructions using Dharmafect® 1 transfection reagent. Control siRNA used—Cat # D-001810-04-20. Mission siRNA universal negative control (SIC001 –Sigma Aldrich) was used according to manufacturer's instructions as a negative control for the experiment.

Detection of telomerase activity

We utilized the TRAPeze RT® Telomerase detection Kit (Merck Millipore) to determine telomerase activity according to manufacturer's instructions with minor modifications. Briefly, cells were harvested and washed in PBS. The cells were then lysed with CHAPS lysis buffer. Protein and RNA were collected in the supernatant. Protein concentration was standardized to 500 ng/μl for all experimental and control reactions. All samples were then subjected to experimental analysis accompanied by two controls; heat treatment at 85°C for 10 minutes and control reaction containing a PCR inhibitor as per the manufacturer's instruction. All reactions were performed in triplicate. The reactions were carried out in the LightCycler LC480 (Roche) under the following cycling conditions: 37°C for 30 minutes, 95°C for 2 minutes and 45 cycles of 95°C for 15 seconds, 59°C for 60 seconds and 45°C for 10 seconds. Telomerase activity was estimated by extrapolation from the standard curve generated by 1:10 serial dilutions (40–0.4 amoles) of TSR8 control as per Merck Millipore instructions. The data was analysed in LightCycler® Software version 1.5.1.

Data analysis and statistics

Statistical analysis was conducted in Graphpad Prism version 5.03. All statistical analyses were performed using a two-tailed Student's *t*-test with a 95% confidence interval. *P*-values of less than 0.05 were considered significant. The linear dependencies between two variables were expressed using Pearson's (*r*) correlation co-efficient.

Results

Human embryonic kidney and metastatic breast cancer cells display LRP/LR and hTERT on the cell surface and intracellularly

Since the overexpression of LRP/LR and hTERT has been observed in numerous cancer cell lines, the levels of LRP/LR and hTERT on the cell surface and intracellularly on HEK293 and MDA_MB231 cells were examined by flow cytometry. HEK293 and MDA_MB231 cells displayed high levels of LRP/LR and hTERT on both the cell surface and intracellularly (Fig 1). Of the assessed HEK293 cell population, 71.22% and 97.98% of the cells expressed intracellular LRP/LR and hTERT, respectively. MDA_MB231 cells exhibited 98.82% and 94.54% of LRP/LR and hTERT intracellularly, respectively (Fig 1). The levels of LRP/LR and hTERT on the cell surface were similarly determined. Flow cytometry revealed that 75.26% and 98.56% of HEK293 cells expressed LRP/LR and hTERT on the cell surface, respectively. MDA_MB231 cells expressed 99.17% and 95.86% of LRP/LR and hTERT on the cell surface, respectively (Fig 1). We confirmed previous studies that HEK293 and MDA_MB231 cells display high levels of LRP/LR. However, this is the first report noting the levels of hTERT both intracellularly and on the cell surface on these two cell lines.

LRP/LR co-localizes with hTERT on the cell surface and in the perinuclear compartments

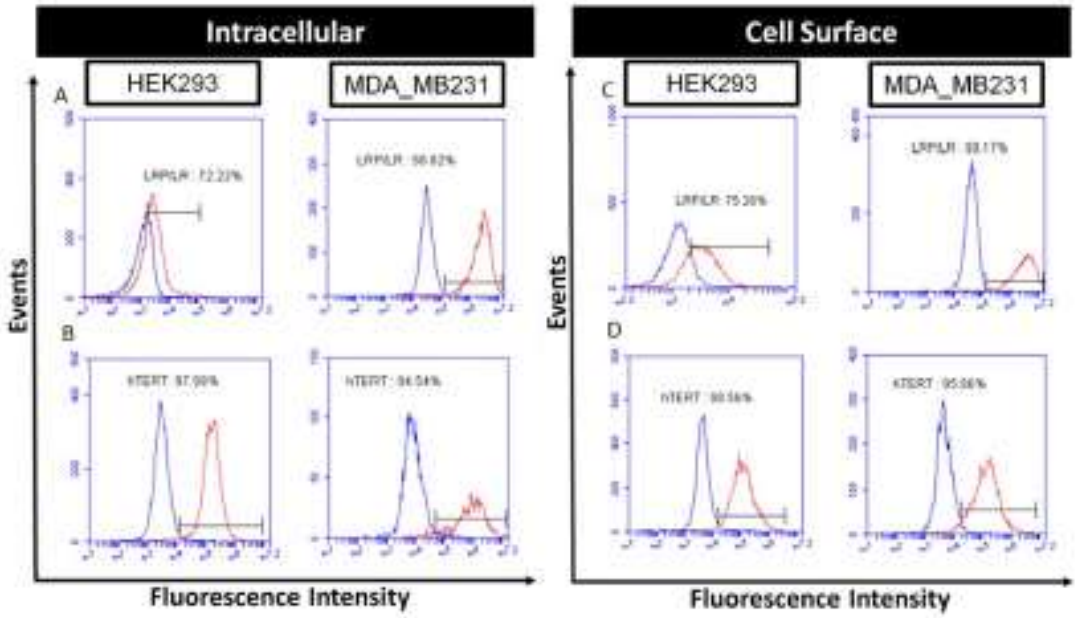
Confocal microscopy was employed to investigate whether LRP/LR and hTERT co-localize on the cell surface as well as intracellularly, as sharing a similar cellular localization may be indicative of a possible association between these proteins. Co-localization of LRP/LR and hTERT was detected on the cell surface of non-permeabilised HEK293 and MDA_MB231 cells (Fig 2b and 2d) and pronounced in the perinuclear compartments of permeabilised HEK293 and MDA_MB231 cells (Fig 2a and 2c). These results demonstrate that LRP/LR and hTERT co-localize in perinuclear compartments and the cell surface but undetectable/no co-localization in the nucleus of the HEK293 and MDA_MB231 cells, respectively.

FLAG$^{®}$ co-immunprecipitation assay of LRP/LR and hTERT confirms interaction

To assess whether the observed co-localization of the two proteins indicated interaction/association with each other, FLAG$^{®}$ co-immunprecipitation/pull down assays were performed (Fig 3). The presence of the LRP-FLAG and hTERT proteins was detected by corresponding antibodies. h-TERT (panel A, bound protein) and LRP-FLAG (panel B, bound protein) both bound to FLAG$^{®}$ M2- beads, in pCI neo-moLRP-FLAG transfected cells, whereas both proteins failed to bind to FLAG$^{®}$-M2 beads in non-transfected cells (bound protein panel A and B, non-transfected cells). This strongly indicates an interaction/association between hTERT and LRP-FLAG.

siRNA-mediated knockdown of LRP/LR expression in HEK293 and MDA_MB231 cells

To assess whether LRP/LR influences telomerase activity, LRP/LR was down-regulated by employing RNA interference technology using small interfering RNAs (siRNAs). The level of LRP/LR expression in HEK293 and MDA_MB231 cells after transfection with siRNA-LAMR1 was determined using western blotting and was quantified by densitometry (Fig 4). The level of LRP was reduced by 90.48% and 92.59% in HEK293 and MDA_MB231 cells respectively, compared to the non-transfected controls.



		HEK293	MDA_MB231
LRP/LR	Surface	75.26%	99.17%
	Intracellular	72.22%	98.82%
hTERT	Surface	98.56%	95.86%
	Intracellular	97.98%	94.54%

Fig 1. Flow cytometric detection of intracellular and cell surface levels of LRP/LR and hTERT on HEK293 and MDA_MB231 cells. A) Intracellular levels of LRP/LR in permeabilised HEK293 and MDA_MB231 cells were determined primarily by incubating the cells with IgG1-IS18 followed by incubation with anti-human-FITC coupled secondary antibodies (Sigma-Aldrich). B) Intracellular levels of hTERT in permeabilised HEK293 and MDA_MB231 cells were determined primarily by incubating the cells with anti-Telomerase reverse transcriptase antibody followed by incubation with goat anti-mouse IgG-APC coupled secondary antibodies (Sigma-Aldrich). C) Cell surface levels of LRP/LR in non-permeabilised HEK293 and MDA_MB231 cells were determined primarily by incubating the cells with IgG1-IS18 followed by incubation with anti-human-FITC coupled secondary antibodies (Sigma-Aldrich). D) Cell surface levels of hTERT in non-permeabilised HEK293 and MDA_MB231 cells were determined primarily by incubating the cells with anti-telomerase reverse transcriptase antibody followed by incubation with Goat anti-mouse IgG-APC coupled secondary antibodies (Sigma-Aldrich). The blue curve represents the no primary antibody control (to account for non-specificity of the secondary antibodies), whilst the red curve represents cells that were treated with both primary and secondary antibodies. The percentage represents the proportion of cells within the population which expressed LRP/LR and hTERT intracellularly and on the cell surface. This was calculated using a linked marker from the point of intersection between the curves to the end of the red curve.

doi:10.1371/journal.pone.0141618.g001

siRNA-mediated knock-down of LRP/LR in HEK293 and MDA_MB231 cells significantly impedes telomerase activity

The telomerase activity in response to the siRNA-mediated down regulation of LRP expression in HEK293 and MDA_MB231 cells was assessed using a TRAPeze RT® telomerase detection kit (Merck Millipore). HEK293 and MDA_MB231 cells were transfected with siRNA-LAMR1

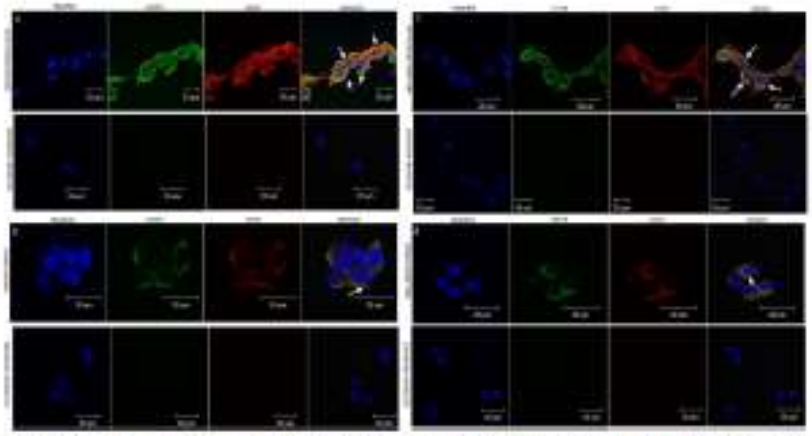


Fig 2. Confocal microscopy analysis of the interaction between LRP/LR and hTERT on MDA_MB231 and HEK293 cells. A) Intracellular LRP/LR and hTERT on immunolabelled HEK293 cells. (B) Endogenous cell surface LRP/LR and hTERT on immunolabelled HEK293. (C) Intracellular LRP/LR and hTERT on immunolabelled MDA_MB231 cells. (D) Endogenous cell surface LRP/LR and hTERT on immunolabelled MDA_MB231. hTERT was detected using anti-telomerase reverse transcriptase and anti-goat to mouse e-APC antibodies. LRP/LR was detected employing anti-IgG-IS18 and anti-human-RTC antibodies. Merge images verified the co-localization. The yellow staining indicates areas of co-localization. Secondary antibody controls are shown beneath each panel. Fluorescence was detected and images were acquired using the Olympus IX 71 Immunofluorescence Microscope and Analysis Get It Research Software. Scale bars are 20μm. White arrows point to areas of co-localization.

doi:10.1371/journal.pone.0141618.g002

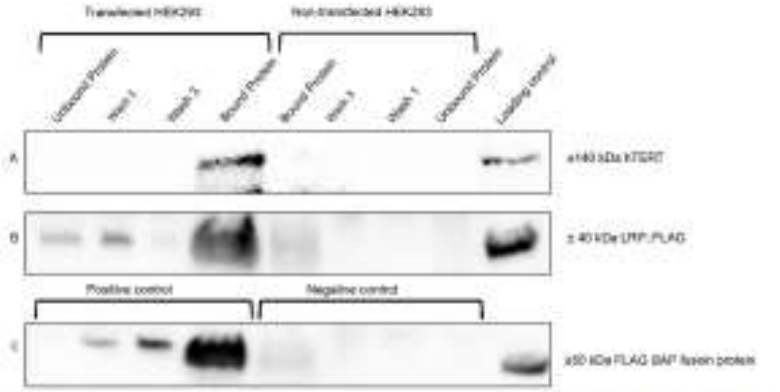


Fig 3. Flag® Immunoprecipitation assays confirming an interaction between LRP/LR and hTERT. Pull down assays were used to detect LRP::FLAG as well as any associated proteins bound to the anti-M2 flag beads. A loading control of crude HEK293 lysate was incorporated to ensure the validity of the blots. Panel C indicates the positive and negative controls, where the Bound protein shows the detection of the BAP fusion protein (50kDa) to the anti-FLAG beads. Panel B indicates that the LRP::FLAG protein was only present in the HEK293 transfected samples, where FLAG was detected on the anti-FLAG beads (Bound protein). Panel A illustrates the detection of a ≥ 140 kDa band (Bound protein) showing a pull down of hTERT for the HEK293 transfected cell line, whereas no signal was detected for the non-transfected HEK293 cell line.

doi:10.1371/journal.pone.0141618.g003

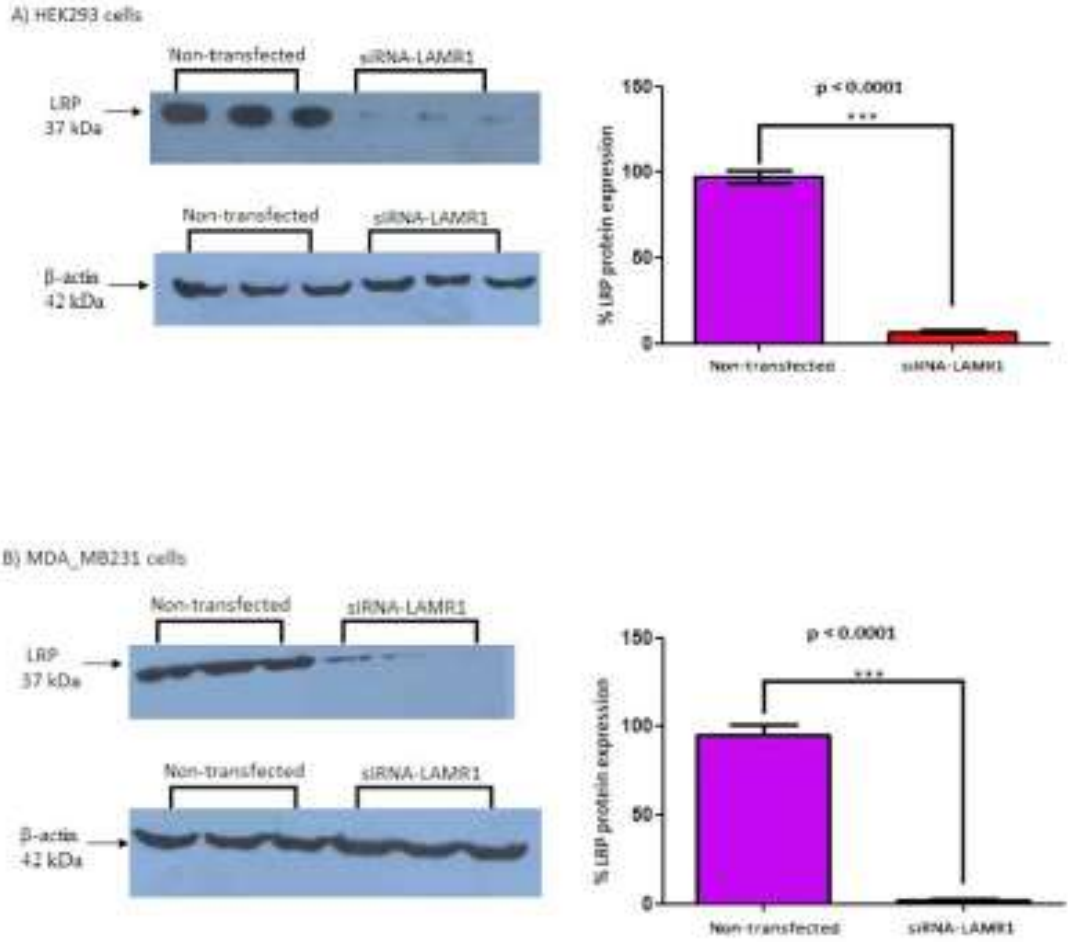


Fig 4. siRNA-mediated knock-down of LRP/LR in HEK293 and MDA_MB231 cells. The expression level in HEK293 and MDA_MB231 cells was investigated 72h post-transfection with siRNA-LAMR1. Densitometric analysis of western blot signals revealed a significant (*** $p < 0.001$) 90.48% and 92.59% reduction in LRP protein expression in A) HEK293 and B) MDA_MB231 cells, respectively, compared to control non-transfected cells (set at 100%).

doi:10.1371/journal.pone.0141618.g004

and siRNA-TFRC/DICER1 (positive control). The level of telomerase activity in HEK293 and MDA_MB231 cells was significantly reduced (Fig 5) after the knock-down of LRP/LR.

Discussion

Numerous studies have implicated LRP/LR and telomerase in the progression of cancer. LRP/LR is overexpressed on the cell surface and intracellularly on a number of cancer cell lines. In these cells, LRP/LR has been shown to confer the ability to metastasize [1–7], hamper apoptosis

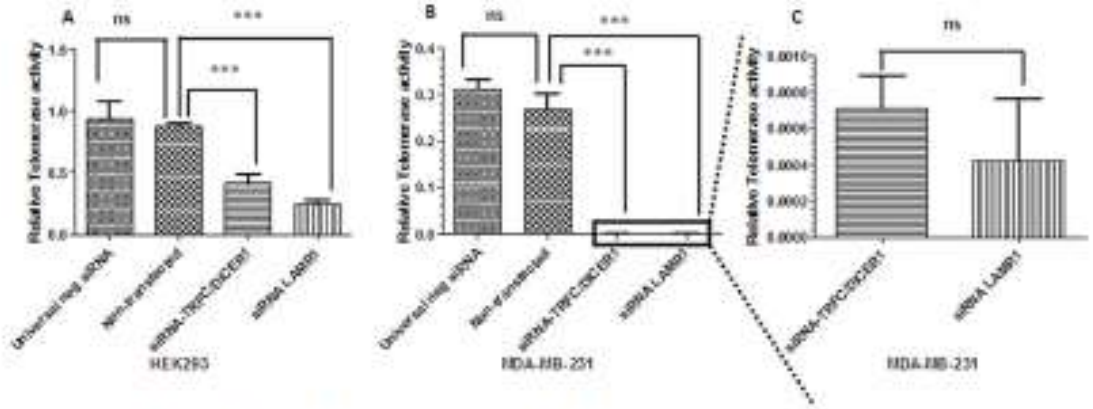


Fig 5. Effect of LRP/LR on telomerase activity in HEK293 and MDA_MB231 cells. The expression levels in HEK293 and MDA_MB231 cells was investigated using TRAPEZE Telomerase kit (Merck Millipore) and qPCR. Analysis of the concentrations revealed a significant (*** $p < 0.001$) reduction in telomerase activity once LRP was knocked down in A) HEK293, B) and C) MDA_MB231 cells., respectively, compared to control non-transfected cells and negative control siRNA transfected cells. Non-significant (ns) at $p > 0.05$.

doi:10.1371/journal.pone.0141618.g005

[38] and promote the induction of tumor angiogenesis [39]. Moreover, telomerase up-regulation enables highly proliferating cancer cells to bypass checkpoint signals during critical telomere shortening which typically induce cellular senescence and cell death (Shay & Wright, 2002). Given that LRP/LR and telomerase are involved in a number of cellular processes and are found in numerous cellular locations (cell surface, nucleus and the perinuclear compartments), an association between these macromolecules warranted investigation.

The tumorigenic breast cancer (MDA_MB231) and human embryonic kidneys (HEK293) cells displayed LRP/LR and hTERT on their cell surface and intracellularly. Flow cytometric analysis revealed that MDA_MB231 cells display higher intracellular levels of LRP/LR and hTERT in comparison to the HEK293 cells. Similarly, the cell surface levels of LRP/LR were higher in the tumorigenic cell line. However, there was no significant difference in the cell surface levels of hTERT between the two cell lines. This is most likely due to the fact that MDA_MB231 cells are tumorigenic and need more LRP/LR and hTERT to maintain their tumorigenic character.

We confirmed previous studies that LRP/LR [3–7] and hTERT are found on the cell surface [40]. The considerably high levels of hTERT on the cell surface may be explained by the presence of an associated peptide known as MHC class1 which is derived from hTERT and is expressed on the cell surface [40]. This peptide may be recognized by hTERT antibodies. These findings demonstrate that LRP/LR and hTERT are found on both the cell surface and intracellularly of both, HEK293 and MDA_MB231 cells.

Confocal microscopy was employed to investigate whether LRP/LR and hTERT co-localize which raises the potential that these proteins may form an association/interaction (Fig 2). The co-localization observed between LRP/LR and hTERT on both HEK293 and MDA_MB231 cells indicates that a spatial overlap occurs between the fluorescent immuno-labelled proteins. Although the close cellular proximity of these proteins on the cell surface of both cell lines has been detected, it does still suggest an association between LRP/LR and hTERT. Confocal microscopy was further utilized to examine whether LRP/LR co-localized with hTERT in sub-

cellular locations other than the cell surface. From Fig 2, it is evident that LRP/LR also shows a high degree of co-localization with hTERT within the perinuclear compartment. LRP/LR and hTERT are known to be present in the cytosol, nucleus and perinuclear compartments. From our results, the intracellular distribution of hTERT and LRP/LR is seen to be fairly widespread throughout the perinuclear compartments. This suggests that LRP/LR could be interacting with hTERT within the perinuclear compartments and on the cell surface.

FLAG®-Co-immunoprecipitation/pull down assays confirmed that LRP/LR and hTERT interact with each other. This interaction can either be direct or indirect. An indirect interaction could be mediated by proteins present in the crude lysate of the HEK293 cells.

To investigate whether LRP/LR has an effect on telomerase activity, LRP/LR expression was significantly decreased in MDA_MB231 and HEK293 cells by employing RNAi methodology. siRNAs directed against LRP were transfected into the aforementioned cells and the degree of LRP down regulation was assessed by western blotting followed by densitometric analysis (Fig 3). The level of LRP expression was significantly reduced by 90.48% and 92.59% in HEK293 and MDA_MB231 cells, respectively. The effect of the knockdown of LRP expression on telomerase activity was investigated by employing the TRAPeze RT® telomerase detection kit (Merck Millipore) and real-time PCR. LRP down regulation resulted in a significant reduction in telomerase activity in HEK293 and MDA_MB231 cells, respectively, suggesting a crucial role of LRP/LR in telomerase activity. These findings therefore suggest that LRP/LR may play a role in maintaining or enhancing telomerase activity.

Similarly, we observed a significant reduction in telomerase activity after transfection with the siRNA-TFRC/DICER1 positive control. According to Baumer et al., 2010, TFRC and DICER1 enhance telomerase activity [41], which clarifies why the down-regulation of TFRC/DICER1 resulted in a significant decrease of telomerase activity.

The functions of LRP/LR and hTERT in cancer progression are numerous. Targeting LRP/LR can therefore be developed as a strategy to hamper cancer progression. Additionally targeting telomerase activity by down regulating LRP/LR could potentially be an alternative target for cancer therapy as high telomerase expression in breast cancer has been associated with increased death risk, disease recurrence and plausible (possible) resistance to chemotherapy [42, 43]. Thus, targeting LRP/LR via RNAi methodology may serve as an alternative method to target telomerase activity and may thus be beneficial as a two-pronged approach to cancer treatment. Ie targeting LRP/LR could also be used in synergy with other cancer drugs to significantly reduce cancer progression.

The fact that the knock-down of LRP resulted in a significant decrease of hTERT activity, suggests that LRP/LR itself increases telomerase activity. This suggests that LRP/LR or fragments thereof which are responsible for hTERT activation may be used as an anti-aging drug since elongation of telomeres is crucial for implementing (impeding) the aging process. Since low-level telomerase activity can also drive age-related diseases and premature aging syndromes, expression of LRP/LR itself or fragments thereof may be utilized to increase telomerase activity and thus may act as potential therapeutics against these diseases.

In conclusion, we have confirmed that HEK293 and MDA_MB231 cells display hTERT and LRP/LR on the cell surface and intracellularly. The LRP/LR-hTERT interaction, confirmed by FLAG® Co-immunoprecipitation, may occur in the perinuclear compartments and on the cell surface. siRNA mediated knockdown of LRP/LR significantly decreased telomerase activity in HEK293 and MDA_MB231 cells. These findings suggest for the first time a novel function of LRP/LR in contributing to hTERT activity. siRNAs targeting LRP/LR may act as a potential alternative therapeutic tool for cancer treatment by (i) blocking metastasis, (ii) impeding tumor angiogenesis (iii) inducing apoptosis and as demonstrated in this study, by (iv) hampering telomerase activity.

Author Contributions

Conceived and designed the experiments: BTL SFTW. Performed the experiments: KN BDCD STM TCO MR. Analyzed the data: KN BDCD STM TCO MR EF. Contributed reagents/materials/analysis tools: UR SK ML. Wrote the paper: KN STM MR TCO BDCD BTL SFTW.

References

1. Omar A, Jovanovic K, Da Costa Dias B, Gonsalves D, Moodley K, Caveney R, et al. Patented biological approaches for the therapeutic modulation of the 37 kDa/67 kDa laminin receptor. Expert Opin Ther Pat. 2011; 21 (1):35–53. Epub 2010/11/30. doi: 10.1517/13543776.2011.538091 PMID: 21110768.
2. Mbazima V, Da Costa Dias B, Omar A, Jovanovic K, Weiss SF. Interactions between PrP(c) and other ligands with the 37-kDa/67-kDa laminin receptor. Front Biosci (Schol Ed). 2010; 1:5:1150–63. Epub 2010/06/03. PMID: 20515747.
3. Chetty C, Khumalo T, Da Costa Dias B, Reusch U, Knedlmusa S, Little M, et al. Anti-LRP/LR-specific antibody IgG1-iS18 impedes adhesion and invasion of liver cancer cells. PLoS One. 2014; 9(5): e96268. Epub 2014/05/07. doi: 10.1371/journal.pone.0096268 PMID: 24796101; PubMed Central PMCID: PMC4010464.
4. Omar A, Reusch U, Knedlmusa S, Little M, Weiss SF. Anti-LRP/LR-specific antibody IgG1-iS18 significantly reduces adhesion and invasion of metastatic lung, cervix, colon and prostate cancer cells. J Mol Biol. 2012; 419(1–2):103–9. Epub 2012/03/07. doi: 10.1016/j.jmb.2012.02.035 PMID: 22391421.
5. Khumalo T, Reusch U, Knedlmusa S, Little M, Veale RB, Weiss SF. Adhesion and invasion of Breast and Oesophageal Cancer Cells Are Impeded by Anti-LRP/LR-Specific Antibody IgG1-iS18. PLoS One. 2013; 8(6):e66237. Epub 2013/07/05. doi: 10.1371/journal.pone.0066237 PMID: 23825539; PubMed Central PMCID: PMC3688981.
6. Zuber C, Knedlmusa S, Zamora G, Reusch U, Vlasova E, Diehl D, et al. Invasion of tumorigenic HT1080 cells is impeded by blocking or down regulating the 37-kDa/67-kDa laminin receptor. J Mol Biol. 2008; 378(3):530–9. Epub 2008/04/05. doi: 10.1016/j.jmb.2008.02.004 PMID: 18395761.
7. Khumalo T, Ferreira E, Jovanovic K, Veale RB, Weiss SF. Knockdown of LRP/LR Induces Apoptosis in Breast and Oesophageal Cancer Cells. PloS one. 2015; 10(10):e0139564. Epub 2015/10/02. doi: 10.1371/journal.pone.0139564 PMID: 26422016.
8. Rieger R, Edenhofer F, Lasmezas CI, Weiss S. The human 37-kDa laminin receptor precursor interacts with the prion protein in eukaryotic cells. Nat Med. 1997; 3(12):1383–8. Epub 1997/12/13. PMID: 9396609.
9. Gauczynski S, Peyrin JM, Haik S, Leucht C, Hundt C, Rieger R, et al. The 37-kDa/67-kDa laminin receptor acts as the cell-surface receptor for the cellular prion protein. Embo J. 2001; 20(21):5863–75. Epub 2001/11/02. doi: 10.1093/emboj/20.21.5863 PMID: 11689422; PubMed Central PMCID: PMC125290.
10. Hundt C, Peyrin JM, Haik S, Gauczynski S, Leucht C, Rieger R, et al. Identification of interaction domains of the prion protein with its 37-kDa/67-kDa laminin receptor. Embo J. 2001; 20(21):5876–86. Epub 2001/11/02. doi: 10.1093/emboj/20.21.5876 PMID: 11689423; PubMed Central PMCID: PMC125293.
11. Gauczynski S, Nikles D, El-Gogo S, Papy-Garcia D, Rey C, Alban S, et al. The 37-kDa/67-kDa laminin receptor acts as a receptor for infectious prions and is inhibited by polysulfated glycans. J Infect Dis. 2006; 194(5):702–9. Epub 2006/08/10. doi: 10.1086/505814 PMID: 16897621.
12. Leucht C, Simonsen S, Rey C, Vana K, Rieger R, Lasmezas CI, et al. The 37 kDa/67 kDa laminin receptor is required for PrP(Sc) propagation in scrapie-infected neuronal cells. EMBO Rep. 2003; 4 (3):290–5. Epub 2003/03/14. doi: 10.1038/sj.embor.embor768 PMID: 12634848; PubMed Central PMCID: PMC1315896.
13. Da Costa Dias B, Jovanovic K, Gonsalves D, Moodley K, Reusch U, Knedlmusa S, et al. Anti-LRP/LR specific antibody IgG1-iS18 and knock-down of LRP/LR by shRNA rescue cells from Abeta42 induced cytotoxicity. Sci Rep. 2013; 3:2702. Epub 2013/09/21. doi: 10.1038/srep02702 PMID: 24048171; PubMed Central PMCID: PMC3776967.
14. Da Costa Dias B, Jovanovic K, Gonsalves D, Moodley K, Reusch U, Knedlmusa S, et al. The 37 kDa/67 kDa laminin receptor acts as a receptor for Abeta 42 internalisation. Sci Rep. 2014; 4:5566. Epub 2014/07/06. doi: 10.1038/srep05566 PMID: 24993253; PubMed Central PMCID: PMC4081222.
15. Jovanovic K, Lorus B, Da Costa Dias B, Penny C, Weiss SF. High resolution imaging study of interactions between the 37 kDa/67 kDa laminin receptor and APP, beta-secretase and gamma-secretase in Alzheimer's disease. PLoS One. 2014; 9(6):e100373. Epub 2014/06/28. doi: 10.1371/journal.pone.0100373 PMID: 24972054; PubMed Central PMCID: PMC4074076.

16. Jovanovic K, Gonsalves D, Da Costa Dias B, Moodley K, Reusch U, Knaus mus S, et al. Anti-LRP1/LR specific antibodies and shRNA antagonize amyloid beta shedding in Alzheimer's disease. Sci Rep. 2013; 3:2659. Epub 2013/09/21. doi: 10.1038/srep02659 PMID: 24045612; PubMed Central PMCID: PMC3776966.

17. Pimplikar EC, Jovanovic K, Pinto MG, Ferreira E, Da Costa Dias B, Penny C, et al. LRP1/LR antibody mediated rescuing of Abeta induced cytotoxicity is dependent on PrPc in Alzheimer's Disease. J Alzheimer's Disease2015.

18. Griffith JD, Comeau L, Rosenfield S, Stansel RM, Bianchi A, Moss H, et al. Mammalian telomeres end in a large duplex loop. Cell. 1999; 97(4):503–14. Epub 1999/05/25. PMID: 10338214.

19. de Lange T. Shelterin: the protein complex that shapes and safeguards human telomeres. Genes Dev. 2005; 19(18):2100–10. Epub 2005/09/17. doi: 10.1101/gad.1346005 PMID: 16166375.

20. Letsolo BT, Rowson J, Baird DM. Fusion of short telomeres in human cells is characterized by extensive deletion and microhomology, and can result in complex rearrangements. Nucleic Acids Res. 2010; 38(6):1861–72. Epub 2009/12/23. doi: 10.1093/nar/gkp1160 PMID: 20026586; PubMed Central PMCID: PMC2847243.

21. Capper R, Britt-Compton B, Tankimanova M, Rowson J, Letsolo B, Man S, et al. The nature of telomere fusion and a definition of the critical telomere length in human cells. Genes Dev. 2007; 21(19):2495–508. Epub 2007/10/03. doi: 10.1101/gad.439107 PMID: 17906915; PubMed Central PMCID: PMC1993879.

22. Palm W, de Lange T. How shelterin protects mammalian telomeres. Annu Rev Genet. 2008; 42:301–34. Epub 2008/08/06. doi: 10.1146/annurev.genet.41.110306.160350 PMID: 18680434.

23. Harley CB, Futcher AB, Greider CW. Telomeres shorten during ageing of human fibroblasts. Nature. 1990; 345(6274):458–60. Epub 1990/05/31. doi: 10.1038/345458a0 PMID: 2342578.

24. Harley CB, Kim NW, Prowse KR, Weinrich SL, Hirsch KS, West MD, et al. Telomerase, cell immortality, and cancer. Cold Spring Harb Symp Quant Biol. 1994; 59:307–15. Epub 1994/01/01. PMID: 7587082.

25. Allsopp RC, Chang E, Kashefi-Aazam M, Rogaev EI, Piatyszek MA, Shay JW, et al. Telomere shortening is associated with cell division in vitro and in vivo. Exp Cell Res. 1995; 220(1):194–200. Epub 1995/09/01. doi: 10.1006/excr.1995.1306 PMID: 7664836.

26. Harley CB, Vaziri H, Counter CM, Allsopp RC. The telomere hypothesis of cellular aging. Exp Gerontol. 1992; 27(4):375–82. Epub 1992/07/01. PMID: 1459213.

27. Shay JW, Wright WE. Senescence and immortalization: role of telomeres and telomerase. Carcinogenesis. 2005; 26(5):867–74. Epub 2004/10/09. doi: 10.1093/carcin/bgh296 PMID: 15471900.

28. Wright WE, Shay JW. The two-stage mechanism controlling cellular senescence and immortalization. Exp Gerontol. 1992; 27(4):383–9. Epub 1992/07/01. PMID: 1330985.

29. Shay JW, Pereira-Smith OM, Wright WE. A role for both RB and p53 in the regulation of human cellular senescence. Exp Cell Res. 1991; 196(1):33–9. Epub 1991/09/01. PMID: 1652450.

30. Greider CW, Blackburn EH. Telomeres, telomerase and cancer. Sci Am. 1996; 274(2):92–7. Epub 1996/02/01. PMID: 8560215.

31. Holt SE, Wright WE, Shay JW. Regulation of telomerase activity in immortal cell lines. Mol Cell Biol. 1996; 16(8):2932–9. Epub 1996/08/01. PMID: 8649404; PubMed Central PMCID: PMC231287.

32. Bodnar AG, Ouellette M, Frolkis M, Holt SE, Chiu CP, Morin GB, et al. Extension of life-span by introduction of telomerase into normal human cells. Science. 1998; 279(5349):349–52. Epub 1998/03/07. PMID: 9454332.

33. Kim NW, Piatyszek MA, Prowse KR, Harley CB, West MD, Ho PL, et al. Specific association of human telomerase activity with immortal cells and cancer. Science. 1994; 266(5193):2011–5. Epub 1994/12/23. PMID: 7605428.

34. Tomas-Loba A, Flores I, Fernandez-Marcos PJ, Cayuela ML, Maraver A, Tejera A, et al. Telomerase reverse transcriptase delays aging in cancer-resistant mice. Cell. 2008; 135(4):609–22. Epub 2008/11/18. doi: 10.1016/j.cell.2008.09.034 PMID: 19013273.

35. Bernardes de Jesus B, Vera E, Schneeberger K, Tejera AM, Ayuso E, Bosch F, et al. Telomerase gene therapy in adult and old mice delays aging and increases longevity without increasing cancer. EMBO Mol Med. 2012; 4(8):691–704. Epub 2012/05/16. doi: 10.1002/emmm.201200245 PMID: 22585399; PubMed Central PMCID: PMC3494070.

36. Zuber C, Knaus mus S, Zermoni G, Reusch U, Wasova E, Diehl D, et al. Invasion of tumorigenic HT1080 cells is impeded by blocking or down-regulating the 37-kDa/67-kDa laminin receptor. Journal of molecular biology. 2008; 378(3):530–9. Epub 2008/04/05. doi: 10.1016/j.jmb.2008.02.004 PMID: 18387633.

37. Vana K, Weiss S. A trans-dominant negative 37kDa/67kDa laminin receptor mutant impairs PrP(Sc) propagation in scrapie-infected neuronal cells. Journal of molecular biology. 2006; 358(1):57–66. Epub 2006/03/07. doi: 10.1016/j.jmb.2006.02.011 PMID: 16516231.

38. Moodley K, Weiss SF. Down-regulation of the non-integrin laminin receptor reduces cellular viability by inducing apoptosis in lung and cervical cancer cells. PLoS One. 2013; 8(3):e57409. Epub 2013/03/09. doi: 10.1371/journal.pone.0057409 PMID: 23472084; PubMed Central PMCID: PMC3589420.

39. Khaial R, Da Costa Dias B, Moodley K, Penny C, Reusch U, Knackmuss S, et al. In vitro inhibition of angiogenesis by antibodies directed against the 37kDa/67kDa laminin receptor. PLoS One. 2013; 8(3): e58389. Epub 2013/04/05. doi: 10.1371/journal.pone.0058389 PMID: 23554901; PubMed Central PMCID: PMC3595224.

40. Langlade-Demoyen P, Garcia Pons F, Addevi O, Cardinaud S, Neuveut C, Inventors. Polynucleotides Encoding MHC Class I-Restricted HTERT Epitopes, Analogues Thereof Or Polyepitopes Patent US 20140056932. 2010.

41. Beumer Y, Funk D, Schlosshauer B. Does telomerase reverse transcriptase induce functional de-differentiation of human endothelial cells? Cell Mol Life Sci. 2010; 67(14):2451–65. Epub 2010/03/31. doi: 10.1007/s00018-010-0349-z PMID: 20352467.

42. Li X, Lewis MT, Huang J, Gutierrez C, Osborne CK, Wu MF, et al. Intrinsic resistance of tumorigenic breast cancer cells to chemotherapy. J Natl Cancer Inst. 2008; 100(9):672–9. Epub 2008/05/01. doi: 10.1093/jnci/djn123 PMID: 18445819.

43. Lu L, Zhang C, Zhu G, Irwin M, Risch H, Menato G, et al. Telomerase expression and telomere length in breast cancer and their associations with adjuvant treatment and disease outcome. Breast Cancer Res. 2011; 13(3):R56. Epub 2011/06/08. doi: 10.1186/bcr2893 PMID: 21645365; PubMed Central PMCID: PMC3218945.

www.oncotarget.com Oncotarget, 2018, Vol. 9, (No. 43), pp: 27059-27073

Research Paper

LRP/LR specific antibody IgG1-iS18 impedes neurodegeneration in Alzheimer's disease mice

Eloise Ferreira[1], Monique J. Bignoux[1], Tyrone C. Otgaar[1], Nicolas Tagliatti[1], Katarina Jovanovic[1,2], Boitelo T. Letsolo[1] and Stefan F.T. Weiss[1]

[1]School of Molecular and Cell Biology, University of the Witwatersrand, Johannesburg, Republic of South Africa

[2]Present address: UCL Institute of Ophthalmology, London, UK

Correspondence to: Stefan F.T. Weiss, email: stefan.weiss@wits.ac.za

Keywords: Alzheimer's disease; amyloid beta; LRP-LR; therapeutic antibody; transgenic mice

Received: September 12, 2017 Accepted: May 08, 2018 Published: June 05, 2018

Copyright: Ferreira et al. This is an open-access article distributed under the terms of the Creative Commons Attribution License 3.0 (CC BY 3.0), which permits unrestricted use, distribution, and reproduction in any medium, provided the original author and source are credited.

ABSTRACT

Alzheimer's disease (AD) is a neurodegenerative disease caused by accumulation of amyloid beta (Aβ) plaque and neurofibrillary tangle formation. We have shown *in vitro*, that knock-down and blockade of the 37 kDa/67 kDa Laminin Receptor (LRP/LR) resulted in reduced Aβ induced cytotoxicity and Aβ accumulation. In order to test the effect of blocking LRP/LR on Aβ formation and AD associated symptoms, AD transgenic mice received the anti-LRP/LR specific antibody, IgG1-iS18 through intranasal administration. We show that this treatment resulted in an improvement in memory, and decreased Aβ plaque formation. Moreover, a significant decrease in $A\beta_{42}$ protein expression with a concomitant increase in amyloid precursor protein (APP) and telomerase reverse transcriptase (mTERT) levels was observed. These data recommend IgG1-iS18 as a potentially powerful therapeutic antibody for AD treatment.

INTRODUCTION

Alzheimer's disease (AD) is the most prevalent form of neurodegenerative disorders afflicting in excess of 47 million people worldwide [1]. Dementia, including AD poses a significant economic cost, estimated at 818 billion USD in 2015, which is expected to reach 2 trillion USD by 2030 [1]. Due to the considerable knowledge gap in the understanding of the disease causing mechanism, currently only palliative treatment options for AD are available. This highlights the pronounced need to advance the present knowledge base and develop therapeutic strategies for the treatment of AD.

There are two key neuropathological hallmarks of AD; the formation of extracellular amyloid beta (Aβ) plaques and the formation of intracellular neurofibrillary tangles consisting of aggregates of hyper-phosphorylated tau (a microtubule associated protein). Accumulation of these proteins eventually lead to neuronal loss [2]. Aβ plaques are predominantly made up of neurotoxic $A\beta_{42}$ [2] which is generated through the sequential cleavage of the amyloid precursor protein (APP) by β-secretase (also known as BACE1–B-site APP cleaving enzyme) and γ-secretase [3], which results in Aβ shedding. The soluble Aβ oligomers play a role in the formation of ion-permissible channels, therefore causing increased ion influx (of Ca^{2+} in particular) with resultant cytotoxicity [4, 5]. Aβ furthermore induces neuronal loss through an interaction with cell components, either through direct interaction with cell surface receptors [6] or indirectly by incorporating into lipid membranes and cell organelles [7]. One such receptor with which Aβ interacts is the 37 kDa Laminin Receptor Precursor/67 kDa high affinity Laminin Receptor (LRP/LR) [8, 9]. LRP/LR is a multifunctional, non-integrin, type II transmembrane receptor which is predominantly situated within lipid raft regions of plasma membranes as well as within the cytoplasm and the nucleus [10]. LRP/LR serves as a receptor for numerous components including viruses, bacteria, prion proteins, extracellular matrix proteins and very importantly, Aβ. LRP/LR therefore has copious functions in cancer [11, 12], angiogenesis [13], prion disorders [14–17], telomerase [18, 19] as well as AD [6, 8, 20–22]. It was recently discovered that LRP/LR co-localises with APP, indirectly interacts with β- secretase

and directly interacts with the catalytic unit (PS1) of γ-secretase to enhance cleavage of APP. In addition, it has been observed that $A\beta_{42}$ interacts with LRP/LR on the cell surface with resultant $A\beta_{42}$ internalisation and accumulation. Treatments targeting LRP/LR, such as the anti-LRP/LR antibody, IgG1-iS18 and shRNAs have shown to result in a significant reduction in Aβ shedding and can furthermore rescue cells from $A\beta_{42}$ induced cytotoxicity [8, 21, 23].

Another such protein with which LRP/LR interacts is the reverse transcriptase ribonucleoprotein, telomerase. Telomerase predominantly plays a role in maintaining telomeres in highly proliferative cells [24, 25] by catalysing the addition of TTAGGG repeats to telomeric DNA to protect telomeres from erosion. Telomerase consists of two essential components, the TERT enzyme which is responsible for the reverse transcriptase activity and the telomerase RNA template component, TERC [26]. Telomerase has furthermore been implicated in the pathological process of AD. It has been shown that people suffering from AD have shorter telomere lengths in their neuronal and T cells [27] and that $A\beta_{42}$ inhibits telomerase activity through the binding of Aβ oligomers to the telomeric DNA-RNA template complex of telomerase [28]. This indicates an antagonistic relationship between telomerase and Aβ within neurons. We have recently discovered that LRP/LR and hTERT interact, both on the cell surface and within the perinuclear compartments [19, 23]. Together with this, it was observed that knockdown of LRP/LR mediated by small interfering RNAs (siRNAs) caused a significant impediment of telomerase activity, indicating that LRP/LR has a function in regulating telomerase activity [18, 23].

TERT furthermore performs extra-telomeric functions, whereby it is known to play a protective role in the mitochondria against apoptosis, mitochondrial DNA damage [29] and is involved in DNA damage responses and repair [30]. It has been observed that DNA damage is an initial and critical contributor for aging and is affected by the accumulation of persistent DNA lesions containing unrepairable double strand DNA breaks (DSBs) [31]. Oxidative damage caused by free radical/ROS formation can lead to formation of DSBs which can trigger a series of repair pathways. These involve replacement of histone H2A with the histone variant H2AX, in nucleosomes which flank DSBs with concurrent or subsequent phosphorylation of a C-terminal serine in H2AX. Phosphorylated H2AX (γH2AX) helps recruit proteins containing phospho-specific interaction domains which in turn help recruit DNA repair factors [32]. Accumulating evidence suggests increased DNA damage, particularly oxidative damage, and deficiencies in the repair of DNA lesions in cells from patients with AD [33]. Importantly, Aβ peptides directly initiate free radical/ROS formation, cellular dysfunction, and subsequent neuronal death [31]. Hence, protection from DNA damage presents a basic approach for treatment of age-related diseases such as AD.

With this information in mind, we aimed to investigate LRP/LR as a potential therapeutic target for the treatment of AD in 5XFAD mice. In order to examine this, LRP/LR was blocked with IgG1-iS18 antibody and the effect of the treatment on AD related brain pathology, memory and the cognitive abilities of the mice were studied. In addition, levels of Aβ and other AD related proteins, γH2AX as well as TERT expression and telomerase activity were determined.

RESULTS

IgG1-iS18 significantly improves short term memory and learning ability of 5XFAD mice

In order to validate whether targeting LRP/LR using IgG1-iS18, in AD transgenic mice would have an effect on their cognitive abilities, the novel object recognition and puzzle box tests were performed. We carried out a intranasal treatment protocol twice a week for 8 weeks in 5XFAD transgenic mice beginning at the age of approximately 4–5 months. Mice received either PBS as control treatment or the anti-LRP/LR specific antibody, IgG1-iS18. After completion of the treatment protocol the novel object recognition test was performed and the percentage time exploring a familiar as well as novel object was recorded. A one-way between subjects ANOVA was conducted to compare the effect of treatment on the time exploring familiar and novel objects. The PBS treated mice showed no significant difference in the time spent exploring the familiar and novel objects [$F(1, 18) = 1.09$, $p = 0.311$]. However, mice that received IgG1-iS18 via intranasal administration spent 16.18% more time exploring the novel objects [$F(1, 16) = 11.36$, $p = 0.0039$] (Figure 1A). Post hoc analysis using the Tukey-HSD test indicated that the mean value for the exploration time (percentage) of the novel object (Mean = 58.09%, SD = 10.18%) was significantly different than the percentage time exploring the familiar objects (Mean = 41.91%, SD = 10.18%). Next, the puzzle box test was performed to determine the effect of intranasal administration on short and long term memory as well as the learning ability of the 5XFAD mice (Figure 1B). When analysing short term memory, the PBS treated mice were significantly impaired on T3 and T6, and had higher latencies to reach the goal zone compared to the mice that received IgG1-iS18 (T3 [$F(1, 20) = 4.69$, $p = 0.0426$] and T6 [$F(1, 21) = 4.49$, $p = 0.0461$]. Post hoc analysis further showed that the IgG1-iS18 treated mice (T3: Mean = 9.34 s, SD = 6.61 s; T6: Mean = 106.21 s, SD = 72.75 s) reached the goal zones in trial T3 and T6 in significantly less time than the PBS treated mice (T3: Mean = 23.77 s, SD = 21.09 s; T6: Mean = 157.82 s, SD = 36.39 s). One-way ANOVA and Tukey-Kramer post hoc analysis furthermore showed that the IgG1-iS18 treated group displayed learning of the open as well as the burrow puzzle with a significant

decrease in latencies from 40.2 s (T2) to 9.3 s (T3) (T2 vs. T3, $p = 0.0388$) and 180 s (T5) to 106.2 s (T6) (T5 vs. T6, $p = 0.0108$) respectively. In addition, PBS treated mice had higher latencies to reach the goal zone on T7, when analysing long term memory, though not significantly when compared to IgG1-iS18 treated mice (Mean (PBS) = 180, SD = 0; Mean (IgG1-iS18) = 146.73, SD = 58.73; $p = 0.06$) (Figure 1B).

Intranasal administration of IgG1-iS18 decreases AD histopathological hallmarks and Aβ levels in brains of AD transgenic mice

After sacrifice at 9 months, histological studies were performed utilizing the Congo red stain. The visual observation of these images revealed that treatment with IgG1-iS18 antibody (Figure 2B) caused a decrease in amyloid plaques in the hippocampus when compared to mice that received PBS (Figure 2A) treatment. Quantitative studies and post hoc analysis of the amyloid load (%) in the hippocampal sections of the PBS and IgG1-iS18 treated mice showed that there was a significant decrease after treatment with IgG1-iS18 (Mean = 0.64%, SD = 0.32%) when compared to the PBS treated mice (Mean = 1.52%, SD = 0.33%) [$F(1, 12) = 25.08$, $p = 0.00031$] (Figure 2C). To confirm the effect of intranasal IgG1-iS18 antibody treatment on amyloid levels, insoluble and soluble Aβ levels of the entire contralateral hemisphere of the mouse brains, from each of the two treatment groups were determined. Insoluble protein was extracted with guanidine hydrochloride (GuHCl) and dot-blot analysis was performed to determine the levels of Aβ per mg brain tissue. It was observed that there was a significant 24.72% [$F(1,30) = 26.46$, $p = 1.55E-05$] decrease in insoluble $A\beta_{1-42}$ after treatment with IgG1-iS18 (Mean = 75.28%, SD = 19.22%) when compared to the PBS control mice (Mean set to 100%) (Figure 3A). Next, we investigated the level of soluble $A\beta_{1-42}$ peptide by performing sandwich ELISAs. A highly significant decrease [$F(1,24) = 37.61$, $p = 2.46E-06$] was observed (Figure 3B) when the average $A\beta_{1-42}$ level of the nasal IgG1-iS18 antibody treated mice (Mean = 227.71 pg/mg, SD = 15.06 pg/mg) was compared with that of the PBS treated mice (Mean = 370.21 pg/mg, SD = 82.41 pg/mg).

Together, these data suggest that there is a significant decrease in Aβ protein levels in the mouse brain homogenates after treatment with IgG1-iS18.

IgG1-iS18 treatment substantially increases APP brain levels

Since we have previously reported that IgG1-iS18 treatment had no effect on cell surface levels of APP, β-secretase and γ-secretase in HEK293 cells, *in vitro*, [20] we wanted to confirm that levels of these proteins in the brain were the same in all treatment groups. Western blotting revealed uniform expression of LRP, β- and γ-secretase among the PBS and antibody treated animals (Supplementary Figure 1). This was expected as IgG1-iS18 blocks the interaction between LRP and β-, and γ-secretase, respectively, and therefore, does not affect protein levels [21, 22]. However, in contrast to these previously published observations, APP levels increased substantially and significantly after antibody treatment of the 5XFAD transgenic mice, with an average elevation of 85.86% [$F(1,14) = 51,11$, $p = 4.94E-06$] observed (Figure 4).

Intranasal IgG1-iS18 treatment significantly increases mTERT expression and phosphorylation of H2AX

We have recently shown that LRP/LR co-localizes with the reverse transcriptase ribonucleoprotein, TERT [18]. It has furthermore been reported that TERT plays a neuroprotective role [34] and that there is a reduction in expression of TERT protein in the brain, during normal aging in mice [35]. Therefore, we decided to investigate mTERT protein expression in the mouse hemi-brain homogenates. Western blot analysis revealed an extensive and highly significant 74.34% [$F(1,14) = 296.29$, $p = 8.14E-11$] increase in mTERT protein levels in the brain tissue of the IgG1-iS18 antibody treated mice compared to the PBS control group (Figure 5). Furthermore, post hoc analysis using the Tukey HSD test confirmed this observation. Moreover, since TERT is responsible for the reverse transcriptase activity of telomerase, we determined the effect of the IgG1-iS18 antibody treatment on telomerase activity in the mouse brain tissue. We detected extremely low levels of telomerase activity in the mouse brain homogenates of both the PBS as well as IgG1-iS18 treated mice and no significant change between control and treated mice was observed (Supplementary Figure 2). This is in agreement with previous findings describing downregulation of telomerase activity in rodent brain postnatally [36].

It has been established that DNA damage is an initial and critical contributor for aging and it has been suggested that the pathogenesis of AD may involve a DNA repair defect [33]. To further substantiate the neuroprotective role of IgG1-iS18 and to investigate the effect of this treatment on the DNA damage response, the levels of phosphorylated H2AX (γH2AX) was determined. These histones are specifically phosphorylated at Ser139 and serve to mark sites of DNA damage and help recruit DNA repair factors [32]. We performed western blot analysis with protein extracted from hemi-brains of mice that received either PBS or IgG1-iS18 antibody treatment to determine the levels of γH2AX. Figure 6 shows there was a significant increase [$F(1,12) = 11.34$, $p = 0.00559$] in levels of γH2AX but not in endogenous levels of total H2AX [$F(1,12) = 1.06$, $p = 0.3246$], in the brain tissue of antibody treated mice when compared to PBS treated control mice.

DISCUSSION

Here we demonstrate the novel finding that intranasal administration of the anti-LRP/LR specific antibody, IgG1-iS18 to 5XFAD transgenic mice results in improved recognition and learning/short term memory as well as decreased Aβ accumulation with a concomitant increase in mTERT levels. Since we have previously observed *in vitro*, that blockade of LRP/LR with IgG1-iS18 reduced Aβ shedding, hampered $A\beta_{42}$ internalization and increased cell survival in the presence of Aβ, we hypothesized that intranasal administration of IgG1-iS18 might lead to reduced Aβ generation and toxicity and alleviate AD associated symptoms. In testing this hypothesis, we found that biweekly nasal administration of IgG1-iS18 for 8 weeks significantly improved recognition and short term memory (Figure 1).

Cognitive impairments in AD are exhibited as deficits in higher-order neurocognitive functions including, planning and problem solving, short term, long term and working memory. There are various potential memory and

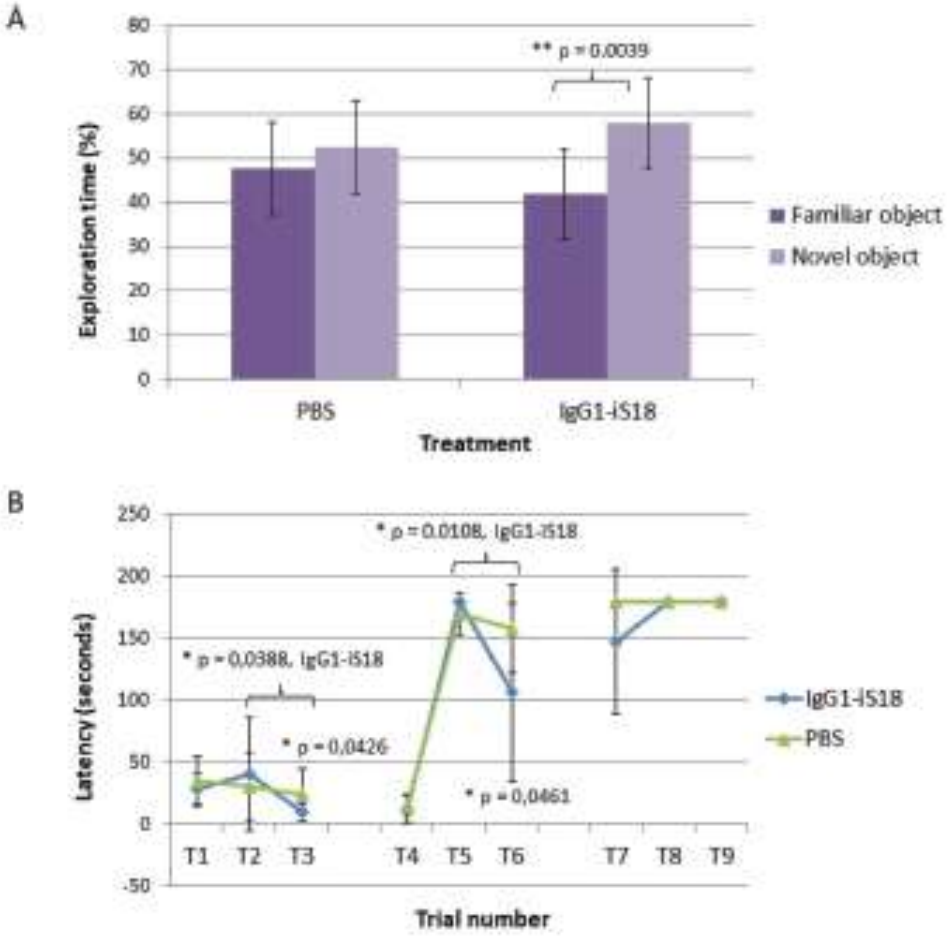


Figure 1: Memory and cognitive function tests performed to assess the effect of treatment with IgG1-iS18. (A) The novel object recognition test was performed with 4–5 month old 5XFAD ($n = 10$) male mice treated with either PBS or IgG1-iS18. The percentage of time that the mice spent exploring the novel and familiar object over the total time spent exploring both objects was calculated. Error bars represent standard deviation, $^{*}p$, 0.05, $^{**}p$, 0.01, $^{***}p$, 0.001; One-way ANOVA. (B) Performance of the AD transgenic mice in the puzzle box test. Latencies scored to reach the goal zone during the 9 trials of the test are shown. Tasks performed during T1–T9 are as follow: Day 1 (training), T1 - underpass un-blocked, and the top of the underpass uncovered, T2 and T3 the top was covered and mice entered the goal box via the underpass. Day 2 (burrowing puzzle), T4 was identical to T2 and T3. T5 and T6 - underpass was filled with sawdust. Day 3 (plug puzzle), T7 was a repetition of T5 and T6. T8 and T9 underpass was obstructed by a plastic object. Error bars represent standard deviation, $n = 12$ per group, $^{*}p$, 0.05, $^{**}p$, 0.01, $^{***}p$, 0.001; One-way ANOVA.

cognitive function assessments routinely used to investigate cognitive decline in neurodegenerative diseases. The object recognition test is now among the most commonly used behavioural tests for mice. This test assesses attention to novelty and exploration of a novel, non-aversive object placed in a familiar environment [37, 38]. The novel object recognition test was therefore used to evaluate the effect of treatment with IgG1-iS18 on recognition memory. We observed that the treated mice exhibited object recognition by preferentially exploring the novel object (58.09%) compared to the familiar object (41.91%) during the testing phase as indicated in Figure 1A. In a study performed by Frydman-Marom *et al.*, [39] they observed that wild type mice that do not express the 5XFAD transgene spent approximately 68% of the total exploration time exploring the novel object. This suggests that treatment of 4–5 month old 5XFAD mice with IgG1-iS18 can improve object recognition but not to baseline levels as observed in wild type mice. It is however possible that initiating treatment at an earlier stage and increasing the number of treatments might decrease Aβ levels even further and improve the memory and cognitive abilities of the AD transgenic mice. Nevertheless, a significant improvement was observed in recognition memory in the 5XFAD transgenic mouse model that shows rapid synthesis of Aβ, neuronal loss and neuroinflammation [40].

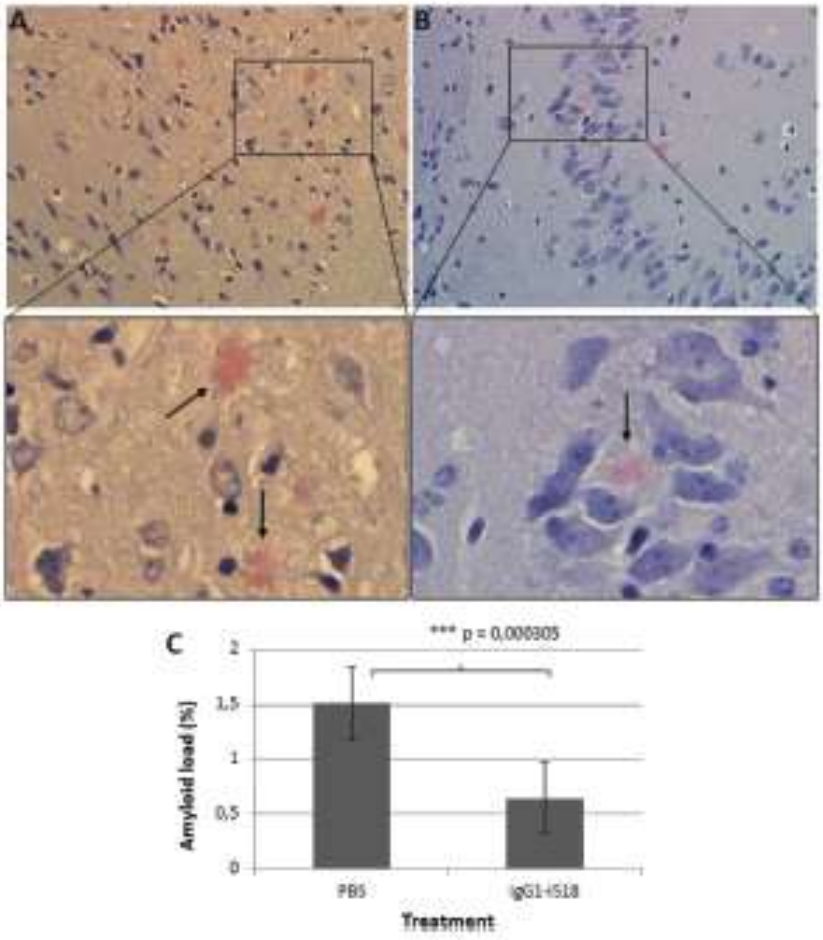


Figure 2: Congo red stain of the hippocampus of AD transgenic mice treated with (A) PBS and (B) IgG1-iS18. Amyloid load (C) is expressed as the proportion (%) of tissue area occupied by amyloid beta plaques in the hippocampal sections of the PBS and IgG1-iS18 treated mice. A decrease in amyloid plaque formation is observed after treatment with IgG1-iS18. Original magnification at 400×. Error bars represent standard deviation, $n = 7$ per group, *p, 0.05, **p, 0.01, ***p, 0.001; One-way ANOVA.

To further investigate the effect on short and long term memory as well as learning ability of the AD transgenic mice, the puzzle box test was performed. This is a problem-solving test in which mice are required to complete escape tasks of increasing difficulty within a limited amount of time. It has previously been shown to be a quick but highly reliable assessment of higher-order cognitive functioning [41]. We determined that the PBS treated control mice had higher latencies to reach the goal zone on T3 and T6, when the underpass was open and blocked with sawdust (burrow puzzle), respectively when compared to mice treated with IgG1-iS18. IgG1-iS18 treated mice furthermore showed a significant decrease in latencies to reach the goal zone in T3 and T6 when compared to T2 (underpass open) and T5 (underpass blocked with sawdust) respectively, whereas, no difference

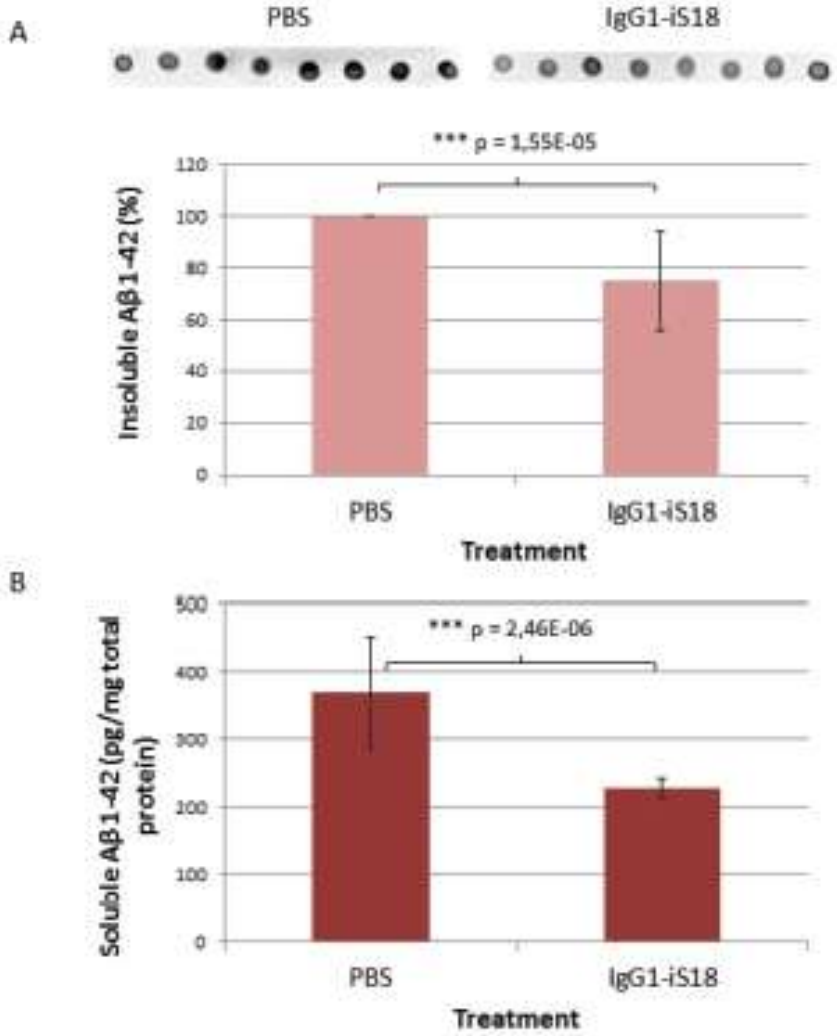


Figure 3: Levels of Aβ in brain tissue of AD transgenic mice after treatment with IgG1-iS18 and PBS. (A) Insoluble Aβ levels were determined by dot blot and calculated as a percentage per mg brain tissue. Data shown (average ± standard deviation) is representative of eight biological repeats (performed in duplicate) per treatment group. *p, 0.05, **p, 0.01, ***p, 0.001; One-way ANOVA. (B) Levels of soluble Aβ in brain tissue of AD transgenic mice after treatment with IgG1-iS18 and PBS as determined by $Aβ_{42}$ ELISA. Data shown (average ± standard deviation) was calculated as pg $Aβ_{42}$ per mg total protein and is representative of seven biological repeats per group (seven mice per treatment group, performed in duplicate). *p, 0.05, **p, 0.01, ***p, 0.001; One-way ANOVA.

was observed for the PBS treated control mice (Figure 1B) This suggests an improvement in learning/short term memory on the immediate problem repeats trials. Girard *et al.*, [42] showed that deficits in learning and memory in 5XFAD transgenic mice started at 4 months with a substantial increase at 6 months of age. This further suggests that treatment should be initiated prior to the onset of cognitive impairment which might explain why no significant improvement was observed in the long term memory or problem solving abilities of the 4–5 month old 5XFAD mice treated with IgG1-iS18 in the current study. Nonetheless, we still observed a significant improvement in recognition and learning/short term memory after intranasal treatment with IgG1-iS18. In light of the improvement in memory after treatment with IgG1-iS18, we decided to investigate the effect on the histopathology of the hippocampus of the AD mice and we observed a marked decrease in amyloid plaque formation (Figure 2). It has previously been ascertained that hippocampal lesions cause moderate memory impairment [43] and altered executive functions in the puzzle box test [41]. We, therefore, suggest that the improvement in memory and cognitive function is due to the improvement in AD brain pathology.

To confirm if the nasal IgG1-iS18 treatment had an effect on Aβ levels, we performed ELISA and dot-blot quantification of Tris-soluble (soluble) and GuHCl-soluble (insoluble) $Aβ_{42}$ peptide levels respectively, in mouse hemi-brain homogenates. We found a significant decrease in the average Aβ burden, selectively in the IgG1-iS18 treatment group (Figure 3). This is in agreement with our previously published observations, whereby, treatment of HEK293 and SH-SY5Y cells with IgG1-iS18 caused a decrease in Aβ levels [20]. In addition, we have previously demonstrated that LRP/LR and $Aβ_{42}$ interact on the cell surface and that the LRP/LR—$Aβ_{42}$ association results in the induction of apoptosis, which may be significantly deterred upon blockade of this association with anti-LRP/LR-specific antibodies. This study further demonstrated that LRP/LR plays a central role in mediating $Aβ_{42}$ internalization and that antibody blockade and shRNA-mediated down-regulation of the receptor significantly impedes cellular $Aβ_{42}$ uptake and consequent apoptosis [44]. Therefore, it is likely that the responses in cognitive ability and brain

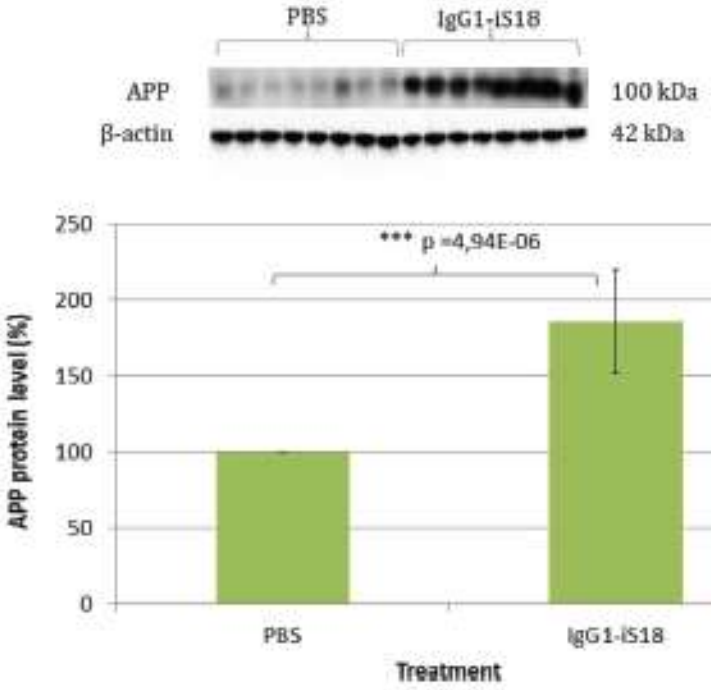


Figure 4: Western blot analysis of APP levels in brain tissue of AD transgenic mice after treatment with IgG1-iS18 and PBS. A significant increase in APP levels was observed after treatment with IgG1-iS18. Error bars represent standard deviation, n = 8 mice per treatment group. *p, 0.05, **p, 0.01, ***p, 0.001; One-way ANOVA.

pathology observed selectively in the IgG1-iS18 antibody treated animals are causally related to the significantly lower brain Aβ levels seen only in these mice. Moreover, we suggest a possible decrease in $Aβ_{42}$ internalization and therefore a subsequent decrease in neurotoxicity.

We have previously shown, by FRET analysis [21], that LRP/LR directly interacts with γ-secretase and indirectly interacts with β-secretase and that blockade of LRP/LR by IgG1-iS18 impedes these interactions and consequent $Aβ_{1-42}$ shedding [22]. This, therefore, suggests that treatment with this antibody does not affect the levels of these AD related proteins but only prevents the sequential cleavage of APP by β- and γ-secretase to prevent formation and shedding of $Aβ_{1-42}$. In light of these previously obtained *in vitro* results, we wanted to confirm that IgG1-iS18 antibody treatment had no significant effect on the levels of LRP/LR, β- and γ-secretase as well as APP in the mouse brain tissue when compared to the PBS treated control mice. Western blotting revealed uniform LRP/LR, β- and γ-secretase expression among the animals (Supplementary Figure 1). However, an interesting finding, in contrast to what we previously observed *in vitro*, was that treatment with the anti-LRP/LR antibody caused a significant 85.86% increase in APP levels *in vivo* (Figure 4). We, therefore, suggest that the increase in APP levels is due to reduced cleavage of this protein, owing to the diminished interaction between LRP/LR, β- and γ-secretase [22], which is concurrent with the reduction in $Aβ_{1-42}$ production that we observed (Figure 3).

In addition to the interactions we have observed between LRP/LR, β- and γ-secretase [22], we have recently shown that LRP/LR and the reverse transcriptase ribonucleoprotein, TERT, co-localizes in tumorigenic as well as non-tumorigenic cells and co-immunoprecipitation assays furthermore confirmed an interaction between these proteins [18]. In rodent brain, telomerase activity is high during embryonic development but rapidly decreases postnatally [36]. However, expression of TERT has been described to persist into adulthood in mouse and rat [36]. In agreement with this, we observed very low levels of

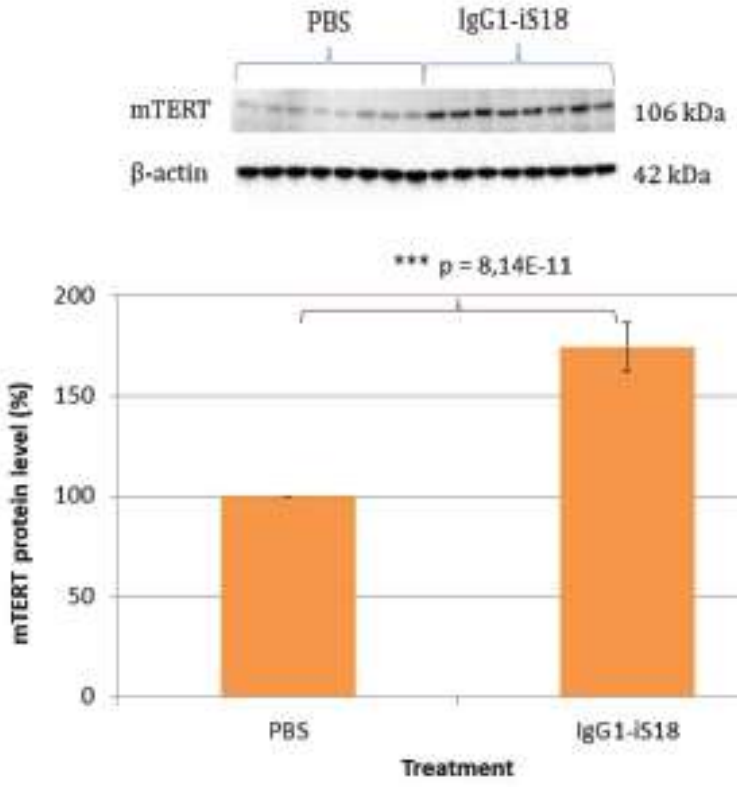


Figure 5: Levels of mTERT in brain tissue of AD transgenic mice after treatment with IgG1-iS18 and PBS. Western blot analysis was performed and a significant increase in mTERT levels was observed after treatment with IgG1-iS18. Error bars represent standard deviation, $n = 8$ mice per treatment group, $^{*}p$, 0.05, $^{**}p$, 0.01, $^{***}p$, 0.001; One-way ANOVA.

telomerase activity in the mouse brain homogenates with no significant change between control and treated mice (Supplementary Figure 2). Besides the role TERT plays as reverse transcriptase ribonucleoprotein in telomerase, TERT also performs extra-telomeric functions. It has been reported that TERT protects neurons from apoptosis induced by various stresses [34] and moreover, is involved in DNA damage responses and repair [30]. Considering the known protective functions of TERT, we hypothesized that an increase in mTERT- levels could confer resistance to amyloid pathology. We, therefore, wanted to determine if the improvement in cognitive ability and decrease in Aβ observed after antibody treatment was accompanied by a concomitant increase in mTERT levels. Interestingly, we discovered a significant increase in mTERT protein levels in the brain tissue of the antibody treated mice when compared to the PBS treated control animals (Figure 5). It is well-known that the incidence rate of AD increases with age and it has recently been shown that the pathological mechanisms of AD are associated with human telomerase. Wang *et al.*, [28] found that $A\beta_{1-42}$ and $A\beta_{1-40}$ inhibit telomerase activity *in vitro* by binding to the telomeric DNA/RNA complex of telomerase. In addition, Zhu *et al.*, [45] demonstrated a neuroprotective function of TERT in an *in vitro* AD experimental model, whereby overexpression of TERT decreased vulnerability to Aβ-induced apoptosis. Therefore, we suggest that in the current study, the blockade of the LRP/LR—$A\beta_{42}$ association by IgG1-iS18 prevented internalization of extracellular $A\beta_{42}$ and subsequent apoptosis. Moreover, the decrease in Aβ levels observed after IgG1-iS18 antibody treatment caused a reduction in neurotoxicity and hence a concomitant increase in mTERT levels. It is also possible that the increase in mTERT levels has a protective function in the brain and may offer further neuronal resistance against pathological Aβ.

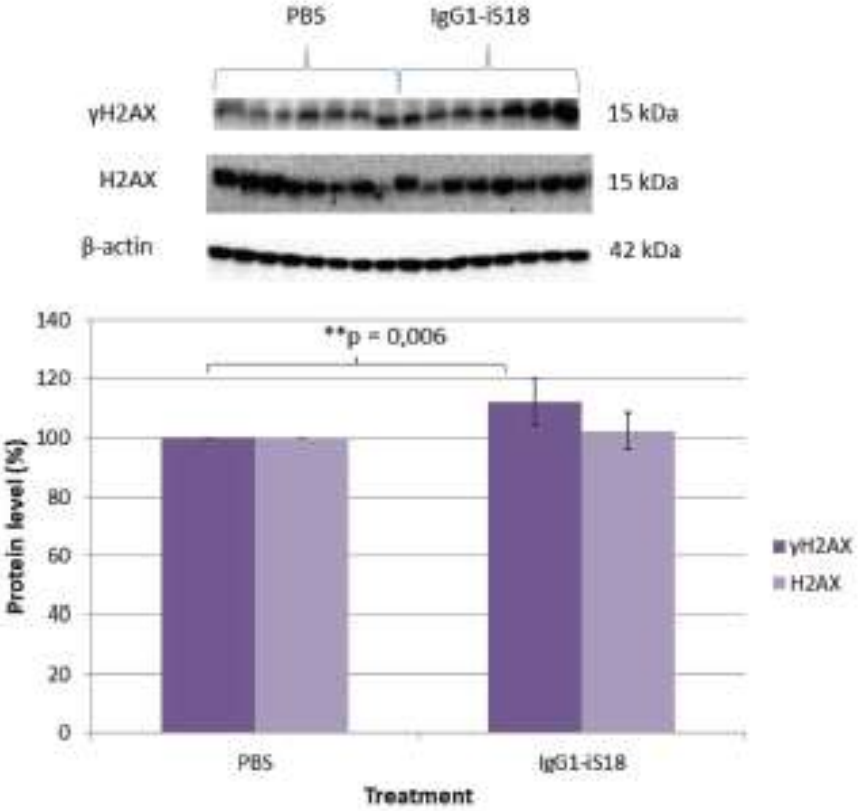


Figure 6: Effect of IgG1-iS18 on phosphorylated (Ser139) γH2AX and total H2AX protein levels in brain tissue of AD transgenic mice as detected by western blot analysis. A significant increase in pSer139 γH2AX levels were observed after treatment with IgG1-iS18. Error bars represent standard deviation, $n = 7$ mice per treatment group. $^{*}p$, 0.05, $^{**}p$, 0.01, $^{***}p$, 0.001; One-way ANOVA.

It has been suggested that TERT likewise plays a role in resistance to tau pathology. Spilsbury *et al.*, [46] recently observed, *in vitro*, that in the absence of TERT, pathological tau increases ROS generation and oxidative damage in neurons. They furthermore observed a mutual exclusion of TERT and neurofibrillary tangles (NFT) in the hippocampus of AD patients, suggesting that TERT expression might further play a role in tau pathology. However, Maarouf *et al.*, [40] observed no elevations in Tris-soluble or GHCl-soluble mouse endogenous tau in 5XFAD transgenic mice with increasing age. No NFT or phosphorylated-tau staining was observed in 5XFAD mouse brain sections using the AT8 antibody. Furthermore they suggested an inability of high Aβ loads to cause NFT in 5XFAD mice [40] and therefore the effect of IgG1-iS18 treatment on NFT and phosphorylated-tau levels was not investigated in the current study.

As previously mentioned, studies have elucidated that Aβ neurotoxicity is associated with Aβ induced neuronal apoptosis via oxidative stress and disrupted cellular calcium homeostasis, which both contribute to DNA damage [47, 48] and mitochondrial dysfunction [49]. Several factors involved in DNA repair and in signalling the presence of damage have shown to accumulate after double-strand DNA breaks. One such important response to DNA damage is the phosphorylation of H2AX (γH2AX) [50] which facilitate the recruitment of a subset of damage response and repair proteins. Masutomi *et al.*, [51] showed that in cells lacking hTERT, the DNA damage response was impaired due to a reduced degree of phosphorylation of H2AX, thus implicating hTERT as a critical regulator of the DNA damage response pathway. Since we observed a decrease in neurotoxicity and an increase in mTERT levels after treatment with IgG1-iS18, we decided to investigate the levels of γH2AX present in the brain tissue. Surprisingly, the antibody treatment significantly increased levels of γH2AX but not total H2AX (Figure 6). This suggests that the increase in γH2AX levels observed was as a result of phosphorylation of H2AX rather than an increase in total endogenous H2AX levels. It is possible that the increase in the γH2AX levels was due to the concomitant increase in mTERT and might contribute to the repair and protection against neurodegeneration as observed in this study due to the involvement of γH2AX in the recruitment of a multitude of DNA damage response proteins.

In summary, this is the first report proposing that intranasal administration of the anti-LRP/LR antibody, IgG1-iS18, is able to reduce levels of soluble and insoluble $A\beta_{42}$ in the whole brain and diminish accumulation of amyloid plaques in the hippocampus. We suggest that, together with this, the increase in mTERT levels and H2AX phosphorylation resulted in a decrease in neurotoxicity and consequently conveyed improvement of cognitive abilities, recognition and learning/short term memory. Therefore, we recommend the anti-LRP/LR specific antibody, IgG1-iS18, as a novel and powerful potential therapeutic strategy for treatment of AD. This therefore prompts the implementation of clinical studies to further investigate the effect of IgG1-iS18 on patients suffering from AD.

MATERIALS AND METHODS

Animals and intranasal treatment

The B6SJL-Tg(APPSwFlLon, PSEN1*M146L*L 286V)6799Vas/Mmj (Tg6799) transgenic line was used and obtained from Jackson Laboratories (Bar Harbour, ME). These 5XFAD transgenic mice overexpress mutant human APP(695) with the Swedish (K670N, M671L), Florida (I716V), and London (V717I) Familial Alzheimer's Disease (FAD) mutations along with human PS1 harbouring two FAD mutations, M146L and L286V. Both transgenes are regulated by the mouse Thy1 promoter to drive overexpression in the brain. 5XFAD mice display major features of Alzheimer's disease amyloid pathology and are useful models of intraneuronal $A\beta_{42}$ induced neurodegeneration and amyloid plaque formation. The high APP expression observed in this model causes accumulation of $A\beta_{42}$ and plaque formation can be observed at 2 months of age. Twenty four male mice (at approximately 4.5 months) were randomized to 2 treatment groups: group 1 ($n = 12$) received PBS as vehicle control and group 2 ($n = 12$) received the anti-LRP specific antibody IgG1-iS18. The treatments were administered intranasally twice a week for 8 weeks and the mice received IgG1-iS18 at a total dose of 288 μg/mouse (9 μg/15 μl/naris = 18 μg/mouse, 2 × week = 36 μg/mouse/week, 8 weeks = 288 μg/ mouse). All procedures were performed with approval by the University of the Witwatersrand Animal Ethics Screening Committee (clearance certificate number 2014/37/C).

Memory and cognitive function tests

Novel object recognition

The novel object recognition test *(for reviews see* [52, 53]) was performed in a 440 mm × 500 mm open field chamber with opaque walls. Each mouse was habituated to an empty novel object recognition open field box for two 10 min sessions 24 hr apart. Twenty four hours after the last habituation session, mice were subjected to training in a 10 minute session of exposure to two identical, non-toxic, hard plastic items in the open field box. After the training session, the animal was returned to its home cage. After a retention interval of 24 hrs, the animal was returned to the arena which contained two objects, one identical to the familiar object and one novel object. The animal was allowed to explore for 10 minutes, during which the amount of time exploring each object

was recorded and tracked employing Panlab Smart video tracking software, Smart 3.0. Objects were randomized and counterbalanced across animals. Objects and arenas were thoroughly cleaned between trials.

Puzzle box test

The protocol was slightly modified from Ben Abdallah *et al*., [41]. The arena consisted of a white box divided by a removable barrier into two compartments: a start zone (67 cm long, 25.5 cm wide) and a smaller dark and covered goal zone (15 cm long, 25.5 cm wide). The mice were introduced into the start zone and allowed to move into the goal zone through a narrow underpass (~4 cm wide) located in the barrier. The mice were subjected to a total of nine trials (T1–T9) over 3 consecutive days, with three trials per day, during which they were challenged with obstructions of increasing difficulty placed at the underpass. On day 1 (training), the underpass was un-blocked, and the top of the underpass was uncovered during T1. During T2 and T3 the top was covered and mice entered via the small underpass. On day 2 (burrowing puzzle), T4 was identical to T2 and T3. During T5 and T6, however, the underpass was filled with sawdust and mice had to dig their way through. On day 3 (plug puzzle), T7 was a repetition of T5 and T6. However, during T8 and T9, mice were presented with the plug puzzle, where the underpass was obstructed by a plastic object that mice had to pull or push with teeth and paws to enter the goal zone. This sequence allowed assessing problem solving ability (T5 and T8), learning and short-term memory (T3, T6, and T9) while the repetition on the next day provided a measure of long-term memory (T4 and T7). Performance of mice in the puzzle box was assessed by measuring the latency to enter the goal zone with all four paws or was ended after a total time of 3 min.

Brain harvest

After all memory and cognitive tests were performed mice were euthanized and transcardially perfused with cold phosphate buffered saline (PBS) (Sigma-Aldrich). A hemibrain from each mouse was dissected, snap-frozen in liquid nitrogen, then stored at –70° C until used for biochemical analysis. The remaining hemibrains were fixed in 4% paraformaldehyde (Sigma-Aldrich) for histological analysis. Briefly, the brains were fixed for 24 h in 4% paraformaldehyde at 4° C where after they were rinsed with PBS. In order to displace all water from the brain samples, 30% sucrose was added and the samples were incubated for approximately 3 days. The samples were then stored at 4° C in 0.1M PBS containing protease inhibitor (Sigma-Aldrich) until further analysis.

Histological analysis

Histological analysis was performed by IDEXX laboratories (Pretoria, South Africa). All brain samples (n = 8) were re-fixed in 10% buffered formalin and sections were made and processed according to routine histological tissue processing in an automated tissue processor with standard operating procedures Idexx-AP-SOP-27. Following tissue processing, sections of 5–6 µm were cut (IdexxSA-AP-SOP-30) and the produced slides were stained in an automated Haematoxylin and Eosin tissue stainer (IdexxSA-AP-SOP-205). Slides were furthermore stained with Congo red to identify amyloid before histological evaluation. The amyloid load was quantified from histological sections by using ImageJ software. Amyloid plaques were manually outlined and the amyloid load corresponded to the ratio (%) of the mean area of amyloid plaques to total area measured in each hippocampal section.

Protein extraction

All steps were completed at 4° C. The frozen brain samples were homogenized in 500 µl cold PBS with protease inhibitors using a Dounce homogenizer. Of each sample, 100 µl homogenate was removed and frozen at –20° C for analysis of telomerase activity. To the remaining homogenate, 400 µl of 2× RIPA buffer was added and the samples were lysed at 4° C for 30 min with gentle agitation. The supernatant, containing the soluble proteins, was collected after centrifugation at 16000 × g for 20 min and stored at –20° C until further analysis. The remaining tissue pellet was then homogenized in 100 µl Guanidine HCl buffer (GuHCl) (5M Guanidine HCl, 50 mM Tris (pH8) containing protease inhibitors (Sigma-Aldrich)) to extract insoluble amyloid beta. After homogenization, 7.9 ml GuHCl was added and the samples were gently rotated overnight at 4° C. The supernatant was stored at –20° C until further analysis. A BCA assay was performed on the soluble protein samples in order to determine the total protein concentration.

Western blot analysis

The soluble protein samples were heated for 5 min at 95° C in Blue Loading Buffer (New England Biolabs) with 40 mM of dithiothreitol and a total of 10 µg (β-actin), 20 µg (γH2AX), 25 µg (PS1), 35 µg (LRP), 40 µg (APP and H2AX), 50 µg (mTERT) and 60 µg (BACE1) of protein was then separated on AnykD™ Criterion™ TGX Stain-Free™ Protein Gels (Biorad). A prestained molecular weight marker (PageRuler Prestained Protein Ladder, Thermo Fisher) was loaded onto each gel. After transferring the proteins onto polyvinylidine fluoride membrane (Pall) with 1 × transfer buffer (20% methanol in 25 mM Tris and 19.2 mM glycine) the membranes were blocked in 3% BSA (Amresco) in PBS and 0.1% Tween 20 (PBST). The primary and secondary antibodies used for western blots are detailed in Supplementary Table 1. The proteins were visualized with Clarity™ Western ECL

Blotting Substrate (Biorad) and the ChemiDoc™ Imaging System (Biorad). Densitometric analysis was performed with Image Lab 5.1 software (Biorad).

Dot blot analysis

In order to determine the effect of IgG1-iS18 treatment on the insoluble Aβ levels, a dot blot was performed. The GuHCl protein extracts were dotted onto a nitrocellulose membrane and allowed to dry. The membrane was blocked in 3% BSA in PBST for 30 min where after it was incubated with rabbit anti-human $Aβ_{1-42}$ (Cell Signaling Technology®, D9A3A) (1:1000) at room temperature for 1 hour. The membrane was washed 3 x with PBST for 5 min and incubated with anti-rabbit HRP secondary antibody (Cell Signalling) (1:2500) at room temperature for 30 min. After the membrane was washed another 3 × with PBST, it was incubated with Clarity™ Western ECL Blotting Substrate (Biorad) and the ChemiDoc™ Imaging System (Biorad) was used for detection. Densitometric analysis was performed with Image Lab 5.1 software (Biorad).

$Aβ_{42}$ ELISA

Soluble human $Aβ_{1-42}$ was measured with the Quantikine® ELISA Human Amyloid β (as1-42) kit (R&D Systems). The manufacturer's instructions were followed. Briefly: The plate was washed twice with Wash Buffer immediately prior to use. Human Amyloid β (as1-42) standard and 100× diluted soluble protein samples were added to the wells (100 µl) and incubated for 2 hours at 2–8° C. Each well was then aspirated and washed four times with Wash Buffer. Cold Human Amyloid β (as1-42) conjugate (200 µl) was added to each well and incubated for 2 hours at 2–8° C. The plate was washed four times with Wash Buffer and 200 µl of Substrate Solution was added to each well. The plate was then incubated for 30 min at room temperature in the dark where after 50 µl Stop Solution was added. The optical density was determined using an ELISA plate reader at 450 nm with wavelength correction at 540 nm.

Telomerase activity

The TRAPeze® Kit, RT Telomerase Detection Kit (Merck), was used to determine the effect of IgG1-iS18 treatment on telomerase activity. Relative telomerase activity was quantified following the manufacturers protocols with minor alterations. Protein and RNA was extracted using 200 µl of CHAPS lysis buffer per 40–100 mg of tissue and incubated on ice for 30 min. In order to obtain the extract, the samples were centrifuged at 16000 × g for 20 minutes at 4° C and the supernatant was snap frozen on dry ice. The protein was quantified with the NanoDrop® ND-1000 (Thermo Scientific) and standardized to 1000 ng/µl for all experimental and control reactions. OneTaq® HotStart Taq Polymerase (5 U/µl) (New England Biolabs) was used and all samples were analysed via qPCR with the Roche LightCycler LC480. The following cycling parameters were applied: 37° C for 30 minutes, 95° C for 2 minutes and 45 cycles of 95° C for 15 seconds, 59° C for 60 seconds and 45° C for 10 seconds. Telomerase activity was calculated from the standard curve generated by 1:10 serial dilutions (20–0.0002 amoles) of TSR8 control template as per Merck Millipore instructions. The data was analysed with LightCycler1 Software version 1.5.1.

Statistical analysis

Statistical analysis was performed using Microsoft Excel 2010 (Microsoft Corporation) and QuickCalcs Outlier Calculator ©2017 GraphPad Software which employs the Grubbs' test (extreme studentized deviate). All experiments were performed with a minimum of 6 biological repeats and error bars represent standard deviation. The One-way ANOVA and Student's *t*-test was performed at a 95% confidence interval; where p values < 0.05 were considered statistically significant ($^{*}p < 0.05$, $^{**}p < 0.01$ and $^{***}p < 0.001$). The Tukey HSD or Tukey-Kramer Post Hoc Test was performed after One-Way ANOVA to confirm significance.

Abbreviations

Aβ: Amyloid Beta; AD: Alzheimer's Disease; APP: Amyloid Precursor Protein; BACE-1: B-site APP cleaving enzyme; BCA: Bicinchoninic Acid Assay; CHAPS: 3-((3-cholamidopropyl)dimethylammonio)-1-propanesulfonate; DDR: DNA Damage Response; DMSO: Dimethyl Sulfoxide; DNA: Deoxyribonucleic Acid; DSBs: Double Stranded Breaks; ELISA: Enzyme-linked Immunosorbant Assay; FAD: Familial Alzheimer's Disease; GuHCl: Guanidine HCl Buffer; HCl: Hydrochloric Acid; HEK293: Human Embryonic Kidney Cells; HRP: Horseradish Peroxidase; hTERT: Human Telomerase Reverse Transcription; kDa: Kilo Dalton; LRP/LR: 37 kDa Laminin Receptor Precursor/67 kDa High Affinity Laminin Receptor; mTERT: Mouse Telomerase Reverse Transcriptase; PBS: Phosphate Buffered Saline; PBST: Phosphate Buffered Saline with Tween; qPCR: Quantitative Polymerase Chain Reaction; RIPA: Radioimmunoprecipitation Assay Buffer; RNA: Ribonucleic Acid; ROS: Reactive Oxygen Species; shRNA: Short Hairpin RNA; siRNA: Small Interfering RNA; TERC: Telomerase RNA Component; TERT: Telomerase Reverse Transcriptase.

Author contributions

E.F. designed and performed all experiments, analysed the data and wrote the manuscript; M.J.B. assisted with experiments, assisted in analysing data and writing

of the manuscript; T.C.O. assisted with experiments; N.T. assisted with experiments; K.J. assisted with design of study; B.T.L. conceptualized the study but sadly passed away whilst study was being performed; S.F.T.W. conceptualized the study and edited the manuscript.

ACKNOWLEDGMENTS

We thank Affimed Therapeutics GmbH, Heidelberg, Germany for providing antibody IgG1-iS18.

We thank the staff at Central Animal Services, University of the Witwatersrand, South Africa, for assistance with animal care and treatments.

CONFLICTS OF INTEREST

The authors declare that they have no competing interests that might be perceived to influence the results and discussion reported in this paper. The authors declare no competing financial interests.

FUNDING

This work is based upon research supported by the National Research Foundation (NRF), the Republic of South Africa (RSA), grant numbers 105832 and 109298. Any opinions, findings and conclusions or recommendations expressed in this material are those of the author(s), and therefore, the National Research Foundation does not accept any liability in this regard thereto. Financial support was further received from the South African Medical Research Council (MRC) under a self-initiated grant awarded to SFTW. Any opinions, findings and conclusions or recommendations expressed in this material are those of the author(s), and therefore, the MRC does not accept any liability in this regard thereto.

REFERENCES

1. Prince M, Wimo AGM, Ali GC, Wu YT, Prina M. World Alzheimer Report 2015: the global impact of dementia: an analysis of prevalence, incidence, cost and trends. London: Alzheimer's Disease International. 2015.
2. Serrano-Pozo A, Frosch MP, Masliah E, Hyman BT. Neuropathological alterations in Alzheimer disease. Cold Spring Harb Perspect Med. 2011; 1:a006189.
3. Caetano FA, Beraldo FH, Hajj GN, Guimaraes AL, Jürgensen S, Wasilewska-Sampaio AP, Hirata PH, Souza I, Machado CF, Wong DY, De Felice FG, Ferreira ST, Prado VF, et al. Amyloid-beta oligomers increase the localization of prion protein at the cell surface. J Neurochem. 2011; 117:538–553.
4. Demuro A, Mina E, Kayed R, Milton SC, Parker I, Glabe CG. Calcium dysregulation and membrane disruption as a ubiquitous neurotoxic mechanism of soluble amyloid oligomers. J Biol Chem. 2005; 280:17294–17300.
5. Lin H, Bhatia R, Lal R. Amyloid beta protein forms ion channels: implications for Alzheimer's disease pathophysiology. FASEB J. 2001; 15:2433–2444.
6. Da Costa Dias B, Jovanovic K, Gonsalves D, Weiss SF. Structural and mechanistic commonalities of amyloid-beta and the prion protein. Prion. 2011; 5:126–137.
7. Verdier Y, Penke B. Binding sites of amyloid beta-peptide in cell plasma membrane and implications for Alzheimer's disease. Curr Protein Pept Sci. 2004; 5:19–31.
8. Da Costa Dias B, Jovanovic K, Gonsalves D, Moodley K, Reusch U, Knackmuss S, Penny C, Weinberg MS, Little M, Weiss SF. Anti-LRP/LR specific antibody IgG1-iS18 and knock-down of LRP/LR by shRNAs rescue cells from Abeta42 induced cytotoxicity. Sci Rep. 2013; 3:2702.
9. Pinnock EC, Jovanovic K, Pinto MG, Ferreira E, Dias BC, Penny C, Knackmuss S, Reusch U, Little M, Schatzl HM, Weiss SF. LRP/LR Antibody Mediated Rescuing of Amyloid-β-Induced Cytotoxicity is Dependent on PrPc in Alzheimer's Disease. J Alzheimers Dis. 2016; 49:645–57.
10. Mbazima V, Da Costa Dias B, Omar A, Jovanovic K, Weiss SF. Interactions between PrP(c) and other ligands with the 37-kDa/67-kDa laminin receptor. Front Biosci. 2010; 15:1150–1163.
11. Omar A, Reusch U, Knackmuss S, Little M, Weiss SF. Anti-LRP/LR-specific antibody IgG1-iS18 significantly reduces adhesion and invasion of metastatic lung, cervix, colon and prostate cancer cells. J Mol Biol. 2012; 419:102–109.
12. Khumalo T, Ferreira E, Jovanovic K, Veale RB, Weiss SF. Knockdown of LRP/LR Induces Apoptosis in Breast and Oesophageal Cancer Cells. PLoS One. 2015; 10:e0139584.
13. Khusal R, Da Costa Dias B, Moodley K, Penny C, Reusch U, Knackmuss S, Little M, Weiss SF. *In vitro* inhibition of angiogenesis by antibodies directed against the 37 kDa/67 kDa laminin receptor. PLoS One. 2013; 8:e58888.
14. Edenhofer F, Rieger R, Famulok M, Wendler W, Weiss S, Winnacker EL. Prion protein PrPc interacts with molecular chaperones of the Hsp60 family. J Virol. 1996; 70:4724–4728.
15. Gauczynski S, Peyrin JM, Haik S, Leucht C, Hundt C, Rieger R, Krasemann S, Deslys JP, Dormont D, Lasmezas CI, Weiss S. The 37-kDa/67-kDa laminin receptor acts as the cell-surface receptor for the cellular prion protein. EMBO J. 2001; 20:5863–5875.
16. Hundt C, Peyrin JM, Haik S, Gauczynski S, Leucht C, Rieger R, Riley ML, Deslys JP, Dormont D, Lasmezas CI, Weiss S. Identification of interaction domains of the prion protein with its 37-kDa/67-kDa laminin receptor. EMBO J. 2001; 20:5876–5886.
17. Rieger R, Edenhofer F, Lasmezas CI, Weiss S. The human 37-kDa laminin receptor precursor interacts with the prion protein in eukaryotic cells. Nat Med. 1997; 3:1383–1388.
18. Naidoo K, Malindisa ST, Otgaar TC, Bernert M, Da Costa Dias B, Ferreira E, Reusch U, Knackmuss S, Little M, Weiss SF, Letsolo BT. Knock-Down of the 37 kDa/67 kDa

Laminin Receptor LRP/LR Impedes Telomerase Activity. PLoS One. 2015; 10:e0141618.

19. Otgaar TC, Ferreira E, Malindisa S, Bernert M, Letsolo BT, Weiss SFT. 37 kDa LRP:FLAG enhances telomerase activity and reduces senescent markers *in vitro*. Oncotarget. 2017; 8:86646–56. https://doi.org/10.18632/oncotarget.21278.

20. Jovanovic K, Gonsalves D, Da Costa Dias B, Moodley K, Reusch U, Knackmuss S, Penny C, Weinberg MS, Little M, Weiss SF. Anti-LRP/LR specific antibodies and shRNAs impede amyloid beta shedding in Alzheimer's disease. Sci Rep. 2013; 3:2699.

21. Jovanovic K, Loos B, Da Costa Dias B, Penny C, Weiss SF. High resolution imaging study of interactions between the 37 kDa/67 kDa laminin receptor and APP, beta-secretase and gamma-secretase in Alzheimer's disease. PLoS One. 2014; 9:e100373.

22. Jovanovic K, Chetty CJ, Khumalo T, Da Costa Dias B, Ferreira E, Malindisa ST, Caveney R, Letsolo BT, Weiss SF. Novel patented therapeutic approaches targeting the 37/67 kDa laminin receptor for treatment of cancer and Alzheimer's disease. Expert Opin Ther Pat. 2015; 25:567–582.

23. Weiss SF. Bad Boy with a Twist: Targeting the 37 kDa/67 kDa Laminin Receptor for Treatment of Cancer and Neurodegenerative Diseases and for Changing Telomere Dynamics. Cell & Cellular Life Sciences Journal. 2017; 2:000114.

24. Greider CW, Blackburn EH. The telomere terminal transferase of Tetrahymena is a ribonucleoprotein enzyme with two kinds of primer specificity. Cell. 1987; 51:887–898.

25. Kim NW, Piatyszek MA, Prowse KR, Harley CB, West MD, Ho PL, Coviello GM, Wright WE, Weinrich SL, Shay JW. Specific association of human telomerase activity with immortal cells and cancer. Science. 1994; 266:2011–2015.

26. Nakamura TM, Cech TR. Reversing time: origin of telomerase. Cell. 1998; 92:587–590.

27. Franco S, Blasco MA, Siedlak SL, Harris PL, Moreira PI, Perry G, Smith MA. Telomeres and telomerase in Alzheimer's disease: epiphenomena or a new focus for therapeutic strategy? Alzheimers Dement. 2006; 2:164–168.

28. Wang J, Zhao C, Zhao A, Li M, Ren J, Qu X. New insights in amyloid beta interactions with human telomerase. J Am Chem Soc. 2015; 137:1213–1219.

29. Cong Y, Shay JW. Actions of human telomerase beyond telomeres. Cell Res. 2008; 18:725–732.

30. Saretzki G. Extra-telomeric functions of human telomerase: cancer, mitochondria and oxidative stress. Curr Pharm Des. 2014; 20:6386–6403.

31. Mao P, Reddy PH. Aging and amyloid beta-induced oxidative DNA damage and mitochondrial dysfunction in Alzheimer's disease: implications for early intervention and therapeutics. Biochim Biop hys Acta. 2011; 1812:1359–1370.

32. Odell ID, Wallace SS, Pederson DS. Rules of engagement for base excision repair in chromatin. J Cell Physiol. 2013; 228:258–266.

33. Coppede F, Migliore L. DNA damage and repair in Alzheimer's disease. Curr Alzheimer Res. 2009; 6:36–47.

34. Li J, Qu Y, Chen D, Zhang L, Zhao F, Luo L, Pan L, Hua J, Mu D. The neuroprotective role and mechanisms of TERT in neurons with oxygen-glucose deprivation. Neuroscience. 2013; 252:346–358.

35. Eitan E, Tichon A, Daniel G, Priel E. Telomerase expression in adult and old mouse Purkinje neurons. Rejuvenation Res. 2012; 15:206–209.

36. Klapper W, Shin T, Mattson MP. Differential regulation of telomerase activity and TERT expression during brain development in mice. J Neurosci Res. 2001; 64:252–260.

37. Misslin R, Ropartz P. Responses in mice to a novel object. Behaviour. 1981; 78:169–177.

38. van Gaalen MM, Steckler T. Behavioural analysis of four mouse strains in an anxiety test battery. Behav Brain Res. 2000; 115:95–106.

39. Frydman-Marom A, Levin A, Farfara D, Benromano T, Scherzer-Attali R, Peled S, Vassar R, Segal D, Gazit E, Frenkel D, Ovadia M. Orally administrated cinnamon extract reduces beta-amyloid oligomerization and corrects cognitive impairment in Alzheimer's disease animal models. PLoS One. 2011; 6:e16564.

40. Mucouf CL, Kokjohn TA, Whiteside CM, Macias MP, Kalback WM, Sabbagh MN, Beach TG, Vassar R, Roher AE. Molecular Differences and Similarities Between Alzheimer's Disease and the 5XFAD Transgenic Mouse Model of Amyloidosis. Biochem Insights. 2013; 6:1–10.

41. Ben Abdallah NM, Fuss J, Trusel M, Galsworthy MJ, Bobsin K, Colacicco G, Deacon RM, Riva MA, Kellendonk C, Sprengel R, Lipp HP, Gass P. The puzzle box as a simple and efficient behavioral test for exploring impairments of general cognition and executive functions in mouse models of schizophrenia. Exp Neurol. 2011; 227:42–52.

42. Girard SD, Jacquet M, Baranger K, Migliorati M, Escoffier G, Bernard A, Khrestchatisky M, Feron F, Rivera S, Roman FS, Marchetti E. Onset of hippocampus-dependent memory impairments in 5XFAD transgenic mouse model of Alzheimer's disease. Hippocampus. 2014; 24:762–772.

43. Broadbent NJ, Gaskin S, Squire LR, Clark RE. Object recognition memory and the rodent hippocampus. Learn Mem. 2009; 17:5–11.

44. Da Costa Dias B, Jovanovic K, Gonsalves D, Moodley K, Reusch U, Knackmuss S, Weinberg MS, Little M, Weiss SFT. The 37 kDa/67 kDa Laminin Receptor acts as a receptor for Aβ42 internalization. Sci Rep. 2014; 4:5556.

45. Zhu H, Fu W, Mattson MP. The catalytic subunit of telomerase protects neurons against amyloid beta-peptide-induced apoptosis. J Neurochem. 2000; 75:117–124.

46. Spilsbury A, Miwa S, Attems J, Saretzki G. The role of telomerase protein TERT in Alzheimer's disease and in tau-related pathology *in vitro*. J Neurosci. 2015; 35:1659–1674.

47. Zhang J, Pieper A, Snyder SH. Poly(ADP-ribose) synthetase activation: an early indicator of neurotoxic DNA damage. J Neurochem. 1995; 65:1411–1414.

48. Deng G, Su JH, Ivins KJ, Van Houten B, Cotman CW. Bcl-2 facilitates recovery from DNA damage after oxidative stress. Exp Neurol. 1999; 159:309–318.

49. Mattson MP. Cellular actions of beta-amyloid precursor protein and its soluble and fibrillogenic derivatives. Physiol Rev. 1997; 77:1081–1132.

50. Paull TT, Rogakou EP, Yamazaki V, Kirchgessner CU, Gellert M, Bonner WM. A critical role for histone H2AX in recruitment of repair factors to nuclear foci after DNA damage. Curr Biol. 2000; 10:886–895.

51. Masutomi K, Possemato R, Wong JM, Currier JL, Tothova Z, Manola JB, Ganesan S, Lansdorp PM, Collins K, Hahn WC. The telomerase reverse transcriptase regulates chromatin state and DNA damage responses. Proc Natl Acad Sci U S A. 2005; 102:8222–8227.

52. Leger M, Quiedeville A, Bouet V, Haelewyn B, Boulouard M, Schumann-Bard P, Freret T. Object recognition test in mice. Nat Protoc. 2013; 8:2531–2537.

53. Antunes M, Biala G. The novel object recognition memory: neurobiology, test procedure, and its modifications. Cogn Process. 2012; 13:93–110.

Journal of Alzheimer's Disease 69 (2019) 729–741
DOI 10.3233/JAD-190075
IOS Press

LRP::FLAG Rescues Cells from Amyloid-β-Mediated Cytotoxicity Through Increased TERT Levels and Telomerase Activity

Monique J. Bignoux, Katelyn Cuttler, Tyrone C. Otgaar, Eloise Ferreira, Boitelo T. Letsolo and Stefan F.T. Weiss*
School of Molecular and Cell Biology, University of the Witwatersrand, Private Bag 3, Wits 2050, Johannesburg, South Africa

Accepted 26 March 2019

Abstract. Alzheimer's disease (AD) represents the most common form of neurodegenerative disorders with only palliative treatments currently available. Amyloid plaque formation caused by amyloid-β (Aβ) aggregation and neurofibrillary tangle formation caused by hyperphosphorylated tau are hallmarks for the development of AD. The 37 kDa/67 kDa laminin receptor (LRP/LR) has been implicated in AD and tools blocking or downregulating LRP/LR impede amyloid plaque formation *in vitro* and *in vivo*. We have recently shown that LRP::FLAG enhances telomerase activity with a concomitant reduction of senescent markers. Here, we overexpressed LRP::FLAG in HEK293 and SH-SY5Y cells, which resulted in an increase in hTERT levels as well as increased telomerase activity and increased cell viability in the presence of cytotoxic levels of exogenous Aβ. LRP::FLAG overexpression decreased Aβ shedding and intracellular Aβ levels in HEK293 cells. This suggests that LRP::FLAG rescues cells from Aβ-induced cytotoxicity through increased telomerase activity. This study recommends LRP::FLAG as a novel alternative therapeutic for AD treatment through activation of telomerase activity.

Keywords: Alzheimer's disease, amyloid-β, 37 kDa/67 kDa laminin receptor (LRP/LR), telomerase, TERT

AUTHOR COPY

INTRODUCTION

Alzheimer's disease (AD) is the most common form of progressive neurodegenerative disorders afflicting in excess of 47 million people globally. This form of dementia predominantly affects the aging population and is a significant socio-economic burden, whereby in 2015, the global cost was estimated at 818 billion USD [1]. There is a considerable knowledge gap which exists in the understanding of the disease-causing mechanism and as a result, only palliative therapeutic options are currently available. This highlights the necessity for disease-modifying treatment strategies for neurodegenerative disorders such as AD. AD is defined by the accumulation of the neurotoxic amyloid-β 42 ($A\beta_{42}$) peptide, resulting in the development of extracellular Aβ plaques [2, 3] and the aggregation of hyperphosphorylated tau (a microtubule associated protein), producing intracellular neurofibrillary tangles [4]. Collectively, it is these factors and their associations that cause the progressive and devastating behavioral and cognitive dysfunction seen in those suffering from AD.

The 4 kDa Aβ peptide is the candidate etiological cause for AD, expressly, it is the 42-amino acid (aa) proteolytic cleavage product which amasses to cause the neurotoxic effects present in AD [5].

*Correspondence to: Stefan F.T. Weiss, School of Molecular and Cell Biology, University of the Witwatersrand, Private Bag 3, Wits 2050, Johannesburg, South Africa. E-mail: stefan.weiss@wits.ac.za.

ISSN 1387-2877/19/$35.00 © 2019 – IOS Press and the authors. All rights reserved

Generation of the Aβ peptide occurs via the amyloidogenic pathway, when the amyloid-β protein precursor (AβPP) is sequentially cleaved by β-secretase and γ-secretase, respectively. AD occurs when the amyloidogenic pathway is inappropriately favored and when $Aβ_{42}$ degradation is reduced, thus leading to the accumulation of these peptides [6]. AD pathology arises as a consequence of Aβ-mediated distortions in the neural morphology. These distortions impede neurotransmission and, correspondingly, cause neural dysfunction [7]. Aβ neurotoxicity has furthermore been linked to Aβ-induced neuronal apoptosis through disruption of intracellular membranes [8, 9] as well as oxidative stress, both of which contribute to mitochondrial dysfunction [10] and DNA damage [11, 12]. The mechanism by which Aβ prompts the characteristic neuronal loss is due to its direct interaction with receptors on the cell surface [13] or through indirect interactions, such as incorporation into cell organelles and lipid membranes [14]. The interaction between Aβ and cell surface receptors, such as with the 37 kDa Laminin Receptor Precursor/67 kDa high affinity Laminin Receptor (LRP/LR) [15], prompts internalization of $Aβ_{42}$, thus causing the intracellular accumulation of $Aβ_{42}$, and subsequent neurotoxic effects [13, 16–18].

LRP/LR, otherwise known as LamR1, RPSA, and p40, is a multifunctional type II transmembrane receptor consisting of 295aa and is principally found within lipid raft regions of the plasma membrane in addition to the cytoplasm and the nucleus [19–21]. LRP/LR is associated with numerous diseases. These include, but are not limited to, cancer, prion disorders, aging, and AD. In cancer, LRP/LR is known to be highly upregulated, leading to enhanced adhesion and invasion and ultimately, metastasis, as well as angiogenesis and the inhibition of apoptosis [22–30]. In addition, LRP/LR is involved in the aging process due to an interaction with telomerase [31, 32]. Furthermore, LRP/LR is implicated in AD, through its interaction with Aβ on the cell surface, as well as its role in Aβ shedding, due to its interaction with the AD-related proteins: AβPP, γ-secretase, and β-secretase [33, 34]. LRP/LR is involved in the internalization of $Aβ_{42}$, which causes accumulation of $Aβ_{42}$ intracellularly [34] and ultimately $Aβ_{42}$-mediated cytotoxicity [15]. Furthermore, the underlying mechanism of the $Aβ_{42}$-induced neuronal cytotoxicity is an indirect result of an interaction between the cellular prion protein (PrP^C) and $Aβ_{42}$ [35]. Antibody (IgG1-iS18) and small hairpin RNA (shRNA) technologies employed to target LRP/LR, to block the receptor and downregulate its expression, respectively, revealed a significant reduction in Aβ-mediated cytotoxicity and $Aβ_{42}$ shedding [15, 33, 36].

Recently, an additional protein found to be associated with AD is telomerase, a ribonucleoprotein with reverse transcriptase activity. Telomerase is principally found in highly proliferative cells and has a key function in protecting DNA from degradation, through the addition of telomeric (TTAGGG) repeats to the ends of telomeric DNA [37, 38]. Telomerase is a multi-subunit protein with two key components, TERT, the catalytic reverse transcriptase and TERC, the RNA component [39]. Telomerase activity has an important role in cellular senescence and immortalization, whereby it is involved in the aging process and the cancerous state [40]. Additionally, TERT has a role in numerous extra-telomeric processes, predominantly for the conservation of cell viability [41]. TERT protects and aids in the functioning of the mitochondria [42–44]. When reactive oxygen species (ROS) are present and conditions become hypoxic, TERT translocates to and protects the mitochondria against DNA (mtDNA) damage, as well as apoptosis [45]. Moreover, telomerase has an essential role in regulation of DNA repair and DNA damage responses by which it is involved in the recruitment of DNA repair proteins [41]. It has been shown that telomerase is implicated in the pathological processes of AD [46–48]. Evidence shows that AD patients have shorter telomere lengths in their neuronal and T cells [47]. Furthermore, *in vitro* studies have demonstrated that telomerase activity is inhibited by $Aβ_{42}$, through the binding of Aβ oligomers to the telomeric DNA-RNA template complex of telomerase [48], representing an antagonistic relationship between telomerase and Aβ within neurons. It has been proposed that upregulation of telomerase provides a potential therapeutic strategy for the treatment of AD, as the resulting overexpression of TERT protects neuronal cells against Aβ-induced apoptosis [46]. A discovery by Otgaar et al. [32] elucidated that overexpression of LRP::FLAG [49] resulted in an increase in TERT expression, telomerase activity, telomere length as well as a reduction in senescent markers [32]. Altogether indicating that LRP/LR has a role in AD and in the regulation of telomerase activity and TERT expression [31, 32, 36].

Therefore, this study focused on stably transfecting HEK293 and SH-SY5Y cells with the pCIneomoLRP::FLAG construct, to assess the effect of

PROOF

overexpression of LRP::FLAG on $A\beta_{42}$ levels, TERT expression, telomerase activity, and cell viability, in an *in vitro* AD setting.

METHODS AND MATERIALS

Tissue culture

Non-tumorigenic, human embryonic kidney cells (HEK293) were used due to their detectable levels of telomerase activity and their common use as an AD model. Human neuroblastoma cells (SH-SY5Y) were used as the secondary AD model, due to their low levels of TERT. HEK293 and SH-SY5Y cell lines were cultured in 1 : 1 Dulbecco's modified eagle medium (DMEM) and Ham's F12 nutrient mixture, supplemented with 15% fetal bovine serum (FBS) and 1% penicillin/streptomycin solution. Cells were incubated at 37°C with 5% CO_2 in a humidified atmosphere.

Cell transfection

Transfection of HEK293 and SH-SY5Y cells with the pCIneo-moLRP::FLAG plasmid was carried out, following the Clontech Xfect™ transfection protocol, once the cells had reached 50–70% confluency. The transfected subconfluent cell culture was incubated for 48 h. Thereafter, all growth media was replenished with fresh complete growth media and subsequently treated with 800 ng/ml Geneticin, as a selective treatment for transfected cells. Thereafter, cells were treated with 400 ng/ml Geneticin to maintain the transfected cell population.

Western blotting

Western blotting was used to confirm expression of LRP::FLAG and to detect total protein levels of LRP and hTERT, post-transfection with pCIneo-moLRP::FLAG, β-actin was used as the loading control. Briefly, cell lysates were prepared with 1X RIPA buffer and protein levels quantified via the bicinchoninic acid assay (BCA). Protein was then resolved on a 12% SDS-PAGE gel for 45–55 min at 150 V per gel. Subsequently, proteins were transferred onto a polyvinylidene fluoride (PVDF) membrane at 350 mV for 50 min, using a semi-dry transferring apparatus. Membranes were thereafter blocked in 3% BSA (Amresco) in 1X PBS and 0.1% Tween 20 (PBST) for 1 h. After blocking, the blots were incubated with the appropriate primary antibody overnight with gentle shaking at 4°C. The membranes were subsequently washed in PBST and further incubated for 1 hour in the dark, in the respective secondary antibody. The membranes were then washed as outlined above. The proteins were visualized with Clarity™ Western ECL Blotting Substrate (Biorad) and the ChemiDoc™ Imaging System (Biorad). Densitometric analysis was performed with Image Lab 5.1 software (Biorad), whereby all values were further normalized against the β-actin loading control. For the list of all antibodies and dilutions, refer to (Supplementary Table 1).

Confocal microscopy with Airyscan™

Cells were seeded at a density of 1.2×10^5 cells/well onto cover slips (Labocare – 18 × 18 mm; 0.19 mm thick) and incubated overnight. All subsequent steps were performed with gentle shaking. Cells were fixed with 4% formaldehyde in PBS for 20 min at room temperature. Cells were washed thrice with 1X PBS and thereafter permeabilized with 0.25% Triton X-100 for 30 min. Coverslips were washed 3 times with 1X PBS and blocked with 0.5% BSA in 1X PBS for 30 min. Cells were incubated with the relevant primary antibody solution (diluted 1 : 200 in 0.5% BSA-PBS) overnight at 4°C. Hereafter, cells were washed 3 times in 0.5% BSA-PBS. Cells were then incubated with the respective secondary antibody diluted (1 : 500) in 500 µl 0.5% BSA-PBS for 2 h in the dark, at room temperature. Coverslips were then washed thrice, in the dark and subsequently incubated in 0.05 µg/ml DAPI diluted in 1X PBS for 5 min in the dark. Coverslips were further rinsed 4 times and mounted onto glass microscope slides with 20 µl Fluoromount (Sigma) and allowed to set in the dark at room temperature for 1.5 h. Thereafter, slides were stored in the dark at 4°C until viewed. Slides were viewed using the Zeiss LSM 780 confocal microscope with the addition of Airyscan™. Subsequently, images were analyzed with Zen 2010 imaging software v2.1. Controls were prepared as above, with the exception of primary antibodies. For the list of all antibodies used for confocal microscopy, (see Supplementary Table 2).

$A\beta_{42}$-ELISA

Total human $A\beta_{1-42}$ was quantified with the use of the Human Amyloid β (aa 1–42) Quantikine ®

AUTHOR COPY

ELISA kit by R&D Systems. The manufacturer's instructions were followed. Briefly: The plate was washed twice with Wash Buffer immediately preceding use. Human Amyloid β (aa1–42) standard, together with extracted protein samples were added to the wells (100 µl/well) and incubated for 2 h at 4°C. Thereafter, each well was aspirated and washed four times with Wash Buffer. Cold Human Amyloid β (aa1–42) conjugate (200 µl/ well) was added and incubated for a further 2 h at 4°C. The plate was subsequently washed four times with Wash Buffer and 200 µl /well of Substrate Solution was added. Following this, the plate was incubated for 30 min at room temperature in the dark, after which 50 µl/ well of Stop Solution was added. The optical density was determined using an ELISA microtiter plate reader at 450 nm with wavelength correction at 540 nm.

Telomerase activity

The TRAPeze® RT Telomerase Detection Kit (Merck), was used to determine the effect of LRP::FLAG overexpression on telomerase activity. Telomerase activity was quantified as per the manufacturer's instructions. Briefly, cells were harvested and lysates prepared by resuspension in CHAPS Lysis Buffer ((3-((3-cholamidopropyl) dimethylammonio)-1- propanesulfonate)). Protein and RNA fractions were collected in the supernatant, where after protein concentrations were quantified with the NanoDrop® ND-1000 (Thermo Scientific) and standardized to 500 ng/µl for all experimental and control reactions. All samples were analyzed via qPCR with the Roche LightCycler LC480, with the following cycling parameters applied: one cycle of 37°C for 30 min, 95°C for 2 min, and 45 cycles of 95°C for 15 s, 59°C for 60 s, and 45°C for 10 s. Telomerase activity was thereafter calculated from the standard curve generated by 1 : 10 serial dilutions (20–0.0002 amoles) of the provided TSR8 control template as per Merck Millipore instructions. All controls were included: a minus telomerase control (CHAPS Lysis Buffer), a no template control (Nuclease free/PCR Grade Water) and a heat-treated telomerase negative control, whereby 10 µl of each 500 ng/µl sample was incubated at 85°C for 10 min prior to detection. A telomerase positive cell extract was provided as a positive control and made up as per the protocol. The data was analyzed with LightCycler1 Software version 1.5.1.

3-(4, 5-Dimethylthiazol-2-yl)-2, 5-Diphenyltetrazolium bromide (MTT) cell viability assay

The MTT assay was used to assess cell viability following transfection and after treatment with cytotoxic levels of $A\beta_{42}$. Briefly, non-transfected and LRP::FLAG transfected HEK293 and SH-SY5Y cells were seeded at 1×10^5 cells/well in a 48 well plate and incubated overnight under normal conditions. Following this, the cells were treated with 500 nM $A\beta_{42}$ (to mimic Aβ-mediated cytotoxicity) for 48 h. Furthermore, all untreated controls and positive controls (cells incubated with 8 mM protocatechuic acid- PCA) were included for all cell lines. Post 48 h incubation, 100 µl of 1 mg/ml MTT was added to each well and subsequently incubated for 2 h at 37°C. Following incubation, all culture media was aspirated, and the resultant formazan crystals were dissolved in 200 µl dimethyl sulfoxide (DMSO). Subsequently, the optical density was determined using an ELISA plate reader at 570 nm. All experimental and control samples were assayed in triplicate and the percentage cell viability was calculated, relative to the untreated controls.

Statistical analysis

Statistical analysis was performed using Microsoft Excel 365 (Microsoft Corporation) and QuickCalcs Outlier Calculator ©2017 GraphPad Software which employs the Grubbs' test (extreme studentized deviate). All experiments were performed with a minimum of three biological repeats and error bars represent standard deviation. The Student's *t*-test was performed at a 95% confidence interval; where values $^{*}p < 0.05$ were considered statistically significant and values $^{**}p < 0.01$ and $^{***}p < 0.001$ were considered highly significant.

RESULTS

This study investigated the effect of overexpressing LRP::FLAG on TERT and Aβ protein levels, as well as the resultant effect on telomerase activity and cell viability in the HEK293 and SH-SY5Y AD cell culture models. Here, we show that, LRP::FLAG is exclusively expressed in the transfected HEK293 (HEK293T) (Fig. 1A) and SH-SY5Y (SH-SY5YT) (Fig. 1B) cells, post-transfection of HEK293 and SH-SY5Y cells with the pCIneo-mLRP::FLAG construct. Furthermore, we reveal a resultant increase

IOS PRESS

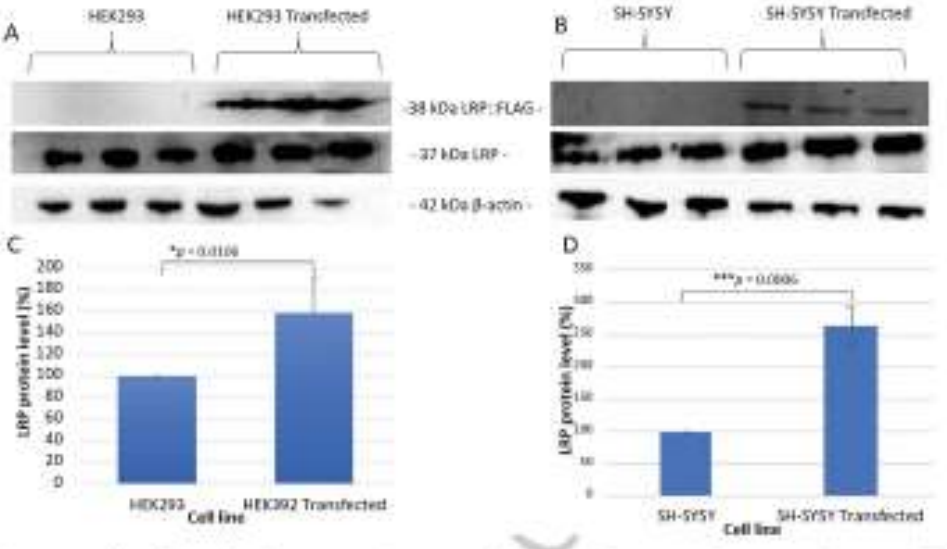


Fig. 1. Western blot analysis confirms that LRP::FLAG is overexpressed in HEK293 and SH-SY5Y cells. HEK293 and SH-SY5Y cells were confirmed to be overexpressing LRP::FLAG after stable transfection with pCIneo-mol.RP::FLAG. A) LRP::FLAG is detected in HEK293 transfected cells and not in non-transfected HEK293 cells. B) LRP::FLAG is detected in SH-SY5Y transfected cells and not in non-transfected SH-SY5Y cells. β-actin is used as the loading control. C) Densitometric analysis indicates a significant 58% increase in LRP protein level after LRP::FLAG overexpression in HEK293 cells. D) Densitometric analysis in SH-SY5Y transfected cells indicates LRP::FLAG overexpression significantly increases LRP protein levels by 165%. Error bars represent standard deviation, $n = 3$ biological repeats. $^{*}p<0.05$, $^{**}p<0.01$, $^{***}p<0.001$; Student's t-test.

in TERT levels and telomerase activity as well as a significant reduction in Aβ levels in the HEK293 and SH-SY5Y cells overexpressing LRP::FLAG.

Overexpression of LRP::FLAG increases hTERT levels with a concomitant decrease in Aβ levels in SH-SY5Y cells

Since we confirmed transfection in SH-SY5Y cells, confocal microscopy with the addition of Airyscan™ was employed to assess the effects on the levels and respective co-localization of LRP, $A\beta_{42}$ and hTERT. In non-transfected SH-SY5Y cells, LRP localizes on the cell surface and intracellularly (Fig. 2A), as we previously reported [19]. Under the same conditions, Aβ tends to localize to the cell surface as has been shown previously [50] and to a lesser extent in the cytoplasm (Fig. 2B). Although Aβ levels are low in SH-SY5Y cells, co-localization (Fig. 2E) was observed between LRP and Aβ on the cell surface and to a lesser extent in the cytoplasmic regions (Fig. 2D–F). This is conducive to what was previously reported [15]. Upon transfection of SH-SY5Y cells with pCIneo-mol.RP::FLAG (Fig. 2H), there is a clear increase in total levels of LRP (Figs. 1D and 2G), attributed to the endogenous LRP as well as the LRP::FLAG proteins, with a concomitant decrease in Aβ levels, whereby levels are almost undetectable (Fig. 2I) in comparison to the non-transfected cells (Fig. 2B). In SH-SY5Y cells, hTERT localizes uniformly across the nuclear and cytosolic regions (Fig. 2N), whereby co-localization occurs between LRP and hTERT (Fig. 2P–R). However, upon overexpression of LRP::FLAG, the SH-SY5YT cells exhibit a clear increase in hTERT levels and cytosolic localization, as observed in (Fig. 2T), which is further shown by the increase in fluorescence intensity indicated in (Fig. 2X).

Since we know of an antagonistic relationship between TERT/telomerase and Aβ in AD, as previously reported [48], confocal microscopy with the addition of Airyscan™ was employed to determine whether these two proteins co-localize in the cell. Here, we observe that hTERT and Aβ do indeed co-localize, predominantly in the cytoplasmic regions, as indicated by white areas in Fig. 3E and as detectable

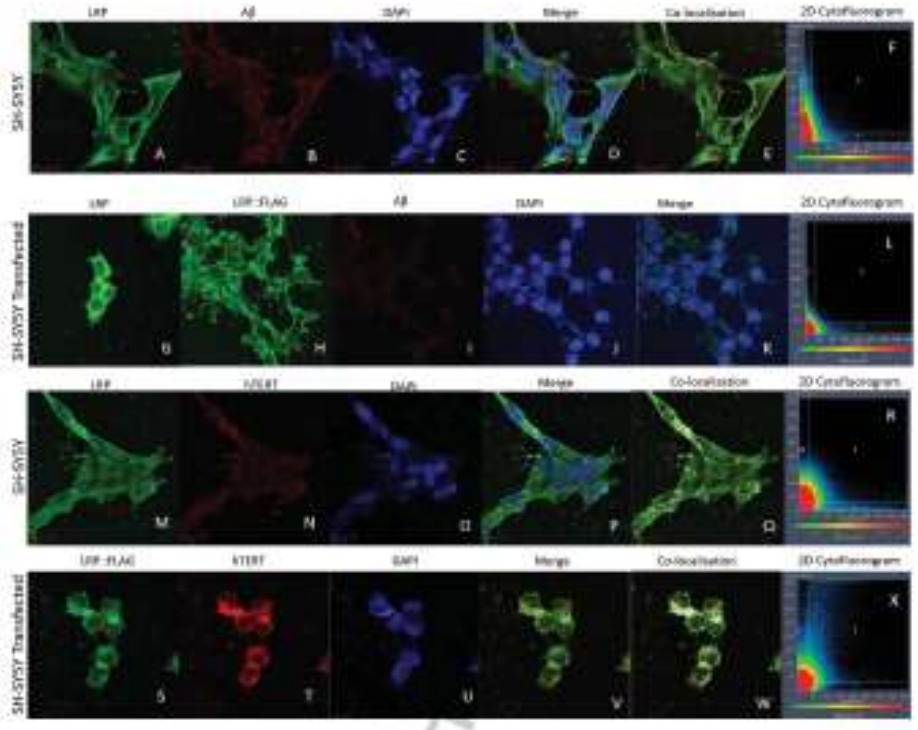


Fig. 2. LRP::FLAG overexpression decreases Aβ levels and increases hTERT levels in SH-SY5Y cells. A–L) Intracellular localization and co-localization of LRP (FITC-Green) and Aβ (APC-Red) as well as LRP::FLAG (FITC-Green) and Aβ in SH-SY5Y and SH-SY5YT cells. M–X) Intracellular localization and co-localization of LRP (FITC-Green) and hTERT (APC-Red) as well as LRP::FLAG (FITC-Green) and hTERT in SH-SY5Y and SH-SY5YT cells. A, M) Endogenous LRP levels in SH-SY5Y cells. H) Endogenous Aβ levels in SH-SY5Y cells. G) LRP levels are increased in SH-SY5YT cells. H, S) LRP::FLAG expression is confirmed in SH-SY5YT cells. I) Aβ expression becomes almost undetectable upon overexpression of LRP::FLAG. C, J, O, U) Nuclei are stained with DAPI (Blue). Co-localization occurs between LRP and Aβ (D, K) and between LRP and hTERT (R, X) represented by yellow fluorescence in merged images, as white areas (H, Q, W) and as fluorescence in the third quadrant of the 2D cytofluorograms (F, L, R, X). All images are at 630 X magnification and a resolution of 140 nm (Airyscan™). Scale bars represent 10 μm.

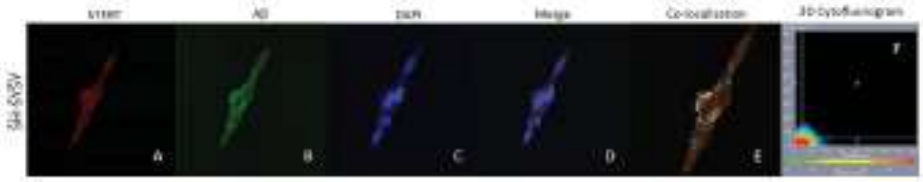


Fig. 3. Immunofluorescence microscopy in SH-SY5Y cells suggests co-localization of hTERT and Aβ. hTERT (APC-Red) (A) and Aβ (FITC-Green) (B) co-localize on the cell surface and intracellularly in SH-SY5Y cells. Nuclei are stained with DAPI (Blue) (C). Co-localization is represented by yellow fluorescence in the merged image (D), as white areas (E) and as fluorescence in the third quadrant of the 2D cytofluorogram (F). All images are at 630 X magnification and a resolution of 140 nm (Airyscan™).

fluorescence in quadrant 3 of (Fig. 3F). This furthermore suggests an interaction and a possible association between the two proteins.

LRP::FLAG overexpression significantly decreases intracellular $A\beta_{42}$ levels and $A\beta_{42}$ shedding in HEK293 and SH-SY5Y cells

An $A\beta_{42}$-ELISA was performed on both the HEK293 and SH-SY5Y cells to further analyze $A\beta_{42}$ levels. Analysis of intracellular $A\beta_{42}$ levels in HEK293 and HEK293T cells, showed a significant reduction of 53.7 % in intracellular $A\beta_{42}$ in the HEK293T cells ($p = 0.0009$) (Fig. 4A). No significant change was observed on analysis of intracellular $A\beta_{42}$ levels in both untreated SH-SY5Y and SH-SY5YT cells (Fig. 4C). Moreover, intracellular $A\beta_{42}$ levels in the SH-SY5Y and SH-SY5YT cells were almost undetectable without $A\beta_{42}$ treatment (Fig. 4C). Therefore, immunofluorescent labelling was used to quantify $A\beta_{42}$ levels in the SH-SY5Y cells and is described as above (Fig. 2A–L). Furthermore, since LRP/LR is involved in the shedding of $A\beta_{42}$ [51], extracellular $A\beta_{42}$ levels were assessed by $A\beta_{42}$-ELISA to determine whether overexpression of LRP::FLAG would cause an increase in $A\beta_{42}$ shedding. Surprisingly, we observed a significant reduction in extracellular $A\beta_{42}$ levels ($p = 0.0105$) in the HEK293T cells, when compared to HEK293 cells (Fig. 4B). This indicates a reduction in Aβ shedding in the HEK293T cells overexpressing LRP::FLAG.

Overexpression of LRP::FLAG significantly increases telomerase activity in HEK293 and SH-SY5Y cells

Multiple studies have reported that an increase in TERT expression induces an increase in telomerase activity [52, 53], therefore, subsequent to observing an increase in hTERT levels post- LRP::FLAG overexpression (Fig. 2T), relative telomerase activity was quantified via qPCR. In addition, since $A\beta_{42}$ is known to have a relationship with hTERT [48], telomerase activity was assayed in both the presence and absence of cytotoxic levels of $A\beta_{42}$. Here, we affirm that, in the absence of $A\beta_{42}$ (0 nM), HEK293T ($p = 0.0067$) and SH-SY5YT ($p = 0.0025$) cells exhibited significantly higher telomerase activity when compared to non-transfected HEK293 and SH-SY5Y cells, respectively (Fig. 5). This is conducive to what we previously reported in HEK293 cells [32]. Upon treatment with cytotoxic levels of $A\beta_{42}$ (500 nM), we observed a significant decrease in relative telomerase activity in both the non-transfected HEK293 ($p = 0.0056$) and SH-SY5Y ($p = 0.0005$) cells, as well as in HEK293T ($p = 1.81E{-}06$) cells. Surprisingly, however, both transfected cell lines displayed significantly higher telomerase activity in comparison to non-transfected HEK293 ($p = 0.03$) and SH-SY5Y ($p = 8.62E{-}05$) cells after treatment with $A\beta_{42}$ (500 nM). This suggests that overexpression of LRP::FLAG increases telomerase activity, despite the presence of high levels of Aβ.

UNDER PEER REVIEW

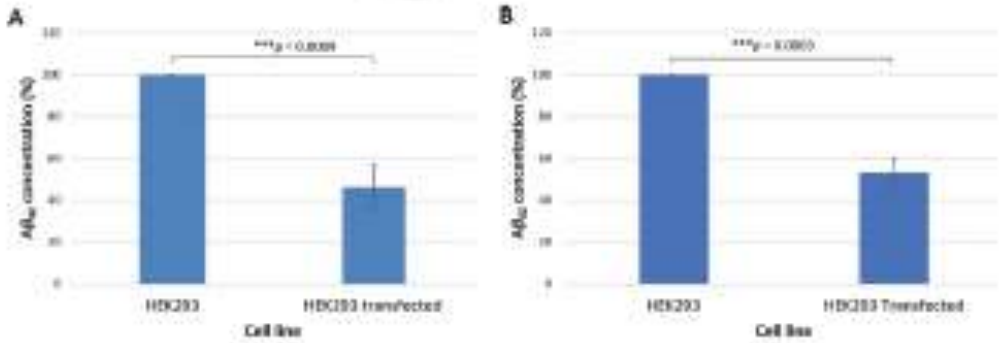


Fig. 4. LRP::FLAG overexpression decreases intracellular $A\beta_{42}$ levels and $A\beta_{42}$ shedding in HEK293 cells. A significant decrease in total intracellular $A\beta_{42}$ levels is observed in HEK293T cells (A). A significant decrease in $A\beta_{42}$ shedding is seen in HEK293T cells (B). $A\beta_{42}$ concentration is expressed as a % pg $A\beta_{42}$ per/mg total protein. Non-transfected HEK293 were set to 100%. Error bars represent standard deviation, n = 3 biological repeats. $^{*}p < 0.05$, $^{**}p < 0.01$, $^{***}p < 0.001$; Student's *t*-test.

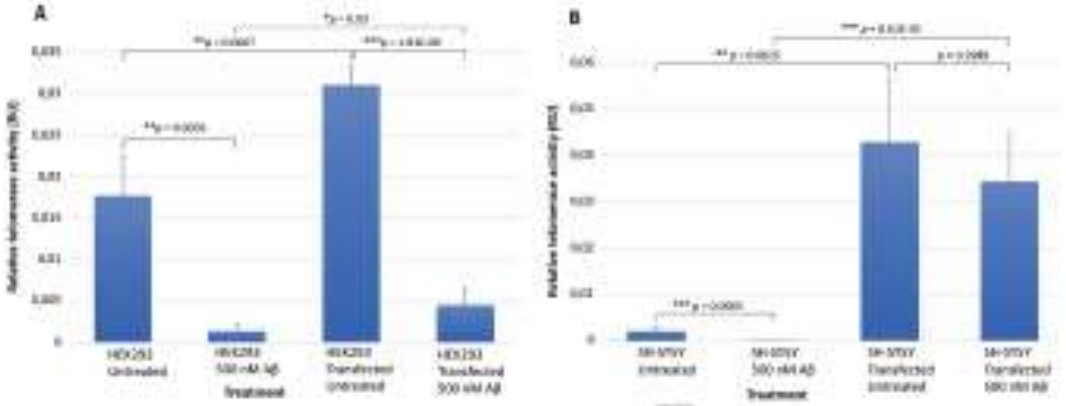


Fig. 5. LRP::FLAG overexpression significantly increases telomerase activity in HEK293 and SH-SY5Y cells. Relative telomerase activity (RU = relative units) is increased in HEK293T compared to non-transfected HEK293 cells (A) and in SH-SY5YT cells compared to non-transfected SH-SY5Y cells (B) both before and after treatment with cytotoxic levels of synthetic $A\beta_{42}$ (500 nM). All values were normalized against the negative controls; all negative control values were subtracted from the signal of each sample. This data is representative of the mean value obtained across all biological repeats for each cell line and each treatment. Error bars represent standard deviation, $n = 3$ biological repeats. $^{*}p<0.05$, $^{**}p<0.01$, $^{***}p<0.001$; Student's *t*-test.

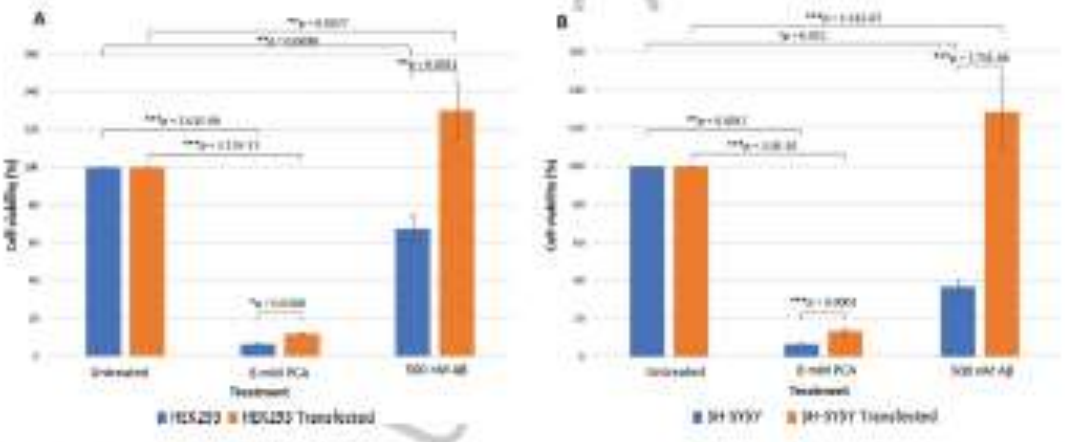


Fig. 6. LRP::FLAG overexpression rescues HEK293 and SH-SY5Y cells from $A\beta_{42}$ induced cytotoxicity. Cellular viability of (A) HEK293 and HEK293T as well as (B) SH-SY5Y and SH-SY5YT cells, as determined by MTT assay. Cell viability was assessed 48 h post-treatment with 500 nM synthetic $A\beta_{42}$ and the untreated set to 100%. PCA was used as a positive control. Error bars represent standard deviation. $n = 3$ biological repeats $^{*}p<0.05$, $^{**}p<0.01$, $^{***}p<0.001$; Student's *t*-test.

Overexpression of LRP::FLAG rescues HEK293 and SH-SY5Y cells from $A\beta_{42}$ – mediated cytotoxicity

We have previously shown that LRP/LR is a receptor for $A\beta_{42}$, whereby it is involved in the internalization and therefore, the accumulation of $A\beta_{42}$ intracellularly, ultimately inhibiting cell proliferation and inducing apoptosis [51]. Since we revealed that LRP::FLAG overexpression increased hTERT levels with a concomitant decrease in $A\beta_{42}$ levels, an MTT assay was performed to determine whether LRP::FLAG overexpression would also influence the viability of the transfected HEK293 and SH-SY5Y cells in the presence of cytotoxic levels of synthetic $A\beta_{42}$ peptides (Fig. 6). We observed that treatment with 500 nM $A\beta_{42}$, reduced cellular viability significantly in both non-transfected HEK293 ($p = 0008$) and SH-SY5Y ($p = 1.31E-07$) cells, with a decrease of 32.68% and 63.33% seen in comparison to untreated HEK293 and SH-SY5Y cells, respectively. (Fig. 6). Simultaneously, we investigated the effect of the 500 nM synthetic $A\beta_{42}$ treatment on cell viability in HEK293T and SH-SY5YT cells

(Fig. 6). Interestingly, we revealed that these cells exhibited a significant 62.62 % ($p = 0.0011$) and 91.44 % ($p = 7.75E-06$) less cell death, respectively, when compared to the non-transfected counterparts treated under the same conditions. Taken together, these data indicate the novel finding that LRP::FLAG overexpression rescues both HEK293 and SH-SY5Y cells from $A\beta_{42}$-induced cytotoxicity.

DISCUSSION

We have recently shown that 5XFAD transgenic mice treated with the anti-LRPLR specific antibody, IgG1-iS18, exhibited an improvement in memory, a decrease in Aβ plaque formation, with a significant reduction in both soluble and insoluble $A\beta_{42}$ levels. This was suggested to be a neuroprotective effect as attributed to a concomitant and significant increase in mTERT levels observed [36]. Despite the previously explained role of LRPLR in the pathological process of disease, we recently elucidated that overexpression of LRP::FLAG [40] resulted in an increase in TERT expression, telomerase activity, telomere length as well as a reduction in senescent markers [32]. Altogether indicating that LRPLR has a role in the regulation of telomerase activity and TERT expression [31, 32, 36]. Furthermore, since telomerase plays a role in AD [46–48], we therefore wanted to determine the effect of overexpressing LRP::FLAG in an AD setting. This present study demonstrates that overexpression of LRP::FLAG increases TERT levels and concurrently reduces intracellular $A\beta_{42}$ levels and $A\beta_{42}$ shedding in HEK293 cells. In addition, we reveal a concomitant increase in telomerase activity and rescue from $A\beta_{42}$-mediated cytotoxicity.

It was previously reported that LRPLR both co-localizes and interacts with hTERT in HEK293 and MDA-MB231 cells [31, 32]. Here, it is seen that LRP and hTERT do indeed co-localize in the SH-SY5Y cells (Fig. 2P, R), as determined by confocal microscopy and that co-localization occurs in the nuclear and cytosolic regions. In addition, we observed a substantial increase in hTERT levels in the SH-SY5YT cells after LRP::FLAG overexpression. Interestingly, we found that the hTERT was localized more abundantly in the cytoplasmic regions, than in the nucleus. Studies have reported that TERT translocates from the nucleus to the mitochondria, where it plays a role in decreasing ROS levels, DNA damage, and apoptosis [42–44]. Spilsbury et al. [54] revealed that TERT preferentially localizes to the mitochondria in neurons upon AD pathology; here, they suggested that TERT decreases ROS levels and improves respiratory chain function. It is well-reported that AD is a multifactorial disease, where many components of the cell play a role; however, it has recently been described that mitochondrial dysfunction is one of the earliest observed pathogenic alterations, which occurs well before the accumulation of amyloid plaques [55, 56]. Numerous studies have reported impairment of mitochondrial function as well as increased production of ROS in AD transgenic mouse models and AD patients [57–59]. Although the mechanism behind mitochondrial dysfunction and AD is not completely understood, it is known that there is a cumulative effect between mitochondrial dysfunction and Aβ accumulation [60].

Since it was previously observed that LRP co-localizes with hTERT and with $A\beta_{42}$, respectively, it was of interest to assess whether hTERT and $A\beta_{42}$ co-localize. We observed co-localization between hTERT and $A\beta_{42}$ in the cytoplasm of the SH-SY5Y cells (Fig. 3), thus, suggesting an interaction between these proteins. Interestingly, we observed a significant decrease in intracellular $A\beta_{42}$ levels in the HEK293T cells, as well as the SH-SY5YT cells overexpressing LRP::FLAG, when compared to the non-transfected cells, respectively. Furthermore, a significant reduction in extracellular $A\beta_{42}$ levels was observed in the transfected HEK293 cells, when compared to the non-transfected HEK293 cells, thereby, representing a significant reduction in $A\beta_{42}$ shedding. Since $A\beta_{42}$ levels were undetectable in the SH-SY5Y cells by $A\beta_{42}$-ELISA, we were unable to assess whether there was a change in $A\beta_{42}$ shedding upon overexpression of LRP::FLAG in these cells. Wang et al. [48] proposed that there is an antagonistic relationship between telomerase and $A\beta_{42}$ within neurons, since $A\beta_{42}$ is involved in the inhibition of telomerase activity, through the binding of the telomeric DNA/RNA template of telomerase. Since we saw an increase in hTERT protein levels, as well as localization to the cytoplasm, we propose this concomitant decrease in $A\beta_{42}$ levels seen in both the SH-SY5Y (Fig. 2) and the HEK293 (Fig. 4A) cells, as well as the reduction in $A\beta_{42}$ shedding (Fig. 4B), is owed to the interaction between TERT and Aβ.

It has been reported by multiple studies, that an increase in hTERT expression causes an increase in telomerase activity, and that TERT behaves as the limiting factor for telomerase activity [52, 53]. Therefore, as we observed an increase in hTERT levels and a decrease in $A\beta_{42}$ levels, we determined the

resulting effect on telomerase activity in both the absence and presence of cytotoxic levels of $A\beta_{42}$. We confirmed a significant increase in telomerase activity in both HEK293 (Fig. 5A) and SH-SY5Y (Fig. 5B) cells overexpressing LRP::FLAG. Furthermore, this follows the trend we previously reported in HEK293 cells [32]. Although telomerase expression is a known hallmark of cancer, it has been shown that ectopic expression of telomerase is not associated with malignancy [61]. It was reported that the introduction of telomerase to fibroblasts did not alter other growth parameters. The telomerase-expressing cells showed no other changes in growth patterns or genomic instability, and these cells did not bypass cell-cycle induced check point controls typical of cancer cells [61]. Indeed, The HEK293 and SH-SY5Y cells overexpressing LRP::FLAG maintained a dependence on standard serum concentrations and exhibited contact inhibition.

Treatment with cytotoxic levels of $A\beta_{42}$, thereby mimicking $A\beta_{42}$-mediated cytotoxicity, caused a consequential reduction in telomerase activity in both transfected and non-transfected HEK293 and SH-SY5Y cells. Since we know $A\beta_{42}$ induces apoptosis [46] and inhibits telomerase activity [48], it is proposed that this reduction in telomerase activity is observed as a combination of these two factors. Remarkably, however, telomerase activity was significantly higher in both the HEK293T and SH-SY5YT cells when treated with synthetic $A\beta_{42}$ peptides and compared to their non-transfected counterparts treated under the same conditions (Fig. 5). Additionally, we performed an MTT assay, subsequent to a 48 h exogenous treatment with 500 nM synthetic $A\beta_{42}$ peptides, to assess the effect on cell viability. Interestingly, less cell death was observed in both the HEK293T (Fig. 6A) and the SH-SY5YT (Fig. 6B) cells, post treatment with cytotoxic levels of $A\beta_{42}$ peptides, when compared to the corresponding non-transfected cells. Thus, these novel findings suggest overexpression of LRP::FLAG significantly increases telomerase activity, despite the presence of $A\beta_{42}$ and furthermore rescues cells from $A\beta$-mediated cytotoxicity. This observation is proposed to be attributable to the fact that the increase in hTERT levels and the resulting increase in telomerase activity after overexpression of LRP::FLAG, is occurring prior to the manifestation of $A\beta_{42}$-mediated cytotoxicity.

The pathological agent of AD, $A\beta$, has a functional role in mitochondrial dysfunction by disrupting calcium homeostasis through the formation of ion-permissible channels in the cell membrane, as well as causing oxidative stress [10]. In addition, ROS-induced alterations in mitochondrial membrane potential have been shown to be caused by p53, thereby, promoting apoptosis [62]. The "mitochondrial cascade hypothesis" can be used to explain sporadic, late-onset AD. It explains how a decline in the efficiency of mitochondrial activities occurs as a result of age-related effects on genetic factors (nuclear and mitochondrial DNA), thus causing an increase in ROS, thereby triggering production of $A\beta$ [63]. Telomerase is responsible for maintaining telomere length [64] and the loss of telomerase activity is pivotal in cellular senescence, whereby it is involved in the aging process [40]. Furthermore, AD sufferers exhibit shorter telomeres in their neuronal cells [47], which is indicative of acceleration of this process. Vera et al. [65] suggested that the rescuing effect of telomerase on short telomeres is sufficient to restore cell and organismal viability as well as genomic stability. Therefore, we propose that the increase in hTERT levels can compensate for the adverse effects caused by the high levels of $A\beta_{42}$, by increasing telomerase activity. Through the increase in telomerase activity, we suggest the age-related effects on the mitochondria are decreased, thereby lowering mitochondrial dysfunction and reducing the production of $A\beta$. In conjunction with this, the increased levels of hTERT seen in the cytoplasm could have an additive effect, to protect the mitochondria from both the internalization of $A\beta$, as well as $A\beta$-induced mitochondrial impairment, as previously described. It is reported that p53 is present at elevated levels in neurons affected by amyloid plaques [66], as well as in transgenic mice overexpressing the $A\beta$ peptide [67]. Fu et al. [68] elucidated that TERT can prevent the activation of caspases, prior to mitochondrial dysfunction and through an interaction with the tumor suppressor, p53 [62]. Therefore, it is likely that TERT is furthermore exerting a protective effect in the cytoplasm, against the aforementioned detrimental effects of $A\beta$, through the modulation of p53-dependent mechanisms. Thus, we suggest the increase in TERT levels and telomerase activity is playing a protective function against apoptotic stresses caused by $A\beta$ and mitochondrial perturbations, which influence each other in a deadly cycle and is thereby, providing a neuroprotective function. However, further studies are being performed to investigate the effect of overexpressing LRP::FLAG on ROS production and mitochondrial function.

PROOF

This study has shown that LRP::FLAG overexpression increases hTERT expression, concomitantly increases telomerase activity, and concurrently decreases intracellular $A\beta_{42}$ levels and shedding in HEK293 and SH-SY5Y AD cell culture models. Together, our results suggest that the telomerase protein, TERT, seems to be a protective factor against AD pathology and may offer resistance against pathological Aβ. We therefore propose that LRP::FLAG overexpression is serving as a telomerase activating compound to reduce AD pathology and is resulting in neuroprotective processes as indicated by the rescue from $A\beta_{42}$ -induced cytotoxicity observed in this study. Thus, overexpression of LRP::FLAG could form the basis for a powerful, novel preventative treatment for neurodegenerative disorders, such as AD.

ACKNOWLEDGMENTS

We thank Affimed Therapeutics GmbH, Heidelberg, Germany for providing the IgG1-iS18 antibody.

This work is based upon research supported by the National Research Foundation (NRF), the Republic of South Africa (RSA). Any opinions, findings and conclusions or recommendations expressed in this material are those of the author(s), and therefore, the National Research Foundation does not accept any liability in this regard thereto. Financial support was further received from the South African Medical Research Council (MRC) under a self-initiated grant awarded to SFTW. Any opinions, findings and conclusions or recommendations expressed in this material are those of the author(s), and therefore, the MRC does not accept any liability in this regard thereto.

Authors' disclosures available online (https://www.j-alz.com/manuscript-disclosures/19-0075r1).

SUPPLEMENTARY MATERIAL

The supplementary material is available in the electronic version of this article: http://dx.doi.org/10.3233/JAD-190075.

REFERENCES

[1] Prince M, Comas-Herrera A, Knapp M, Guerchet M, Karagiannidou M (2016) *World Alzheimer Report 2016. Improving healthcare for people living with dementia: coverage, quality and costs now and in the future*. Alzheimer's Disease International, London, UK.

[2] Xiao Y, Ma B, McElheny D, Parthasarathy S, Long F, Hoshi M, Nussinov R, Ishii Y (2015) Aβ (1–42) fibril structure illuminates self-recognition and replication of amyloid in Alzheimer's disease. *Nat Struct Mol Biol* **22**, 499.

[3] Serrano-Pozo A, Frosch MP, Masliah E, Hyman BT (2011) Neuropathological alterations in Alzheimer disease. *Cold Spring Harb Perspect Med* **1**, a006189.

[4] Avila J (2006) Tau phosphorylation and aggregation in Alzheimer's disease pathology. *FEBS Lett* **580**, 2922-2927.

[5] Choi SH, Kim YH, Hebisch M, Sliwinski C, Lee S, D'Avanzo C, Chen H, Hooli B, Asselin C, Muffat J (2014) A three-dimensional human neural cell culture model of Alzheimer's disease. *Nature* **515**, 274.

[6] Kakiya N, Saito T, Nilsson P, Matsuba Y, Tsubuki S, Takei N, Nawa H, Saido TC (2012) Cell surface expression of the major amyloid-β peptide (Aβ)-degrading enzyme, neprilysin, depends on phosphorylation by mitogen-activated protein kinase/extracellular signal-regulated kinase kinase (MEK) and dephosphorylation by protein phosphatase 1a. *J Biol Chem* **287**, 29362-29372.

[7] Hyman B, West H, Rebeck G, Hulette S, Mantegani R, Uhlinja M, Havlin K, Stanley H (1995) Quantitative analysis of senile plaques in Alzheimer disease: observation of log-normal size distribution and molecular epidemiology of differences associated with apolipoprotein E genotype and trisomy 21 (Down syndrome). *Proc Natl Acad Sci U S A* **92**, 3586-3590.

[8] Demuro A, Mina E, Kayed R, Milton SC, Parker I, Glabe CG (2005) Calcium dysregulation and membrane disruption as a ubiquitous neurotoxic mechanism of soluble amyloid oligomers. *J Biol Chem* **280**, 17294-17300.

[9] Lin H, Bhatia R, Lal R (2001) Amyloid β protein forms ion channels: implications for Alzheimer's disease pathophysiology. *FASEB J* **15**, 2433-2444.

[10] Mattson MP (1997) Cellular actions of beta-amyloid precursor protein and its soluble and fibrillogenic derivatives. *Physiol Rev* **77**, 1081-1132.

[11] Zhang J, Pieper A, Snyder SH (1995) Poly (ADP-ribose) synthetase activation: An early indicator of neurotoxic DNA damage. *J Neurochem* **65**, 1411-1414.

[12] Deng G, Su JH, Ivins KJ, Van Houten B, Cotman CW (1999) Bcl-2 facilitates recovery from DNA damage after oxidative stress. *Exp Neurol* **159**, 309-318.

[13] Da Costa Dias B, Jovanovic K, Gonsalves D, Weiss SF (2011) Structural and mechanistic commonalities of amyloid-β and the prion protein. *Prion* **5**, 126-137.

[14] Verdier Y, Penke B (2004) Binding sites of amyloid β-peptide in cell plasma membrane and implications for Alzheimer's disease. *Curr Protein Pept Sci* **5**, 19-31.

[15] Dias BDC, Jovanovic K, Gonsalves D, Moodley K, Reusch U, Knackmuss S, Penny C, Weinberg MS, Little M, Weiss SF (2013) Anti-LRP/LR specific antibody IgG1-iS18 and knock-down of LRP/LR by shRNAs rescue cells from Aβ 42 induced cytotoxicity. *Sci Rep* **3**, 2702.

[16] Stefani M (2010) Biochemical and biophysical features of both oligomer/fibril and cell membrane in amyloid cytotoxicity. *FEBS J* **277**, 4602-4613.

[17] Bartzokis G (2011) Alzheimer's disease as homeostatic responses to age-related myelin breakdown. *Neurobiol Aging* **32**, 1341-1371.

[18] Marchesi VT (2011) Alzheimer's dementia begins as a disease of small blood vessels, damaged by oxidative-induced inflammation and dysregulated amyloid metabolism: implications for early detection and therapy. *FASEB J* **25**, 5-13.

[19] Mbianima V, Da Costa Dias B, Omar A, Jovanovic K, Weiss S (2010) Interactions between PrP (c) and other ligands with the 37-kDa/67-kDa laminin receptor. *Front Biosci* **15**, 366-7.

[20] Jovanovic K, Chetty CI, Khumalo T, Da Costa Dias B, Ferreira IL, Malindisa ST, Caveney R, Letsolo BT, Weiss SF (2015) Novel patented therapeutic approaches targeting the 37/67 kDa laminin receptor for treatment of cancer and Alzheimer's disease. *Expert Opin Ther Pat* **25**, 567-582.

[21] Weiss SF (2017) Bad boy with a twist: targeting the 37 kDa/67 kDa Laminin receptor for treatment of cancer and neurodegenerative diseases and for changing telomere dynamics. *Cell Cell Life Sci J* **2**, 000114.

[22] Rao C, Castronovo V, Schmitt MC, Wewer UM, Clayzeith AP, Liotta LA, Sobel ME (1989) Evidence for a precursor of the high-affinity metastasis-associated murine laminin receptor. *Biochemistry* **28**, 7435-7440.

[23] Zaber C, Knackmuss S, Zamora G, Reusch U, Vlasova E, Diehl D, Mick V, Hoffmann K, Niklas D, Pröhlich T (2008) Invasion of tumorigenic HT1080 cells is impeded by blocking or downregulating the 37-kDa/67-kDa laminin receptor. *J Mol Biol* **378**, 530-539.

[24] Omar A, Reusch U, Knackmuss S, Little M, Weiss SF (2012) Anti-LRP/LR-specific antibody IgG1-i518 significantly reduces adhesion and invasion of metastatic lung, cervix, colon and prostate cancer cells. *J Mol Biol* **419**, 102-109.

[25] Moodley K, Weiss SF (2013) Downregulation of the non-integrin laminin receptor reduces cellular viability by inducing apoptosis in lung and cervical cancer cells. *PloS One* **8**, e57409.

[26] Khumalo T, Reusch U, Knackmuss S, Little M, Veale RB, Weiss SF (2013) Adhesion and invasion of breast and oesophageal cancer cells are impeded by anti-LRP/LR-specific antibody IgG1-i518. *PloS One* **8**, e66297.

[27] Khanal R, Dias BDC, Moodley K, Penny C, Reusch U, Knackmuss S, Little M, Weiss SF (2013) In vitro inhibition of angiogenesis by antibodies directed against the 37kDa/67kDa laminin receptor. *PloS One* **8**, e58088.

[28] Chetty C, Khumalo T, Dias BDC, Reusch U, Knackmuss S, Little M, Weiss SF (2014) Anti-LRP/LR specific antibody IgG1-i518 impedes adhesion and invasion of lung cancer cells. *PloS One* **9**, e96268.

[29] Rebelo TM, Chetty CI, Ferreira IL, Weiss SF (2016) Anti-LRP/LR-specific antibody IgG1-i518 impedes adhesion and invasion of pancreatic cancer and neuroblastoma cells. *BMC Cancer* **16**, 917.

[30] Vania L, Chetty CI, Ferreira IL, Weiss SF (2016) Anti-LRP/LR-Specific antibody IgG1-i518 significantly impedes adhesion and invasion in early- and late-stage colorectal carcinoma cells. *Mol Med* **22**, 66-8.

[31] Naidoo K, Malindisa ST, Olgasr TC, Bernert M, Dias BDC, Ferreira IL, Reusch U, Knackmuss S, Little M, Weiss SF (2015) Knock-down of the 37kDa/67kDa laminin receptor LRP/LR impedes telomerase activity. *PloS One* **10**, e0141618.

[32] Olgasr TC, Ferreira IL, Malindisa S, Bernert M, Letsolo BT, Weiss SF (2017) 37 kDa LRP-/- PI-AG enhances telomerase activity and reduces senescent markers in vitro. *Oncotarget* **8**, 86646.

[33] Jovanovic K, Gonsalves D, Dias BDC, Moodley K, Reusch U, Knackmuss S, Penny C, Weinberg MS, Little M, Weiss SF (2013) Anti-LRP/LR specific antibodies and shRNAs impede amyloid beta shedding in Alzheimer's disease. *Sci Rep* **3**, 2699.

[34] Jovanovic K, Loos B, Dias BDC, Penny C, Weiss SF (2014) High resolution imaging study of interactions between the 37 kDa/67 kDa laminin receptor and APP, beta-secretase and gamma-secretase in Alzheimer's disease. *PloS One* **9**, e100373.

[35] Pansock DC, Jovanovic K, Pinto MG, Ferreira IL, Dias BDC, Penny C, Knackmuss S, Reusch U, Little M, Schatzl HM (2016) LRP/LR antibody mediated rescuing of amyloid-β-induced cytotoxicity is dependent on PrPc in Alzheimer's disease. *J Alzheimers Dis* **49**, 645-657.

[36] Ferreira IL, Bignon MJ, Olgasr TC, Taglialti N, Jovanovic K, Letsolo BT, Weiss SF (2018) LRP/LR specific antibody IgG1-i518 impedes neurodegeneration in Alzheimer's disease mice. *Oncotarget* **9**, 27059.

[37] Greider CW, Blackburn EH (1987) The telomere terminal transferase of Tetrahymena is a ribonucleoprotein enzyme with two kinds of primer specificity. *Cell* **51**, 887-898.

[38] Kim NW, Piatyszek MA, Prowse KR, Harley CB, West MD, Ho PL, Coviello GM, Wright WE, Weinrich SL, Shay JW (1994) Specific association of human telomerase activity with immortal cells and cancer. *Science* **266**, 2011-2015.

[39] Nakamura TM, Cech TR (1998) Reversing time: origin of telomerase. *Cell* **92**, 587-590.

[40] Shay JW, Wright WE (2004) Senescence and immortalization: role of telomeres and telomerase. *Carcinogenesis* **26**, 867-874.

[41] Santos JH (2014) Extra-telomeric functions of human telomerase: cancer, mitochondria and oxidative stress. *Curr Pharm Des* **20**, 6385-6403.

[42] Ahmed S, Passos JF, Birket MJ, Beckmann T, Brings S, Peters H, Birch-Machin MA, von Zglinicki T, Saretzki G (2008) Telomerase does not counteract telomere shortening but protects mitochondrial function under oxidative stress. *J Cell Sci* **121**, 1046-1053.

[43] Haendeler J, Dröse S, Büchner N, Jakob S, Altschmied J, Goy C, Spyridopoulos I, Zeiher AM, Brandt U, Dimmeler S (2009) Mitochondrial telomerase reverse transcriptase binds to and protects mitochondrial DNA and function from damage. *Arterioscler Thromb Vasc Biol* **29**, 929-935.

[44] Singhapol C, Pal D, Czapiewski R, Porika M, Nelson G, Saretzki GC (2013) Mitochondrial telomerase protects cancer cells from nuclear DNA damage and apoptosis. *PloS One* **8**, e52989.

[45] Cong Y, Shay JW (2008) Actions of human telomerase beyond telomeres. *Cell Res* **18**, 725.

[46] Zhu H, Fu W, Mattson MP (2000) The catalytic subunit of telomerase protects neurons against amyloid β-peptide-induced apoptosis. *J Neurochem* **75**, 117-124.

[47] Franco S, Blasco MA, Siedlak SL, Harris PL, Moreira PI, Perry G, Smith MA (2006) Telomeres and telomerase in Alzheimer's disease: Epiphenomena or a new focus for therapeutic strategy? *Alzheimer Dement* **2**, 164-168.

[48] Wang J, Zhao C, Zhao A, Li M, Ren J, Qu X (2015) New insights in amyloid beta interactions with human telomerase. *J Am Chem Soc* **137**, 1213-1219.

[49] Yuan K, Weiss S (2006) A trans-dominant negative 37 kDa/67 kDa laminin receptor mutant impairs PrPSc propagation in scrapie-infected neuronal cells. *J Mol Biol* **358**, 57-66.

[50] Vetrivel KS, Thinakaran GJ (2010) Membrane rafts in Alzheimer's disease beta-amyloid production. *Biochim Biophys Acta* **1801**, 860-867.

[51] Dias BDC, Jovanovic K, Gonsalves D, Moodley K, Reusch U, Knackmuss S, Weinberg MS, Little M, Weiss SF (2014) The 37kDa/67kDa laminin receptor acts as a receptor for Aβ 42 internalization. *Sci Rep* **4**, 5556.

[52] Bodnar AG, Ouellette M, Frolkis M, Holt SE, Chiu C-P, Morin GB, Harley CB, Shay JW, Lichtsteiner S, Wright WE

ARTICLE

(1998) Extension of life-span by introduction of telomerase into normal human cells. *Science* **279**, 349-352.

[53] Counter CM, Hahn WC, Wei W, Caddle SD, Beijersbergen RL, Lansdorp PM, Sedivy JM, Weinberg (1998) Dissociation among in vitro telomerase activity, telomere maintenance, and cellular immortalization. *Proc Natl Acad Sci U S A* **95**, 14723-14728.

[54] Spillantini A, Miwa S, Attems J, Saretzki G (2015) The role of telomerase protein TERT in Alzheimer's disease and in tau-related pathology in vitro. *J Neurosci* **35**, 1659-1674.

[55] Rhein V, Song X, Wiesner A, Ittner LM, Baysang G, Meier F, Ozmen L, Bluethmann H, Dröse S, Brandt U (2009) Amyloid-β and tau synergistically impair the oxidative phosphorylation system in triple transgenic Alzheimer's disease mice. *Proc Natl Acad Sci U S A* **106**, 20057-20062.

[56] Yao J, Irwin RW, Zhao L, Nilsen J, Hamilton RT, Brinton R (2009) Mitochondrial bioenergetic deficit precedes Alzheimer's pathology in female mouse model of Alzheimer's disease. *Proc Natl Acad Sci U S A* **106**, 14670-14675.

[57] Crouch PJ, Harding S-ME, White AR, Camakaris J, Bush AI, Masters C (2008) Mechanisms of Aβ mediated neurodegeneration in Alzheimer's disease. *Int J Biochem Cell Biol* **40**, 181-198.

[58] Akandi A, Benard G, Augereau O, Malgat M, Talbot J, Mazat J, Letellier T, Dachary-Prigent J, Solaini G, Rossignol R (2005) Gradual alteration of mitochondrial structure and function by β-amyloids: importance of membrane viscosity changes, energy deprivation, reactive oxygen species production, and cytochrome c release. *J Bioenerg Biomembr* **37**, 207-225.

[59] Calkins MJ, Manczak M, Mao P, Shirendeb U, Reddy P (2011) Impaired mitochondrial biogenesis, defective axonal transport of mitochondria, abnormal mitochondrial dynamics and synaptic degeneration in a mouse model of Alzheimer's disease. *Hum Mol Genet* **20**, 4515-4529.

[60] Petersen CAH, Alikhani N, Behbahani H, Wiehager B, Pavlov PF, Alafuzoff I, Leinonen V, Ito A, Winblad B, Glaser E (2008) The amyloid β-peptide is imported into mitochondria via the TOM import machinery and localized to mitochondrial cristae. *Proc Natl Acad Sci U S A* **105**, 13145-13150.

[61] Morales CP, Holt SE, Ouellette M, Kaur KJ, Yan Y, Wilson KS, White MA, Wright WE, Shay JW (1999) Absence of cancer-associated changes in human fibroblasts immortalized with telomerase. *Nat Genet* **21**, 115.

[62] Li H, Cao Y, Berndt MC, Funder JW, Liu J-P (1999) Molecular interactions between telomerase and the tumor suppressor protein p53 in vitro. *Oncogene* **18**, 5785.

[63] Swerdlow RH, Khan SM (2004) A "mitochondrial cascade hypothesis" for sporadic Alzheimer's disease. *Med Hypotheses* **63**, 8-20.

[64] Blackburn EH (2000) Telomere states and cell fates. *Nature* **408**, 53.

[65] Vera E, Blasco M (2012) Beyond average: potential for measurement of short telomeres. *Aging* **4**, 379.

[66] de la Monte SM, Sohn YK, Wands JR (1997) Correlates of p53- and Fas (CD95)-mediated apoptosis in Alzheimer's disease. *J Neurol Sci* **152**, 73-83.

[67] Lafuente JM, Hall CK, Ngo L, Jay G (1996) Extracellular deposition of beta-amyloid upon p53-dependent neuronal cell death in transgenic mice. *J Clin Invest* **98**, 1632-1638.

[68] Fu W, Begley JG, Killen MW, Mattson MP (1999) Anti-apoptotic role of telomerase in pheochromocytoma cells. *J Biol Chem* **274**, 7264-7271.

AUTHOR COPY

Appendix H

Co-authored Patents

(12) INTERNATIONAL APPLICATION PUBLISHED UNDER THE PATENT COOPERATION TREATY (PCT)

(19) World Intellectual Property Organization
International Bureau

(43) International Publication Date
11 May 2017 (11.05.2017)

WIPO | PCT

(10) International Publication Number
WO 2017/077516 A2

(51) International Patent Classification:
A61K 38/17 (2006.01) *A61P 9/10* (2006.01)
C07K 14/705 (2006.01) *A61P 17/06* (2006.01)
A61P 39/00 (2006.01) *A61P 3/10* (2006.01)
A61P 35/00 (2006.01) *C07K 16/28* (2006.01)
A61P 37/04 (2006.01) *A61K 39/395* (2006.01)
A61P 21/00 (2006.01) *C12N 15/11* (2006.01)
A61P 19/10 (2006.01) *C12N 15/113* (2010.01)
A61P 17/00 (2006.01)

(21) International Application Number:
PCT/IB2016/056686

(22) International Filing Date:
7 November 2016 (07.11.2016)

(25) Filing Language: English

(26) Publication Language: English

(30) Priority Data:
1519557.1 5 November 2015 (05.11.2015) GB

(71) Applicant: **UNIVERSITY OF THE WITWATERSRAND, JOHANNESBURG** [ZA/ZA]; 1 Jan Smuts Avenue, BRAAMFONTEIN, 2000 Johannesburg (ZA).

(72) Inventors: **WEISS, Stefan Franz Thomas**; 12 Melrose Gate, 5 Noordhoek Close, Melrose North, 2196 Johannesburg (ZA). **LETSOLO, Boitelo Theresiah**; 33 Menton Road, Melville, 2092 Johannesburg (ZA). **NAIDOO, Kerrilyn**; 291a South Ridge Road, Glenwood, 4001 Durban (ZA). **OTGAAR, Tyrone Chad**; 959 Bushbuck Street, Allensnek, 1709 Roodepoort (ZA).

(74) Agent: **DESSINGTON & ASSOCIATES, INC.**; Summit Park, 495 Summit Road, Morningside, 2196 Johannesburg (ZA).

(81) Designated States *(unless otherwise indicated, for every kind of national protection available)*: AE, AG, AL, AM, AO, AT, AU, AZ, BA, BB, BG, BH, BN, BR, BW, BY, BZ, CA, CH, CL, CN, CO, CR, CU, CZ, DE, DJ, DK, DM, DO, DZ, EC, EE, EG, ES, FI, GB, GD, GE, GH, GM, GT, HN, HR, HU, ID, IL, IN, IR, IS, JP, KE, KG, KN, KP, KR, KW, KZ, LA, LC, LK, LR, LS, LU, LY, MA, MD, ME, MG, MK, MN, MW, MX, MY, MZ, NA, NG, NI, NO, NZ, OM, PA, PE, PG, PH, PL, PT, QA, RO, RS, RU, RW, SA, SC, SD, SE, SG, SK, SL, SM, ST, SV, SY, TH, TJ, TM, TN, TR, TT, TZ, UA, UG, US, UZ, VC, VN, ZA, ZM, ZW.

(84) Designated States *(unless otherwise indicated, for every kind of regional protection available)*: ARIPO (BW, GH, GM, KE, LR, LS, MW, MZ, NA, RW, SD, SL, ST, SZ, TZ, UG, ZM, ZW), Eurasian (AM, AZ, BY, KG, KZ, RU, TJ, TM), European (AL, AT, BE, BG, CH, CY, CZ, DE, DK, EE, ES, FI, FR, GB, GR, HR, HU, IE, IS, IT, LT, LU, LV, MC, MK, MT, NL, NO, PL, PT, RO, RS, SE, SI, SK, SM, TR), OAPI (BF, BJ, CF, CG, CI, CM, GA, GN, GQ, GW, KM, ML, MR, NE, SN, TD, TG).

[Continued on next page]

(54) Title: COMPOUNDS FOR USE IN THE TREATMENT OF TELOMERE RELATED DISEASES AND/OR TELOMERE RELATED MEDICAL CONDITIONS

WO 2017/077516 A2

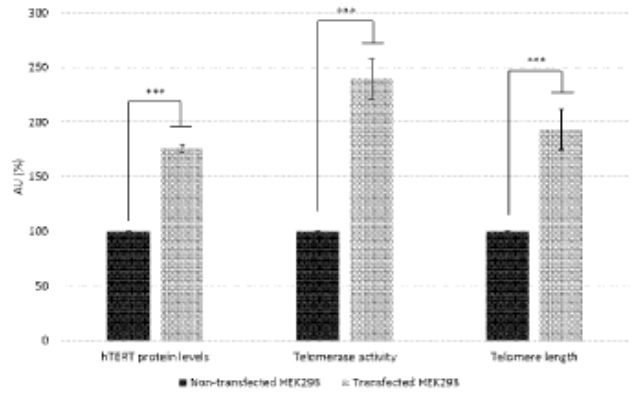


FIGURE 6

(57) Abstract: The invention relates to compounds for use in the treatment of telomere related diseases and/or telomere related medical conditions, particularly wherein said telomere related diseases and/or telomere related medical conditions are cancer and cellular ageing. Particularly, herein is disclosed 37 kDa/67 kDa laminin receptor precursor/ high affinity laminin receptor (LRP/LR) and/or a fragment thereof for use in the treatment and/or prevention of cellular ageing.

WO 2017/077516 A2

Declarations under Rule 4.17:

— *as to applicant's entitlement to apply for and be granted a patent (Rule 4.17(ii))*

Published:

— *without international search report and to be republished upon receipt of that report (Rule 48.2(g))*

— *with sequence listing part of description (Rule 5.2(a))*

WIPO PCT
The International Patent System

WORLD INTELLECTUAL PROPERTY ORGANIZATION

Receipt of Electronic Submission

The Receiving Office (RO/IB) acknowledges the receipt of a PCT International Application filed using ePCT-Filing. An Application Number and Date of Receipt have been automatically assigned (Administrative Instructions, Part 7).

Submission Number:	066788	
Application Number:	PCT/IB2019/066788	
Date of Receipt:	08 July 2019	
Receiving Office:	International Bureau of the World Intellectual Property Organization	
Your Reference:	P1181PC	
Applicant:	UNIVERSITY OF THE WITWATERSRAND, JOHANNESBURG	
Number of Applicants:	1	
Title:	BIOPHARMACEUTICAL AGENTS FOR USE IN REDUCING LIPID CONTENT IN CELLS	
Documents Submitted:	P1181PC-appb-000004.pdf (P1181PC - Weiss 8 - PCT DRAWINGS AS FILED - 8 July 2019.pdf)	1044206
	P1181PC-appb-000006.pdf (P1181PC - Weiss 8 - PCT AS FILED - 8 July 2019.pdf)	1028239
	P1181PC-appb.xml	942
	P1181PC-decl-000001.pdf (P1181PC - Signed Assignment.pdf)	181151
	P1181PC-decl.xml	6098
	P1181PC-dpcf-000001.zip (P1181PC - Preconversion format.zip)	3398029
	P1181PC-feer-000001.pdf (P1181PC - Small Entity Status Letter - 8 July 2019.pdf)	427326
	P1181PC-fees.xml	2298
	P1181PC-poat-000001.pdf (P1181PC - PCT Power of Attorney.pdf)	271164
	P1181PC-requ.xml	8116
	P1181PC-seql-000001.txt (Sequence Listing P1181PC.txt)	9067
	P1181PC-vlog.xml	2808
Submitted by:	Charl MARAIS (Customer ID: user_ZA_MARAIS_CHARL_3104)	
Timestamp of Receipt:	08 July 2019 13:17 UTC+2 (CEST)	
Official Digest of Submission:	1A:E5:69:16:40:B0:C2:EF:DD:0C:44:97:91:E0:E4:2A:82:AD:F1:34	

REPUBLIC OF SOUTH AFRICA

PATENTS ACT, 1978

APPLICATION FOR A PATENT AND ACKNOWLEDGEMENT OF RECEIPT

[Section 30 (1)-Regulation 22]

The granting of a patent is hereby requested by the undermentioned applicant on the basis of the present application.

Official Application No.			Applicant's or Agent's Reference
21	01	**2019/02879**	Weiss 11 - P2001P

71	Full Name(s) of Applicant(s)
University of the Witwatersrand, Johannesburg 1 Jan Smuts Avenue, Braamfontein, 2050, South Africa	

54	Title of Invention
A METHOD OF DECREASING CONCENTRATION OF TAU (T) PROTEIN AND/OR PHOSPHORYLATED TAU (T) PROTEIN	

The applicant has claimed priority (if any) as set out in the abovementioned international application

~~This application is for a patent of addition to patent application No:~~

21	01	

~~This application is a fresh application in terms of section 37 and based on Application No.~~

21	01	

This application is accompanied by:

	1.	A single copy of a provisional specification of _____ pages.
	2.	Drawings of _____ sheet(s).
	3.	Publication particulars and Abstract(Form P8)
	4.	A copy of Figure of the drawings (if any) for the abstract
	5.	Assignment of invention
	6.	Certified priority document(s)
	7.	Translation(s) of the priority document(s)
	8.	Assignment of priority rights
	9.	A copy of the Form P.2 and the specification of S.A Patent Application (if applicable).
	10.	A declaration and power of attorney on Form P3
	11.	Statement on the use of Indigenous Biological Resource, Genetic Resource, Traditional Knowledge or Use on Form P26
	12.	Request(s) for ante-dating/delay of acceptance on Form P4
	13.	Request for classification on Form P4

CONFIRMATION

REPUBLIC OF SOUTH AFRICA | **REGISTER OF PATENTS** | PATENTS ACT, 1978

Official application No.	Lodging date: Provisional	Acceptance date
21 01 **2019/02879**	22 2019/05/09	47
International classification	Lodging date: Complete	Granted date
51	23	

71 Full name(s) of applicant(s)/Patentee(s):

University of the Witwatersrand, Johannesburg

71 Applicant substituted:	Date registrered

71 Assignee(s):	Date registrered

72 Full name(s) of inventor(s):

WEISS, Stefan Franz Thomas
CUTTLER, Catelyn
OTGAAR, Tyrone Chad
VAN DER MERWE, Eloise
BIGNOUX, Monique J.

Priority claimed:	Country	Number	Date

54 Title of invention

A METHOD OF DECREASING CONCENTRATION OF TAU (T) PROTEIN AND/OR PHOSPHORYLATED TAU (T) PROTEIN

Address of applicant(s)/patentee(s):

1 Jan Smuts Avenue, Braamfontein, 2050
SOUTH AFRICA

74 Address for service

University of the Witwatersrand, Johannesburg c/o Dr. R. J. CAVENEY
1 Jan Smuts Avenue, Braamfontein, 2050
SOUTH AFRICA
Reference No. Weiss 11 - P2001P

61 Patent of addition No.	Date of any change

Fresh application based on.	Date of any change

CONFIRMATION

Companies and Intellectual Property Commission

a member of the dti group

Duplicate

Sales Journal

POSTAL ADDRESS
P.O. Box 429
PRETORIA
0001

PHYSICAL ADDRESS
THE DTI Campus (Block F-Entfufukweni)
77 Meintjes Street
SUNNYSIDE
PRETORIA
0001

CALL CENTER
0861 843 384 (South Africa)
+27 11 284 9405 (International)

Sales Journal Number : 47621976
Date : 2019/05/10

Debit Code CAVEN4
Agent R J CAVENEY
Postal Address PO BOX 3106 CRAMERVIEW 2060 SOUTH AFRICA
Document Reference P3696915
File Reference 2019\02879

Form Code Application for a patent accompanied by a provisional specification in terms of section 30(1) {reg. 22(1)(a) and (e)}

Debit Amount -R60

CONFIRMATION

FOR OFFICE USE ONLY

Duplicate Sales Journal

Sales Journal Number : 47621976 **Date :** 2019/05/10

Debit Code CAVEN4
Agent R J CAVENEY
Postal Address PO BOX 3106 CRAMERVIEW 2060 SOUTH AFRICA
Document Reference P3696915
File Reference 2019\02879

Form Code Application for a patent accompanied by a provisional specification in terms of section 30(1) {reg. 22(1)(a) and (e)}

Debit Amount -R60

WIPO PCT
The International Patent System

WORLD INTELLECTUAL PROPERTY ORGANIZATION

Receipt of Electronic Submission

The Receiving Office (RO/IB) acknowledges the receipt of a PCT International Application filed using ePCT-Filing. An Application Number and Date of Receipt have been automatically assigned (Administrative Instructions, Part 7).

Submission Number:	064443	
Application Number:	PCT/IB2020/064443	
Date of Receipt:	11 May 2020	
Receiving Office:	International Bureau of the World Intellectual Property Organization	
Your Reference:	P2001PCWeiss11	
Applicant:	UNIVERSITY OF THE WITWATERSRAND, JOHANNESBURG	
Number of Applicants:	1	
Title:	A METHOD OF DECREASING CONCENTRATION OF TAU (T) PROTEIN AND/OR PHOSPHORYLATED TAU (T) PROTEIN	
Documents Submitted:	P2001PCWeiss11-appb-000004.pdf (P2001PC - Weiss 11 - 11 May 2020 - AS FILED - FIGURES bw.pdf)	1249806
	P2001PCWeiss11-appb-000005.pdf (P2001PC - Weiss 11 - 11 May 2020 - AS FILED - SPEC.pdf)	648199
	P2001PCWeiss11-appb.xml	970
	P2001PCWeiss11-decl-000001.pdf (P2001PC - Confirmation of Assignment Weiss.pdf)	1236902
	P2001PCWeiss11-decl.xml	9700
	P2001PCWeiss11-dpcf-000001.zip (P2001PC - Preconversion format.zip)	4130487
	P2001PCWeiss11-feer-000001.pdf (P2001PC - Small Entity Status Letter.pdf)	427326
	P2001PCWeiss11-fees.xml	2301
	P2001PCWeiss11-poat-000001.pdf (PoA.pdf)	120297
	P2001PCWeiss11-requ.xml	7950
	P2001PCWeiss11-seql-000001.txt (Sequence Listing P2001PC - Weiss 11.txt)	9277
	P2001PCWeiss11-vlog.xml	2318
Submitted by:	Charl MARAIS (Customer ID: user_ZA_MARAIS_CHARL_3104)	
Timestamp of Receipt:	11 May 2020 21:52 UTC+2 (CEST)	
Official Digest of Submission:	29:C6:FC:95:63:EE:87:D9:F3:1B:19:F9:F6:87:F7:CC:E8:B6:6E:83	

Appendix I

Animal Ethics and Cell line Waivers



agriculture,
forestry & fisheries

Department:
Agriculture, Forestry and Fisheries
REPUBLIC OF SOUTH AFRICA

Genetic Resources, Department of Agriculture, Forestry and Fisheries
Private Bag X973, Pretoria 0001

Enquiries: Bathobile Mahlangu • Tel: 012 319 6185 • Fax: 012 319 6298 • E-mail: BathobileM@daff.gov.za •Ref: 39.2/University of Witwatersrand -18/216

Prof SFT Weiss
University of Witwatersrand
School of Molecular and Cell Biology
1 Jan Smuts Ave
Braamfontein
Johannesburg
2050

+27 (0) 11 717 6346 (Tel)
+27 (0) 11 717 6351 (Fax)
Stefan.Weiss@wits.ac.za (email)

Dear Prof Weiss

RE: REGISTRATION OF FACILITY

With reference to the application to register a facility, submitted in terms of the Genetically Modified Organisms Act, 1997 (Act No. 15 of 1997). Registration number **39.2/University of Witwatersrand -19/146.**

The facility is hereby registered; please find attached your certificate which serves as proof of registration. Please familiarize yourself with the Standard Operating Procedure approved for Regulation 2(2) to determine whether your current activities or any future activities would require an additional contained use permit or not.

Please consult the website of the Department at www.daff.gov.za (Branches, Agricultural Production, Health & Food Safety/ Genetic Resources/ Biosafety) for the latest application forms and the SOP document referred to in the above paragraph.

If any of the provisions of the Genetically Modified Organisms Act, 1997 (Act No. 15 of 1997), including any condition of any permit issued in terms of the GMO Act, is not complied with at all times, you will be subject to prosecution in terms of Section 21 of the GMO Act, 1997.

Yours sincerely

Ms N L Mkhonza
Registrar: Genetically Modified Organisms Act, 1997 (Act No. 15 of 1997)

agriculture,
forestry & fisheries

Department:
Agriculture, Forestry and Fisheries
REPUBLIC OF SOUTH AFRICA

CERTIFICATE OF REGISTRATION

Registration Number: **39.2/UNIVERSITY OF WITWATERSRAND - 19/146**

It is hereby certified that the facility situated at:

UNIVERSITY OF WITWATERSRAND
SCHOOL OF MOLECULAR AND CELL BIOLOGY
1 JAN SMUTS AVE
BRAAMFONTEIN
JOHANNESBURG
2050

has been registered in the name(s) of: **PROF SFT WEISS**

on behalf of: **UNIVERSITY OF WITWATERSRAND**

In terms of Regulation 8 of the Genetically Modified Organisms Act, 1997 (Act No. 15 of 1997) in respect of the following-

type of facility: **LABORATORY**

containment level: **ONE (1) & TWO (2)**

for period: **15 MAY 2019 – 15 MAY 2022**

Date issued: **15 MAY 2019**

Registrar for Genetically Modified Organisms

Date

Research Office

INSTITUTIONAL BIOSAFETY COMMITTEE
(R 14/16)

CLEARANCE CERTIFICATE PROTOCOL NUMBER: 20150350Lab

BRIEF DESCRIPTION OF APPLICATION:

Laboratories situated in rooms 612 and 617 in Gate House

APPLICANT: Professor S Weiss

SCHOOL/DEPARTMENT : Molecular & Cell Biology

DATE CONSIDERED: By circulation

DECISION OF COMMITTEE:

These laboratories are considered to meet the standards of the Institutional Biosafety Committee (IBC) as specified in the IBC's published Standard Operating procedures.
Any change to the type of biohazardous agent(s) being handled should be reported to the IBC

1. This clearance certificate expires on 1 March 2016 and may be renewed on application

Radiation and Health Physics Unit
University of Witwatersrand
Johannesburg, Republic of South Africa
Tel: +27 (0) 11 717 6931

DATE: 2 March 2015 CHAIRPERSON: (Mr J Larkin)

DECLARATION OF APPLICANT:

To be completed in duplicate and **one copy** returned to the Secretary, Room 10005, 10th floor, Senate House, University.

1. I have read, understood and accepted the approval conditions above
2. I agree to submit a yearly progress report to the Committee and to submit an interim report on the form provided, in the event of any significant unforeseen event, e.g. suspension of a drug trial, temporary closure or relocation of my laboratory, etc.
3. I note that the University Safety Officer, or his/her representative, may at any reasonable time inspect my laboratory or trial site to ensure compliance with current Health and Safety legislation. I undertake to offer my full co-operation in any such inspection.
4. I have read, understood and will comply with the *recommended standard operating procedures for the handling of biohazardous materials* posted at http://web.wits.ac.za/Academic/Research/Biosafety.htm
5. I declare (delete as appropriate) that:
   a. I have all the approvals required by statute or regulation and by the funding agencies supporting this work, or
   b. that I will not begin work until such approvals are obtained

Signed: Date: 3-Nov-2015

MSWorks2000\Iaq\2015\IBCClear.wpd

Prof S FT Weiss

PLEASE QUOTE THE PROTOCOL NUMBER IN ALL ENQUIRIES

University
of the Witwatersrand,
Johannesburg

Human Research Ethics Committee (Medical)
(formerly Committee for Research on Human Subjects (Medical)

Secretariat: Research Office, Room SH10006, 10th floor, Senate House • Telephone: +27 11 717-1234 • Fax: +27 11 339-6708
Private Bag 3, Wits 2050, South Africa

Ref: W-CJ-130520-1

20/05/2013

TO WHOM IT MAY CONCERN:

Waiver: This certifies that the following research does not require clearance from the Human Research Ethics Committee (Medical).

Investigator: **Professor Stefan F T Weiss.**

Project title: **Targeting the 37 kDa/67 kDa laminin receptor for Alzheimer's Disease treatment.**

Reason: This is a laboratory study using commercial cell lines including - SHSY5Y N2a and HEK293. No humans are involved.

UNIVERSITY OF THE WITWATERSRAND
PROF PE CLEATON-JONES
HREC (MEDICAL)
2013 -05- 20
JOHANNESBURG

Professor Peter Cleaton-Jones
Chair: Human Research Ethics Committee (Medical)

copy: Anisa Keshav, Research Office, Senate House, Wits

Human Research Ethics Committee (Medical)

Research Office Secretariat: Senate House Room SH10005, 10th floor. Tel +27 (0)11-717-1252
Medical School Secretariat: P V Tobias Building, Room 304, 3rd floor Tel +27 (0)11-717-2700
Private Bag 3, Wits 2050, www.wits.ac.za. Fax +27 (0)11-717-1265

Ref: W-CJ-140804-1 04/08/2014

TO WHOM IT MAY CONCERN:

Waiver: This certifies that the following research does not require clearance from the Human Research Ethics Committee (Medical).

Investigator: **Prof ST Weiss.**

Project title: **Antibodies and shRNA targeting the 37kDa LRP/LR for cancer treatment.**

Reason: This is a laboratory study using commercially available or established cell lines at Wits including USHSY5Y, A375, MDA-MB231, HT-29, LNCaP, WHCO1, HEP G2, HPAC, HUVEC, MCF-7, HeLa and HEK-293 or similar. There are no human participants

UNIVERSITY OF THE WITWATERSRAND
PROF PC CLEATON-JONES
HREC (MEDICAL)
2014 -08- 04
JOHANNESBURG

Professor Peter Cleaton-Jones

Chair: Human Research Ethics Committee (Medical)

Copy - HREC(Medical) Secretariat : Anisa Keshav, Zanele Ndlovu.

STRICTLY CONFIDENTIAL

ANIMAL ETHICS SCREENING COMMITTEE (AESC)

CLEARANCE CERTIFICATE NO. 2016/06/38/C

APPLICANT: Professor S F T Weiss

SCHOOL: School of Molecular and Cell Biology
DEPARTMENT:
LOCATION:

PROJECT TITLE: In vivo investigation of the effect of LRP:: FLAG overexpression on the ageing process and telomere dynamics in C57BL/6J mice

Number and Species

40 Female C57BL/6J mice

Approval was given for the use of animals for the project described above at an AESC meeting held on 2016/06/30. This approval remains valid until 2018/11/01.
Unreported changes to the application may invalidate the clearance given by the AESC
An annual progress report must be provided

The use of these animals is subject to AESC guidelines for the use and care of animals, is limited to the procedures described in the application form and is subject to any additional conditions listed below:

There should be no physical contact of the mice that results in injuries during the social behaviour tests

Signed: _____ (Chairperson, AESC) Date: 23/06/2017

I am satisfied that the persons listed in this application are competent to perform the procedures therein, in terms of Section 23 (1) (c) of the Veterinary and Para-Veterinary Professions Act (19 of 1982)

Signed: _____ (Registered Veterinarian) Date: 23 June 2017

cc: Supervisor: N/A
Director: CAS

Works 2003\div2016\AESCCert.wpd